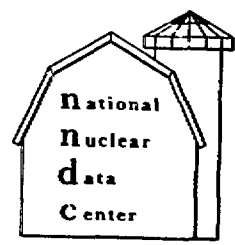# PROCEEDINGS OF THE CONFERENCE ON NUCLEAR DATA EVALUATION METHODS AND PROCEDURES

HELD AT
BROOKHAVEN NATIONAL LABORATORY
UPTON, NEW YORK 11973
September 22-25, 1980

March 1981

INFORMATION ANALYSIS CENTER REPORT

NATIONAL NUCLEAR DATA CENTER
BROOKHAVEN NATIONAL LABORATORY
UPTON, NEW YORK 11973

National
Nuclear
data
Center

$(CONF - 8009979 - (Vol 2)$

PROCEEDINGS OF THE CONFERENCE ON NUCLEAR DATA EVALUATION METHODS AND PROCEDURES

HELD AT
BROOKHAVEN NATIONAL LABORATORY
UPTON, NEW YORK 11973
September 22-25, 1980

Conference Chairman:
R.J. Howerton
Lawrence Livermore National Laboratory

Proceedings Editors:
B.A. Magurno and S. Pearlstein
Brookhaven National Laboratory

March 1981

NATIONAL NUCLEAR DATA CENTER

BROOKHAVEN NATIONAL LABORATORY

ASSOCIATED UNIVERSITIES, INC.

PREFACE

The Conference on Nuclear Data Evaluation Methods and
Procedures organized under the auspices of the Division of High
Energy and Nuclear Physics, the Division of Reactor Research and
Technology, and the Office of Fusion Energy, of the U.S.
Department of Energy and the Electric Power Research Institute
(EPRI) was held at Brookhaven National Laboratory, Sept. 22-25,
1980. The Proceedings are presented in these volumes. The
Conference was held in the format of a workshop in which review
papers were presented by particularly knowledgeable persons in
each aspect of nuclear data evaluation. Following each review
paper there was a discussion period which proved, in most cases,
to be lively.

Both written versions of the reviews and transcribed versions
of the discussion periods are included in this report. It is
hoped that it will serve the double purpose of describing the
state-of-the-art and of providing a handbook of methods that can
be referred by both experienced and new evaluators.

The organization and implementation of this conference
required a large amount of work on the part of many persons.
Quite clearly, the success of the effort depended primarily upon
the reviewers who provided the technical substance. The
organizing committee, made up of the session chairman, selected
the reviewers so an acknowledgment of their efforts is likewise
appropriate. A special word of thanks is due to Dr. J.J. Schmidt
of the IAEA Nuclear Data Section who provided a masterful summary
of each day's discussion as the last item on the day's program.

On the first evening of the meeting there was a "mixer" and a
banquet was held at the end of the second day. Our after-dinner
speaker, Professor H.H. Barschall, recounted his personal
experiences during the early days of discovery of the fission
process and his subsequent experiences with the Manhatten District
Project.

The National Nuclear Data Center of Brookhaven National
Laboratory was the host organization for the conference. Dr. Sol
Pearlstein, Director of the NNDC, and his staff provided excellent
support to the participants by taking care of the details of
travel and housing, by insuring that the session were taped and by
obtaining the use of the excellent auditorium in Berkner Hall.

Finally, I extend my personal thanks and those of the
organizing committee to Mr. Benjamin Magurno of the NNDC. He
handled the myriad of tasks associated with announcing the
conference, pre-registration, organization of the banquet, and
editing and expediting the publication of these proceedings.

<div align="center">

Robert J. Howerton, Chairman
Livermore, California

</div>

TABLE OF CONTENTS

ORGANIZING COMMITTEE

R.J. Howerton, Chairman	LLNL
T.R. England	LANL
H. Henryson, II	ANL
S.F. Mughabghab	BNL
R.W. Peelle	ORNL
R.E. Schenter	HEDL
F. Schmittroth	HEDL
A.B. Smith	ANL
P.G. Young	LANL

LIST OF ATTENDEES

R.A. Anderl, EG&G
E.D. Arthur, LANL
H.H. Barschall, WIS
M.R. Bhat, BNL
R.C. Block, RPI
R.L. Bunting, EG&G
R.F. Chrien, BNL
L. Carter, HEDL
P. Collins, ANL
C.L. Cowan, GE-SU
C.L. Dunford, BNL
C. Durston, BNL
T.R. England, LANL
F. Froehner, KFK
C.Y. Fu, ORNL
M.A. Gardner, LLNL
Y. Gohar, ANL
L. Greenwood, ANL
H. Gruppelaar, ECN
P.T. Guenther, ANL
G.H. Hale, LANL
H. Henryson, II., ANL
R.J. Howerton, LLNL
G. Kegel, U of Lowell
Ch. Lagrange, BRC
D. Larson, ORNL
H. Lemmel, IAEA
H. Liou, BNL
R.C. Little, LANL
M.A. Lone, CRC
C.R. Lubitz, KAPL
R. MacFarlane, LANL
B.A. Magurno, BNL

D.G. Madland, LANL
J.H. Marable, ORNL
M. Mattes, USTUT
E. Menapace, CNEN
G.H. Miley, UI
P.A. Moldauer, ANL
M.S. Moore, LANL
S.F. Mughabghab, BNL
D. Nethaway, LLNL
D. Oberg, HEDL
O. Ozer, EPRI
B. Patrick, HAR
S. Pearlstein, BNL
R.W. Peelle, ORNL
F.G.J. Perey, ORNL
C. Philis, BRC
W.P. Poenitz, ANL
P. Reeder, BNWL
C.W. Reich, EG&G
B.F. Rider, GE-V
J. Rowlands, WIN
J.J. Schmidt, IAEA
F. Schmittroth, HEDL
R. Sher, STAN
A.B. Smith, ANL
L. Stewart, ORNL
H. Takahashi, BNL
N. Tubbs, NEADB
R.J. Tuttle, RI-AI
H. Vonach, IRK
H. Weigmann, CBNM
L. Weston, ORNL
N. Yamamuro, TIT
P.G. Young, LANL

Dup

USE OF R-MATRIX METHODS FOR LIGHT ELEMENT EVALUATIONS

G. M. Hale

Los Alamos Scientific Laboratory, University of California
Theoretical Division
Los Alamos, New Mexico 87545

ABSTRACT

Some general aspects of parameterizing nuclear re-
action data with a unitary, multichannel theory are
discussed. The special case of R-matrix theory is con-
sidered, where the explicit separation of long- and
short-range forces and the natural occurrence of energy
pole terms afford a number of advantages in describing
data for light-element reactions. Examples are given
for both neutron- and charged-particle-induced reac-
tions which illustrate multichannel R-matrix tech-
niques, including the use of charge symmetry to relate
data for mirror systems. The limitations of conven-
tional R-matrix methods are discussed briefly.

INTRODUCTION

Nuclear data evaluation often involves the parametric repre-
sentation of experimental measurements to produce smooth func-
tions of incident energy and scattering angle. To build in even
the simplest of the conservation laws for nuclear interactions,
e.g., flux, total angular momentum, and parity, one needs to pa-
rameterize the unitary collision matrix, U. [1] The most famil-
iar of these is a direct parameterization of U in terms of phase
shifts, absorptions, and mixing angles. However, the unitary
realizations of U in terms of these parameters becomes increas-
ingly cumbersome as the number of coupled states exceeds two.
Furthermore, the energy dependence of these parameters, which
comes in great part (especially at low energies) from the known
long-ranged parts of the interactions, remains unspecified.

These difficulties with the direct parameterization of the
collision matrix can be circumvented by using R-matrix theory.
[2] Following a simplified illustration of multi-reaction data
analyses using a unitary description, we shall introduce the pa-
rameters of R-matrix theory in a brief summary of the formalism.

Unitary Description of Nuclear Reactions

At sufficiently low energies, a system of interacting nuclear particles eventually separates into pairs of clustered fragments which mutually interact only through Coulomb forces (if present). In regions of configuration space where this separation holds (the "external region"), the radial wavefunction describing the relative motion of any possible two-body arrangement channel c can be expressed as

$$u_c(r_c) = I_c(r_c) - \sum_{c'} O_{c'}(r_c) U_{c'c} \quad , \tag{1}$$

where the collision matrix elements $U_{c'c}$ are amplitudes of outgoing spherical waves $O_{c'}$ in each of the channels c' for incoming spherical waves I_c normalized to unit flux incident in channel c. Conservation of the (unit) incident flux in all the outgoing channels implies unitary of the collision matrix,

$$UU^\dagger = U^\dagger U = 1 \quad . \tag{2}$$

The results of any scattering measurement done on the system can be expressed as bilinear combinations of the elements of U. In particular, the differential, integrated, and total cross sections for uncharged incident particles are given by

$$\frac{d\sigma_{\alpha'\alpha}}{d\Omega_{\alpha'}} = F_\alpha \sum_L B_L P_L (\cos \theta_{\alpha'}) \quad , \tag{3}$$

with

$$B_L = \frac{1}{4} \sum_{s's} (-1)^{s'-s} \sum_{J_1 J_2 \ell'_1 \ell'_2 \ell_1 \ell_2} \bar{Z}(\ell'_1 J_1 \ell'_2 J_2, s'L)$$

$$\bar{Z}(\ell_1 J_1 \ell_2 J_2, sL) \text{Re}(U_{c'_1 c_1} - \delta_{c'_1 c_1})(U_{c'_2 c_2} - \delta_{c'_2 c_2})^* \quad ,$$

$$\sigma_{\alpha'\alpha} = \pi \underset{Js's\ell'\ell}{F_\alpha} \sum (2J+1) |U_{c'c} - \delta_{c'c}|^2 \quad , \tag{4}$$

$$\sigma_{T,\alpha} = 2\pi F_\alpha \sum_{Js\ell} (2J+1) \left[1 - \text{Re}(U_{cc}) \right] \quad , \tag{5}$$

where the factor $F_\alpha = [k_\alpha^2 (2s_{1\alpha}+1)(2s_{2\alpha}+1)]^{-1}$ is defined in terms of the incident center-of-mass wave number k_α and spins $s_{1\alpha}$ and $s_{2\alpha}$. The channel label c contains an arrangement index α and the quantum numbers s, ℓ, and J, for spin, orbital angular momentum, and total angular momentum, respectively. The coefficients $\bar{Z}$ are related to those of Blatt and Biedenharn, as defined in Ref. [3].

The unitary conditions (2) satisfied by the collision matrix impose strong constraints on data for different reactions calculated from relations like Eqs. (3)-(5) for the cross sections. To illustrate this, we consider the simple case of only two coupled states, each of which belongs to a different arrangement α. The 2 x 2 collision matrix is conveniently parameterized in terms of Stapp's "nuclear-bar" parameters [4] by

$$
U = \begin{bmatrix} \eta \, e^{2i\delta_1} & i\sqrt{1-\eta^2} \, e^{i(\delta_1+\delta_2)} \\ i\sqrt{1-\eta^2} \, e^{i(\delta_1+\delta_2)} & \eta \, e^{2i\delta_2} \end{bmatrix} \tag{6}
$$

In addition to being unitary, the matrix is symmetric as is required by time-reversal invariance. [1]

We see the unitary and time-reversal conditions allow a parameterization of U in terms of only three real parameters, δ_1, δ_2, and η, which are, in principle, completely determined by analyzing (1,1) and (2,2) scattering data. Thus, in this simple case, data for the (1,2) reaction are <u>completely</u> <u>redundant</u> with (1,1) and (2,2) scattering data. Of course, in most cases of interest, other states must be taken into account that dilute these simple results, but the tendency of unitarity to relate data for different reactions remains, particularly near resonances where the dominance of a few states more closely approximates the simple situation described above.

The ability to include redundant data from different sources has clear statistical advantages in the determination of parameters by fitting experimental measurements. The parameters are better defined simply because their over determination is increased, and they are influenced less by systematic errors in the measurements, assuming these errors occur in random, uncorrelated ways among data for different reactions. Including measurements of observables other than cross sections (polarizations, etc.) has much the same effect, and in addition, since they depend on different bilinear combinations of the collision matrix elements, tends to eliminate multiple solutions for the parameter values, a well-known problem which plagues phase-shift analyses of cross sections.

From the considerations above, it is clear that evaluation purposes are well served by a parameterization of nuclear reactions having a simple multichannel generalization which, at a minimum, builds in the unitarity and symmetry of the collision matrix. R-matrix theory provides such a parameterization which,

moreover, explicitly contains the dependence of the collision matrix on the known, long-ranged forces. A brief, formal summary of this theory is given in the following section.

R-Matrix Formalism

We outline here, for the sake of completeness, dicussion which has appeared in previous contributions [5], [6] to cross section and evaluation meetings, and which is equivalent to that found in the literature. [2], [3], [7] R-matrix theory presumes there exists a set of finite relative coordinates, called "channel radii," beyond which short-ranged forces vanish, and the wavefunction has the form given in Eq. (1). These channel radii (a_c) define a "channel surface," inside of which (i.e., the "internal" region) the wavefunction can be expressed as a formal solution of the Schroedinger equation

$$\Psi = (H-E + \mathcal{L})^{-1} \mathcal{L} \Psi \quad , \tag{7}$$

with the addition of a "boundary condition" operator

$$\mathcal{L} = \sum_c |c)(c| \left(-\frac{\partial}{\partial r_c} r_c - B_c\right) \quad , \tag{8}$$

which projects onto the channel surface and makes the internal hamiltonian operator H hermitian. [7] The "channel surface" functions $|c)$ in Eq. (8) are defined in terms of channel spin-angle eigenfunctions of total angular momentum and parity, $Y_c(\hat{r}_c)$ and the channel reduced masses, m_c, by

$$|c) = \left(\frac{\hbar^2}{2m_c a_c}\right)^{1/2} \frac{\delta(r_c - a_c)}{r_c} Y_c(\hat{r}_c) \quad , \tag{9}$$

and B_c are the real, energy-independent boundary condition numbers which characterize the theory of Wigner and Eisenbud. [2]

Using Eq. (8) in the projection of Eq. (7) on the channel surface gives

$$(c'|\Psi) = \sum_c (c'|G|c)(c|\frac{\partial}{\partial r_c} r_c - B_c \tag{10}$$

where the Green's function operator

$$G = (H + \mathcal{L} - E)^{-1} \tag{11}$$

is hermitian due to the choice (8) for $\mathcal{L}$. But because the wavefunction and its first derivative are continuous across the channel surface, the projection $(c|\Psi)$ is simply Eq. (1) evaluated at $r_c = a_c$. Thus, Eq. (10) leads to a relation between elements of the R matrix,

$$R_{c'c} \equiv (c'|G|c) \quad , \tag{12}$$

and elements of the unitary collision matrix $U_{c'c}$ appearing in Eq. (1). In matrix form, this relation is [3]

$$U = 2I0^{-1}[1-R(L-B)]^{-1}RO^{-1} + IO^{-1} \cdot , \tag{13}$$

where the incoming and outgoing spherical waves are evaluated at $r_c = a_c$, as is the logarithmic derivative $L_c = a_c \frac{\partial}{\partial r_c} O_c/O_c$.

The unitarity of the collision matrix U follows from the hermiticity of the R matrix. Furthermore, R, being surface matrix elements of the internal Green's function (11) depends only upon the properties of the internal hamiltonian H, which is dominated by nuclear forces. External Coulomb and angular momentum effects are separated out in Eq. (13) and contained in the surface functions O, I, and L. The real and imaginary parts of $L = S + iP$ are usually called the "shift" and "penetrability" functions, respectively, while the phase of O is termed the "hard sphere" phase shift, ϕ.

The hermiticity of G allows a simple and familiar expansion for the R matrix. Since the eigenfunctions $|\lambda)$ satisfying

$$(H + \mathcal{L})|\lambda) = E_\lambda |\lambda) \quad , \tag{14}$$

for real eigenvalues E_λ form a complete orthonormal set in the internal region, G has the spectral expansion

$$G = \sum_\lambda \frac{|\lambda)(\lambda|}{E_\lambda - E} \quad . \tag{15}$$

from which it follows immediately that

$$R_{c'c} = (c'|G|c) = \sum_\lambda \frac{\gamma_{c'\lambda} \gamma_{c\lambda}}{E_\lambda - E} \quad , \tag{16}$$

where $\gamma_{c\lambda} = (c|\lambda)$ is the "reduced width" amplitude.

Equations (13) and (16) constitute the simple unitary, symmetric, multichannel description of nuclear reactions desired for parametric fits to experimental data. The parameters of R-matrix theory, the $\gamma_{c\lambda}$ and E_λ, depend in principle upon the channel radii a_c and boundary conditions B_c. But since one can transform the parameters $\gamma_{c\lambda}, E_\lambda$ analytically from one boundary condition to another [8], the values of B_c are of no practical consequence (although they can be important in interpretations of the $\gamma_{c\lambda}$ and E_λ). In principle, the same is true of the channel radii a_c, provided that they always exceed the range of the short-ranged inter-cluster forces. But in practice, the sum over levels in (16) is always truncated, and the correspondence of the $\gamma_{c\lambda}$ and E_λ for different radii is difficult to establish. Fortunately, it appears in most cases that truncated level expansions can give good descriptions of the data over finite energy regions if the channel radii are close to the sizes of the interacting nuclei $[a \sim r_0(A_1^{1/3} + A_2^{1/3})]$

The simple pole terms of the R-matrix expansion can be made to correspond with resonances of the interacting system of particles. However, distant-level, or "background" (sometimes called R_∞) poles usually identified with shorter-lived "direct" processes can also be included. Both types of terms are important in describing reactions in light nuclei, and the off-diagonal distant-level contributions to the R matrix usually cannot be neglected since they correspond to direct stripping and pick-up mechanisms.

R-MATRIX CODES AND METHODS

Several codes have been developed to fit experimental data with R-matrix parameters. The emphasis of some of the work done with these codes is on nuclear structure studies, where the main interest is in the values of the parameters; and of others, evaluation, where the fits to the data are of primary concern. In either case, the calculational procedures are much the same. One chooses for a set of two-body channels in the system of interest (usually the open channels in the energy range under consideration) values of channel radii and maximum orbital angular momentum quantum numbers (ℓ_{max}). This defines a finite number of states for the problem, coupled according to their values of total angular momentum and parity (J^P). For each J^P, a finite number of levels is specified by choosing level eigenenergies E_λ and channel reduced widths $\gamma_{c\lambda}$. Starting values for many of these parameters can be obtained from compilations of nuclear structure data [9] or from theoretical calculations. The R-matrix elements are formed according to Eq. (16) and combined with the surface quantities derived from Coulomb wavefunctions to give the collision matrix elements of Eq. (13), which are then used in Eqs. (3)-(5) (or in corresponding relations) to calculate the cross sections (or other observables). The R-matrix

parameters are adjusted to achieve a "best" fit in some sense to the experimental data included in the analysis.

Characteristics of some of the R-matrix codes currently being used are listed in Table I. MULTI [10] has been used in nuclear-structure studies for neutrons incident on a variety of heavy and light elements. Codes in the ORMAP sequence [11] have been used to analyze and extract nuclear-structure information from neutron elastic and inelastic measurements done on light targets between ^{6}Li and ^{13}C at Ohio University.

The RFUNC program is a single-channel (R-function) code used at ORNL to evaluate the n-^{12}C cross sections at energies below 2 MeV [12] for ENDF/B. A similar R-function program is used at Yale University and at ANL. EDA [13] has been used to analyze data for both neutron- and charged-particle-induced reactions in light systems between A_6 = 4 and A_{15} = 17. The ENDF/B evaluation for ^{4}He, and those for ^{6}Li, ^{10}B, ^{15}N, and ^{16}O at low energies, were based on R-matrix analyses using this code. EDA is the most general R-matrix program available, but it requires large computers, whereas most of the other codes can be run on a PDP-10.

Different methods of preparing the input data are used in analyses done with these codes. MULTI and EDA use the data directly, weighted in most cases by the quoted experimental errors, assuming no correlations (other than overall normalizations) exist among the measurements. ORMAP analyzes Legendre coefficients derived from the experimental data, neglecting correlations among the input coefficients. In their ^{12}C evaluation, Fu and Perey [12] first estimated averaged values and covariances for six individual sets of total cross-section measurements, then combined them using Bayes' theorem to obtain a significantly reduced number of points and associated covariances for input to their R-matrix analysis.

Three of the codes (MULTI, RFUNC, and EDA) use automated search routines to minimize the χ^2 of their fits to the input data, thereby obtaining information about the second derivatives of χ^2 with respect to the R-matrix parameters. Twice the inverse of the matrix of these second derivatives evaluated at the parameter values which minimize the χ^2 gives the covariance matrix C for the parameters p. A straightforward application of first-order error propagation gives for the covariances among the calculated cross sections,

$$\text{cov} (\sigma_i, \sigma_j) = \sum_{k\ell} \frac{\partial \sigma_i}{\partial p_k} C_{k\ell} \frac{\partial \sigma_j}{\partial p_\ell} \, , \tag{17}$$

where σ_i and σ_j, can be cross sections for different reactions, for different energies, and for different angles, and the derivatives $\partial\sigma/\partial p$ are evaluated at the parameter values which minimize χ^2. Such calculations were used to provide the covariance files at low energies for the ENDF/B evaluations of ^{6}Li, ^{10}B, and ^{12}C.

EXAMPLES

In this section, we present specific examples from analyses done with EDA to enlarge on some of the points made in the introductory sections and to illustrate R-matrix techniques which appear to account rather successfully for a large body of data from reactions among light nuclei.

Low-Energy Behavior of Cross Sections

At low energies, one expects the incident particle to be affected mainly by the long-ranged parts of the interaction due to its long wavelength. These are the parts of the interaction (i.e., Coulomb and angular momentum effects) that are treated "exactly" in R-matrix theory. Indeed, all the simple dependencies one expects for low-energy cross sections--"1/v" for exoergic neutron-induced reactions, "constant" for neutron elastic scattering with hard-sphere s-waves, "Gamow" for charged-particle induced reactions, etc.--come automatically from the penetrability functions P of the theory. These simple dependencies are modified by the short-ranged effects contained in the R matrix itself, which can be significant in the case of low-lying resonances.

As a first example, we show in Fig. 1 the ratio of the $^{10}B(n,\alpha)$ and $^6Li(n,\alpha)$ cross sections as calculated from the R-matrix analyses of reactions in the ^{11}B and ^7Li systems to provide $n-^{10}B$ and $n-^6Li$ cross sections at low energies for ENDF/B-V, compared to recent measurements done at NBS. The measured and calculated shapes are normalized to 1 at 15 eV, so that one has only a comparison of the shapes of the cross sections as a function of energy. If both cross sections were strictly 1/v, the ratio would plot as a horizontal straight line, and in fact, one sees about a 2% deviation from this behavior up to 1 keV in both the measurements and the calculation. In the calculations, the deviation comes from a broad $7/2^+$ s-wave resonance which causes the $^{10}B(n,\alpha)$ cross section to drop below 1/v. The $^6Li(n,\alpha)$ cross section, having no low-lying s-wave resonances, remains close to 1/v in this region. The break in the measurements at energies below 10 eV is not yet understood, but is believed to be a molecular effect in the $^{10}BF_3$ crystal.

A similar plot in Fig. 2 shows the ratio of the $^{10}B(n,\alpha)$ to $^3He(n,p)$ cross sections at energies below 50 keV. Again, the data are recent measurements by the NBS group, the solid curve is the R-matrix calculation, and the dashed curve is the present ENDF/B evaluation. A significant departure from 1/v is caused in this case by a 0^+ resonance in the $^3He(n,p)$ cross section located just below the $n-^3He$ threshold. The departure enters gradually in the R-matrix calculation, as the data indicate, whereas the evaluation, without the guidance of low-energy data, was forced to make a rather abrupt transition between regions of 1/v and non-1/v behavior in the cross section.

Fig. 3 shows an example for an important charged-particle fusion process, the $T'(d,n)^4$He reaction. The Gamow penetrability and $1/k^2$ factors have been removed from the cross section, leaving an "astrophysical S-function" which presumably behaves as a constant at low energies. In fact, the dashed horizontal line labeled "Gamow extrapolation" corresponds to the cross-section values reported by Arnold et al. [14] in place of their own experimental measurements [15] at energies below 20 keV. The R-matrix calculation clearly does not follow the Gamow dependence at low energies due to a $3/2^+$ s-wave resonance at 100 keV, and tends to confirm the behavior of the original measurements [15].

Unitary Constraints Near Resonances

As was mentioned in the introduction, unitary constraints near resonances can approach the simple situation illustrated by the single 2 x 2 collison matrix. A good example is the cross sections for $n-^6$Li near the 245 keV resonance, which has two states coupled to $J^P = 5/2^-$. A quick look back at Eqs. (4), (5), and (6) will show that for δ_1 resonant ($\approx \pi/2$), the peak total and reaction cross sections are both determined by the η parameter alone. Thus, the failure of the ENDF/B-IV R-matrix analysis to fit both Diment's [16] relatively precise total cross sections and measurements [17,18] of the ^{6}Li(n,t) cross section near the peak, as shown in Fig. 4, signaled a severe (>15%) unitary inconsistency between measurements of the neutron cross sections. Additional input on the values of η was gained from precise (2,2) t-α elastic scattering measurements [19] over the resonance, which indicated that the calculated peak total cross section needed to be raised and the peak (n,t) cross section somewhat lowered (the anti-correlation between the peak total and (n,t) cross sections is also a consequence of unitarity). Cross sections from the revised analysis (ENDF/B-V) including the precise t-α data are seen in Fig. 5 to agree well in the peak of the resonance with later measurements of the total cross section [20] and of the (n,t) cross sections [21,22], achieving unitary consistency among the cross sections for this system near the peak of the resonance to the order of $\lesssim 3\%$.

Charge-Symmetric Techniques

The fact that the R-matrix has the same symmetries as the internal hamiltonian, which is dominated by nuclear forces, can be exploited to introduce symmetry properties not shared by the collision matrix. One of these is the charge symmetry of nuclear forces, which means that nuclear forces in a system are unchanged by the interchange of protons and neutrons. This implies that the R-matrix parameters for mirror systems are essentially the same if the boundary condition numbers B_c are taken to be the same. The parameters need to be corrected for internal Coulomb effects which can be treated perturbatively, as was described at the Harwell meeting [23].

We have used charge-symmetric R-matrix analyses to describe successfully data from mirror reactions in the 4-, 5-, and 7-nucleon systems. The ENDF/B ^{4}He evaluation, for instance, comes from an R-matrix analysis which describes n-α and p-α data simultaneously with essentially the same parameters. The example shown in Fig. 6 is a charge-symmetric prediction for the n-T total cross section from an R-matrix analysis of p-^{3}He scattering data below 20 MeV. The differences between the prediction (solid curve) and the ENDF/B evaluation (dashed curve), which is representative of all but the most recent data, are quite large at energies below 1 MeV. However, a precise new measurement of the total cross section done at LLL [24] appears to confirm the prediction at low energies, which resolves a long-standing conflict between measurements of the low-energy n-T cross section and those of the coherent scattering length [25].

LIMITATIONS OF CONVENTIONAL R-MATRIX THEORY

The first limitation one encounters in applying R-matrix theory to the description of light nuclear reactions is the restriction to two-body channels. Especially when deuterons are involved, the thresholds for three- (and more) body channels occur at relatively low energies. Such channels can be accounted for approximately by treating them as pseudo two-body channels in which pairs of the particles are resonant. This treatment is usually adequate to account for absorption in the two-body channels due to three-body states and can even be used to fit three-body spectra if the widths of the resonating sub-structures are properly taken into account.

The second limitation of the theory that is important in applications to light nuclei is the assumption that the channels for different arrangements are orthogonal at finite channel radii. This orthogonality is automatic for channels having the same two-body arrangement, and holds for channels from different arrangements if the channel radii are infinite, but in general the overlap is non-zero for channels from different arrangements at finite channel radii.

Including channel non-orthogonality affects the relation (13) between the R matrix and the collision matrix, U, in that the quantities I and O no longer remain simple, diagonal matrices of Coulomb wavefunctions. Unfortunately, the off-diagonal elements of these matrices become complicated integrals that cannot be evaluated in a model-independent manner. However, taking such contributions into account with a simple three-particle model, for instance, would build into R-matrix theory the particle-exchange effects that have been speculated to be important in explaining, for example, the large 1/v cross section at low energies in the ^{6}Li(n,t)^{4}He reaction.

CONCLUSIONS

The introductory discussion and examples given were intended to present two main points; first, that unitarity is a necessary and useful theoretical constraint to impose upon the evaluation of microscopic nuclear data, and second, that R-matrix theory provides a unitary framework particularly well-suited for describing reactions in light nuclei. The full advantages of this approach for evaluation purposes are realized only by doing multi-reaction analyses, including data for a variety of observable types. This has been done, wherever possible, for the R-matrix-based evaluations for ^{4}He, ^{6}Li, ^{10}B, ^{12}C, ^{15}N, and ^{16}O, and perhaps should be used to update evaluations for some of the other light elements in ENDF/B.

Users of R-matrix codes for data evaluation appear to agree on the desirability of diluting the influence of any one data set on the final results, either by including a large number of data sets directly in the analysis or by precombining measurements of the same quantity. The second approach, if it is done in a statistically unbiased fashion, obviously has merit when some of the data sets contain unmanageably large numbers of points. The complication in this case, however, is that covariances must be supplied with the input data.

Finally, we conclude with the observation that this basically successful approach to describing charged-particle and neutron-induced reactions has some interesting areas for further study. A more sophisticated treatment of the internal Coulomb corrections we are making to R-matrix parameters would improve the predictive capability of this technique and possibly allow a better assessment of the consistency of data for mirror reactions with charge symmetry of nuclear forces. An approximate accounting for three-body channels and for channel non-orthogonality at finite radii could result in more detailed agreement with experimental measurements and a better undertanding of the origin of certain non-resonant features in the data.

Most of the analyses described here using EDA were done in collaboration with D. C. Dodder and K. Witte. I am grateful to C. Bowman and A. Carlson at the National Bureau of Standards for providing Figures 1 and 2 showing some of their recent measurements prior to publication.

REFERENCES

1.   G. Breit, Phys. Rev. 58, 1068 (1940).

2.   E. P. Wigner and L. Eisenbud, Phys. Rev. 72, 29 (1947).

3.   A. M. Lane and R. G. Thomas, Rev. Mod. Phys. 30, 257 (1958).

4.   H. P. Stapp, T. J. Ypsilantis, and M. Metropolis, Phys. Rev. 105, 302 (1957).

5. G. M. Hale, "R-Matrix Methods for Light Systems, IAEA-90, Vol. II, p. 1 (1976).

6. G. M. Hale and D. C. Dodder, "R-Matrix Analyses of Light-Element Reactions for Fusion Applications," Proc. Int. Conf. on Nuclear Cross Sections for Technology, Knoxville (1979), to be published, and LA-UR-79-2896 (1979).

7. A. M. Lane and D. Robson, Phys. Rev. 51, 774 (1966).

8. F. C. Barker, Aust. J. Phys. 25, 341 (1972).

9. F. Ajzenberg-Selove, "Energy Levels of Light Nuclei," Nucl. Phys. A320 (1979), A336 (1980).

10. G. F. Auchampaugh, "MULTI, A FORTRAN Code for Least Squares Fitting of Neutron Cross Section Data Using the Reich-Moore Multilevel Formalism," LA-5473-MS (1974).

11. R. Lane and collaborators, ORMAP (Ohio R-Matrix Program), unpublished.

12. C. Y. Fu and F. G. Perey, Atom. Data and Nucl. Data Tables 22, 249 (1978).

13. D. C. Dodder, K. Witte, and G. M. Hale, EDA (LASL Energy Dependent Analysis Code), unpublished.

14. W. R. Arnold et al., Phys. Rev. 93, 483 (1954)

15. W. R. Arnold et al., "Absolute Cross Section for the Reaction T(d,n)He^4 from 10 to 120 keV," LA-1479 (1953).

16. K. M. Diment and C. A. Uttley, "The Total Cross Section of ^{6}Li," AERE-PR/NP 15, 12 (1969).

17. M. S. Coates, G. J. Hunt, and C. A. Uttley, "Measurements of the Relative ^{6}Li(n,α) Cross Sections in the Energy Range 1 keV to 7500 keV," Neutron Standards Reference Data, IAEA, Vienna, p. 105 (1974).

18. W. P. Poenitz, Z. Phys. 268, 359 (1974).

19. R. A. Hardekopf et al., "^{4}He(t,t)^{4}He Elastic Scattering: Analyzing Powers and Differential Cross Sections," LA-6188 (1977).

20. P. Guenther, A. Smith, and J. Whalen, "Neutron Total and Scattering Cross Sections of ^{6}Li in the Few MeV Region," ANL/NDM-52 (1980), and personal communication from A. Smith (1980).

21. G. P. Lamaze, R. A. Schrack, and O. A. Wasson, Nucl. Sci. Eng. 68, 183 (1978).

22. C. Renner et al., Bull. Am. Phys. Soc. 23, 526 (1978).

23. D. C. Dodder and G. M. Hale, "Applications of Approximate Isospin Conservation in R-Matrix Analyses," in Neutron Physics and Nuclear Data, Proceedings (Harwell), p. 490 (1978).

24. T. W. Phillips, B. L. Berman, and J. D. Seagrave, Phys. Rev. C22, 384 (1980).

25. H. Rauch, "The Low Energy Neutron Scattering Lengths of ^{3}He and T and Their Relation to the Four-Body Problem," in Few Body Systems and Nuclear Forces I, (Proceedings, Graz), p. 289 (1978).

TABLE I

CHARACTERISTICS OF SOME R-MATRIX CODES IN CURRENT USE

Code:	MULTI	ORMAP	RFUNC	EDA
Developed at:	LLL(LASL)	Ohio U	ORNL	LASL
Incident particles:	neutrons	neutrons	neutrons	general
No. arrangements:	3	3	1 (spin) target	no limit*
No. levels/J^P:	no limit*	5	10	no limit*
ℓ_{max}:	6	3	3	no limit*
Types of data analyzed:	Int. cross sections for (n,n), (n,n'), (n,γ), (n,f)	Legendre coeffi- cients for σ,P up thru L=5	σ,P	general
Search Method:	Automated Levenberg- Marquardt algorithm	Manual	Automated grid	Automated rank-1 variable metric
Fits on:	PDP-10	PDP-10	PDP-10	CDC-7600

*

Subject to overall storage limitations
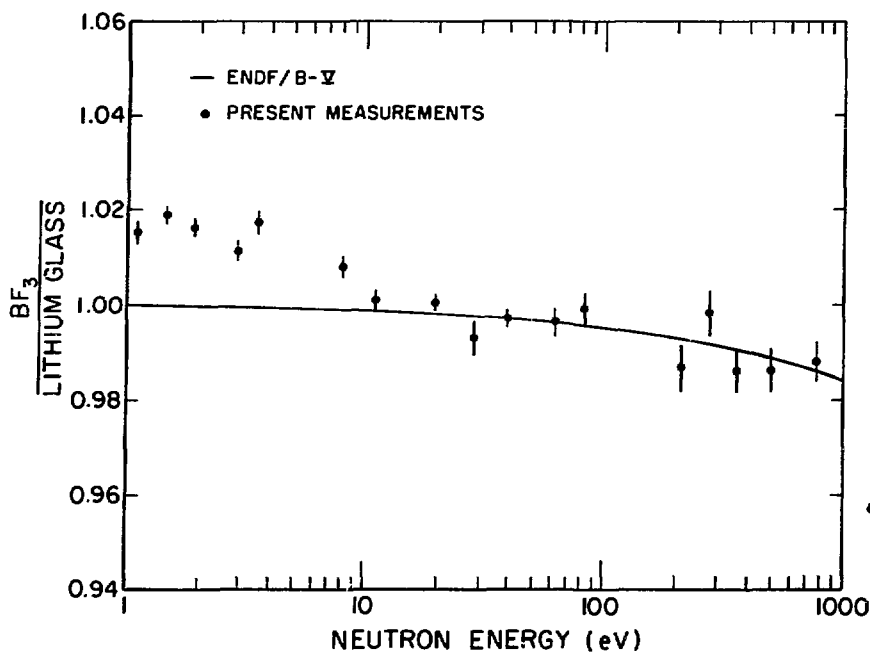
Fig. 1.
Ratio of the relative shapes of the $^{10}B(n,\alpha)$ and $^{6}Li(n,\alpha)$
cross sections at energies between 1 eV and 1 keV. The
points are recent measurements from NBS, and the curve is
from R-matix calculations used in the ENDF/B-V evaluations
for ^{10}B and ^{6}Li.
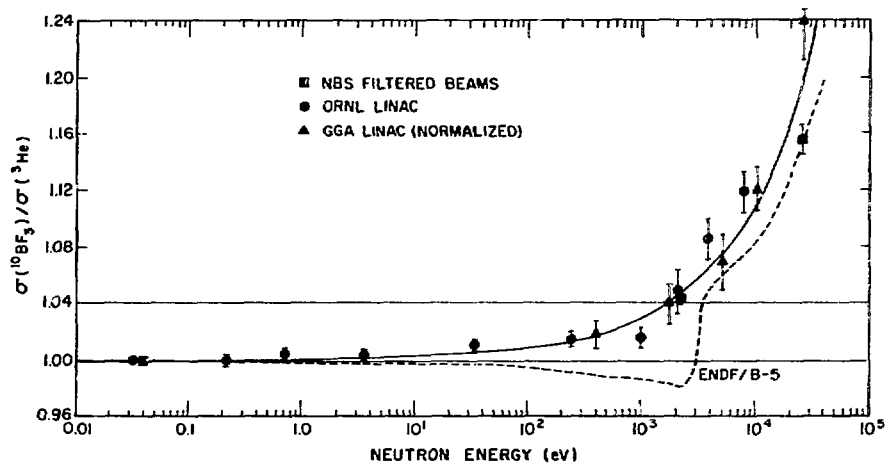
Fig. 2.

Ratio of the relative shapes of the $^{10}B(n,\alpha)$ and $^{3}He(n,p)$ cross sections at energies between 10 eV and 50 keV. All the points are measurements by the NBS group. The solid curve is a calculation of the ENDF/B-V $^{10}B(n,\alpha)$ cross section relative to the $^{3}He(n,p)$ cross section obtained from an R-matrix analysis of reactions in the ^{4}He system; the dashed curve is for the same $^{10}B(n,\alpha)$ cross section relative to the ENDF/B-V $^{3}He(n,p)$ cross section.
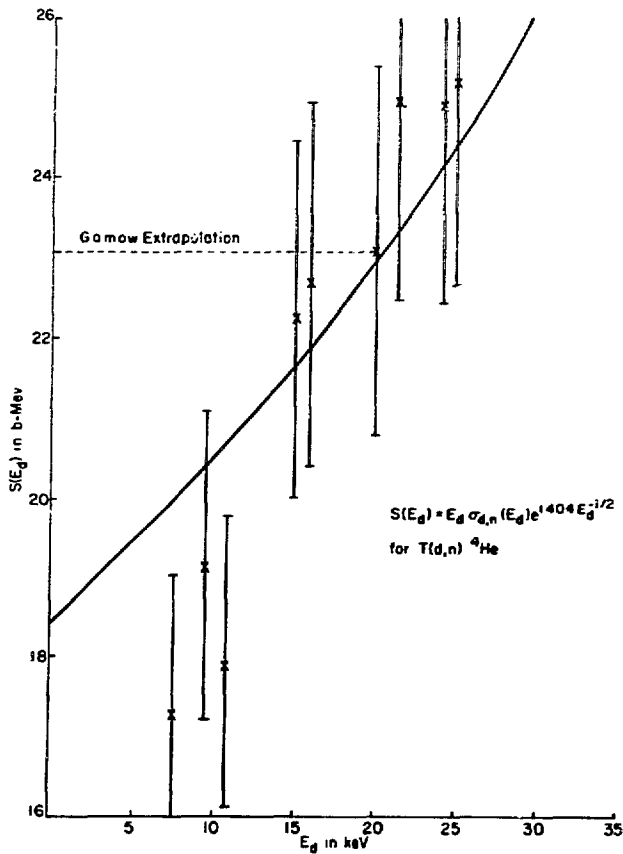
Fig. 3.
Astrophysical S-function for T(d,n)^{4}He as a function of
laboratory energy. The solid curve is the R-matrix calcu-
lation, and the dashed line is the Gamow extrapolation re-
ported by Arnold et al. [14] in place of their measured
points [15] at energies below 20 keV.
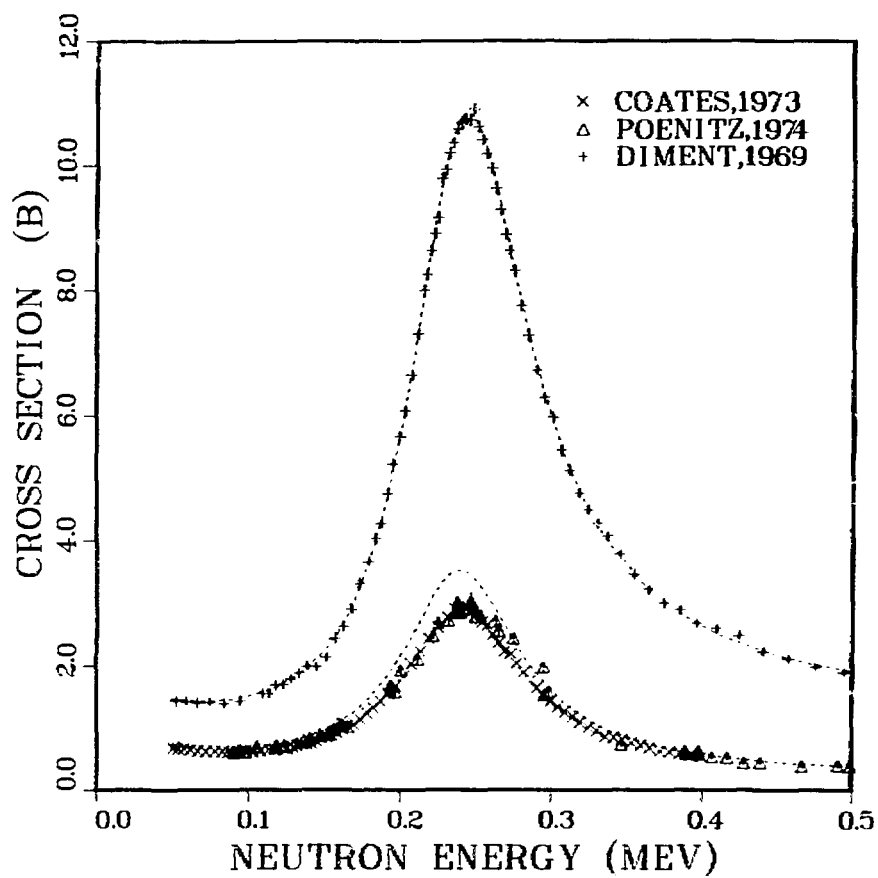
Fig. 4.
Measurements of the n-^{6}Li total cross section by Diment [16] and of the ^{6}Li(n,t) reaction cross section by Coates [17] and by Poenitz [18] compared to calculated values (dashed curves) from the R-matrix-based ENDF/B-IV evaluation.
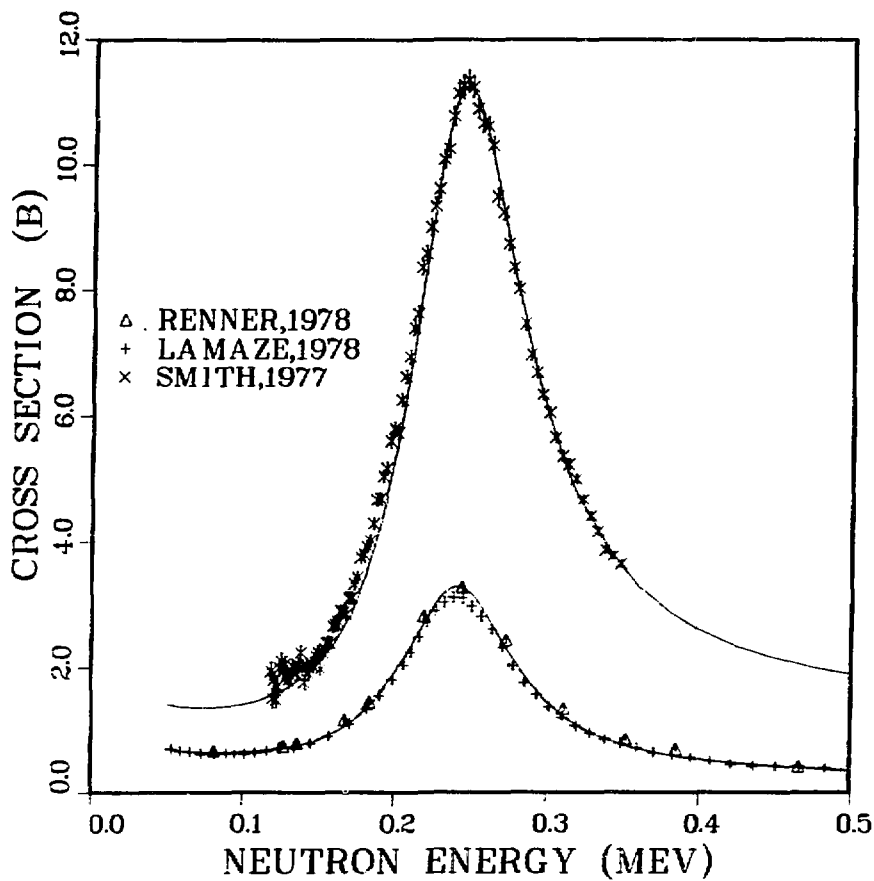
Fig. 5.
Recent measurements of the n-6Li total cross section by
Smith [20] and of the 6Li(n,t) reaction cross section by
Lamaze [21] and by Renner [22] compared to calculated values
(solid curves) from the R-matrix-based ENDF/B-V evaluation.
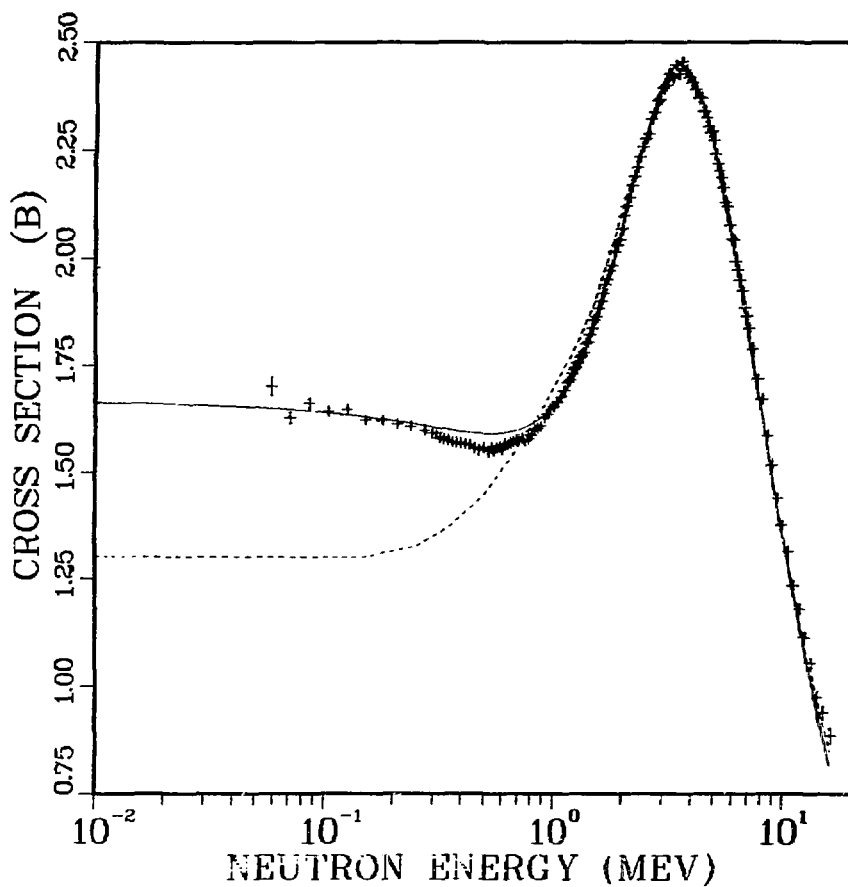
Fig. 6.
Coulomb-correct d, charge-symmetric prediction of the n-T total cross section (solid curve) from an R-matrix analysis of p-^{3}He scattering, compared with recent measurements by Phillips [24] and with the ENDF/B-V evaluation (dashed curve), which is representative of all previous measurements.

Discussion

Young

To how heavy a nucleus is it possible to carry out such detailed and thorough analyses?

Hale

It depends, of course, upon how rapidly the number of two-body channels that must be taken into account increases with mass numbers, but I would guess that the present method would work without having to make approximations for neglected channels up to mass numbers in the region of Na.

Schmidt

Did I understand correctly, that your R-matrix calculation of the T(d,n) cross section below about 30 keV disproves the Gamow extrapolation.

Hale

Yes.

Schmidt

Your R-matrix curve has significantly smaller slope than the approximately 10% accurate experimental data. This low energy part of the T(d,n) reaction is very important for the ignition phase of fusion.

Hale

Yes, I agree. It should be emphasized, however, that our calculation deviates from the experimental points only at energies below about 11 keV. In this energy region, the experimentalists were so unsure of the reliability of the data that they published values from the Gamow extrapolation in place of their measured points. I would say that the R-matrix extrapolation, which is determined mainly by fitting the higher energy data, is certainly more reliable than the Gamow extrapolation, and probably more reliable than the measurements at the lowest energies. Once the parameters of the s-wave level are determined by fitting data over the resonance, then the low-energy behavior of the cross section is pretty well defined by the interaction of penetrability effects with the broad resonance.

Perey

If I understand correctly, EDA still does not use covariance matrices in the input data. That is to say you assume every data point to be uncorrelated. I believe this is a serious limitation which I would urge you to attempt to remove as early as possible.

As an example, I suspect that you and possibly many people are concerned about the apparent lack of agreement of your R-matrix curve for the D-T reaction below 30 keV with data. It is impossible to gauge what is the level of agreement or disagreement between the calculation and the data without consideration of the off-diagonal elements of the covariance matrix of the data. The agreement could be much better or much worse than it appears to be by considering the data points as uncorrelated.

Hale

I agree this is something we should worry about in principle, but I am concerned about the practical aspects of increasing the size and complexity of an already large and complicated code by taking into account covariances among the input data. The overall normalization uncertainties are already handled separately from the statistical errors.

As I mentioned before, the T(d,n) measurements at low energies were very difficult, and the impression I have from talking to some of the participants in the experiment is that they are surprised the calculation agrees as well as it does with their measured points at energies below 20 keV. In particular, they feel that the lowest three points (E_d = 7-11 keV) could have considerably larger uncertainties than they assigned.

Poenitz

Which ^{6}Li(n,α) cross sections were shown in the two figures? It appears that not only the latest experimental data came up in the peak but also the R-matrix fit came down.

Hale

In the first figure (circa ENDF/B-IV), I showed your data (labeled Poentiz) and those of Coates. In the comparison with the ENDF/B-V results, the data of Lamaze and Renner were shown. Yes, it is correct that the calculated ^{6}Li(n,α) cross section decreased somewhat in the peak for Version V and the calculated peak total cross section increased--by a substantial amount, actually, as compared to Diment's errors.

Poenitz

In what sense do you use the x^2 fit? If you have two data sets
as input, one with 100 data points and the other with 10, do you
use them such that the one with 100 points has a factor of 10
higher weight?

Hale

Yes, we would include both data sets with the number of points
given. Except, as mentioned earlier, we do handle the
normalization separately, and each experimental data set would
only have one normalization factor.

Vonach

Where are the high energy limits for the R-,matrix techniques?
Would you discuss them?

Hale

The upper energy limit depends on the specific reaction or channel
in an analysis. For some reactions, we cover ranges of
(laboratory) energy from 0 to 20 or 30 MeV; for others, we only go
up to a few MeV. This is because generally we try to avoid going
above the thresholds for three-body states, although there are
approximately ways of treating these in terms of pseudo two-body
channels (i.e., sequential decay) that we sometimes use. A
typical measure of the energy range we cover would be 10-15 MeV
excitation energy in a compound system.

METHODS USED IN EVALUATING DATA FOR THE INTERACTION OF NEUTRONS WITH LIGHT ELEMENTS (A < 19)*

Leona Stewart [†]

Los Alamos Scientific Laboratory, Theoretical Division
University of California
Los Alamos, New Mexico 87545

ABSTRACT

In the interaction of neutrons with light nuclei, many anomalies are observed. In particular, the probability for gamma-ray production is generally small over most of the neutron energy range. On the other hand, ^6Li, ^3He, ^{10}B, and ^7Be have thermal "absorption" cross sections which range from 940 to 48,000 barns. ^{10}B is the only light isotope which has a positive Q for a 3-body reaction, the $(n,t2\alpha)$. As the neutron energy increases, however, 3- and 4-particle direct breakup and sequential formation cross sections dominate the nonelastic for D, T, ^6Li, ^7Be, ^{10}B, and ^{12}C above a few MeV. For higher-mass isotopes, particle emission (protons and α's) are often the preferred mode for deexcitation of levels excited via (n,n') reactions, where energetically possible. Very few of these partial cross sections have been measured with the necessary precision. Problems are particularly inherent in experiments on negative Q reactions near the 3-body threshold. The many-body problem must be treated as several two-body sequential steps in a theoretical analysis; the emitted particle angular distribution is required as input, but is rarely known. Precise knowledge about individual partial cross sections is often important, especially when neutron multiplication, breeding of fusion fuel, radioactive contamination, depletion or buildup of the target, energy transfer, or time-dependent parameters are required. Specific examples are described for the evaluation of neutron interactions with light elements which employ isotopic spin, inverse reactions, charge-conjugate reactions, and the elastic scattering of charged particles (with Wick's Limit).

INTRODUCTION

The evaluation of neutron interactions with light nuclei is of interest for a broad range of applications. Light nuclei are widely used in flux monitors for cross-section standards applications, in the production and use as fusion fuels, as absorbers of low-energy neutrons, as neutron moderators, and as neutron multipliers. Air and water are common neutron shields. Compounds containing hydrogen, carbon, nitrogen, and oxygen are widely employed in research and industry. Of the light stable nuclei, only fluorine plays a minor role in applied programs. Since standards applications are included elsewhere in these proceedings, these cross sections are not covered in this review. Evaluations performed using theoretical models are described in the previous paper, therefore this review includes a tabular summary only of those data (See Table 1). This paper will be concerned mainly with briefly describing the many "tools" which can be employed in the evaluation of neutron interactions with light element reactions which greatly enhance the reliability where precise theoretical analyses are not yet available.

METHODS EMPLOYED AS "AIDS"

Various tools can be employed in the evaluation of neutron cross sections. They vary in complexity and detail and several are equally valid for the higher-mass range, though rarely used. These aids are briefly outlined in this section. Examples are chosen to show the results of the use of these tools in the following section. In the context of this review, it would be impossible to give a concise derivation for each theoretical method employed but it is hoped that the simple formulation chosen here will appeal to a wider audience.

Wick's Limit

A minimum value of the zero-degree elastic scattering cross section[7] is called Wick's Limit. It is obtained by assuming that the real part of the scattering amplitude at zero degrees can be neglected. The imaginary part of the scattering amplitude, squared, is simply related by:[7]

$$\sigma(E,0°) > \frac{k^2[\sigma_{TOT}(E)]^2}{(4\pi)^2} > 3.03\times10^{-2} \left(\frac{m_t}{m_n+m_t}\right)^2 [\sigma_{TOT}(E)]^2 \, E_{lab}.$$

In evaluating neutron elastic scattering angular distributions to zero degrees, this limit is very useful especially when using charged-particle experimental data and when neutron measurements do not include small angles. It also provides a check on the zero-degree cross sections obtained from Legendre fits to experimental data.

A note of caution should be borne in mind, however, if the zero-degree cross section is automatically set to Wick's Limit. When the real part of the scattering amplitude is identically zero at energy E, the neutron polarization is also identically zero at all scattering angles at that energy.

Charge-Conjugate Reactions

Charge conjugation results from the exchange of the charge of the projectile and target nuclei. Since (n-n), (n-p), and (p-p) forces are related by charge independence,* charge-conjugate reactions can be used to great advantage in the evaluation of neutron cross sections and angular distributions for the light nuclei. For ENDF/B-V, the following evaluations widely employed charge-conjugate reactions:

Reaction	Charge-Conjugate	Types of Data
n + D	p + D	Elastic and Non Elastic
n + T	p + ^{3}He	Elastic and Non Elastic
n + ^{3}He	p + T	Elastic and Non Elastic
n + ^{4}He	p + ^{4}He	Elastic †

In the evaluation of the elastic scattering of neutrons by deuterons, n-d data were scarce in number and often of poor quality. Figure 1 shows how the p-d experiments were employed, along with Wick's Limit, in obtaining the shape and magnitude of the n-d angular distribution. A Legendre fit to the n-d data alone left much to be desired. In this case, the minimum in the cross section and the forward-backward peaking were reasonably well represented by p-d scattering, neglecting Coulomb interference at small angles. It was fortuitous that the integral of this curve agreed with $\sigma_{TOT} - \sigma_{NON}$ to within a few mb at 5.6 MeV.

Phase-Space

To complete the evaluation of the n-d interaction, an n-body code was designed to calculate the energy and angle for the D(n,2n) reaction. By assuming equal probability in phase space, the energy distribution in the center-of-mass system of any one of the "n" particles emitted can be represented by:

$$N(E_i) \, dE_i = \text{Constant} \sqrt{E_i} \, [E_i(\text{max}) - E_i]^{(3n/2)-4} \, dE_i$$

---

*Neglecting Coulomb effects and proton-neutron mass differences.

†For n + ^{4}He, only the elastic channel is open up to 20 MeV.

where E_i(max) is the maximum energy available to particle "i" and depends only on the incident neutron energy and the Q-value of the reaction. The angular distributions, translated into the laboratory reference system, are derived from the above equation. Experimental data for D(n,p)2n and D(p,2p) are essentially all of the (n,2n) spectral information available for the light nuclei. A direct comparison of the experimental D(n,p)2n proton spectra with phase space calculations is shown in Figure 2 for 14.4-MeV neutrons. These calculations are normalized assuming the evaluated $\sigma_{n,2n}$ cross section is 180 mb. In Figure 3, D(p,2p) calculated spectra at 13.9 MeV are compared with the extensive experimental data. The data were smoothed to obtain the solid lines. Note that the experimental data indicate final-state interactions and charge effects between the two identical protons emitted. The general agreement in magnitude is quite good, especially at small angles.

Finally, the sum over neutron energies produces a strong forward peaking of the emitted neutrons as seen in Figure 4. The important conclusion to be drawn is that the assumption of isotropy in the center-of-mass system produces large anistropic distributions in the laboratory system. Near 14 MeV, the 0°/180° ratio is almost 100 for D(n,2n) neutrons.

Inverse Reactions

A reaction and its inverse are directly related through the reciprocity theorem and time reversal invariance. The translation of a reaction to its inverse (or vice versa) involves only the density of states, and the spins and angular momenta of each particle in the entrance and exit channels. Both the cross sections and angular distributions of the reaction products are translated in the same manner.

No experiments were available on the ^{3}He(n,p) reaction below 1 MeV even though the cross section is 5327 barns at thermal energy. Although a 1/v shape and magnitude could be determined from measurements of total cross sections at low energies, it was important to extend the shape to high energies.

Measurements had been made, however, on the inverse reaction:[10,11]

$$p + T \longrightarrow n + {}^3He - 0.764 \text{ MeV},$$
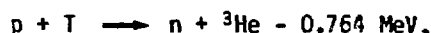
which, when translated into the n + ^{3}He system covered the energy range from approximately 5 keV to 2 MeV. These results showed the deviation from 1/v in addition to a plateau near 1 MeV. The measurements are described in Ref. 1.

The classic example of inverse reactions concerns the photo-disintegration of the deuteron. Again, cross-section data on this reaction were translated into the $^1H(n,\gamma)D$ system in order to extend the evaluation from thermal to 20 MeV. This example was taken from the evaluation of Horsley.[12] The calculations from the inverse reaction compared well with a direct measurement near 14 MeV.

Isospin

The concept of isospin* was first introduced by Heisenberg as a method for labelling two alternative charge states, neutron and proton, by applying the Pauli spin matrix notation. Simply stated, isospin is a shorthand way of representing the charge independence of nuclear forces. A complete derivation cannot be included in this review,[†] instead, use is made of the formula:

$$T_\zeta = \frac{1}{2}(N - Z),$$

where N is the number of neutrons and Z the number of protons in the nuclei whose mass number is A, usually referred to as "isobaric nuclei". As in physical spin, T_ζ takes on all integer (or half-integer) values between -T and +T.

A diagram[13] for the mass-six isobaric nuclei is shown in Fig. 5. From Eq. (1), the lowest value of isospin (T = 0) is assigned to the ground state of ^6Li, which is the stable nucleus. ^6He and ^6Be form a (T = 1) triplet with the second excited state in ^6Li with $J^\pi = 0^+$. Since ^6H and ^6B do not exist, isospin states with T > 1 have not been observed. Note that isospin states T = 0 and T = 1 are allowed in ^6Li while states in ^6He and ^6Be have only T = 1. States with the same isospin have the same J^π and there-fore the same wave function. Since isospin is a good quantum number, it has become a powerful tool in the interpretation of experimental data needed for the evaluation of neutron interac-tions with nuclei.

COMPARISON OF ENDF/B-V CROSS SECTIONS

The evaluated total cross sections for hydrogen and helium isotopes are shown in Fig. 6. Except for the well-known $P_{3/2}$ resonance in ^5He, only broad structure is observed. The broad maximum near 3.4 MeV in ^4H has been assigned as a 2^-, T=1

---

*The terms isospin, isotopic spin, and isobaric spin are used interchangeably throughout the literature.

[†]See the previous paper by G. M. Hale for additional information.

state consistent with its isobaric analogue in ^{4}He and ^{4}Li although a phase-shift analysis implies two and possibly four states to this level (See Ref. 14). Since all of these levels decay by particle emission, unique assignments are difficult. The nonelastic cross sections for D, T, and ^{3}He are smooth.

Total cross sections for ^{6}Li, ^{7}Li, and ^{9}Be are compared in Fig. 7. The peak in ^{9}Be near 2.8 MeV ascribed to two levels is not seen in the evaluation for the (n,2n) cross section (Fig. 8), although the (n,2n)2α reaction threshold is well below this energy, and all levels in ^{9}Be decay by neutron emission. The shape of the evaluated total cross section for ^{9}Be above 10 MeV is not borne out by available experimental data or theory. ^{6}Li is the lowest mass nucleus for which inelastic scattering is possible but all except the 2nd level decay by the emission of α + d. The (n,n'γ) cross sections for the second level were not available except as upper limits but the values assumed are small due to its J^π and T assignment. This T = 1 state corresponds to the isobaric ground states of ^{6}He and ^{6}Be, therefore the shape and magnitude of the ^{6}Li(n,p)^{6}He cross section were assumed. ^{7}Li is the lightest nucleus which shows a significant (n,n'γ) cross section (Fig. 9). This 478-keV level is rarely separable from the elastic peak in a neutron scattering experiment except at low energies so this evaluation was based on γ-ray measurements. Due to the spin and parity of the level, γ-ray emission is isotropic so that an angular distribution measurement was not required. Several problems pertaining to the nonelastic cross sections and the energy-angular distributions of neutron production will be discussed in more detail in the next section.

The total cross sections for ^{10}B, ^{11}B, and C are shown in Fig. 10. Here the structure is significant, especially for C. As noted in Table I, an R-matrix analysis was used for the evaluation of C up to 4.8 MeV. Above this energy, the inelastic scattering from the 4.44-MeV level comes in very strongly and, in fact, shows resonance effects as seen from Fig. 11. The anomaly near 15 MeV is not real. Since ^{10}B is used as a standard and as an absorber at low energies and ^{11}B is not very important, C has been chosen to represent the various partials which make up the total nonelastic cross sections. As seen from Fig. 12, the total (n,n') is made up of the (n,n'γ) and (n,n'3α) reactions. All of the partials show structure below 10-12 MeV. Note the large 4-body cross section which dominates the nonelastic cross section above 14 MeV. In the evaluation, various ^{12}C levels were assigned to allow correlation between the (n,n') neutron energy and angle so that a very small part of the cross section is left in the so-called "continuum" where energy-angle effects are lumped.

The nonelastic cross sections for ^{14}N, ^{16}O, and ^{19}F are shown in Fig. 13. Although (n,n'γ) cross sections become much larger for these nuclei, it should be noted that, at high-excitation

energies, the target often decays via particle emission and these
are labeled in ENDF/B-V by flags. Otherwise it would be
impossible to check the gamma-ray production cross sections or to
calculate hydrogen and helium isotope production induced by
neutrons.

CONTINUUM REACTIONS

As mentioned previously, the representation of continuum
neutrons for 3- and 4-body reactions is a difficult task for light
nuclei. Improvement can be obtained by assuming that a target has
bands of excitation energies (E ± ΔE), with the "real" levels
superimposed. These bands can then represent sequential modes of
formation and decay of the levels and they preserve the energy-
angular distributions of the emitted neutrons. Similar treatment
is often made for heavier nuclei when a band of levels could not
be effectively separated into each composite part.

The treatment of the $^6Li(n,n'd)$ reaction for 5.74-MeV neutrons
is compared with experimental measurements in Fig. 14 at two
angles. The experimental data[16] contain the elastic peak while
the calculations include several bands of levels plus two real
levels at 2.2 and 3.5 MeV. Note that the Version IV evaluation
took no account of the energy and angular correlation of the
neutrons so that neutrons could be emitted at 134° with energies
higher than "allowed" by kinematics for the elastically scattered
neutrons. This type of analysis certainly allows energy to be
conserved and energy-angular correlations to be used, thereby
improving the quality of the evaluation. For more details, see
Ref. 17.

The same treatment has been applied in representing the
$^9Be(n,2n)2\alpha$ reaction with the results for 5.9-MeV neutrons com-
to Version V in Fig. 15. The curve labeled "present evaluation"
is described in Ref. 15. The Version V evaluation allows only a
few levels so that the "first" neutron emitted is directly corre-
lated in energy and angle. The "second" neutron emission is then
calculated from the kinematics of the reaction and combined as a
"continuum" which extends in Fig. 15 to about 2 MeV. The Version
V representation was severely handicapped by format restrictions as
described in Ref. 18. The present evaluation which contains
uncertainty information is available in the Version V format from
the National Neutron Cross Section Center with the only require-
ment that the (n,n') cross sections be multiplied by two to obtain
the total number of neutrons in the exit channel.

For the light isotopes, several problems remain of which a few
are important and others are interesting. First, and foremost, is
the need for a format to represent the error files for the hydro-
gen and carbon standards. Hydrogen and carbon are scattering
standards which infers that the angular distributions of the
neutrons must have some statement of error and correlation.

Second, it is important to note the difference between data measured for an isotope and for a material. For example, is the ^{13}C resonance included in the analysis for ^{12}C? Is the material labeled C or ^{12}C? One knows, a priori, that most of the measurements are made on a material while an R-matrix analysis considers ^{12}C and ^{13}C separately. The reaction cross sections, are usually attributed by virtue of the Q-value to ^{12}C. These comments are not restricted to the carbon evaluation. They are directed, instead, to a clear and concise method for labelling, if one can be found.

Third, a better method is needed for representing (n,2n) and (n,3n) energy and angular spectra for the light nuclei. The data can certainly be calculated today better than they can be represented in the ENDF files. In fact the representation for all continuum reactions for light nuclei needs improvements.

Fourth, to the author's knowledge, several isotopic evaluations are not in reliable condition. The "correct" way to improve the evaluations is not at all obvious from recent measurements. Perhaps the most important are the fuel-breeding reactions, $^6Li(n,n'd)$ and $^7Li(n,n't)$, above a few MeV.

The $^6Li(n,n'd)$ reaction is compared with measurements of the total emission cross section and the Version V evaluation in Fig. 16. While the errors on the measurements are considerable, they certainly do not overlap each other nor, above 6 MeV, the evaluated curve. The Drake data suggest that the evaluation should be higher and the Rosen measurements imply that the evaluation should be lower. Perhaps it should be noted that both Hopkins and Drake measured the total emission spectrum, including the (n,2n) reaction which has a 4.3-MeV threshold, while the α-d star was observed by Rosen.

A consistency check was made by comparing the ^6Li elastic scattering measurements with ENDF/B-V (Fig. 17) since all other partials are small compared to the cross sections shown in Fig. 16. This comparison indicates that the elastic could be lowered below about 5.5 MeV, remain the same near 5.5 MeV, and could be lowered appreciably at higher neutron energies, except 14 MeV. The only other obvious alternative would be a large (n,2n) cross section which would be contrary to the imprecise data available and hardly seems likely. It should be noted, however, that energy spectra of the emitted neutrons have been compared among these measurements and the largest discrepancies among the data appear for the emission of neutrons below 1 MeV.

The $^7Li(n,n't)$ reaction is shown in Fig. 18. Again, a high and low data set exist except that now the Rosen data are high rather than low. The Swinhoe experiments involved recovering and

measuring the tritium produced in the samples, as did the measurement by Wyman (not represented). The Wyman data reproduced the Rosen data near 14 MeV. Rosen observed the t + α star in emulsions.

When compared to experiment, the ENDF/B-V evaluation on the elastic scattering of neutrons by ⁷Li (Fig. 19) does not fare so badly since all of the measurements except the first point by Hopkins include the 478-keV inelastic level in the elastic angular distributions. A successful method for correctly representing the angular distributions of the neutrons scattered from this level, is not yet clear.

The nitrogen evaluation could stand some updating for various partial cross sections but these are small contributions to the total nonelastic cross section. The ¹¹B evaluation has not been updated properly since Version I and is perhaps the least reliable of all the evaluations of the light isotopes.

CONCLUSIONS

Although most evaluators of ENDF materials are not particularly concerned with light nuclei, the methods outlined here are often useful in many applications. For example, the $X(\alpha,n)Y$ reaction gives a lower limit on alpha-particle production for the

$$n + Y \longrightarrow \alpha + X$$

inverse reaction for all nuclei since it corresponds to the ground-state transition.

In this review, it has been shown that isospin, charge-conjugate reactions, phase-space arguments, and charged-particle cross sections can often be used to improve the evaluations for light isotope reactions. A precise, theoretical treatment of the complete system, however, is the recommended procedure, where practical.

ACKNOWLEDGMENTS

REFERENCES

1. P. G. YOUNG, "Summary Documentation of LASL Nuclear Data Evaluations for ENDF/B-V," LA-7663-MS, Los Alamos Scientific Laboratory.

2. R. KINSEY, "ENDF-201 ENDF/B Summary Documentation,"BNL-NCS-17541, UC-80, Brookhaven National Laboratory.

3. Brookhaven National Laboratory, "ENDF-300 Standard Reference and Other Important Nuclear Data by the Cross Section Evaluation Working Group," BNL-NCS-51123, UC-34c, ENDF-300.

4. C. Y. FU and F. G. PEREY, "Neutron Scattering Cross Sections of Carbon Below 2 MeV Recommended From R-Matrix Fits to Data," Atomic Data and Nuclear Data Tables 22, 249-267 (1978).

5. D. G. FOSTER, JR. and P. G. YOUNG, "A Preliminary Evaluation of the Neutron and Photon Production Cross Sections of Oxygen," LA-4780 (1972).

6. P. G. YOUNG and E. D. ARTHUR, "GNASH: A Preequilibrium, Statistical Model Code for the Calculation of Cross Sections and Emission Spectra," LA-6947 (1977).

7. E. WANTUCH, "The Scattering of 4.5- and 5.5-MeV Neutrons by Deuterons," Phys. Rev. 84, 169 (1951).

8. J. E. BROLLEY, JR., T. M. PUTNAM, L. ROSEN, AND L. STEWART, "Hydrogen-Helium Isotope Elastic Scattering Processes at Intermediate Energies," Phys. Rev. 117, 1307 (1960).

9. A. HORSLEY and L. STEWART, "Evaluated Neutron Cross Sections for Deuterium," LA-3271 (1967).

10. J. H. GIBBONS and R. L. MACKLIN, "Total Neutron Yields from Light Elements Under Proton and Alpha Bombardment," Phys. Rev. 114, 571 (1959).

11. R. L. MACKLIN and J. H. GIBBONS, "On the Absolute Value and Energy Dependence of the ^{3}He(n,p)T Reaction," Proceedings of the International Conference on the Study of Nuclear Structure with Neutrons, Antwerp, 19-23 July 1965, (North-Holland Publishing Co., 1966), p. 498.

12. A. HORSLEY, "Neutron Cross Sections of Hydrogen in the Energy Range 0.001 eV - 20 MeV." Nucl. Data, vol. 2, 243, (1966)

13. F. AJZENBERG-SELOVE, "Energy Levels of Light Nuclei A = 5-10," Nucl. Phy., A320 1-224 (1979).

14. S. FIARMAN and W. E. MEYERHOF, "Energy Levels of Light Nuclei A = 4," Nucl. Phy. A206, 1-64, (1973).

15. P. G. YOUNG and L. STEWART, "Evaluated Data for n + ^{9}Be Reactions," LA-7932-MS (ENDF-283) UC-34c, (1979), Los Alamos National Laboratory.

16. J. C. HOPKINS, D. M. DRAKE, and H. CONDE, "Elastic and Inelastic Scattering of Fast Neutrons from ^{6}Li and ^{7}Li," Nucl. Phys., A107, 139 (1968); and LA-3765, Los Alamos Scientific Laboratory. (Nov. 1967).

17. L. STEWART and P. G. YOUNG, "Evaluated Nuclear Data for CTR Applications," Transactions of ANS Annual Meeting, Toronto, Canada, June 14-18, 1976.

18. R. J. HOWERTON and S. T. PERKINS, "Comments on Beryllium (n,2n) Cross Sections in ENDF/B-IV and -V," Nucl. Sci. Eng. 65, 201 (1978).

TABLE I. EVALUATIONS PERFORMED BY THEORETICAL ANALYSES

Target/ MAT #	Quantity Predicted	Energy Range	Method Used	Covariance File	Comments	Primary References for Evaluation
1-H-1 1301	$\sigma_{ELAS}(E)$ and $\sigma_{ELAS}(E, \theta)$	200 keV to 20 MeV	Yale Phase Shifts	Yes	Actually σ_{tot} was input assuming $\sigma_{tot} = \sigma_{ELAS}$	LA-7663-MS (Ref 1 ENDF-201 (Ref 2) ENDF-300 (Ref 3)
2-He-4 1270	$\sigma_{ELAS}(E)$ $\sigma_{ELAS}(E, \theta)$ P(E,)**	10^{-5} to 20 MeV	R-Matrix Multi-level	No	Analysis performed using both n + ^{4}He and p + ^{4}He	LA-7663-MS (Ref 1 ENDF-201 (Ref 2)
3-Li-6 1303	σ_{tot}, σ_{ELAS} $\sigma_{n,t}$, $\sigma_{ELAS}(E, \theta)$ $\sigma_{n,t}(E,), P(E,)^{**}$	10^{-5} eV to 2 MeV	R-Matrix Multi-level Multi-channel	Yes	$t +$ elastic included and P	LA-7663-MS (Ref 1 ENDF-201 (Ref 2) ENDF-300 (Ref 3)
5-B-10 1305	σ_{ELAS}, $\sigma_{n,\alpha}$, $\sigma_{n,t}$ σ_{ALL} P	10^{-5} eV to 1 MeV	R-Matrix Multi-level Multi-channel	Yes	$+ ^7$Li inverse B total	LA-7663-MS (Ref 1 ENDF-201 (Ref 2) ENDF-300 (Ref 3)
6-C-12 1306	$\sigma_{ELAS}(E)$ $\sigma_{ELAS}(E,)$ P(E,)**	10^{-5} to 4.8 MeV	R-Matrix Multi-level Multi-chan.	Yes	Actually σ_{tot} was input assuming $\sigma_{tot} = \sigma_{ELAS}$	Published (Ref 4) ENDF-201 (Ref 2)
7-N-14 1307	$\sigma_{ELAS}(E)$ $\sigma_{ELAS}(E,)$ σ ***	10^{-5} eV to 5.4 MeV 6-20 MeV	R-Matrix GNASH COMNUC	No	Only input data available were σ_{tot} and P	LA-7663-MS (Ref ENDF-201 (Ref 2) LA 6947 (Ref 6)
8-O-16 1276	$\sigma_{ELAS}(E)$ $\sigma_{ELAS}(E,)$ $\sigma_{n,\alpha}(E)$ $\sigma_{n,\alpha}(E,)$	10^{-5} eV to 6.7 MeV	R-Matrix Multi-level Multi-channel	Yes	α data included in analysis. Also σ_{tot} assumed equal to σ_{ELAS} at energies below the n,α threshold	LA-6780 (Ref 5 LA-7663 (Ref 1

* See these primary references which refer to previous references and often fail documentation. A complete list of the appropriate references would number in the hundreds and is therefore omitted here.

For n + ^{4}He, σ_{ELAS} not over this energy range.

** Although P(E,) data were used as input and calculated values output, the ENDF/B format has no provision for this information.
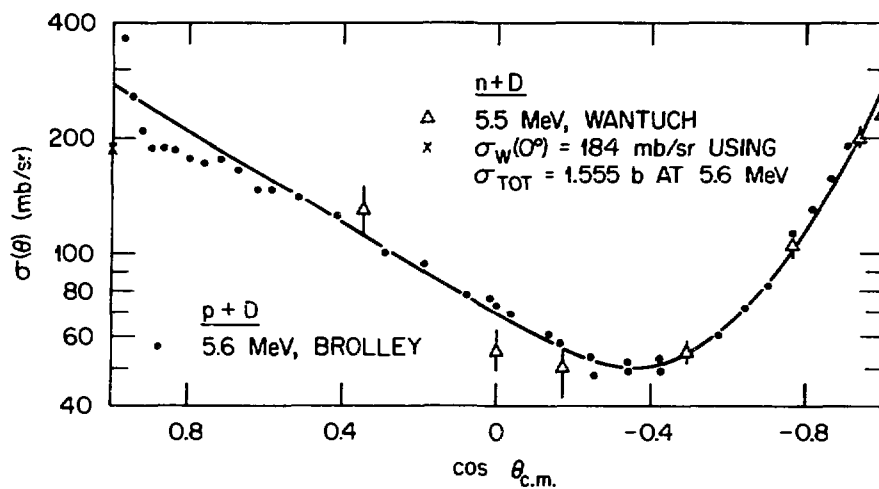
Fig. 1. Elastic scattering of deuterons by neutrons and protons
near 5.5 MeV. The experimental data are given in Ref. 7
and Ref. 8.
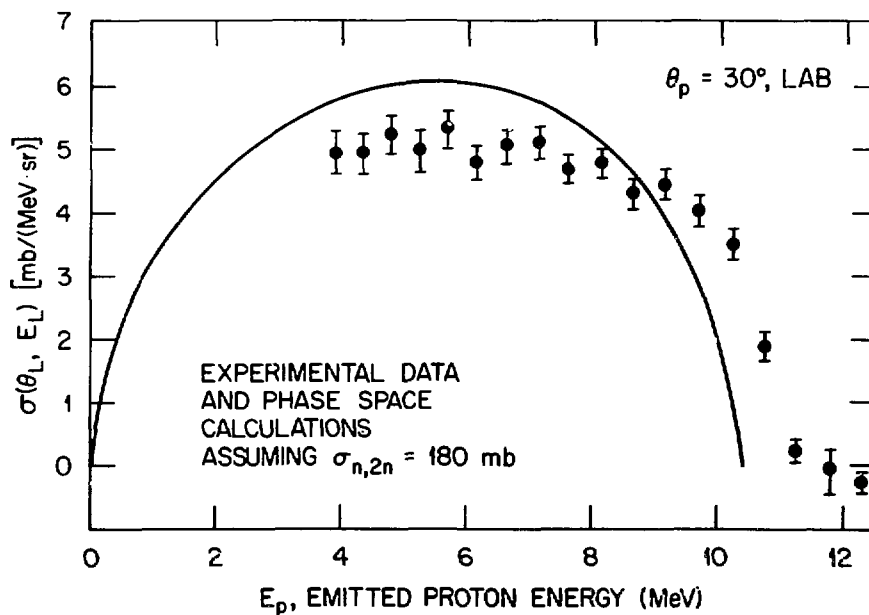
Fig. 2. Proton spectra from the D(n,p)2n reaction at 14.4 MeV
compared to 3-body Phase Space Calculations (See Ref. 9
for complete details).
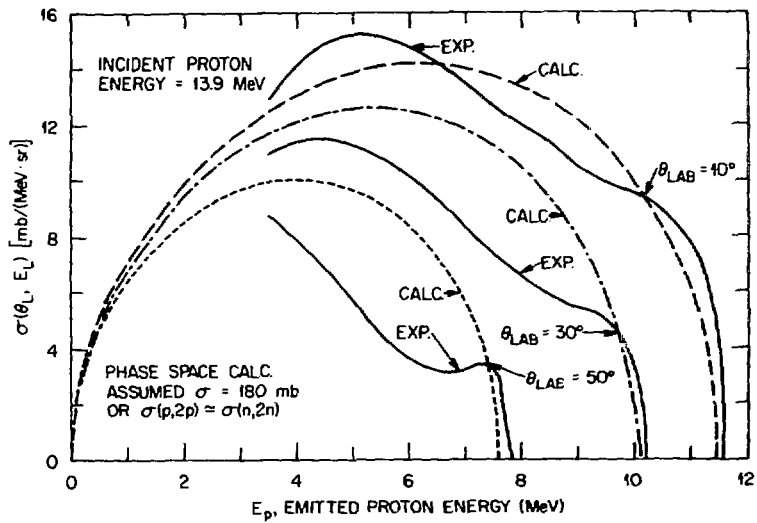
Fig. 3. Proton spectra from the D(p,2p)n Charge-Conjugate
Reaction for 13.9-MeV protons compared to Phase Space
Calculations (See Ref. 9 for complete details).
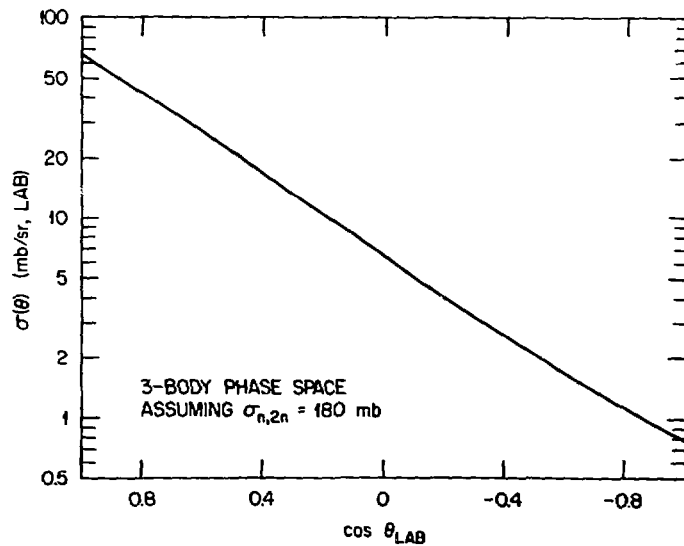
Fig. 4. Angular distribution of the D(n,2n) neutrons near 14 MeV
in the laboratory reference system, assuming isotropy in
the center-of-mass system.

6He

6Li

6Be

β⁻

0.973
⁴He + 2n   [4.05]

1.80

(2)⁺   1.87
⁵He + n

0⁺;1

5.65   1⁺;0
3⁻   2⁺;1   5.66
4.59   2⁺;0   ⁵Li + n
⁵He + p
3.563   0⁺;1   3.6981
⁴He + n + p

2.185   3⁺;0

1.4735
⁴He + d

1⁺;0

1.67   (2)⁺

[3.09]
0⁺;1

0.59
⁵Li + p

-1.372
⁴He + 2p
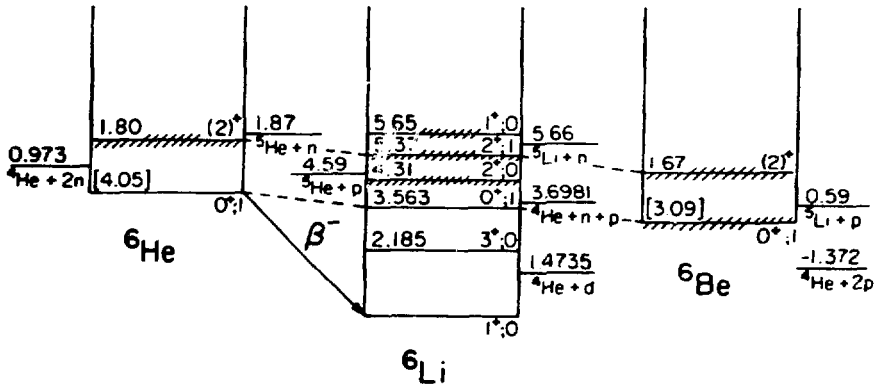
Fig. 5. Comparison of the Isospin Configuration for A = 6 (These
data were taken from Ajzenberg-Selove, Ref. 13).
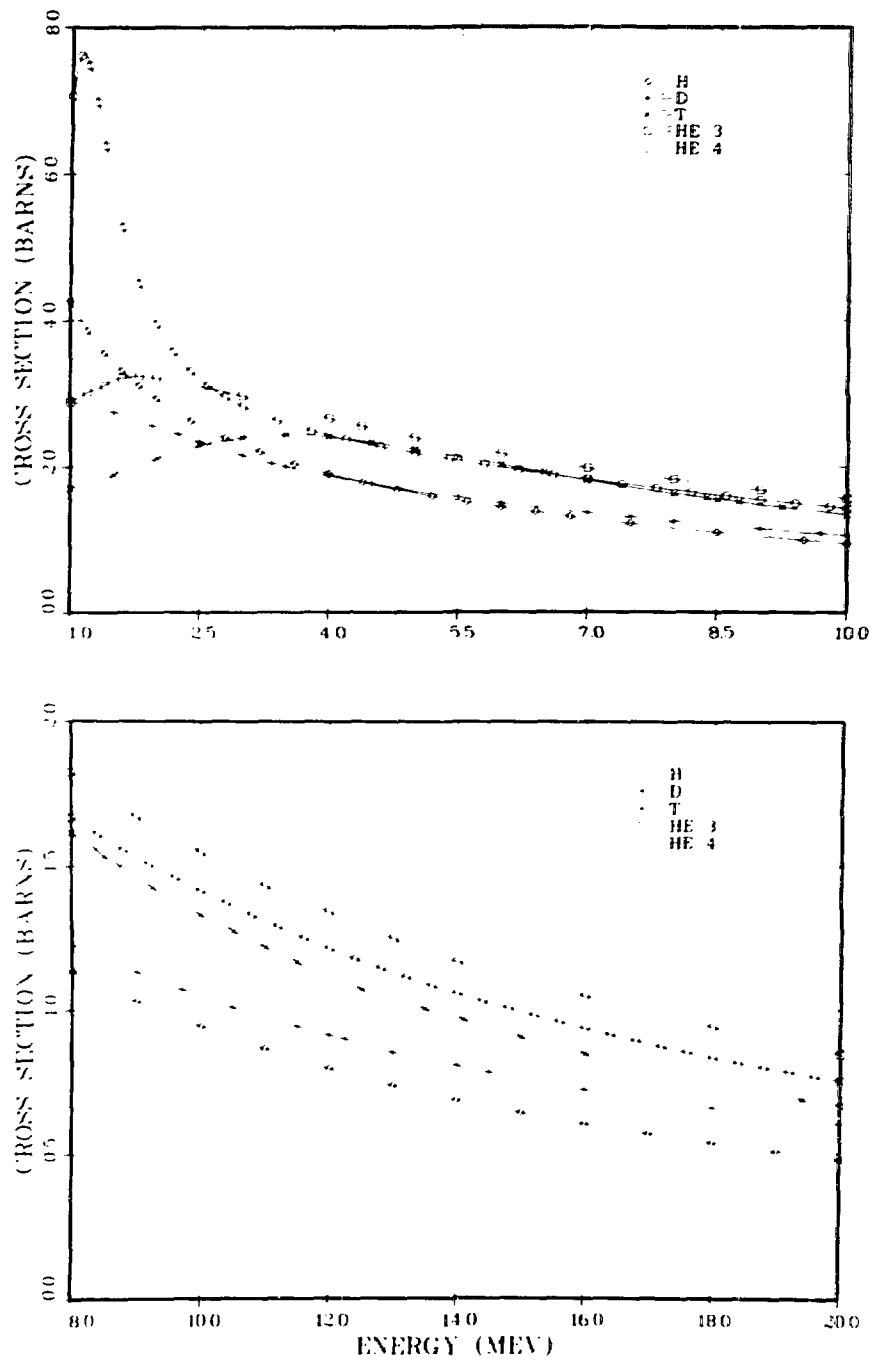
Fig. 6. Evaluated total cross sections for ENDF/B-V for the
hydrogen and helium isotopes.
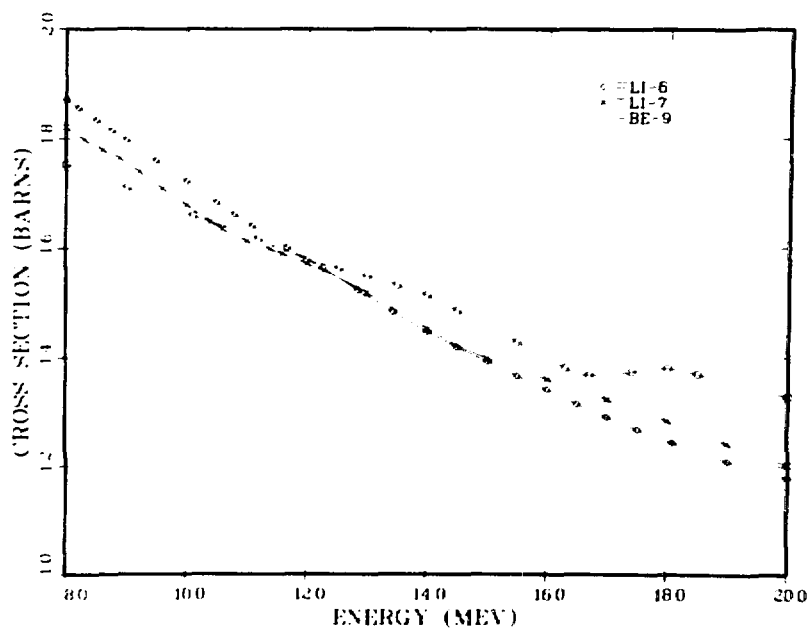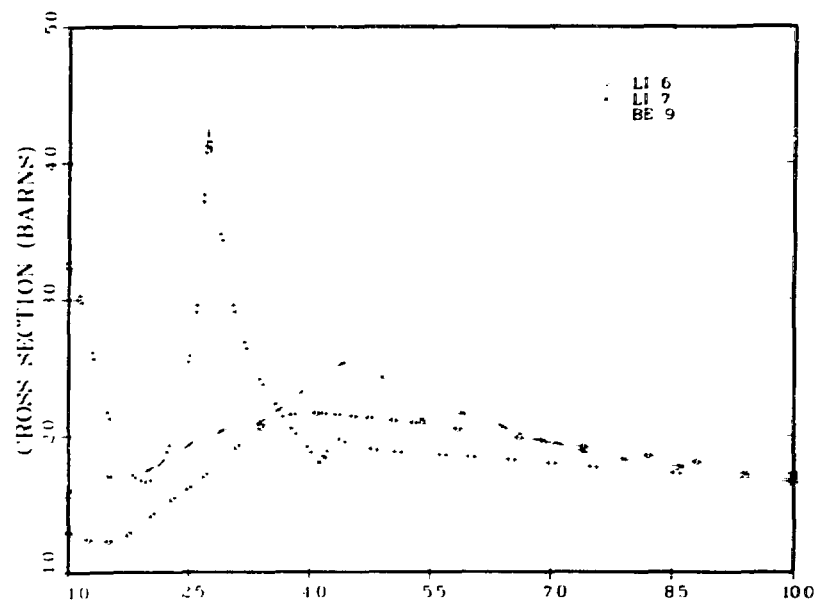
Fig. 7. Evaluated total cross sections for ENDF/B-V for ^{6}Li, ^{7}Li, and ^{9}Be. The structure in ^{9}Be above 12 MeV is not corroborated by the experimental data or theory.

CROSS SECTION (B)

1.0
0.9
0.8
0.7
0.6
0.5
0.4
0.3
0.2
0.1
0.0

- ASHBY, 1958
- SAKISAKA, 1959
- MYACHKOVA, 1961
- ROSEN, 1957
- FLEROV, 1958
- CHUAN, 1959
- PHILLIPS, 1964
- CATRON, 1961
- DRAKE, 1977
- FOWLER, 1955
- ZUBOV, 1961
- FISCHER, 1957
- BLOSER, 1972
- HOLMBERG, 1969

0.0   2.5   5.0   7.5   10.0   12.5   15.0   17.5   20.0

NEUTRON ENERGY (MEV)
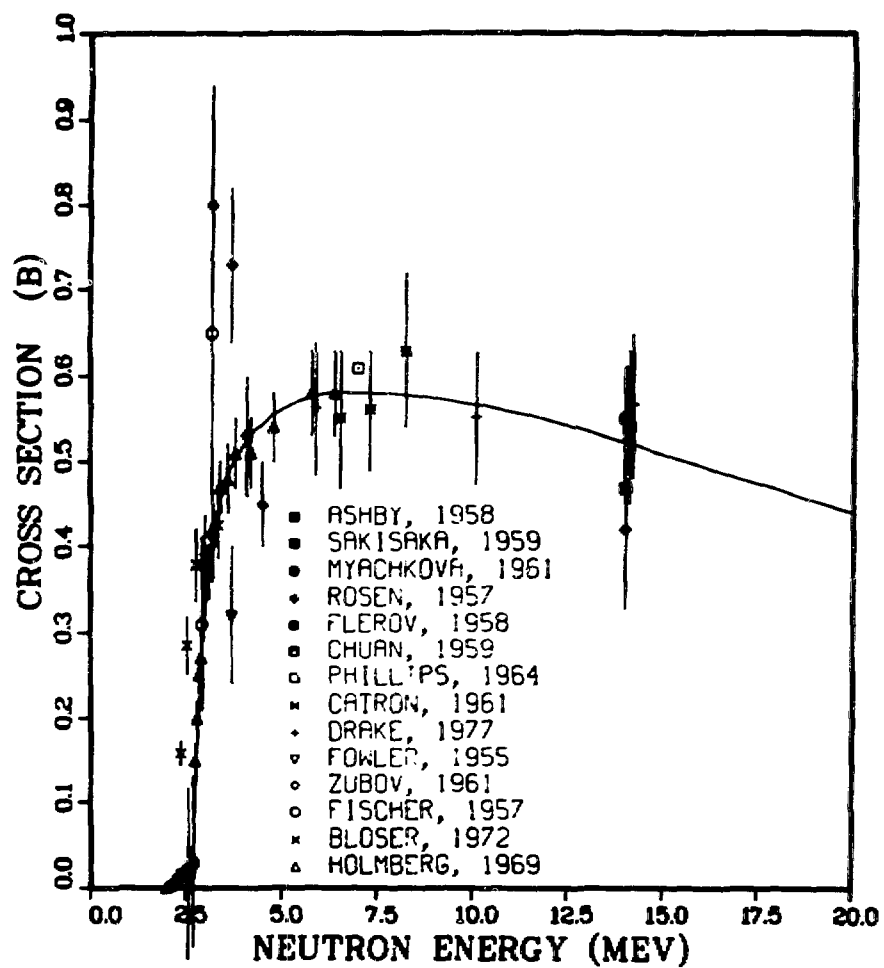
Fig. 8. Measured and evaluated $^9Be(n,2n)$ cross sections from
threshold to 20 MeV. The solid curve is ENDF/B-V. The
experimental data presented here are described in Ref. 15.
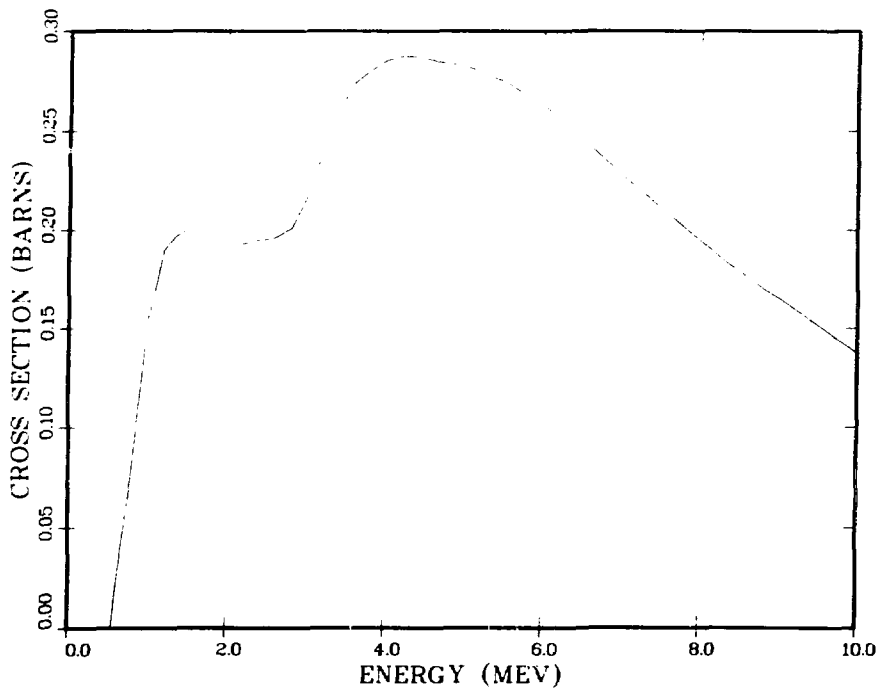
Fig. 9. The ^{7}Li(n,n'γ) cross section corresponding to the first
excited state in ^{7}Li at 478 keV. All other levels in ^{7}Li
decay via particle emission. This cross section steadily
decreases to approximately 70 mb at 20 MeV.
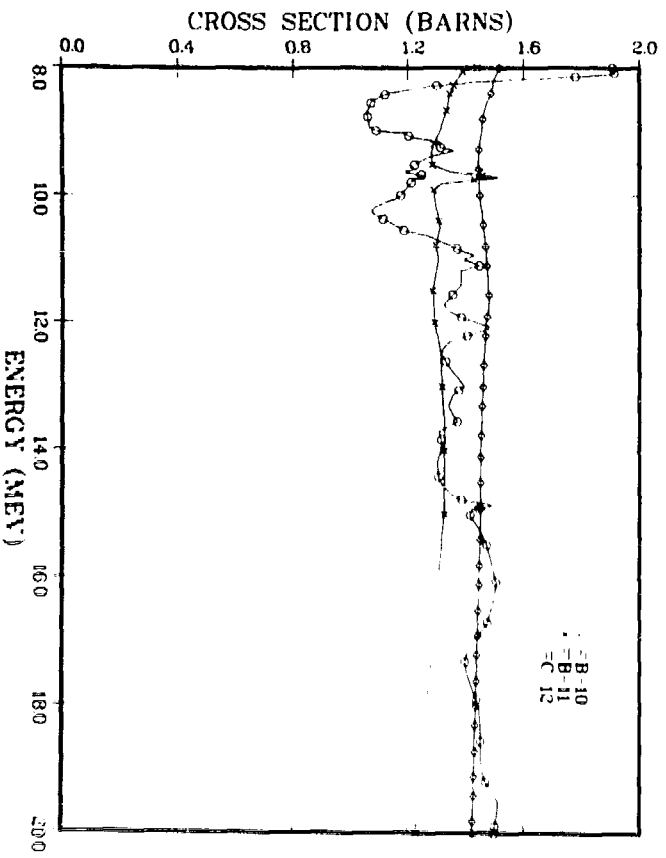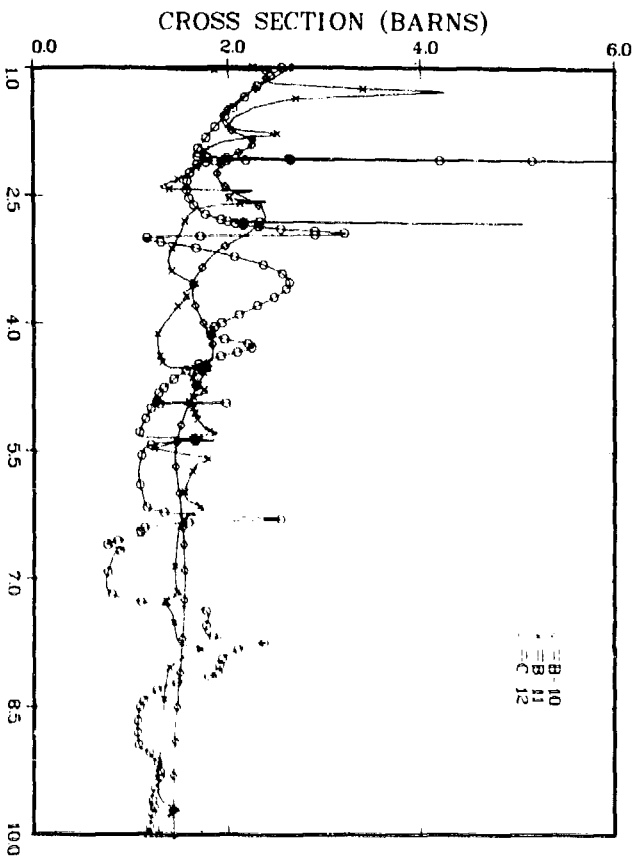
Fig. 10. Evaluated total cross section for ENDF/B-V for ¹⁰B, ¹¹B, and ¹²C.
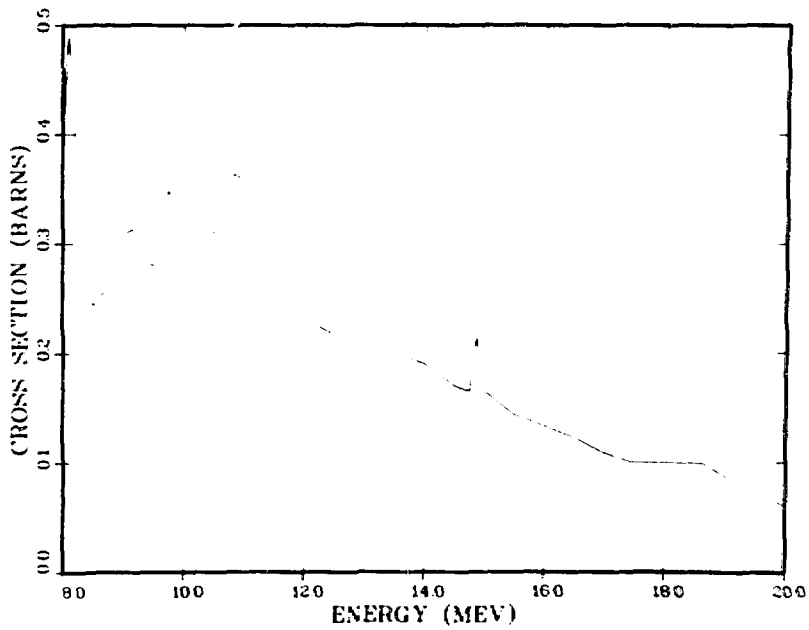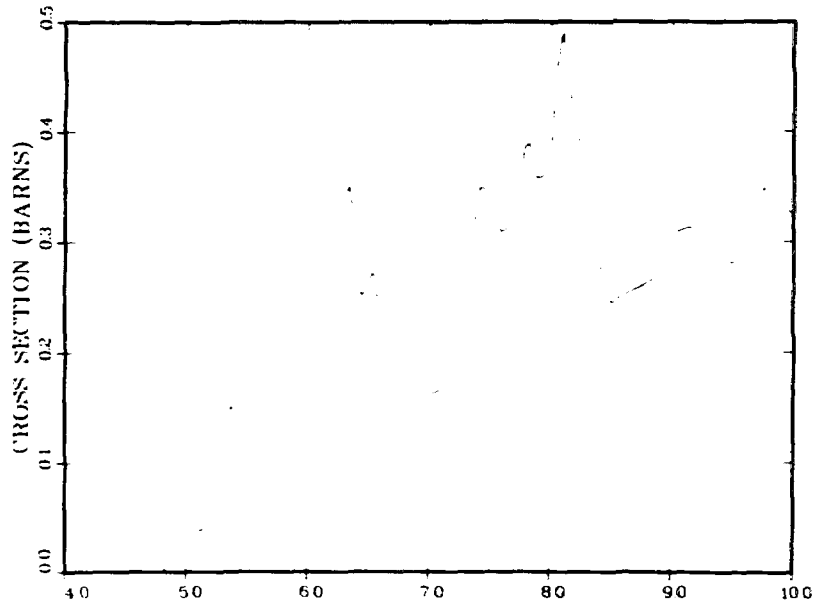
Fig. 11. The $^{12}C(n,n'\gamma)$ cross section corresponding to the first
excited state in ^{12}C at 4.4 MeV. All other states decay
via particle emission.
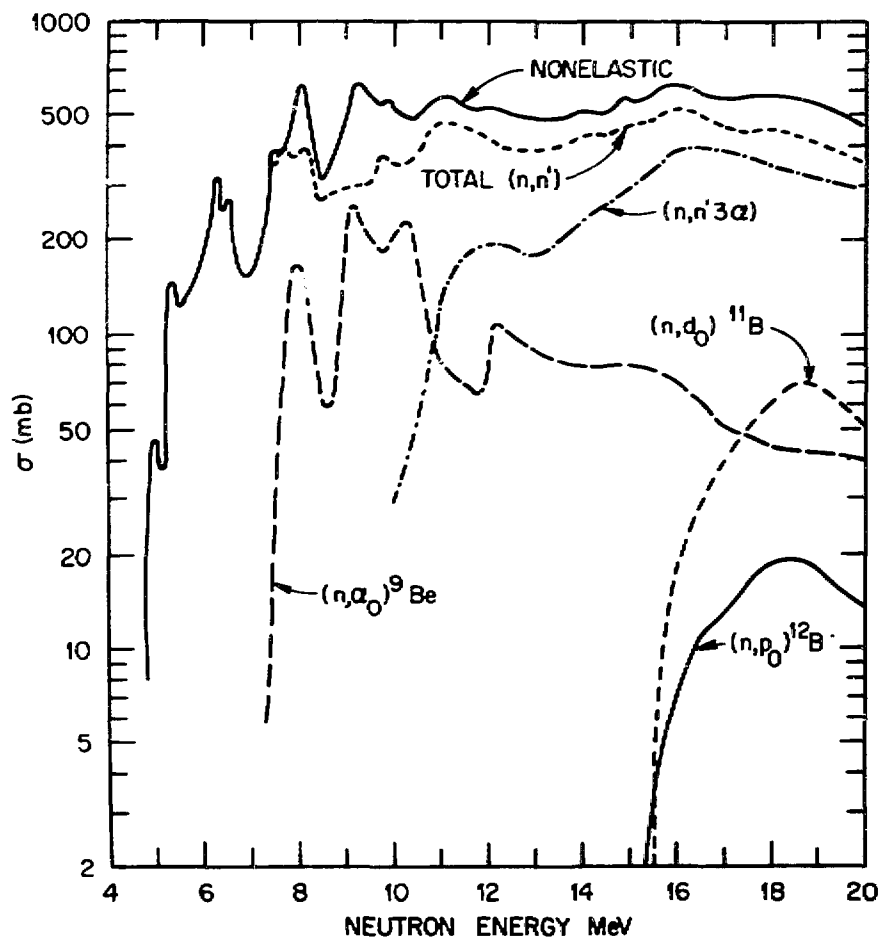
Fig. 12. The evaluated nonelastic cross sections for ^{12}C showing
structure in the individual partials at low energies and
the large cross section for 4-body breakup at high
neutron energies.
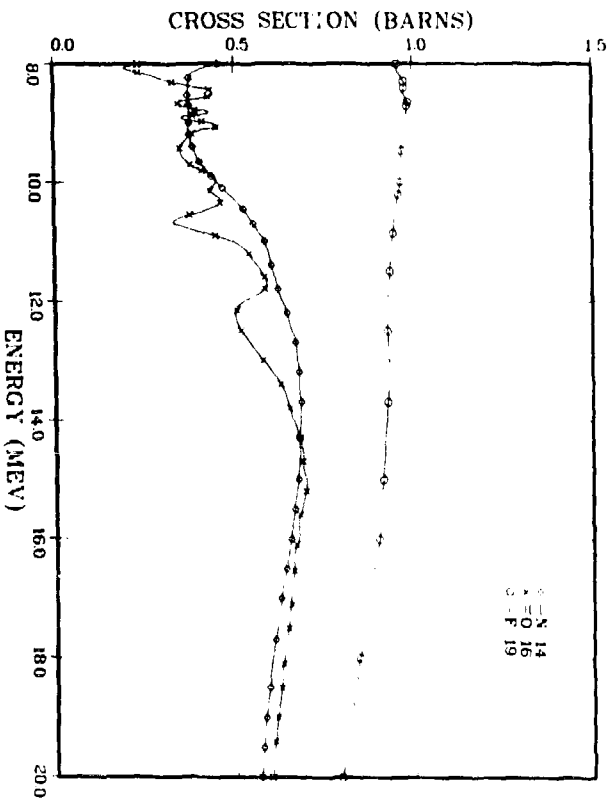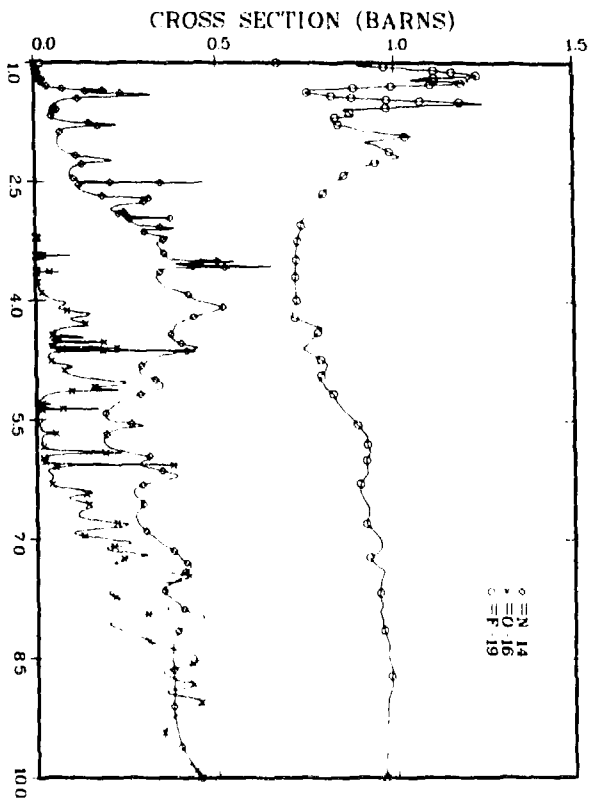
Fig. 13. Structure observed in the nonelastic cross sections for ^{14}N, ^{16}O, and ^{19}F.
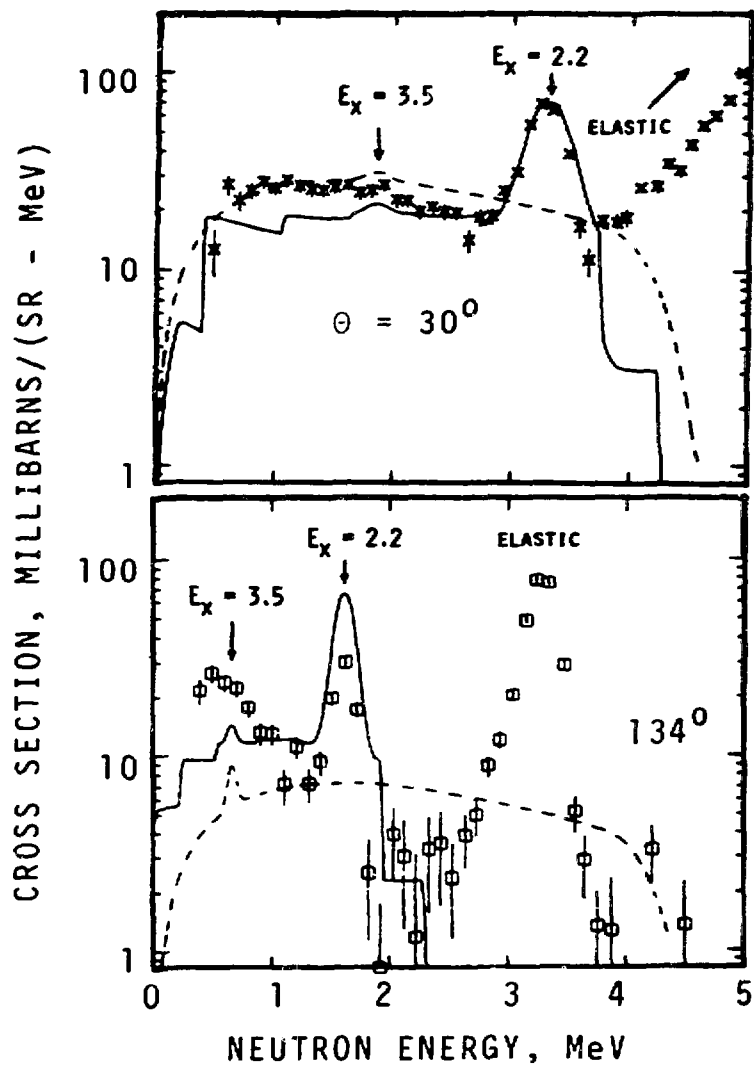
Fig. 14. Experimentally observed neutron spectra from 5.74-MeV neutrons scattered by ^{6}Li. The solid curve (ENDF/B-V) was obtained by assuming bands of excitation energies in addition to the "real" levels at 2.2 and 3.5 MeV. The experimental data[16] include the elastic peak while the curves represent only the (n,n'). The dashed curve was taken from ENDF/B-IV.
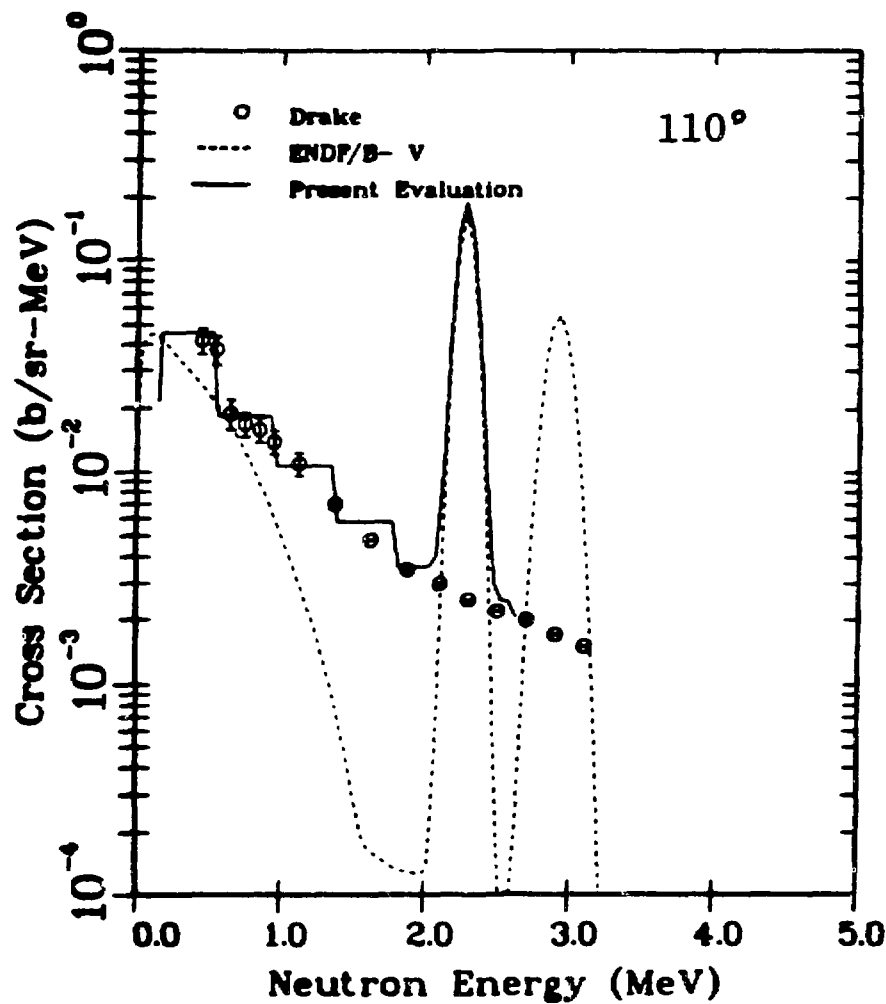
Fig. 15. The neutron emission spectrum at 110° for beryllium
scattered by 5.9-MeV neutrons. For Version V, two
levels in ⁹Be are assumed at excitation energies of 1.68
and 2.43 MeV, which then decay by neutron emission. The
"present" evaluation assumes "bands"of excitation
energies with "real" levels superimposed. Good
agreement is obtained with all of the data at several
incident neutron energies (Ref. 15).
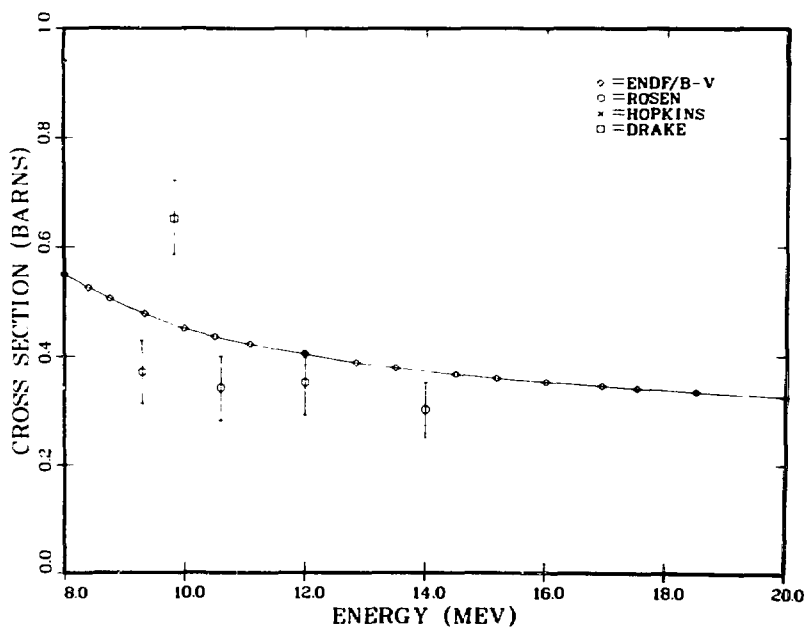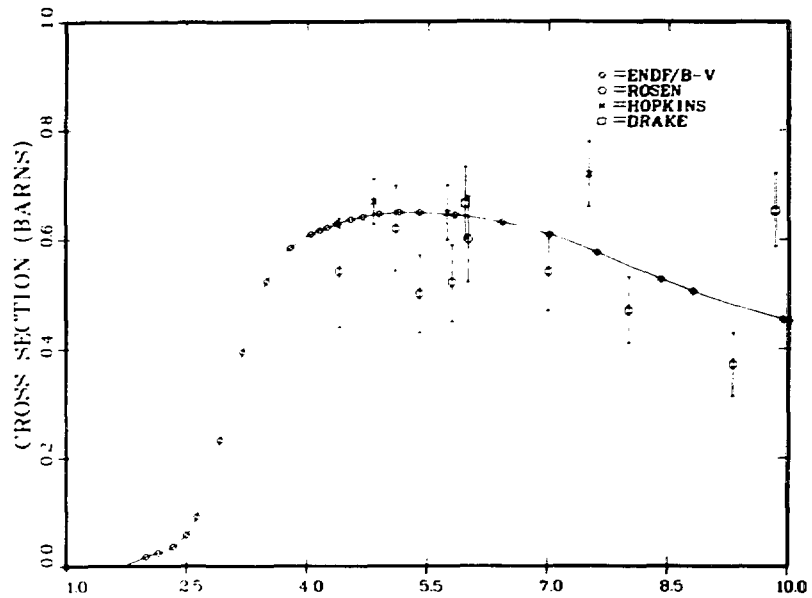
Fig. 16. Comparison of ENDF/B-V with experimental measurements on the $^6Li(n,n'd)$ cross sections.
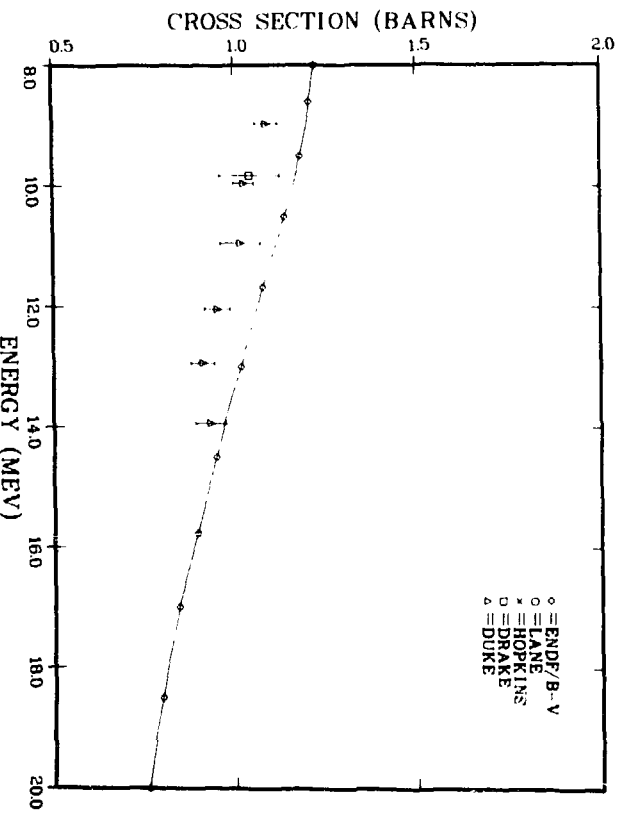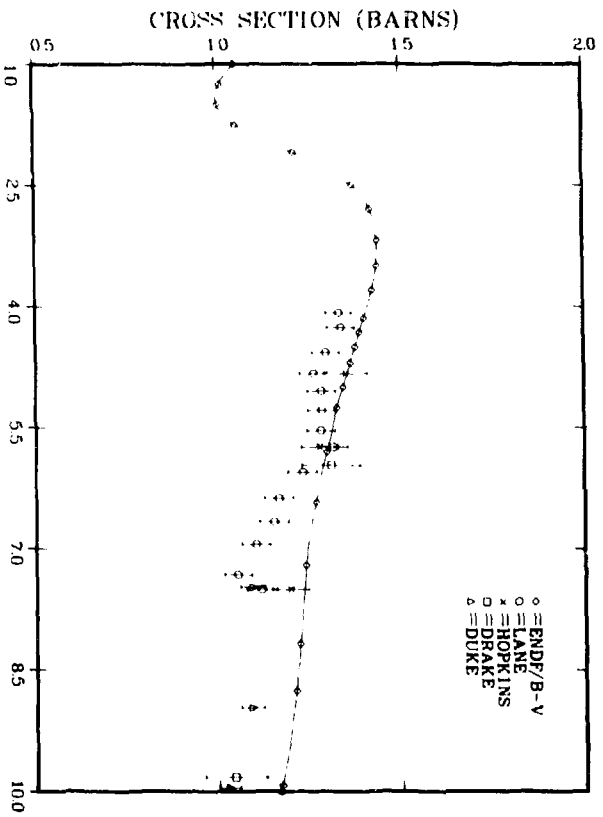
Fig. 17. Comparison of the ENDF/B-V evaluation with the experimental data on neutron elastic scattering by ^{6}Li
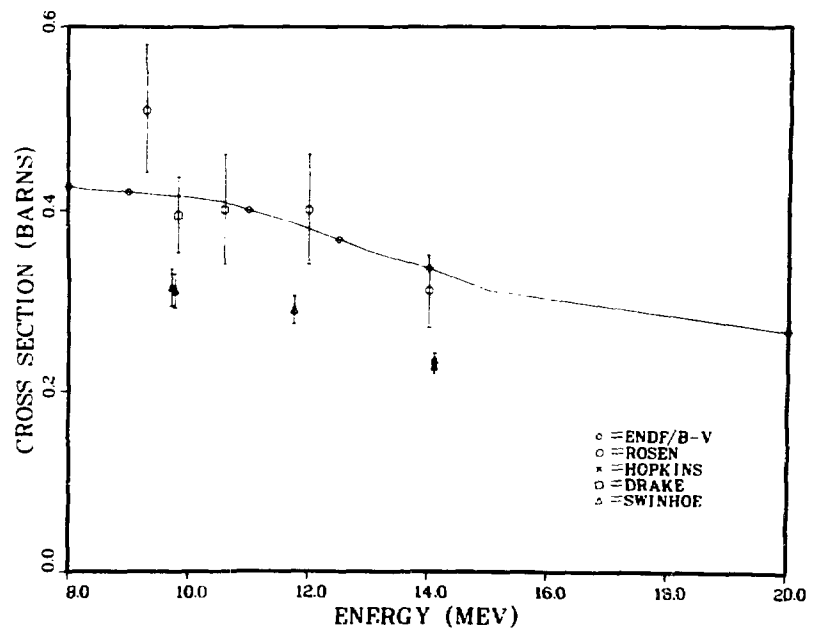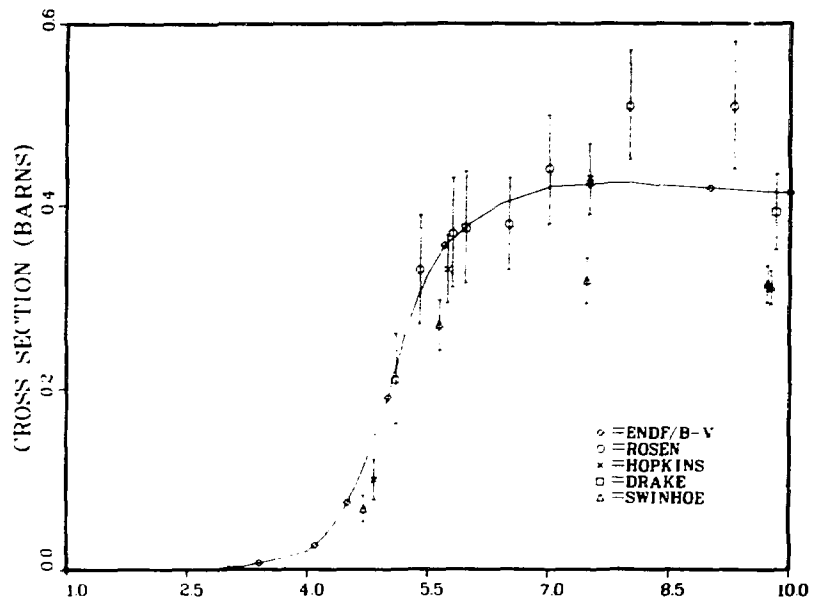
Fig. 18. Comparison of the experimental data on the ^{7}Li(n,n't)
reaction with ENDF/B-V.
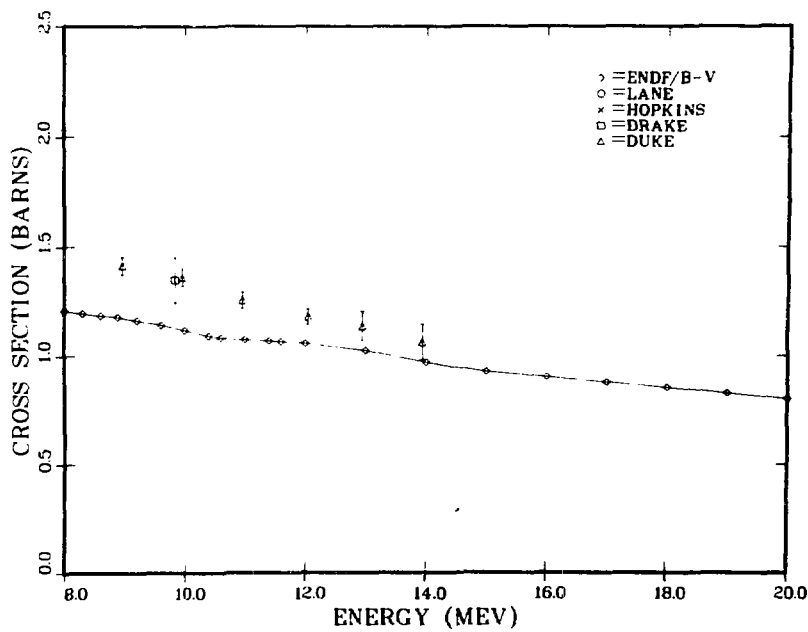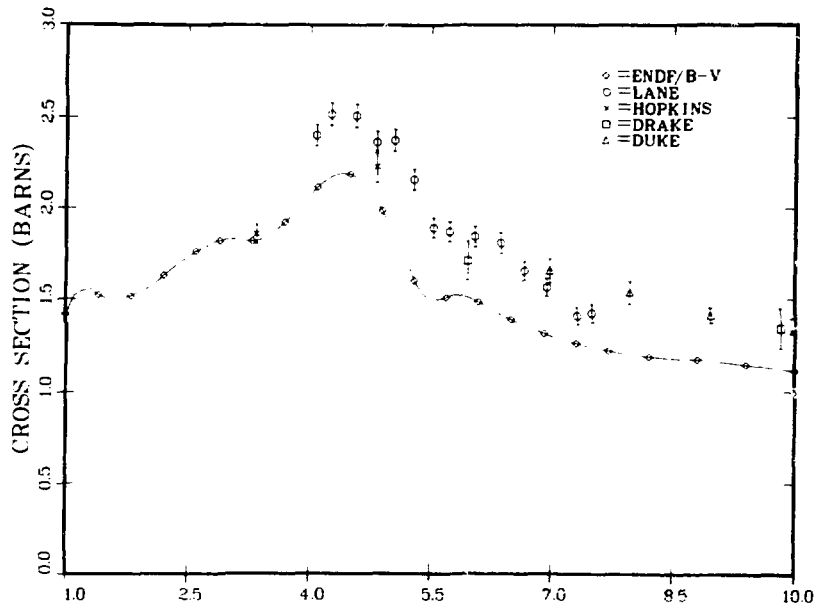
Fig. 19. Comparison of measurements of the elastic scattering of
neutrons by ^{7}Li with ENDF/B-V. Here the experiments
include the (n,n'γ) reaction shown in Fig. 9, except for
the point of Hopkins[16] at the lowest energy.

Discussion

Mughabghab

Were the total cross section measurements of Harvey included in the ^{7}Li evaluation?

Stewart

Yes, but only the total cross section was updated in the evaluation and that only above the 200-keV resonance.

Froehner

I did not catch whether the R-matrix fits reported by G. Hale in the preceeding talk were fully utilized. To what extent were they? How were the ENDF/B-V curves at higher energies in the last slides obtained?

Stewart

The curves at lower energies, such as the ^{6}Li to 1 or 2 MeV, were the R-matrix predictions of Gerry Hale. Above that energy, they were obtained by "brute force," using all the information that we know.

Smith

I have a comment and a question. First, regarding tritium production from ^{7}Li, a paper is presently being typed that describes a new experiment performed at ANL including full blown correlation matrices. The substance of it is that the cross section is slightly larger than the British measurement (Swinhoe and Uttley), but the two experiments are consistent. It is a very carefully done measurement, and I have confidence in it. It was made by Donald Smith and James Meadows, who are both very careful experimentalists.

Now for my question, which I address to you and to the previous speaker. I am a rather dull-minded experimentalist who likes to try and get some physics out of his measurements rather than just sending the numbers to the evaluator. In doing so, I have blundered about occasionally with things like R-functions and R-matrices. The R-matrix is a beautiful formalism, and it has certain physical laws built into it, like unitarity. I am sure I have done things very crudely, but I have run into problems, and I will give two examples.

An R-function analysis of a very good data (n + ^{12}C) leads to a result which is in agreement with the excellent one by Perey and Fu; I believe, to within 1% at 4 MeV. However, in some cases where the resonances are not all that well defined, the parameters

are quite different. That is, they are not at all unique, and this is for the simplest thing I can think of--a spin 0 target and just an R-function analysis.

A more complex case of the same problem of physical definition is this ^{6}Li business. In a 1979 paper (I believe the reference is Z. Physik A227), it is proposed that this whole business of the L = 0 contribution to thermal energies is due to a deutron exchange mechanism by a direct process. I played games with that, too, and as Dr. Hale pointed out, you can mock up this direct reaction with the R_∞ components. I get a very good looking result doing this. Now what do I do? I looked at the ^{7}Li system and, following Dr. Hale's guidance, I struck an L = 0 state in at about 2.5 MeV. This works well, but there is no other evidence for it that I can find except the n + ^{6}Li thermal cross section. I look at the mirror nucleus, ^{7}Be, and I cannot find the L = 0 state there either.

Now how do I use these results? They are beautiful parameterizations and they knit together different reactions. But how do I get the physics of reaction mechanisms out of them? How do I determine whether it is a direct reaction, a resonant reaction, where the resonances really are, and what is the physics involved?

Stewart

I believe that Gerry Hale should address this question.

Hale

The interpretation of R-matrix parameters for light nuclei is complicated by the fact that even most of the "resonances" are essentially single-particle states which are so broad that they seldom show up as well-defined "bumps" or anomolies in the measurements. In the case of ^{6}Li, however, I think the 3/2$^+$ state is well estabalished--not because it is required to explain the 1/v cross section at low energies, since that comes mainly from the 1/2$^+$ s-wave--but because it is the lowest order positive parity quartet-doublet transition which can interfere with the famous 5/2$^-$ resonance to give the observed asymmetric behavior of the ^{6}Li(n,t) cross section at low energies. I think it is quite likely that the bulk of the 1/v cross section in ^{6}Li comes from a direct process, like the deuteron-exchange term proposed by Weigmann, which is approximated in our analysis by distant levels, and not by any s-wave resonances close to the n-^{6}Li threshold.

Stewart

If the Swinhoe experiments are correct on the total tritium production, as far as I know there is no other reaction in Li-7 that can absorb the excess cross section except the elastic, and the elastic scattering experiments are much too low to allow me to

choose any total cross section that has ever been measured. That
is the only thing I would like to leave you with, that is, I must
have the partials add up to the total cross section. The only
other possibilities for the excess cross section are the (n,p) and
(n,2n) reactions. They are both small, however,. and not likely
candidates.

SESSION X

UNRESOLVED RESONANCE REGION $< E_n \leq$ 3 MeV; $19 \leq A \leq 220$
Chairman: A.B. Smith   ANL

Dup

INTERPRETATION AND NORMALIZATION OF EXPERIMENTAL DATA
FOR TOTAL, SCATTERING AND REACTION CROSS SECTIONS[*]

P. T. Guenther, W. P. Poenitz and A. B. Smith

Applied Physics Division
Argonne National Laboratory
Argonne, Illinois 60439, U.S.A.

ABSTRACT

Problem areas in the interpretation of fast-neutron
data are discussed. Their impact on experimental uncer-
tainties and hence the evaluation process are reviewed in
the context of user needs. Contributions of supplementary
information such as nuclear models and applications tests
are explored. Specific means for resolving difficulties
cited are proposed and illustrated.

INTRODUCTION

The derivation of an adopted "best value" of a given
physical parameter involves three mutually interactive, but
approximately separable, entities: The Evaluator, the Data
Base, and the Auxiliary Information.

The Evaluator deduces - from the Data Base and Auxiliary
Information - the "best value" in compliance with some theory or
philosophy. Over the years evaluation techniques have varied in
sophistication from the artistic hand guided by a french curve
and a good bit of insight, inspiration, or prejudice, to dogged
persistence with immense computer-manipulated data files.

The Data Base (hopefully) comprises a maximal ensemble of
relevant experimental information. The essential point here is
that somehow the various contributing data sets have been put on
compatible footing by uniform assignment of correlated and uncor-
related errors, energy resolution, and so forth.

Auxiliary Information is supplied by systematics, theoret-
ical estimates, nuclear models, and the like. In short, it is
any knowledge that might augment that of the Data Base.

The sum total of knowledge is contained in the Data Base
and Auxiliary Information. The Evaluator cannot change that.
However, he can change perception of that knowledge. From this
perspective a particular data set may appear to be discrepant.
If rational search reveals a shortcoming in the interpretation
of a physical measurement, so that the data set can be corrected
or its uncertainty increased, the knowledge of the Data Base
will have been improved.

The purpose of this paper is to highlight a few problem
areas arising in the interpretation of fast-neutron data.
The discussion is by no means complete, but rather reflects
what the authors believe to be a few topics of contemporary
concern in data reduction, analysis and evaluation. It is
hoped that the examples given help those facing the task of
compiling and evaluating a Data Base to assess the importance
and extent of certain experimental parameters, correction
procedures and supplementary information. Such judgment is
essential both before the evaluation process as well as in
reviewing its results.

Although it might be satisfying to produce evaluated files
well ahead of user needs, constraints on financial and human
resources may prove such a goal over-ambitious. Thus it is
appropriate to inquire about typical applications of nuclear
microscopic data and to review its utility in this context.

In the present mass-energy region the user interest is
primarily in Fast Breeder Reactor neutronics and, secondarily,
in fusion-blanket design. The relevant integral calculations
employ diffusion, transport or monte-carlo methods. The evaluator
should be cognisant of these uses and methods. The diffusion and
transport calculations are generally of a multi-group nature as
illustrated, for example, by MC^2-2 [1] where the calculation is

carried out within the framework of 2000 ultra-fine lethargy groups. Such group structure implies an energy-bin width of ten to a few tens of keV as illustrated in Fig. 1. The data emphasis is on cross section magnitude averaged over the bin width, with far less concern with angular dependence. The bin-energy mesh is much coarser than the underlying physical fluctuations and some of the better-resolution measurements. Precisions within an intermediate resolution equivalent to that employed by the user are sought in the evaluation. More detail is at best a burden and at worst can compromise the intermediate resolution accuracies.

In principle, monte-carlo techniques, such as VIM [2], can utilize unlimited detail. In special cases dealing with small regions this may be true in practice. However, it is frequently pointed out [3] that full-scale-system monte-carlo calculations employing a very detailed evaluated data base will rapidly exhaust the storage and computational budget of the largest present (or conceived) computational facility. Thus, in practice, full-scale-system monte-carlo procedures employ energy definitions very similar to those used in the multi-group methods.

The above leads us to conclude that the evaluation process should give primary emphasis to angle-integrated cross-section values and intermediate energy resolutions.

NEUTRON TOTAL CROSS SECTIONS

The total cross section is of central importance for several reasons. It is the envelope to which a given file of partial cross sections must conform. In fact, because of its potential accuracy, it is often used to determine some particular partial cross section. It is also a critical input to nuclear model parameterization.

The total cross section is, in principle, perhaps the simplest parameter to determine both in regard to experimental procedure as well as interpretation of the physical measurement. This would appear to be true particularly for energy-averaged cross sections.

Yet what in fact is measured is the energy-averaged transmission, i.e.,

$$\langle T \rangle = \langle \exp(-n\sigma(E)) \rangle \quad . \tag{1}$$

In the presence of fluctuations the averaging process cannot pass through the exponential and one is forced to define the effective cross section

$$\sigma_{eff} = n^{-1} \, \ln\langle T \rangle \quad . \tag{2}$$

The identification of σ_{eff} as the energy-averaged total
cross section $\langle\sigma(E)\rangle$ is only as valid as a linear representation
of the exponential in Eq. (1). Thus any finite-sample measure-
ment which does not fully resolve the underlying resonance
structure only determines σ_{eff}.

The importance of this effect (sometimes referred to as
resonance self-shielding) over large mass and energy regions
has been recently realized [4].

Presently there are three methods for determining $\langle\sigma(E)\rangle$.

A.   Obtain transmissions for a thin sample and/or resolve the
resonance structure (in which case there is no average
involved).

B.   Measure concurrently transmissions for a set of sample
thicknesses and extrapolate the deduced cross sections
to "zero thickness".

C.   Correct for the fluctuations by calculational means.

Option A is subject to obvious physical limitations, yet
has been successful in a very few isolated cases (e.g., probably
for Fe).

Option B is realizable provided a sample set is available.
Here one obtains a family of σ_{eff} curves which gradually con-
verge with increasing incident neutron energies. They decrease
in magnitude with increasing sample thickness. These effective
cross sections may then be extrapolated – energy by energy – to
the zero thickness value.

This procedure is illustrated, in Fig. 2, in detail for a
Cr measurement [5] with an energy resolution of ~50 keV on a
small energy interval (1-1.5 MeV) where a linear least-squares
fit was used to approximate the true sample-thickness dependence,
which is a function of the underlying resonance structure. (If
its shape were known, the data could be used to scale its magni-
tude, – a very satisfactory procedure). Evidently the correction
varies considerably with clustering of levels and the effective
energy – average used.

Figure 2b shows the fits to simulated effective cross section.
They were derived from energy-average transmissions for various
sample thicknesses computed with the Cr ENDF/B-V total cross
section [6] under the assumption that the latter fully resolves
the energy-dependent structure. It is apparent that in this case
the dependence on sample thickness is appreciably weaker and more
uniform in energy. This would indicate that perhaps the under-
lying structure is not fully resolved and that in fact the file
contains an effective cross section. Indeed, as Fig. 2a shows,
the ENDF/B-V totals lie somewhat below the experimental values.
On the whole this is true up to about 3 MeV, after which the ex-
periment confirms the file to within experimental error.

In contrast, as indicated in Fig. 2c, an identical simulation based on the high-resolution Fe total cross section of Harvey [7] is qualitatively similar to the experiment. As the resolution becomes finer the overall correction becomes smaller. However, there are dramatic fluctuations in its behavior as Fig. 2d attests. The simulation was done in the same manner as above except with an energy resolution of 10 keV.

A more serious discrepancy between the ENDF/B-V file and experiment arises in the case of elemental nickel. Figure 3a displays a recent measurement interpreted by the above method [8]. It consistently exceeds a similar average of the corresponding ENDF-B/V [9] values by amounts attributable to the correction. The corresponding comparison made for Fe in Fig. 3b indicates agreement within experimental uncertainty.

Approach C must be employed if a set of samples is unavailable (as in the case of rare isotopes). A number of calculated resonance self-shielding corrections have been used [10]. The method explored by Poenitz in connection with actinide total cross sections [11] will be illustrated.

To briefly summarize this scheme we note that, under the assumption that the self-shielding effect depends on the fluctuating cross section, he derives the total and potential cross sections and the average resonance parameters from the optical model phase shifts [12]. Using the single-level Breit-Wigner resonance formulation, average level spacings from the Fermi-gas model, Wigner and Porter-Thomas distributions for level spacing and width fluctuations, respectively, he simulates by monte-carlo methods effective resonance cross sections, from which the corrections can be inferred.

This procedure was used to predict the self-shielding effect in natural tungsten. Calculations were performed for the isotopes of tungsten. An example of the results is shown in Fig. 4a. The appropriate corrections for the elemental samples were constructed by superimposing "diffuse samples" with thicknesses in proportion to the isotopic abundance. The corrected values for the various samples are displayed in Fig. 4b. They are mutually consistent within <±1%. The isotopic correction factors thus verified have been applied to the isotopic total cross section of tungsten [13] as shown in Fig. 5.

From what has been said it should now be clear that a reasonable intercomparison of fluctuating cross sections, and totals in particular, can only be made after a common resolution has been established. A procedure which attempts to exploit the information inherent in the better-resolution subsets is proposed in Ref. [14].

To outline the method, we recognize that among the sets there will be one of highest and one of lowest resolution. The latter will be the common resolution. The highest resolution data is now averaged to the resolution function of the lowest resolution set. Similar averages are constructed for

the intermediate resolution sets using their resolution functions
on the high resolution data. The ratios of these averages to the
broad average are employed to reduce the intermediate sets to the
common resolution.

After the evaluation process has run its course, the struc-
ture may be reimposed upon the evaluated broad-average resolution
recalling the self-normalized ratios previously determined.

NEUTRON SCATTERING CROSS SECTIONS

Since many applications require only a crude definition
of angular distributions, the emphasis here will be on angle-
integrated cross sections.

Fluctuations are also of concern in the scattering experi-
ment, although self-shielding is of lesser importance. First,
the uncertainty in the attenuation corrections due to a fluctua-
ting σ_T is reduced in proportion to the sample transmission.
Secondly, the deduced cross section is linearly related to the
observed count rate, N: $d\sigma = \varphi\epsilon$ CN (φ, ϵ, and C are the incident
flux, detector efficiency and correction factors, respectively).
However, if a fluctuating cross section is to serve for comparison
with an energy-averaged nuclear model or for an evaluation, the
measurement program must be sufficiently comprehensive to permit
meaningful averaging.

Some important problems limiting the potential accuracy of
the experiment are:

- Detector efficiency definition

- Source-sample geometry

- Multiple event corrections.

Probably more than any other single parameter detector efficiency
determines the accuracy of the many fast-neutron interaction
studies. At ANL we find this to be the largest error contribu-
tion in an elastic scattering measurement. If a substantial
reduction of uncertainty is demanded, considerable progress must
be made in this area.

Source-sample geometry affects both angular as well as flux
determination accuracies, and thus the angle-integrated cross
section. First, zero-degree reaction can contribute substantial
errors, perhaps as high as 5% in highly anisotropic distributions.
Secondly, large samples put a heavy burden on correction procedure.
Suppose one doubles the size of the samples we use at ANL (typi-
cally 2x2 cm. cylinders > 10 cm from source target). This would
increase the effective scattering angle at 20° by 2°. If in
addition the source-sample distance were halved, the effective
scattering angle would increase 7°. Now add a fluctuating σ_T and,
depending on the energy resolution selected for the experiment,

one may have to augment the uncertainty by another 1/2° or so.
Note that these changes may have all been motivated by the aim
to better define the cross section by increased count rates.

Large sample geometries demand meticulous corrections. For
example, estimates for the influence of sample size on multiple
event corrections are given in Table I. The importance of these
corrections is generally acknowledged and most reports of scat-
tering results indicate that they have been made, without, however,
specifying any detail. The prospective evaluator groping to ap-
preciate the impact of these corrections on the quality of his
Data Base may find the following exercise of interest.

Table I. The Effect of Sample Size on
Multiple-Event Correction Factors in 186 W.

R = H/2[a] (cm)	Elastic Cross Section (b)	2+ Inelastic Cross Section (b)
Uncorrected Experimental Value	3.93	0.525
0.5	4.36	0.572
1.0[b]	4.88	0.631
2.0	6.34	0.761

[a] Samples are right circular cylinders of height H and radius R.

[b] Typical ANL size.

Comparison of Multiple-Event Scattering Corrections

Input data. The illustrative example is constructed about
a real and typical measurement of scattering from a heavy rota-
tional nucleus, ^{186}W. The experimental observations include
the elastic distribution, the differential cross sections for
the first 2+ rotational state ($E_x=0.122$ MeV) and the excitation
of fifteen higher-lying levels at an incident neutron-energy
of 3.05 MeV [15]. The scattering samples were right cylinders
2 cm in diameter and 2 cm long. (This illustration is relevant
to a wide range of fission product and actinide measurements.)

Correction factors. Given the observables, a number of
approaches were used to correct for multiple events using a
detailed point monte-carlo calculation [15,16]. The emphasis
was on the impact of correction procedures upon angle integrated
cross sections. Obviously, there is also an impact upon dif-
ferential values, particularly significant in connection with
model comparisons. Six alternatives were explored ranging from

the very crude to the most detailed possible from the available
experimental information. Those cases and attendant angle-
integrated results are summarized in Table II.

Case-A. This is the crudest assumption assuming only elas-
tic scattering, i.e., implying that the total cross section
equals the elastic cross section. The resultant "corrected"
observed elastic-scattering cross-section falls 13% short of the
true value. This is the consequence of the failure to consider
inelastic removal processes.

Case-B. This computation uses a non-elastic removal cross
section derived from the difference between measured total and
elastic-scattering cross-sections. The resulting "corrected"
cross-section is in very close agreement with the most detailed
result F. The inelastic removal cross section was evidently
reasonably approximated.

Case-C. This calculation considers only the elastic scat-
tering and the inelastic excitation of the prominent first (2+)
state. The inelastic removal cross-section is under-estimated
and hence the elastic cross-section is too low by approximately
10%. Too many neutrons have been scattered into the first
inelastic component, resulting in a cross-section excessively
small.

Case-D. Here the non-elastic cross section, in addition
to the 2+ inelastic contribution, is introduced into the cal-
culations giving a reasonable approximation of the inelastic
removal from both the elastic and 2+ inelastic components. The
results are again very close to those predicted by the most
detailed input.

Case-E. This calculation makes use of the full experimental
data base; the elastics, the 2+ inelastic component, and 15 addi-
tional inelastic excitations. It is very comprehensive, but
there remains an appreciable non-elastic cross section that was
not observed. The latter still has a strong effect on the
resulting "corrected" values.

Case-F. This final example makes use of all the available
experimental information and includes the unobserved non-elastic
cross section that is still significant. The resulting cor-
rected cross sections are accepted as the most reliable given
the available information. They differ considerably from some
of the alternatives considered.

Thus, given an excellent scattering measurement one can
deduce reliable scattering results only if care is taken to
properly define the multiple event correction factors. This is
particularly true when observed components make significant con-
tributions to the interaction. That is so for nearly all heavy
nuclides in the MeV region and particularly so when fission is
involved. Improper correction procedures can lead to errors
far larger than sought --or quoted-- and destroy the internal
consistency of the evaluation process. Despite this, almost
all experimental results reported in the literature give essen-
tially no definition of the character of the correction factors
referring only to a simple statement that they were made.

Table II. Comparisons of Multiple Event Corrections to Scattering Cross Sections

Case	Inelastic Removal Processes	Elastics %[a] Q = 0.0		Inelastics % Q = -0.122	
Exp.	---	3.93 b	19%	0.525 b	17%
A	---	4.25	13%	---	
B	$\sigma_T - \sigma_{e\ell}$	4.85	1%	---	
C	R	4.40	10%	0.439	30%
D	R+N	4.89	0%	0.626	1%
E	R+I	4.67	4%	0.464	26%
F	R+I+U	4.88	--b	0.631 b	--

[a] Percent deviation from Case F.

[b] Assumed correct reference point.

R 2+ rotational, Q = -.122

I 15 discrete inelastic excitations

N Non-elastic less R

U Non-elastic less R and I

A carefully executed contemporary elastic scattering experiment is capable of defining angle-integrated cross sections with overall uncertainties of 3-5%. This compares favorably with the uncertainty range of 1-3% for total cross sections and certainly qualifies the elastic cross section for full membership in the Data Base.

The accuracies attainable for inelastic cross sections, on the other hand, are in general substantially lower. For example, even though (n,n') measurements enjoy the simplicity of a direct observation (in contrast to a (n,n'γ) measurement whose interpretation requires knowledge of branching ratios, etc.) some of the experimental difficulties encountered are

- Poorer counting statistics

- Definition of detector efficiency over a wide dynamic range

- Inability to separate close lying levels due to finite energy resolution

- Increased sensitivity to multiple even corrections.

These as well as other problems lead to uncertainties in angle-integrated inelastic cross sections of 5-10% in favorable cases, but more typically of 15-25% or more.

In view of these uncertainties (and of course of the basic principle of maximal knowledge) it seems inappropriate to evaluate the elastic cross section as the difference between total and non-elastic cross sections. Often, evaluated inelastic cross sections are given smooth excitation functions (although fluctuations in prominent inelastics are frequently observed [17]). As a consequence the elastic cross section (for the sake of internal file consistency) is endowed with a fluctuating component which may not only be inaccurate in detail but also may exceed reasonable magnitudes attributable to the compound elastic contribution.

The way out of this dilemma is, of course, to reduce all partial (as well as total) cross sections to a common resolution in the Data Base. Now the Evaluator can determine consistent "best values". A possible averaging procedure and retention of structure detail was previously discussed.

A reasonably complex and representative example (though short of a rigorous evaluation) illustrative of the above concept has been prepared using Poenitz's Evaluator CMA [18] which was presented earlier on in this workshop. Table III summarizes the constituent cross sections which were considered [19]. A sampling of the result is shown in Fig. 6a-c. The residual structure displayed is consistent throughout all cross sections, and particularly in evidence in the 2+ vibrational excitation of ^{60}Ni (Ex = 1.33 MeV). See Fig. 6b.

Table III. Elemental Nickel Data Base

Elemental Cross Sections	Isotopic Inelastic Contributions[a,c]		
Total	58	60	62
Elastic	1.454	1.334	1.173
Capture	2.459	2.159	--
(np)	2.775	2.285	--
(n,α)	3.0[b]	2.506	--
Continuum inelastics (includes ^{61}Ni Contributions)	3.264[b] 3.420[b]	2.626 3.15[b]	--

a   Adjusted for isotopic abundance.

b   Average of several levels.

c E_x in MeV.

Note that this example is internally consistent making
use of all components and best judgments of their respective
uncertainties in a proper logical manner. The evaluated
results and associated uncertainties are consistent with the
input Data Base as illustrated in Fig. 6b and c. Although
this example is only illustrative, it is clear that the
results are very inconsistent with ENDF/B-V [9] in many of the
most prominent components as illustrated in Fig. 6a. The
discrepancies are far larger than sought by the user. They
are traceable to variations in the physical interpretation of
the Data Base, differences in the data base (some improved
recent measurements) and to entirely different approaches to
the evaluation process.

AUXILIARY INFORMATION

The usefulness of the optical model as a source of supple-
mentary information will be illustrated. The reliability of
such calculations depends on the quality and comprehensiveness
of the experimental foundation of its parameterization.
A simple applications test has been included in the fol-
lowing remarks.

Total and Scattering Cross Sections

The interpretation of angular distributions by means of
the optical model requires a data set of sufficient range and
sampling density to define the necessary energy-averaged behavior.
Angular distribution for ^{60}Ni reported in Ref. [20] are
shown in Fig. 7a. The mean experimental energy resolution was
20-50 keV over the indicated energy range. Even so, considerable
residual fluctuations persist. The spherical optical model fit is
compared to a 200 keV average of the data in Fig. 7b. A concern
at the time of this analysis was the discrepancy between the com-
puted and measured total cross section evidenced in Fig. 8. Since
only one isotopic ^{60}Ni sample was available, the sample thickness
correction was investigated by transmission experiments employing
several thicknesses of elemental nickel as discussed in a previous
section. When the properly corrected elemental cross sections
where compared with calculations using the original ^{60}Ni parameters,
good agreement was found (Fig. 3a, [21]).
Figure 9 exposes an inconsistency between an experimental set
of ^{242}Pu totals and the corresponding optical model calculation
based on a potential that had been derived from a comprehensive
set of actinide and heavy element total cross sections [22]. Since
the potential successfully summarized the systematics of its base,
the extrapolation to ^{242}Pu could be done with confidence.

Capture Cross Sections

A good knowledge of capture cross sections of a large
number of nuclei is important for technological applications.
The fertile nuclei play a predominant role, but capture cross
sections of structural materials, fission products, fissile
nuclei, and other transactinides are important as well. The
evaluation of such data is hampered by a generally poor dif-
ferential Data Base with 10-20% differences between newer
measurement results being common, and uncertainties usually
not better than 5-10%. This naturally suggests utilization
of other sources of information as well, for example, nuclear
model calculations and integral data. Unfortunately, the
capture cross sections calculated in terms of the statistical
and optical models depend on a large number of parameters
which are not well defined by other experimental data either.
The consequences of this problem are large differences of
theoretically calculated capture cross sections, which in the
case of fission product nuclei amount to factors of 2-5 at
2 MeV [24,25]. Perhaps the situation is not as bad in the
lower keV region (10-100 keV) which is more important for
practical applications. The parameter dependence was inves-
tigated for $^{238}U(n,\gamma)$ and the results are shown in Figs. 10a-e.

Values obtained from experimental data, measured in the
resolved resonance range, are usually employed to normalize the
theoretically calculated Γ_γ/D. The sensitivity of the cal-
culated capture cross section between 10 keV and 1 MeV to a
1 percent change of Γ_γ/D is shown in Fig. 10a. Assuming
that a value for Γ_γ/D is available for normalization, the
sensitivity of the calculated cross section to the level
density formula parameters, A and σ, is small below 100 keV,
but increases rapidly at higher energies (see Figs. 10b and c).

The fluctuation correction (Moldauer [26]) is unfortunately
largest in the energy range of greatest interest for the cap-
ture cross sections. Figure 10d shows the uncertainty caused
by this correction, assuming that it amounts to 10% of the
size of the correction.

The optical model parameters can be obtained from fitting
total and scattering cross sections, a data base which is
reasonably good for ^{238}U. The difference for the calculated
capture cross section obtained with two different sets of
optical model parameters is shown in Fig. 10e. One parameter
set was obtained by fitting total cross sections and elastic
and inelastic scattering cross sections of ^{238}U. The other
set was obtained from a optical model fit of the total cross
sections alone.

We see from Fig. 10a-e that the predominant uncertainty of
the calculated capture cross sections in the 10-100 keV range
is due to Γ_γ/D, the optical model parameters, and the fluctua-
tion correction. The total uncertainty of the calculated cross
sections can be estimated to be ~6% at 10 and 30 keV, and ~7%

at 100 keV for ^{238}U(n,γ). These uncertainties are not much
larger than those obtained from an evaluation of differential
experimental data in this energy range. Thus, computed values
could serve as useful input to the evaluation. Unfortunately,
the situation is not quite that favorable in the fission product
range. Uncertainties for Γ_γ/D are generally larger as
values are not available at all. A good data base of total and
scattering cross sections required to derive optical model
parameters does not exist. However, measurements for such data
are presently underway at Argonne.

The lack of good data for the fission product range suggests
the inclusion of integral data together with differential data
as a basis for evaluations in this energy range. The theoret-
ically calculated cross sections provide a physical shape to
be normalized with the integral and/or differential data. This
approach is successfully used by Schenter et al. [27].

Applications Guidance

Evaluated data files are extensively tested using a series
of integral benchmarks for which such indices as eigenvalue,
reaction rates, etc., are well known [28]. These are very com-
plex tests that have, to some extent, influenced the basic file
and in doing so may have masked and/or confused the nature of
the uncertainties. Far simpler application comparisons can
give guidance to the evaluator at an early stage without dis-
tortion. Such simple tests are familiar to the dosimetry
fraternity [29].

As an example consider the neutron inelastic scattering
cross section of a typical FBR structural material. That cross
section is dominated by contributions from 2+ rotational or
vibrational states in a single isotope or several even isotopes.
The cross sections are large and fluctuating with thresholds at
~1 MeV. Thus the structural inelastic cross sections appear to
impact only upon the relatively low intensity and higher energy
portion of a typical FBR spectrum. This is illustrated in
Fig. 11a where one such ENDF/B-V inelastic scattering cross sec-
tion is convoluted with the BIG-10 spectrum [30]. Clearly, it
is the low energy and threshold region that should receive
attention when dealing with the FBR spectrum. This implies
that the inelastic scattering cross sections of very minor odd
isotopes should be given careful attention, as their isotopic
cross sections are large and their inelastic thresholds very
much lower in energy than those of the even isotopes.
Taking these cross sections into consideration one gets a
very different picture as shown in Fig. 11b. The contribution
of the minor isotope inelastic cross section is large, increas-
ing the one-group-averaged inelastic cross section of this
structural material in the BIG-10 spectrum by 17%. The
increase is even larger in the softer FBR spectra. Sensitivity

estimates suggest a large impact [28]. The component was ignored
in ENDF-V. How one relates such an oversight to quantitative
error specification is an open question.

The above example is not an isolated case. The unfortunate
and long standing uncertainties in the heavy element cross sec-
tions, outlined above, are another illustration of strong data
impact near the very peak of typical FBR spectra.

Evaluators should carefully examine their qualitative con-
tent and representation in the context of primary applications
usage employing simple estimates of importance such as weighted
broad-group cross sections.

SUMMARY

The intent of the foregoing dicussions was to alert the
evaluator of fast-neutron data to typical application needs, ex-
perimental uncertainties, and uses of supplementary information.
These particular issues were addressed in connection with total,
elastic, inelastic, and capture cross sections:

- Many neutronic calculations require only a rudimentary
  definition (i.e., the "transport cross section") of
  angular distributions and intermediate energy resolu-
  tions.

- Most transmission measurements determine an effective
  cross section and must be corrected to define the energy-
  averaged σ_T.

- Factors influencing the accuracies of elastic and in-
  elastic angular distributions and hence the angle-
  integrated cross sections were discussed. The
  importance of proper treatment of inelastic removal
  processes in multiple-event corrections was demonstrated.

- A comparison of accuracies for elastic and inelastic
  cross sections indicates that it is inappropriate to
  define σ_{el} as a free adjustable parameter (i.e.,
  $\sigma_{el} = \sigma_T - \sigma_{inel}$).

- The need to simultaneously evaluate partial and total
  cross sections at the same energy resolution was stressed
  and such an evaluation was illustrated.

- A method for retaining "structure information" was out-
  lined.

- The ability of the optical model to delineate data in-
  consistencies was demonstrated.

- The use of simple applications test was illustrated by
  demonstrating a serious shortfall of a typical structural
  inelastic file in the spectrum of the "BIG 10."

- The sensitivity of calculated capture cross sections to
  various input parameters was explored. It was found that
  such calculations may contribute valuable knowledge to
  the evaluation of capture cross section provided para-
  meterization can be based on reliable experimental in-
  formation from other neutron interaction studies.

Finally, one point must be emphasized. In the introduction
it was noted that a consistent treatment of the information em-
bodied in the Data Base might lead to an improvement of its
knowledge content. The detailed discussions of this paper were
carried on in that spirit. However, the evaluation process can-
not obviate the need for new experimental information, for it is
after all the foundation of all knowledge both in the Data Base
as well as the Auxiliary Information. The tremendous human
and computational effort of digging into the past and putting
the Data Base on a uniform footing (through reassignment of er-
rors, inclusions of newly understood corrections, and so forth)
on a massive scale should be carefully weighed against the bene-
fits derived from a new generation of comprehensive improved
measurements, taking care to exploit the lessons learned from
the evaluation process.

NOTE

The evaluation of neutron cross sections for elemental
nickel was intended for illustrative purposes only. GMA results
may change with improved input and should not be used or quoted.

REFERENCES

1. H. HENRYSON II, B. J. TOPPEL, and C. G. STENBERG, "MC^2-2: A Code to Calculate Fast Neutron Spectra and Multigroup Cross Sections," Argonne National Laboratory Report, ANL-8144 (ENDF 239) (1976).

2. E. M. GELBARD and R. E. PRAEL, "Monte Carlo Work at Argonne National Laboratory," in Proc. NEACRP Meeting Monte Carlo Study Group, July 1-3, 1974, Argonne, Illinois, ANL-75-2 (NEA-CRP-L-118), Argonne National Laboratory (1975), p. 201.

3. R. HOWERTON, private communication.

4. A. SMITH et al., "Fast-neutron Total and Scattering Cross Sections of Cr, Fe and ^{60}Ni," NEANDC Topical Conference, Geel (1979), also A. SMITH and J. WHALEN, "Comments on Energy-averaged Neutron Total Cross Sections," Argonne National Laboratory Report, ANL/NDM-33 (1977).

5. P. GUENTHER et al., to be published.

6. Evaluated Nuclear Data File-B, Version V, Mat. No. 1328.

7. J. A. HARVEY et al., private communication, data available from the National Nuclear Data Center, Brookhaven National Lab.

8. A. B. SMITH, P. T. GUENTHER, and J. F. WHALEN, "The Non-elastic Scattering Cross Sections of Elemental Nickel," Argonne National Laboratory Report ANL/NDM-54.

9. Evaluated Nuclear Data File-B, Version V, Mat. No. 1324.

10. H. W. SCHMITT, Oak Ridge National Laboratory Report, ORNL-2883 (1960), also L. DRESNER, Nucl. Instr. and Methods, 16 176 (1962), also R. L. MACKLIN, Nucl. Instr. and Methods, 26 213 (1964), also D. BOGARD and T. SEMLER, Conf. on Neutron Cross Sections and Technology, CONF-660303, 502, Vol. -1 (1966), also L. B. MILLER and W. P. POENITZ, Nucl. Sci. and Eng., 35 295 (1969), also F. H. FROEHNER, Gulf-General Atomic Report GA-8380 (1968).

11. W. P. POENITZ et al., "Total-Neutron Cross Sections of Heavy Nuclei, International Conference on Nuclear Cross Sections for Technology, Knoxville, Tennessee, Oct., 1979. To be published.

12. P. A. MOLDAUER, Phys. Rev. Lett. 177 1841 (1976).

13. J. WHALEN and J. MEADOWS, Argonne National Laboratory
    Report ANL-7210 (196t).

14. W. P. POENITZ, "Fast-Neutron Capture Cross Sections of
    Importance in Technological Applications," International
    Conference on Nuclear Cross Sections for Technology,
    Knoxville, Tennessee, October 1979. To be published.

15. P. T. GUENTHER, Univ. of Ill. Thesis, Elastic and Inelastic
    Neutron Scattering from the Even Isotopes of Tungsten (1977).

16. E. Cashwell and C. Everett, A Practical Manual on the Monte-
    Carlo Method for Random Walk Problems, Pergamon Press (1959).

17. For example P. T. KARATZES et al., NSE 67, 34 (1978), also
    F. VOSS, et al., Proc. Conf. on Nuclear Cross Sections &
    Technology, NBS 425, 916 (1975).

18. W. P. POENITZ, "Data Interpretation, Objective Evaluation
    Procedures and Mathematical Techniques for the Evaluation
    of Energy-dependent Ratio, Shape and Cross Section Data,"
    Workshop on Evaluation Methods and Procedures, Brookhaven
    National Laboratory, Sept., 1980.

19. A. B. SMITH, private communication.

20. A. B. SMITH et al., "The Interaction of Fast Neutrons with
    ^{60}Ni," Argonne National Laboratory Report, ANL/NDM-44.

21. CLEMENT et al. (1971), data as provided by the National
    Nuclear Data Center, Brookhaven National Laboratory.

22. W. P. POENITZ et al., NSE, to be published.

23. C. LaGRANGE and J. JARY, INDC Report, INDC (FR) -30/L
    (1978).

24. S. IIJIMA et al., J. Nucl. Sci. and Tech., 14, 161 (1977).

25. W. P. POENITZ, Proc. Spec. Meeting on Neutron Cross Sec-
    tions of Fission Product Nuclei, Bologna, 1979, p. 85.

26. P. A. MOLDAUER, Statistical Theory of Neutron Nuclear
    Reactions, Argonne National Laboratory Report, ANL/NDM-40
    (1978).

27. R. E. SCHENTER and T. R. ENGLAND, Proc. Spec. Meeting on
    Neutron Cross Sections of Fission Product Nuclei, Bologna
    1979, p. 253.

28. Benchmark Testing of ENDF/B-IV, ENDF-230, March 1976.

29. D. L. SMITH, "Neutron Dosimetry for Radiation Damage in Fission and Fusion Reactors," International Conference on Nuclear Cross Sections for Technology, Knoxville, Tennessee, October 1979. To be published.

30. E. J. DOWDY, E. J. LUZITO, and E. A. PLASSMANN, Nucl. Technol., 25, 381 (1975).
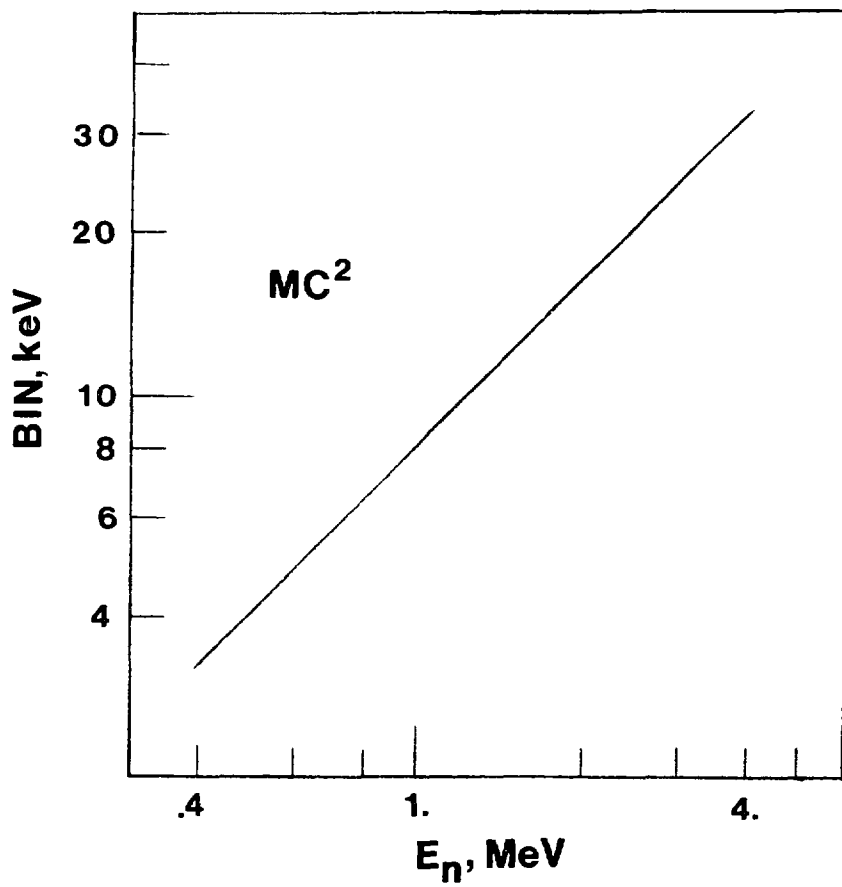
Fig. 1. Energy Bin Widths vs Energy for Multi-Group
Calculations of MC^2-2 [1].
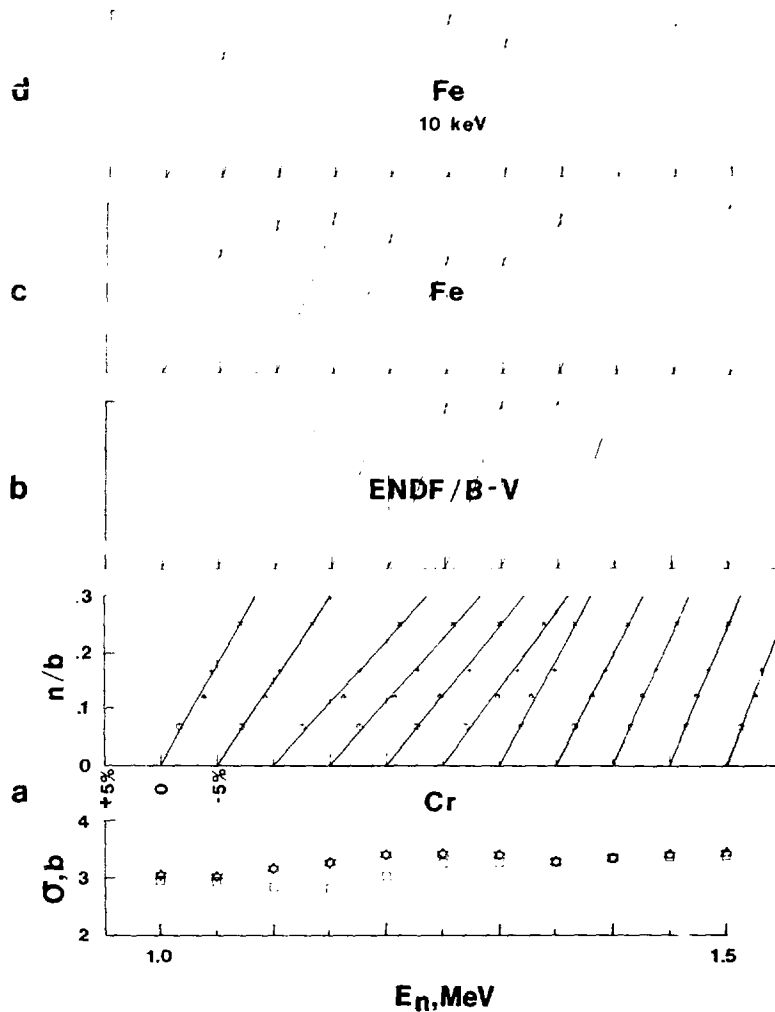
Fig. 2.   Extrapolation of Effective Neutron Total Cross Sections.

a) The lower portion of the figure shows the extrapolated
   energy-averaged cross sections of elemental Cr [5] as stars,
   those of the Cr ENDF/B-V as squares (see text for details).
   The upper portion of the figure details the linear fit to the
   effective cross sections at each energy point as deviation from
   from the extrapolated (i.e., "zero thickness") values in percent
   vs sample thickness in nuclei per barn.

b) Simulated extrapolation derived from the Cr ENDF/B-V totals
   using the energy resolution of [6].

c) As in b) but using the high-resolution Fe data of [7].

d) As in c) but with a 10 keV resolution.
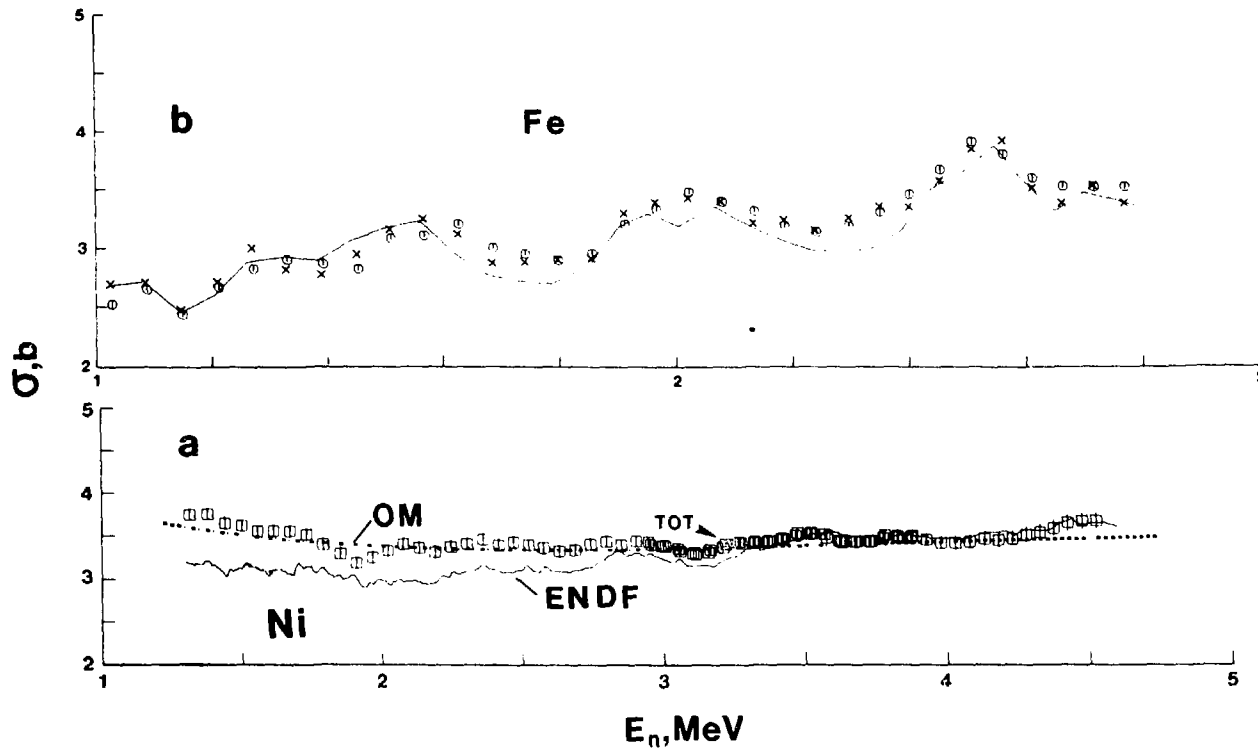
Fig. 3.   The Neutron Total Cross Sections of Elemental Nickel and Iron.

a) Experimental points of [8] are
   indicated by squares, the equiv-
   alent energy-averaged ENDF/B-V
   values by a light line, the
   optical model calculation defined
   in [20] by a heavy, dashed line.
   Note the discrepancy below ~3 MeV.

b) Iron total cross sections. Circles
   indicate the experimental values
   of [4], crosses those of [7]
   averaged to the energy resolution
   of [4]. The line is a similiar
   energy-average of the ENDF/B-V
   values.
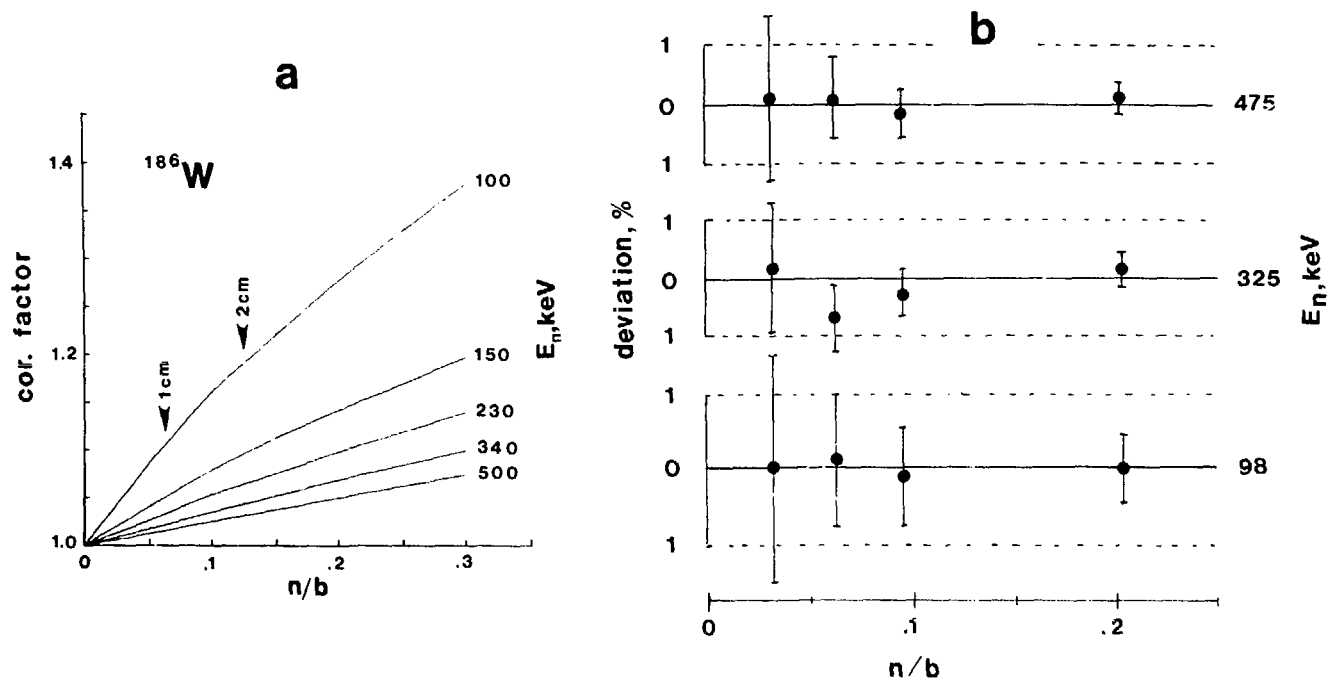
Fig. 4. Effective Neutron Total Cross Section Correction for Elemental Tungsten.

a) The isotopic correction factors for ^{186}W at several energies calculated by the method of [11].

b) The results of correcting the experimental effective cross sections obtained for several sample thicknesses. They are displayed as deviations from the mean in percent at the given energy vs sample thickness in nuclei per barn.
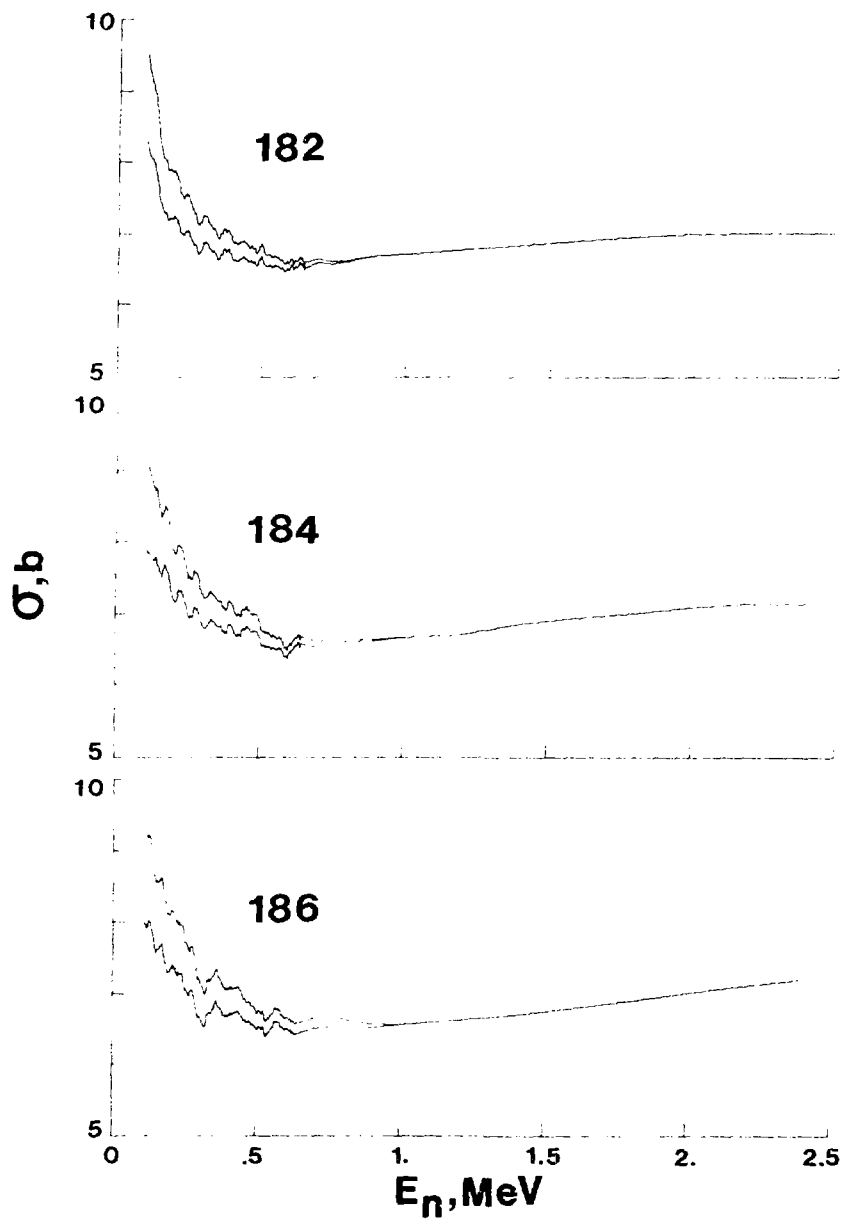
Fig. 5. Isotopic Neutron Total Cross Sections of Tungsten.
The experimental effective cross sections of [13]
(lower curve) and the values (upper curve) obtained
by the correction procedure of [11].
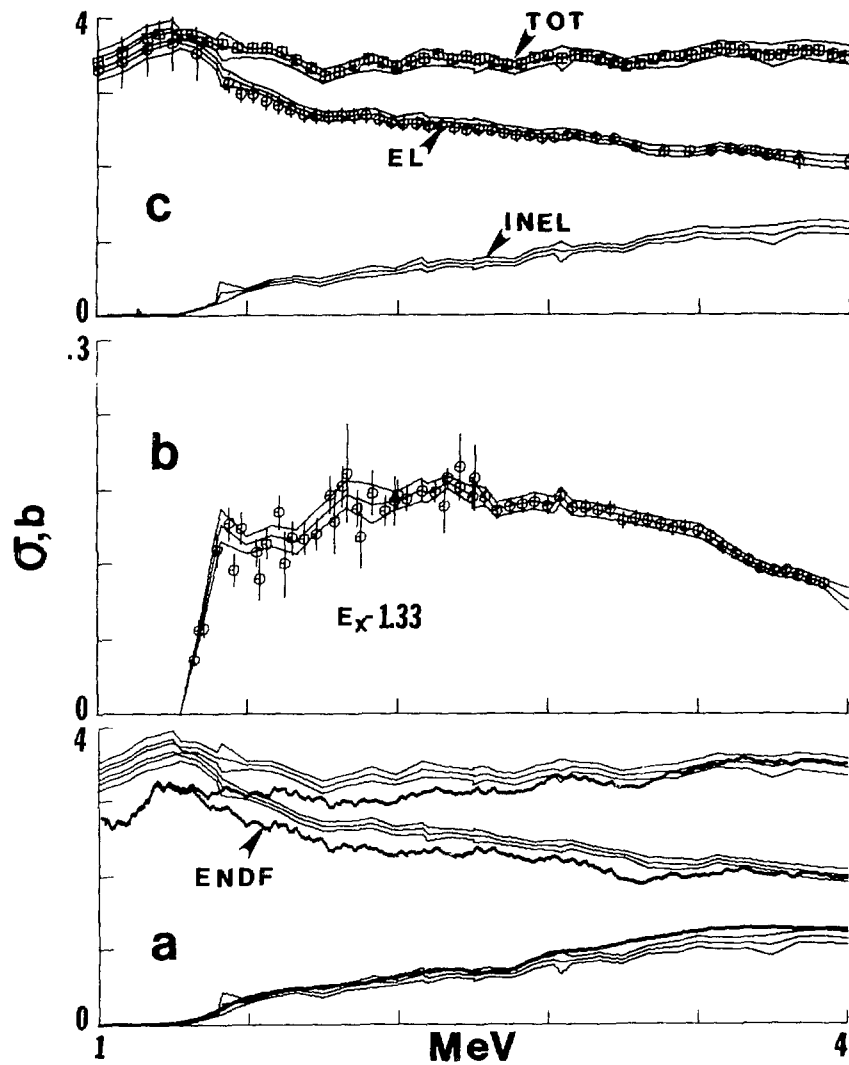
Fig. 6. The Evaluation of Neutron Cross Sections for Elemental Nickel.

a) Total, elastic, and non-elastic evaluated cross sections
compared with the Ni ENDF/B-V values.

b) Evaluation results for the Ex = 1.33 MeV excitation function of ^{60}Ni.

c) Evaluation results for total and elastic cross sections. Symbols
indicate Data Base specified in Table III.

a) Least squares Legendre-polynomial fit for experimental data of 20-40 keV resolution. $d\sigma$ in barns per steradian, angle in laboratory degrees. Note residual fluctuations.
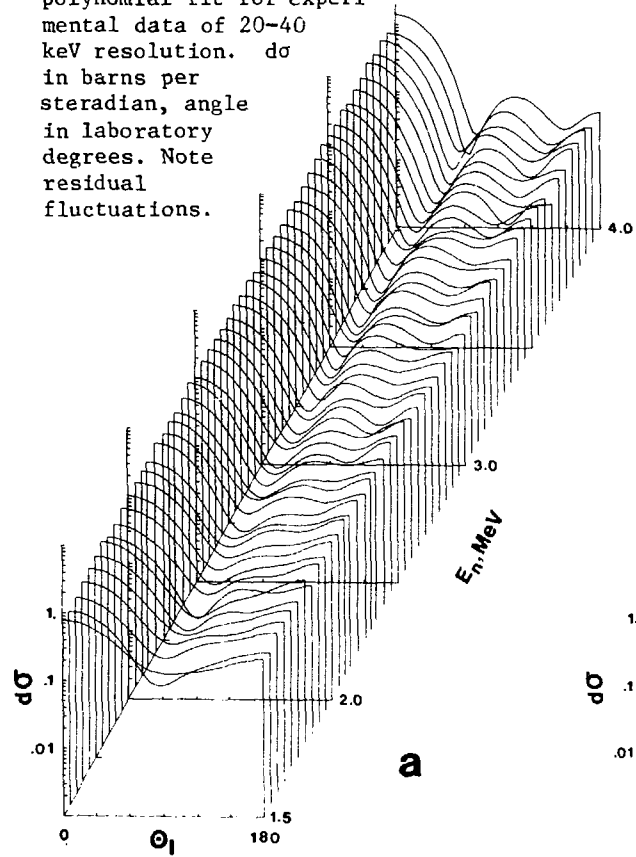
b) The data of a) averaged of 200 keV is shown as circles. The curves are optical model calculations defined in [20].
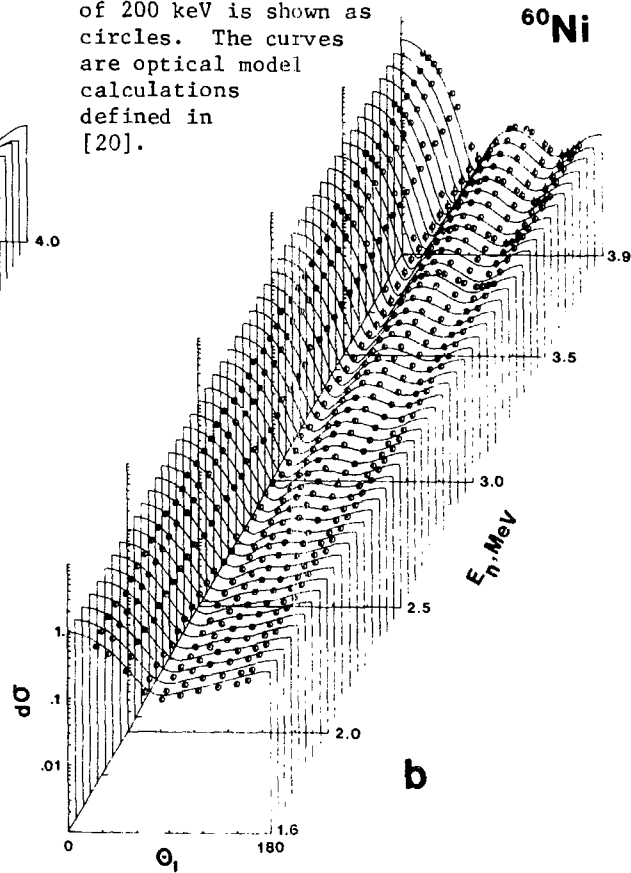
^{60}Ni

Fig. 7. Neutron Elastic Scattering Angular Distribution for ^{60}Ni [20].
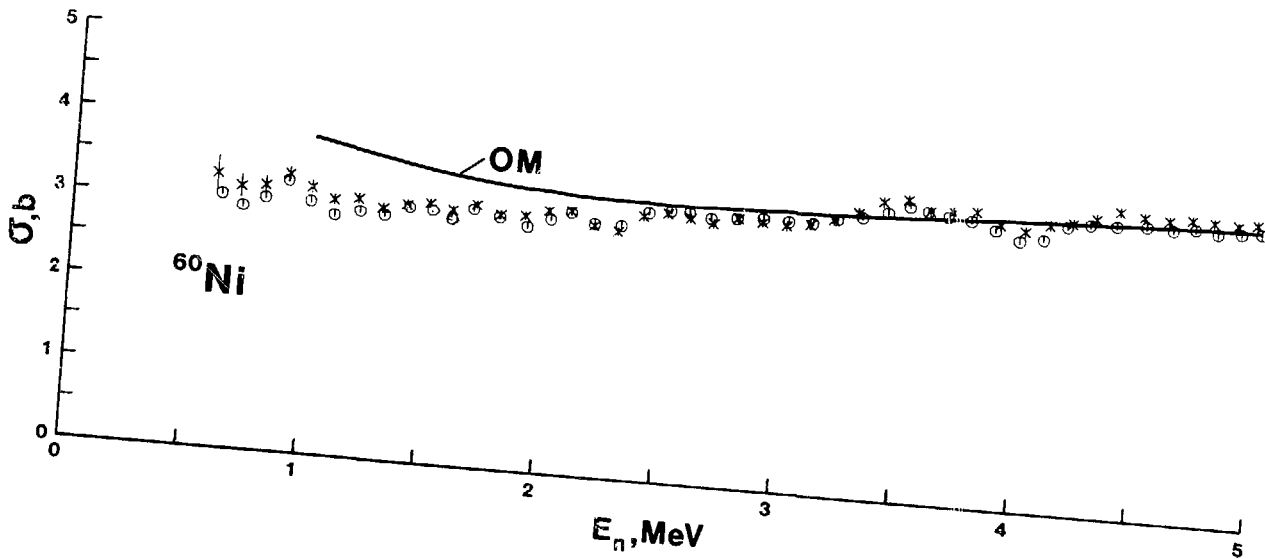
Fig. 8. Neutron Total Cross Sections of ^{60}Ni. Experimental values of [20] shown as circles, those of [21] appropriately averaged as crosses. The heavy line is the optical model calculation defined in [20].
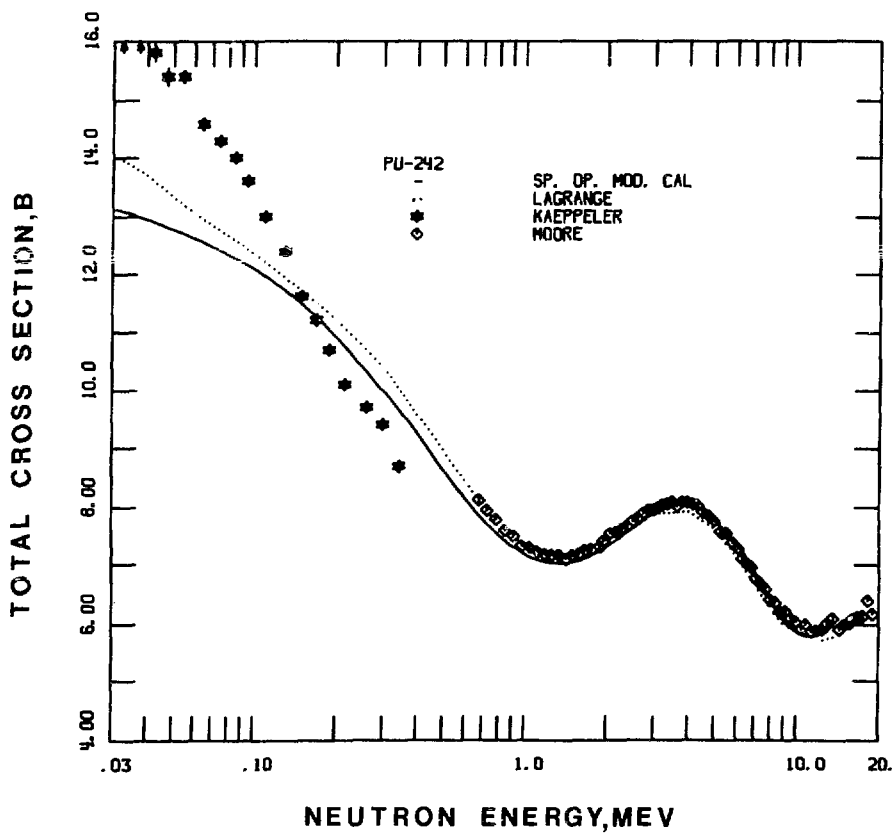
Fig. 9. The Neutron Total Cross Sections of ^{242}Pu. Symbols refer to experimental values. The heavy solid line is a spherical-optical-model calculation using the potential of [11]. The dotted line is a coupled-channels calculation defined in [23].
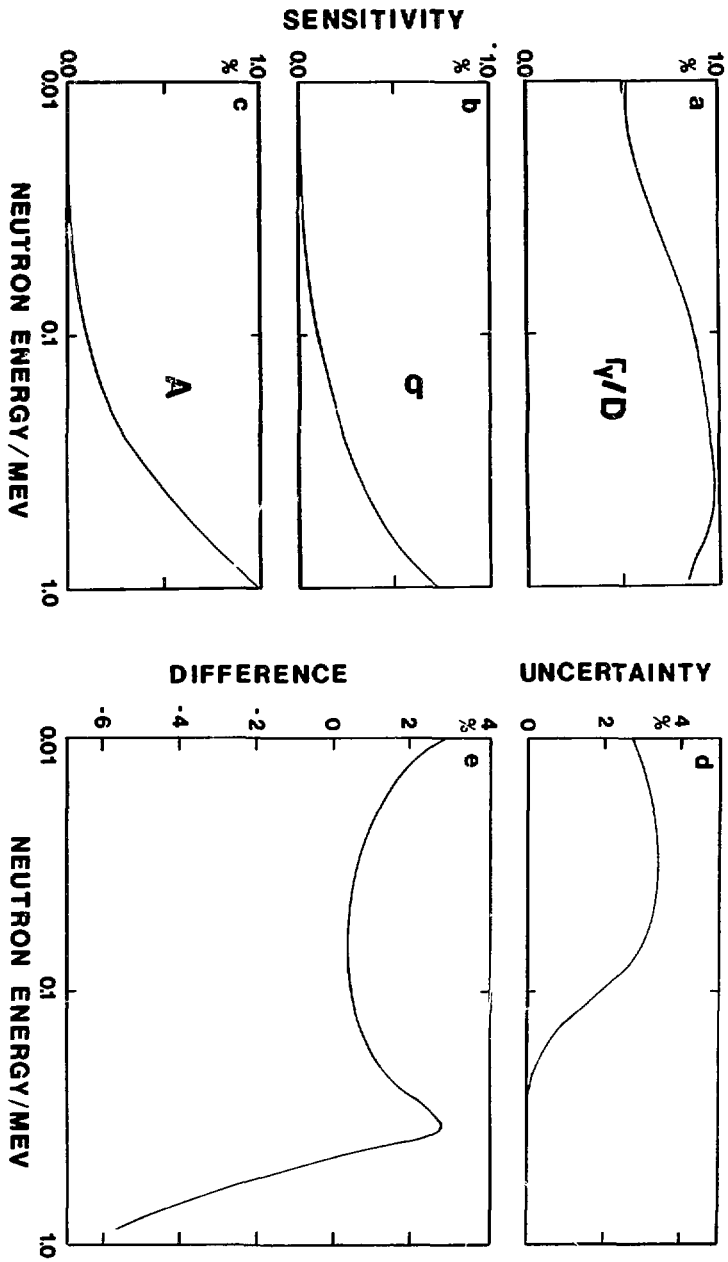
Fig. 10. Sensitivity of Calculated Capture Cross Sections of ^{238}U
to Various Input Parameters.

a) $\Gamma\gamma/D$,

b) and c) level density parameters

A and σ, respectively,

d) fluctuation correction,

e) optical model parameters.
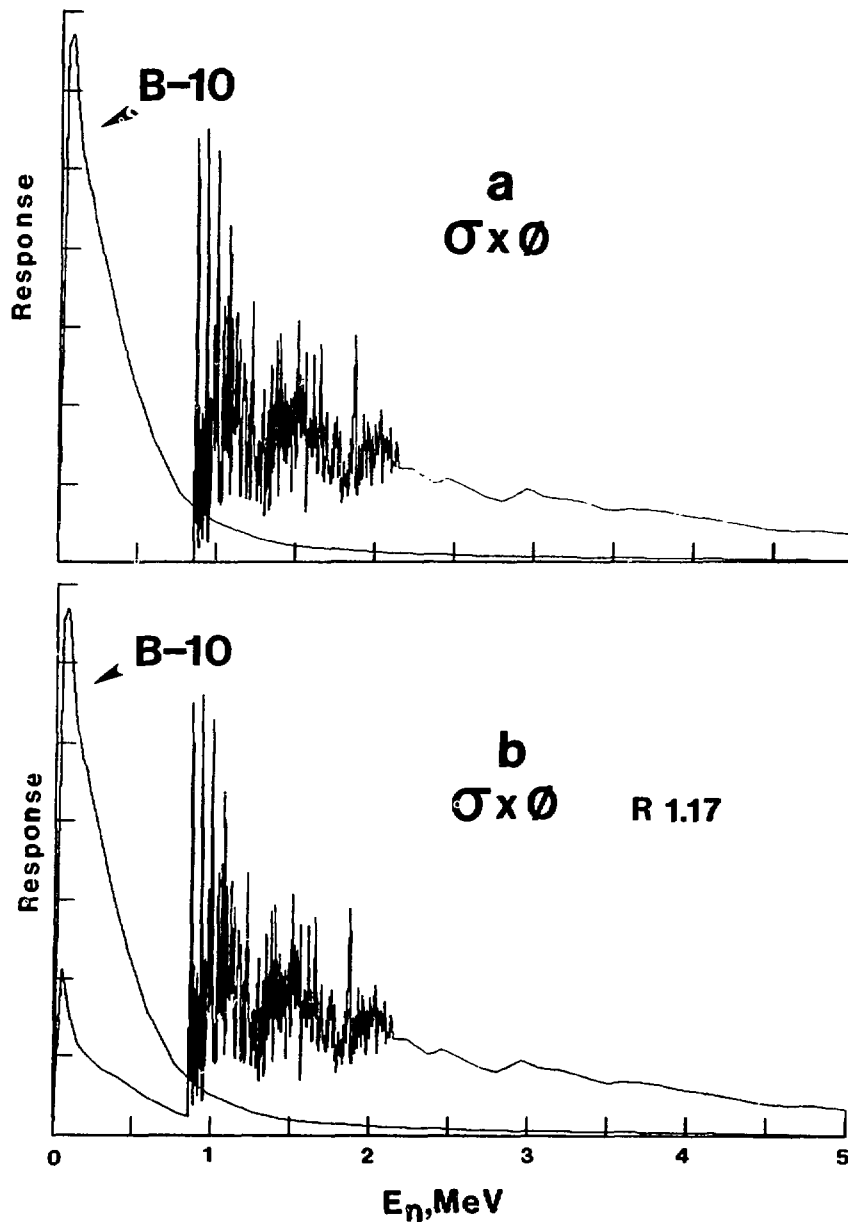
Fig. 11. Convolution of Illustrative FBR Inelastic Cross Section
with BIG-10 Spectrum.

a) Result as obtained from ENDF/B-V.

b) Result including minor-isotopic composition. The latter
increases the spectrum average quantity by 17%. The
curves denote the spectrum-weighted cross sections and the
BIG-10 spectrum.

Discussion

Smith

I must confess to a somewhat incestuous relation with this paper
for which I apologize. The authors are Drs. Guenther, Poenitz--
and the Chairman had a finger in it too.

Froehner

This is a comment rather than a question. The speaker stated that
there is a question as to whether the error introduced in energy-
averaged cross section measurements due to cross section
fluctuations is really a linear function of sample thickness. In
fact, it is linear to the first approximation; the slope being
just half the variance of the cross section multiplied by the
sample thickness.

Guenther

Recently, several of us at our Laboratory have considered this
problem and concur with what you have just said. Never-the-less,
the correction factors I have illustrated, as formulated by Dr.
Poentiz, do show some deviation from the linearity of the first
approximation. This is the higher-order effect.

Perey

I very much concur with one of the final statements you have
made. There is a general perception that if we would exploit our
extensive data files using our new evaluation techniques we would
be in much better shape. We only need to evaluate i* all
properly. I think you have properly pointed out that detailed
corrections are demanding of a comprehensive experimental
knowledge that is very often not available. It has been my
experience that one can spend a great deal of time attempting to
correct old data for effects we are now aware of with little
success. You often end up having to re-measure it anyway and you
are not much ahead until you do so. You have express such a view;
it is one I very much concur with.

Rowlands

Your measurements dealing with broad-resolution sample-size
effects provide valuable information for applications. However,
they may not provide all the required information. There are
problems associated with moderation effects and the relationship
between resonance widths and the mean energy loss in scattering
from different materials in a reactor core or shield. The
question is equivalent to knowing whether the narrow resonance
approximation applies or if the intermediate-resonance

approximation must be used. I think it would be very valuable if the information on the distribution of cross section values about the broad-resolution average (or sample-size effects) could be included in the evaluations.

Guenther (Comment)

Moderation was not a concern in the microscopic measurements I outlined. I believe you are focusing on lower energies than those I dealt with but we are attempting at Argonne to experimentally relate the dispersions to the variances Dr. Froehner mentioned. It is too soon to make any comments on these latter results.

Schmidt

I would like to address a general question to the "users". How are the considerable differences in resolutions associated with different types of data (e.g., total and partial cross sections, etc.) reflected in the evaluated data files affecting the use of this data? What is the effect of these inconsistencies in resolutions appearing in the evaluations?

Guenther (Comment)

I did show one illustration for the case of nickel and there are many others. In the time available I was not able to discuss the consistency of the evaluation of total, elastic-scattering and non-elastic cross sections. The point is that one commonly finds a very smooth behavior for the evaluated non-elastic cross section. The latter is subtracted from the highly fluctuating total cross section to obtain the elastic-scattering cross section which then contains all the structure of the total cross sections. The elastic-scattering structure is thus not correct in detail and if we need the structure its fidelity should be reasonably good. Furthermore, this common procedure results in a nonsensical compound-elastic component. These may be serious concerns.

Howerton

In response to Dr. Schmidt's question to the "user"; there is no general definition of the "user". He is drawn from a diverse community of interest and we cannot define any class of data that will "a priori" fit all his needs. Therefore, the evaluator attempts to provide all the information he can. Presumably the evaluator has some knowledge of those things that should be treated and how they should be handled. I do emphasize that we cannot difine a single uniqe "user"

COMMENTS ON SOME ASPECTS OF THE USE OF OPTICAL STATISTICAL MODEL FOR EVALUATION PURPOSES

Ch. Lagrange

Service de Physique Neutronique et Nucléaire
Centre d'Etudes de Bruyères-le-Châtel
B.P. n° 561
92542 MONTROUGE CEDEX, France

ABSTRACT

At the present time theoretical nuclear models are
being used increasingly to complete evaluated data files
in cases when measured data are deficient, or to pro-
vide neutron cross sections when no data are available
or even measurable. In this context what is really
required concerning theoretical evaluation tools is a
treatment as simple and physical as possible so as to
allow extrapolations with reasonable confidence. In
this paper only the optical and statistical models are
considered in the frame of their practical applications
in the energy range from unresolved resonance region to
about 3 MeV. We will outline the advances that have
occured in the recent past concerning some techniques
for obtaining reasonable parametrisations.

INTRODUCTION

Theoretical model calculations remain an essential tool, in
the case when experimental data are not available, in order to
fill the gaps by interpolation, extrapolation or prediction. For
this reason recent lectures about the role and efficiency of
nuclear models including the optical and statistical ones were
given in the recent past. We mention for example those given in
the IAEA Consultants Meeting on the use of Nuclear Theory in
Neutron Nuclear Data Evaluation held at Trieste [1] during the
winter 1975. More recently a course on Nuclear Theory for Applica-
tions was organized by the IAEA during the winter courses (1978)
on Nuclear Physics and Reactors [2]. The theoretical foundations
of the optical and statistical models were there presented by
C. Mahaux [3] and P.A. Mauldauer [4] respectively, whereas the
practical applications of these models for evaluation purposes

were presented by A. Prince [5] and G. Reffo [6]. The proceedings
of these various meetings were published and are available in
the laboratcries represented at the present workshop. Consequently
we refer to these detailed lectures for the conceptual and the
practical applications of these models. The main objective of this
paper is thus to present and comment the procedures used in the
parametrisation of the models, and the main difficulties usually
met. The various examples of parametrisation and problems pres-
ented below must be considered as material for further discussion
in the various workshop sessions.

OPTICAL MODEL PARAMETRISATION

As the "non local" optical model potential (OMP) requires
"complicated" computer programs not available in all the Labora-
tories, we consider here only the parametrisation of the "local
equivalent" one which is generally used. However the parametri-
sation procedure here described can be easily employed for more
realistic OMP.

In the energy range considered here from unresolved resonance
region up to 3 MeV neutron incident energy, the main experimental
constraints taken generally into account in the parametrisation
procedures are the neutron strength functions and total cross
sections. The theoretical elastic and inelastic cross sections are
the incoherent sum of direct and compound cross sections. These
compound components are calculated using the statistical model
and it still remains, as explained in the second part of this pa-
per, many uncertainties in the practical applications of this
model. Moreover the elastic and inelastic scattering cross sec-
tions above the unresolved region are characterized by fine struc-
tures which cannot be reproduced by the phenomenological models.
An example of such an inadequate parametrisation of the phenome-
nological model is shown in Figs.1 and 2. In Fig. 1 the experi-
mental [7] differential elastic scattering neutron cross sections
at 2.5 MeV incident energy for ^{208}Pb are reported. The experimen-
tal resolution was less than 25 keV. The upper solid curve is the
sum of the compound (CN) plus direct interaction (D.I) phenomeno-
logical calculations, whereas separated contributions are shown
as dashed curves. The fit observed is not good on the angular
region 45-90 degrees. This can be understood (cf. Fig. 2) consid-
ering the microscopic calculations of the optical potential in
the frame of the intermediate structure model performed by
M.J. Dufour and J. Salvy [8]. These last calculations were done
for testing the role of the particle vibration coupling in
various nuclear data. The effects of the "doorway state" in the
neutron channels p 3/2 and f 5/2 are reflected in the calculated
elastic cross sections reported in Fig. 2. From this example the
comparisons of model calculations have to be made with experi-
mental data of sufficiently large resolution. However this reso-
lution must be good enough so as to resolve elastic and inelastic

scattering data.

Coupled channels or spherical optical model calculations

The most crucial problem is the choice between coupled chan-
nels and spherical optical model calculations. We refer to the
talk given at this workshop by Dr Moldauer concerning the effect
of nuclear deformation on neutron strength functions and scat-
tering lengths, and to the one of Dr. Guenther concerning direct
inelastic cross sections. However the experimental values of the
neutron total cross sections can also be considered as a crucial
guide for the choice of the model parameters. The fast neutron
total and scattering cross sections of ^{107}Ag from 0.25 to 4.5 MeV
were analysed by Smith et al. [10] using spherical optical model
calculations. Their calculations are in a reasonable agreement
with the experimental data, and no significant dependence of the
inelastic scattering process on deformation was found. However,
as can be seen in Fig. 3 our calculated values of the total cross
sections depend greatly, at low energies, on the choice of the
deformation parameters. These calculations were performed assuming
for ^{109}Ag a vibrational model, and coupling together the ground
state and the first $3/2^-$ and $5/2^-$ states.

As the optical model involves a relatively great number of
parameters it is easy to obtain spherical optical model (SOM)
calculations in good agreement with some experimental data. But
if the parameter set thus obtained present some anomalous behav-
iour a more careful investigation of the model has to be under-
taken, and possible deformation effects must be considered. For
example SOM calculations of neutron cross sections for iron give
neutron total cross sections at 3-4 MeV which are within a few
percent of the measured values, but as the energy decreases cal-
culated values become increasingly larger than the experimental
data (10% at 1 MeV). A good fit is obtained assuming that the
diffuseness of the imaginary well can be energy dependent [11].
The same problem seems to occur in the case of Ti and Cr [12].

Wave functions and deformation parameters

For "vibrational" nuclei, deformation parameters obtained from
neutron inelastic scattering data and electromagnetic excitations
data are almost equal. Madsen, Brown and Anderson [13] have presen-
ted some theoretical explanations of the small differences between
deformation parameters obtained using various probes. An example
of such differences is shown in Table I, where experimental deter-
minations are reported from Ref.[14] and Ref.[15].

For rotational nuclei, instead of comparing the deformation
parameters β_2 β_4, comparisons have to be made using the multipole
moments of the OMP which are defined as :

$$q_\lambda = Z \int V(r) \; Y_\lambda^0 \; (\theta) \; r^\lambda \; \vec{dr} \; / \int V(r) \; \vec{dr} \qquad (1)$$

From the results presented in Ref.[16] and Ref.[17] the quadrupole moments obtained from nucleon scattering and electromagnetic excitations are in a very good agreement. Moreover useful informations can be obtained from the systematic trends of the 2nd and 4th order moments of the matter distribution obtained from Hartree-Fock-Bogolyubov (H.F.B) calculations.

For transitional nuclei, the simple collective models such as the vibrational or rotational ones are inadequate to a good description of energies and electromagnetic properties of the low lying collective states. Kumar [18], [19] and his co-workers have developed and tested a generalized optical model. In this formalism the microscopic wave functions calculated from the dynamic deformation theory or from H.F.B methods are used. The choice of the deformation is thus avoided and the possibility of shape coexistence can be taken into account. Using this formalism a quite satisfactory agreement was obtained in the case of ^{76}Ge (p,p')[18] and in the case of neutron cross section calculations for the even Samarium isotopes [19].

Coupled channels calculations for odd-mass nuclei

Coupled channels calculations are very time consuming when applied to odd-mass target nuclei using the actual level schemes. In the case of actinide nuclei an approximation called "the fictitious even-even nucleus" was recently presented [20].

In this approximation calculations are performed for a fictitious even-even nucleus (rotational model) with the same mass number and deformation parameters obtained from a systematic available in this mass region. Direct elastic and inelastic scattering cross sections are then shared among the ground state band levels of the odd-mass nucleus following the prescription of the "strong coupling rotational model [21]":

$$\frac{d\sigma}{d\Omega}(I_i) = \sum_{\lambda=0,2,4} <I_0 \ \lambda \ K \ 0|I_i \ K>^2 \ \frac{d\sigma}{d\Omega} \ (\lambda) \qquad (2)$$

where K is the Z' projection of the angular momentum of the last nucleon and I, λ are the spins for the levels of the real and fictitious nuclei respectively. It is suggested that the above simple model is tested in the mass number region $A = 19-220$.

We present for odd-A vibrational nuclei a similar model. This model is derived from the weak coupling model of De-Shalit [22]. Using this model the direct inelastic cross sections are given by :

$$\frac{d\sigma}{d\Omega} \ (I_i) = \frac{(2I_i+1)}{(2I_0+1)(2\lambda+1)} \ \frac{d\sigma}{d\Omega} \ (\lambda) \qquad (3)$$

Calculations are performed for ^{109}Ag using the real coupling
basis $1/2^-$, $3/2^-$, $5/2^-$ and the fictitious one 0^+, 2^+. The percen-
tage changes in the calculated total cross section resulting from
the choice of the model are shown in Fig. 4 for various values
of the deformation parameters. The model predicts (cf. Eq. 3) the
following direct inelastic scattering ratio :

$$R = \frac{\sigma(5/2^-)}{\sigma(3/2^-)} = 1.5 \qquad (4) \qquad .$$

The calculated values of this ratio deduced from coupled channels
calculations results, using the $1/2^-$, $3/2^-$, $5/2^-$ basis, are re-
ported in Fig. 5. The predictions given by the weak coupling
models are in a relative agreement with realistic calculation
near or above 8 MeV. We mention however that for energies less
than 2 MeV the calculated direct inelastic cross sections are much
smaller than those calculated using the statistical model.

Distorded wave Born approximation (D.W.B.A) or coupled channels (C.C) calculations

The calculations shown for ^{109}Ag in Figs 3,5 illustrate the
difference between D.W.B.A. and C.C. calculations. The D.W.B.A.
calculations give essentially the same results than those report-
ed in Fig. 3 (β = 0.0) for the total cross sections and in Fig. 5
(R = 1.5) for the direct inelastic cross sections. From these
results it appears that this approximation cannot be used with
confidence in the energy region below 5 MeV. We mention that
this lower energy limit has to be increased when the mass number
decreases or when the value of the deformation parameter
increases.

Optical model parametrisation procedures

The optical parameters sets deduced (cf. Ref.[23] for more
details) from systematic analyses of proton scattering data over
a large range of energies and mass number are quite useful for
providing us with general trends of the empirical parameters :
dependence on mass number, neutron excess, energy... . But for
evaluation purposes a particular parameter set has to be tailored
to each individual case.
The procedure employed by the Argonne Laboratory Group [24]
emphasizes elastic scattering at energies where the compound
elastic cross sections can be well determined and the neutron
total cross sections over a wide energy range (0.1 - 20 MeV).
Using this procedure the effect of coupling on the elastic and
inelastic cross sections was investigated. We mention for example
the theoretical extrapolation to ^{238}U of coupled channels param-
eters deduced for ^{186}W. Using this procedure the model was used
to provide extrapolated or interpolated nuclear data for fission
products, structural materials, and actinide nuclei.

The SPRT procedure developed at Bruyères-le-Châtel [25] emphasizes the neutron strength and scattering radius as well as the neutron total cross sections over a wide energy range. Moreover all the nucleon-nucleus scattering data are taken into account. The weight of these various experimental data is deduced from the sensitivity of calculated results to small variation of the parameters. We require to obtain a satisfactory agreement with all of the data by using an unique physically coherent parameter set. In the case when the experimental data are scarce, the predictions are based on an adequate readjustment (potential depths, deformation parameters) of a parameter set previously tailored for a neighbouring nucleus. As many experimental constraints are included in the parametrisation procedure the uncertainties in calculated results are relatively small. We mention for example less than 5% for the total cross sections. The uncertainties on the calculated compound nucleus cross sections are near 5% for neutron energies less than 10 MeV, and near 10% at greater energies.

STATISTICAL MODEL CALCULATIONS

As mentioned by Barnard and Reitmann [26] in the case of ^{103}Rh and by Vladuca et al. [27] in the case of ^{89}Y and ^{93}Nb, accurate neutron inelastic scattering model tests can be obtained only when the neutron transmission coefficients are calculated from a potential specially selected for a nucleus or a family of isotopes in the same mass region.

Choice of the neutron transmission coefficients

We present statistical model calculations of neutron cross sections for ^{103}Rh performed with transmission coefficients deduced from SOM parameters sets adopted for ^{93}Nb : set B [28] and ^{103}Rh : set A [29]. The calculated values of the neutron strength functions and scattering radius are reported in Table II together with the experimental values [30]. Due to the peaking of the p-wave strength function (S_1) and the low values of the s-wave one (S_0) the p-waves neutron transmission coefficients are quite large whereas the s-wave one is unusually small. As the ground state of ^{103}Rh has $J^\pi = 1/2^-$, the negative parity levels are more strongly excited than the positive-parity ones. Calculated results of the neutron elastic cross sections are presented in Fig. 6 together with the experimental values of Ref. [26]. The calculated cross sections for the production of the 40 keV isomer state ($7/2^+$) were deduced from the sum of inelastic cross sections of individual positive-parity-levels. These are reported in Fig. 7 together with the experimental data of Ref. [31].

The results presented in Figs. 6 and 7 clearly indicate the uncertainties obtained in optical statistical model calculations of neutron elastic and inelastic cross sections.

Choice of proton transmission coefficients

The transmission coefficients for sub-Coulomb protons can be calculated using the selected OMP parameters sets deduced by Johnson et al. [32] for example. As the phenomenological model neglects the imaginary coulomb correction term (ΔW_c), such parameters sets cannot be simply related to those derived at higher energies or to the neutron ones [29]. Recently Rapaport [33] carried out an empirical determination of ΔW_c for proton energies greater than 15 MeV. Using the microscopic calculations of the OMP such as those presented by Jeukenne, Lejeune and Mahaux (J.L.M. Model) [34] ΔW_c can be calculated. In this context the new analytical expression of the J.L.M. model obtained by Lejeune for nucleon energies less than 10 MeV are of a fundamental interest [35].

Calculations of the width fluctuation correction factor (W.F.C.)

The W.F.C. has the following expression :

$$W_{c,c'} = (1 + 2\,\delta_{c,c'}/\nu_{c'})\int_0^\infty f_{c,c'}(t)\cdot g_n(t)\ dt \qquad (5)$$

with

$$f_{c,c'}(t) = \left[\left(1 + \frac{2t\ T_c}{T\nu_c}\right)\left(1 + \frac{2t\ T_{c'}}{T\nu_{c'}}\right)\right]^{-1} \qquad (6)$$

and

$$T = \sum_{e=1}^{n} T_e + T_\gamma \qquad (7)$$

$$g_n(t) = \exp\left(-\frac{T_\gamma\ t}{T}\right)\prod_{e=1}^{n}\left[1 + \frac{2t\ T_e}{T\nu_e}\right]^{-\frac{\nu_e}{2}} \qquad (8)$$

In these expressions ν_c and $\nu_{c'}$ respectively refer to the entrance and exit channels, with n being the number of open neutron channels, T_γ is the total radiative transmission coefficient and ν the number of degrees of freedom for the distributions of neutron transmission coefficients.

The main common problems are the evaluation of the integral and the choice of the various ν. The values of ν have been determined in Ref. [36] from Monte Carlo calculations but no analytical expression, suitable for practical applications, was there derived. Tepel et al. [37] proposed an algebraic evaluation

of $W_{c,c'}$ valid only when n is sufficiently large (n > 10), where-
as using the same formalism Hofmann et al. [38] derived an empi-
rical formula for the practical calculations of ν. For these
reasons, as suggested by Gruppelaar and Reffo [39], the practical
calculations were usually performed by using the classical inte-
gration method at low energies ($\nu = 1$ for all the nucleon chan-
nels) and the approximation of Tepel et al. at higher energies.

As mentioned in Ref. [40] the numerical procedure of the eva-
luation of the integral (eq. 5) is very fast if the function
$g_n(t)$ is calculated only once. Recently Moldauer [41] proposed
the following result for the calculation of ν

$$\nu = 1.78 + (T_e^{1.212} - 0.78) e^{-0.228T} \qquad (9)$$

This formula is of great interest in view of calculating cross
sections using over the full energy range the same coherent for-
malism. We have already made some calculations for ^{92}Mo using this
formula and the one proposed by Hofmann et al. In that case the
calculated capture cross sections differ by less than 2% and the
inelastic scattering cross sections differ near the threshold by
about 5%. Finally we mention that useful calculational tests on
the width fluctuation correction involving continuum level
excitations were presented by G. Reffo and F. Fabbri in Ref. [42].

CONCLUSION

Considering the progress accomplished on the recent past
concerning microscopic theoretical calculations and parametrisa-
tion procedures of the OMP we think that this model may be used
successfully for evaluation purposes. As for the statistical model,
although recent progress has been made concerning width fluctua-
tion correction calculations it still remains many difficulties in
the practical applications. These lie in the determination of
the radiative widths and level density parameters. In this context
the theoretical calculations such as those undertaken by Benzi
and co-workers [43] : "B C S level density calculations and
consistent estimate of radiative widths by means of a thermodyna-
mic model" are of a fundamental interest.

REFERENCES

1. "Nuclear Theory in Neutron Nuclear Data Evaluation",
    Vol. I - II - IAEA-190 , Vienna (1976).

2. "Nuclear Theory for Applications" - IAEA-SMR-43 (1980).

3. C. MAHAUX, in Ref.[2], p. 97.

4. P.A. MOLDAUER, in Ref. [2], p. 165.

5. A. PRINCE, in Ref. [2], p. 149 and p. 231.

6. G. REFFO, in Ref. [2], in Ref. [2], p. 205.

7. G. HAOUAT et al., NEANDC(E) 180"L" - INDC(FR)13/L

8. J.M. DUFOUR and J. SALVY, CEA-N-2080 (1979) and private communication.

9. Ch. LAGRANGE et al., Phys. Lett. 58B, 293 (1975).

10. A. SMITH et al., Nucl. Phys. A332, 297 (1979).

11. A. SMITH and P. GUENTHER, ANL/NDM 47 (1979).

12. A. SMITH, Argonne National Laboratory, Private communication (1980).

13. V.A. MADSEN et al., Phys. Rev. Lett. 34, 1388 (1975).

14. J. RAPAPORT and R.W. FINLAY, IEEE Transactions on Nuclear Science, Vol. NS-26 n° 1 (February 1979).

15. J. RAPAPORT et al., Nucl. Phys. A296, 95 (1978).

16. R.S. MACKINTOSH, Nucl. Phys. A266, 379 (1976).

17. Ch. LAGRANGE and J.P. DELAROCHE, Proc. of an Int. Conf. on Neutron Physics and Nuclear Data (Harwell U.K. 1978) p. 355.

18. A. AASE et al., Proc. of an Int. Conf. on Nuclear Physics (Berkeley U.S.A. 1980) p. 305.

19. Ch. LAGRANGE et al., Proc. of an Int. Conf. on Nuclear Physics (Berkeley U.S.A. 1980) p. 352.

20. Ch. LAGRANGE and O. BERSILLON, in Progress Report on Actinide Nuclear Data Evaluation Works - B.R.C. (Period from 1st April 1979 to March 31st 1980) to be published.

   D. MADLAND, Los Alamos National Laboratory, Private communication (1979).

21. J.S. BLAIR, Phys. Rev. 115, 928 (1959).

22. A. De SHALIT, Phys. Rev. 122, 1530 (1961).

23. P.E. HODGSON, Nuclear Reactions and Nuclear Structure, Clarendon Press, Oxford (1971).

24. P. GUENTHER et al., JAERI-M-5984 (1975) 269.

25. Ch. LAGRANGE, JAERI-M-5984 (1975) p. 58.
    J.P. DELAROCHE et al., same as Ref. [1], Vol. I, p. 251.
    Ch. LAGRANGE, RT/FIS-LDN(80) 1, NEANDC(E) 209 "L" (1979),
    p. 233.

26. E. BARNARD and D. REITMANN, Nucl. Phys. A303, 27 (1978)

27. G. VLADULA et al., Z. Physik A - Atoms and Nuclei 295,
    (1980) 235.

28. Ch. LAGRANGE, Bull. Am. Phys. Soc. 24, 870 (1979).

29. Ch. LAGRANGE, Phys. Rev. C 22, 896 (1980).

30. P. RIBON, CEA-N-1149 (1969).

31. D.C. SANTRY and J.P. BUTLER, Can. J. Phys. 52, 1421 (1974).

32. C.H. JOHNSON et al. Phys. Rev. C 20, 2052 (1979).

33. J. RAPAPORT, Phys. Lett. 92B, 233 (1980).

34. J.P. JEUKENNE, A. LEJEUNE and C. MAHAUX, Phys. Rev. C16, 80
    (1977).

35. A. LEJEUNE, Phys. Rev. C21, 1107 (1980).

36. P.A. MOLDAUER, Phys. Rev. C11, 426 (1975) and C12, 744
    (1975).

37. J.W. TEPEL, H.M. HOFMANN and H.A. WEIDENMÜLLER, Phys. Lett.
    49B, 1 (1974).

38. H.M. HOFMANN et'al. Ann. Phys. 90, 403 (1975).

39. H. GRUPPELAAR and G. REFFO, Nucl. Sc. Eng. 62, 756 (1977).

40. Ch. LAGRANGE, in Proc. of a Specialist's Meeting held at
    the Central Bureau of Nuclear Measurements, Geel, Belgium,
    (1977), Ed. by C.H. Böckhoff, Pergamon Press (1979).

41. P.A. MOLDAUER, Nucl. Phys. A344, 185 (1980).

42. G. REFFO and F. FABBRI, Nucl. Sc. Eng. 66, 251 (1978).

43. V. BENZI et al., RT/FIS-LDN (80) 1 - NEANDC(E) 209"L"
    (1979) p. 215.

TABLE I

Quadrupole deformation parameters for N = 50 and Z = 50
single-closed shell nuclei

β	Nuclei N = 50			Nuclei Z = 50				
	^{88}Sr	^{90}Sr	^{92}Mo	^{116}Sn	^{118}Sn	^{120}Sn	^{122}Sn	^{124}Sn
$\beta_{nn'}$	0.133(7)	0.085(8)	0.099(5)	0.120(10)	0.109(7)	0.106(5)	0.100(6)	0.092(6)
$\beta_{pp'}$	0.110	0.070(5)	0.080(6)	0.133	0.134(10)	0.119(10)	0.112(7)	0.108(7)
β_{em}	0.14 (2)	0.094(5)	0.116(8)	0.118(7)	0.108(2)	0.106(2)	0.102(2)	0.096(2)

TABLE II

Neutron strength functions and scattering radius
for ^{103}Rh

	$S_0 \ 10^{+4}$	$S_1 \ 10^{+4}$	R' fm
RIBON P.	$0.54 \ {}^{+\ 0.07}_{-\ 0.06}$	$6.0 \ {}^{+1}_{-1.5}$	6.56 ± 0.06
OMP B	0.424	10.28	6.27
OMP A	0.64	5.75	6.600
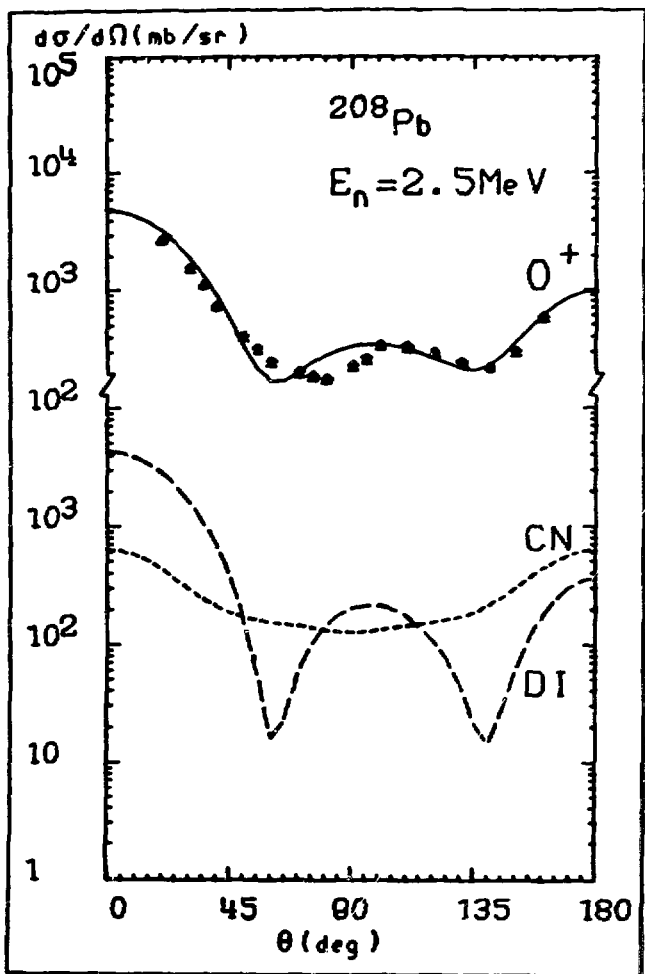
Fig. 1 Elastic differential cross sections for the scattering of 2.5 neutrons from ^{208}Pb.
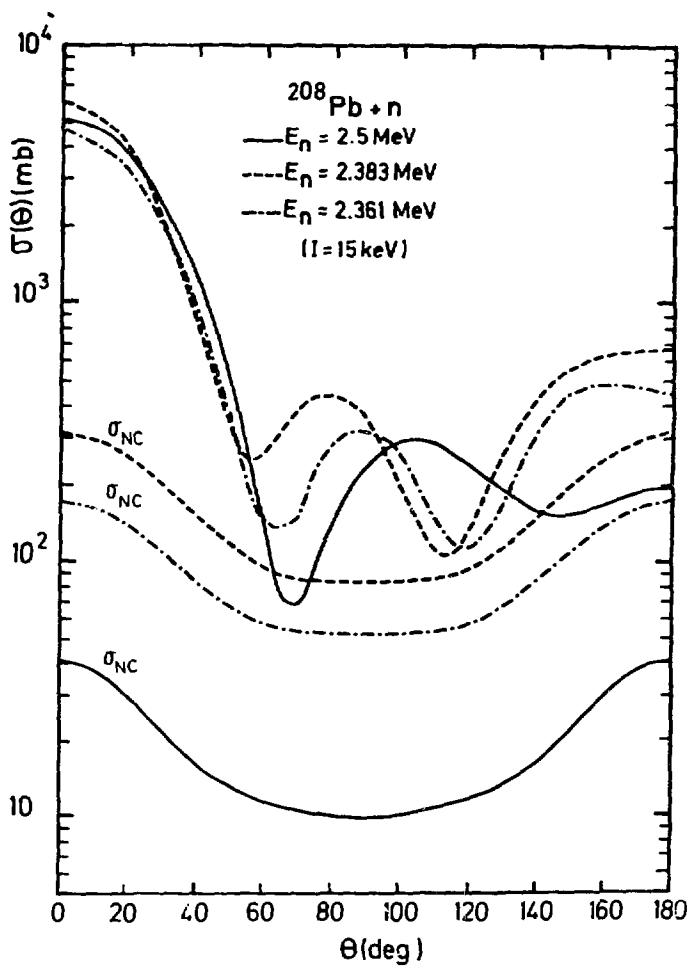
Fig. 2   Microscopic calculation of neutrons elastic differential cross sections for ^{208}Pb.
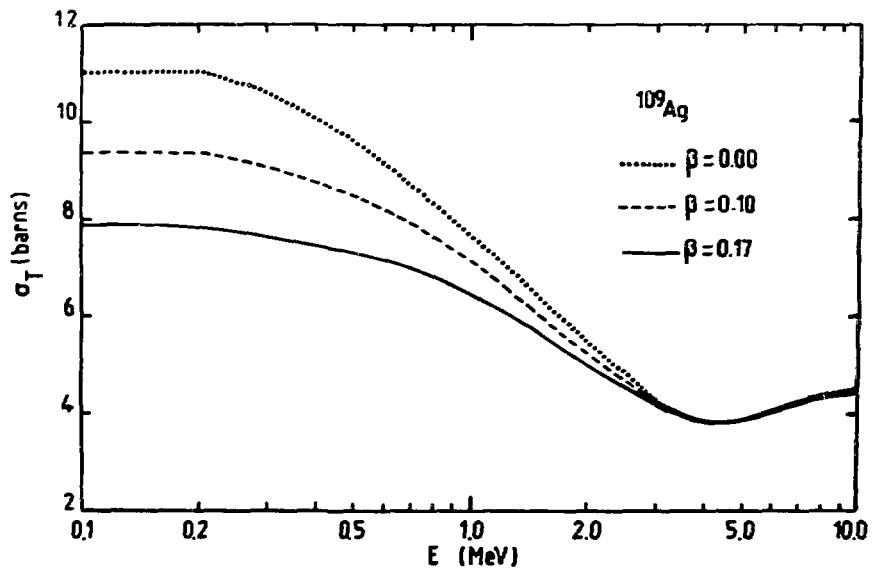
Fig. 3   Calculated neutron total cross sections for ^{109}Ag.
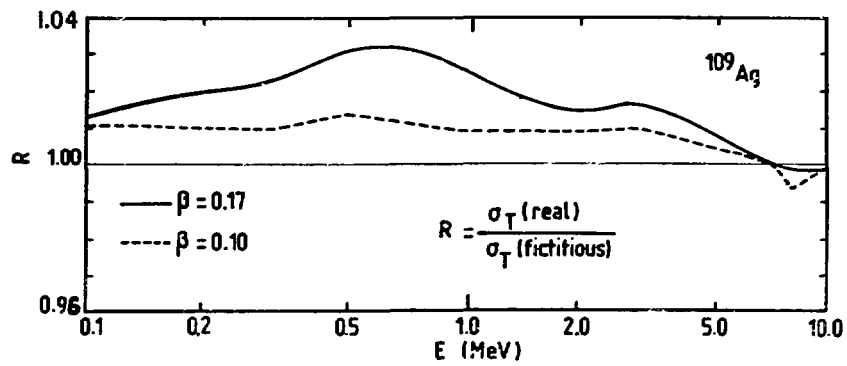
Fig. 4 Ratio of the calculated values of the neutron total cross sections for ^{109}Ag.
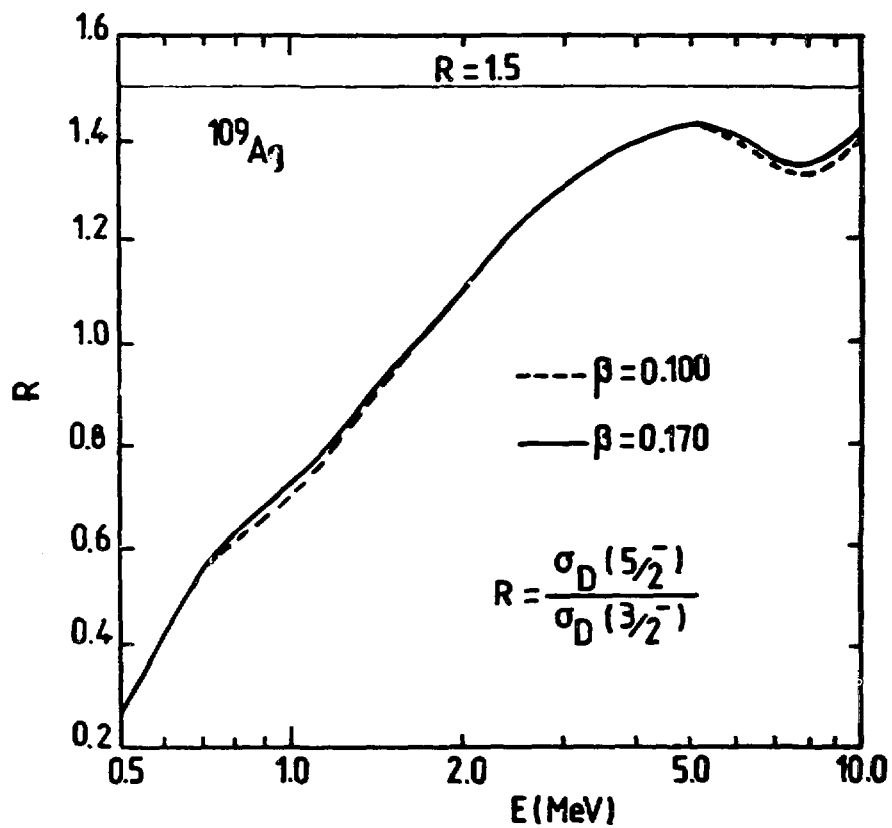
Fig. 5   Simplified comparisons of calculated direct inelastic cross
          sections for ^{109}Ag.
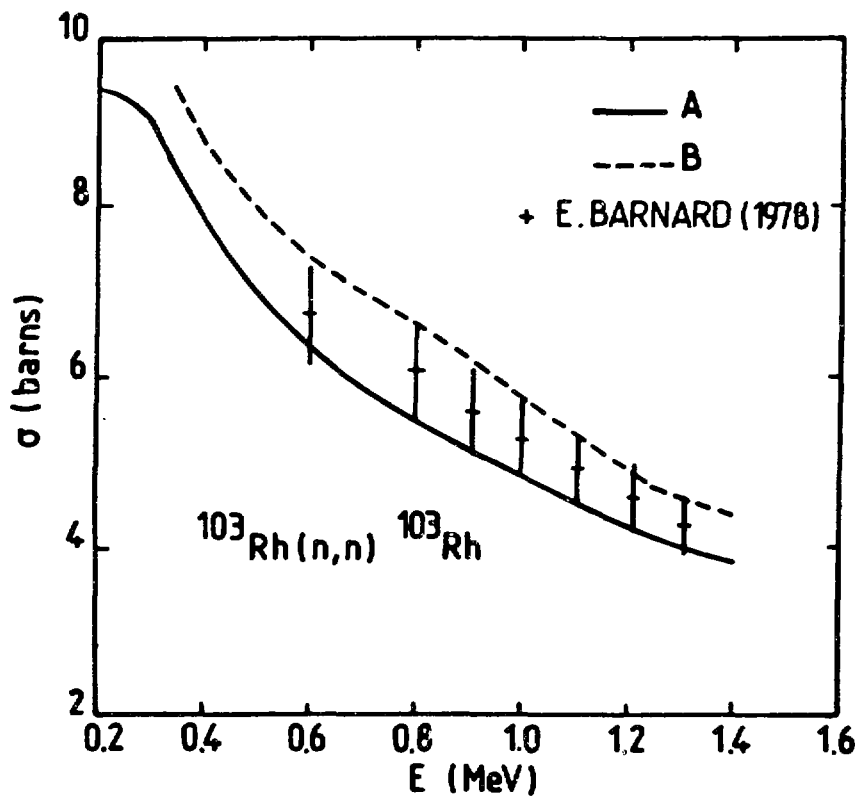
Fig. 6   Neutron elastic scattering cross sections for [103]Rh.
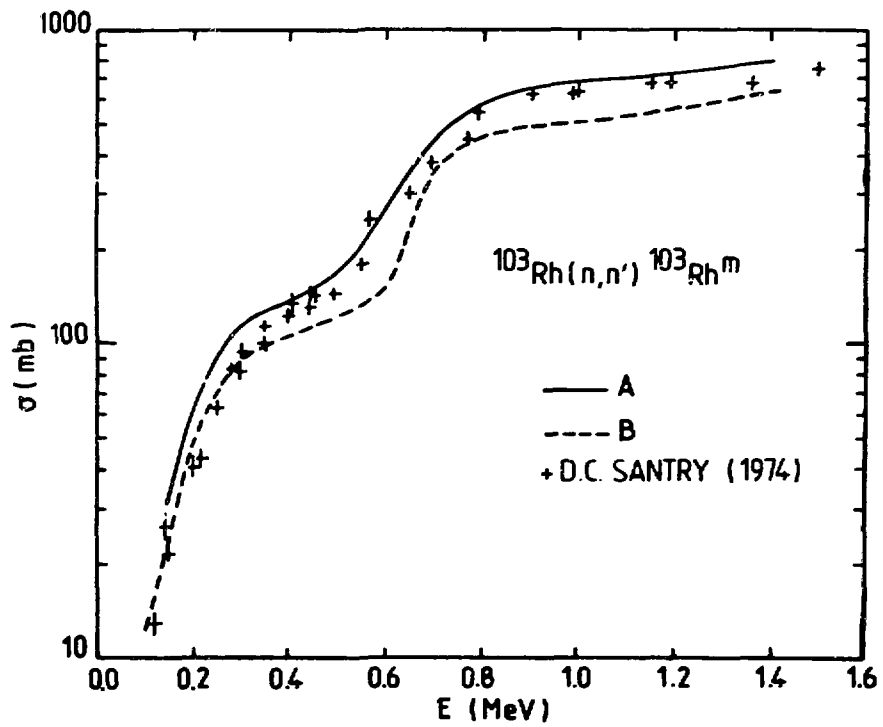
Fig. 7   Cross sections for the production of the 40 keV isomeric
          state in ^{103}Rh by inelastic scattering of neutrons.

Discussion

Moldauer (Comment)

I will make a brief remark on the effect of direct reactions in compound-nucleus cross sections. We conventionally have the average cross section for many-many competing channels expressed as the Hauser-Feshbach cross section times a correction factor. Usually, the partial widths of the various channels are uncorrelated and you only have an enhancement of the elastic channel--the so called elastic-enchancement factor. However, in the case of directly coupled channels the partial widths can be correlated leading to an enhancement of the compound-inelastic cross sectins for the coupled channels. In some circumstances and particular choices in parameter space the inelastic enhancement can be as large as that for the elastic channel e.g., by a factor of two or so. Usually, the effect is much smaller but one should be aware of the potential for a relatively large inelastic enhancement factor. I have recently set forth the details of the mechanism in a paper which I refer you to.

Gruppelaar

I would like to add a comment. We have employed such an expression in the treatment of valence capture in molybdenum. We did a calculation for this case where there was a large valence component but still the effect upon the capture cross section was only a small percentage; it was not a very important contribution. Maybe it could be more important for some other isotopes.

Lagrange

Yes, I have read your paper. I agree that the choice of the effective number of degrees of freedom for the neutron channels does not greatly effect the capture cross section. However, I would like to emphaiize the importance of a comprehensive model which is applicable over a wide energy-range of interest.

Poenitz

I would like to point out that new total cross sections in the light fission-product mass region have recently been measured at Argonne. These data will be released for use soon. I was surprised that you could fit the Rhodium total cross section data which you had available. Did you fit total, elastic and inelastic data at the same time or the total alone?

Lagrange

The analysis of ^{103}Rh was based upon the total cross section (2.5-
15.0 MeV) and the reported strength functions. Problems were
encountered in attempting to fit the low energy total cross
sections as given in BNL-325. I do not know if these problems
were associated with the model or the experimental data--perhaps
channel coupling is a factor. New and precise experimental values
could help resolve the problem.

Smith (Comment)

I would like to note that silver results are a part of the recent
Argonne measurements cited by Dr. Poenitz. They should make
possible a clear test of the very nice predictions of coupling
schemes that the Speaker has given in the context of ^{109}Ag.

EVALUATION METHODS AND PROCEDURES WITH EMPHASIS ON HANDLING EXPERIMENTAL DATA

H. Vonach and S. Tagesen

Institut für Radiumforschung und Kernphysik der Österr. Akademie der Wissenschaften, Wien, Austria

ABSTRACT

A review is given on the procedures and methods used in the evaluation of the cross-sections for neutron induced reactions in the mass-range $19 \leq A \leq 209$ and the energy region of overlapping resonances up to 20 MeV. Thus the central topic are the evaluation methods for (n,p), (n,α), (n,2n) and

$A(n,n')^m A$ cross-sections, mostly derived from activation measurements. In the first part we will address the evaluator's task to do thorough critical review of the experimental data base especially the problems connected with renormalization of cross-section values, re-assesment of cross-section errors, estimating the degree of correlation present in the cross-section uncertainties, rejection of obviously wrong data, normalization of relative cross-section measurements and handling of inconsistencies between different data sets. In the second part the various methods used for deriving evaluated cross-sections and their variances and covariances from the experimental data base will be reviewed and discussed. Finally recommendations will be made how to proceed in future evaluations.

1. INTRODUCTION

Cross-section evaluations for neutron induced reactions e.g. (n,2n), (n,p) or (n,α) reactions are

mainly needed for fast neutron dosimetry that is for
measurement of neutron flux distributions by means of
the multi-foil activation technique and for estimates
of radiation damage and activation of materials in
fission reactors and in future also fusion or fusion-
fission devices. Especially for neutron dosimetry
rather accurate ($\sim$ 5%) evaluated cross-section values
with reliable uncertainty information are needed, a
goal which has not been achieved completely at present.
    In order to improve this situation I will in the
following try to review and discuss the methods used
so far for such evaluations and try to give some re-
commendations for the procedures to be used in future
evaluations. As light and fissionable nuclei and also
the resonance region are delt with in other reviews,
I will restrict myself to reactions on nuclei in the
mass-range 19 < A < 209 and neutron energies in the
continuum region (starting typically at some 100 keV
to a few MeV) to 20 MeV. Restriction to this energy
however, does not necessarily mean that we can assume
the cross-sections to be smooth functions of energy.
For nuclei up to about A > 60 irregular structure in
the excitation functions is observed especially in the
few MeV neutron energy range due to level density
fluctuation and for nuclei below A = 40 in addition
Ericson fluctuation may show up at higher neutron
energies (up to about 15 MeV) and this has to be kept
in mind in the discussion of the evaluation procedures.
    Furtheron I will restrict myself to the question
of deriving evaluated cross-sections from existing ex-
perimental data, as the supplementary use of theoreti-
cal calculations will be discussed in the following
lecture.
    The subject being defined in this way the review
will address two main areas:
    1) The problem of establishing and critical review
       of the experimental data base.
    2) The procedures used to derive evaluated cross-
       sections and estimates of their variances and
       covariances from an accepted data base.

    2. ESTABLISHMENT AND CRITICAL REVIEW OF THE
       EXPERIMENTAL DATA BASE

2.1. Introductory remarks

    The problems connected with the critical review
of the experimental data used for an evaluation have
so far received much less attention than the formal

procedures subsequently used to derive the evaluated
cross-sections from the accepted data base. This is
a serious deficiency as it is this first stage which
really needs the professional expertise of an ex-
perienced evaluator and as the decisions made in the
critical review of the data base determine to a large
extent the output of an evaluation whatever procedures
are subsequently used in actually deriving the evalua-
ted cross-section values.
    Thus in the following I will address in some de-
tail the problems of
    - renormalization of cross-sections
    - reassesment of cross-section errors
    - deriving of estimates of the correlations bet-
      ween the cross-section errors
    - rejection of data and handling of inconsistent
      data
    - quantitative consistency checks

2.2. Check of experimental data for renormalization

    All experimental data should be checked whether
the cross-sections depend on nuclear data which have
subsequently been revised and should be renormalized
in all such cases. In detail the following renormali-
zations should be applied to the data in case of
activation cross-sections which constitute the main
part of the data base for the reactions considered in
this review.
a) Cross-sections measured relative to some standard
   cross-sections other than the n-p scattering cross-
   section should be renormalized to the most recent
   ENDF/B values of the cross-section for the used
   standard reactions except for few specific cases
   where the INDC standards subcommitties may make
   other recommendations. If there is no ENDF/B evalua-
   tion existing for the standard in question, other
   recent evaluations such as evaluations for the IRDF
   should be used. If however, a cross-section is
   measured relative to another cross-section, which
   itself had been measured absolutely by the same
   author such measurements may also be considered to
   be absolute as in that case the standard cross-
   section served only as an intermediate step in the
   measurement and renormalization must not be done in
   those cases.
b) Cross-section measurements based on the angular
   distributions of the neutron production reactions
   (D(d,n); T(d,n); T(p,n)) should be renormalized
   according to the evaluations of Liskien and Paulsen
   /1/ resp. to that of Drosg /2/ for charged particle

energies above 3 MeV for the D(d,n) and above 5 MeV for the T(p,n) and T(d,n) reactions. For the angular distribution in the ^{7}Li(p,n) reaction the evaluation by Liskien and Paulsen /3/ should be used.

c) The decay data (half-lives, branching ratios, positron fraction etc.) used for calculation of the absolute activities should be checked for subsequent revisions.

d) Relative cross-section measurements (excitation functions without absolute normalization or excitation functions normalized to some other cross-section measurement of the reaction to be evaluated itself at one energy) should be renormalized in the following way: As a first step the whole evaluation procedure is executed without such relative measurements and a preliminary evaluated excitation function is determined. Then all relative excitation functions are normalized to this preliminary excitation function, the normalization factor being determined by a least square fit which is also used to check the compatibility of each relative excitation function with the rest of the data.

In some cases a reported excitation function (absolute cross-sections) actually consists of a relative cross-section measurement normalized by just one absolute cross-section measurement at one energy. In such cases the reported result should be decomposed into its two parts and both the absolute and the relative measurement treated independently according to the rules described before.

As an example for the effect of the described procedures column 4 of table 2 gives the cross-section renormalizations applied by the authors to the various data sets in their evaluation of the ^{90}Zr(n,2n) cross-section /4/.

2.3. Establishment of a set of experimental errors of equal confidence level for all experimental data

If the different experimental data sets are to be given proper weight in the further evaluation process it is necessary to estimate effective uncertainties (that is uncertainties including contributions from random errors and all identified sources of systematic error) on the same e.g. 1σ confidence level for all measured cross-section values. Using the errors quoted by the authors will in general not be sufficient as the quoted errors may refer to different confidence levels (e.g. 1σ or 2σ) and more important, as systematic errors have been neglected or underestimated in

many papers. Therefore it is one of the most important
tasks of evaluators to check the error statements
given by the measurers and change them if necessary in
order to establish a set of experimental errors of
equal 1σ confidence level for all experiments.

For this purpose we suggest the following proce-
dure:
1) It is checked whether a confidence level different
   from 1σ was assumed by the authors. If so, the error
   estimates are changed accordingly. If no information
   can be obtained it appears safe to assume a 1σ con-
   fidence level.
2) It is checked whether all relevant sources of
   systematic errors have been accounted for. If not,
   estimated values for the missing error contri-
   butions are added quadratically to the authors'
   error estimates. As an example how to do this in
   practice table 1 shows a check list indicating the
   error contributions to be expected in measurement
   of activation cross-sections. If cross-section
   measured relative to some standard cross-section
   were renormalized to the present value of that
   standard also the error contribution due to the
   standard should be changed accordingly.
3) In addition to the cross-section errors there is al-
   ways an error δE_n in the average neutron energy
   corresponding to a specific data point which may be
   important for steeply increasing or decreasing ex-
   citation functions. It should be taken into account
   by adding a contribution $\frac{d\sigma}{dE_n} \cdot \delta E_n$ quadratically
   to the error estimated according to 1-3.
4) For relative measurements normalized as described
   in section 2.2. the error of the normalization
   factor has of course to be added to the error of
   the relative measurements.

Reassesment of experimental errors according to the
described procedures is discussed for many specific
cases in the evaluation work of the authors /4,5/. As
an example column 5 and 6 of table 2 show the error
reassesment applied by the authors in their ^{90}Zr(n,2n)
evaluation /4/.

2.4. Correlations between the cross-section uncertain-
     ties

In addition to the knowledge of the effective 1σ
uncertainties of all input data it is necessary to have
at least a rough estimate of the degree of correlation

present between these uncertainties.

The experimental cross-section errors are largely due to the systematic uncertainties in the fluence and absolute activity measurements and therefrom the following correlations result:

a) The error due to the uncertainty of the efficiency of the detector used for the measurement of the induced activity influences each cross-section within one excitation function measurement in the same way and thus produces a "long range" correlation within each excitation function.

b) The uncertainties in the neutron fluence measurements for different neutron energies also have strong positive correlations in most cases. This produces both additional correlation within each excitation function and correlation between the cross-section uncertainties for different reactions if several reactions were measured by one group using the same neutron fluence measuring device.

Thus the complete uncertainty information about an experiment requires the full covariance matrix $<\sigma_{nk}(E_i).\sigma_{n'k}(E_{i'})>$ between all pairs of cross-sections measured in the particular experiment k (n,n' are used to indicate different reactions studied in one experiment). In some most recent experiments this information is given explicitly. As an example table 3 shows the relative covariance matrix $\dfrac{<\sigma(E_i).\sigma(E_{i'})>}{<\sigma(E_i)><\sigma(E_{i'})>}$ for the recent measurements of the $^{63}Cu(n,\alpha)^{60}Co$ excitation function of G. Winkler et al. /6/ at ANL. As the table shows the average size of the non-diagonal elements is ~ 0.5, indicating that correlations between cross-section measurements of one reaction at different neutron energies are in general quite large and have to be considered in the evaluation process, because they produce corresponding correlations between the uncertainties of the evaluated cross-section values.

In general these correlation matrices are not given by the experimenters and the evaluator has to estimate them from the uncertainty information given in the papers. Lack of detailed information and restricted manpower will however in most cases not allow to derive detailed correlation matrices for each data set.

The problem becomes managable if we approximate the relative correlation matrices by use of a constant value for its non-diagonal elements (for the matrix of table 3 this would mean approximating all off-diagonal

elements by their average value of $\sim$ 50%). As this specific but typical example shows this approximation will not be too bad in most cases and allow to handle the bulk of the correlations in a rather simple way.

Using the above approximation the evaluator has to estimate this average correlation coefficient

$$B_{nnkk} = \frac{<\Delta\sigma_{nk}(E_i) \cdot \Delta\sigma_{nk}(E_{i'})>}{<\Delta\sigma_{nk}(E_i)><\Delta\sigma_{nk}(E_{i'})>}\Bigg|_{E_i, E_{i'}} \qquad (1)$$

$(\sigma_{nk}(E_i)$ = cross-section value observed for reaction of type n at energy E_i in data set k) for each data set k.

This has to be done by detailed investigation of the uncertainties in the respective data (s. table 1) and dividing them into parts correlated and uncorrelated for measurements at different neutron energies. Having done this one gets

$$B_{nnkk} = \frac{\Delta_{nk}{}^2\sigma_{corr}}{\Delta_{nk}{}^2\sigma_{total}} \qquad (2)$$

For relative measurements normalized to the absolute cross-section as discussed in section 2. B_{nnkk} is obviously given by

$$(B_{nnkk})_{rel.meas} = \frac{\Delta^2\sigma_{norm}}{\Delta^2\sigma_{rel.meas} + \Delta^2\sigma_{norm}} \qquad (3)$$

$\Delta\sigma_{norm}$ = rel. uncertainty of the normalization factor
$\Delta\sigma_{rel}$ = rel. uncertainties of the relative measurements.

Values of the average correlation coefficients B_{nnkk} derived in this way for the excitation functions of 8 threshold reactions /4,5/ are given in table 4. As the table shows there are typically correlations of the order of 50% in measurements of excitation functions of neutron induced reactions determined by the activation method.

In addition to the discussed correlations within each data set there are in principle additional correlations between the cross-section measurements of different experiments mostly due to the use of common standards, e.g. $^{235}U(n,f)$, $^{238}U(n,f)$, $^{27}Al(n,\alpha)$ etc.

However, in our evaluation work it turned out that the effect of such correlations could be neglected compared to the discussed correlations within the data sets. This is due to the fact that in most cases only a small fraction of the data has been measured relative to anyone particular standard as shown in table 4. Thus it should be checked whether a substantial fraction of the data base for some reactions to be evaluated was measured relative to one specific standard cross-section. If so, the correlations due to the uncertainty of that standard cross-section should be considered, otherwise such correlations may be neglected.

Finally we have to deal with the correlations existing between the cross-sections for different reactions n and n'. Again such correlations will exist both within the results of one experiment in which several cross-section measurements were performed in the same neutron flux and between the results of different experiments due to the use of common standards.

In order to deal quantitatively with these correlations one again has to approximate the corresponding relative correlation matrices by matrices with constant elements $B_{nn'kk}$ resp. $B_{nn'kk'}$ with

$$B_{nn'kk} = \frac{<\Delta\sigma_{nk}(E_i)\cdot\Delta\sigma_{n'k}(E_{i'})>}{<\Delta\sigma_{nk}(E_i)><\Delta\sigma_{n'k}(E_{i'})>}\Bigg|_{E_i,E_{i'}} \tag{4}$$

and

$$B_{nn'kk'} = \frac{<\Delta\sigma_{nk}(E_i)\cdot\Delta\sigma_{n'k'}(E_{i'})>}{<\Delta\sigma_{nk}(E_i)><\Delta\sigma_{n'k'}(E_{i'})>}\Bigg|_{E_i,E_{i'}} \tag{5}$$

As before $B_{nn'k}$ and $B_{nnkk'}$ can be estimated from an analysis of the uncertainties of the corresponding experiments k resp. k and k'. $B_{nn'kk}$ values for a number of experiments were estimated by the authors in their evaluation work /4,5/ and typically values around 0.5 were found. $B_{nn'kk'}$ values probably are considerably smaller in most cases.

These correlations will however in most cases produce only rather small correlations between the corres-

ponding evaluated cross-sections. This is due to the
fact that in general only a small part of the data for
a specific reaction n will arise from experiments
simultaneously measuring also the cross-sections for
reaction n and because as mentioned before the effect
of correlations from use of common standards is also
rather small.

Thus in many cases it will be justified to neg-
lect these cross-section correlation between different
reactions. If however one decides to consider in de-
tail, both the correlations due to common experiments
and due to common standards in different experiments
have to be considered as either of them may dominate
in different cases.

2.5. Rejection of data

Obviously wrong data should be rejected.
If a sufficiently large data base exists such
wrong data may easily be identified by their large de-
viation from the main body of the data. Quantitatively
different criteria may be used, in our evaluation work
/4,5/ we use the condition that the accepted data
should deviate by not more than 3σ from the weighted
average of all other data. Fig. 1 shows an example for
data rejection according to that condition.

If only a few data sets e.g. two mutually incon-
sistent data sets exist data rejection becomes much
more difficult (s. fig. 2). In some cases a decision
may become possible on the bas s of model calculations,
systematics or by identifying overlooked error contri-
butions in the measurements; otherwise it will be ne-
cessary to retain all measurements and increase all
errors by a common factor until the data become mutual-
ly consistent.

Finally after the question arises how to treat
partially wrong measurements. In our work /4,5/ we
have rejected the whole excitation function if one of
the measurements was found to be obviously wrong
according to the criteria described above, but this
question is open for discussion.

2.6. Checks on the consistency of the accepted data
     base

By means of applying the procedures described in
the previous subsections we get the final accepted
data base.

This accepted data base may still contain incon-
sistencies and thus the degree of internal consistency

achieved can and should be checked in the following way:

The excitation function to be evaluated is divided into energy bins of suitable size and the weighted average of all cross-section measurements within each bin as well as the internal ($\Delta\sigma_{int}$) and external error ($\Delta\sigma_{ext}$) of this average is calculated according to standard statistical procedures (s. fig. 3). From the ratio $R = \sigma_{ext}/\sigma_{int}$ we can judge the degree of consistency achieved. If the ratio fluctuats around one the data base is consistent.

In energy regions where R is considerably larger than one, data are inconsistent and either the inconsistency should be traced to some specific data sets by repeating step 3. (error reassesment) or all errors should be increased by a factor of R. If R is not too large, e.g. < 2, this approach will in generally be acceptable.

In doing this consistency check, 2 technical points have to be taken care of:

a) The division of the excitation curve into energy groups for the calculation of weighted averages is always a compromise between the demand for having enough data points within each interval and the demand that the cross-section should be approximately constant within each interval and thus the group size has to vary both for different reactions and also within one excitation curve according to the amount of data available, the neutron energy resolution of the existing cross-section data and the slopes of the excitation curves. It is unavoidable that cross-section changes of 10 - 20% (and occasionally even more) are admitted within the group and therefore all cross-sections have to be renormalized to the energy at the group center (s. fig. 3b).

b) In some cases of excitation functions measured at small energy increments two or more data points may be situated within one of the chosen energy groups (s. fig. 3b). The errors of such cross-section measurements for adjacent energy values must be considered to be almost completely correlated and it would be incorrect to treat them as independent measurements.

Therefore prior to the averaging process described above within each group all cross-section data of each author are combined to one cross-section value by calculating the average cross-section and the (linear) mean error.

As a typical result of such inconsistency checks
table 6 shows the results obtained for the ^{90}Zr(n,2n)
reaction with the energy bin structure shown in fig. 3a.
In this specific example the observed ratios R do in-
dicate that the accepted data base is internally con-
sistent and the critical review of the experimental
data base has been successfully completed.

3. PROCEDURES FOR GENERATING EVALUATED CROSS-
   SECTIONS AND ESTIMATES OF THEIR UNCERTAIN-
   TIES FROM AN ACCEPTED DATA BASE

3.1. Procedures for generating evaluated cross-sections

Evaluated cross-section values have been derived
from an accepted data base (e.g. fig. 3a) in
a number of different ways. The procedures most
frequently used are
a) doing an "eye-guide" smooth line fit
b) fitting a suitable smooth curve (e.g. polynomial)
   to the data by a least square fitting procedure
   /7,8/
c) fitting a theoretical cross-section curve (e.g.
   from statistical model calculations) to the measure-
   ments by appropriate parameter adjustment
d) use of the average group cross-sections derived
   according to section 2.6. as evaluated cross-section
   values at the corresponding energies (s. fig. 3b)
   and completion of the evaluation by suitable inter-
   polation procedures /4,5/.
Method c) fitting of a theoretical excitation function
is always necessary if experimental data are lacking
or of poor quality for a considerable part of the ex-
citation function because in that case the theoretical
curve is needed for extrapolation resp. interpolation
of the experimentally known part of the excitation
function over the whole energy region to be covered
by the evaluation. For example in case of ^{90}Zr(n,2n)
the energy region from threshold to 13.3 MeV has to be
evaluated by means of model calculations with para-
meters fitted to the experimentally known part of the
excitation function /4/. As this subject is covered
in the talk of Dr. Arthur I will not further discuss
it here.
For these energy regions where reliable and accu-
rate cross-section measurements exist (e.g. for ^{90}Zr)
in the energy region 13.3 - 17 MeV covered in fig. 3a)
model calculations can add little further information

and the evaluation should be based entirely on the experimental data b⌐se using methods a, b or d. If method a (drawing of smooth line) is used, it will be preferable to use the preaveraged data base that is the values $\bar{\sigma}(E_i)$ and their uncertainties $\Delta\bar{\sigma}(E_i)$ derived according to figure 3 as starting point. If this is done the result of all three approaches will be very similar and method a may very well be used for simplicity.

3.2. Estimates of the variances of the evaluated cross-section values

For characterizing the uncertainties of the evaluated cross-section values up to now mostly rather crude approximations have been used mainly of two types

a) Use of so called "dispersion indicators" /9/ that is specification of a "band" around the final evaluation within which the majority of the experimental data points for a given energy range can be found.

b) Derivation of uncertainties of their evaluated values from the scatter of the data points from a smooth polynomial fit as for example extensively used by Lapenas et al. /7/.

These approaches have serious shortcomings. Method a) tends to overestimate the uncertainties as the demand that most of the data points should lie within the uncertainties of the evaluated cross-section curve is obviously wrong. If we combine N data sets of about equal accuracy in an evaluation the uncertainties of the evaluated cross-sections will be smaller than the uncertainties of the input data by a factor of $\sqrt{N}$, in practice typically 2-3 and thus only a small part of the data points can be expected to fall within the limits of the (1σ) uncertainties of the evaluated cross-section curve.

On the other hand Lapenas' method tends to seriously underestimate the uncertainties of the evaluated cross-sections as it is only sensitive to the random error of the input cross-sections.

A rather realistic estimate of the uncertainties of the evaluated values however can be easily obtained from the results of the consistency checks described in section 2.6. Using the larger of the two quantities $\Delta\bar{\sigma}_{int}$ and $\Delta\bar{\sigma}_{ext}$ (s. fig. 3b) will in most cases give a safe and rather accurate measurement for the uncertainty of the evaluated cross-section values for the corresponding energy bins. This procedure for deriving

uncertainties of evaluated cross-section values has
been used by the authors /4,5/ and also been checked
in some cases as shown in fig. 4 and 5. Fig. 4 shows
an evaluation of the ^{63}Cu(n,2n) cross-section using
only data up to 1964 with uncertainties according to
our prescription and the results of the same procedure
using all data up to 1979. As apparent from the figure
the changes in the evaluated cross-sections due to in-
clusion of the recent more accurate data are of the
order of the estimated uncertainties of the 1964
evaluation. Fig. 5 compares the results of our eva-
luation of the ^{90}Zr(n,2n) reaction with new precision
measurements of that cross-sections performed after
completion of the evaluation /10/. Again there is
agreement within the estimated uncertainties of the
evaluation.

It has to be kept in mind, however that the des-
cribed simple procedure for estimating the uncertain-
ties of the evaluated data is based on two assumptions
the validity of which has to be checked in each case.
a) no correlations between the measured cross-sections
   from different experiments
b) smooth behaviour of the cross-section within the
   chosen energy bin structure.

If substantial correlations between different
data sets exist as for example found for the ^{235}U(n,f)
cross-section measurements /11/, these correlations
have to be taken into account explicitely in the cal-
culation of the weighted averages and their uncertain-
ties (s. section 2.6.) as described in ref. 11 and 12.

If we expect cross-section fluctuations (e.g.
from systematics or from theory) in some region of an
excitation function and the quality of the experimen-
tal data (energy resolution and density of measure-
ments) is insufficient to resolve such fluctuations it
should be stated that the uncertainties derived in the
described way only apply to cross-sections averaged
over the bin width and for cross-sections at sharp
energies the estimated "amplitude" of the fluctuations
has to be added to the error estimates for the avera-
ged cross-sections.

This consideration will apply to many reactions
on light nuclei (up to A=40).

3.3. Procedures for estimating the correlations bet-
     ween the uncertainties of the evaluated cross-
     sections

The correlations in the uncertainties of the

measured cross-sections discussed in section 2.5. do
produce substantial correlations between the uncertain-
ties of the evaluated cross-sections especially within
each excitation function. Thus a number of methods
have been developed to get at least a rough estimate
of the non-diagonal elements of the covariance matri-
ces of the evaluated cross-sections. The most frequent-
ly used procedures are

1.) The correlation coefficients of the measured ex-
citation functions are estimated as discussed in
section 2.4..For the measured excitation functions
the assumption is made that the relative correla-
tion coefficients of the evaluated cross-sections
are of equal size. This procedure is apparently
used in many of the uncertainty estimates for
ENDFB/V dosimetry file.

2.) The average correlation coefficients for the
measured cross-sections are estimated from the
deviation of the measurements from the evaluated
cross-section curve and again it is assumed that
the correlations in the evaluated cross-sections
are of equal size. This procedure implemented in
the computer code SUR has been extensively used at
Oak Ridge /13/.

3.) The relative covariance matrix

$$
B_{nnii'} = \frac{<\Delta_n\sigma_{eval}(E_i) \cdot \Delta\sigma_{n\ eval}(E_{i'})>}{<\Delta_n\sigma_{eval}(E_i)><\Delta\sigma_{n\ eval}(E_{i'})>}
\tag{6}
$$

$(\Delta\sigma_{n\ eval}(E_i)$ = uncertainty of evaluated cross-
sections for reaction of type n at energy E_i) of
the evaluated cross-sections is calculated by
standard statistical methods from the estimated
correlation coefficients $B_{nn;ii';kk'}$ (s. section
2.5.) in the input data.

   This method was first proposed by Sukhovitskij
and Konshin /11/ and has been used by these authors
in an evaluation of the $^{235}U(n,f)$ cross-section
taking into account both the correlations within
each data set k and the substantial correlations
existing in that case between different data sets.

   We have used this formalism in our evaluation
work /4,5/ neglecting correlations between diffe-
rent data sets and assuming constant relative cor-
relation coefficients B_{nnkk} within each data set

(s. section 2.5.). With these assumptions the elements $B_{nnii'}$ of the covariance matrix of the evaluated excitation function is given by the relation /4/

$$B_{nnii'} = \frac{<\Delta\sigma_{n\ eval}(E_i) \cdot \Delta\sigma_{n\ eval}(E_{i'})>}{<\Delta\sigma_{n\ eval}(E_i)><\Delta\sigma_{n\ eval}(E_{i'})>} =$$

$$= \frac{\sum_k a_{nik}a_{ni'k}\Delta\sigma_{nk}(E_i) \cdot \Delta\sigma_{nk}(E_{i'})B_{nnkk}}{\Delta\sigma_{n,eval}(E_i) \cdot \Delta\sigma_{n,eval}(E_{i'})} \qquad (7)$$

whereby the sum extends over all data sets k containing measurements both in energy bins E_i and $E_{i'}$. The quantities a_{nik} and $a_{ni'k}$ are the statistical weights which the data set k possesses in the evaluation at the energies E_i resp. $E_{i'}$. These are of course given by

$$a_{nik} = \frac{(\frac{1}{\Delta\sigma_{nik}})^2}{\sum_k (\frac{1}{\Delta\sigma_{nik}})^2} \qquad (8)$$

Methods 1.) and 2.) give a reasonable estimate of the correlation matrix of an evaluated excitation curve, if most of the input data sets cover the full energy range. If however - as usual - the data base consists of a number of data sets covering different parts of the excitation function and in addition measurements for single energy points, the correlation matrix of the evaluated excitation functions will show strong structures and will be very different from the correlation matrices of the input data sets. In such data cases only method 3.) will be applicable. As an example for such cases table 7 shows the correlation matrix for the $^{19}F(n,2n)$ reaction derived in /5/ using equ. (7) and (8).

Very little work has up to now been done on correlation matrices between evaluated cross-sections for different reactions. They can also be handled with the formalism given in ref. 11; however as already mentioned correlations between different data sets due to use of common standards will often be important and thus the simplified formalism of ref. 4 will in

general not be applicable.

4. CONCLUSIONS

As already discussed in this workshop the best use of the existing information on cross-section measurements and their uncertainties can be made by the generalized least square method of Perey /14/ as for example implemented in the computer-code BAYES /15/.

If however use of this method is not possible because of restricted man-power and computer capabilities there is still the possibility of doing evaluations (including reliable uncertainty estimates) for the evaluated cross-sections which are much superior to the mostly qualitative evaluations which have been performed in the past.

For such evaluations trying to give the best obtainable result without using the full covariance formalism we would like to make the following recommendations:

1.) All experimental data should be critically reviewed as described in detail in section 2 of this paper.
2.) If sufficient experimental data exist the evaluated cross-sections may be derived in two ways:
   a) weighted cross-section averages are calculated for suitable energy bins as described in ref. /4,5/, these cross-sections can to good approximation be assigned to the center of the energy bins and the evaluated cross-sections at any energy are obtained by suitable (so far mostly linear) interpolations between these energy-group averages.
   b) a suitable smooth function is fitted to the whole accepted data base as for example in ref. 8.
   If the cross-section is known to be smooth method b) may be preferable, wheras method a) has to be used if the excitation does have some experimentally well-proven structure which cannot be reproduced by the smooth functions approach. For example this is the case for the ^{24}Mg(n,p) reaction where such strcuture have definitely been found in the 12-15 MeV range /4/.
3.) The most simple and reliable method to estimate the uncertainties of the evaluated cross-sections seems to be the following: External and internal errors of cross-sections averaged over a suitable energy bin structure are calculated as discussed

in section 2.6. and the larger of the two errors
is used as uncertainty of the evaluated cross-
section.

4.) If experimental data are either lacking or highly
discrepant in some energy region the purely ex-
perimental evaluation procedure recommended so far
should be supplemented by calculational methods in
those energy regions making use as much as possible
of   the constraints on the calculations by the
existing measurements /5/. The purely experimental
method should be retained in those energy regions
where the quality of the measurements is suffi-
cient.

5.) A reasonably accurate estimate of the relative
correlation matrix of the evaluated excitation
functions can be obtained from estimates of the
correlation in the input data sets using the
formalism of ref. 4 (equ. 7 of this paper).

6.) Correlations matrices between evaluated excitation
functions for different reactions are rather diffi-
cult to estimate. Using the formalism of ref. 11
one might be able to decide whether such correla-
tions are negligible. If not, reliable estimates
will probably be possible only by use of the full
least square covariance formalism /14,15/.

REFERENCES

/1/ H. Liskien and A. Paulsen: Neutron production
cross-sections and energies for the reactions
$T(p,n)^3He$, $D(d,n)^3He$ and $T(d,n)^4He$. Nuclear Data
Tables 11, 569 (1973)

/2/ M. Drosg: Unified absolute differential cross-
sections for neutron production by the hydrogen
isotopes for charged particle energies between
6 and 17 MeV. Nucl. Science & Eng. 67, 190 (1978)

/3/ H. Liskien and A. Paulsen: Neutron Production
cross-sections and energies for the reactions
7Li(p,p)7Be and Li'(p,n)*7Be*. Atomic and Nuclear
Data Tables 15, 57 (1975)

/4/ S. Tagesen, H. Vonach and B. Strohmaier:Evaluation
for the reactions 24Mg(n,p)24Na, 64Zn(n,p)64Cu,
63Cu(n,2n)62Cu and 90Zr(n,2n)89Zr. Physics Data
Nr. 13-1 (1979)

/5/ B. Strohmaier, S. Tagesen and H. Vonach:Evaluation
of the cross-sections for the reactions 19F(n,2n),
31P(n,p)31Si, 93Nb(n,n')93mNb and 103Rh(n,n')103mRh
Physics Data Nr. 13-2 (1980)

/6/ G. Winkler, G.L. Smith and J.W. Meadows: Measure-
ment of cross-sections for the 63Cu(n,α)60Co
reaction from threshold to 10 MeV. Nucl. Sci. &
Eng. (in print)

/7/ A.A. Lapenas, Kh.Ja. Bondars and Ja.K. Vejnbergs:
Izmerenie Spektrov Nejtronov Aktivycionnym Metodom,
Zinatne, Riga, USSR (1975)

/8/ H.I. Bak and A. Lorenz: Review of the current status
of the U-238, NP-237 and Th-232 fission cross-
sections. Journal of the Korean Nucl. Society 3,
77 (1971)

/9/ D.L. Smith: Evaluation of the 115In(n,n')115mIn
reaction for the ENDF/B dosimetry file, ANL/NDM 26
(1976)

/10/ A. Pavlik, H. Vonach and G. Winkler: priv. comm.

/11/ V.A. Konshin, V.F. Zharkov and E.Sh. Sukhovitskij:
Evaluation of the 235U fission cross-sections in
the energy range 0.1 keV - 20 MeV, INDC (CCP)-
148/L (1980)

/12/ E.Sh. Sukhovitskij and V.A. Konshin: Report INDC
(CCP)-113/U, Vienna 1977

/13/ F.C. Defilippo: A program to generate error co-
variance files. ORNL/TM-5223 (1976)
J.D. Drischler and C.R. Weisbin: Covariance
matrices for several important reactor materials.
ORNL-5318 (1977)

/14/ F.G. Perey: Contributions to few channel un-
     folding. ORNL/TM-6267 (1978)
     C.Y. Fu, D.M. Hetrik and F.G. Perey: Simultaneous
     evaluation of the 32S(n,p), 56Fe(n,p) and
     65Cu(n,2n) cross-sections. Proc. of Conf. for
     nuclear cross-sections and technology, 1979, to
     be published by National Bureau of Standards
/15/ D.M. Hetrick and C.Y. Fu, Bayes: A generalized
     least squares program for updating of cross-
     section evaluations with correlated data sets.
     ORNL/TM-7341

TABLE 1

Sources of error important in measurements of
activation cross-sections

1.) Neutron flux measurement resp. standard cross-
    section
2.) Angular distribution of source neutrons (if angular
    dependence of neutron energy is used for simultan-
    eous measurements of cross-sections at various
    energies)
3.) Irridiation geometry
4.) Contribution of scattered neutrons to the activation
    of the samples
5.) Neutron scattering and absorption in the samples
    itself
6.) "Contamination" of neutron source by non-monochroma-
    tic neutrons (breakup neutrons, neutron production
    in windows and backing)
7.) Absolute efficiency of counter used to detect in-
    duced activity (including self-absorption effects
    in samples)
8.) Statistical error
9.) Error contributions from decay data used to calcu-
    late the cross-section

TABLE 2

Cross-section renormalization and error reassesment in the evaluation of the 90Zr(n,2n) reaction / 4/.

Reference	E_n Range	Nr. of Data Pts.	C.S.Renormal.	Error reassesment	
	(MeV)		(%)	from %	to %
Reed 60	14.1	1	-	4.	9.9
Prestwood 61A	12.13-19.76	4	0 - 1	5.	5.
Prestwood 61B	14.3 -14.93	1	1	5.	5.
Rayburn 61	14.4	1	1	7.5	3.1
Rieder 66	14.05-14.7	2	5	5.7	7.5
Csikai 67	15.07	1	3	15.	15.8
Minetti 68	14.7	1	1	8.8	8.8
Abbond 69	13.57-18.18	13	-	1.1	10.
Barral 69	14.6	1	3	7.6	7.6
Lu 70	14.4	1	8	4.7	6.8
Kanda 72	13.44-14.87	6	0 - 1.5	14.8	14.8
Nethaway 72	13.67-14.91	13	1	4.9	4.9
Araminowics 73	14.6	1	1	9.4	10.6
Quaim 74	14.7	1	8	10.2	10.2
Bayhurst 75	14.1 -28	11	0 - 3	4.2	5.7
Sigg 75	14.8	1	3	6.3	6.3
Karolyi 68	14.8	1	3	7.5	9.0

TABLE 3

The relative covariance matrix for the cross section ratios $\sigma[^{63}Cu(n,\alpha)^{60}Co] / \sigma[^{238}U(n,f)]$.
Correlations are given in per cent.

Data point number	1	2	3	4	5	6	7	8	9	10	11	12	13	14	15	16	17	18	19	20	21	22	23	24	25	26	27	28	Energy (MeV)
1	100	2	4	5	5	5	3	3	3	3	5	5	4	5	5	5	6	5	4	5	5	5	5	5	4	4	1	4	3.56
2		100	17	17	23	23	11	13	13	14	21	24	18	24	24	21	24	23	12	24	20	20	20	21	19	16	17	17	4.80
3			100	37	39	45	28	23	26	27	39	44	36	43	43	41	44	44	33	43	40	39	38	39	32	32	34	35	4.07
4				100	42	48	29	26	28	29	44	48	38	48	48	44	49	19	35	43	41	41	42	40	34	36	35	35	4.35
5					100	50	31	26	29	30	45	50	40	49	50	46	50	50	37	49	44	43	43	43	41	36	38	37	4.56
6						100	35	30	33	34	51	56	46	56	56	52	57	57	12	56	51	49	49	49	47	41	43	42	4.95
7							100	22	21	24	36	40	32	40	40	32	41	41	30	40	36	36	36	32	35	31	33	32	5.12
8								100	18	21	33	32	28	37	37	32	32	37	26	36	31	31	31	33	30	27	28	29	5.19
9									100	20	30	33	27	33	33	31	34	33	25	33	30	29	29	29	28	24	25	24	5.27
10										100	35	39	31	39	39	36	40	39	29	39	35	35	35	36	34	30	32	31	5.46
11											100	62	47	62	62	54	63	62	43	61	53	53	53	56	51	45	48	47	5.68
12												100	52	69	69	60	70	69	18	68	58	59	58	62	57	50	53	52	5.86
13													100	52	52	48	53	53	39	52	47	47	48	46	40	43	42		5.87
14														100	69	60	69	69	48	68	58	58	58	62	57	50	53	52	6.07
15															100	60	20	69	48	68	58	59	58	62	57	50	54	52	6.35
16																100	61	61	41	60	54	54	54	55	53	46	49	48	6.40
17																	100	70	49	69	60	60	59	63	58	51	54	53	6.60
18																		100	48	60	59	59	59	62	57	50	53	55	6.84
19																			100	18	43	43	43	44	42	37	39	38	6.91
20																				100	58	58	58	62	57	50	53	51	7.09
21																					100	52	52	54	51	45	40	42	7.42
22																						100	54	56	53	47	50	48	7.92
23																							100	56	54	47	50	49	8.41
24																								100	56	50	53	52	8.43
25																									100	48	51	50	8.70
26																										100	49	49	9.35
27																											100	52	9.42
28																												100	9.07

(G. Winkler, D.L. Smith and J.W. Meadows, "Measurement of Cross Sections for the $^{63}Cu(n,\alpha)^{60}Co$ Reaction from Threshold to 10 MeV", Nucl. Sci. Eng. (1980), in print)

TABLE 4

Estimates of the relative correlation coefficients B_{nnkk} in the measurements of excitation functions of fast neutron induced reactions (from ref. 4 and 5).

Reaction	Nr. of data sets	Range of correlation coefficients	Average correlation coefficients
^{19}F(n,2n)	10	0.10-0.95	0.52
^{24}Mg(n,p)	8	0.15-0.90	0.55
^{31}P(n,p)	7	0.05-0.70	0.41
^{63}Cu(n,2n)	22	0.01-0.90	0.33
^{64}Zn(n,p)	7	0.30-0.80	0.70
^{90}Zr(n,2n)	7	0.50-0.80	0.65
^{103}Rh(nn')^{103m}Rh	6	0.30-0.97	0.67

TABLE 5

Distribution of cross-section measurements with respect to absolute measurements, relative measurements and measurements relative to different standards (ratio measurements)

Type of meas. \ Reaction	$^{19}F(n,2n)$	$^{24}Mg(n,p)$	$^{31}P(n,p)$	$^{63}Cu(n,2n)$	$^{64}Zn(n,p)$	$^{90}Zr(n,2n)$	$^{103}Rh(nn')\ ^{103m}Rh$
	number of data sets						
Abs. measurement	4	7	3	15	5	2	2
Rel. measurement	5	2	6	10			1
rel. to $^{235}U(n,f)$	1				1		
rel. to $^{238}U(n,f)$			1		1	1	
rel. to $^{56}Fe(n,p)$	3	1	1		2		
rel. to $^{27}Al(n,a)$	2	3		2	4	5	1
rel. to $^{27}Al(n,p)$				2			
rel. to $^{32}S(n,p)$		1			1		i
rel. to $^{63}Cu(n,2n)$	1	1	1			3	1
rel. to $^{65}Cu(n,2n)$	1	1		1	2	1	
rel. to $^{31}P(n,p)$					1		
rel. to $C(n,n)$							1
rel. to $^{115}In(n,n')^{115m}In$							1

TABLE 6

Results of the consistency check for the accepted
90Zr(n,2n) data base

Energy bin	$\Delta\bar{\sigma}_{ext}$	$\Delta\bar{\sigma}_{int}$	$R = \dfrac{\Delta\bar{\sigma}_{ext}}{\Delta\bar{\sigma}_{int}}$
(MeV)	(mb)	(mb)	
13.3-13.7	22	14.6	1.5
13.7-14.1	19.6	17.8	1.1
14.1-14.5	19.	13.1	1.45
14.5-14.9	22.2	17.4	1.28
14.9-15.4	20.1	29.7	0.67
15.4-16.6	30.3	36.8	0.82
16.6-17.7	10.7	59.1	0.18
17.7-19.0	45	43.1	1.04
19.0-20.0	12	45.1	0.27

$$\bar{R} = 0.91$$

TABLE 7

Correlation matrix for the evaluated $^{19}F(n,2n)$ cross-sections (from ref. 4)

Correlation matrix														Group boundary (MeV)
100	18	33	0	0	1	0	0	7	47	19	20	18	25	12.40
	100	13	0	1	1	0	0	13	20	8	8	7	11	12.80
		100	3	3	4	4	2	12	33	14	14	13	18	13.20
			100	46	67	68	31	4	0	0	0	0	0	13.60
				100	40	40	18	3	1	0	0	0	0	14.00
					100	64	27	7	1	0	0	0	0	14.20
						100	28	8	0	0	0	0	0	14.40
							100	2	0	20	20	23	21	14.60
								100	8	3	3	3	5	14.80
									100	19	19	18	25	15.00
										100	48	46	46	16.00
											100	45	45	17.00
												100	50	18.00
													100	19.00
														20.00

Fig. 1. Rejection of obviously wrong measurements in
case of the 9OZr(n,2n) reaction /4/

Fig. 2. Experimental situation where the problem of data
rejection becomes extremely difficult

$^{90}Zr(n,2n)^{89}Zr$

＋ Reed	60
o Prestwood	61
⟂ Rayburn	61
⟂ Mangal	63
O Rieder	66
⊂⊃ Csikai	67
✕ Minetti	69
∽ Karolyi	68
⊙ Barral	69
✕ Abboud	69
□ Lu	70
• Qaim	71
∧ Kanda	72
□ Nethaway	72
∼ Araminowicz	73
▽ Qaim	74
◇ Bayhurst	75
✕ Sigg	75

12.5 – 16.4 MeV

mb

— MeV —
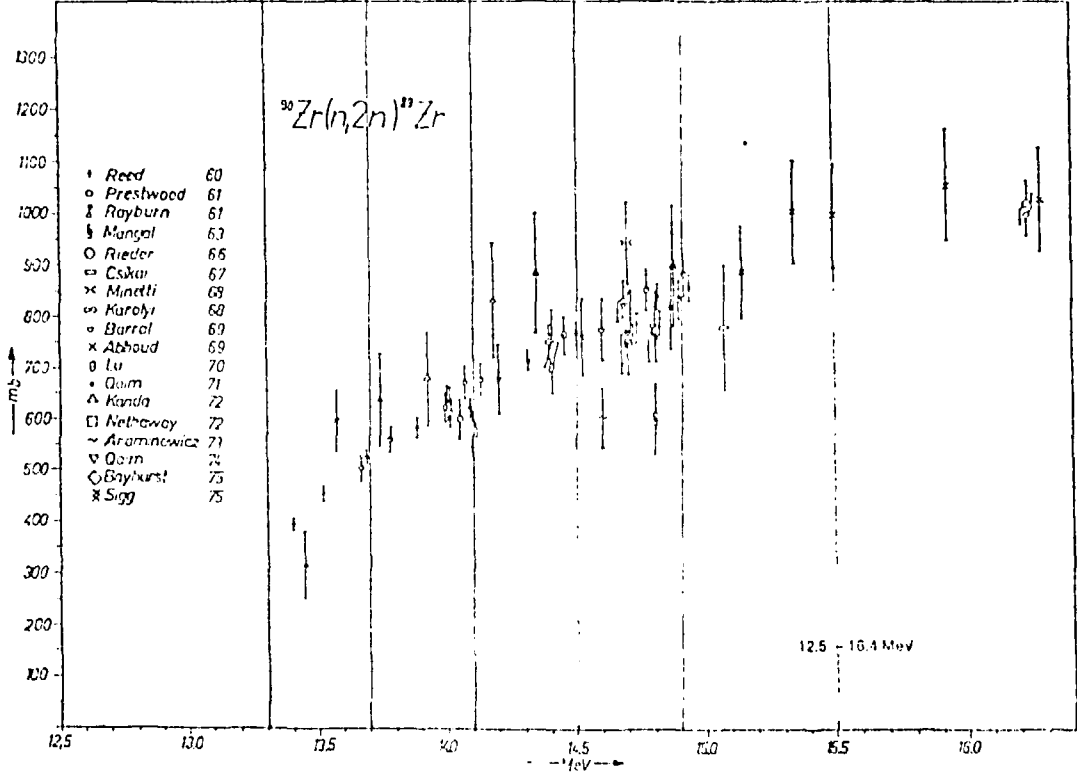
Fig. 3a. Consistency check on accepted experimental
data base accepted data base for the
90Zr(n,2n) reaction with energy group struc-
ture chosen to calculate average cross-sections
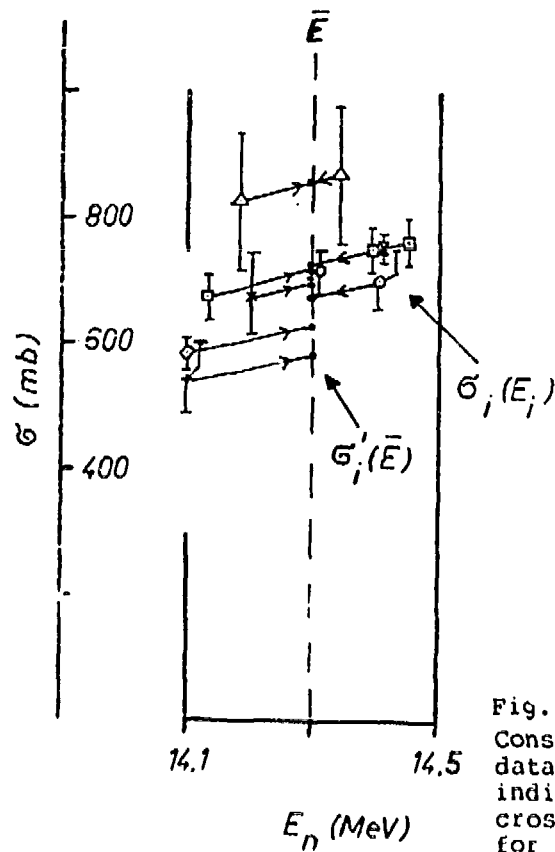
$$\bar{\sigma}(\bar{E}) = \frac{\sum \sigma_i' / \Delta^2 \sigma_i'}{\sum 1 / \Delta^2 \sigma_i'} = 692 \, mb$$

$$\Delta\bar{\sigma}_{int} = \frac{1}{(\sum \frac{1}{\Delta^2\sigma_i'})^{1/2}} = 13 \, mb$$

$$\Delta\bar{\sigma}_{ext} = \frac{[\sum\{(\sigma_i' - \bar{\sigma})^2 / \Delta^2\sigma_i'\}]^{1/2}}{(\sum \frac{1}{\Delta^2\sigma_i'})} = 19 \, mb$$

Fig. 3b.

Consistency check on accepted experimental data base enlarged view of 14.1-14.5 MeV bin indicating method used to calculate average cross-section and internal and external errors for center of energy bin
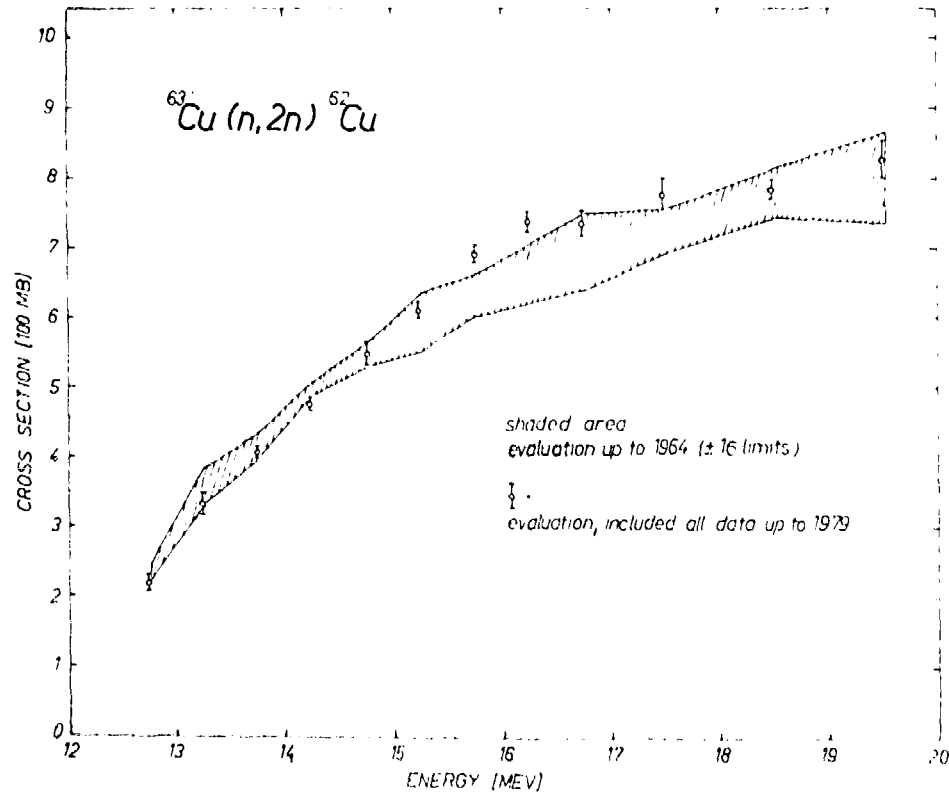
Fig. 4. Comparison of 63Cu(n,2n) evaluations based on
experimental data available at different times.
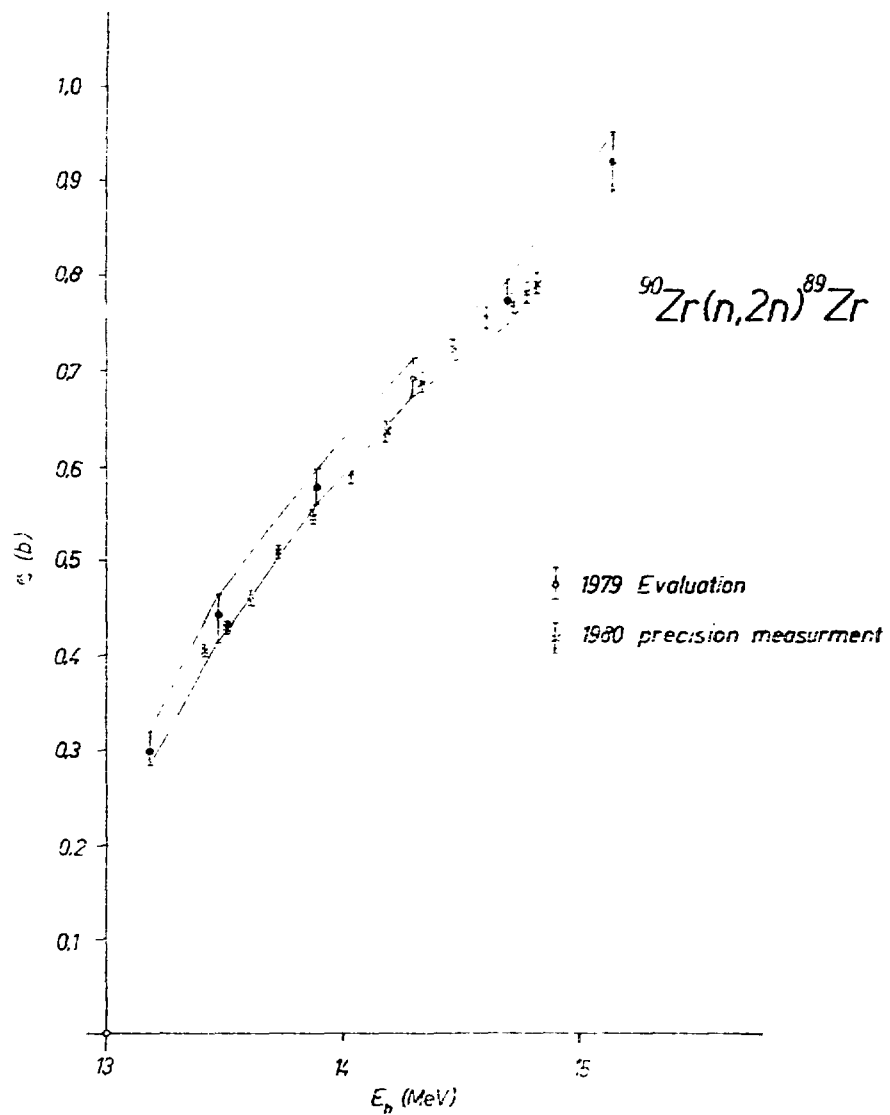
Fig. 5. Comparison of the 1979 90Zr(n,2n) evaluation
with new precision measurements.

Discussion

Poentiz

I should point out tnat the usefulenoss o. looking at internal and external errors was discus-ed in a paper by Birge in 1932. (See Reference in the paper by Poenitz in these proceedings).

The problem you pointed out for ^{64}Zn(n,p) does not create a problem if one uses general L-S fit procedure. It also is not critical if one separates the evaluation of the shape from the normalization.

Vonach

I agree to that. There are a number of points where one has to be more careful if one does not or cannot use the full L-S fitting procedure.

Perey

I think that your method has the appeal that each step appears to be very clean but the whole method is highly inconsistent with the techniques advocated by Poenitz and myself. For instance, when you make a ratio measurement to a standard cross section, you don't make it to an evaluation. it is to nature's cross section. You cannot possibly include the uncertainty of what you know about the cross section. It was the true cross section that was acting in the measurement, not the evaluated cross section or your knowledge of it. All you did was make a ratio measurement and it should be handled as a ratio measurement

Vonach

I completely agree that the joint evaluation of all reactions connected by ratios is the most desirable thing but if you have the task to evaluate one reaction and don't have the possibility to evaluate all the other reactions that are correlated, then by knowing all the ratio measurements and by knowing what the cross section is for the standard, you can put this information in. I don't see any violation of principle.

Gruppelaar

You showed us a case in which there were two series of discrepan. (n,2n) cross section measurements. I wonder whether in this case it is possible to use theory to check these data with perhaps the possiblity to reject one of the data sets. I think that a little more credit should be given to theory. For instance, in the case

of radiative capture in the MeV range the fine structure due to inelastic scattering competition is mostly not observed in experiments. In this and other cases the evaluator really needs the theory.

Vonach

In cases such of such discrepancies we always try to get additional information by model calculations. In the special example, I have discussed (^{66}Zn(n,p)), the uncertainties in the level densities did not allow a decision.

Froehner

I would like to amplify what Harm Gruppelaar just said. In most of my work which is concerned with the resolved resonance region and in what is apparent in what we heard in Gerry Hale's talk, we rely very heavily on a formalism that can give us guidance in very many cases and it is certainly better to use R-Matrix theory than to follow a prescription like the one you presented and spurn what theory can tell us, so one has to be careful about sweeping statements. I realize that in some energy regions, and probably at higher energies, theory is not of much help. For my own concerns, theory is of definite help and improve the data a little, at least, over what you showed in your example.

Howerton

I don't think that Dr. Vonach needs any defense and I don't intend to make any. I only want to point out that the title of his paper is "...With Emphasis on Handling Experimental Data". Had he been asked to talk, in general, about providing evaluations he might well have given another talk.

Menapace

I would remark that even for experiments with uncertainties of 5% or less, theoretical calculations are of main importance in order to deduce a good model parameterization for use in the cases, where experimental data are lacking or discrepant.

Vonach

I agree completely that an accurate excitation function will always give a good opportunity to test models, but the evaluation itself should remain based on the measurements.

CALCULATIONAL METHODS USED TO OBTAIN EVALUATED DATA ABOVE 3 MeV

Edward D. Arthur

Los Alamos Scientific Laboratory, University of California
Theoretical Division
Los Alamos, New Mexico 87545

ABSTRACT

Calculational methods used to provide evaluated neutron data for nuclei between A = 19 and 220 at incident energies above several MeV range from empirical techniques based on cross-section systematics to sophisticated nuclear-model codes that describe the major mechanisms governing neutron reactions in this mass and energy range. Examples of empirical approaches are given along with discussion concerning regions of applicability and accuracies that can be expected. The application of more sophisticated nuclear models (Hauser-Feshbach statistical, preequilibrium, and direct-reaction theories) is discussed, particularly with regard to improved parameter determinations that can be used in such calculations. Efforts to improve the consistency and to unify these theoretical approaches are addressed along with benefits to evaluated data that can be realized through careful application of such nuclear-model techniques.

INTRODUCTION

Evaluated neutron data libraries often rely on calculational techniques to provide necessary cross section, spectral, or angular distribution information. Such instances may involve the need to supplement measured results; to provide data for energy ranges or reaction types lacking experimental data; and, in the most extreme case, to provide data for a nucleus (such as an unstable fission product) where no measurements exist or will likely exist. For medium and heavy nuclei (defined as $19 \leq A \leq 220$ for the purpose of this paper), these techniques range from empirical representations of the systematic behavior of experimental data to more basic approaches employing the Hauser-Feshbach

statistical, preequilibrium, and direct-reaction theories supplemented by use of the spherical or deformed optical model.

In the following sections these techniques are reviewed and their validity examined over the neutron energy range between 3 and 20 MeV. In addition, because of interest in higher energy data motivated by d + Li radiation damage sources, the extension of these techniques up to neutron energies of 50 MeV will be discussed briefly. Because of the wide range in mass and energy covered by this paper, detailed discussions are not feasible; instead examples are provided to illustrate general methods and techniques or to illustrate problem areas. For more detailed discussions, the reader is referred to reviews by Frehaut, [1] Cindro, [2] Qaim, [3] Young et al., [4] and Gardner, [5] as well as the proceedings from various symposiums [6-8] dealing with nuclear theory for applications.

PHENOMENOLOGICAL METHODS BASED ON SYSTEMATIC DATA TRENDS

Interactions of fast neutrons with nuclei in this mass region occur chiefly through elastic and inelastic scattering along with reactions involving the emission of one or more nucleons. Among this latter cross-section type, the (n,2n), (n,p), and (n,α) reactions have been extensively studied over a wide range in mass, albeit restricted to the energy region around 14-15 MeV. From these measurements, parameterizations of cross-section trends as a function of mass or more often as a function of neutron excess, (N-Z)/A, have been developed. Expressions for (n,2n) cross sections have been determined by Lu and Fink [9] that predict such data to within 20% around 14 MeV, while equivalent expressions [10] for (n,p) and (n,α) cross sections exist also having accuracies in the 20-30% range. Recently, Qaim [11-13] and his coworkers have improved such systematics through use of more reliable techniques such as Ge(Li) detectors and isotopically pure samples. Similar efforts [3] have led to systematic studies of the behavior of (n,t), (n, ^{3}He), (n,np), and (n,nα) cross sections as a function of mass in the 14-MeV energy range. For the latter two reaction types, the relative paucity of measurements prevent cross-section prediction to better than a factor of two.

Such systematic behavior of cross-section trends are often used in neutron data evaluation, particularly in the absence of experimental data for the given nucleus of interest. In the Livermore ENDL evaluated data library [14] the expressions of Lu and Fink, [9] Gardner and Rosenblum, [15] and Gardner and Yu [16] are often used to provide information concerning the 14-MeV values of (n,2n), (n,p), and (n,α) cross sections, respectively. Where such 14-MeV systematics are used, there occurs the difficulty of extending cross-section information to other incident energies. For example, in the Lawrence Livermore Laboratory (LLL) ENDL library, the (n,2n) excitation function is

constructed as follows. From threshold the cross section rises
in a sigmoid shape until it reaches a plateau value generally de-
fined (for medium and heavy weight nuclei) by the Lu and Fink
formula. Competition from the (n,3n) reaction causes the (n,2n)
cross section to smoothly decrease with the maximum (n,3n) cross
section set equal to 60% of the maximum (n,2n) cross-section val-
ue. Recent measurements [17-19] of t..e (n,2n) excitation func-
tion from threshold up to 28 MeV provide the opportunity to test
this parameterization. In Fig. 1 the ratios of calculated to ex-
perimental cross sections for nuclei between ^{89}Y and ^{209}Bi are
presented for three ranges of thè energy U_R, which is defined
as the difference between the incident neutron energy and the
(n,2n) threshold. The first region, U_R = 2 MeV, lies fairly
close to the (n,2n) threshold; the second, U_R = 6 MeV, occurs
for these nuclei in the 14-15 MeV incident energy range; and the
third region lies above the (n,2n) plateau region where competi-
tion from (n,3n) reactions occur. As to be expected, the agree-
ment is best around U_R = 6 MeV, corresponding to energies for
which systematics have been most thoroughly developed. Above and
below this energy region, the agreement worsen: with a systematic
underprediction of 30-40% in the calculated cross section.

Other efforts to parameterize the shape of such cross-
section curves appear to be sparse although there have been at-
tempts by Krivan and Munzel [20,21] regarding shapes for (n,p),
(n,α), and (n,2n) excitation functions. To do so, the position
and value of the maximum cross sections, the half width, and an
asymmetry parameter were determined as a function of mass. Such
systematics appear to work reasonably well for (n,2n) reactions,
but for (n,p) and (n,α) cross sections, there are significant de-
viations from experimental data.

Empirical parameterizations of 14-MeV cross sections have
been supplemented by the use of evaporation theory to provide in-
formation concerning cross-section shapes. The foremost example
of such a technique is the THRESH code developed by Pearlstein
[22] which has been used in almost 50% of the current evaluations
in the ENDF library [23] to provide information (either relative
shapes or absolute cross sections) for one or more reaction
types. As an example, the (n,2n) cross section is calculated
from the expression

$$\sigma_{n,2n}(E) = \sigma_{ne} \frac{\sigma_{n,M}}{\sigma_{ne}} \frac{\sigma_{n,2n}(E)}{\sigma_{n,M}} \qquad (1)$$

where σ_{ne} is the nonelastic cross section, and the second factor
represents the portion of the nonelastic cross section resulting
in neutron emission that is parameterized as a function of the
neutron excess, (N-Z)/A. The third factor is calculated from
evaporation model theory [24]

$$\frac{\sigma_{n2n}(E)}{\sigma_{n,M}} = \frac{\int_0^{E-B_n} \varepsilon\sigma_c(E)e^{\sqrt{4a(E-\varepsilon)}}d\varepsilon}{\int_0^E \varepsilon\sigma_c(E)e^{\sqrt{4a(E-\varepsilon)}}d\varepsilon} \quad , \tag{2}$$

where E, B_n, and ε are the excitation energy of the compound system, the neutron binding energy, and the exit energy of the neutron, respectively; a is the level density parameter; and σ_c is the compound nucleus formation cross section.

The advantages of such a technique as embodied in the THRESH code are its simplicity, (Z and A are the only required input parameters although others may be provided); its speed; and, since the model has been fit to experimental data sets, it is possible to obtain errors and their correlations. The range of uncertainties [25] for (n,p), (n,α), and $(n,2n)$ reactions appear in Table I where they are presented as a function of neutron excess.

A common use of THRESH is to normalize (if necessary) to experimental data at 14 MeV and to then use its calculated results to represent a cross-section excitation function in a given evaluation. To test its ability to predict cross-section shapes, a similar analysis has been performed with THRESH results as was done for ENDL systematics in Fig. 1. Again, the $(n,2n)$ reaction was chosen because of the wide mass range in which experimental excitation functions exist; although in this case the range in neutron excess was expanded to include lighter nuclei (^{45}Sc). Similarly, three regions of U_R were chosen to represent incident energy regions near threshold, near the energy at which the maximum cross section occurs, and at energies lying above this plateau region. The results are shown in Fig. 2. For $U_R = 2$ MeV, the calculated cross sections for heavy nuclei lie 25-50% higher than the data, indicating the possible effects of gamma-ray competition, angular momentum, or population of discrete levels, none of which are included in THRESH. For lighter nuclei [smaller $(N-Z)/A$ values], such effects are generally absent. (Note that some calculated values deviate systematically over the three U_R ranges, indicating a need to renormalize to better fit the experimental data.) For $U_R = 6$ MeV, there is generally good agreement, particularly for heavier nuclides (within 10%). However, at $U_R = 10$ MeV, the code consistently underpredicts the $(n,2n)$ cross section with the most likely cause being that preequilibrium effects [important in $(n,2n)$ reactions at these energies] are not included. From Fig. 2 it appears that use of these techniques to provide cross sections on heavier nuclei above 20 MeV should be exercised with a caution if results are desired to better than within a factor of two.

Phenomenological models play roles in data evaluation other than those connected with cross-section needs. For example, evaluated angular distribution information must be provided for continuum neutron emission, a situation that is made difficult because of the paucity of such experimental measurements and because theoretical models are generally not enough developed to

accurately predict such data. Recently Kalbach and Mann [26] have developed a phenomenological model which with four fitted parameters, knowledge of the energy of the outgoing particle, and division of the cross section into multistep-direct and multistep compound parts can reasonably predict angular distributions in a wide mass range and for secondary energies extending to 60 MeV. Figure 3 compares the predictions of this model to data measured on iron by Hermsdorf et al. [27] for 14.6-MeV neutrons. Sums over three regions of secondary energy are presented, the first representing low emission energies governed mainly by compound nuclear processes, the second dominated by multistep direct processes (here approximated by a total preequilibrium emission fraction), and finally a sum over the range of emission energies from 2 to 11 MeV as may be used to describe the gross angular distribution associated with a total emission spectrum. The overall agreement is good, even within the approximation that the total preequilibrium emission cross section was used in place of the multistep direct component. This indicates the usefulness of this phenomenological representation, particularly at higher incident energies where energy-angle correlations become more important.

NUCLEAR MODELS AND THEIR APPLICATION TO DATA EVALUATION

An application of one or more of the theoretical models that describe neutron reactions in this mass and energy region (optical, Hauser-Feshbach statistical, preequilibrium, and direct) has generally been used to provide some portion of evaluated data files. Most often, this has been through use of the optical model to supplement experimental data regarding total, nonelastic, and elastic cross sections as well as angular distributions from elastic scattering. Likewise, the Hauser-Feshbach statistical model has been used to provide similar data for neutron inelastic scattering from discrete levels. Recently, more sophisticated applications have occurred in which simultaneous calculations of cross sections and spectra have been made for a number of reaction types over a wide incident energy range using consistent input parameter sets.

The optical model and the coupled-channel direct reaction theory are discussed in another contribution to this Workshop. Thus, discussion here will concentrate chiefly on the Hauser-Feshbach statistical and preequilibrium models with particular emphasis placed on the parameters that are used with them. The development of improved techniques for parameter determination along with new model codes that handle tertiary (and higher-order) reactions strengthens the role such techniques will play in future data evaluation. These improvements will be discussed along with problems occurring in the use of such models.

The calculation of cross sections for particle or gamma-ray emission through the Hauser-Feshbach statistical model occurs by use of the expression [28]

$$\sigma_{cc'} = \frac{\pi \lambda^2}{(2i+1)(2I+1)} \sum_{J\pi} \frac{\sum_{s\ell} T_c \sum_{s'\ell'} T_{c'}}{T} W_{cc'}$$ (3)

where i and I are the projectile and target spins, respectively. The term $W_{cc'}$ represents width-fluctuation [29] corrections that must be applied at low energies. Since $W_{cc'} \to 1$ at energies above a few MeV, it will not be described here. To evaluate components appearing in this schematic expression one must have information from optical-model calculations regarding transmission coefficients that describe the compound nucleus formation at a given incident energy as well as ones that described particle emission over a wide secondary energy range. Gamma-ray transmission coefficients must be obtained generally through the use of the Weisskopf [30] single particle or Brink-Axel [31] giant dipole resonance models. Discrete level data must generally be provided, and if a continuum of excitation energies is assumed (because of the lack of sufficient discrete level data) then a level density model and its associated parameters must be employed. Thus application of the Hauser-Feshbach model to data evaluation generally requires a complexity of input parameters much greater than other calculational techniques discussed earlier.

Generally for incident neutron energies above 10 MeV, cross section and spectral results from the statistical model must be modified for nonequilibrium effects through use of the preequilibrium model. To calculate preequilibrium emission, the master equations exciton model [32] has been widely used in evaluations, although some applications of the geometry-dependent hybrid model have also occurred. (For more detail concerning the hybrid model, see the review by Blann. [33]) Within the master equations exciton model, a reaction is assumed to proceed through a variety of particle-hole configurations, starting with simple ones and advancing through more complicated ones until equilibrium is achieved. At each stage during the process there occurs some probability for particle emission. To obtain cross sections and spectra with this model, the following coupled equations must be solved.

$$\frac{dP}{dt}(n,t) = P(n-2,t)\lambda_+(n-2,E) + P(n+2,t)\lambda_-(n+2,E)$$

$$- P(n,t)[\lambda_+(n,E) + \lambda_-(n,E) + \sum_b \int W_b(n,\epsilon)d\epsilon] \quad , \quad (4)$$

where n is the exciton number (n=p+h), the quantities λ_+ and λ_- represent transition rates to produce increasingly (or decreasingly) complex p-h configurations and W_b is the probability to emit at each stage particles of type b having energy ε. To obtain these rate expressions, the square of the average matrix element for the effective two-body interaction $|M|^2$ must be calculated. In the exciton model this is done empirically through assumption of the form

$$|M|^2 = kA^{-3} E^{-1} \quad . \qquad\qquad (5)$$

The constant k appearing on the above expression has been determined by Kalbach [34] from the analysis of particle-induced reaction data at energies of tens of MeV. Remaining quantities needed to calculate preequil'brium emission are the compound nucleus formation cross section, inverse cross sections at secondary energies ε, and state densities used to represent p-h configurations.

Recently several new codes employing statistical preequilibrium theories have been developed that should greatly aid in data evaluation. A selected number of these along with their characteristics appear in Table II; a more complete overview has been given by Prince in Ref. 35. The STAPRE, [36] TNG, [37] HAUSER, [38] and GNASH [39] codes carry out multistep reaction calculations with full allowance for angular momentum effects along with preequilibrium corrections. Others like MSPQ [40] and ALICE [41] use evaporation theory for the statistical portion of the calculation along with preequilibrium emission based on the exciton and geometry-dependent hybrid models, respectively. The AMALTHEE [42] and PREANG [43] codes both use matrix methods to solve exactly the master equations of the exciton model without artificial division between preequilibrium and equilibrium components.

Optical, Gamma-ray, and Level-Density Parameters

Transmission coefficients used in Hauser Feshbach calculations should produce accurate compound nucleus formation cross sections while also realistically describing particle emission over a spectrum of emission energies. Such conditions lead to considerable constraints on the optical parameters used so that transmission coefficients obtained from global optical parameter sets can be inadequate for the problem or energy range of interest. Recently improvements in optical model parameters have occurred through the use of the "SPRT" technique developed by Lagrange and co-workers [44] and now used extensively in calculations for evaluated data. The technique employs s- and p-wave strengths to supplement total cross section and elastic angular distribution data so that neutron optical parameters that are typically applicable over the energy range from 10 keV to 20 MeV can be determined. Neutron data are often augmented by the

the use of proton data to extend the range over which such parameters are valid. Figure 4 shows an example of this technique in which coupled-channel calculations of the neutron total cross section for ^{197}Au have been made using the parameters of Delaroche. [45] For ^{197}Au, the parameters are valid up to energies around 60 MeV because of the availability and use of higher energy proton data in the parameter determinations.

The applicability of such optical parameter sets can be verified indirectly through Hauser-Feshbach calculations of processes such as (n,2n) reactions on medium and heavy nuclei from threshold up to energies around 15 MeV. Generally the cross section rises rapidly and if gamma-ray competition is determined using gamma-ray strength functions (see next paragraph), then the calculated shape depends heavily on the neutron transmission coefficients. In addition the calculated cross section can be often determined by transitions to discrete levels in the A-1 nucleus so that level density effects are minimal. Figure 5 illustrates such a case for the ^{89}Y(n,2n) reaction where the optical parameters of Lagrange [46] determined by the SPRT Method and used in GNASH calculations [47] produce good agreement with available experimental data. A similar situation exists for the ^{90}Zr(n,2n) reaction near threshold. However, for incident energies up to 15 MeV, greater than 75% of the calculated cross section results from direct transitions to the 9/2+ ground state of ^{89}Zr. This situation allows the behavior of higher order transmission coefficients to be tested through comparison to experimental data.

As mentioned above, the use of gamma-ray strength functions may offer improvements in the calculation of multistep reactions such as (n,2n), particularly around thresholds where gamma-ray competition is important. Gamma-ray strength functions and their systematics have recently been the subject of an extensive investigation by D. G. and M. A. Gardner [48] to which the reader is referred. In many statistical-model calculations, gamma-ray transmission coefficients are normalized to the $2\pi\langle\Gamma_\gamma\rangle/\langle D\rangle$ ratio where $\langle\Gamma_\gamma\rangle$ and $\langle D\rangle$ are the average gamma-ray width and spacing for s-wave resonances. Such techniques pose little problems for stable nuclei where these data are available experimentally. However, for compound systems lacking this data, these quantities must be deduced from their systematic behavior. This can lead to large errors particularly around closed shell regions where there are large variations in resonance spacings. The use of strength functions to determine gamma-ray transmission coefficients should help alleviate this problem since their normalization should vary slowly between nearby nuclei. Figure 6 illustrates this behavior by showing results of ^{85}Rb and ^{87}Rb capture calculations[48] using identical E1 and M1 strength functions (shown at the left) that reproduce experimental capture cross sections differing by a factor of more than 25.

Progress in improvement of level density parameters and representations has lagged behind the advances described above for optical and gamma-ray strength parameters. Most calculations performed for data evaluations use phenomenological models--generally the constant temperature and Fermi-gas expressions due to Gilbert and Cameron [49] or the back-shifted Fermi-gas model developed by Dilg et al. [50] Mention should also be made concerning the use by Jary [51] in (n,2n) calculations of the Ignatuyk [52] expressions that include an excitation energy dependent level-density parameter. Some improvements in the parameters used with such models have occurred recently due to the work of Reffo [53] on spin cut-off parameters and by Cook [54] regarding updated fits to determine the remaining parameters. Even after these parameter improvements, such models are deficient in describing high excitation energy regions or predicting the ratio of positive to negative parity states as a function of excitation energy. From this point of view, model codes would benefit by the implementation of microscopic level densities using methods such as those of Morretto [55] or Grimes. [56]

Applications

In spite of these shortcomings, nuclear models have been applied successfully to many evaluation problems. Complete and consistent calculations of neutron reactions on barium isotopes from 20 keV to 20 MeV have been made by Strohmaier et al. [57] using the STAPRE code listed in Table II. The TNG code has been used by Fu in the evaluation of neutron cross sections for Ca, Fe, and Pb, [58-60] and most recently by Larson [61] to calculate neutron reactions on ^{23}Na. Mann et al. have used the HAUSER code to calculate cross sections for the ^{54}Fe(n,p) dosimetry reaction [62] and to calculate alpha-particle production from neutron reactions on copper up to 40 MeV. [63] The GNASH multistep statistical code has been used to calculate reaction cross sections on Fe, Co, [64-65] and most recently on Ni isotopes [66] up to energies of 40-50 MeV. An example of such a calculation is shown in Fig. 7 for the ^{58}Ni(n,2n) reaction. Neutron optical parameters were obtained through the SPRT method while proton and alpha optical parameters were verified through calculation and comparison to proton and alpha induced reaction data up to 40 MeV. Data from $^{58,60-62}$Ni capture reactions provided gamma-ray strength function information. These parameters were then used in preequilibrium-statistical calculations along with direct inelastic scattering cross sections obtained from DWBA calculations. The ^{58}Ni(n,2n) cross section constitutes only a small portion of the total reaction cross section, but reasonable agreement is obtained principally because of the input parameter determinations. Previous calculations [18,67] that relied on global input parameter sets have faired poorly, often missing the experimental results by greater than a factor of two.

Nuclear model calculations can be used to correct some inaccuracies that often exist in evaluated data files. One such area is the representation of neutron emission spectra induced by neutrons in the 10-20 MeV range. Deficiencies in evaluated data have been pointed out by Hetrick et al. [68], occurring most often in cases where evaporation formulas using temperatures determined from level-density parameters are employed for such spectra representation. One such example is the evaluated spectra for tungsten isotopes appearing in ENDF/B-V. In Fig. 8, the evaluated ^{184}W spectrum is compared to measurements by Hermsdorf [27] on natural tungsten using 14.6 MeV neutrons. A large discrepancy exists most noticeably in the secondary energy region where pre-equilibrium emission and direct reaction effects are most important. Such behavior is corroborated by comparison of calculated neutron spectra [69,70] to results from integral measurements such as those from the pulsed sphere program at Livermore (see Fig. 9). Comparisons to such integral data have proven to be a valuable complement to microscopic data in the 14 MeV region. The calculated emission spectrum that will be used in a new evaluation [71] for tungsten isotopes currently under preparation is shown in Fig. 10. Much better agreement is obtained although some underprediction still exists in the upper end of the spectrum. This would possibly be improved if calculated direct reaction cross sections were included in the comparison.

A consistent application of nuclear models could alleviate another problem occurring in evaluated data files. For example, calculational techniques are sometimes used to provide evaluated neutron cross sections but experimental results are used directly to provide evaluated gamma-ray production data. Inconsistencies between these evaluated data types can lead to energy imbalance problems that can be solved through a consistent use of nuclear-model calculations matched to experimental data. Such problems have been addressed by MacFarlane [71] and Young [4] through energy balance tests of various ENDF evaluations. Some results from these studies are presented in Table III for energies in the 2-20 MeV range. A poor rating indicates that significant (up to 10%) violations occur for conservation of total energy.

As evaluated data libraries are extended to higher energies, the demands placed upon model calculations will increase because of the general consensus that experimental measurements cannot satisfy all of the data needs for energies above 20 MeV. In such instances, calculations must be performed in which complicated reaction chains must be followed to include all major neutron and charged-particle producing reactions. Figure 11 shows such a chain that was used for GNASH calculations on iron [64] up to 40 MeV. Calculated cross sections using this chain are shown in Fig. 12, indicating that contributions for reactions such as (n,2np) [sum of (n,npn) + (n,pnn) + (n,2np)] dominate at higher energies over those involving solely neutron emission, again illustrating the need for such detail in the calculation.

Problems that occur in model calculations below 20 MeV are magnified considerably at higher energies, particularly with regard to level density representations and parameters. This is due in part to the higher excitation energies involved and because nuclei are reached that lie further away from the line of stability at which most experimental information exists. Such deficiencies can be compensated to some degree through comparison to higher energy charged-particle induced reaction data that can be used to verify and optimize parameters for level density, preequilibrium, and other ingredients needed in such calculations.

Improvements in Nuclear Models

There are several areas of theoretical improvements that will be useful for future data evaluation. One such example is the extension, for preequilibrium emission, of the generalized master equations of Mantzouranis et al. [73] by Gruppelar and Akkerman [74] to the theoretical analysis of angular distributions induced by 14.6 MeV neutrons. Satisfactory results were obtained over a wide mass range (berylium to bismith) after adjustment of two global parameters.

The unification of preequilibrium and the Hauser-Feshbach statistical model has been pursued by Fu [75] at ORNL through incorporation of angular momentum effects into the preequilibrium model. The result is a form that becomes compatible with standard Hauser-Feshbach techniques when equilibrium is reached. A part of this is achieved through the determination and use of level and state density parameters that are consistent between the two models, a situation that has generally been lacking in the past. This unified model, after determination of two parameters through comparison to 14.6 MeV neutron emission data for iron, has been applied to calculation of the neutron and charged-particle emission spectra on 12 isotopes having recent experimental data. Initial results from such calculations have proven satisfactory as shown in Fig. 13 where comparisons are made to experimental neutron production spectra. This model, in addition to providing cross sections and spectral information, also allows angular distribution information to be obtained for continuum particle emission.

UNCERTAINTIES RESULTING FROM APPLICATION OF CALCULATIONAL TECHNIQUES

Along with the evaluated data that can be obtained using the calculational methods outlined in this paper, there is a need to provide information about uncertainties arising from use of such techniques, especially in areas lacking experimental data. By

use of the empirical techniques discussed at the beginning of this paper, fits can be made to experimental data using a given parameter set, from which uncertainties and their correlations can be ascertained. An example of such results appeared in Table I. However, if a model is extended significantly beyond the region where its parameters and their errors were obtained, then the confidence that can be placed upon calculated results and errors declines considerably.

If nuclear models are used to determine evaluated data where no experimental measurements exist then the error problem becomes increasingly more difficult. In such cases, the number of input parameters is greater and often because of lengthy computational times it is not possible to vary each input parameter to examine the sensitivity of the calculated results to it. Also, for some excitation energy regions or nuclei far removed from stability, the theoretical models used may have little or no validity. There are however cases where meaningful errors and their correlations can be obtained for parameters used in theoretical analyses. One such example is the use of chi-square minimization methods to obtain optical parameters from fits to experimental data. Also, some nuclear-model codes require relatively little computer time, and studies of the sensitivity of calculated results can be made as a function of a significant number of parameters. One such example is the analysis by Pearlstein [76] of neutron emission spectra induced by 14 MeV neutrons over the mass range from sodium to bismuth. The preequilibrium-evaporation code ALICE [41] was used to obtain covariances and correlations for several fitted parameters. The result was a global parameter set that could produce agreement to within 30% of the measured results in over 70% of the cases studied.

The estimation of errors using more complicated Hauser-Feshbach techniques (with preequilibrium corrections) generally is more vague and relies on the systematic behavior of input parameters within some realm of physically acceptable values. The error estimates made in calculations of neutron reactions on barium isotopes by Strohmaier [57] follow this pattern where relatively small estimates (10%) were made for neutron emission cross sections because of well-determined neutron parameters and a good supply of experimental data. For other cases such as charged-particle reactions lacking well-determined input parameters or data, estimated errors were significantly larger (40%).

CONCLUSIONS

Some of the calculational techniques used to provide evaluated data for medium and heavy mass nuclei in the neutron energy range above 3 MeV have been reviewed. Empirical techniques play a role when cross-section estimates are desired based on systematic data trends or in situations where more basic models are not sufficiently developed to produce adequate agreement with

experimental results. However, the improvement in input parameters and the availability of new, sophisticated nuclear model codes have resulted in an increased use of theoretical methods to provide cross sections and spectral information. The extension of evaluated data to higher energies promises further improvement in these theoretical techniques. It should be remembered, however, that underlying these discussions of empirical and theoretical methods is the realization of the importance of having adequate experimental data with which to verify and improve such techniques.

REFERENCES

1. J. Frehaut, "Neutron-Induced Cascade Reactions," in Proc. Int. Conf. on the Interactions of Neutrons with Nuclei, Lowell, MA (1976), p. 336.

2. N. Cindro, "(n,x) Reactions on Medium and Heavy Nuclei," Proc. Int. Conf. on the Interactions of Neutrons with Nuclei, Lowell, MA (1976), p. 348

3. S. M. Qaim, "Recent Advances in the Study of Some Neutron Threshold Reactions," Proc. Int. Conf. on Neutron Physics and Nuclear Data, Harwell (1978), p. 1088.

4. P. G. Young et al., "Application of Nuclear Models," Int. Conf. on Nuclear Cross Sections for Technology, Knoxville, TN (1979).

5. D. G. Gardner, "Recent Developments in Nuclear Reaction Theories and Calculations," in Proc. of Sym. on Neutron Cross Sections from 10-50 MeV, Brookhaven (1980).

6. T. Fuketa, Ed., Proc. of the EANDC Topical Discussion on "Critique of Nuclear Models and Their Validity in the Evaluation of Nuclear Data," NEANDC(J)38L (1975).

7. "Nuclear Theory in Neutron Nuclear Data Evaluation," Vols. 1 and 2, IAEA-190 (1976).

8. A. Salam, Ed., "Nuclear Theory for Applications, Proceedings of a Course," IAEA-SMR-43, Trieste (1978).

9. Wen-deh Lu and R. W. Fink, Phys. Rev. C4, 1173 (1971).

10. V. N. Levkovskii, Sov. J. Nucl. Phys. 18, 361 (1974).

11. S. M. Qaim, Nucl. Phys. A185, 614 (1972).

12. N. I. Molla and S. M. Qaim, Nucl. Phys. A283, 269 (1977).

13. S. M. Qaim, "Nuclear Data Needs for Radiation Damage Studies," in Proc. of Advisory Group Mtg. on Nuclear Data for Fusion Reactor Technology, IAEA-TECDOC-223 (1979).

14. R. J. Howerton et al., "The LLL Evaluated Nuclear Data Library (ENDL)," UCRL 50400, Vol. 15A (1975); M. A. Gardner and R. J. Howerton, "ACTL: Evaluated Neutron Activation Cross-Section Library," UCRL-50400, Vol. 18 (1978).

15. D. G. Gardner and S. Rosenblum, Nucl. Phys. A96, 121 (1967).

16. D. G. Gardner and Y. W. Yu, Nucl. Phys. 60, 49 (1964).

17. J. Frehaut and G. Mosinski, "Measurement of (n,2n) and (n,3n) Cross Sections for Incident Energies between 6 and 15 MeV," in Nuclear Cross Sections and Technology Conference Proceedings NBS-S425, p. 855 (1975).

18. B. P. Bayhurst et al., Phys. Rev. C12, 451 (1975).

19. L. R. Veeser et al., Phys. Rev. C16, 1792 (1977).

20. V. Krivan and H. Munzel, J. Inorg. Nucl. Chem. 34, 2093 (1972).

21. V. Krivan and H. Munzel, J. Inorg. Nucl. Chem. 34, 2989 (1972).

22. S. Pearlstein, J. Nucl. Energy 27, 81 (1973); S. Pearlstein, "Program THRES2, A Revision of THRESH," Brookhaven National Laboratory report (1975).

23. R. Kinsey, "ENDF/B Summary Documentation, 3rd Edition, (ENDF/B-V)," Brookhaven report BNL-NCS-17541 (1979).

24. J. M. Blatt and V. Weisskopf, Theoretical Nuclear Physics (Wiley, New York, 1952), p. 365.

25. S. Pearlstein, "Neutron Cross Sections and Their Uncertainties Obtained from Nuclear Systematics," in Nuclear Cross Sections and Technology Conference Proceedings NBS-S425, p. 332 (1975).

26. C. Kalbach and F. M. Mann, "Phenomenology of Preequilibrium Angular Distributions," in Proc. Symp. on Neutron Cross Sections from 10-50 MeV, Brookhaven (1980).

27. D. Hermsdorf et al., "Differentielle Neutronenemissionsquerschnitte," ZFK-277, Dresden, DDR (1974).

28. W. Hauser and H. Feshbach, Phys. Rev. 87, 366 (1952).

29. P. A. Moldauer, Phys. Rev. C12, 744 (1975).

30. J. M. Blatt and V. F. Weisskopf, Theoretical Nuclear Physics (John Wiley, New York, 1952), p. 627.

31. D. M. Brink, Thesis, Oxford University (1955), unpublished; P. Axel, Phys. Rev. 126, 671 (1962).

32. C. Kalbach, Acta. Phys. Slov. 25, 100 (1975).

33. M. Blann, Annual Reviews of Nuclear Science 25, 123 (1975).

34. C. Kalbach, Z. Phys. A287, 319 (1978).

35. A. Prince, "Statistical Theory Applications and Associated Computer Codes," p. 231; and "Computer Codes Incorporating Preequilibrium Decay," p. 305, in Proc. of the Course on Nuclear Theory for Applications, IAEA-SMR-43, Trieste (1978).

36. M. Uhl and B. Strohmaier, "STAPRE: A Computer Code for Particle-Induced Activiation Cross Sections," IRK 76/01 (1976).

37. C. Y. Fu, "Development of a Two-Step Hauser-Feshbach Code With Precompound Decays and Gamma-Ray Cascades," Nuclear Cross Sections and Technology Conference Proceedings, NBS-S425, p. 328 (1975).

38. F. M. Mann, "HAUSER-4: A Computer Code to Calculate Nuclear Cross Sections," HEDL-TME-76-80 (1976).

39. P. G. Young and E. D. Arthur, "GNASH: A Preequilibrium-Statistical Nuclear Model Code for Calculation of Cross Sections and Emission Spectra," LA-6947 (1977).

40. J. Jary, "MSPQ: A FORTRAN Code for Cross Section Calculations Using a Statistical Model with Preequilibrium Effects," INDC(FR)10L (1977).

41. M. Blann, "Overlaid ALICE," University of Rochester report COO-3494-29 (1975).

42. O. Bersillon and L. Faugere, "AMALTHEE" A Code for Spectra and Cross Section Calculations within the Exciton Model," NEANDC(D)191L (1977).

43. J. M. Akkermans and H. Gruppelaar, "Calculation of Preequilibrium Angular Distributions with the Exciton Model Code PREANG," ECN-60 (1979).

44. J. P. Delaroche, Ch. Lagrange, and J. Salvy, "The Optical Model with Particular Considerations of the Coupled-Channel Optical Model," IAEA-190, p. 251 (1976).

45. J. P. Delaroche, "Potential Optique Nucleon - ^{197}Au entre 10 keV et 57 MeV," Proc. of the Int. Conf. on Neutron Physics and Nuclear Data, Harwell (1978), p. 366.

46. Ch. Lagrange, "Optical Model Parameterization between 10 keV and 20 MeV - Applicable to the ^{89}Y and ^{93}Nb Spherical Nuclei," in Proc. 3rd National Soviet Conf. on Neutron Physics, Kiev (1975) CONF-75061154 Atomizdat (1976).

47. E. D. Arthur, "Calculations of Neutron Cross Sections on Isotopes of Yttrium and Zirconium," LA-7789-MS (1979).

48. D. G. Gardner et al., "A Study of Gamma-Ray Strength Functions," UCID-18759 (1980).

49. A. Gilbert and A. G. W. Cameron, Can. J. Phys. 43, 1446 (1965).

50. D. Dilg et al., Nucl. Phys. A217, 269 (1973).

51. J. Jary and J. Frehaut, "Level Density Dependence of (n,γ), (n,n'), and (n,2n) Reaction Cross Sections," in Progress Report of the Neutron and Nuclear Physics Division for the Year 1979, CEA-N-2131, p. 185 (1980).

52. A. V. Ignatyuk et al., Sov. J. Nucl. Phys. 21, 255 (1975).

53. G. Reffo, "Parameter Systematics for Statistical Theory Calculations of Neutron Reaction Cross Sections," CNEN-RT/FI-80 (1980).

54. J. L. Cook and E. K. Rose, "An Evaluation of the Gilbert-Cameron Level Density Parameters," AAEC/E419 (1977).

55. L. G. Sargent, Nucl. Phys. A44, 145 (1972).

56. S. M. Grimes et al., Phys. Rev. C19, 2378 (1979).

57. B. Strohmaier et al., Nucl. Sci. Eng. 65, 368 (1974).

58. C. Y. Fu, Atomic Data and Nucl. Data Tables 17, 127 (1976).

59. C. Y. Fu and F. G. Perey, ENDF/B-V MAT 1326 (1979).

60. C. Y. Fu and F. G. Perey, Atomic Data and Nucl. Data Tables 17, 409 (1975).

61. D. C. Larson, to be published.

62. R. E. Schenter et al., "Evaluation of the ^{58}Fe(n,γ) and ^{54}Fe(n,p) Reactions for the ENDF/B-V Dosimetry File," in Proc. of Int. Conf. on Nuclear Cross Sections for Technology, Knoxville, TN (1979).

63. D. W. Kneff et al., Nucl. Technology 49, 498 (1980).

64. E. D. Arthur and P. G. Young, "Evaluation of Neutron Cross Sections to 40 MeV for ^{54,56}Fe," in Proc. Symp. on Neutron Cross Sections from 10-50 MeV, Brookhaven (1980).

65. E. D. Arthur et al., "Calculation of ^{59}Co Neutron Cross Sections between 3 and 50 MeV," in Proc. of Symp. on Neutron Cross Sections from 10-50 MeV, Brookhaven (1980).

66. R. C. Harper and E. D. Arthur, to be published.

67. A. Marcinkowski, "Measurements and Evaluation of Fast Neutron Cross Section Data for Reactor Dosimetry," INDC(NDS)103/M (1979).

68. D. M. Hetrick et al., "Status of ENDF/B-V Neutron Emission Spectra Induced by 14 MeV Neutrons," ORNL/TM 6637 (1979).

69. G. P. Estes and R. E. Seamon, "More Integral Testing of ENDF/B-V Data," to be presented at the ANS Winter Meeting (Nov. 1980).

70. R. J. Howerton, "Data Testing Results for the ENDF/B-V Evaluated Neutron Data File," UCID-18731 (1980).

71. E. D. Arthur, C. A. Philis, P. G. Young, and A. B. Smith, to be published.

72. R. E. MacFarlane, Trans. Am. Nuc. Soc. 33, 681 (1979).

73. G. Mantzouranis et al., Phys. Lett 57N, 220 (1975).

74. H. Gruppelaar and J. M. Akkermans, "Comparison of Experimental and Calculated Neutron Emission Spectra and Angular Distributions," in Proc. Symp. on Neutron Cross Sections from 10-50 MeV, Brookhaven (1980).

75. C. Y. Fu, "A Consistent Nuclear Model for Compound and Precompound Reactions with Conservation of Angular Momentum," ORNL/TM 7042 (1980).

76. S. Pearlstein, Nucl. Sci. and Eng. 68, 55 (1978).

TABLE I

UNCERTAINTY RANGES (%) FOR THRESH CROSS SECTION RESULTS AS
A FUNCTION OF NEUTRON EXCESS (Ref 25)

Reaction	Neutron Excess (N-Z)/A			
	0.03-0.05	0.05-0.1	0.1-0.15	0.15-0.2
(n,2n)	20-50	10	10	10
(n,p)	20-25	20-30	20-40	30-150
(n,α)	25	25-40	30-60	40-150

TABLE II

SOME RECENT NUCLEAR MODEL CODES USED FOR EVALUATION PURPOSES

Code	Author	Method	$\frac{d\sigma}{d\varepsilon}$	$\frac{d\sigma_\gamma}{d\varepsilon}$ (a)	$\frac{d\sigma}{d\Omega}$	$\frac{d^2\sigma}{d\varepsilon d\Omega}$	σ^m (b)	σ_f (c)
ALICE	Blann	Evaporation and geometry-dependent hybrid preequilibrium	x					
AMALTHEE	Bersillon & Faugere	Matrix solution of master equations exciton model for t → ∞	x					
GNASH	Young & Arthur	Multistep Hauser-Feshbach, master equations exciton model	x	x			x	x
HAUSER5	Mann	Multistep Hauser-Feshbach, master equations exciton model	x	x	x		x	x
MSPQ	Jary	Evaporation and exciton model preequilibrium	x					x
PREANG	Akkermans, Gruppelaar & Luider	Matrix solution of generalized master equation exciton model	x			x		
STAPRE	Uhl & Strohmaier	Multistep Hauser-Feshbach, master equation exciton model	x	x			x	x
TNG	Fu	Unified multistep Hauser-Feshbach and preequilibrium with angular momentum conservation	x	x	x	x	x	

(a) gamma-ray spectra and cross sections

(b) isomeric state cross sections

(c) fission cross sections

TABLE III

QUALITATIVE RATING OF ENERGY BALANCE FOR ENDF/B-V
MATERIALS IN THE ENERGY RANGE 2-20 MeV (Ref. 72)
(G = good, F = fair, P = poor)

^{19}F	F	^{55}Mn	P
^{23}Na	F	Fe	P
Mg	F	^{59}Co	P
^{27}Al	F	Ni	F
Si	G	Cu	*
^{31}P	F	Mo	*
^{32}S	F	^{138}Ba	F
Cl	*	^{181}Ta	P
K	P	^{182}W	P
Ca	G	^{183}W	P
Ti	F	^{184}W	P
V	F	^{186}W	P
Cr	P	Pb	F

*Masked by element effect
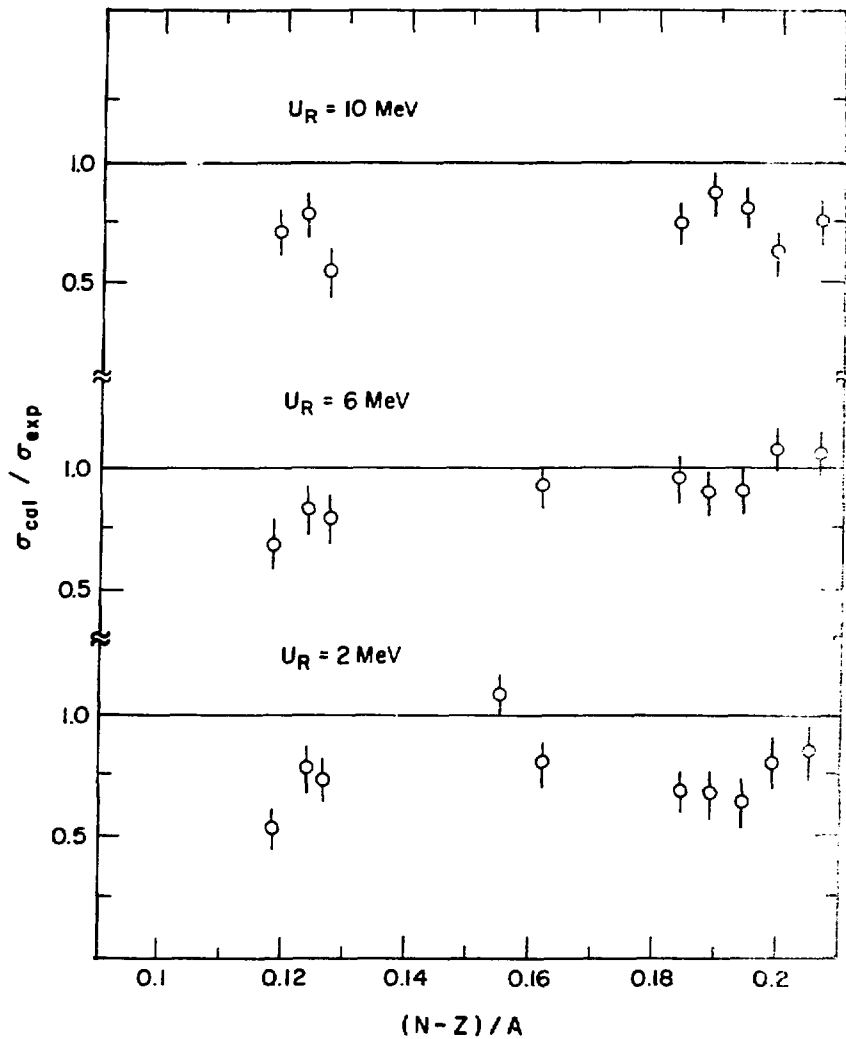
Fig. 1.

The ratio of (n,2n) cross sections calculated using the LLL
ENDL empirical methods to experimental results for nuclei
ranging from ^{89}Y to ^{209}Bi are presented for three regions of
U_R [U_R = incident energy - (n,2n) threshold energy].
These regions correspond to energies slightly above the
(n,2n) threshold, to energies where the (n,2n) cross sec-
tions reach a maximum, and to energies above the plateau
region where (n,3n) competition occurs.
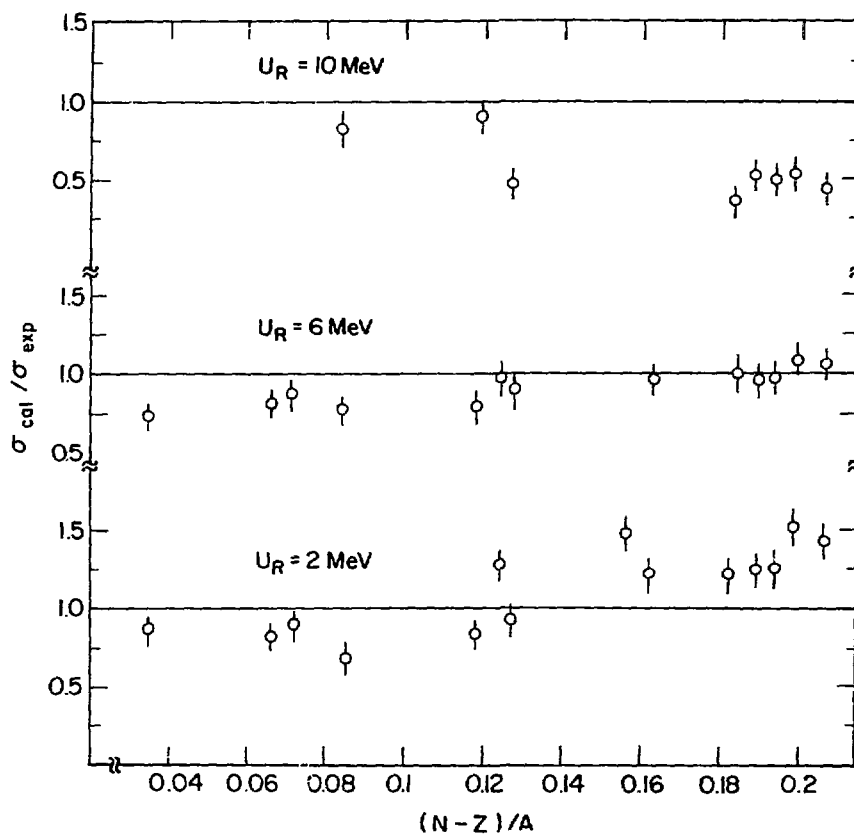
Fig. 2.
The ratio of (n,2n) cross sections calculated using the
THRES2 [22] code to data for nuclei ranging from ^{45}Sc to
^{209}Bi. The same U_R regions are used as were defined in
Fig. 1.
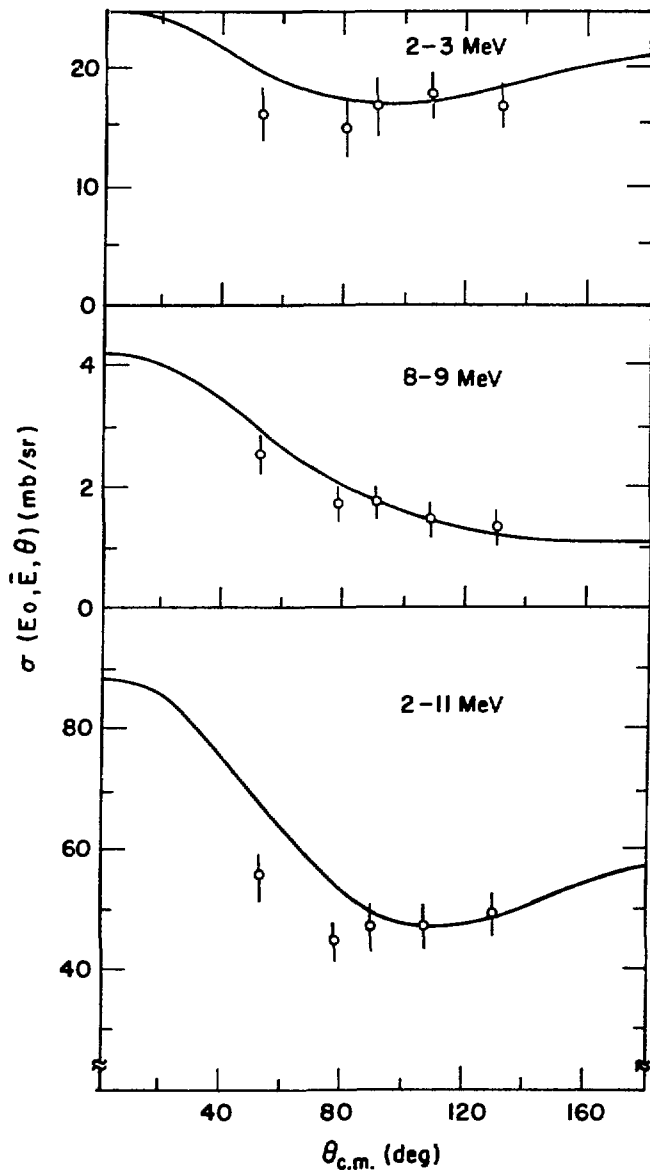
Fig. 3.
Angular distributions of emitted neutrons from 14.6 MeV
neutron interactions with iron calculated using the Kalbach-
Mann [26] expressions are compared to the Hermsdorf [27]
data for several ranges of secondary energy.

AU TOTAL CROSS SECTION
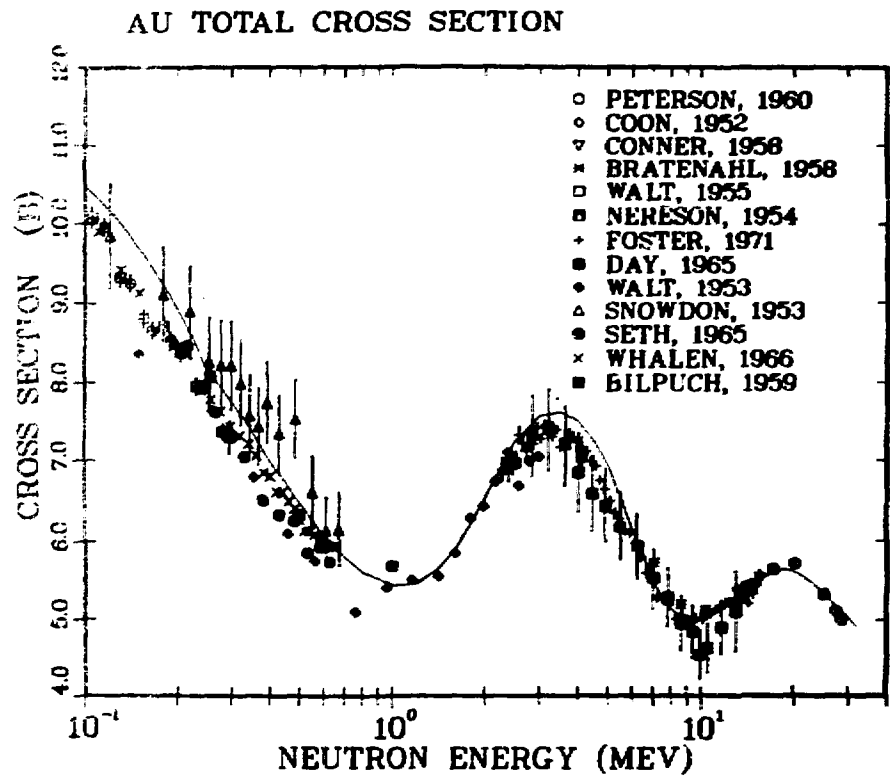
Fig. 4.
The [197]Au total cross section determined from coupled-
channel calculations using the Delaroche optical parameters
[45] are compared to experimental data.
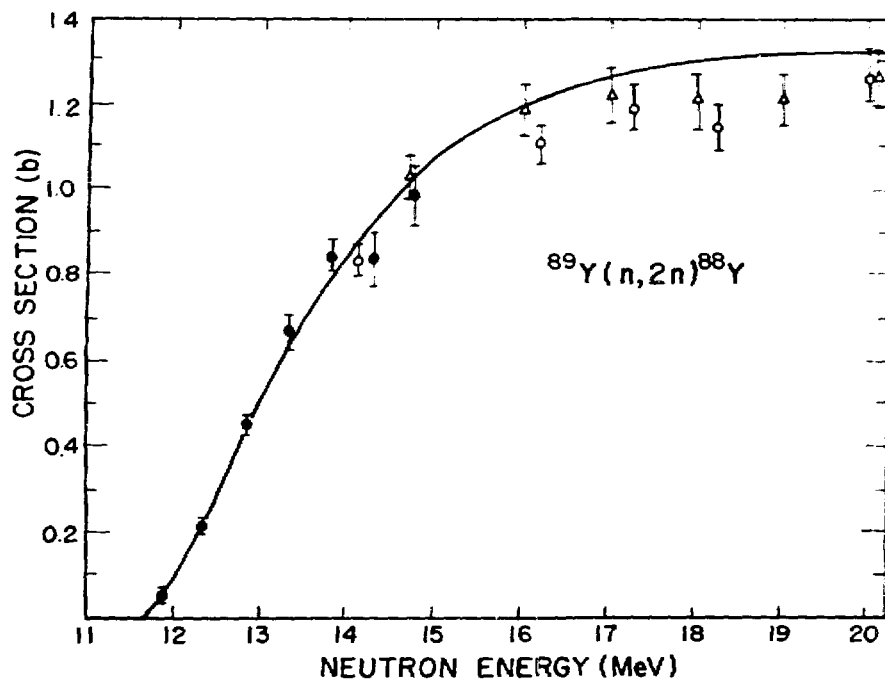
Fig. 5.
Cross sections for the ^{89}Y(n,2n) reaction obtained from
GNASH calculations using the Lagrange optical parameters
[46] are compared to recent measurements [17-19] of this
reaction.
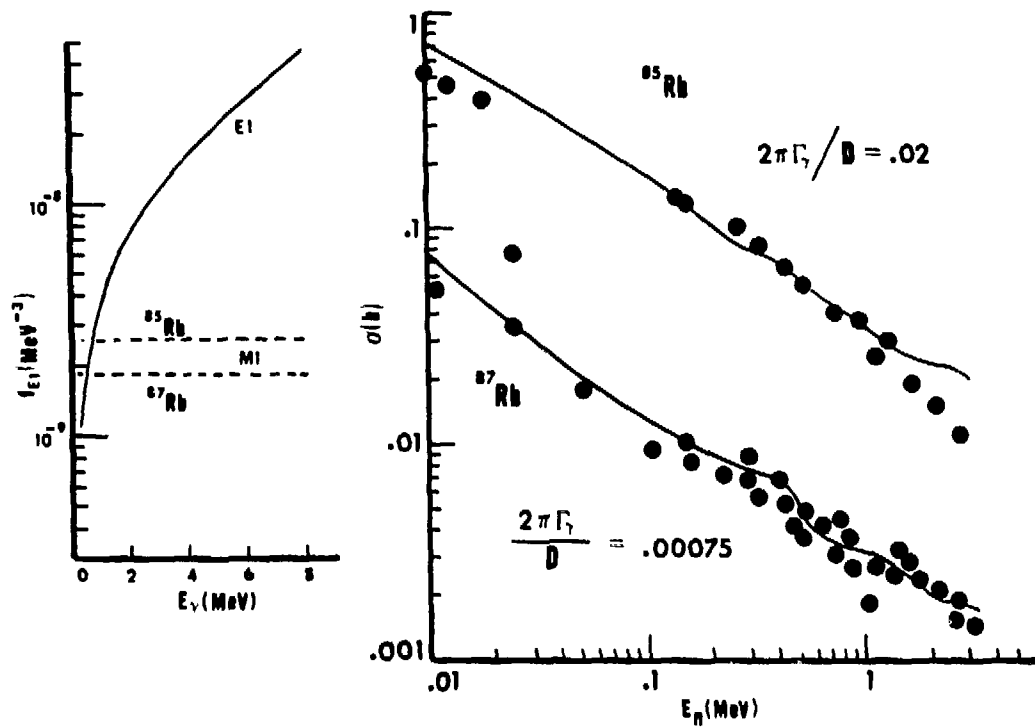
Fig. 6.
Calculated ^{85,87}Rb(n,γ) cross sections [48]. The same E1
strength function (shown at the left) used for both isotopes
produces good agreement with experimental results.
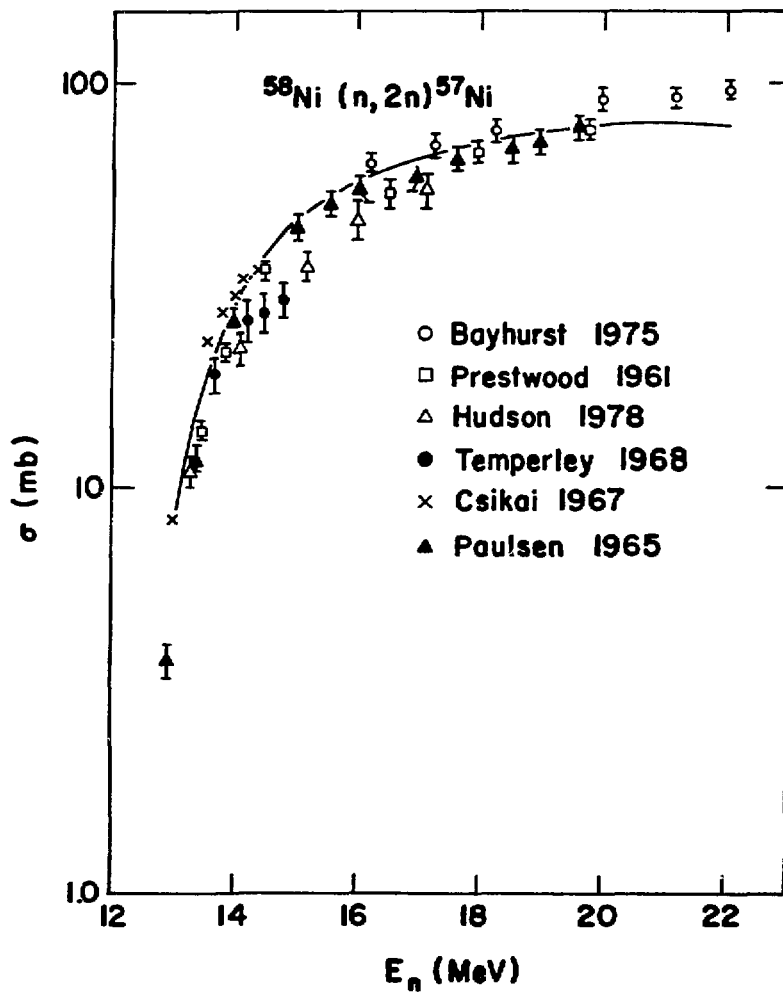
Fig. 7.
Cross sections calculated for the ^{58}Ni(n,2n) reaction using
consistent sets of input parameters are compared to
experimental data.
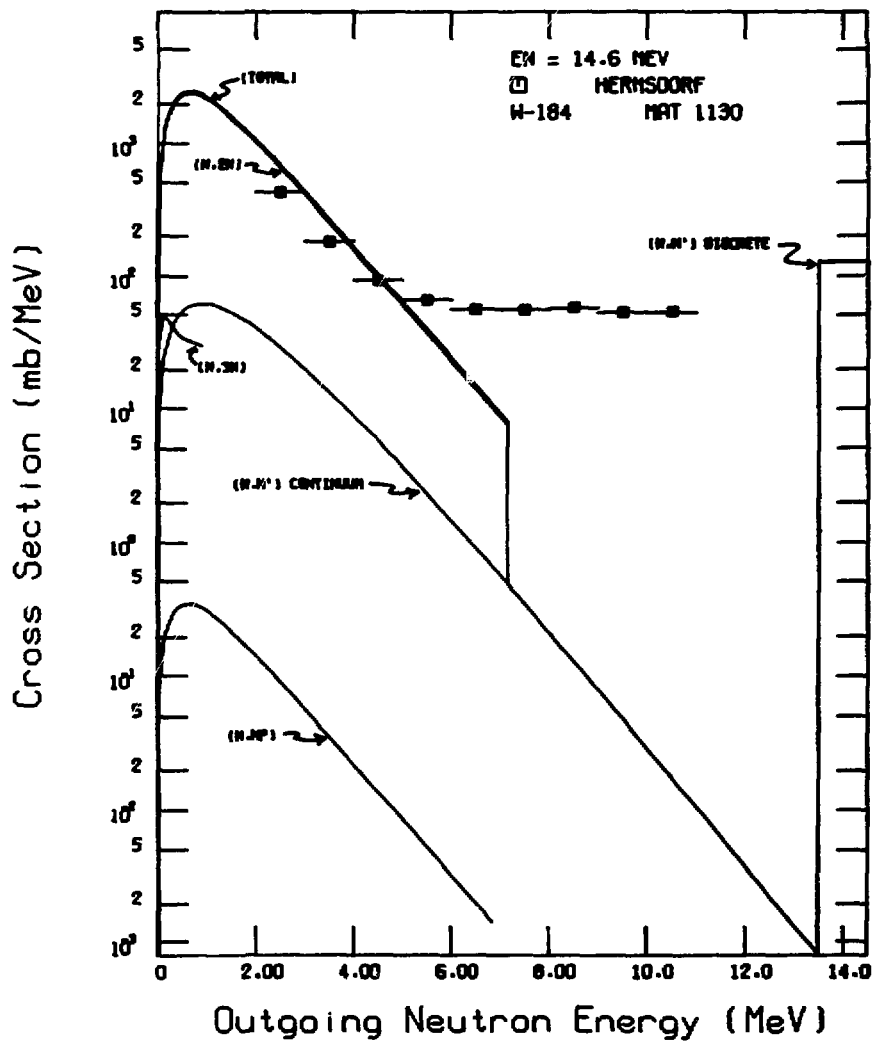
Fig. 8.
The partial and total neutron emission spectra from the
ENDF/B-V ^{184}W evaluation are compared to the data of
Hermsdorf [27] measured at 14.6 MeV for natural tungsten.

TUNGSTEN , ENDF/B
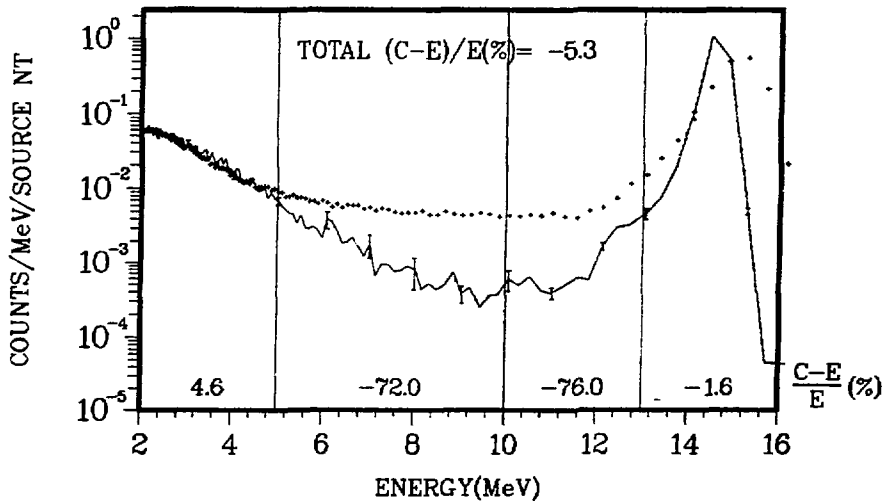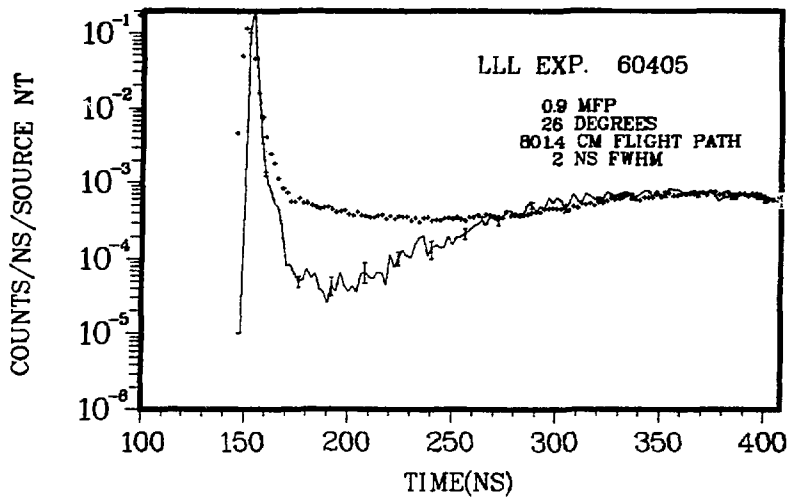
Fig. 9.

Calculated spectra (solid curves) obtained through use of
the ENDF/B-V evaluated tungsten data are compared to experi-
mental results from 14-MeV pulsed-sphere measurements.
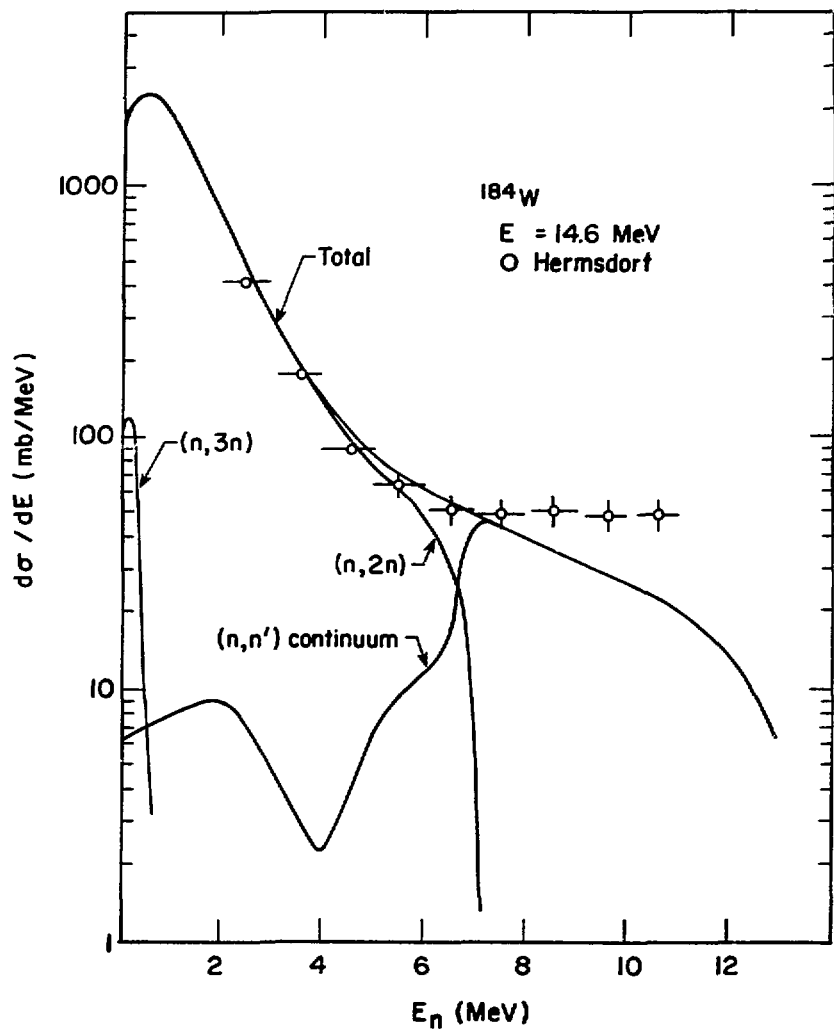
Fig. 10.
The partial and total neutron emission spectra obtained from
new calculations [71] on ^{184}W are compared to the Hermsdorf
data. Direct reaction contributions included in the calcula-
tions do not appear in this comparison.
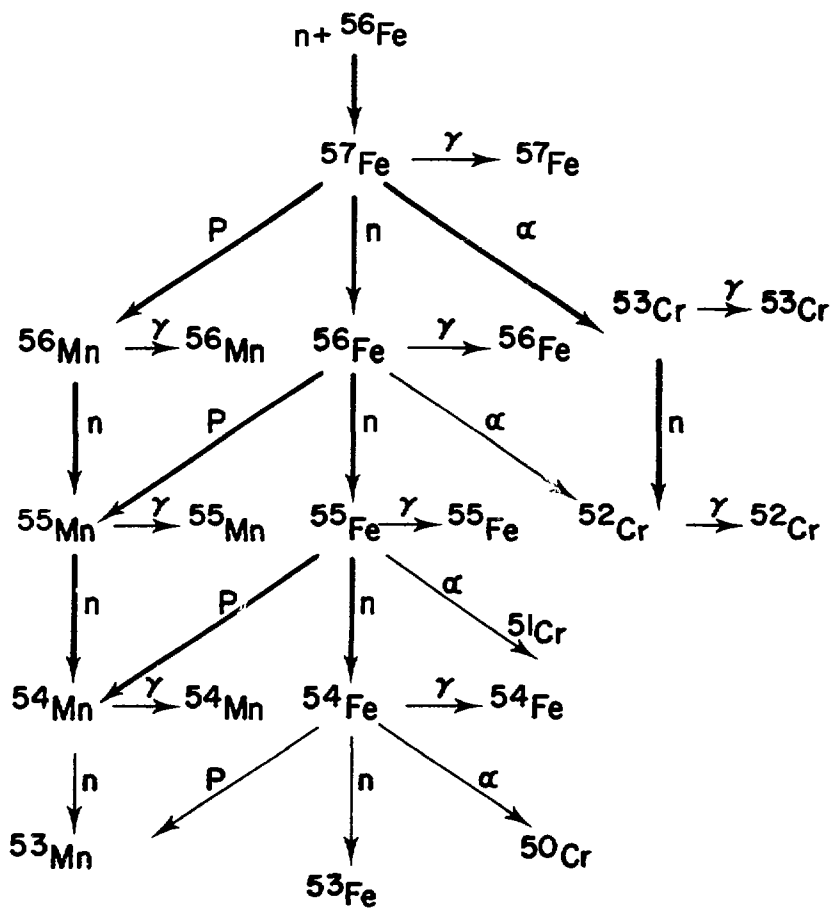
Fig. 11.
The reaction chain used for the calculation of neutron
reactions on iron [64] up to energies of 40 MeV.
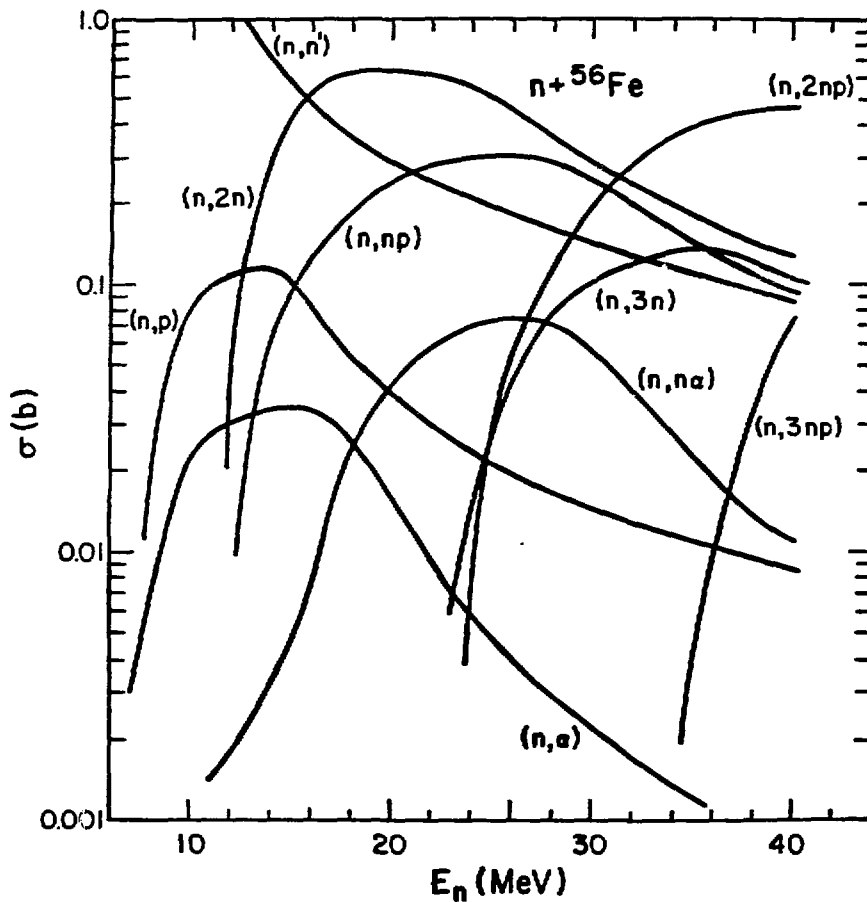
Fig. 12.

Theoretical n + ^{56}Fe cross sections obtained from GNASH
calculations using the reaction chain shown in Fig. 11.
Note that above 30 MeV, processes such as (n,np) and (n,2np)
compete with and begin to dominate over reactions involving
solely neutron emission.
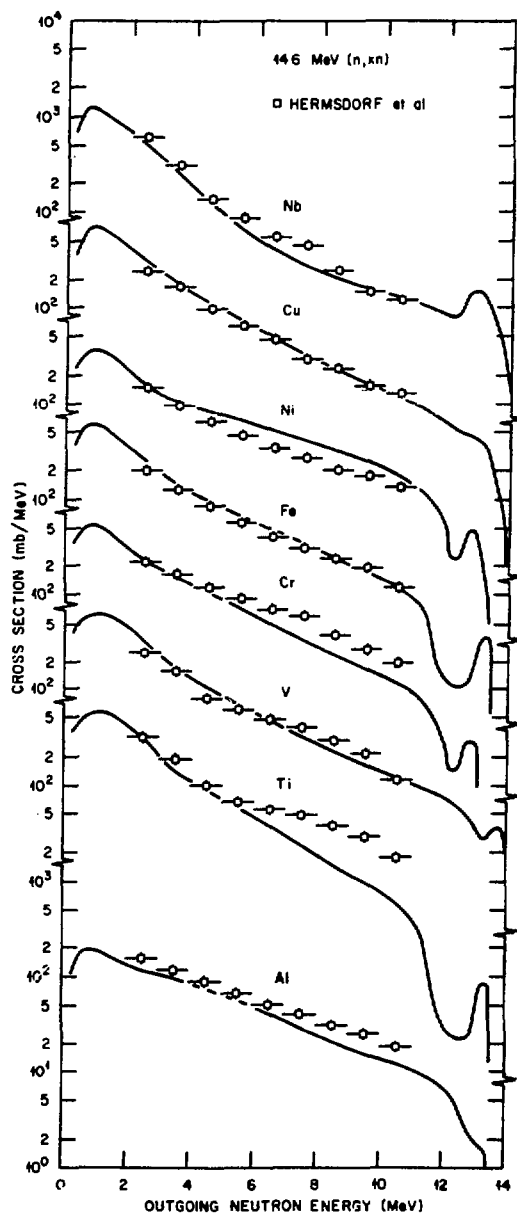
Fig. 13.

Neutron production spectra obtained through calculations using the unified Hauser-Feshbach-preequilibrium model of Fu [75] are compared to the 14.6 MeV Hermsdorf data for eight natural elements.

Discussion

Peelle

Now that evaluation tools employing nuclear model codes are becoming rather well developed, how does one or how might one assess uncertainty in cross section values obtained with their help?

Arthur

Up to now the assessment of errors from nuclear model calculations has generally been rather crude and subjective relying mainly on estimates made by the calculator based on a confidence placed on the input parameters. There have been recent analyses made by Vonach et al., of the errors on calculated cross sections after systematic variation of input parameters within physically accepted limits. At higher neutron energies such efforts can be difficult because of the long computational times needed for some of these models. Also there may be instances where a given model is not applicable so that the errors obtained may be meaningless.

Vonach

In our evaluation work we have made studies to estimate the uncertainties of model calculations by studying the sensitivity of the calculations to parameter variation within their estimated uncertainties. From the results of such calculations, a covariance matrix can be obtained and subsequently treated in the same way as covariance matrices for measurments. We intend to continue to follow this line of bringing calculational results and measurements into the same formal framework.

Poenitz

I looked at the same question for $^{238}U(n,\gamma)$. One can partition the problem in two parts, the first part is easy: one determines the uncertainty of model parameters from the uncertainty of the experimental data on which they are based. Investigating the sensitivity of the calculated quantity leads to the estimate of the uncertainty. The second part, that is the uncertainty from the model approximations, is much more difficult to estimate. This is related to the philosophical point that these are all empirical models and they can be only as good as the measured data. We can use them to fill in the gaps but utimately they can be only as good as the best experimental data. It is only following new experiments that improvements to models are made. The best example of this can be seen if one follows the development of the optical model.

Menapace

I would like to point out possible limitations arising, in this kind of calculation, from the use of the presently available microscopic formulas for level density at high excitation energies. As a consequence, the equilibrium contribution can be underestimated, with a questionable parameterization of the adopted pre-equilibrium model resulting.

Arthur

That's true. In the higher energy calculations, preequilibrium emission dominates and you are back to the state densities that were derived from Gilbert-Cameron or Fermi Gas Model.

Gruppelaar

What kind of description would you like to adopt for emission spectrum files? Do you think of a mixed description by an evaporation expression and a point-wise representation or would you like to adopt unequal bin sizes in your model code to obtain a fine-grid representation at low emission energies?

Arthur

Up to now we have employed histogram representation with some crude effort to provide a fine grid representation in energy regions where thresholds occur. I see nothing wrong with using such a mixed form representation however.

Mughabghab

What optical model parameters did you use to obtain your transmission coefficient? Did you vary these parameters to obtain the good fits in the case of ^{89}Y in the threshold region?

Arthur

The optical parameters of Lagrange were used with no adjustment to fit the $^{89}Y(n,2n)$ cross section data around threshold

SESSION XII

EVALUATION OF SMOOTH CROSS SECTIONS IN THE PRESENCE OF FISSION
Chairman: R.W. Peelle ORNL

EVALUATION OF NEUTRON CROSS SECTIONS FOR FISSILE AND FERTILE NUCLIDES IN THE keV RANGE[*]

L. W. Weston

Oak Ridge National Laboratory
Oak Ridge, Tennesseee 37830

ABSTRACT

Procedures for evaluation of radiative capture, elastic and inelastic processes, and fission in the keV region of neutron energies are described. The use of theoretical tools along with the available ENDF utility codes allows the evaluator to extend and expand upon the experimental data which are often sparse or discrepant. A few problems with the utility codes are noted and suggestions made for improvement and extension. Some ENDF/B-V cross sections for important nuclei are plotted in detail and show significant need for improvement in the shape of the individual partial cross sections to be consistent with theoretical predictions within the constraints of the experimental data. In particular, uranium and plutonium isotopic evaluations, which are of critical importance to fast reactors, deserve careful attention using improved methodology.

INTRODUCTION

Since detailed documentation of the procedures used for evaluations of the cross sections for ENDF/B in the keV region for the fissile and fertile isotopes are sparse, available techniques will be discussed in this paper with emphasis upon obtaining consistent results for the partial cross sections. In the past, partial cross sections have often been evaluated by different evaluators with little consideration of the interactions between the individual cross sections. A more unified approach to evaluation

---

should yield improved results because theory places constraints upon the partial cross sections within the uncertainty of the experimental data.

FISSION CROSS SECTION

Usually more experimental data on the fission cross section exist in the energy region of concern than on the other cross sections. Because of the ample data, evaluations are normally based almost completely upon these measurements rather than model calculations. As an example, the fission cross section data and evaluation [1,2] for Pu-241 are compared in Fig. 1. At first inspection one would consider a simple least-squares fit to all the data to be the obvious solution. Unfortunately this is seldom practical because it is common for the experimental data to be discrepant by many standard deviations. This is understandable when it is considered that the experimentalist can usually reduce the measurement uncertainties of which he is aware to the point where these uncertainties are smaller than the unknown systematic uncertainties.

In practice much intuition and renormalizing of data is used in the evaluation of fission cross sections. There are always uncertainties in the absolute magnitude of the cross section so that internormalization of data sets is commonly carried out in order to evaluate the shape of the cross section. In the keV region the fission cross section is usually measured relative to those of $^{10}B(n,\alpha)$ or the $^{6}Li(n,\alpha)$ up to about 100 keV and relative to $^{235}U(n,f)$ at higher neutron energies. Exceptions to this are a few absolute measurements and measurements relative to the (n,p) scattering in hydrogen. Examples of shape fitting techniques is the least squares code being developed by M. Bhat [3] and W. P. Poenitz [4].

The uncertainty file for a fission cross section evaluation may be obtained with a code such as SUR [5] by F. C. Difilippo. This code assumes the various input data sets are independent and computes the uncertainty file directly from the experimental data. The uncertainty in the standard cross section used to measure the flux must also be considered in determining the uncertainty file. When there are only one or two experimental data sets available for a partial cross section, then the uncertainty file must be evaluated from the uncertainties quoted by the experiments.

TOTAL CROSS SECTION

The total cross section in the keV neutron energy region for the fissile and fertile nuclei normally has less structure than the partial cross sections and is the most consistent among the nuclides. The level spacing for these nuclei is usually not large

compared to the Doppler width of the resonances in the keV neutron energy region; therefore the total cross section is smooth.

The average total cross section is composed of potential scattering which is smooth and slowly varying with the phase shift; the resonance term which is dependent upon the neutron strength function which varies slowly with neutron energy, and a term due to many-level interference [6]. Since the total cross section is not dependent on the parameters of the exit channels, it is not expected to show the rapid variation as do the partial cross sections.

The evaluation of the average total cross section is useful since it limits the sum of the partial cross sections. Since only the entrance neutron channel and not the exit channels effects the total cross section, a new channel which opens, such as inelastic scattering, must compete with other channels which are already open. For evaluations of the fissile and fertile nuclei accurate average total cross section measurements from the keV region up to 20 MeV are needed.

CAPTURE CROSS SECTION

In most cases fewer measurements of the capture cross section than the fission cross section are available. The experimental measurements are appreciably more difficult and uncertainties much larger. When the nuclide has a large fission cross section only measurements of the ratio of the capture cross section to the fission cross section (alpha) are usually made.

In evaluating the capture cross section in the keV region there is another important consideration in addition to average capture cross section measurements. One should also consider the average resonance parameters determined from the resolved resonance region. For many of the nuclides under consideration, the s-wave strength function and level spacing have been derived from measurements in the resolved resonance region. The average capture cross section can be expressed [7] approximately as:

$$\sigma_{n,\gamma}^{\ell} = \frac{2\pi^2}{k^2} \sum_{J}^{NJS_{\ell}} \frac{g_J}{\bar{D}_{\ell,J}} \left\langle \frac{\Gamma_n \Gamma_\gamma}{\Gamma} \right\rangle_{\ell,J} \tag{1}$$

where $\bar{D}$ is the average level spacing, Γ_n the neutron width, Γ_γ the radiation width and Γ is the total width. The total width is the sum of the partial widths;

$$\Gamma = \Gamma_n + \Gamma_f + \Gamma_\gamma + \Gamma_{xr} \quad , \tag{2}$$

where Γ_{xr} is a competitive width such as inelastic scattering. The expression for the fission cross section is identical to that for capture upon substitution of the fission width, Γ_f, for the radiation width, Γ_γ. The average in Eq. (1) is over the proper statistical distribution for each partial width.

There is a code, UR, written by E. Pennington which is available from the National Nuclear Data Center, which will calculate average resonance parameters to describe a capture and fission cross section at a given neutron energy. Unfortunately, this code calculates on a point-by-point basis by varying $\bar{\Gamma}_n$ and $\bar{\Gamma}_f$ but does not fit with energy independent parameters. This lack of flexibility makes the code difficult to use when considering average parameters from the resolved resonance region for use in an evaluation. In the keV region one must also include p-wave and d-wave parameters which are usually not available from the resolved resonance region analysis. These parameters may be estimated approximately, however.

Figure 2 shows an evaluation of the average capture cross section for Pu-240 where the average resonance parameters from the resonance region strongly influenced the evaluation [1]. Without such an influence the evaluation of the capture cross section in the 5- to 80-keV region would have been higher. The data of Wisshak and Käppeler [8] were not available at the time of the evaluation. Another example [9] of this type of fitting is shown for the capture cross section of Np-237 in Fig. 3. In this example, the average resonance parameters from the resolved resonance region, the experimental data in the keV region and theory were all used to obtain an average resonance parameter fit.

INELASTIC SCATTERING

Inelastic scattering is a competitive reaction which usually makes a significant contribution in the neutron energy range of concern in this paper. There are known discrete inelastic scattering levels in all the fissile and fertile nuclides below a half MeV. At higher neutron energies inelastic scattering will not be considered in this paper.

Inelastic scattering to discrete levels has been measured for a few discrete levels in the fissile and fertile nuclei but in most cases model calculations must be relied upon for estimates of these cross sections and their angular distributions. A good example of the treatment of inelastic scattering in an evaluation [10] is shown in Fig. 4 for U-238. Both experimental measurements and model calculations have been used to evaluate the inelastic scattering from the 45-keV level and the effect on the capture and scattering cross sections have been taken into account properly. Note there is a decrease in the capture cross section which corresponds to the onset of inelastic scattering.

The effect of inelastic scattering on the elastic scattering, capture, and fission cross section is through the average total width, Γ, shown in Eq. (1). The inelastic scattering width, $\Gamma_{n'}$, is summed with the other partial widths to form the total width as given in Eq. (2). It should be noted that inelastic scattering affects capture, fission, and elastic scattering proportionally but does not affect the total cross section.

Unfortunately, the ENDF/B format allows only one discrete inelastic scattering channel in the unresolved resonance region [11] and many processing codes do not allow the average total width to be neutron energy dependent. Thus the first inelastic scattering channel must be carefully handled and usually the unresolved resonance region in ENDF is ended before the onset of the second and higher inelastic levels which have a major contribution.

For many of the important nuclides, the other partial cross sections are evaluated independently of the inelastic scattering with the corresponding loss of information and physical meaningfulness. An example [2] of this is Pu-241 as shown by the data in Fig. 5. Often in such cases the elastic scattering is considered as a free parameter to force the partial cross sections to add to the total. In the author's opinion, the experimental data and model calculations should be fit with unresolved resonance parameters up to the point in neutron energy where the density of inelastic channels makes this procedure impractical. The ENDF format does not allow the use of the parameters to such a high neutron energy, however, a more physically meaningful evaluation could be obtained in this manner. There is a need for a code to implement such a procedure.

EXAMPLES OF ENDF/B-V EVALUATION

The ENDF/B-V evaluations for U-238 and Pu-241 have been illustrated in Figs. 4 and 5. For U-238 the inelastic scattering was taken into account properly which was not the case for Pu-241. The structure in the Pu-241 cross sections between 100 and 1000 eV was indicated in the experimental data [12] and is an example of structure in the unresolved resonance region. The details of this structure are surprising since it would normally be expected in the fission but only weakly in the capture channel. This structure is apparently a modulation of the strength function and not the more commonly found intermediate structure in the fission widths.

The ENDF/B-V evaluation [13] of U-235 is shown in Fig. 6. The evaluation exhibits structure in the cross sections up to 100 keV as was indicated by the experimental data. Because of the importance of U-235 as a standard cross section as well as a fuel, this structure was represented in the evaluation. As a standard cross section, U-235 is only accepted above 100 keV because of this structure.

The inelastic scattering for U-235 shown in Fig. 6 was carried over from Version IV and there are plans [14] for a new evaluation.

When this evaluation is performed the interaction on the other partial cross sections should also be considered.

The Pu-239 evaluation [15] for ENDF/B-V is shown in Fig. 7. The structure in the fission and capture cross sections from 100 to 300 eV is an attempt to reproduce the fluctuations which appear in the fission cross section measurements and the measurements of the ratio of capture-to-fission cross sections. The shape of this structure was carried over from ENDF/B-IV and could be improved if more recent data were considered. Figure 8 illustrates part of the experimental data [16] on alpha in this neutron energy range.

The unresolved resonance region for Pu-239 extends up to 25 keV, however, the 7.85-keV inelastic scattering level was not handled in a systematic manner by means of average resonance parameters. The structure in the capture cross section at about 50 keV is mysterious, since the experimental measurements of alpha, the ratio of capture-to-fission, do not indicate such structure. The inelastic thresholds at 57.3 and 75.7 keV could affect the capture but not in this manner.

CONCLUSIONS

The procedures for the evaluation of neutron cross sections for some of the fissile and fertile nuclei in the keV neutron energy region have been discussed and examples shown. The general conclusion must be that the ENDF evaluations have considered the available data and are reasonably acceptable; however, much opportunity for improvement is an unavoidable conclusion. Whether such improvements are needed is best left to the users of ENDF for practical applications, but one has difficulty supporting results obtained by techniques now known to be inappropriate. If one judges by the request list [17] for these neutron cross sections for applied uses then the need is inescapable.

The recommendation of the author is that more versatile evaluation tools should be developed which employ as much theory as practical and will fit the experimental data in such a manner that all the partial cross sections will be consistent. Uncertainty files for the unresolved resonance parameters could be produced by these same evaluation tools. The development of such evaluation tools would not be trivial, but should measurably improve future evaluations.

ACKNOWLEDGMENTS

REFERENCES

1. L. W. WESTON, "Evaluation of the Fission and Capture Cross Sections of Pu-240 and Pu-241 for ENDF/B-V," Proc. Intern. Conf. on Nuclear Cross Sections for Technology, Knoxville, Tennessee (1979) to be published.

2. ENDF/B-V data file for Pu-241 (MAT 1381), evaluated by L. W. Weston, R. Q. Wright, and R. J. Howerton, BNL-17541 (ENDF-201), edited by D. Garber, available from the National Nuclear Data Center, Brookhaven National Laboratory, Upton, N. Y. (1975).

3. M. BHAT, Brookhaven National Laboratory, private communication.

4. W. P. POENITZ, J. W. MEADOWS, and R. J. ARMANI, "The Evaluation of ^{235}(n,f) above 100 keV for ENDF/B-V and the Implications of a Unified ^{235}U Mass Scale," Proc. Intern. Conf. on Nuclear Cross Sections for Technology, Knoxville, Tennessee (1979), to be published.

5. F. C. DIFILIPPO, "SUR, A Program to Generate Error Covariance Files," ORNL/TM-5223 (1976).

6. J. E. LYNN, "The Theory of Neutron Resonance Reactions," Claredon Press, Oxford (1968), p. 217.

7. ENDF-102, "Data Formats and Procedures for the Evaluated Nuclear Data File, ENDF," BNL-NCS-50496 (1979), p. D.15.

8. K. WISSHAK and F. KÄPPELER, Nucl. Sci. Eng. 69, 39 (1979).

9. L. W. WESTON and J. H. TODD, "Neutron Capture Cross Section of Neptunium-237," to be published.

10. W. P. POENITZ, "Fast-Neutron Capture Cross Sections of Importance in Technological Applications," Proc. Intern. Conf. on Nuclear Cross Sections in Technology, Knoxville, Tennessee (1979), to be published.

11. ENDF-102, "Data Formats and Procedures for the Evaluated Nuclear Data File, ENDF," BNL-NCS-50496 (1979), p. D.36 - D.39.

12. L. W. WESTON and J. H. TODD, Nucl. Sci. Eng. 65, 454 (1978).

13. ENDF/B-V data file for ^{235}U(MAT 1395), principal evaluator M. R. Bhat, BNL-17541 (ENDF-201), edited by D. Garber, available from the National Nuclear Data Center, Brookhaven National Laboratory, Upton, N. Y. (1975).

14. L. STEWART, Los Alamos Scientific Laboratory, private communication.

15. ENDF/B-V data file for ^{239}Pu (MAT 1399), principal evaluators E. Kujawski and L. Stewart, BNL-17541 (ENDF-201), edited by D. Garber, available from the National Nuclear Data Center, Brookhaven National Laboratory, Upton, N. Y. (1975).

16. R. GWIN et al., Nucl. Sci. Eng. 59, 79 (1976).

17. Compilation of Requests for Nuclear Data, BNL-NCS-51005 (1979).
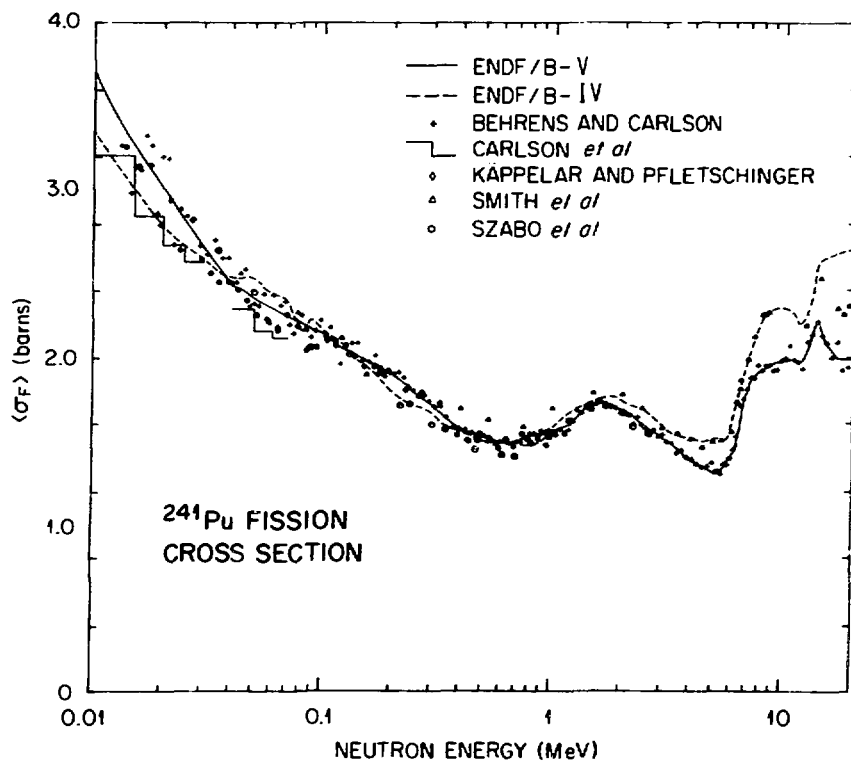
Figure 1. The Fission Cross Section of Pu-241; Experimental Data and ENDF/B-V Evaluation.
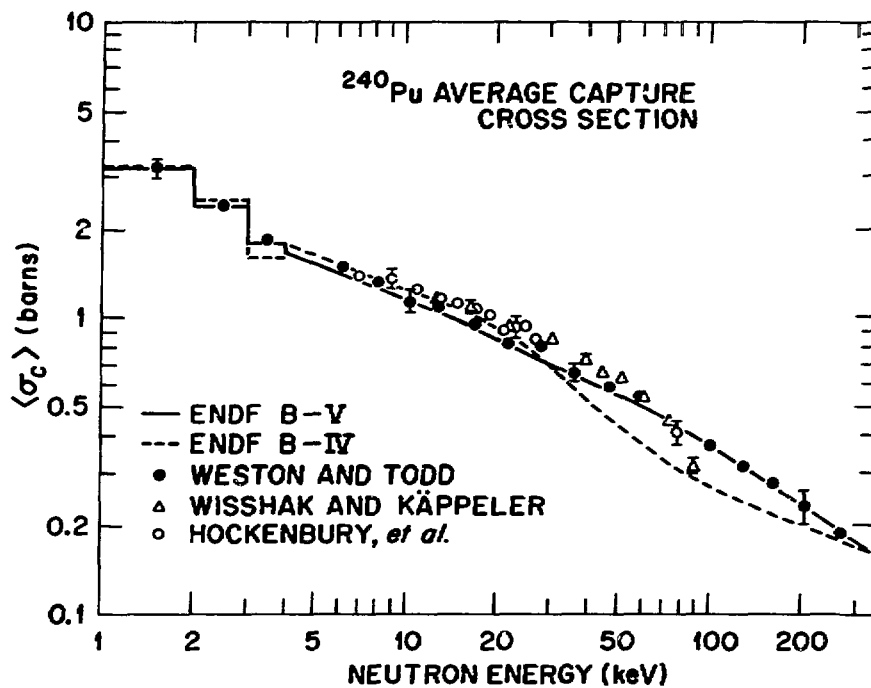
Figure 2. The Pu-240 Average Capture Cross Section; Experimental
Data and ENDF/B-V Evaluation. An example of the use of
average resonance parameters from the resolved reso-
nance region.
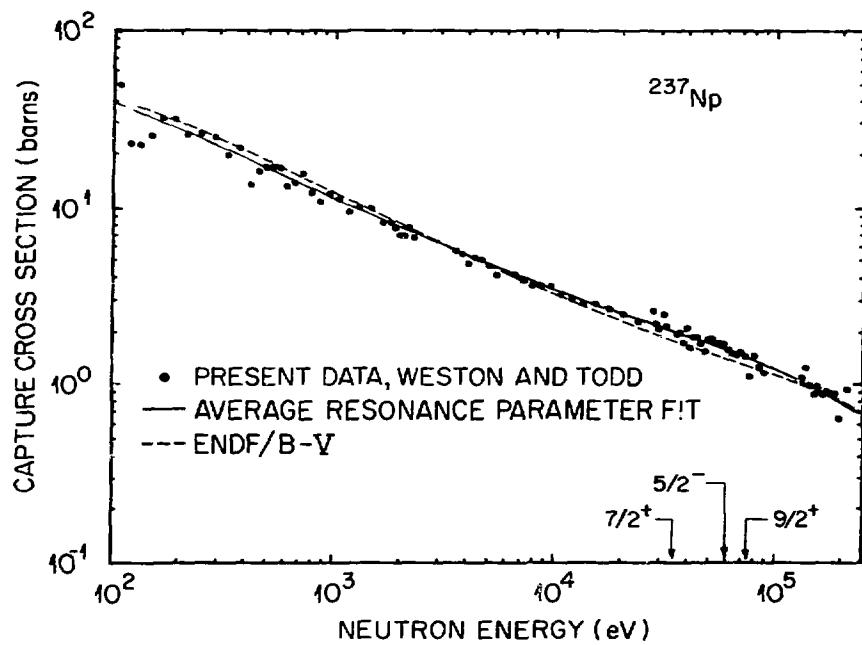
Figure 3. The Np-237 Average Capture Cross Section. An example
of an average resonance parameter fit to experimental
data.
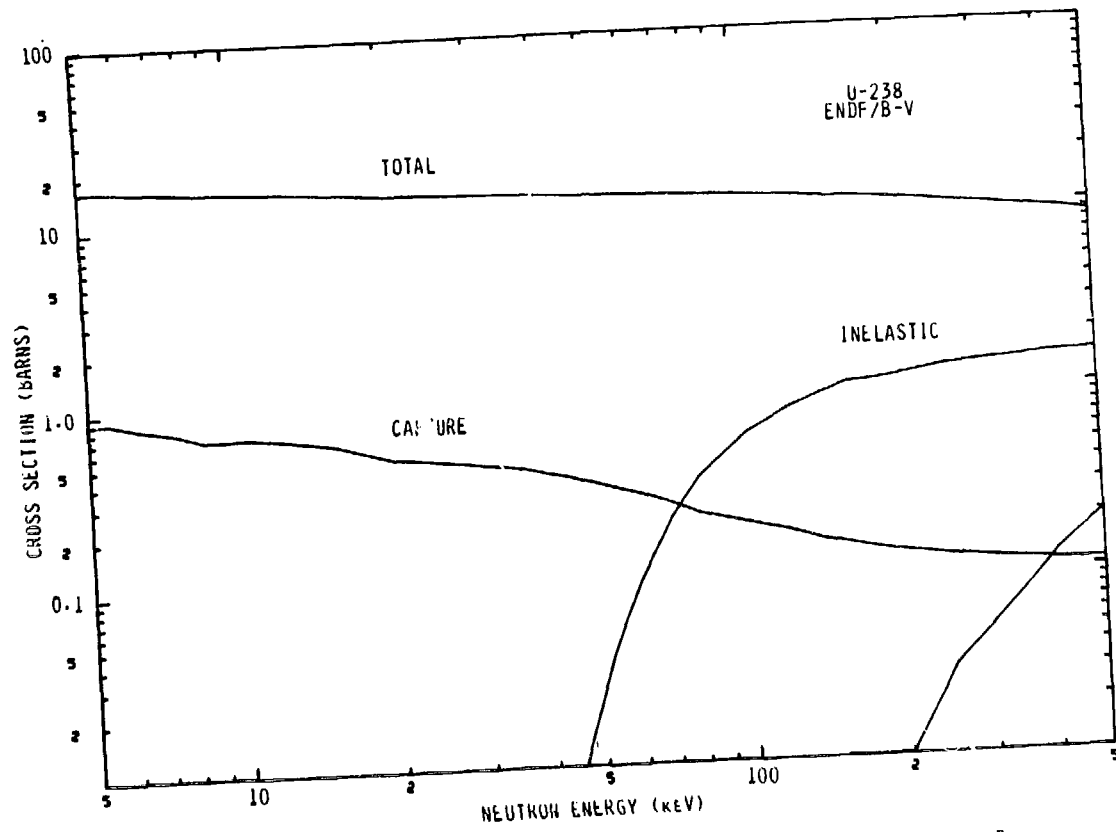
Figure 4. The ENDF/B-V Evaluation of the U-238 Cross Sections from 5 to 500 keV Neutron Energy.
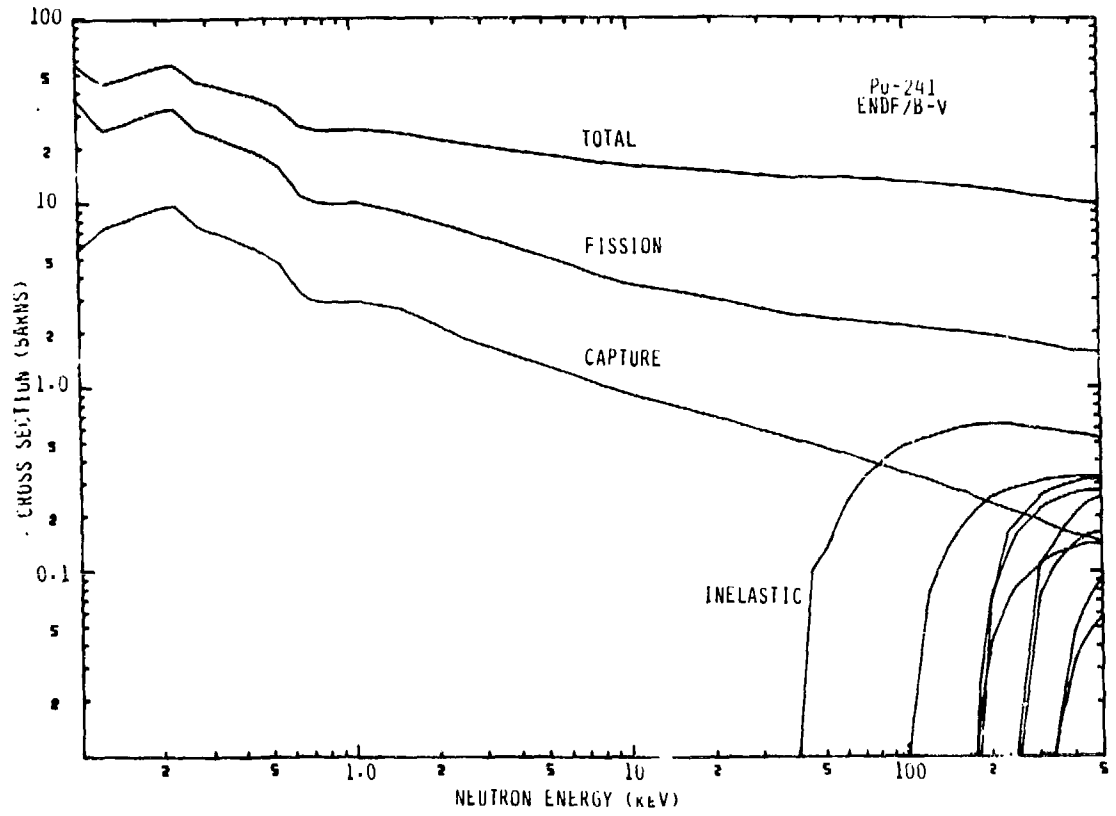
Figure 5.   The ENDF/B-V Evaluation of the Pu-241 Cross Sections from
1 to 500 keV Neutron Energy.
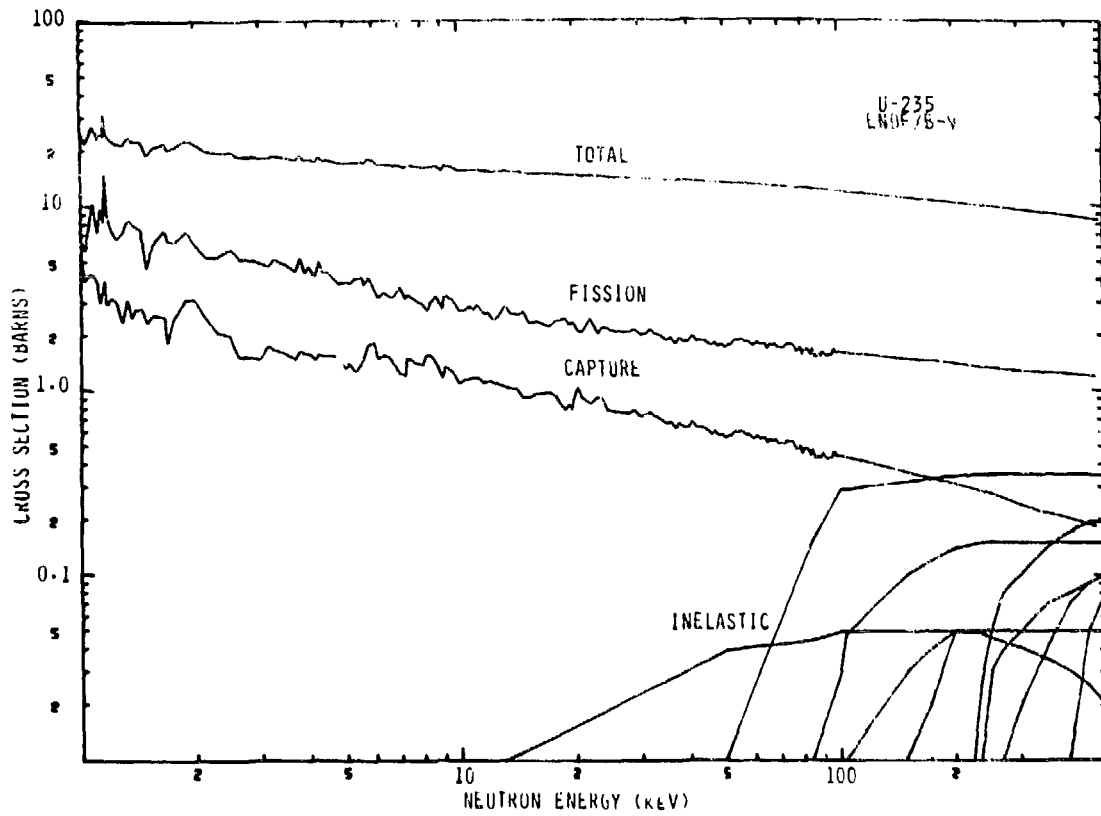
Figure 6. The ENDF/B-V Evaluation of the U-235 Cross Sections from 1 to 500 keV Neutron Energy.
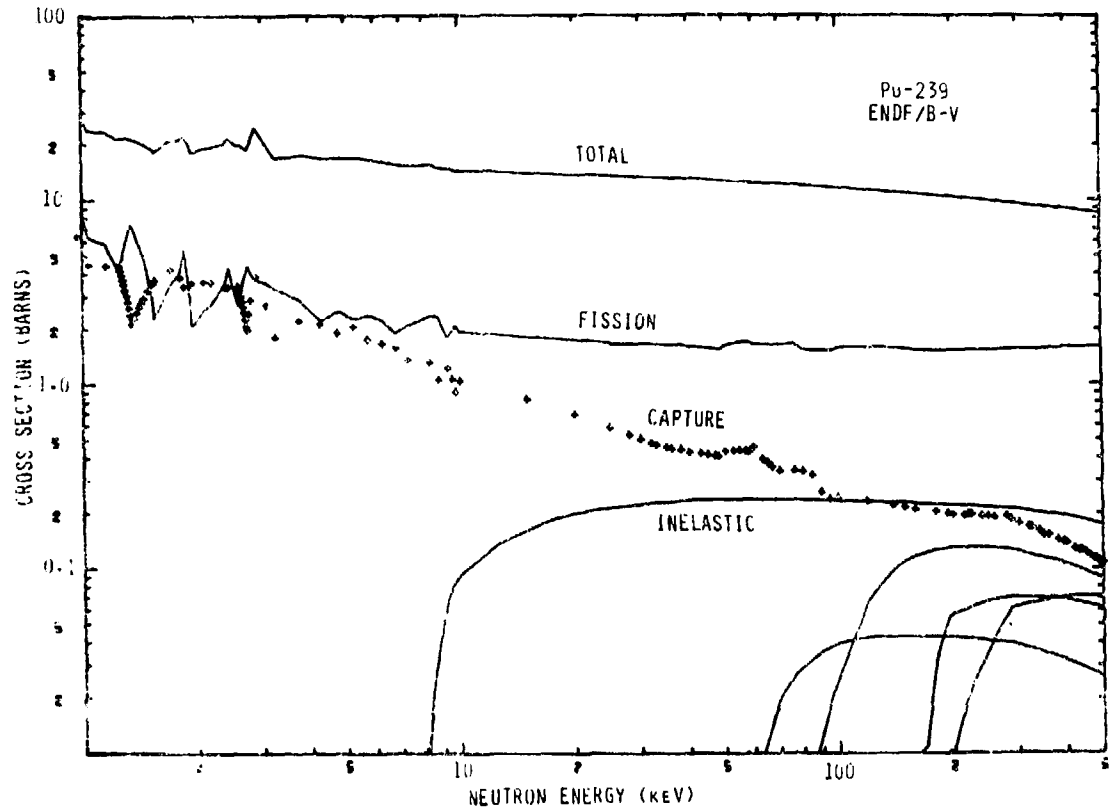
Figure 7. The ENDF/B-V Evaluation of the Pu-239 Cross Sections from 1 to 500 keV Neutron Energy.
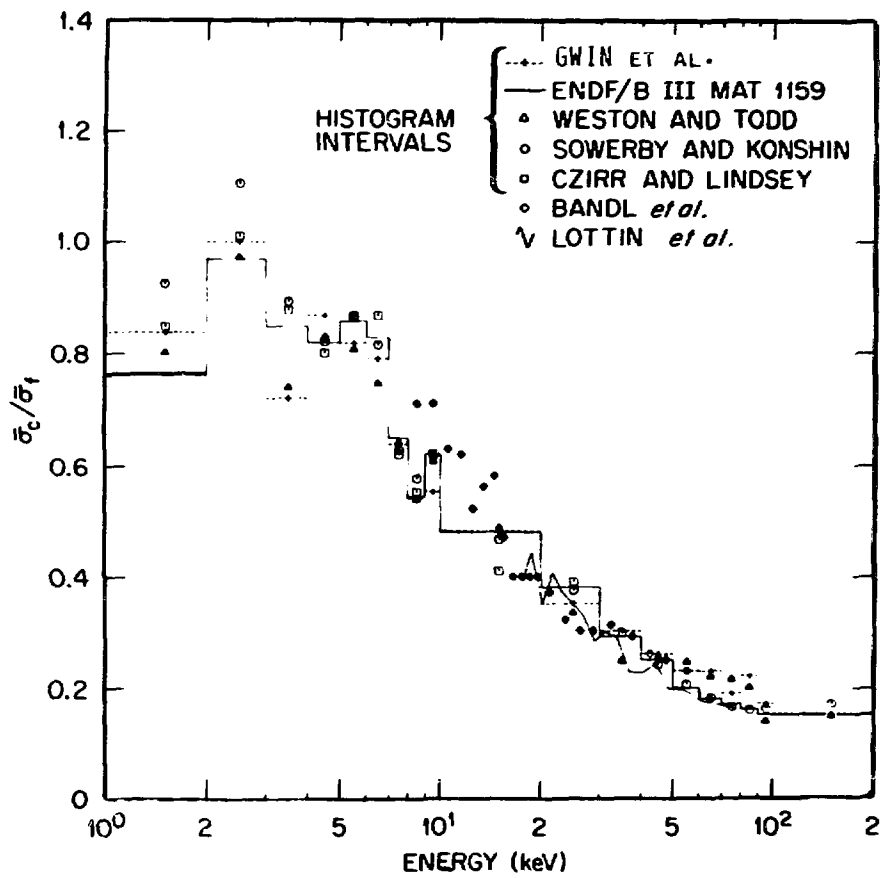
Figure 8. Experimental Measurements of $\bar{\sigma}_c/\bar{\sigma}_f$ for Pu-239 from 1 to 200 keV Neutron Energy.

Discussion

Poenitz

I certainly agree that the models should be used to obtain con-
sistency between the reactions. However, I feel somewhat insecure
to use resonance parameters obtained in the resolved resonance
range for the unresolved resonance range. The problem is the
fluctuations, and parameters obtained in a limited energy range may
not be average values.

Weston

It is true that one must be careful with the use of resonance re-
gion average parameters, however, it is added information which
should not be ignored.

Moore

I am not sure what the objection is to the competitive width when
there is more than one inelastic channel. You can sum up and get
an energy-dependent effective width. You are not supposed to use
the output of that competitive width calculation anyway. So you
can lump more than one inelastic channel there if you want to.

Weston

Yes, I was only pointing out that one cannot put all this informa-
tion into ENDF, but having it helps one fit and understand the
cross section.

Howerton

Are you advocating requiring using unresolved region resonance
parameters in the data files or are you advocating that the eval-
uator use these parameters as an evaluation tool with pointwise
data being entered, as has been done in the past?

Weston

I am advocating that the evaluator should use unresolved resonance
parameters to as high a neutron energy as possible in order to ob-
tain an accurate, consistent evaluation which is physically mean-
ingful. The results can be entered in ENDF as unresolved param-
eters up to the second important inelastic scattering level and
then pointwise data. No format change would be required.

<u>Peelle</u>   (to assembly)

Are inconsistencies among and within actinide evaluations, like
those mentioned here for ENDF/B-V, also present in other sets of
evaluations?

<u>Howerton</u>

There are some minor and major inconsistencies in the ENDL files.

<u>Froehner</u>

In response to Bob Peelle's question, I can say this about KEDAK.
There used to be inconsistencies with theoretical concepts like
resonance formulae. These were gradually weeded out in recent
years by generating cross sections with R-matrix and level-
statistical codes in a consistent manner, i.e., all competing
cross sections from one set of parameters. New inconsistencies
threaten to creep in, however. For example, a level-statistical
calculation of the ^{235}U fission cross section below 100 keV is
certainly inconsistent with the best data, in particular with
the pronounced fluctuations of those. One is again confronted
with the questions of whether the file should be general, con-
taining all detail, or applications-oriented, containing simpli-
fied data. At present we try to keep KEDAK general, storing
data in detail, but also furnishing average parameters for aver-
age cross section generation.

<u>Rowlands</u>

Covariance data are needed for the resonance structure in the
unresolved region for a number of isotopes, primarily ^{238}U, but
also other isotopes. Because of this it seems to me to be better
to represent the mean resonance parameters and their uncertainties
explicitly in the files. However, quite detailed energy repre-
sentations might be needed to reproduce the broad-resolution
("intermediate" - ed.) structure.

<u>Smith</u>

1. Comment - Inconsistencies above about 100 keV in σ_T for acti-
nides are partly due to the experimentalists failing to measure
consistent sets across a breadth of targets and make proper cor-
rections (e.g., for self shielding).

2. At higher energies (e.g.,$\geq$ 1.0 MeV), the elastic component can
no longer be treated as a tree parameter in actinide evaluation
(because measurements are now good to 3-5%).

Weston

The use of average resonance parameters in a proper manner in an evaluation would prevent the elastic scattering or even the total cross section from being used as a free parameter. Accurate total cross sections with proper corrections are needed by evaluators.

Poenitz

I do not quite see whether there is a real need to represent the fluctuations on the file. I know only of two examples when this was considered: Rowland discussed a "fluctuation" of $\bar{\nu}$ around 400 keV and found no practical importance. Burns and Weisbin (Trans. Am. Nucl. Soc. 22, 724, November 1975) considered the fluctuations of $^{238}U(n,\gamma)$ in the unresolved resonance range and found that any effects are negligible compared with the importance of the absolute values of the cross section.

Peelle

Those fluctuations up to now have been more important to the evaluator in making sure that he combines the various data sources correctly than they have proven to be to most users. That is, so far they are mostly important in the intermediate phase in helping the evaluator obtain the correct average behavior.

Weston

Fluctuations which are of no importance to the users of the evaluations should be omitted but effects such as the drop in the capture and other partial cross sections at the onset of inelastic scattering are important and must be represented.

Stewart:

Some of the structure and deviations shown were large and structure shown in some of the files is often incorrect due to the fact that the cross section may be measured with good resolution compared to the resolution of the ratio measurement. Then the conversion of the ratio to the cross section needs to be handled correctly. In fact, some of the figures look like the structure may be inverted.

SOME METHODS USED IN EVALUATIONS OF NEUTRON CROSS SECTIONS FOR THE ACTINIDES IN THE MeV ENERGY REGION

B.H. Patrick

Nuclear Physics Division, Atomic Energy Research Establishment,
Harwell, Didcot, Oxon., U.K.

ABSTRACT

Evaluations of neutron cross sections of actinide
nuclei are derived from consideration of experimental
data where possible and the application of theory or
systematics to fill the gaps. The extent of the
actinide data base is shown. Methods used in the
evaluation of experimental data are examined and ways
of determining errors and correlations in evaluations
discussed. The theoretical methods which are applied
in the absence of measured data are outlined.

1. INTRODUCTION

This paper is intended to cover methods used in evaluations
of neutron cross sections in the presence of fission. In
consequence, the nuclei to be considered are those with atomic
number greater than or equal to that of actinium, which means
that discussion can be limited to the actinides, these being
defined as the nuclei with $Z = 89$-103 inclusive. In practice,
the actinium isotopes are of little or no interest and the
actinide region is generally taken to begin at thorium. The
primary importance of the actinides lies in their use in fission
reactor cores and in their presence as constituents of irradiated
fuel.

The paper considers the incident neutron energy range from
0.5 MeV up to ~20 MeV, although some flexibility will be allowed
in the low energy limit. The region below 0.5 MeV is being dealt

with in a paper by Larry Weston at this meeting.

Inevitably, the scope of the paper has to be limited. It has
not been possible to examine all actinide evaluations but it is
hoped that a fairly representative sample of methods used is
included, drawn, in general, from the more recent evaluations.
The paper examines techniques used in evaluations of measured
data but it will be shown that due to a dearth of experimental
data, much use is made of calculations based on theory and
systematics to produce the required cross section values. The
theoretical methods employed to fill in the gaps are outlined,
but for a more detailed account of the application of theory to
the evaluation of actinide nuclear data, see, for example, Lynn
[1] (and other papers in the same proceedings) or Konshin [2].

The use to which evaluations are put must always be borne in
mind when examining the methods employed by evaluators. In this
context, the main (and virtually only) reason for performing
evaluations of actinide cross sections is for purposes associated
with fission reactors or nuclear devices. As a result, there
will be cases in which, for example, cross sections in some
energy ranges are totally unimportant from a practical viewpoint
but which may have significance in the understanding of nuclear
structure or reaction mechanisms. In these cases, it may be
perfectly justifiable for the evaluator to ignore fine or
unimportant detail, although users should be made aware of such
treatment. Similarly, the accuracy to which specific data are
needed must always be an important consideration when producing
an evaluation. There is usually no great sense in applying very
sophisticated and expensive calculational methods where the
resulting accuracy is not justified, and where a simpler
technique will produce acceptable results. It follows that
evaluations which partly fall into these categories will not be
the subject of criticism.

It has already been noted that evaluations in the actinide
region are based on considerations of measured data and on
theoretical methods, the latter varying from arbitrary
assumptions about the behaviour of a particular cross section,
through phenomenological studies of systematics to detailed model
calculations. In general, as a result of the accuracy
limitations of theoretical calculations, evaluations are based on
measured data where they exist but, of course, this is by no
means an absolute rule. However, the importance of measured data
extends well beyond their usefulness in evaluations which are
based directly on them, since the parameters which comprise the
theoretical descriptions are obtained from the analysis of
measurements. For these reasons, the data base is very important
and worth some examination.

It is difficult to present a full picture of the extent and
size of the data base in a simple table but an attempt has been
made as given in Table I. The table supplies information on the
amount of measured data available for the most important cross
sections of actinide nuclei ranging from Th-230 to Cf-252.

Although $\bar{\nu}$ and the fission neutron spectrum are not actually part of this review (they will be dealt with by other reviewers), they have also been included in the table for added interest. Since the table includes only differential data, there may be additional information on the fission neutron spectrum in the form of nuclear evaporation temperatures which were not extracted by the search. The numbers contained in the table are in the form A(B), where A is the number of measured data points for which the incident neutron energy was >0.5 MeV and B is the number of experiments which contribute to A. The information was obtained from a search through the data stored in the NEA Data Bank at Saclay as at July, 1980. An upper energy limit of 50 MeV was also placed on the retrieval.

The numbers shown in Table I should not be taken too seriously. All evaluators know that, when the data on any particular quantity are examined with a view to performing an evaluation, it is frequently necessary to exclude some of the measurements for one reason or another, and the number of data points which are actually accepted can become quite small. The table does not show the energy distribution of the data points and even where there appear to be large numbers of values, there may be energy regions in which data are very scarce. It also became apparent when producing the table, that some data sets are included more than once in the compilation. For example, values may have been revised by the measurers at a later date and the original ones not removed when the new ones were added to the files. Some instances of this were eliminated but undoubtedly some are still included. The usefulness of the table lies as much, if not more, in the blank spaces which indicate a total lack of data above 0.5 MeV. The sparseness of the data base becomes clear and the minimum extent to which theory must be applied becomes apparent.

Table I shows that there are data on all the important cross sections for only four actinides, viz. Th-232, U-235, U-238 and Pu-239. As expected, the fission cross section is the most widely measured quantity, reflecting the relative ease with which measurements can be made on small quantities of material. Apart from the four actinides just mentioned, there are few capture measurements and the situation is even worse for the other cross sections. As for $\bar{\nu}$ and the fission neutron spectrum, there appears to be a reasonable amount of information on the former but for the latter, the only existing data for an incident neutron energy above 0.5 MeV seem to be for U-235.

The conclusions to be drawn from Table I are that while there is in general a reasonable amount of data for the major actinides, the situation for the less important actinides is fairly poor and much reliance has to be placed on theoretical calculations to provide the necessary values. It is true that the data base is somewhat enlarged, in so far as theory is concerned, by studies other than neutron interactions. For example, much information on fission probabilities and barrier

heights has been obtained from charged particle induced fission measurements, and details of nuclear energy levels lying below the neutron separation energy are found in other ways, but the bulk of the parameters have to be obtained by theoretical interpretation of the measured data which comprise the entries in Table I.

The remainder of this paper will be split into three main sections, the first dealing with methods used in evaluations of measured data and the second covering situations based on theory or systematics. In the last section, brief mention will be made of some non-statistical effects which occur at the higher energies and which have a bearing on actinide evaluations.

2. METHODS USED IN EVALUATIONS OF MEASURED DATA

It is not intended that this paper should deal with the processes by which an evaluator chooses acceptable data and which eventually lead to the values on which the evaluation is based. It is sufficient to record here an evaluator's obligation to revise measured values to take account of up-to-date standards and to assign errors (which may or may not be those defined by the measurers) to the data values. We shall begin the discussion at the point where an evaluator has a set of cross sections from which he must produce his recommended values.

At this stage, it is quite possible that the measured data fall into two categories (a) absolute cross sections and (b) relative cross sections i.e. measurements of the shape or energy dependence. The simplest procedure, adopted in many evaluations, is to normalise the relative data in the best possible way (i.e. at a suitable energy where the error in the absolute data is least), to plot all the data together and to draw a curve through the points by eye. In such cases, the errors in the evaluated data are usually assigned by observation of the spread in the measured values about the curve. While these procedures might be acceptable in cases where the accuracy of the data is not very high, more sophisticated treatments are being sought for situations in which the errors are small ($\leqslant 5\%$).

In the last year or so, two more elaborate methods have been applied to the U-235 fission cross section. In the first, Poenitz [3] divided the evaluation into two distinct parts (a) the establishment of the cross section shape and (b) the normalisation of the cross section. In part (a), a 63 point energy grid was set up and experimental data points extrapolated to the grid energy using second degree polynomials below 1 MeV and linear interpolation above, based on the shape of the cross section obtained from an earlier evaluation [4]. Uncertainties were also assigned to each value at a grid energy taking into account the total uncertainty in the measured values, together

with contributions to allow for uncertainties in the energy
determination and fluctuations in the cross section.

Cross section ratios between any two energy grid points are
formed for each contributing data set, thus eliminating any
dependence on arbitrary or absolute normalisation. After
weighted averaging, a system of equations of ratios is
established which can be solved, starting with an arbitrary value
for the cross section at the highest energy grid point, to yield
the cross section shape. A curve was then drawn by eye through
the resulting values, a calculation by Moore [5] being used to
give guidance on the shape to be expected.

A normalisation factor was then derived for each set of
measured absolute data and an overall normalisation factor
obtained from the weighted average.

Poenitz, in his report [3], does not seem to have carried
through the estimates of the errors to be assigned to the cross
section as a function of energy throughout the range of the
evaluation from 100 keV to 20 MeV. Undoubtedly the errors can be
assessed in this type of analysis and it is known that a
covariance file is included in the U-235 fission cross section
evaluation in ENDF/B V, which was based on the Poenitz method.

A method based on correlations between the errors in
different experimental results has been proposed by Sukhovitskij
and Konshin [6] for determining errors in evaluated data, and the
method applied by Konshin et al [7] to the fission cross section
of U-235 between 100 eV and 20 MeV. The evaluation itself
employed no special techniques, the authors beginning with an
accepted cross section value at thermal energy and working their
way up in energy, establishing values in specific energy regions
which are used for the normalisation of data extending up to
higher energies. Konshin et al argue that special attention must
be paid to the errors because of the fairly strong correlations
which exist between some measurements due to the use of similar
methods and standards. The basis of the method lies in
considering the partial errors (assumed to be uncorrelated in a
given experiment), which make up the total error, and estimating
the correlations between them. The total errors in the various
sets of measurements are correlated with each other through the
partial errors. Sukhovitskij and Konshin derived an expression
for the difference between the estimated cross section σ_{est}
and the actual (but unknown) cross section σ_0

$$\overline{|\sigma_{est} - \sigma_0|}^2 = \sum_{k=1}^{NS} \sum_{i=1}^{NA} \sum_{j=1}^{NA} a_i\, a_j\, K_{kij} \sqrt{\overline{|\Delta\sigma_{ik}|^2}\,\overline{|\Delta\sigma_{jk}|^2}} \quad (1)$$

where the correlation coefficient between the kth partial
error of the ith and j^{th} experiments is

$$K_{kij} = \frac{\overline{\Delta\sigma_{ik}\ \Delta\sigma_{jk}}}{\left[\overline{|\Delta\sigma_{ik}|^2}\ \overline{|\Delta\sigma_{jk}|^2}\right]^{1/2}} \qquad (2)$$

and $\Delta\sigma_{ik}$ is the kth partial error in the ith experiment, NS is the number of partial errors, NA is the number of experiments involved in the evaluation and a_i is a weight given to the ith experiment, with

$$\sum_{i=1}^{NA} a_i = 1 \qquad (a_i > 0) \qquad (3)$$

The weights (a_i) are adjusted by an iterative method in a computer code to minimise the value of $|\sigma_{est} - \sigma_o|^2$ [this is equivalent to a least squares procedure (i.e. $a_i = 1/(\Delta\sigma_i)^2$) when there are no correlations present]. The formalism also gives expressions for the error in the estimated value (σ_{est}) and also the correlation coefficient between values at one energy and another.

In their analysis of the U-235 fission cross section data, Konshin et al consider 12 types of partial error and the correlations between different experiments arising from each of these. The 12 error types are listed in Table II. The authors find that the error obtained by their method can be more than a factor of two higher than that calculated if correlations are neglected, this being particularly true in the region below 10 keV. Above that energy the differences are generally smaller and above 100 keV they are typically less than 20%. A comparison of this evaluation with ENDF/B V data shows agreement to within 1-3% between 0.1 and 15 MeV.

In recent years, no one has argued more strongly than Perey for the inclusion of covariance information in evaluated cross section files. Mainly as a result of his efforts, a framework for covariance data has been established [8] within the ENDF/B file system and such information exists for some nuclides in ENDF/B V. Processing codes have been written to take advantage of the covariance files and there is no doubt that the additional information provided by the covariance files will lead to an improvement in the estimation of the uncertainties in calculated integral quantities.

The U-235 fission cross section data used in most evaluations include those obtained from measurements relative to the accepted standard cross sections [i.e. H(n,p), ^{6}Li(n,α) and ^{10}B(n,α)] but not measurements against, for example, Pu-239 fission or U-238 capture. It is generally felt that the latter types of data provide information on the other cross section and not on U-235 fission. Thus when a new version of ENDF/B is required, the first task is to evaluate the standards and to use

the results to convert, for example, Pu-239/U-235 fission cross section ratio values to Pu-239 fission cross sections. But such ratio data can be measured with a precision which is comparable to or even better than measurements employing the normal standards and therefore they have potentially as much bearing on the U-235 fission cross section as on the other cross section.*

In an attempt to take advantage of the additional information contained in ratio data, Sowerby et al [9] performed an evaluation in which data on U-235, U-238 and Pu-239 fission, and U-238 capture, together with ratios of any two of these cross sections, were considered simultaneously. Curves were drawn by eye through the various types of data and values read off at selected energies. At a given energy, weights were assigned to each value, based on the estimated accuracy of the data, and a least squares procedure used to find the best values of the cross sections.

In summary, the situation appears to be that Poenitz has devised a method for dealing quantitatively with absolute and relative data, Konshin et al have formulated a procedure for assessing errors and correlations in evaluated data, Sowerby et al have shown that more than one cross section can be considered at a time and Perey has developed a formalism for introducing covariance information into evaluated data files. Perhaps the ideal evaluation procedure lies in using elements from each of 'ese and as the accuracy of measurements increases, this is a allenge which may have to be faced.

Before leaving this section, three further points should be made. The first concerns the fitting of curves to experimental data in order, for example, to obtain interpolated values at other energies. It has been noted that Poenitz used both linear and non-linear interpolation methods while others have been content with curves drawn by eye. The question arises as to whether theory could provide a better representation of the shape of a cross section for use in such cases. It is extremely unlikely that in the forseeable future theoretical calculations will provide the basis for the evaluations of the fission cross sections of the major actinides, as is now the case in the ENDF/B V evaluations of parts of the light element standards, but perhaps such calculations could assist in the fission evaluation procedures. At present, the accuracy with which fission cross sections can be estimated may not be sufficient for this purpose although, as has been seen, Poenitz has taken the first step in this direction in using the calculation by Moore to give guidance on the U-235 fission cross section shape. However, the possible presence of effects not included in the theoretical description (e.g. intermediate structure) must be recognised and discretion

---

*The need to consider several cross sections simultaneously is possibly even more apparent in the dosimetry field where there is a greater variety of ratio measurements and proportionately fewer relative to the accepted standard cross sections.

exercised.

The second point to be made concerns the use to which integral data should be put in producing an evaluated file based on differential data. There is general agreement that clean, accurate integral measurements can, and should, be used to assist in the selection of cross section values in situations where there are significant discrepancies among the measurements. The differences in philosophies appear when it comes to deciding if the evaluated file should itself be adjusted (within the assessed uncertainty) to give better agreement with more complex integral data, or whether the adjustment should be incorporated at the group constant stage. The former procedure is used in ENDF/B while the latter is employed in the UK treatment, it being felt that in this way the evaluated data files are more application independent.

The last point is related to the form of construction of the evaluated data file. In the UK Nuclear Data Library (UKNDL), the cross section values are given pointwise at all energies and the evaluator does not have to concern himself with the processing codes. But this is not the case with ENDF/B, where it is legitimate, for example, to describe the low energy region in the form of resolved and unresolved resonance parameters. The evaluator must be aware of the way in which the processing code will treat the parameters so that a user will obtain the cross section values which the evaluator intended. To illustrate this point, consider the situation arising when average parameters are used to describe the unresolved resonance region. It is very important for the evaluator to know whether the processing code will interpolate the parameters or the cross sections.

3. METHODS USED IN EVALUATIONS BASED ON THEORY OR SYSTEMATICS

The extent to which theory, ranging from its purest form to simple systematic trends, has to be used to produce the values needed to complete evaluated data files is illustrated in Table I. With the exception of the four major actinide nuclei (Th-232, U-235, U-238 and Pu-239) and in a few particular cases, there are insufficient or no measured data at all on the total, elastic, differential elastic, inelastic, differential inelastic, capture and (n,2n) cross sections and on $\bar{\nu}$, for incident neutron energies above 0.5 MeV. The situation for fission cross sections is considerably better, but even here there are some minor actinides with few or no measured values, the nuclei beyond Am-241 being particularly noteworthy in this respect. In addition, only for U-235 are there any data on the fission neutron spectrum for this energy range. So theory has a very important and extensive role to play. Let us now consider some of the methods used by evaluators for each of the above mentioned cross sections in turn.

(a) Total Cross Sections

       One of the simplest methods used in cases where there is a
lack of measured total cross section data is to make use of the
fact that above the unresolved region, the differences between
the values for one actinide nuclide and a nearby one are likely
to be small. This is illustrated in Fig. 1 where the total cross
sections for U-235, U-238 and Pu-239, as measured by Schwartz et
al [10], are shown from 0.5 to 15 MeV. It is clear that the
shapes and magnitudes are very similar. Little error is
introduced therefore by adopting the measured total cross section
values of a neighbouring nuclide and this method was used by
Konshin et al [11] in an evaluation of Pu-241 in which they
assumed that the total cross section could be represented by the
data for Pu-239. This treatment was chosen because the
evaluators were unhappy with optical model calculations which did
not give satisfactory agreement with the low energy behaviour of
the cross section as represented by the strength functions.
       A somewhat better prescription has been suggested by Moore
and Auchampaugh [12] for obtaining the total cross section of
certain actinide nuclei in the absence of measurements. This is
best illustrated by the following example showing how the Pu-242
cross section could be deduced with high precision from measured
data on nearby nuclides.

$$\sigma_{nT} \text{ (Pu-242)} = \sigma_{nT} \text{ (U-238)} + [\sigma_{nT} \text{ (Pu-239)} - \sigma_{nT} \text{ (U-235)}]$$

This is particularly useful if the cross sections within the
square brackets can be obtained from a common source so that
systematic effects in the difference tend to cancel. The authors
suggest that this method could be used as a constraint on optical
model calculations, but it is not clear if use has been made of
this idea in an actual evaluation.
       The most commonly used tool for estimating total cross
sections in the absence of measured data is the optical model and
a great deal of literature exists on its various forms. Many
aspects of this model will be covered in reasonable detail by
others at this meeting (notably Moldauer and Salvy), but at the
risk of repeating some of their statements, a brief outline of
some aspects will be given here.
       The optical model exists in two distinct forms, the
spherical and deformed (or coupled channel) models. Since the
actinide nuclei are permanently deformed, it would appear
reasonable to apply the coupled channel model. But as this model
often requires considerable computational time, many evaluators
prefer to use the simpler and faster spherical model, accepting
the limitations in accuracy which this introduces. The
parameters for the model are derived from fits to measured data
but, although it is generally fairly easy to obtain satisfactory
agreement over a limited energy range, it can prove difficult to
find a set of parameters which are suitable over a wide energy

range. In their simplest form, the real and imaginary depths of the potential well are taken to be energy independent (see, for example, Caner et al [13]) but for greater accuracy, the depths of the potential well are functions of the incident neutron energy (see, for example, Kikuchi [14]). The inadequacies of the spherical model have been discussed by Lagrange [15] and Fig. 2, taken from his paper, shows the differences between spherical model calculations by Matsunobu et al [16] and deformed model calculations by Lagrange and Jary [17] for the compound nucleus formation cross sections of Th-232 and Pu-240. The differences in the magnitudes and energy dependences of the cross sections are very significant. Lagrange notes that for a precise determination of actinide cross sections, the effects of quadrupole and hexadecapole deformations must be taken into account. In conclusion, Lagrange recommends that for even-even nuclei, where no coupled channel code is available, interpolation or extrapolation of deformed optical model calculations should be used to give greater reliability than can be obtained from spherical models, and to aid this suggestion, he intends to make available results on Th-232, U-234, U-238 and Cm-248 to add to those already published [17] for Pu-240 and Pu-242.

A slightly different approach has been taken by Madland and Young [18]. They have sought to derive global potentials which will be applicable in fairly narrow ranges of nuclear mass, the actinide region receiving first attention. Their method begins with the determination of an optimum spherical potential by fitting the total and differential elastic cross sections of a range of actinide nuclei. An iterative procedure is then used to transform from spherical values to coupled channel parameters by requiring that these should also reproduce measured differential inelastic cross section data. Using the global coupled channel parameters, calculations of the total cross sections of a range of actinide nuclei up to 10 MeV compare quite well with measured values although the authors felt that further work was required before the parameters could be considered to be final.

(b) Elastic Scattering Cross Section

The methods used to determine elastic scattering cross sections are essentially the same as for total cross sections. That is, the measured data for a nearby nucleus can be adopted, as for example in the Pu-241 evaluation by Konshin et al [11], or an optical model calculation can be performed to obtain the direct elastic component which is essentially equal to the total elastic cross section, as the compound elastic part is very small in the energy region being considered here (see, for example, Kikuchi [14]).

In principle, a more straightforward statistical treatment can be used to estimate values of the shape elastic cross section, using the expressions

$$\sigma_{SE} = \pi \lambda^2 \sum_1 (2l + 1) \left| 1 - \bar{U}_l \right|^2 \qquad (4)$$

$$\bar{U}_l = e^{-2i\varphi_1} \left[\frac{1 - \pi P_l S_l}{1 + \pi P_l S_l} \right] \qquad (5)$$

where φ_1 is the hard sphere phase shift for neutron waves of orbital angular momentum l, P_l, is the penetration factor and S_l is the neutron strength function. The total elastic scattering cross section is obtained by adding the compound elastic component but, above ~1 MeV, this part can usually be neglected. However, this approach requires a good knowledge of the various l-wave strength functions and, in general, sufficiently accurate information is not available. When the equivalent expression to (4) was used by Lynn (see ref. [19]) to calculate the total cross sections of Th-232 and U-238, the results were significantly larger than the measured values in the energy range 0.3 to 2.5 MeV. These procedures are therefore not expected to lead to reliable elastic scattering cross section data. However, a similar statistical treatment can be used to obtain the total compound nucleus formation cross section (see Lynn [20]) and the shape elastic cross section found by subtracting this from the total cross section arrived at in another way. Such a method was used by Lynn et al [19] in an evaluation of Am-241.

(c) Differential Elastic Scattering Cross Section

The ways in which evaluators deduce the angular distributions of elastic scattering follow very closely the methods used for determining total cross sections and little more needs to be said. However, it is possibly worth noting that care must be exercised in comparing calculations with measurement, particularly at the higher neutron energies. The finite energy resolution in measurements sometimes results in some inelastic effects (usually almost isotropic) being included in "elastic" determinations (true elastic is strongly forward peaked at higher energies) and this can have very significant effects on the angular distributions.

(d) Inelastic Scattering Cross Section

Up to about 5 MeV, compound nucleus formation is the principal reaction mechanism and therefore statistical treatments are generally applied to the calculation of the components of the non-elastic cross section. The usual method consists of applying the Hauser-Feshbach formalism (allowing for the effects of fluctuations in the neutron and fission widths, and also of interference between levels), the neutron transmission

coefficients being obtained from an optical model calculation.
The Hauser-Feshbach calculations are normally carried out for
discrete levels up to a specified energy, the parameters of the
levels (energy, spin and parity) being taken from experimental
observation where possible but, in the event of the level scheme
not being fully known, an appropriate set of discrete levels may
be invented. Above the highest energy discrete level, the levels
may be grouped into bands, say 100 keV wide, and average cross
sections calculated. At some higher energy, it is usual to
consider the energy levels in the residual nucleus as forming a
continuum.

In the case in which the energy levels are presumed to form
a continuum (high incident neutron energy), the amount of
computer time required to calculate the inelastic cross section
in detail may not be justified by the achievable accuracy. Lynn
has used [19] a simple semi- empirical formula for use in such
conditions, based on the spectral form of the neutron evaporation
to a residual nucleus with a constant temperature (θ) level
density law. His expression is

$$\frac{\delta \sigma_{nn' \to E'}}{\delta E'} \cdot \Delta E' = C(E_n) \, (E_n - E') \, e^{-(E_n - E')/\theta} \, \Delta E' \quad (6)$$

for inelastic scattering from initial energy E_n to an energy
group of width $\Delta E'$ at excitation energy E' in the residual
nucleus. The normalisation factor $C(E_n)$ is determined
empirically from statistical calculations of the total inelastic
scattering cross section at a number of energies. The method was
applied to Am-241 and the results using equation (6) were found
to agree with the more detailed calculations within ~10%.

The calculation of cross sections for reactions involving a
continuum of exit channels requires a knowledge of level
densities and this is an area in which detailed quantitative
understanding is very unsatisfactory. Generally, experimental
information is restricted to the low-lying levels and to a region
just above the neutron separation energy (typically ~5-7 MeV)
where slow neutron resonances can be studied. Nuclear models or
semi-empirical methods must be used to interpolate or extrapolate
to other energies. The most commonly used formulation of level
density is that due to Gilbert and Cameron [21], who specified a
constant temperature form up to a certain energy (typically
between 3 and 5 MeV for actinide nuclei) and above that energy,
the standard Fermi gas formula was adopted. In studying the
systematics of neutron reactions of the actinide nuclei, Lynn
[20] found it necessary to modify the values of the parameters
given by Gilbert and Cameron to obtain better agreement with
experimental data and also to alter the low energy form to take
account of the energy gap.

Before leaving inelastic scattering in the region below ~5
MeV, it is to be noted that the results obtained from the
Hauser-Feshbach method are not independent of the way in which

the transmission coefficients for other partial cross sections
are calculated. This is a natural consequence of the compound
nucleus reaction in which various partial cross sections compete
for a share of the total formation cross section and it means,
for example that the inelastic scattering cross sections depend
on the way in which the transmission coefficients are estimated
for the fission channels.

Above ~5 MeV, direct and pre-compound processes begin to
appear, although in many evaluations these are ignored and the
statistical model continues to be applied. However, Konshin et
al [11] have devised a method of including pre-equilibrium
effects, assuming that statistical equilibrium is established
after the emission of the first neutron. These authors also
applied the formalism to the (n,2n), (n,3n), (n,n'f) and (n,2nf)
cross sections.

(e) Differential Inelastic Cross Section

The angular distribution of inelastically scattered neutrons
is usually assumed to be isotropic in the centre of mass system
for the compound nucleus formation part of the reaction. Any
non-isotropic effects usually appear through direct processes
which are generally calculated using a coupled channel code. For
example, above 100 keV, Konshin et al [11] assumed that all the
anisotropy arose from direct excitation of the first level only.

(f) Capture Cross Section

In general, the capture cross sections of the actinides
become very small above a few MeV due to strong competition by
other compound nucleus partial cross sections and, from a
practical point of view, there is little incentive to make
detailed calculations above that region. The usual method of
estimating the cross section is to apply the Hauser-Feshbach
formalism, the problem then becoming one of calculating the γ-ray
transmission coefficients. In principle, this calculation should
take account of all γ-ray multipolarities but the level density
is normally assumed to be independent of parity and only electric
dipole transitions are considered. The values of the average
radiation width, $\langle \Gamma_\gamma \rangle$, are sometimes taken from measurements on
low energy resonances (using the strong coupling dipole model to
extrapolate to higher energies) or from the giant dipole
resonance model, with one or (more frequently) two Lorentz shaped
lines. In the latter case, the estimated total radiation width
at low energies is often found to be larger than experimental
measurement by about a factor of two and the calculation has to
be renormalised.

At high neutron energies, the direct capture process comes
into play and to take account of this, Lynn et al [19] allowed
the capture cross section to remain constant at 10 mbarn once it
had fallen to this level, in an evaluation of Am-241.

(g) Fission Cross Section

It is only in recent years that it has been possible to calculate reasonably accurate fission cross sections but even at the present time, although barrier heights are known from basic theory to within ~0.5 - 1 MeV, an accuracy of ~100 keV is needed to meet the cross section requirements.

Although the existence of the double-humped fission barrier has been known for a considerable time, many evaluations assume a single barrier and use the Hill-Wheeler formula to determine the transmission coefficients. The effective number of fission channels, the barrier height and the penetrability parameter $\hbar\omega_F$ are generally adjusted to give agreement with measured values. The NEARREX code, as adopted by Caner et al [13], uses this treatment. However, this method is really only useful for situations where there is a reasonable quantity of measured data and moreover, each nuclear mass is usually treated individually. But data must be calculated for nuclei for which there is no experimental information and so attempts have been made to combine systematics with the double-humped barrier.

The most comprehensive study of the systematics of fission is that by Lynn [20], based on a Hauser-Feshbach statistical treatment and the double-humped fission barrier. At sub-barrier excitation energies, the shape and magnitude of the fission cross section is mainly determined by the heights and penetrability parameters of the two barriers while at energies above the barriers, the densities of intrinsic deformation states at the barriers also become important. Lynn [20] has deduced the values of the various parameters needed to calculate actinide fission cross sections by analysing both neutron cross section measurements and charged particle transfer reactions, such as (d,pf), (t,pf) and (^{3}He,df). He has written two computer codes to perform the calculations of actinide cross sections, both employing Hauser-Feshbach methods. The first, AVXS, applies to situations in which there is detailed information on the decay channels of the compound nucleus and the second, EVAPF, is used where the knowledge of the decay channels is of a statistical nature. It is found that such calculations produce cross section estimates with an accuracy typically 25-30% for energies above the fission barrier. However in the region below the barrier, where intermediate structure is likely to be present, the accuracy will be much worse.

It is to be noted that the application of Lynn's systematics to the thorium mass region produces some anomalies. These may be due to the presence of a third potential well, as suggested by Möller and Nix [22], implying that caution is needed when applying systematics to this mass region.

The behaviour of the first chance fission cross section above the second chance fission threshold (and correspondingly for the first and second chance fission above the third chance threshold) cannot be determined by experiment but must be

obtained entirely by theoretical means. In some cases, this is
simply achieved by assuming that the (n,f) cross section is
constant above the (n,n'f) threshold, with a magnitude equal to
the fission cross section just below the threshold. The (n,n'f)
cross section is then given by the difference between the total
fission cross section and the (n,f) part. This procedure was
adopted for much of the actinide file of ENDF/B V.

A more plausible model of the (n,n'f) and (n,2nf) reactions
has been developed by Lynn and incorporated in a simplified
version of EVAPF, called EVAPS. This latter code was used [19]
in an evaluation of Am-241. Briefly, the decay of a highly
excited nucleus is assumed to occur through a single value of the
total angular momentum only, the value being defined as the
average spin of the initially formed compound nucleus. Schematic
statistical model formulae are used to estimate the neutron
transmission coefficients. A constant temperature level density
form is employed, the temperature being a function of, among
other quantities, energy and total spin. Barrier level
densities, needed for the estimation of the fission transmission
coefficients, have been determined empirically by fitting the
calculated fission cross sections of Np-237, U-235, U-238 and
Pu-239 to measured data. As an example of this calculational
procedure, the fission cross sections of Am-241 are shown in Fig.
3, where it can be seen that the various fission cross section
components appear to fall at the onset of the next-chance
threshold rather than staying constant.

A different method of calculating the (n,n'f) and (n,2nf)
cross sections has been adopted by Konshin et al [11] and applied
to Pu-241. They assume that the first neutron is emitted before
the nucleus has reached statistical equilibrium and only
subsequent neutrons are emitted from the equilibrium state. They
estimate that the fraction of pre-equilibrium contribution to the
total non-elastic cross section is 6% at an incident neutron
energy of 7 MeV, rising to 19% at 15 MeV. The nuclear excitation
probabilities for emission of one, two and three neutrons are
obtained from the assumed distributions of the emission spectra
and the probabilities are used in specified formulae to calculate
the (n,n'f), (n,2nf), (n,2n) and (n,3n) cross sections as a
function of neutron energy.

(h) (n,2n) and (n,3n) Cross Sections

The experimental data on (n,2n) cross sections are rather
sparse and the situation for (n,3n) is much worse, although the
high threshold energy of the latter (typically 12-14 MeV) means
that this is of little practical consequence since there are very
few neutrons above 12 MeV in the fission neutron spectrum. A
number of methods have been devised for the calculation of these
cross sections.

A statistical model approach has been used by Jary [23] on
uranium isotopes. Neutron transmission coefficients were

obtained from a coupled-channel model, while the neutron, fission
and radiative widths were estimated by the statistical model,
level densities being given by the Fermi gas model. Comparisons
with experimental data where possible show fairly satisfactory
agreement.

The statistical methods employed by Lynn and by Konshin et
al have already been mentioned in sub-section (g) dealing with
the fission cross section and no further discussion will be
given.

A simple prescription for the (n,2n) and (n,3n) cross
sections was devised by Pearlstein [24], based on the statistical
model applied to an empirical relation for the non-elastic cross
section, and the work was later extended by the same author [25].
The effects of direct reactions, not included in the statistical
model but which are important at high energies, were accounted
for by choosing input parameters to give agreement with
experimental trends. Although the Pearlstein recipe was not
intended to take the place of detailed nuclear model
calculations, its simplicity and the existence of a computer
code, THRESH, has resulted in the prescription being used in a
number of evaluations, for example, Np-237 in ENDF/B V and Pu-241
by Kikuchi [14].

An alternative method of calculating (n,2n) and (n,3n) cross
sections has been produced by Segev and Caner [26]. This is also
based on the compound nucleus model and the authors claim that it
gives a better account of (n,2n) and (n,3n) competition than
Pearlstein's prescription. Closed expressions are arrived at
from which the cross sections can be calculated but these have to
be normalised to experimental data.

The statistical model was also used by Jhingan et al [27],
who, like Segev and Caner, calculated the (n,2n) cross section
above the (n,3n) threshold in a more plausible way. The effects
of fission competition were also included, together with a factor
to take care of competition from γ-ray emission. The latter
factor is provided as a parameterisation depending on the value
of (N-Z)/A and has a magnitude of about 0.88, independent of
energy. The results obtained with this prescription agree quite
well with those calculated by Jary [23].

3. NON-STATISTICAL PROCESSES

Although it has been recognised for a considerable time that
non-statistical processes play a part in neutron reactions above
a few (~5) MeV, the discussion in the previous section has shown
that the vast majority of actinide evaluations ignore this fact
and simply assume that compound nucleus formation is the only
process of any importance. This can be largely justified on the
grounds that the accuracy obtained from the application of the

statistical model is not very high (typically ~25-30%) and, in general, the non-statistical effects on the important actinide cross sections are smaller (≤10%) below 15 MeV. However, if neutron energy spectra are to be calculated for secondary energy distributions, quite significant errors may result by assuming that all emission can be described by the statistical model. It is important therefore to continue the development of models which deal with non-statistical processes in the actinide region but in any case. As the accuracy of model calculations improves, so it will be necessary to take account of such processes also for cross sections.

At the energies of interest for applications of actinide neutron reaction data (< 20 MeV), the most important non-statistical effect is pre-equilibrium emission. This arises, following neutron absorption by a nucleus, from particles which are emitted before the compound nucleus has reached an equilibrium state i.e. when only a few collisions have occurred among the nucleons. Particles emitted before equilibrium have a significantly higher average energy than those released from a fully developed compound nucleus, which accounts for the effect on particle energy spectra. In consequence, if the first particle emitted is a neutron, there is on average less excitation energy for emission of a second neutron and hence pre-equilibrium emission tends to reduce the (n,2n) cross section.

A number of different approaches to the calculation of pre-equilibrium effects have been made, but the one most frequently adopted for neutron reaction calculations appears to be the exciton model originally proposed by Griffin [28]. A recent review of this model from the point of view of fast neutron reactions has been given by Seeliger [29] at an IAEA Consultants Meeting on Nuclear Theory in Neutron Nuclear Data Evaluation and the proceedings of that meeting also contain other papers on the subject, the references being given in Seeliger's paper. However, all the examples quoted in these papers pertain to the mass region below A = 210 and the same is true of a study of pre-equilibrium effects in (n,2n) cross sections at 14.5 MeV by Gupta and Chatterjee [30]. But as we have seen in Section 2, some authors (most notably Konshin et al [11]) have attempted to include pre-equilibrium effects in actinide evaluations but as yet these are at a fairly crude level. However, the direction of theoretical calculations for fast neutron nuclear data evaluation has been indicated and undoubtedly more emphasis will be placed on this aspect in the future.

ACKNOWLEDGEMENTS

REFERENCES

1.   J.E. LYNN, "Theoretical Calculation of Transactinium Isotope Nuclear Data for Evaluation Purposes" in Proc. Advisory Group Meeting on Transactinium Isotope Nuclear Data, International Atomic Energy Agency, Vienna, IAEA-186, 201 (1976).

2.   V.A. KONSHIN, "Applications of the Nuclear Theory to the Computation of Neutron Cross Sections for Actinide Isotopes," in Proc. of Winter College on Nuclear Phys. and Reactors, International Centre for Theoretical Phys., to be published by IAEA, (1980).

3.   W.P. POENITZ, "Evaluation of ^{235}U(n,f) Between 100 keV and 20 MeV," Argonne National Lab. Rep. ANL/NDM-45 (1979).

4.   W.P. POENITZ, "The U-235 Neutron Fission Cross Section from 0.1 to 20 MeV," in Proc. Symp. on Neut. Standards and Applications, U.S. Dept. of Commerce, NBS Special Publication SP 493, 261 (1977).

5.   M.S. MOORE, "Measurement, Analysis, and Implications of the Fission Cross Section of the Important Fissionable Isotopes," in Proc. Conf. on Nuc. Cross Sections and Technology, U.S. Dept. of Commerce, NBS Special Publication NBS 425, Vol. 1, 129 (1975).

6.   E.Sh. SUKHOVITSKIJ and V.A. KONSHIN, "The Use of Correlations for Determining Errors in Evaluated Data," Izv. Akad. Nauk BSSR, Seriya Fiziko-ehnergeticheskikh Nauk, 3, 19 (1976).

7.   V.A. KONSHIN, V.F. ZHARKOV and E.Sh. SUKHOVITSKIJ, "Evaluation of the ^{235}U Fission Cross Section in the Energy Range 0.1 keV - 20 MeV," IAEA Rep. INDC(CCP)-148/L (1980).

8. F.G. PEREY, "Estimated Uncertainties in Nuclear Data – an
    Approach," in Proc. Conf. on Nuc. Cross Sections and
    Technology, U.S. Dept. of Commerce, NBS Special Publication
    NBS 425, Vol. II, 842 (1975).

9. M.G. SOWERBY, B.H. PATRICK and D.S. MATHER, "A Simultaneous
    Evaluation of the Fission Cross Sections of U-235, Pu-239
    and U-238 and the Capture Cross Section of U-238 in the
    Energy Range 100 eV to 20 MeV,", Ann. Nuc. Sci. Eng. $\underline{1}$, 409
    (1974).

10. R.B. SCHWARTZ, R.A. SCHRACK and H.T. HEATON, II, "Total
    Neutron Cross Sections of Uranium-235, Uranium-238 and
    Plutonium-239 from 0.5 to 15 MeV," Nucl. Sci. Eng. $\underline{54}$, 322
    (1974).

11. V.A. KONSHIN et al., "Evaluation of Nuclear Data for Pu-241
    in Neutron Energy Range from 10^{-3} eV to 15 MeV," IAEA
    Report INDC(CCP)-142/GJ (1980).

12. M.S. MOORE and G.F. AUCHAMPAUGH," Techniques for the
    Determination of Capture Cross Sections of Radioactive
    Fission Product Nuclides," in Proc. Spec. Meeting on Neutron
    Cross Sections of Fission Product Nuclei, CNEN Bologna,
    Relazione Tecnica Interna, NEANDC (E) 209 'L' (1979).

13. M. CANER, Y. BARTAL and S. YIFTAH, "Curium-246 Neutron Data
    Evaluation," Israel Atomic Energy Commission Rep. IA-1358
    (1980).

14. Y. KIKUCHI, "Evaluation of Neutron Cross Sections of
    Pu-241," J. Nucl. Sci. Tech. $\underline{14}$, 467 (1977).

15. Ch. LAGRANGE, "On the Usefulness of Coupled Channel
    Calculations for Actinide Nuclei," in Progress Report on
    Actinide Nuclear Data Evaluation Works (Period from April
    1st 1979 to March 31st 1980) to be published as an INDC and
    NEANDC report from Bruyères-le-Châtel.

16. H. MATSUNOBU et al., "A Simultaneous Evaluation of Nuclear
    Data for Heavy Nuclides," to be published in Proc. Int.
    Conf. on Nuc. Cross Sections for Technology, Knoxville
    (1979).

17. Ch. LAGRANGE and J. JARY, "Coherent Optical and Statistical
    Model Calculations of Neutron Cross Sections for Pu-240 and
    Pu-242 between 10 keV and 20 MeV," IAEA Rep. INDC(FR)30/L
    (1978).

18. D.G. MADLAND and P.G. YOUNG, "Neutron-Nucleus Optical
    Potential for the Actinide Region," in Proc. Int. Conf. on
    Neut. Phys. and Nuc. Data for Reactors and other Applied
    Purposes (AERE, Harwell) OECD Nuclear Energy Agency, Paris,
    349 (1978).

19. J.E. LYNN et al., "Evaluation of Differential Nuclear Data
    for Americium Isotopes. Part I: Am-241," UKAEA Rep.
    AERE-R8528, Atomic Energy Research Establishment, Harwell
    (1979).

20. J.E. LYNN, "Systematics for Neutron Reactions of the
    Actinide Nuclei," UKAEA Rep. AERE-R7468, Atomic Energy
    Research Establishment, Harwell (1974).

21. A. GILBERT and A.G.W. CAMERON, "A Composite Nuclear-Level
    Density Formula with Shell Corrections," Can. J. Phys. $\underline{43}$,
    1446 (1965).

22. P. MOLLER and J.R. NIX, "Calculation of Fission Barriers,"
    in Proc. Symp on Physics and Chemistry of Fission
    (Rochester, N.Y.) IAEA, Vienna, Vol. I, 103 (1974).

23. J. JARY, "Methode de Calcul par Modele Statistique des
    Sections Efficaces des Reactions (n,xn) et (n,xnf) pour les
    Isotopes de l'Uranium ^{232}U à ^{239} dans le Domaine d'Energie
    2 MeV - 15 MeV," CEN Saclay Rep. CEA-R-4647 (1975).

24. S. PEARLSTEIN, "Analysis of (n,2n) Cross Sections for Medium
    and Heavy Mass Nuclei," Nucl. Sci. Eng. $\underline{23}$ 238 (1965).

25. S. PEARLSTEIN, "Neutron-Induced Reactions in Medium Mass
    Nuclei," J. Nucl. Ener. $\underline{27}$, 81 (1973).

26. M. SEGEV and M. CANER, "A New Formalism for (n,2n) and
    (n,3n) Cross Sections of Heavy Mass Nuclei," Ann. Nucl.
    Ener. $\underline{5}$, 239 (1978).

27. M.L. JHINGAN et al., "(n,2n) and (n,3n) Cross Sections on
    the Basis of Statistical Model for Fissionable Nuclei," in
    Proc. Int. Conf. on Neut. Phys. ani Nuc. Data for Reactors
    and other Applied Purposes (AERE, Harwell) OECD Nuclear
    Energy Agency, Paris, 1049 (1978).

28. J.J. GRiFFIN, "Statistical Model of Intermediate Structure,"
    Phys. Kev. Lett. $\underline{17}$, 478 (1966).

29. D. SEELIGER, "Pre-equilibrium Emission in Neutron-Induced
    Reactions," in Proc. Consultants Meeting on Nuclear Theory
    in Neutron Nuclear Data Evaluation (Trieste), IAEA, Vienna,
    Technical Document IAEA-190, Vol. I, 313 (1976).

30. S.K. GUPTA and A. CHATTERJEE, "Pre-equilibrium Effects in
    (n,2n) Cross Sections at 14.5 MeV," in Proc. Int. Conf. on
    Neut. Phys. and Nuc. Data for Reactors and other Applied
    Purposes (AERE, Harwell) OECD Nuclear Energy Agency, Paris,
    1044 (1978).

										Fis. Neutr.
Nuclide	σ_{total}	$\sigma_{elastic}$	Diff. Elastic	$\sigma_{inelastic}$	Diff. Inelastic	$\sigma_{capture}$	$\sigma_{fission}$	σ_{n2n}	$\bar{\nu}$	Spec.
Th-230	–	–	–	–	–	–	239(3)	–	5(1)	–
Th-232	1764(16)	25(6)	304(17)	44(6)	23(2)	136(19)	1586(28)	52(11)	176(17)	–
Pa-231	–	–	–	–	–	–	153(7)	–	–	–
Pa-233	–	–	–	–	–	–	1(1)	–	–	–
Pa-234	–	–	–	–	–	–	–	–	–	–
U-232	–	–	–	–	–	–	15(1)	–	–	–
U-233	996(5)	–	–	–	–	4(1)	560(29)	2(2)	254(28)	–
U-234	–	–	–	–	–	–	1197(13)	–	4(1)	–
U-235	5136(16)	41(4)	396(10)	24(4)	93(6)	5(2)	1197(64)	20(2)	414(37)	210(4)
U-236	–	–	–	–	–	11(2)	1968(15)	–	21(1)	–
U-237	–	–	–	–	–	–	11(1)	–	–	–
U-238	3957(14)	17(7)	383(24)	51(19)	22359(82)	157(30)	2486(72)	110(16)	323(35)	–
Np-236	–	–	–	–	–	–	–	1(1)	–	–
Np-237	–	1255(1)	–	–	–	31(7)	877(25)	16(7)	46(10)	–
Np-239	–	–	–	–	–	–	–	–	–	–
Np-240	–	–	–	–	–	–	–	–	–	–
Pu-236	–	–	–	–	–	–	–	–	–	–
Pu-237	–	–	–	–	–	–	–	–	–	–
Pu-238	–	–	–	–	–	1(1)	338(11)	–	–	–
Pu-239	3793(12)	118(3)	809(16)	3(1)	83(5)	5(2)	1115(54)	5(2)	271(30)	–
Pu-240	39(1)	26(1)	130(26)	57(5)	–	1(1)	510(9)	–	48(3)	–
Pu-241	6(1)	–	–	–	–	1(1)	207(13)	–	53(4)	–
Pu-242	–	–	–	–	–	2(2)	527(9)	–	4(1)	–
Pu-243	–	–	–	–	–	–	–	–	–	–
Am-241	31(1)	–	–	–	–	12(5)	300(13)	–	–	–
Am-242	–	–	–	–	–	1(1)	7(3)	–	–	–
Am-243	–	–	–	–	–	26(4)	181(3)	11(1)	–	–
Cm-242	–	–	–	–	–	1(1)	1(1)	–	–	–
Cm-243	–	–	–	–	–	1(1)	57(3)	–	–	–
Cm-244	–	–	–	–	–	1(1)	30(4)	–	–	–
Cm-245	–	–	–	–	–	–	25(2)	–	–	–
Cm-246	–	–	–	–	–	–	25(2)	–	–	–
Cm-247	–	–	–	–	–	–	21(2)	–	–	–
Cm-248	–	–	–	–	–	–	25(2)	–	–	–
Bk-249	–	–	–	–	–	–	55(4)	–	–	–
Cf-249	–	–	–	–	–	–	89(7)	–	–	–
Cf-250	–	–	–	–	–	–	–	–	–	–
Cf-251	–	–	–	–	–	–	–	–	–	–
Cf-252	–	–	–	–	–	–	38(2)	–	–	–

TABLE I

Data Base ($E_n > 0.5$ MeV) for Actinide Evaluations

Numbers given as A(B), where A = number of data points above 0.5 MeV and B = number of experiments with data above 0.5 MeV incident neutron energy.

The entries in this table were obtained from a search through the data files of the NEA ·ta Bank as at July, 1980.

TABLE II

Types of error considered by Konshin et al [11] in their
analysis of the correlations between partial errors in
experimental measurements of the U-235 fission cross
section from 100 eV to 20 MeV

1. Error in determination of number of U-235 nuclei in foil.

2. Error in extrapolation of fission fragment spectrum to zero pulse height.

3. Error associated with absorption of fragments in foil.

4. Error associated with scattering in the chamber walls, foil backing and target structure.

5. Error associated with neutron attenuation in air.

6. Error in determination of neutron flux.

7. Error in background determination.

8. Error in efficiency of fission counting.

9. Error in geometrical factors.

10. Error in the cross section used as a standard.

11. Statistical error.

12. Normalisation error.
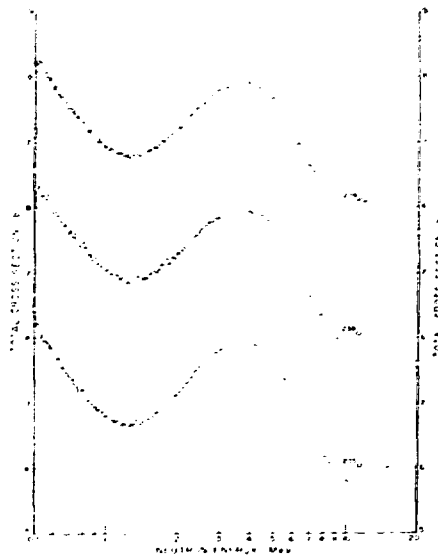
Fig. 1   The total cross sections of U-235, U-238 and Pu-239 from
0.5 to 15 MeV, as measured by Schwartz et al [10].
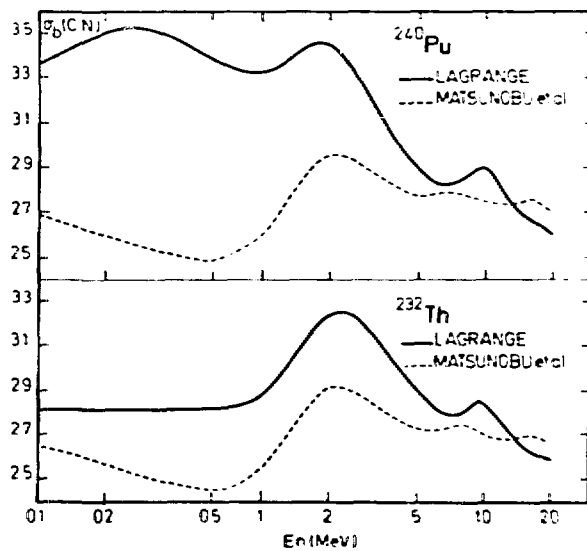
Fig. 2   A comparison of the compound nucleus formation cross
sections of Th-232 and Pu-240 as calculated by Lagrange
[15], using a coupled channel model and by Matsunobu et
al [16], using a spherical optical model.
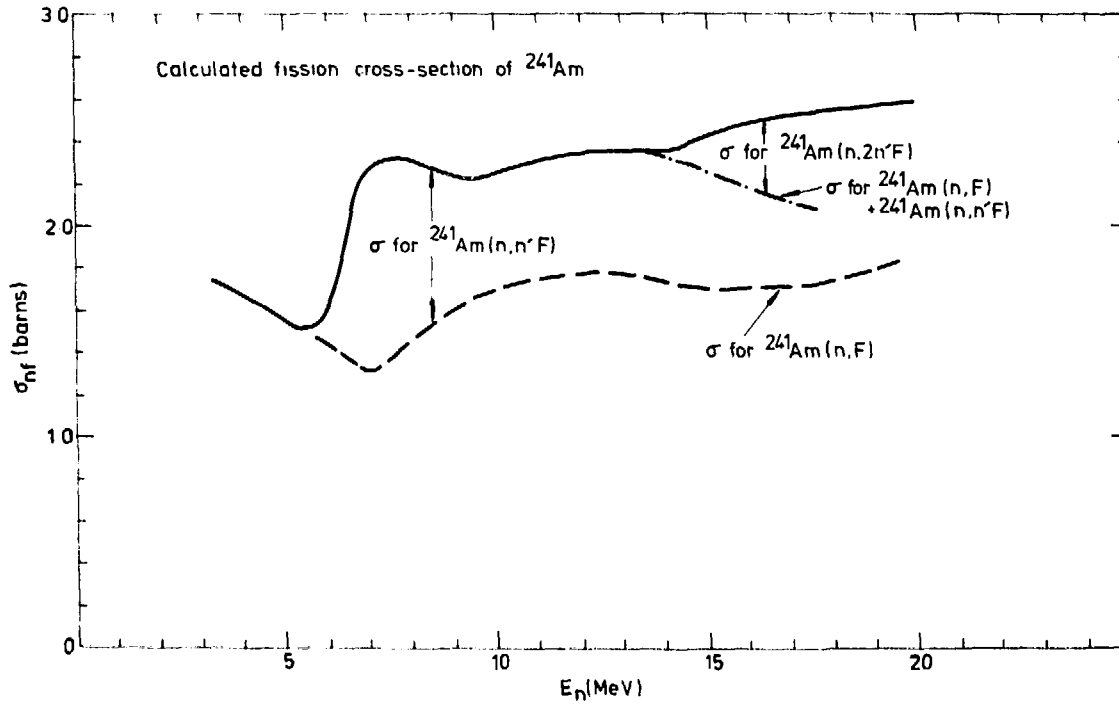
Fig. 3   The (n,f), (n,n'f) and (n,2nf) cross sections of Am-241
as calculated by Lynn in reference [19].

Discussion

Menapace:

An effort has been made at the Bologna Centre to take into account
a preequilbrium contribution in actinide cross section calcula-
tions, and the results were presented at the Knoxville Conference,
October 1979. In particular, for ^{235}U and ^{239}Pu (n,2n) cross
sections, taking into account the preequilibrium component we were
able to reproduce the experimental data of Aldermaston which
cannot be reproduced by only statistical model calculations.

Patrick

Thank you for that information. I was unaware of that work.

Vonach

Concerning level density, I would like to make a comment. There
is to my knowledge no big difference between the use of either
the back-shifted Fermi-gas or the Gilbert-Cameron model, the
differences being probably smaller than the uncertainty of each
model due to the uncertainties in the model parameters. However,
these parameters were derived a rather long time ago and need to
be updated. The new BNL-325 (giving new resonance spacings) in
conjunction with the new table of isotopes (giving new discrete
levels) will give a very good collection of the input data for
that purpose. In Vienna we might do this updating for the back-
shifted Fermi-gas parameters.

Madland

Two Comments: 1. Los Alamos has done recent work (Madland and
Nix) that shows smooth variation other than the usual, assumed,
flat response for the first-chance fission cross section hidden
"underneath" the second-chance fission, the second-chance fission
flat response below the third-chance, etc. We have found that the
second-chance fission cross section drops smoothly, initially,
when the third-comes up and that the first-chance fission cross
section drops smoothly, initially, when the second comes up.
This work will be published shortly.
  2. With regard to the Madland and Young iterative method to
obtain a coupled-channel deformed optical potential: The present
status is that we are awaiting further, resolved, inelastic scat-
tering angular distribution data for low-lying collective states
from actinide nuclei.

Stewart

Preequilibrium neutrons are treated in an <u>ad hoc</u> manner in ENDF/B-V for ^{235}U, ^{239}Pu, and ^{240}Pu. ENDF/B-IV had a similar treatment, which was removed for Version V, for ^{238}U. LLL uses a similar but not identical treatment. Hopefully, this will be treated in a better manner in the next version.

Howerton

<u>Clarification</u>: The ENDF/B-V ^{238}U evaluation was jointly done by ANL and LLL. The preequilibrium component was included using the LLL prescription so it was not a matter of removing anything from a previous evaluation.

Lagrange

My comment concerns inelastic scattering cross sections for low-lying collective states. At incident neutron energies near 2.5 MeV and above, the compound process is negligible in comparison with the direct one. It seemed to me that you have said such compound components were not negligible. Is that true?

Patrick

You are quite correct in saying that the compound inelastic scattering cross sections for low-lying states are very small above $E_n \sim 2.5$ MeV.

Moore

This is the first time I have heard that model calculations can give σ_f to 25% to 30%. Did I understand correctly, or is it σ_γ?

Patrick

The accuracy quoted is Lynn's estimate and applies to the fission cross section in the energy region above the barrier.

GENERAL REVIEW AND DISCUSSION (SESSIONS IX-XII)

J.J. Schmidt, IAEA

.

SUMMARY REVIEW THIRD DAY (24 September)

(Light Isotopes, Unresolved Resonance Region,
Smooth Fission Cross Sections)

J.J. Schmidt

Nuclear Data Section
International Atomic Energy Agency
Vienna, Austria

Let me start today's summary review considering the first two fine papers on light nuclei presented this morning by Hale and Stewart. Hale emphasized the theoretical side whereas Stewart emphasized the actual evaluation problems. There is, however, a common message to be brought home from both papers which "mutatis mutandis" also holds for heavier nuclei: in the computation and evaluation of data for light nuclei one should not be restricted to data on the particular reaction or sets of reactions one has to evaluate, but should take into account all available information from inverse reactions, charged particle reactions, nuclear structure etc. This auxiliary information helps to achieve consistency between data for different reactions, to clarify discrepancies and even to fill gaps in the knowledge. Now let me come to the individual papers.

Hale reminded us first of the principles and practicalities of the R-matrix theory as applied to light nuclei cross sections. There is an important difference between light and medium/heavy nuclei, the latter of which Froehner used as examples in his review talk yesterday. In the energy range of interest to nuclear applications (except e.g., biomedical or FMIT uses), below 10-15 MeV, light nulcei have only a small number of levels. This means mathematically that one cannot average or integrate out the contributions of distant resonances to the cross sections of a given resonance, as one does for heavy nuclei. One has to know exactly the position, decay and quantum properties of a few positive and "negative" energy levels and to take the interference between levels of equal spin and parity into account, in order to satisfactorily describe the low-energy neutron cross sections of a light nucleus such as ^{6}Li. In another example, application of R-matrix theory disproved the so-called Gamow limit of the $T(d,n)^3$He cross section at low keV energies, and was in satisfactory agreement with the scarce experimental data. This example is of considerable practical importance, since these low energy $T(d,n)$ cross sections govern the ignition phase in (d,t)-fuelled fusion reactors.

With the example of a consistent description of the best available total and (n,α) cross section measurements on ^{6}Li, Hale illustrated the importance of retaining the unitarity of the R-matrix. More generally, I feel that Hale demonstrates with an increasing degree of confidence the suitability of the R-matrix

theory to describe in a consistent manner multiples of two-body multi-channel reactions for light nulcei.

You may remember yesterday's question of how to decide between a new evaluation and a new measurement. Hale's specific answer for light nuclei is that, before a new measurement is started, a careful check should be made on the existing evaluations to be sure all pertinent available nuclear information has been taken into account in order to remove data inconsistencies. Only if this has been done and inconsistencies still persist would new measurements be warranted. Certainly in the case of gaps measurements are always needed and valuable, with priorities governed by user's needs, if only, as in the case of light nuclei, to verify theoretical predictions.

Lee Stewart introduced us to the intricacies of evaluation of experimental cross sections for light nuclei up to A = 20, intricacies caused by discrepancies between different measurements, usually due to systematic errors. As a global impression I must confess that I was rather shocked to see that even after years of research some old well-known data discrepancies and gaps in knowledge still prevail. In a number of cases the experimental data base still seems very poor. Rather large discrepancies can be seen in MeV data of ^{6}Li and ^{7}Li. It is needless to underline the importance of these data for reliable prediction of tritium breeding in (d,t)-fuelled fusion reactors. In another example, if I remember correctly, the resonance structure in ^{12}C is known to energies well above 10 MeV, and I wonder why this knowledge is not reflected in the evaluated data files.

In several well-chosen examples Stewart showed how the knowledge of charge-conjugate and inverse reactions and of physical principles such as the charge independence of nuclear forces can be successfully used as a guide in resolving discrepancies or to convey an idea of what the energy shape of a particular cross section should be.

In conclusion Stewart underlined the necessity of adding error files to the evaluated data particularly for the hydrogen and carbon cross section standards; a necessity which I would like to extend to all nuclear standard reference cross sections.

With Guenther's talk we entered the region of fluctuating neutron cross sections for medium-weight nuclei. Guenther stressed some of the experimental uncertainties in this region, described procedures for handling such uncertainties and how to use auxiliary information to pinpoint inconsistencies. I should like to underline two important points he brought out in his talk. First, a least squares fitting procedure as described by Poenitz yesterday is really meaningfully applied only if all the experimental data and their errors have previously been put on an equal footing. Secondly, an evaluator must look at his own work in the context of his environment. He should not try (and is actually never in such a position) to derive data of "eternally lasting truth," since he will then never finish, but instead has

to orient himself to the time schedule and priorities of users' demands. In a nutshell an evaluator is a truly historical human being.

An illustration for the first point is the need for sample thickness corrections which must be applied in order to be able to compare data of different origin. In this context Guenther showed an interesting example of the applicability of nuclear theory consistency. A consistent optical model description of total neutron cross sections of neighboring actinides led to the belief that certain experimental data below about 1 MeV had not been corrected for sample thickness.

As another illustration for the first point Guenther underlined the requirement to reduce data of different origin to the same energy resolution. This brings me to one of the enduring problems in evaluated nuclear data files in energy ranges of fluctutating cross sections: the inconsistency in energy resolution fine structure between different cross sections of the same element or isotope. Consistency between different cross sections is usually reached in the regions of resolved resonances at lower energies and of "truly" smooth cross sections at higher energies. At intermediate energies, however, a highly resolved and strongly fluctuating inelastic excitation cross section may be found together with a poorly resolved (n,p) cross section, to quote only one of many examples. While this inconsistency is in itself not satifactory, it can have the bad consequence, that missing data which have to be deduced by subtraction of known but inconsistently resolved data may become physically meaningless. Extending Guenther's advice, to reduce different measured data for the same cross section to the same i.e., the lowest available energy resolution (the opposite way would be ambiguous and physically meaningless) to the reduction of different evaluated cross sections for the same nuclide to the lowest available energy resolution would entail a loss in physical information, the importance of which can only be judged by the users of the data. I wonder to what extent such inconsistencies affect the users and, whether someone in the audience, for example John Rowlands, might wish to comment on this question?

J. Rowlands: Is it necessary for σ_T to be equal to $\sum_x \sigma_x$ (sum of partial reactions) in applications was your question, I think. σ_T determines how far a neutron travels before making a collision, and σ_x what happens when it collides (reaction (n,x)). After group averaging $\sigma_T \neq \sum_x \sigma_x$ because σ_T is averaged with neutron <u>current</u> and σ_x is averaged with neutron <u>flux</u>. What about Monte Carlo though? I think they already have to cope with the fact that log-log interpolation does not preserve $\sigma_T = \sum_x \sigma_x$.

R. Howerton: The brute-force method of handling the latter point is that one need not use log-log interpolation. The computers are large enough that this problem can be handled. I am not aware of any problems that come about.

R. Peelle: I think there is a problem in that the inconsistency leads to error, blunder, mistakes in some of those partial cross sections, or the total cross section that is used, rather than some bookkeeping problem.

J.J. Schmidt: (continuing):   Let me now turn to the two nuclear theory talks by Lagrange and Arthur.   The important message which I would like you to take home from these two talks is the enormous recent progress in the theoretical understanding and detailed model description of partial nuclear reaction cross sections and of angular distributions and energy spectra of secondary emitted particles.   This development is also reflected in more and more sophisticated nuclear model computer codes which follow a nuclear reaction in great detail and make full use of contemporary large computer capacities.   One example of this development is the way the various models describe pre-equilibrium decay (such as the exciton model or the hybird model).   Secondary particle spectra above, say, 10 MeV can be described satifactorily only if,in addition to compound-nuclear evaporation, pre-compound decay is taken into account.   Multistep cascade calculations are another example of the progress in applied nuclear theory. Theoretical (appropriately parameterized) model calculations come much closer to experimental data than in the past.

As a consequence, as I explained briefly in my first day's summary, the importance of nuclear model calculations as part of the evaluation process has significantly increased.   I should like to bring this importance into perspective

First, no model is satisfactory without using some empirical data.   As a consequence absolute predictions are not possible but often satisfactory descriptions of the shape of cross sections, angular or energy spectra are obtained.   On the basis of the uncertainties of the model parameters one can estimate the uncertainties of the model calculations.   Such calculations can thus rather safely be used to inter- or extrapolate known experimental data.   Furthermore, they can be used (as illustrated today on several occasions) to test the inner consistency of certain evaluations to help to decide between discrepant data and to serve as a guide in solving inconsistencies.

In the discussion Vonach suggested the possibility of putting theory and experiment on the same footing and combining the errors of both in the final result.   Poenitz objected to this suggestion by observing that theoretical calculations entail two types of uncertainties, one due to the uncertainties of the parameters entering the theory and a second one, the uncertainty of the model itself.   While the first uncertainty can be estimated and quantified, it will be much more difficult to assess the accuracy of a model in quantitative terms, though a certain progress may be possible in future.   In summary, as Poenitz concluded, a good parameterization makes the success of a model, and a model can be only as good as the best available experimental data.

Let me stress at this point the crucial importance of a least two parameters which are still not well known and, which time and

again are mentioned during this Workshop, namely, nuclear level
density and fission parameters. A third important parameter was
discussed yesterday i.e., the energy and spin dependence of
neutron radiative capture widths. There is an urgent need for an
adequate representation of the energy dependence of nuclear level
densities. Without going into detail let me just mention again
that, following a strong recommendation by the International
Nuclear Data Committee, the IAEA Nuclear Data Section plans to
convene an expert meeting on basic and applied level densities in
about 1983 where the above-mentioned problem will certainly form
one of the major topics.

A second important parameter is the spin-dependent fission
width at higher energies (pointed out by Patrick) which is crucial
in calculating not only fission cross sections but also cross
sections for competing reactions such as capture and inelastic
scattering for those actinide nuclei for which no or only very
crude experimental data exist. In this context I would also like
to refer you to the recent systematic reviews of the present
theory and knowledge of double-humped fission barrier parameters
presented by Lynn and Weigmann at the Nuclear Theory Courses held
at the International Centre for Theoretical Physics in Trieste in
1978 (reference: IAEA-SMR-43) and 1980 (to be published).

Vonach reported on a very valuable experience in the
evaluation of a limited set of threshold cross sections of
importance in the estimation of reactor radiation damage and
associated error correlation matrices. He reminded us that one of
the most important tasks in evaluation consists of the careful
checking of the experimental errors as given by the authors. He
introduced us to correlations between different energies and
different reactions, showed on the basis of practical
calculations, that the correlations can perhaps be simplified to
constant non-diagonal elements, and finally outlined methods for
deriving evaluated data from a corrected experimental data base.

A basic and very practical question remains to be answered:
what is the limit for taking correlations into account? Everyone
would be happy if for a limited set of reactions for a well-
defined application one could confine oneself to correlations
between just these reactions. However, there usually exist ratio
measurements between these reactions and standard reactions such
as Au(n,γ). These in turn, again through ratio measurements, are
related to other standards and other reactions, and so on. Where
to stop? There is no easy straight-forward answer to this
question. Vonach and Poenitz pointed out some of their own
practical experience where non-diagonal covariance matrix elements
for correlations between different reactions dropped out or became
very small in their specific evaluations. If this observation
would hold more generally, this would certainly ease the problem
considerably. This would give some justification for a purely
practical approach to the variance-covariance problem which I
would recommend i.e., to limit the range of correlations to those
of direct and immediate relevance, for example, the cases of

reactions of interest to radiation damage estimates, i.e. dosimetry and related standard cross sections only.

The last two papers presented today by Weston and Patrick dealt with evaluation problems of actinide neutron cross sections. Weston mentioned some inconsistencies in the current version of ENDF/B, for example, a rather strange shape of ^{235}U inelastic excitation cross sections and a difference in total cross sections between neighboring actinide nuclei which one would not expect from optical model systematics. One should be fair and add that such types of inconsistencies occur in other evaluated data libraries. They have to be understood and removed where ever necessary.

Weston's paper again raises a basic question which was touched upon in previous days: must one really put into evaluated data files all the unresolved resonance detail appearing in contemporary measurements, or smooth curves where the fluctuations have been averaged out? This question is related to the problem how to determine s- and p-wave resonance parameters so as to obtain a reasonable theoretical description of the cross sections in the unresolved resonance range. Even though for many medium and heavy nuclei we know a great many resolved resonances, they normally still represent only a small fraction as well as an incidental sample of the total resonance range. As a consequence average parameters deduced from resolved resonances may not be adequate to describe unresolved resonance cross sections. A typical example is the s-wave neutron strength function. Considerable fluctuations from one resonance subrange to another have been observed, so that in those cases the resolved resonance S_o value cannot be applied in the unresolved resonance range. This is an illustration of the remark made yesterday by Peelle, that resolved resonance investigations do not provide much guidance to unresolved resonance cross sections and parameters.

The question I mentioned before can only be answered from the users' point of view. If the cross section fine structure represents only statistical fluctuations and is not important for the user, i.e., has no influence on the outcome of his calculations, then one should follow Poenitz's advice to save data points and store only smooth averaged cross sections. For some nuclides such as heavy fissionable isotopes the fluctuations may reflect intermediate structure superimposed on statistical fine structure and be of importance to Doppler coefficient calculations, and should thus be retained.

Patrick reviewed one of the most fascinating problem areas in contemporary evaluation i.e., that of the actinides, where for quite a few secondary actinides experimental evidence is poor and one has to rely largely on theoretical predictions. On the one hand Patrick concurred with Lynn, that, with reasonable parameterization of the double-hump barrier and with extrapolation from known actinide cross sections, one can predict the more important unknown actinide cross sections with an uncertainty of 25-30% (an assertion which Weigmann contested in his report on the

fourth Workshop day: see also my summary remarks of that day). On
the other hand he pointed out that the methods used to derive
unknown actinide coss sections should not be more sophisticated
than warranted by the accuracy requirements of the users.
Personally, in the years to come I would still expect an increase
in these accuracy requirements so that the considerable effort,
which is currently going into actinide cross section evaluations,
may still have to be strengthened.

Let me conclude by bringing out two general observations
which were implicitly contained in various discussions and in my
summaries so far.   First, evaluation should not become too
academic and isolated.   This is strongly related to the second
observation that evaluation is not an independent exercise, but
essentially a service to users.   Specialization into different
methodical approaches, nuclide ranges etc. as is apparent at this
workshop   is   certainly   necessary   and   useful.   These
specializations, however, should not lead to isolation.   We can
all learn from each other and we have numerous examples where only
the   combination   of   various   specialized   efforts   led   to   a
satisfactory end result.

SESSION XIII

PHOTON PRODUCTION, $E_n > 0$
Chairman: R.J. Howerton LLNL

EVALUATION OF PHOTON PRODUCTION DATA FROM NEUTRON-INDUCED REACTIONS

C. Y. Fu

Oak Ridge National Laboratory
Oak Ridge, Tennessee 37830, U.S.A.

ABSTRACT

The evaluation methods and procedures used for
generating the photon production data in the current
Evaluated Nuclear Data File (ENDF/B, Version V) are
reviewed. There are 42 materials in the General Pur-
pose File of ENDF/B-V that contain data for prompt
photon production. Almost all evaluations had sub-
stantial experimental data bases, but less than half
of them employed any of the following evaluation
methods. Only a few used theoretical techniques that
are sophisticated enough to ensure internal consis-
tency with other particle production data. Comments
are made on four evaluation methods: the empirical
formalism of Howerton et $al.$, the Troubetzkoy model,
the multi-particle Hauser-Feshbach/Precompound model,
and the Yost method. Critiques are also made on three
procedures used for conserving photon energies in neu-
tron capture reactions. The presence of photon pro-
duction data in the file is useful for studying energy
balance, since photon production generally accounts
for a large portion of the reaction energy output.
Problems found in energy balance checks are discussed.

INTRODUCTION

The evaluation methods used for generating the photon produc-
tion data in ENDF/B-IV [1] were reviewed by Young [2] in 1975. At
that time there were 38 materials in the General Purpose File which
included data for prompt photon production. Four new materials
with photon production data were added for ENDF/B-V [3]. These
are ^{15}N, ^{51}V, ^{59}Co, and ^{232}Th. About half of the materials with
photon production data in ENDF/B-IV were reevaluated or updated
for ENDF/B-V.

The improvement of the photon production data in ENDF/B-V over those in ENDF/B-IV was made essentially through the use of better experimental data and additional applications of the empirical method of Howerton *et al.* [4,5] and the multi-particle Hauser-Feshbach/Precompound model [6]. No new methods or procedures were introduced for ENDF/B-V.

Three of the evaluation methods, the exception being the Yost method, were covered by Young's review [2]. It is perhaps more useful and efficient for the present review to emphasize new topics and new examples. We seriously urge the reader, if interested, to study the previous review beforehand. Little repetition, if any, is made here.

EVALUATION METHODS

The Empirical Method of Howerton *et al.*

This method [4,5] was based on the observation that the photon production spectra from (n,γ) and $(n,x\gamma)$ reactions for heavy elements are evaporation-like. Because of its simplicity, it has been applied to the evaluation of photon production data for a wide range of materials, including ^{31}P, S, Ti, Nb, Mo, Ta, ^{232}Th, and ^{238}U. Its application for the lighter materials may be problematical. As shown by Young [2], it works fine for Ta but not Mo. We reinforce this point by showing in Figs. 1-3 some comparisons of the Ti evaluation with recent data [7]. It is clear that there are structures as functions of both E_γ and E_n that are beyond the method.

The Troubetzkoy Model

The model [8] is based on the compound nucleus assumption without spin and parity considerations. Therefore, one can only include in the calculation multipolarities of the gamma-ray transitions but not their types (E or M). The method was used to calculate the photon production distributions from $(n,x\gamma)$ reactions in Cu and the W isotopes for ENDF/B-V. It was shown by Young [2] that the method works reasonably well for W if one is given some freedom in the adjustment of level density parameters. As for the lighter element, Cu, we do not expect it to work quite as well. Figure 4 illustrates this point by showing some comparisons of the ENDF/B-V Cu evaluation with recent measurements [9].

The Multi-Particle Hauser-Feshbach/Precompound Model

This is the Hauser-Feshbach model with precompound effects. Several model codes have been developed with the aim of computing cross sections for emission of a few outgoing particles, including gamma rays. The Los Alamos code, GNASH [10], was used for the evaluation of ^{15}N. The Oak Ridge code, TNG [11], was used for

the evaluation of Si and Ca from 1 to 20 MeV with complete internal consistency, and for ^{19}F and ^{23}Na to supplement experimental data. Both codes allow the use of externally calculated direct interaction cross sections in the gamma-ray cascades calculations. Some calculated results for Ca [11] are compared in Figs. 5-7 with the measurements of Dickens *et al.* [12]. It is clear that the model is capable of reproducing the more pronounced structures in the photon distributions as a function of incident neutron energies except for high-energy transitions involving the continuum. Recently Gardner *et al.* [13] analyzed several photon production cross sections and spectra for the (n,γ) and (n,xγ) reactions in the mass 90 region and the Ta-Au region. Although their aim was to study parameter (level spacing, radiative width, giant dipole parameter) systematics, their results generally confirm the usefulness and versatility of the multi-particle Hauser-Feshbach/Precompound model.

The Yost Method

The Yost method [14,15] was used for generating the neutron energy-dependent capture gamma-ray yields up to 1 MeV incident neutron energy for Fe, Ta, and W. The results for Fe and W were adopted for ENDF/B-V. The method represents a judicious combination of experimental data and theories:

1. In the resolved resonance region, the R-matrix theory was used to average partial photon spectra that are ℓ-dependent at each incident neutron energy.

2. In the unresolved resonance region, the Hauser-Feshbach model was used for the averaging.

3. All photon transition probabilities evaluated from experimental data, whether primary or secondary from thermal or resonance captures, are used as input to the calculation. This procedure ensures reproduction of evaluated experimental data.

4. Known level properties (spins, parities, and branching ratios) are supplemented by nuclear structure calculations consistent with the experimental photon properties and transitions.

5. Model parameters such as the M1/E1 ratio and level density are varied to fit approximately the experimentally-observed transitions for the purpose of filling in unmeasured transitions and for extrapolating to unmeasured energy regions.

Table I illustrates some characteristics of the evaluated capture gamma-ray distributions as a function of incident neutron energies.

The part of the distribution for $E_\gamma > 8$ MeV is mainly from capture in ^{54}Fe. The distribution in the E_n group of 1.0-1.4 keV is predominantly due to capture in the 1.167-keV resonance ($J^\pi = 1/2^-$) in ^{57}Fe. That in $E_n = 6.5$-9.0 keV is mainly from capture in a s-wave resonance in ^{55}Fe, thus having large yields in the part for $E_\gamma > 8$ MeV. It is clear that the photon distribution in the last neutron group is very different from the other two.

EVALUATION PROCEDURES

Energy Conservation for the Capture Reaction

For the capture reaction, three procedures are in use for conserving the photon energies as the incident neutron energy increases.

LP Flag [16]. Primary photon transitions can be identified by $LP = 2$. When this is the case, the primary photon energy is computed as

$$EG'_k = EG_k + \frac{AWR}{AWR + 1} E_n$$

where EG_k is the energy of the k'th primary photon for $E_n = 0$, and AWR is the ratio of the target mass to neutron mass.

This procedure is used to conserve energy where primary transitions are reasonably well known, as in the cases of H, ^{2}H, ^{3}H, ^{6}Li, ^{7}Li, ^{10}B, ^{12}C, and ^{14}N. In all these cases, only one photon distribution is given and assumed valid for all incident neutron energies. This latter assumption is generally incorrect except for the hydrogen isotopes.

Varying Multiplicity. The multiplicity of photons produced in the capture reactions may be increased with increasing incident neutron energy to conserve energy:

$$M(E_n) = M(0)(E_{cm} + Q_{n,\gamma})/Q_{n,\gamma}$$

where $Q_{n,\gamma}$ is the Q-value for the capture reaction and E_{cm} is center-of-mass energy of the incident neutron.

This procedure is used for ^{9}Be, Mg, ^{31}P, Cr, Nb, Mo, Ta, and ^{232}Th. In all cases, only one photon distribution is given and assumed valid for all incident neutron energies. This procedure is also incorrect but can perhaps be tolerated for heavy materials.

Explicit Energy Conservation. For ^{19}F, Si, Fe, W, and Pb, some efforts were made to evaluate the photon distributions as a function of incident neutron energies. This is the better procedure if some resonance capture photon yields are available experimentally.

Energy Balance for (n,xγ) Reactions

There is no simple procedure to ensure energy balance in (n,xγ) reactions except in special cases. For example, in light nuclides, the origin of each photon may be known and cross sections for producing a particular photon can be related through branching ratios with cross sections of the associated particle-producing reaction. The errors in the branching ratios do not affect energy balance. Another example of insuring energy balance

is found in the application of advanced nuclear model calculations. As in the cases for Si and Ca [11], all experimental data above 1 MeV were interpreted through consistent (n,x) and (n,xγ) calculations. Energy balance is implicit with this method, so problems never arise. In addition, experimental data for (n,x) and (n,xγ) reactions reinforce each other in such consistent model calculations.

In all other cases in which (n,x) and (n,xγ) cross sections were evaluated independently, the energy balance in an evaluation can be checked approximately with the relation:

$$\sigma_t E_n + \sum_i \sigma_i Q_i = \sum_i \sigma_i M_{ni} E_{ni} + \sum_i \sigma_i M_{\gamma i} E_{\gamma i} + KERMA \quad . \quad (1)$$

In Eq. (1), σ_t is the total cross section; E_n is the incident neutron energy in the laboratory system; σ_i, Q_i, M_i, and E_i are respectively the cross section, Q-value, multiplicity, and the average energy of the outgoing neutron or photon for the i'th reaction. Similar terms due to charged particle emission and nucleus recoil are lumped into the factor KERMA, the Kinetic Energy Release in Material. The KERMA factor is usually less than a few percent of the total energy output. Equation (1) can be used to compute KERMA if all the other terms are obtainable from the evaluated file. However, the result can be extremely erroneous because of the subtraction of two large numbers whose errors may be much larger than the KERMA factor itself. On the other hand, if the KERMA factor can be estimated from other means such as nuclear model calculations, then Eq. (1) may be used to check energy balance of the evaluation. This has been done by MacFarlane [17] and energy imbalances were found in nearly all materials containing photon production data except ^{16}O, Si, and Ca, and those materials with mass numbers less than 15.

The extent to which photon production data can affect KERMA factor calculations or the energy balance checks is illustrated for Cu at 14-MeV incident neutron energy. First we look up the KERMA factor estimated from a nuclear model calculation [18] as 0.28 MeV-barns. Then we show in Figs. 8 and 9 comparisons of the ENDF/B-V Cu photon production cross sections and average energies with the recent measurements of Morgan [9]. If we assume that the Morgan data are correct, then errors in the evaluated photon production data alone already exceed 0.28 MeV-barns in the vicinity of 14 MeV. However, this error cannot be brought out by energy balance checks if similar errors exist in the opposite direction in the neutron production data.

Elemental Q-Value Problem

The elemental Q-value problem is a procedural problem. As can be seen from Table 1, there is no single Q-value that can be used to conserve energy for all three photon distributions for the (n,γ) reaction. Similar situations exist for all reactions in all elemental materials that contain two or more isotopes with non-

negligible cross sections. One solution is to provide isotopic cross section evaluations.

PROMPT PHOTONS FROM FISSION

Prompt photon production following thermal-neutron fission of ^{235}U and ^{239}Pu have been measured by Verbinski and Sund [19] and of ^{235}U by Peelle and Maienschein [20]. The measurement of Verbinski and Sund for ^{235}U was used for the ENDF/B-V evaluations for both ^{235}U and ^{238}U. That for ^{239}Pu was adopted for both ^{239}Pu and ^{240}Pu. However, the measurement for ^{235}U by Peelle and Maienschein was used for ^{232}Th and ^{241}Pu. In all cases, one photon distribution is assumed valid for all incident neutron energies. In most cases, photons emitted within 100 nsec after fission are defined by evaluator as prompt.

RECOMMENDATIONS

The multi-particle Hauser-Feshbach/Precompound model is applicable for all reactions and energy ranges except the resolved resonance range. For photon production in the resolved resonance range, the Yost method is the only feasible one. The empirical formalism of Howerton *et al.* and the Troubetzkoy model are useful for heavy elements, perhaps for target mass greater than 100.
If only one photon distribution due to capture is used for a wide range of incident neutron energies, the LP flag method seems more appropriate for conserving energy for light nuclides while the varying-multiplicity method seems better for heavy nuclides.
Energy balance checks should be the evaluator's responsibility in the future so that corrections or adjustments can be made before turning in the evaluation. Perhaps standard checking codes should be written and distributed to all evaluators. Standard evaluation of the KERMA factors should be undertaken and used as input to these checking codes.
The "elemental Q-value" problem, illustrated in Table 1 for the E_n-dependent capture photon yields for elemental iron, is a long-recognized problem that still needs to be resolved.

ACKNOWLEDGEMENT

REFERENCES

1. ENDF/B Summary Documentation, compiled by D. Garber, BNL 17541 (ENDF-201), second Edition (October 1975).

2. P. G. Young, "Nuclear Models and Data for Gamma-Ray Production," in Proc. Conf. Nuclear Cross Sections and Technology, Washington, D. C., March 3-7, 1975, NBS Special Publication 425.

3. ENDF/B Summary Documentation, compiled by R. Kinsey, BNL-NCS-17541 (ENDF-201), Third Edition (July 1979).

4. R. J. Howerton and E. F. Plechaty, Nucl. Sci. Eng. 32, 178 (1968).

5. S. T. Perkins, R. C. Haight and R. J. Howerton, Nucl. Sci. Eng. 57, 1 (1975).

6. See, for example, C. Y. Fu, "Development of a Two-Step Hauser-Feshbach Code with Precompound Decays and Gamma-Ray Cascades," in Proc. Conf. Nuclear Cross Sections and Technology, Washington, D. C., March 3-7, 1975, NBS Special Publication 425.

7. G. L. Morgan, "Cross Sections for the Ti(n,xn) and Ti(n,xγ) Reactions Between 1 and 20 MeV," ORNL-5563 (1979).

8. E. S. Troubetzkoy, Phys. Rev. 122, 212 (1961).

9. G. L. Morgan, "Cross Sections for the Cu(n,xn) and Cu(n,xγ) Reactions Between 1 and 20 MeV," ORNL-5499 (1979).

10. P. G. Young and E. D. Arthur, LA-6947 (1977).

11. C. Y. Fu, Atom. Data and Nucl. Data Tables 17, 127 (1976). Also, C. Y. Fu, "A Consistent Nuclear Model for Compound and Precompound Reactions with Conservation of Angular Momentum," ORNL/TM-7042 (1980) and submitted to Physical Review C.

12. J. K. Dickens, T. A. Love and G. L. Morgan, Nucl. Sci. Eng. 53, 277 (1974).

13. D. G. Gardner, M. A. Gardner and F. S. Dietrich, "A Study of Gamma-Ray Strength Functions," UCID-18759 (1980).

14. K. J. Yost, J. E. White, C. Y. Fu and W. E. Ford, III, Nucl. Sci. Eng. 47, 209 (1972).

15. J. E. White, C. Y. Fu and K. J. Yost, Nucl. Sci. Eng. 51, 496 (1973).

16. D. Garber, C. Dunford and S. Pearlstein, "Data Formats and Procedures for the Evaluated Nuclear Data File, ENDF," BNL-NCS-50496 (ENDF-102), October, 1975.

17. R. E. MacFarlane, "Energy Balance of ENDF/B-V," Trans. Am. Nucl. Soc. 33, 681 (1979).

18. J. B. Roberto, M. T. Robinson and C. Y. Fu, J. Nucl. Mater. 63, 460 (1976).

19. V. V. Verbinski and R. E. Sund, "Measurement of Prompt Gamma-Rays from Thermal-Neutron Fission of ^{235}U and ^{239}Pu, and from Spontaneous Fission of ^{252}Cf," GA-9148 (1969).

20. R. W. Peelle and F. C. Maienschein, "The Absolute Spectrum of Photons Emitted in Coincidence with Thermal-Neutron Fission of Uranium-235," Nucl. Sci. Eng. 40, 485 (1970) and ORNL-4457 (1970).

TABLE I

E_n-Dependent Capture Gamma-Ray Yields for Iron
(Photons per 100 Captures)

E_γ (MeV)	E_n (eV)		
	Thermal	1.0-1.4 keV	6.0-9.0 MeV
1.5	7.0	6.9	3.2
2.0	14.7	7.9	4.5
2.5	6.1	7.5	7.7
3.0	9.3	11.8	5.3
3.5	11.2	12.1	6.8
4.0	3.2	4.6	7.0
4.5	9.1	7.8	5.6
5.0	4.4	6.1	5.8
5.5	1.2	2.2	2.8
6.0	9.3	3.9	6.2
6.5	9.3	15.2	4.3
7.0	0.2	0.2	2.4
7.5	4.8	0.8	2.2
8.0	49.9	54.1	1.8
8.5	0.0	0.0	0.06
9.0	0.8	0.02	10.6
9.5	4.3	0.09	59.7
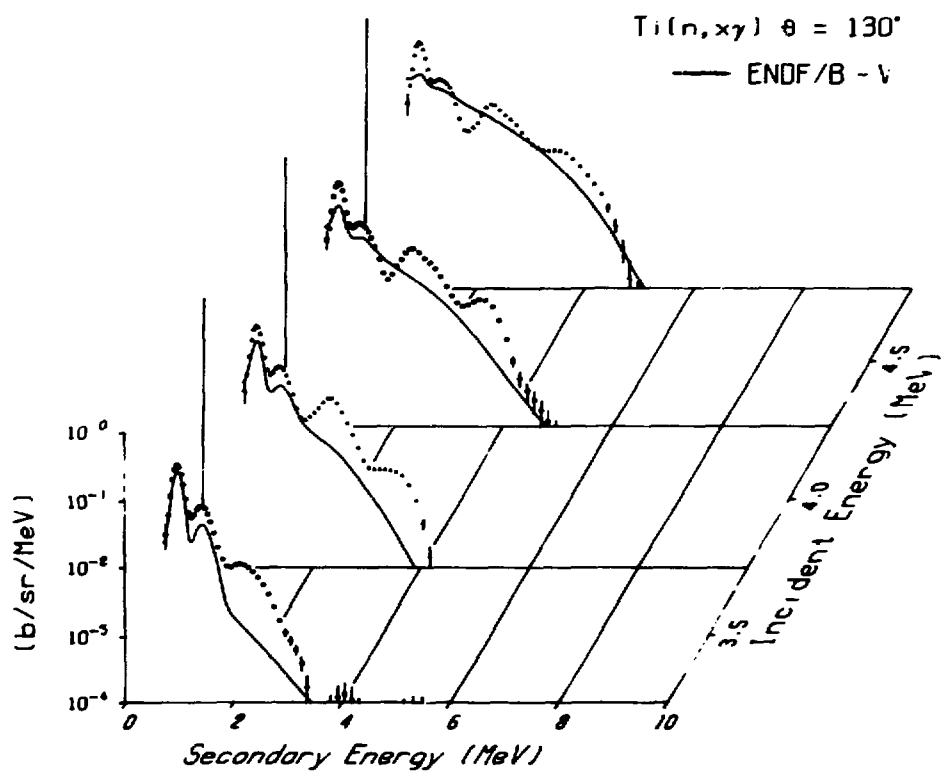
Fig. 1. Comparisons of ENDF/B-V evaluation for Ti with recently
measured [7] photon production spectra versus photon and incident
neutron energy.
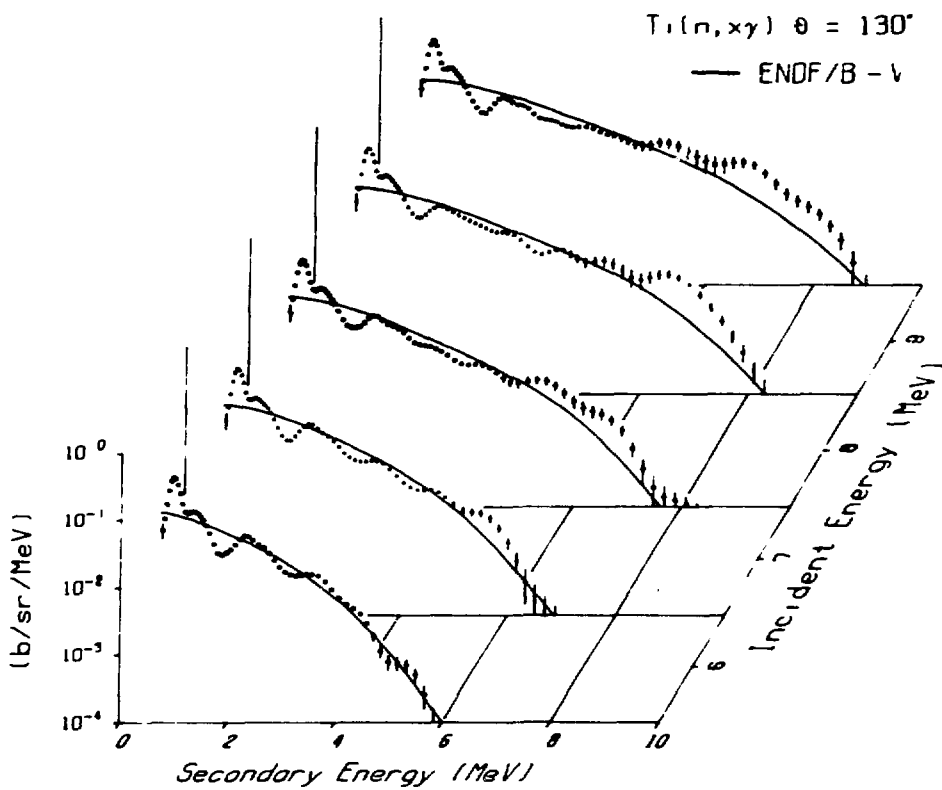
Fig. 2. Comparisons of ENDF/B-V evaluation for Ti with recently measured [7] photon production spectra versus photon and incident neutron energy.
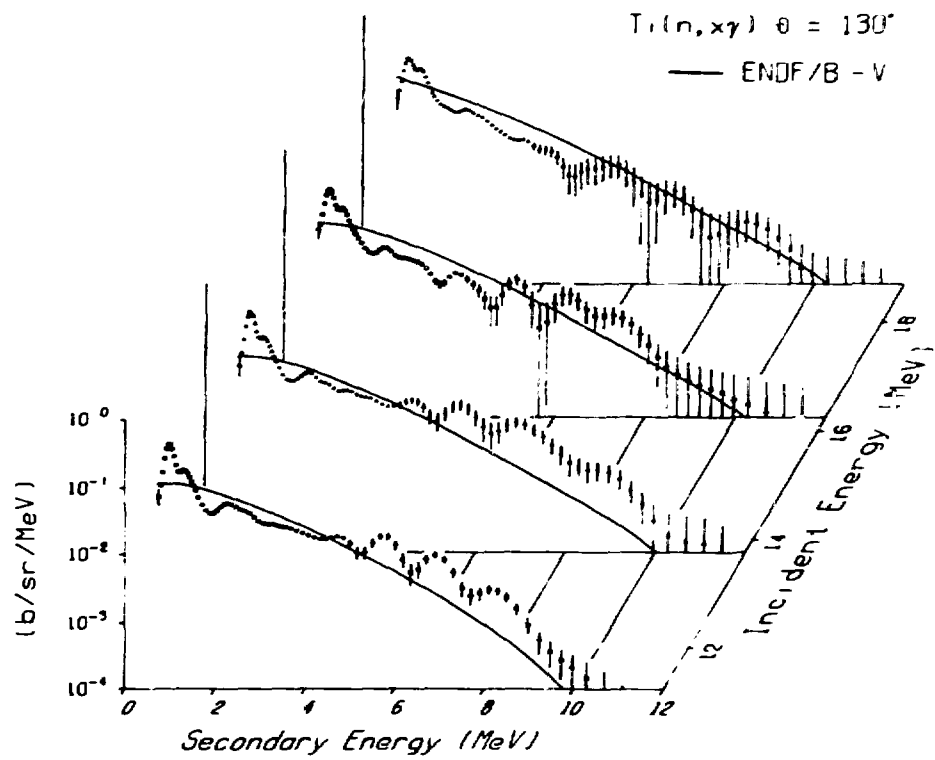
Fig. 3. Comparisons of ENDF/B-V evaluation for Ti with recently measured [7] photon production spectra versus photon and incident neutron energy.
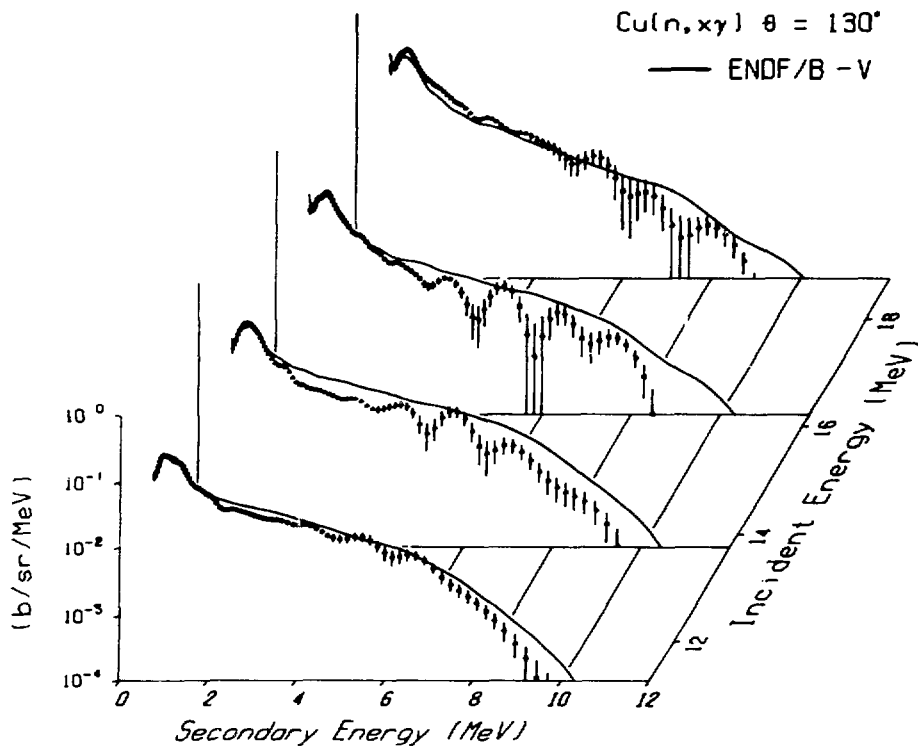
Fig. 4. Comparisons of ENDF/B-V evaluation for Cu with recently measured [9] photon production spectra versus photon and incident neutron energy.
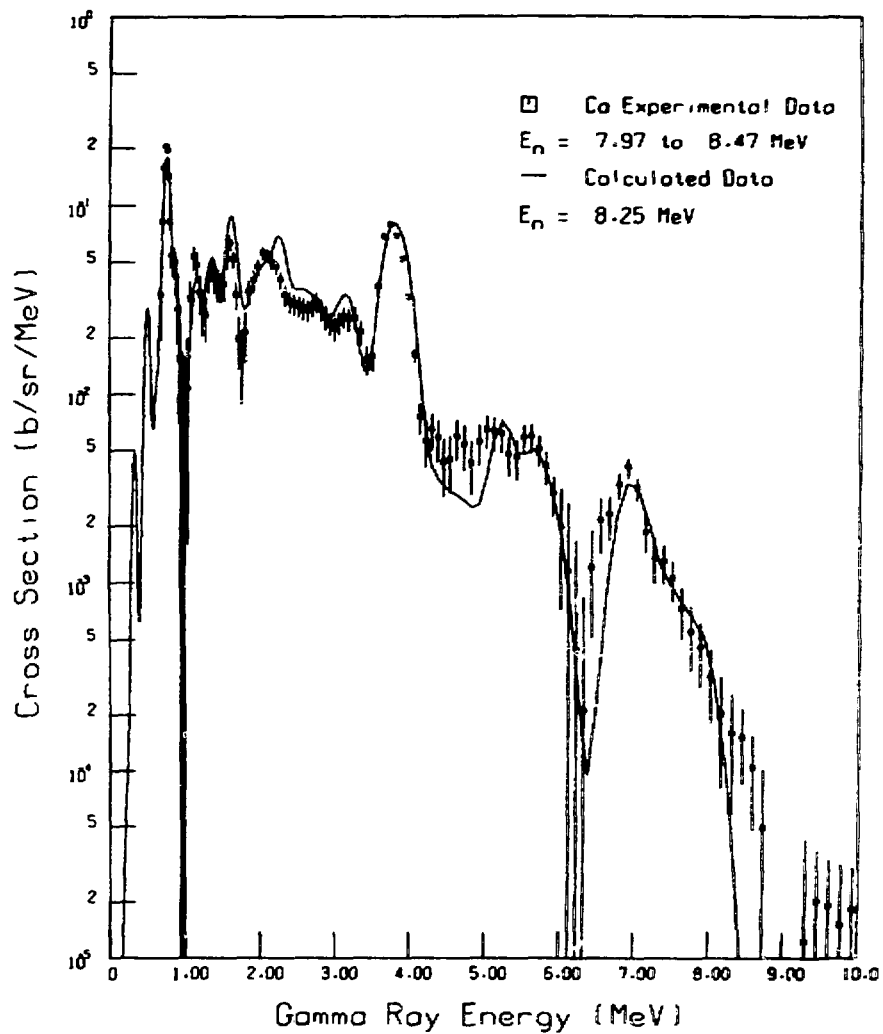
Fig. 5. Comparison of calculated photon production spectrum with measured data [12] for Ca. The calculation was based on the multi-particle Hauser-Feshbach/Precompound model and was adopted for ENDF/B-V to ensure energy conservation.
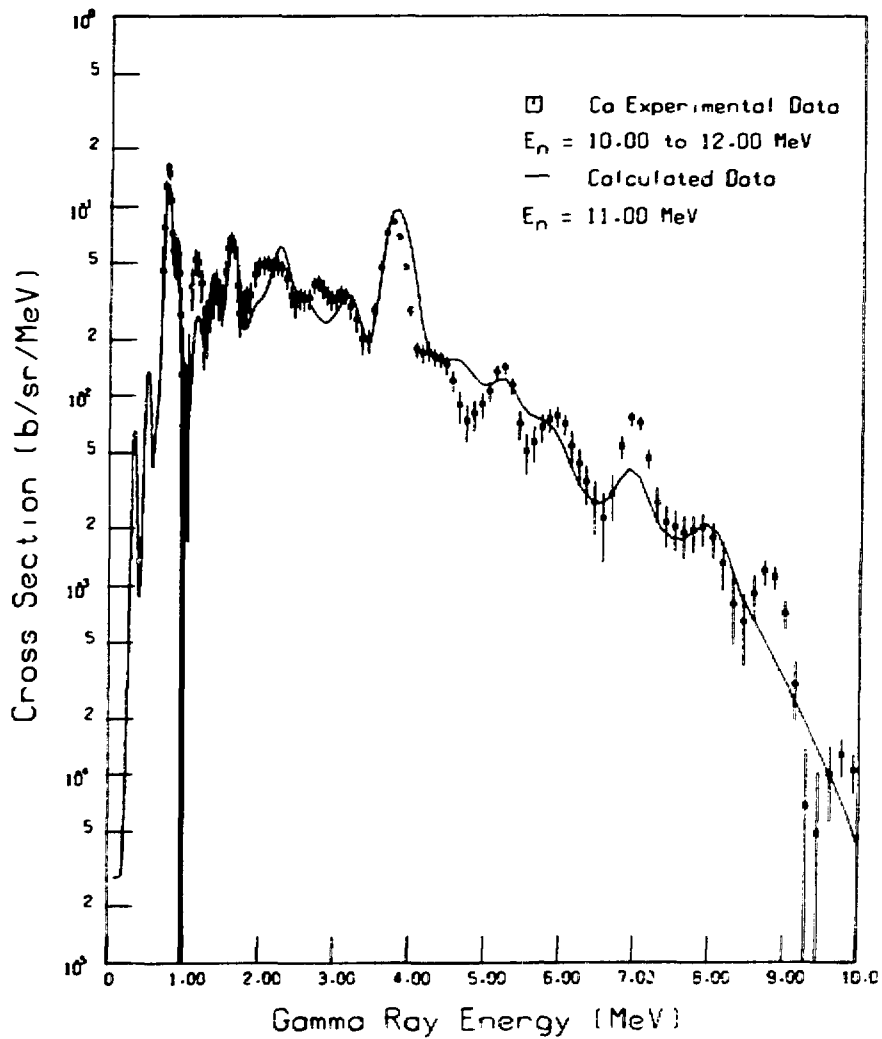
Fig. 6. Comparison of calculated photon production spectrum with measured data [12] for Ca. The calculation was based on the multi-particle Hauser-Feshbach/Precompound model and was adopted for ENDF/B-V to ensure energy conservation.
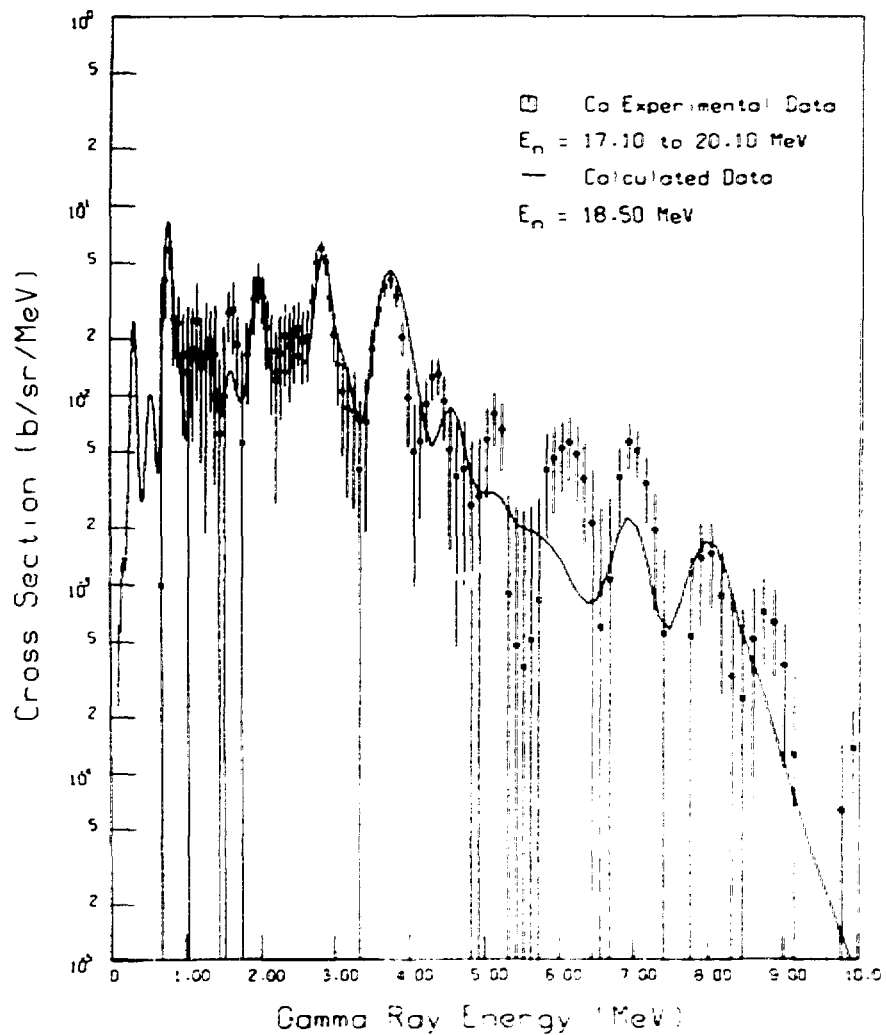
Fig. 7. Comparison of calculated photon production spectrum with measured data [12] for Ca. The calculation was based on the multi-particle Hauser-Feshbach/Precompound model and was adopted for ENDF/B-V to ensure energy conservation.
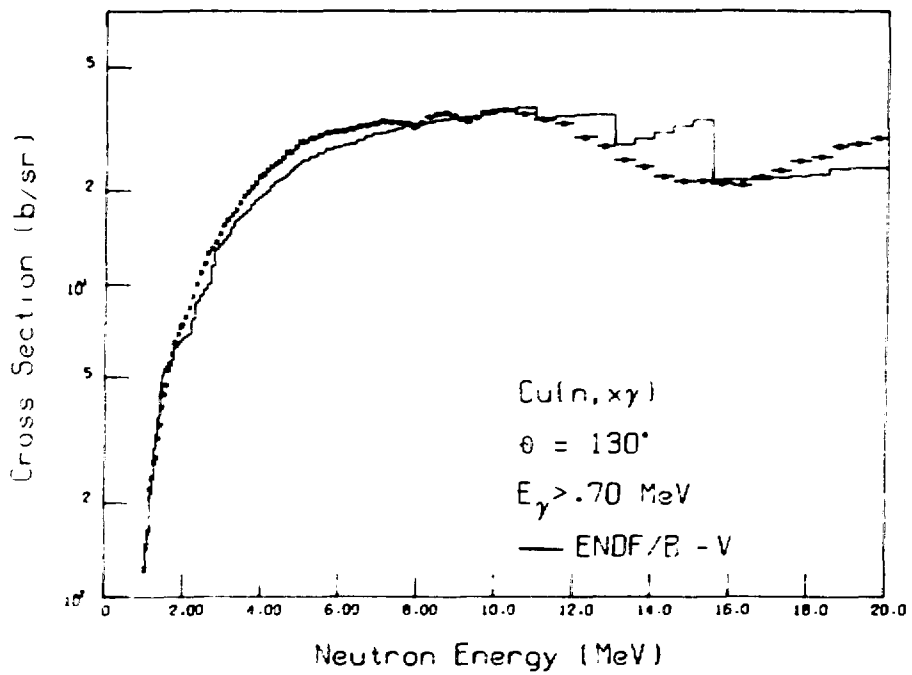
Fig. 8. Integrated yield of secondary photons with $E_\gamma > 0.7$ MeV as a function of the incident neutron energy for Cu.
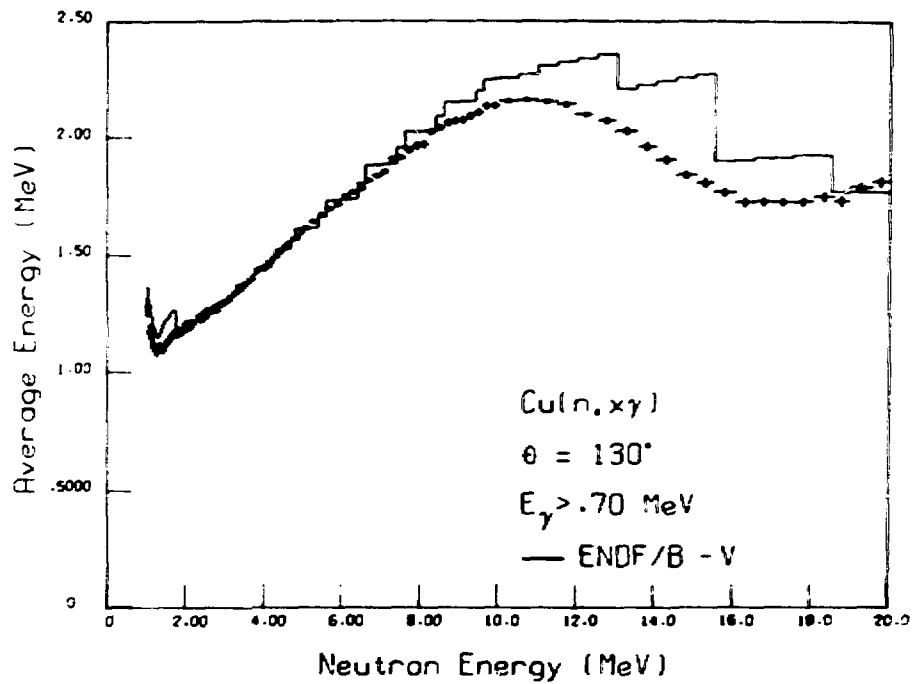
Fig. 9. Average energy of secondary photons with $E_\gamma > 0.7$ MeV as a function of the incident neutron energy for Cu.

Discussion

Howerton

Before the questions I would like to make a comment about some of
the discrepancies associated with energy balance in the ENDF/B
files since I am partially responsible for these but, in a sense,
innocent of culpability. When it was decided that the ENDF/B-IV
library should have photon production data for general purpose
evaluations, there were several materials that did not have such
data. There were photon production data in the ENDL files for
those materials. I agreed that ENDL data could be married onto
the ENDF/B-IV evaluations but with the Caveat that method 1 that
Peter described was used to produce the ENDL values. This method
insures an energy balance if, and only if, the neuton
distributions are those of the file for which the photon data were
produced. Since the ENDF/B-IV neutron energy distributions were
not the same as the neutron energy distributions of the ENDL file,
this adding-on of ENDL photon production data to ENDF/B-IV files
insured, in general, an energy imbalance. This was well-known and
considered at that time. It was decided that having ENDF/B-IV
photon production data with an energy imbalance was better than
having no photon production data in the files for those materials.

Mughabghab

I note in the figure which you showed on the photon production
cross neutron of Ti that there is an excess of strength at high
γ -ray energies. These may be due to "direct" processes. Have
you made any attempt to include these effects in the calculations?

Howerton

I have to answer that question since I was responsible for the
titanium evaluation. The answer is no. The model is complete as
you saw it described so these effects would not be taken into
account. I would like to add that I prefer not to call that which
you saw described under Item 1 a model, I would much rather call
it a recipe.

Fu

The higher γ -ray cross sections you saw in the measurements are
probably not associated with direct capture. The direct capture
can contribute at most about one millibarns at these energies and
the remainder of the $(n,x\gamma)$ reactions can contribute up to several
barns.

Vonach

I should like to comment that complete photon-production cross sections for Barium have been calculated by Uhl and Strohmaier using their multi-step Hauser-Feshbach code STAPRE.
    What is the origin of the discontinuties in the evaluated production cross section of Cu shown in Fig. 8 which do not occur in the measured spectrum?

Fu

I suspect that a mistake was made by the person who did the calculation, but I really don't know.

Stewart

We should bear in mind the importance of the fact that the Q-value upon which KERMA is based has no real counterpart when performing evaluations for elemental mixtures of isotopes. For Cu, for example, the (n,γ) and $(n,2n)$ Q-values differ by as much as 2 MeV for ^{63}Cu and ^{65}Cu. Therefore, it is very difficult to balance energy in all cases for elemental files.

Froehner

For the sake of completeness I'd like to mention that even before Yost's method was published there was a gamma-ray cascase code by Poenitz, published in Zeitschift fur Physik, which gave good results for the populations of low-lying states and is, in modified form, also used in the calculations of Uhl and Strohmaier.

Smith

I would like to comment that attention should be given to the need for isotopic experimental input. The requisite sample supply is under pressure. If there is a need for measured data, an isotopic sample supply must be assured so I strongly urge evaluators to make their needs known and thus establish pressures to reestablish a supply of samples.

Perey

I would like to expand a little on Alan Smith's comment. It is extremely important because it is strongly relevant to the interaction between users, evaluators, and measurers. For some users, we as evaluators (and measurers) can provide what the user wants in terms of measurements and evaluations that are done for elemental mixtures of isotopes. For other users, specific activations may be required and for these, isotopic measurements and evaluations will be necessary. I am concerned that measurements are made for elements of such things as neutron

emission spectra; then an evaluator tries to take the measurements apart and assigns subsidiary spectra to individual reactions and/or to individual isotopes. Then the user who needs evaluated data for the element puts it all back together again. These processes may mix it all up so that what the user eventually has is not very closely related to what was measured. I don't know what what we can do about this.

SESSION XIV

SPECIAL PROBLEMS
Chairman: R.J. Howerton LLNL

PROBLEMS IN THE EVALUATION OF FISSION CROSS SECTIONS

H. Weigmann

CEC-JRC, Central Bureau for Nuclear Measurements
B-2440 Geel, Belgium

ABSTRACT

This contribution concentrates on a few specific
problems which are encountered in the evaluation of
fission cross sections. They are related to the present-
day picture of the fission barrier shape and its conse-
quences for the mechanism of the fission reaction.
For the major fissile isotopes for which a large
amount of high quality experimental data exist, only
minor basic problems are encountered which are connected
with the detailed application of R-matrix theory for the
description of the cross section in the resonance region,
and, especially in the case of ^{239}Pu, with the possible
influence of intermediate structure on resonance self-
shielding and Doppler coefficients.
The main emphasis will be put on nuclei for which
little experimental information is available, and thus
theory is the only handle to evaluate the fission cross
sections or at least to bridge large gaps in the experi-
mental data base. Several problems exist : There are
systematic discrepancies in fission barrier parameters as
obtained from different experimental sources. As is well
known, in the region of the fission threshold, the average
fission cross section is strongly influenced by the
presence of intermediate structure; however, the simul-
taneous occurence of intermediate structure and statisti-
cal parameter fluctuations has not been dealt with ana-
lytically; Monte-Carlo simulations are used here to assess
the magnitude of the effect. At energies above the
fission barrier, the question of the density of barrier
transition states comes into play; this is an outstanding
problem which deserves special interest and care in
future work.

INTRODUCTION

Reactor physics calculations require the knowledge of cross sections for neutron induced nuclear reactions for a large variety of nuclei. For many of these, transactinides in particular, experimental information on cross sections is sparse. Nuclear theory and systematics is the only way to evaluate these cross sections or to fill large gaps in the experimental data base. It is hoped that this can ultimately be done with an accuracy of the order of 25% which is a typical figure for the requirements for the so-called "minor" transactinides. In the case of fission cross sections, some typical problems are encountered which are related to the detailed structure of the fission barrier and its conse-quences for the mechanism of the fission reaction. The discussion of some of these problems is the main subject of this paper.

Before we enter the discussion of evaluations based on syste-matics, two minor basic difficulties should be mentioned which exist in the description of the resonance region also for the common fissile nuclei.

PROBLEMS WITH THE COMMON FISSILE ISOTOPES

In the case of the major fissile isotopes, for which a large amount of accurate experimental data is available, the goal of an evaluation is twofold : At higher energies, where cross sections are smooth functions of energy, it is mainly a critical judgement of the experimental data, and the definition of a recommended "best" data set. However difficult the judgement of the quality of an experimental cross section may be, there are no fundamental difficulties. At low energies, i.e. in the (resolved and unresolved) resonance region, the additional aim is to obtain a handable parametrization of the cross section and to provide the necessary information for the calculation of secondary effects like resonance self-shielding and Doppler-coefficients.

The Resolved Resonance Region

In the resolved resonance region a description of the cross section in terms of resonance parameters is desired which should serve for both, the required parametrization of the cross section curve as well as a basis for the statistical description of the unresolved resonance region. Besides the well known difficulties in using the various approximations to R-matrix theory for a description of the experimental cross section, a more fundamental problem exists with respect to the definition of a partial fission width :

When one was considering a simple (single-humped) fission barrier, the partial fission width was simply given as

$$\Gamma_{f,i} = \frac{D}{2\pi} P_{f,i} \qquad (1)$$

(D is the spacing of compound nuclear resonances)
where   was the penetrability of the fission barrier for a given
"Bohr channel" characterised by the quantum number J (total angu-
lar momentum) and K (its projection onto the symmetry axis). For
the simple approximation of a parabolic fission barrier, the pene-
trability was given as

$$P_{f,i} = \left[1 + exp\left(\frac{2\pi(E_f + \epsilon_i - E)}{\hbar\,\omega_f}\right)\right]^{-1} \qquad (2)$$

where E_f is the height of the lowest fission barrier and ϵ_i is the
excitation energy of the Bohr channel i with respect to that
barrier. The total fission width for a resonance with total angu-
lar momentum J was then

$$\Gamma_f^{(J)} = \sum_i \Gamma_{f,i} \qquad (3)$$

where the sum is over all Bohr channels with total angular momentum
J.

The definition of partial fission widths in terms of penetra-
bilities for individual Bohr channels was essential for the inter-
pretation of the statistical distribution of the total fission
widths $\Gamma_f^{(J)}$ resembling a small number (1 to 4) of degrees of free-
dom.

Equations (1-3) may still be a good approximation also for a
double-humped barrier if the two barriers are sufficiently
different in height such that the lower one may essentially be
neglected. However, for the most important fissile isotopes this
is not expected to be the case. For a true double-humped barrier,
the total fission width for above barrier fission is usually
written as

$$\Gamma_f^{(J)} = \frac{D}{2\pi} T_f^{(J)} \quad ; \qquad T_f^{(J)} = \frac{T_A^{(J)} T_B^{(J)}}{T_A^{(J)} + T_B^{(J)}} \qquad (4)$$

where $T_x^{(J)}$ (X=A,B) are the total transmission coefficients for
the two separate barriers

$$T_x^{(J)} = \sum_i \left[1 + exp\left(\frac{2\pi(E_x + \epsilon_i - E)}{\hbar\,\omega_x}\right)\right]^{-1} \qquad (5)$$

where the sums again are over "Bohr channels".

Although equations (4,5) give a valid definition of the total
fission width of a resonance (for above barrier fission where
intermediate structure effects can be ignored), the partial fission
width is not consistently defined. A definition of a partial
fission width analoguous to equ.(4) with T_A, T_B referring to indi-
vidual Bohr channels would be incorrect since it would ignore the

possibility of K-mixing in the second well. On the other hand, partial widths are of course required by R-matrix theory for the description of interference effects which play an important role in the cross sections of the fissile isotopes. Thus, here one is dealing with a deficiency of the basic theory.

The quality of fits obtained with a definition of the partial fission width as in equ.(1) shows that the difficulty is not too serious as far as the parametrization of the cross section is concerned, but the physical interpretation of the "resonance parameters" obtained may be different from what it was believed to be.

The Unresolved Resonance Region

Whereas the average cross section of the common fissile isotopes in the unresolved resonance region is well known experimentally, the unknown detailed structure of the cross section is of importance only in a statistical sense as far as it influences resonance self-shielding and Doppler effects. The usual method [1,2] to assess the latter is to generate resonance parameters from their respective distribution laws, to construct mock-up cross sections from such resonance sequences and then calculate self-shielding and Doppler coefficients. The problem with this procedure is that the extrapolation of average fission widths and their apparent distribution laws as obtained from the resolved resonance region, into the unresolved resonance region, may be in error if intermediate structure is present. In particular in the case of ^{239}Pu it is well known due to the work of James and Patrick [3] that marked intermediate structure occurs in the J=1$^+$ channel. Consequently, in their evaluation of ^{239}Pu data for ENDF/B-V, Kujawski and Stewart [4] adopt an energy dependence of $< \Gamma_f >$ for J=1$^+$ (and also of $< \Gamma_n^o >$ for J=0$^+$,1$^+$) adjusted such as to fit the pointwise average cross section data in the unresolved resonance region. Problems remain, however, e.g. with the separation of the observed (in the resolved region) width fluctuations into changes of the average value due to intermediate structure, and statistical fluctuations of the individual parameters around their averages. A detailed critical discussion of the statistical treatment of the unresolved resonance region has been given by de Saussure and Perez [5].

EVALUATIONS BASED ON THEORY AND SYSTEMATICS

The starting point for the evaluation of an experimentally insufficiently known cross section (at not too low energies) is the Hauser-Feshbach type statistical model. In the case of neutron induced fission the average cross section reads :

$$\overline{\sigma}_{n,f} = \pi \lambda^2 \sum_{J} g(l,J) \sum_{l,s} \frac{T_{n,l_s}^{(J)} \, T_f^{(J)}}{\sum_{c'} T_{c'}} \, f_{n,l_s;f}^{(J)} \qquad (6)$$

where the summations are over total angular momentum J and orbital angular momentum l and spin s ; the T's are transmission coefficients, $g(l,J)$ is the spin-statistical weight factor and $f_{n,l_s;f}^{(J)}$ is the width fluctuation correction [6].
Here,we are concerned with the fission transmission co-efficient $T_f(J)$. For above-barrier fission where effects of inter-mediate structure may be ignored, it can be written as

$$T_f^{(J)} = \frac{T_A^{(J)} \, T_B^{(J)}}{T_A^{(J)} + T_B^{(J)}} \qquad (7)$$

where, as before, the T_A and T_B are total transmission coefficients for the two separate barriers and are principally given by equ.(5). Of course, individual barrier transition states ("Bohr channels") are known only for very low excitation energies ϵ_i ; at higher energies only their density can be estimated and the generalised expression for the barrier transmission coefficient becomes (X = A,B) :

$$T_X^{(J)} = \sum_i \left[1 + exp\left(\frac{2\pi(E_X + \epsilon_i - E)}{\hbar \omega_X} \right) \right]^{-1} + \int_{J}^{\infty} d\epsilon \, f_X(\epsilon,J) \left[1 + exp\left(\frac{2\pi(E_X + \epsilon - E)}{\hbar \omega_X} \right) \right]^{-1} \qquad (8)$$

In the following subsection we will separately discuss the problems of determining the barrier parameters (mainly E_X), the replacement of equ.(7) for situations with intermediate structure, and the estimate of barrier state densities $f_X(\epsilon,J)$.

Fission Barrier Parameters

Fission barrier parameters for most actinides, including many nuclei which are difficult to study by neutron-induced reactions, have been obtained by Britt [7] from a statistical model analysis of charged particle induced fission reactions. Do these parameters lead to consistent results when applied in the calculation of neutron induced fission? Unfortunately, this is far from being obvious. This may be seen from fig. 1 which, for a few nuclei, compares barrier heights obtained from three different sources, i.e. charged particle reaction data [7], the analysis of average neutron iduced fission cross sections in the threshold region by Lynn [8], and the analysis of sub-barrier intermediate structure

data. The latter yield widths of class II doorway states $\Gamma^\downarrow$ and $\Gamma^\uparrow$ which under the assumption of complete damping are related to the barrier penetrabilities by

$$\Gamma^\downarrow = \frac{D_{\tilde{u}}}{2\pi} T_A \quad ; \quad \Gamma^\uparrow = \frac{D_{\tilde{u}}}{2\pi} T_B \quad ; \quad T_x = \left[1 + exp\left(\frac{2\pi (E_x - E)}{\zeta \, \omega_x} \right) \right]^{-1} \quad (9)$$

where D_{II} is the class II level spacing. Only the lowest barrier transition state is important for sub-barrier fission ($\epsilon_i = 0$ in equ.(8)). For the same values as given by Lynn [8] have been used. For details, numerical values and references to experimental work see ref. [9].

The problems are obvious from Fig. 1, the differences between the results from sub-barrier resonance data and average cross sections being even larger than those between average neutron- and charged particle induced cross sections. It has to be remembered that a 0.2 MeV difference in barrier height produces about a factor of 5 in the transmission coefficient at energies 0.5 MeV below the barrier top.

Let us first examine whether the analysis of sub-barrier intermediate structure resonances could be in error. There are certainly problems : The penetrabilities obtained from intermediate structure data are very uncertain due to Porter-Thomas fluctuations of the widths $\Gamma^\downarrow$ and $\Gamma^\uparrow$ (in most cases they are based on the analysis of only one cluster), and due to the assumption of complete damping, thus differences of up to 0.2 MeV or even 0.3 MeV in barrier heights could be understood if they were random. However, the observed discrepancies are often much larger and they are too systematic in the sense that the intermediate structure analysis yields much lower values usually for one of the two barriers.

Some support for the analysis of the intermediate structure data comes from the observed fission widths of a few resonances at very low energies (far below the first intermediate structure group). If these fission widths are interpreted by direct tunnelling through both barriers, they may be related to the penetrabilities according to

$$\Gamma_{f, min} = \frac{D_{\tilde{u}}}{2\pi} \frac{T_A \, T_B}{4} \quad (10)$$

Table 1 compares the experimental fission widths of very low energy resonances (column 3) to those calculated from the barrier parameters obtained from the intermediate structure analysis (column 2). The agreement is satisfactory.

The main difference thus arises between barrier heights obtained from sub-barrier resonance fission widths in general and

those from the analysis of average cross sections. A possible
reason for large differences between these two sources lies in the
fact that in the case of intermediate structure and low energy
resonance data one looks at the barrier for a specific spin
(corresponding to s-wasve neutron interaction), whereas the average
cross section data are sensitive to a comparatively broad spectrum
of spin values and essentially the lowest barrier is effective.
This fact could thus explain why much higher barriers may result
from resonance data than from average cross sections. However, the
observed discrepancies generally have the opposite sign.

Thus, there exists a discrepancy between resonance data and
average cross section data with respect to barrier parameters,
which at present is not understood.

Effect of Intermediate Structure on Fission Cross Sections

Equation (7) for the fission transmission coefficient is valid
only as long as no intermediate structure is present, i.e. well
above the lower barrier. It becomes invalid as soon as inter-
mediate structure develops in sub-barrier or near barrier
situations, even if the structure is not resolved. The reason is
that due to intermediate structure the overall fission strength
is concentrated in a small number of resonances whereas the bulk
of resonances has a fission width which is much reduced as compared
to the average; the contribution to the cross section of the few
resonances with very large fission width on the other hand is
limited by their neutron widths. The net effect is a reduction of
the average fission probability.

The problem of determining the average fission probability in
this situation has been treated by Lynn and Back [14] in a double
picket fence model approximation : A uniform sequence of class I
resonances is assumed with constant neutron widths and fission
widths following a Lorentzian distribution with a width repre-
senting the total width of an isolated class II state. Then a
uniform sequence of class II states is assumed with constant fission
($\Gamma^\uparrow$) and coupling ($\Gamma^\downarrow$) widths given by equ.(9). The result
obtained by Lynn and Back for the average fission probability
reads :

$$ P_f = \left[1 + \left(\frac{\Gamma'}{\overline{T}_f} \right)^2 + 2 \left(\frac{T'}{\overline{T}_f} \right) coth \left[\frac{1}{2} \left(T_A + T_B \right) \right] \right]^{-1/2} \tag{11} $$

where $\overline{T}_f$ is given by equ.(7) and T' is the sum of transmission
coefficients for all decay channels other than fission.

Thus whenever intermediate structure effects are expected to
be important in the average fission cross section, the fission
transmission coefficient entering the statistical model expression
equ.(6) should be replaced by an effective transmission

coefficient

$$T_{l',+H}^{(7)} = \frac{P_l^{(7)}}{1 - P_l^{(7)}} \sum_{c'} T_{c'}^{(7)} \tag{12}$$

where the sum c' includes all non-fission channels.

As mentioned, equ.(11) is valid in a double picket fence model approximation. Also, the assumption of a Lorentzian distribution for the fine structure fission widths implies $\Gamma + \Gamma > D_I$. The opposite situation in which a perturbation approach is valid, is also treated in ref.[14], and the influence of statistical fluctuations of the class I and class II level parameters are separately and essentially qualitatively discussed.

In order to get a more quantitative insight into the combined effect of the statistical fluctuations of class I and class II level parameters, a series of numerical cross section calculations from Monte Carlo simulations of level sequences has been performed: First, a sequence of class II levels with average spacing D_{II} = 500 eV is generated and their fission (Γ^f) and coupling (Γ^+) widths are independently sampled from Porter-Thomas distributions (valid for sub-barrier energies) with average values given by equ.(9). Then, a sequence of class I levels with average spacing D_I = 10 eV is generated; their neutron widths are sampled from a Porter-Thomas distribution with average value $D_I/2\pi$ x T_n; and a constant capture width $\Gamma_c = D_I/2\pi$ x T_c is assumed. For each class II level, depending on whether $\Gamma^f + {}^c\Gamma^+$ is smaller or larger than 0.5 D_I, it is decided whether its coupling to the class I resonances is treated in perturbation theory or whether a Lorentzian energy dependence of the fine structure fission widths is assumed. In the latter case, the Lorentzian profile

$$\langle \overline{\Gamma}_f \rangle = \frac{D_I}{2\pi} \frac{\Gamma^+ \Gamma^f}{(E-E_s)^2 + \frac{1}{4}(\Gamma^+ + \Gamma^f)^2} \tag{13}$$

defines the expectation value of the fine structure fission widths and individual values are sampled from Porter-Thomas distributions with this energy-dependent expectation value. In the perturbation case the class II coupling width defines an average squared coupling matrix element as

$$\overline{H_c^2} = \frac{D_I}{2\pi} \Gamma^+ \tag{14}$$

and individual values are sampled from a Porter-Thomas distribution with this average.

From the sequence of resonances constructed this way the average cross section for a given compound nuclear spin is

calculated and the procedure repeated a sufficient number of times to obtain a reasonably accurate average. The whole calculation has been done for a number of combinations of T_A and T_B and the results plotted in Fig. 2 as a function of P_F (equ.(11)); in fact, different combinations of T_A and T_B corresponding to the same P_F yielded very similar results as long as both T_A and T_B are smaller than 0.5, i.e. one is dealing with a sub-barrier case (above the lower barrier the assumption made in these model calculations, e.q. Porter-Thomas distributions for the class II widths, would be invalid anyhow).

The full curve in Fig. 2 represents the ratio

$$W_{nf} = \frac{\sigma_{nf}\ (\text{simulation})}{\sigma_{nf}\ (\text{stat. model without fluct. corr.})} \qquad (15)$$

of the fission cross section obtained from the Monte-Carlo simulation and the one calculated from equ.(6) with $T_f^{(J)}$ as given in equ.(12), and $f_{ncl,f}^{(J)} = 1$. For comparison, the broken line gives the width fluctuation factor calculated in the usual way [6] with the value obtained from equ.(12) for T_f.

For one value of P_F ($P_F = 0.054$) Fig. 2 also gives the result obtained when only the parameter distributions for the class I levels are kept and those for the class II levels are replaced by δ-functions (point marked $\triangle$) and when the distributions for the class II levels are kept and the ones for class I levels replaced by δ-functions (point); it is seen that the parameter fluctuations for both classes of levels contribute almost equally strong to the net effect in this case.

The fixed parameters of Fig. 2 (D_{II}, D_I, T_C) were chosen such as to be characteristic of an even-even actinide target nucleus. The T_n of Fig. 2 may correspond to s-wave neutrons at about 100 keV neutron energy. Similar results for two other choices are shown in Fig. 3 ; the large T_C for one of these choices may be thought of as crudely representing a larger number of inelastic neutron channels the fluctuations of which roughly cancel.

The common feature of all three parameter combinations in Figures 2 and 3 is that the actual suppression of the fission cross section due to statistical fluctuations of level parameters as obtained from the Monte Carlo simulation, is much larger than the one which would be calculated from the usual fluctuation correction factor. It is not excluded that this effect has contributed to the discrepancies between fission barrier parameters as deduced from average cross sections on the one hand and from resonance data on the other hand, as described in the previous sub-section.

Density of Barrier Transition States

Once fission barriers and other reaction thresholds are known, nuclear level densities are the most important quantities for the calculation of cross sections. Level densities for several

different situations are required : the density of compound nuclear
resonances, the density of low lying states in the compound nucleus
for the calculation of radiative widths, the density of low lying
states in the target nucleus for the calculation of transmission
coefficients for inelastic scattering; and for the calculation of
fission transmission coefficients (equ.(7) and (8)) the densities of
transition states on top of both fission barriers.

Level densities for normal deformation and their energy- and
spin-dependence may, at least in principle, be obtained from experi-
mental observation, but the density of barrier transition states can
only be inferred indirectly from the analysis of fission cross
sections or probabilities, or estimated on theoretical grounds. For
a long time it was believed, however, that errors in the assumptions
on level densities would tend to cancel because mainly ratios of
level densities enter into fission probability and cross section
calculations. However, serious difficulties were met already in the
attempts to fit measured fission probabilities [7].

These difficulties are probably connected to the question of
the so-called collective enhancement of nuclear level densities :
Thermodynamic theories, the more advanced of which today are based
on realistic Nilsson-model single particle level schemes, calculate
the density of intrinsic excitations of the nucleus as a function of
excitation energy; although principally this intrinsic state density
depends on the single particle level density and thereby on
deformation, it turns out [7] that this dependence is rather weak
due to a cancellation effect : an increased single particle level
density (at barrier deformation) leads to an increased intrinsic
state density at given effective excitation, but it also leads to an
increased pairing gap and therefore to a reduced effective excitation
energy.

To the density of intrinsic states the effect of collective
excitations, mainly rotations, has to be added. It has been pointed
out by Bjørnholm, Bohr and Mottelson [15] that the density of
collective states depends critically on the spatial symmetry
properties of the nucleus. Whereas the nucleus is axially and
reflection symmetric at deformations corresponding to the first well,
it is now assumed that it is axially asymmetric at the first saddle
and reflection asymmetric at the second one. Thus, according to
ref. [15], the final level densities at the first and second
barriers would exceed the one at normal deformation by factors of
about 7 and 2, respectively.

The effect which the symmetry properties may have on fission
probabilities is shown in Fig. 4, which has been taken from Britt
[7]. It compares the fission probability for 237Np calculated with
an axially asymmetric first saddle to the one obtained for the same
barrier parameters but assuming axial symmetry. It is seen that
even if the latter calculation is renormalized to the experimental
data at about 6 MeV, it would give very bad results at higher
energies.

The asymmetric deformations at the saddle points are due to
shell effects, and it is well known that with increasing excitation

energy shell effects tend to disappear. Thus, with increasing excitation energy the nucleus will become axially symmetric again also at barrier deformations, and the extra enhancement of the level density due to lacking symmetry will disappear. The question of at what energies this will actually happen, needs further investigation.

An argument frequently brought forward against collective enhancement factors, is that it means double counting of degrees of freedom. The answer probably is that again this is a matter of excitation energy. What collective motion does is to shift levels down in energy; thus the additional levels at low energy will be missing at some higher energy where there are so many levels anyhow that this deficiency will be unimportant. Still, above some critical value of the excitation energy collective motion and thereby the collective enhancement to the nuclear level density may cease to exist.

Collective enhancement factors to the nuclear level density are still a much debated subject. But the discussion of the previous paragraphs and the example of Fig. 4 may show that it is a very important one which deserves special attention in future work.

REFERENCES

1. C.N. Kelber and P.H. Kier, Nucl. Sci. Eng., 26, 67 (1966)

2. M.W. Dyos, Nucl. Sci. Eng., 34, 181 (1968)

3. G.D. James and B.H. Patrick, Physics and Chemistry of Fission, IAEA, Vienna (1969), p. 391

4. E. Kujawski and L. Stewart, Trans. Am. Nucl. Soc., 26, 591 (1977)

5. G. de Saussure and R.B. Perez, Nuclear Cross Sections and Technology, Vol. I, p. 371, NBS Special Publication 425, Washington 1975

6. L. Dresner, Rep. ORNL-2659, Oak Ridge National Laboratory (1959)

7. H.C. Britt, Physics and Chemistry of Fission 1979, Vol. I, p. 3, IAEA, Vienna 1980

8. J.E. Lynn, UKAEA Report AERE-R 7468 (1974)

9. H.Weigmann, Proceedings of the Course on Nuclear Theory for Application, Trieste 1980, IAEA, Vienna, to be published

10. F.C. Difilippo et al., Phys. Rev., C21, 1400 (1980)

11. S. Plattard, J. Blons and D. Paya, Nucl. Sci. Eng., 61, 477 (1976)

12. G.F. Auchampaugh and L.W. Weston, Phys. Rev., C12, 1850 (1975)

13. D.W. Bergen and R.R. Fullwood, Nucl. Phys. A163, 577 (1971)

14. J.E. Lynn and B.B. Back, J. Phys., A7, 395 (1974)

15. S. Bjørnholm, A. Bohr and B.R. Mottelson, Physics and Chemistry of Fission 1973, Vol. I, p. 367, IAEA, Vienna 1974

TABLE 1

Comparison of fission widths of very low energy resonances
to those calculated with P_A and P_B obtained from the
analysis of intermediate structure

compound nucleus	$\Gamma_{f,min}$ (calc.) [eV]	$\Gamma_{f,min}$ (exper.) [eV]
^{239}U	$12 \cdot 10^{-8}$	$7 \cdot 10^{-8}$ [10]
$^{238}N_D$	$19 \cdot 10^{-6}$	$3 \cdot 10^{-6}$ [11]
^{241}Pu	$3.8 \cdot 10^{-4}$	$4 \cdot 10^{-4}$ [12]
^{243}Pu	$4 \cdot 10^{-5}$	$5 \cdot 10^{-5}$ [13]
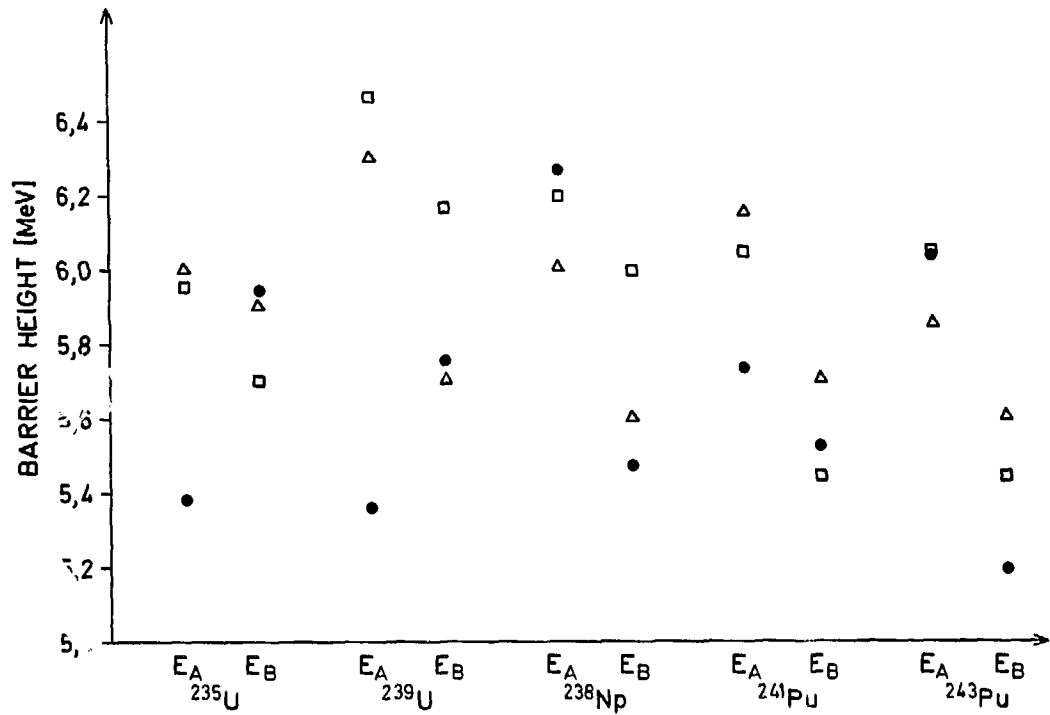
Fig. 1   Fission barrier heights as obtained from three different sources :

△   charged particle induced fission [7]

□   average neutron induced fission cross sections [8]

●   intermediate structure in sub-barrier resonances
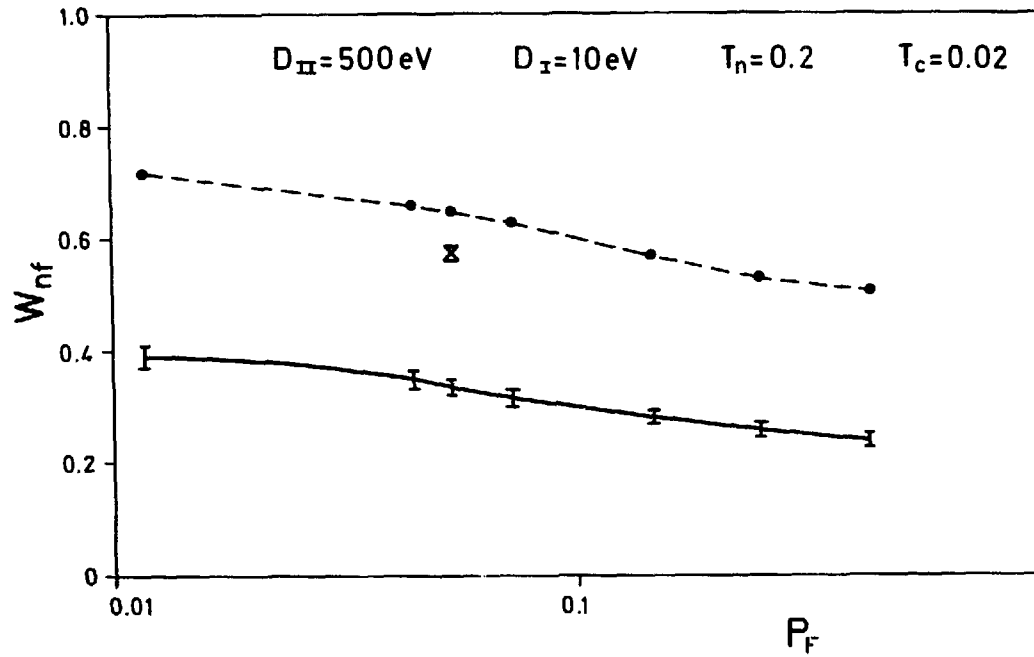
Fig. 2   Reduction of fission cross section due to statistical
         fluctuation of level parameters in a case with inter-
         mediate structure

————   Results of Monte Carlo simulation

------   usual fluctuation correction for purely
        statistical fluctuations
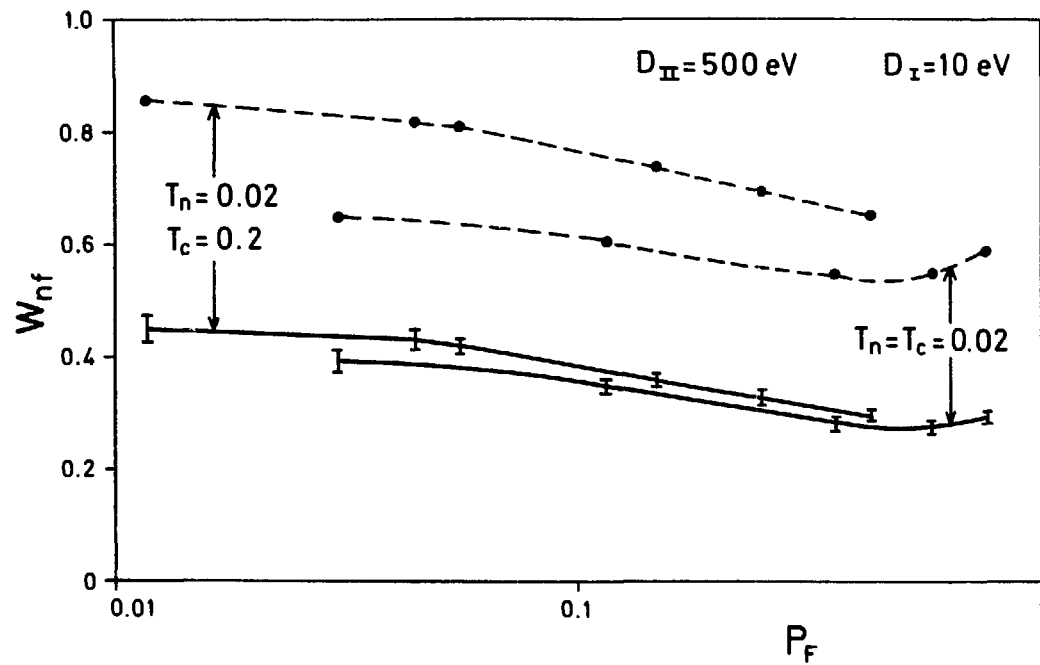
Fig. 3   Same as Fig. 2 for two further sets of average parameters
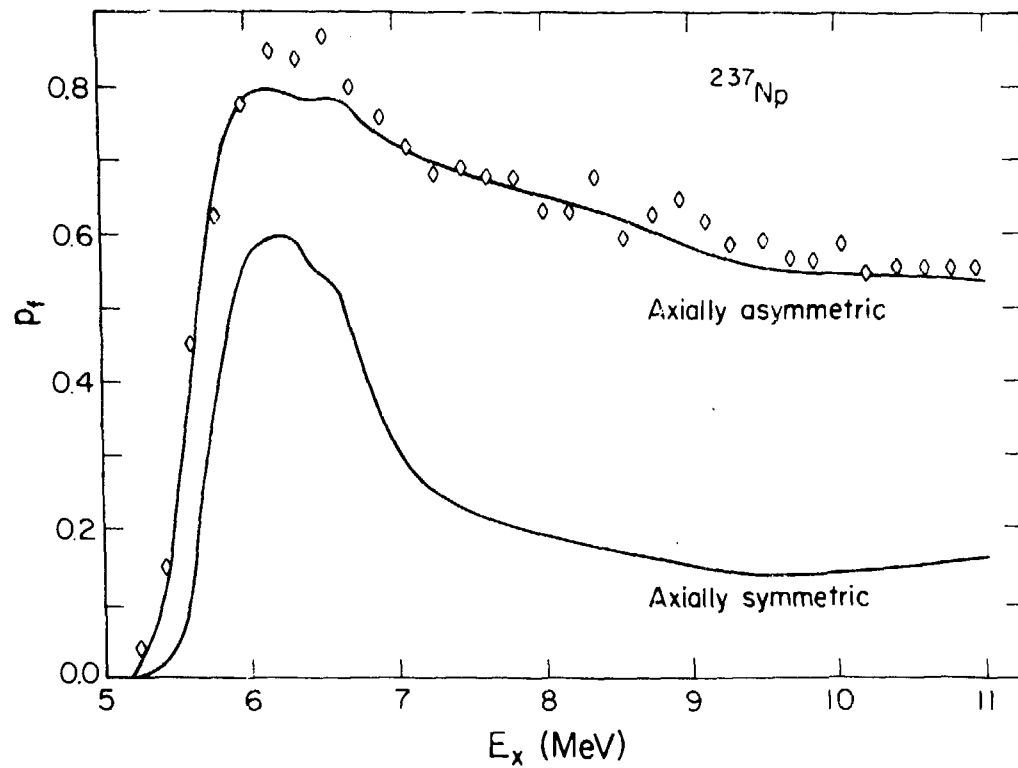
Fig. 4. Comparison of fission probability calculations for ^{237}Np
assuming axially asymmetric and symmetric first saddle
points (after H.C. Britt [7])

Discussion

Moldauer

Could you please tell us what is known about the angular momentum dependence of fission barrier parameters?

Weigmann

I think this is another point where not very much is known but I am glad you asked the question because I forgot to mention one point in connection with the apparent discrepancy shown here. We are looking at different angular moments when we compare average cross sections and resonance data. In the average cross sections we see a rather broader spectrum of angular momentum and the fission barrier which we see would be some kind of weighted average but effectively it would be the lowest barrier for the angular momentum spectrum which is coming into play. But for resonances we are looking at a barrier for a given spin, namely the spin of the resonance we are considering, so these two different observed phenomena could account for a difference, but in the opposite sense, because for the average cross section you would see the lowest barrier while for an individual resonance you would, in general, see a higher barrier. Since the experimental discrepancy is the opposite, this argument serves to enhance the observed discrepancy.

Menapace

On what do the discrepancies in barrier parameter estimates from different methods depend? How much do they depend at the saddle on the adopted level density formulas? How much do they depend on the estimate obtained from average fission cross sections?

Weigmann

They do indeed depend on the adopted level density expression. This is also discussed by Britt. The LASL data have been analyzed with different level density expressions. The latest analysis uses a level density routine by Moretto. The barrier parameters are different, but their dependence on the level density expression is certainly not sufficient to explain the discrepancies discussed in this paper.

Oup

EVALUATION OF FISSION PRODUCT YIELDS
FOR THE U.S. NATIONAL NUCLEAR DATA FILES

B. F. Rider

G.E. Vallecitos Nuclear Center
Pleasanton, California 94566, U.S.A.

T. R. England and D. G. Madland

Los Alamos Scientific Laboratory
Los Alamos, New Mexico 87545, U.S.A.

J. R. Liaw

Argonne National Laboratory
Argonne, Illinois 60439, U.S.A.

R. E. Schenter

Hanford Engineering Development Laboratory
Richland, Washington 99352, U.S.A.

ABSTRACT

Accurate knowledge of fission product decay heat is an important input to the design of quality emergency core cooling systems for nuclear power plants. The General Electric Company has prepared an evaluated set of fission product yields for use in calculation of decay heat curves with improved accuracy. These evaluated yields are based on all known experimental data through mid-1980. Unmeasured fission product yields are calculated from charge distribution, pairing effects, and isomeric state models developed at Los Alamos Scientific Laboratory. Numerous tests of the data have been made at General Electric, Los Alamos Scientific Laboratory, Hanford Engineering Development Laboratory, and the Argonne National Laboratory before incorporating them into Version V of the Evaluated Nuclear Data File (ENDF/B-V).

The 1980 version incorporates ∿88,000 yields and their uncertainties in 40 sets of ∿1100 values for independent yields before delayed neutron (DN) emission by 102 precursors, and a like number of cumulative yields after DN emission. The sets include 27 fissionable nuclides at one or more neutron fission energies. The models used, data sources, evaluation methods, the integral tests made, and the role of accurate fission product yields in reactor design will be discussed. The 1980 yields are available as ENDF-292 (1980) from the National Nuclear Data Center at Brookhaven National Laboratory, Upton, N.Y., or one of the authors, B. F. Rider, General Electric Company, Vallecitos Nuclear Center, P. O. Box 460, Pleasanton, CA 94566.

INTRODUCTION

Since the discovery of fission in 1939, many fission product yield measurements have been made and published. Such yields are useful for many purposes including understanding of the nature of the fission process, determining uranium burnup, calculating fission product inventory, performing shielding calculations, evaluation of neutron absorption effects, and calculating decay heating power. Of these, the most demanding is the calculation of decay heat power because a complete set of independent (direct) fission yields for all fission products with a half-life longer than a few tenths of a second, their half lives, and Q values (heat liberated with each disintegration) and errors associated with each are required.

For reliable and consistent nuclear calculations, it is highly desirable to have a single evaluated set of nuclear data. The United States National Nuclear Data Center at Brookhaven National Laboratory publishes such an Evaluated Nuclear Data File (ENDF/B-V). The General Electric Company has published evaluated fission yield data in a document, NEDO-12154. This fission yield evaluation has been expanded in cooperation with the Fission Yield Subcommittee and the Decay Heat and Actinide Subcommittee of CSEWG (Cross Section Evaluation Working Group) for inclusion in the ENDF/B files. Figure 1 shows the areas expanded specifically for ENDF/B-IV and ENDF/B-V.

GENERAL APPROACH

In the case of U-235 thermal fission, only 243 of the 1153 required independent fission product yields have been measured. All of the unmeasured values have been calculated from the best available models. All chain yields are normalized to 100% for the light and heavy mass peaks separately. Within each mass, a

Gaussian charge distribution has been assumed about the most
probable charge, Zp, with a standard deviation of 0.560 charge
units. Odd-even proton and neutron pairing effects are super-
imposed. The magnitudes of these pairing effects are shown in
Figure 2. All Zp values have been adjusted within their limits
of error to obtain an acceptable proton material balance from the
sum of binary and ternary fission yields. The extent of this
adjustment and the closeness of the balance can be seen in
Figure 3. To give further validity to the decay heat calcula-
tions, the direct yields to the metastable and ground state
isomers, which are nuclear spin dependent, are apportioned to
each isomer (where the spins are known) in accordance with the
equation in Figure 4. Delayed neutron emission is now treated by
including for the first time a proper treatment for fission yields
of 102 delayed neutron emitters. As a result, all independent
fission yields are now appropriately given before delayed neutron
emission and all cumulative fission yields are given after
delayed neutron emission in the traditional manner. All
recommended yields are the result of weighted averages of experi-
mental values, a systematic error of 2% is combined with the
reported random error of each absolute fission yield measurement.
Mass spectrometric measurements, because of possible mass dis-
crimination, have been assigned errors no smaller than 0.5%
relative.

Radiochemical measurements, because of the uncertainties in
absolute accuracies of decay schemes and the counting efficiencies
have been assigned errors no smaller than 20% in the years before
1955, 10% in the years from 1955 to 1965, and 5% in the years
since 1965. A few discrepant measurements were rejected on the
basis of traditional statistical criteria such as the Dixon Range
Test.

TESTS APPLIED

A number of tests were applied to the final yields. A plot
of the mass yields gives the familiar double peaked curve in
Figure 5. The effect of the fission-inducing neutron is seen in
Figure 6. For fission spectrum neutron energy fission, the
fission yields increase in the wings and the valley regions
relative to thermal neutron fission. These valley and wing
yields are all very rare events and taken together represent 0.5
to 1% of the total fission yield. Absolute increases in the
valley and wings with energy are exactly compensated by a corres-
ponding decrease of the values in the peaks, but these changes of
fission yield with neutron energy represent only a 1-3% decrease
in fission yields in the peaks going from thermal neutron fission
to fission spectrum fission, which in many cases, is less than
the experimental error of the measurements.

The number of neutrons contained in the fission products was
compared to the number of neutrons in the compound nucleus before

fission. The difference is the number of neutrons left over and available to carry on a chain reaction, designated nubar. This value closely agrees with the values of nubar obtained by direct measurement as seen in Figure 7. A Terrell plot of fission yield integrals gives curves for the heavy and light mass peaks which are separated by a value equal to nubar as in Figure 8. Any large errors in fission yields cause easily recognized aberrations in the curves. Another useful test is a three-dimensional pin plot of independent fission yields superimposed on the Chart of the Nuclides. In general appearance, the plot in Figure 9 appears as two mountains. From viewing this plot in different directions one can see the distributions of the light and heavy fission fragments as a function of neutron numbers, proton numbers, mass distribution, or charge distribution. Any sharply inconsistent value can be readily seen. The ultimate test is a comparison of decay heat power calculated from these fission yields with direct experimental measurement as shown in Figure 10.

DISCUSSION OF ERRORS

The chain yields in the peak region are known to about 5% in the well measured fissionable nuclides to about 14% in the less well measured fissionable nuclides as seen in Figures 11A and 11B. The chain yields in the wings and valley are less well known ranging from about 16%-25%. The U-235T yields are strikingly better known. Figure 12 looks at the makeup of the better known U-235T chain yield errors. It can be seen that these smaller errors are the result of many determinations rather than abnormally small errors assigned to individual measurements. The average individual measurement is about ±2% but in these cases about an average of 19 measurements result in the deviation of the mean being smaller than 1%.

Figures 13A and 13B show the consistency of these same well-known chain yields for U-235T and Pu-239T over a period of four compilations (revisions 0, 1, 2, 3 to NEDO-12154) from 1972 to 1980. Most noticeably in Pu-239T yields in Figure 13B, the xenon yields have tended to increase as the older measurements in which xenon was incompletely recovered have been corrected by later measurements using isotope dilution mass spectrometry. The non-xenon heavy mass peak nuclides have tended to decrease to compensate for the amount that the xenons have increased since each peak must total 100%. Because of just such unforeseen effects, it has been concluded that current yield recommendations should not be given accuracy assignments smaller than ±1% in the ENDF files in the future.

PROBLEM AREAS

1. Yields have been evaluated for thermal, fission spectrum energy, and 14 MeV induced fission. However, little has been done to model the yields induced by neutrons of energies outside these three neutron spectral regions.

2. Assignment of realistic uncertainties remains judgmental. Except for one case out of every 200 measurements (where a larger uncertainty was assigned by the evaluator) the uncertainty of each measurement was assigned by the one who made the measurement. A more objective method has not yet been found.

3. Merging experimental independent yields and experimental cumulative yields with modelled values for unmeasured independent yields has been a problem area. The method adopted is the powerful and constrained merging technique and resulting error analysis recommended by Spinrad (77SPI1). Independent yields are taken from a calculated charge distribution model. The model independent yields are normalized so their sum equals the chain yield. Large errors are given to the model yields. These model yields are merged statistically with weighted averages of measured yields. One set of cumulative yields is calculated by adding independent yields starting with the initial nuclide in a chain and ending with the chain yield. A second set of cumulative yields is calculated by starting with the chain yields and subtracting independent yields ending with the initial nuclide. These two sets are averaged using reciprocal variance weighting. The first set dominates the initial nuclide yield averages. The second set dominates the final chain member yield averages because of the small errors caused by the constraint imposed at 0% and 100% of the chain yield, respectively.

CONCLUSIONS

The full 983-page 1980 evaluation of fission product yields is now available on microfiche as Report No. NEDO-12154-3(B) from one of the authors (B. F. Rider, General Electric Company, Vallecitos Nuclear Center, P. O. Box 460, Pleasanton, CA 94566). These evaluated fission yields have been further extrapolated to include additional unmeasured low yield (<0.23%) nuclides and renormalized by a maximum of 0.23% to a total of 200% for both fission product peaks combined. The resulting independent and cumulative fission yields are available on computer tape from the U.S.A. National Nuclear Data Center, Brookhaven National Laboratory, Upton, New York 11973, as a part of the Evaluated Nuclear Data File (ENDF/B-V). Finally, the tables of mass chain yields are given in Figures 14A through 14H.

REFERENCES

62TER1   J. TERRELL, "Neutron Yields from Individual Fission
          Fragments," Phys. Rev. 127, 880-904 (1962).

76MAD1   D. G. MADLAND, T. R. ENGLAND, "The Influence of Pairing
          on the Distribution of Independent Yield Strengths in
          Neutron Induced Fission," ENDF-240 (1976).

76MAD2   D. G. MADLAND, T. R. ENGLAND, "Distribution of Indepen-
          dent Fission Product Yields to Isomeric States,"
          ENDF-241 (1976).

77YAR1   J. L. YARNELL, P. J. BENDT, "Decay Heat from Products
          of 235U Thermal Fission by Fast Response Boil-Off
          Calorimetry," LA-NUREG-6713 (Feb., 1977).

77SPI1   B. 1. SPINRAD, "The Sensitivity of Decay Power to
          Uncertainties in Fission Product Yields," Nucl. Sci.
          and Engr., 62, 35-44 (1977).

77MAD1   D. G. MADLAND, T. R. ENGLAND, "The Influence of Isometric
          States on Independent Fission Product Yields," Nucl. Sci.
          and Engr., 64, 859-865 (1977).

EVALUATION	PRE-ENDF	ENDF/B-IV	ENDF/B-V	ENDF/B-VI
REPORT NEDO-	12154	12154-1	12154-2E	12154-3B
YEAR	1972	1974	1978	1980
NUCLIDES	10	10	20	40
CUM. YIELDS	YES	YES	YES	YES
IND. YIELDS	NO	YES	YES	YES
ISOMER RATIOS	NO	NO	YES	YES
ODD-EVEN PAIRING	NO	YES	YES	YES
DELAYED NEUTRON	NO	NO	YES	YES
CHARGE BALANCE	NO	YES	YES	YES
TERNARY FISSION	NO	NO	YES	YES
REFERENCES	812	956	1119	1176
INPUT VALUES	6000	12400	18000	25200
FINAL YIELDS	11000	22000	44000	88000

FIGURE 1. Evaluation Evolution

NUCLIDE	PROTON EFFECT	NEUTRON EFFECT	FOOTNOTE
U235T	0.228	0.044	A
U235F	0.151	0.029	A
U235HE	0.015	0.003	A
U238F	0.329	0.063	A
U238HE	0.018	0.003	A
Pu239T	0.171	0.033	A
Pu239F	0.124	0.024	A
Pu241T	0.206	0.040	A
U233T	0.210	0.041	A
Th232F	0.327	0.063	A
U233F	0.143	0.028	A
U233HE	0.015	0.003	A
U236F	0.166	0.032	A
Pu239H	0.015	0.003	A
Pu240F	0.244	0.047	A
Pu241F	0.141	0.027	A
Pu242F	0.364	0.070	A
Th232H	0.018	0.003	A
Np237F	0.000	0.000	C
Cf252S	0.050	0.010	B

A = 76MAD1   B = 76LIP1   C = ASSUMED   D = UNKN

FIGURE 2A. Magnitude of Pairing

NUCLIDE	PROTON EFFECT	NEUTRON EFFECT	FOOTNOTE
U234F	0.079	0.015	A
U237F	0.102	0.020	A
Pu240H	0.117	0.023	A
U234HE	0.016	0.003	A
U236HE	0.017	0.003	A
Pu238F	0.000	0.000	D
Am241F	0.000	0.000	D
Am243F	0.000	0.000	D
Np238F	0.000	0.000	D
Cm242F	0.067	0.013	A
Th227T	0.000	0.000	D
Th229T	0.274	0.053	A
Pa231F	0.000	0.000	D
Am241T	0.000	0.000	D
Am241H	0.000	0.000	D
Am242MT	0.000	0.000	D
Cm245T	0.000	0.000	D
Cm249T	0.109	0.021	A
Cf251T	0.000	0.000	D
Es254T	0.000	0.000	D

A = 76MAD1   B = 76LIP1   C = ASSUMED   D = UNKN

FIGURE 2B. Magnitude of Pairing (concluded)

NUCLIDE	SUM Z*YIELD	ATOMIC NO.
U235T	92.03	92
U235F	92.00	92
U235HE	92.00	92
U238F	92.00	92
U238HE	91.99	92
Pu239T	93.98	94
Pu239F	94.00	94
Pu241T	94.00	94
U233T	92.04	92
Th232F	90.00	90
U233F	91.98	92
U233HE	92.00	92
U236F	92.00	92
Pu239H	94.00	94
Pu240F	94.00	94
Pu241F	94.00	94
Pu242F	94.00	94
Th232H	90.00	90
Np237F	93.00	93
Cf252S	97.99	98

FIGURE 3A.   Charge Balance Test

NUCLIDE	SUM Z*YIELD	ATOMIC NO.
U234F	92.00	92
U237F	92.00	92
Pu240H	93.99	94
U234HE	92.00	92
U236HE	92.00	92
Pu238F	94.00	94
Am241F	95.00	95
Am243F	95.00	95
Np238F	93.00	93
Cm242F	96.00	96
Th227T	90.00	90
Th229T	90.00	90
Pa231F	91.00	91
Am241T	94.99	95
Am241H	94.99	95
Am242MT	94.99	95
Cm245T	95.99	96
Cf249T	97.99	98
Cf251T	97.99	98
Es254T	98.99	99

FIGURE 3B. Charge Balance Test (concluded)

$$P(J) = P_0(2J+1)EXP[-(J+\tfrac{1}{2})^2/\langle J^2 \rangle] \qquad \text{(Eq 1)}$$

WHERE: $P(J)$ = ANGULAR MOMENTUM DENSITY DISTRIBUTION

$\sqrt{\langle J^2 \rangle}$ = J_{rms} (ANGULAR MOMENTUM OF INITIAL FRAGMENT)

$$\frac{IY(m)}{IY(g) + IY(m)} = \frac{\int_{J_c}^{\infty} P(J)dJ}{\int_{0 \text{ or } \frac{1}{2}}^{\infty} P(J)dJ} \qquad \text{(Eq 2)}$$

WHERE: $IY(m)$ = INDEPENDENT YIELD OF META-STABLE STATE

$IY(g)$ = INDEPENDENT YIELD OF GROUND STATE

FIGURE 4. Isomer Yields are Spin Dependent (76MAD2)
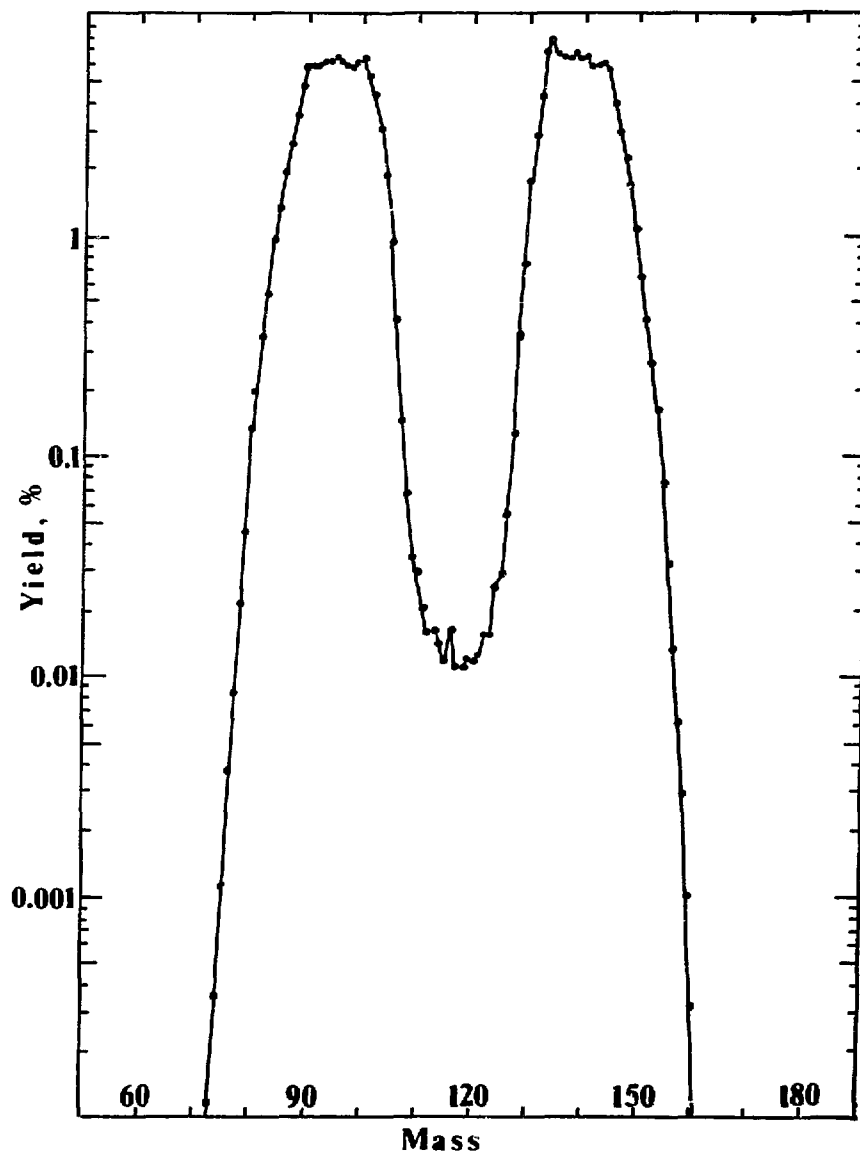
FIGURE 5. U235T Mass Yield Curve
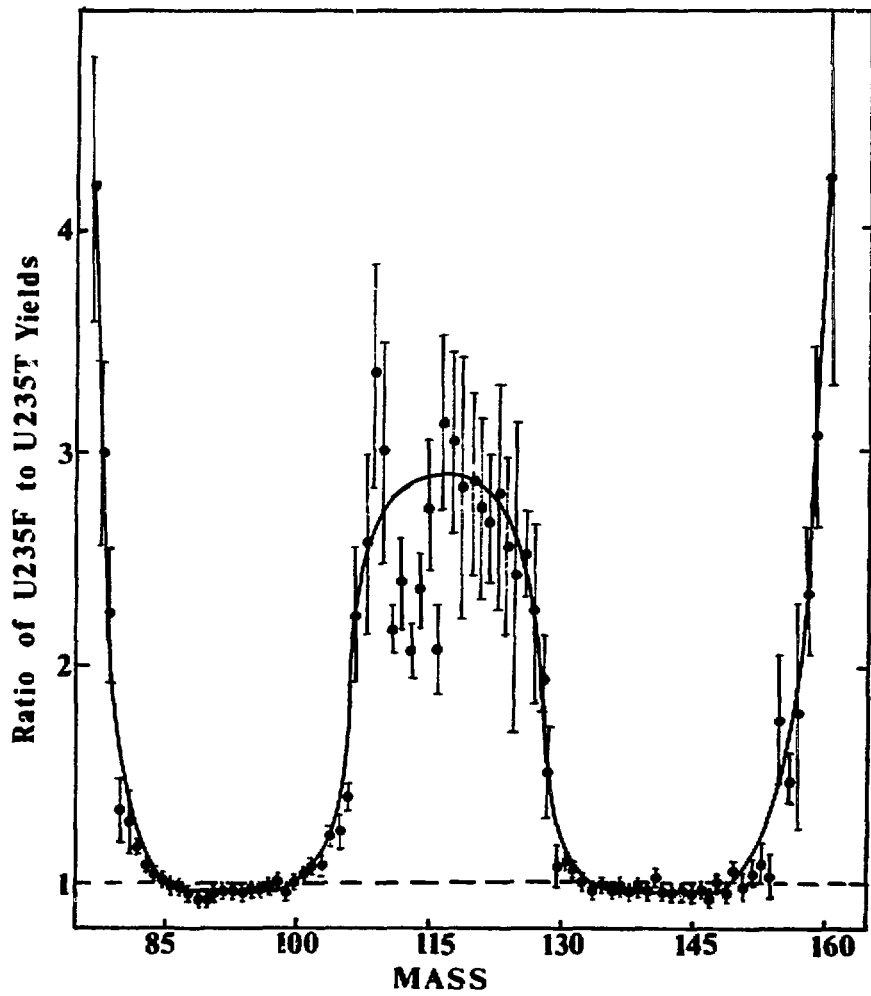
FIGURE 6. Effect of Neutron Energy

COMPOUND NUCLEUS		LESS LIGHT MASS AVE.	LESS HEAVY MASS AVE.	APPARENT NUBAR	EVALUATED NUBAR
U235T	236	- 94.91	-138.67	2.42	2.42
U235F	236	- 95.10	-138.45	2.45	2.47
U235HE	236	- 96.47	-135.28	4.25	4.38
U238F	239	- 97.32	-138.72	2.96	2.79
U238HE	239	- 97.90	-136.65	4.45	4.42
Pu239T	240	- 98.97	-138.09	2.94	2.88
Pu239F	240	- 99.08	-138.07	2.85	2.94
Pu241T	242	-100.26	-138.77	2.97	2.87
U233T	234	- 93.43	-138.09	2.48	2.49
Th232F	233	- 91.07	-139.65	2.23	2.42
U233F	234	- 93.64	-137.88	2.48	2.51
U233HE	234	- 95.97	-134.55	3.48	3.86
U236F	237	- 95.71	-138.54	2.75	2.78
Pu239H	240	-100.15	-135.25	4.60	4.90
Pu240F	241	- 99.46	-128.20	3.24	2.94
Pu241F	242	-100.36	-138.66	2.98	2.95
Pu242F	243	-100.56	-138.98	3.46	--
Th232H	233	- 93.64	-135.48	3.88	3.92
Np237F	238	- 97.09	-138.27	2.64	2.81
Cf252S	252	-105.78	-142.06	4.16	3.82

FIGURE 7A. Apparent Nubar Test

COMPOUND NUCLEUS		LESS LIGHT MASS AVE.	LESS HEAVY MASS AVE.	APPARENT NUBAR	EVALUATED NUBAR
U234F	235	- 93.9103	-138.3548	2.735	--
U237F	238	- 96.5461	-138.7627	2.691	--
Pu240H	241	-100.3365	-136.0433	4.620	--
U234HE	235	- 96.2210	-134.6664	4.113	--
U236HE	237	- 97.2751	-135.5433	4.182	--
Pu238F	239	- 98.4969	-138.4932	2.010	--
Am241F	242	-100.3269	-138.8086	2.865	--
Am243F	244	-101.0840	-138.9098	4.006	--
Np238F	239	- 98.0967	-138.5934	2.310	--
Cm242F	243	-100.7079	-138.7099	3.582	--
Th227T	228	- 88.9180	-137.7275	1.354	--
Th229T	230	- 87.7296	-139.3161	2.954	--
Pa231F	232	- 91.1452	-138.3934	2.461	--
Am241T	242	-100.6776	-138.5665	2.756	--
Am241H	242	-102.0451	-135.4407	4.514	--
Am242MT	243	-100.9789	-139.1229	2.898	--
Cm245T	246	-102.8020	-139.6723	3.526	--
Cf249T	250	-105.7141	-140.0609	4.225	--
Cf251T	252	-107.5475	-140.8272	3.625	--
Es254T	255	-110.8792	-140.2267	3.894	--

FIGURE 7B. Apparent Nubar Test (concluded)
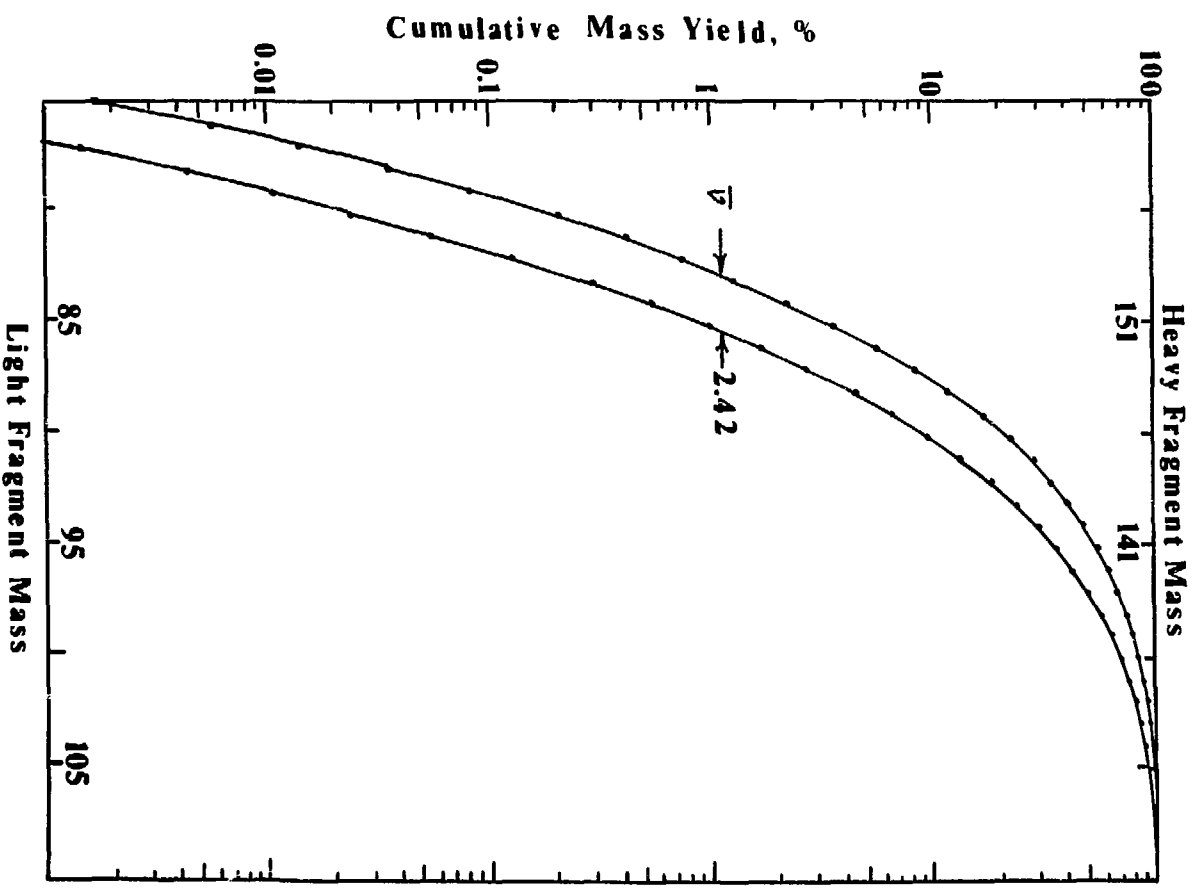
FIGURE 8. Terrell (62TER1) Plot
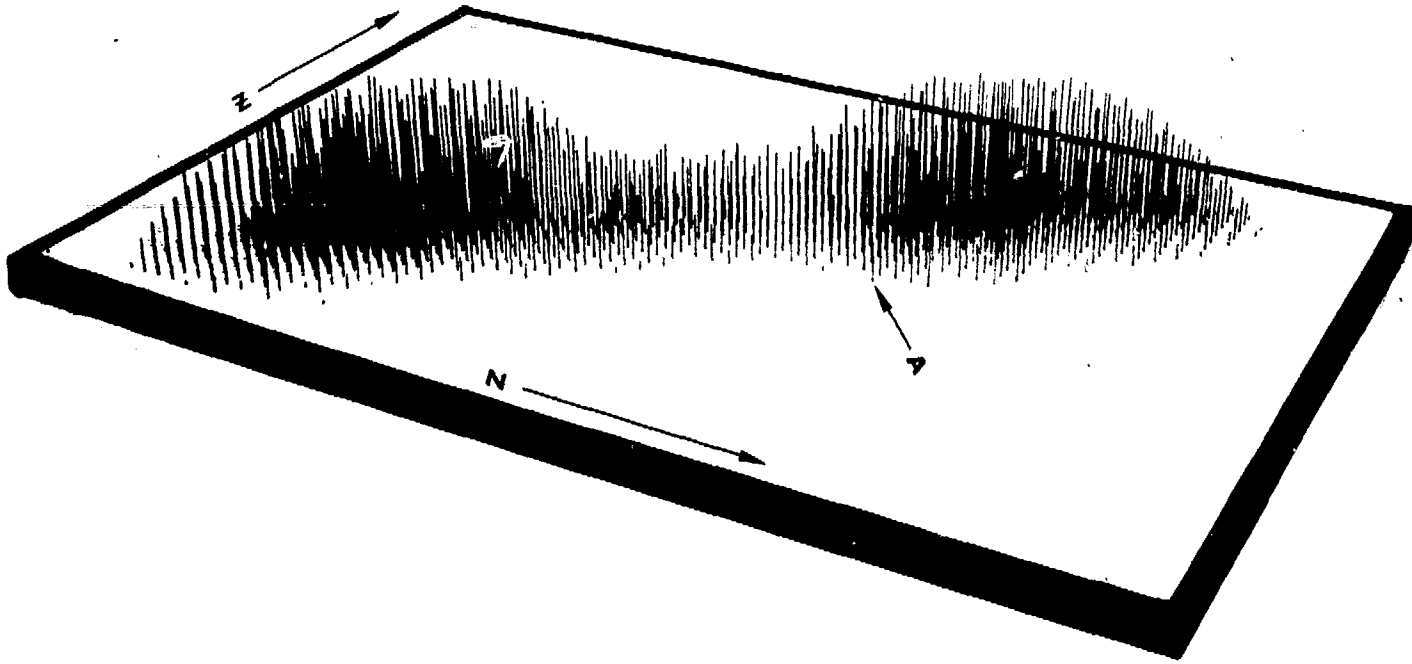
FIGURE 9.   Direct Yield Pin Plot
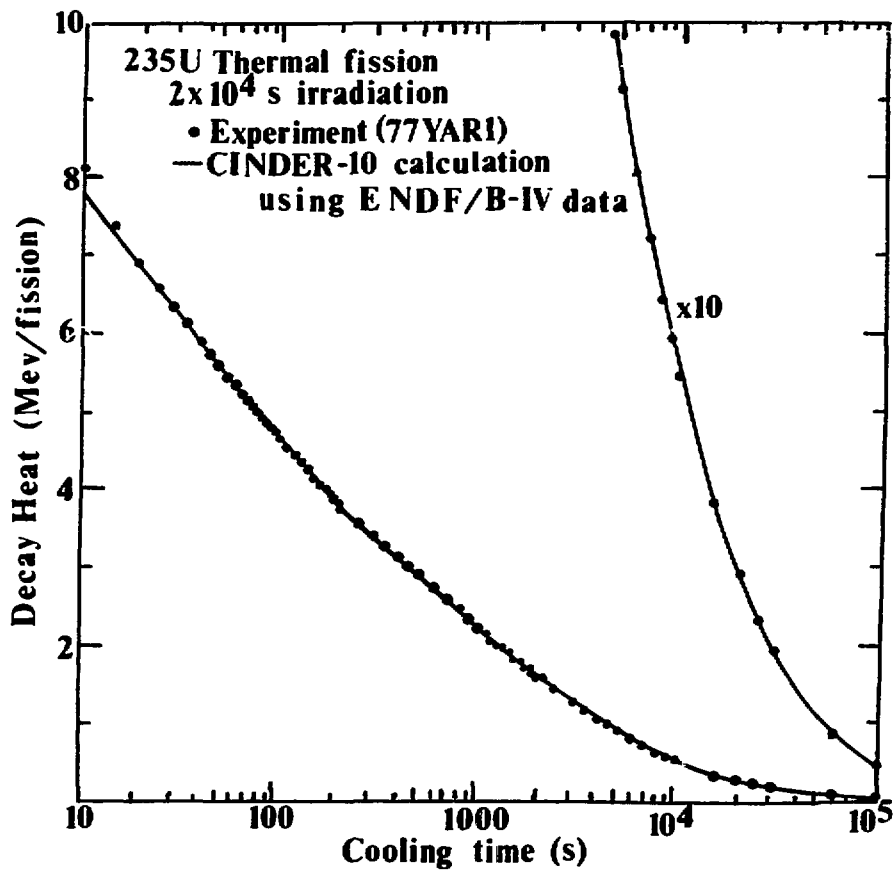
FIGURE 10. LASL Experimental Results with ENDF Calculations

NUCLIDE	MEAN σ PEAKS, %	MEAN σ VALLEY, %
U235T	0.6	15.8
U235F	1.7	14.1
U235HE	6.3	11.2
U238F	2.6	17.0
U238HE	5.4	12.2
Pu239T	2.6	17.9
Pu239F	2.2	16.5
Pu241T	2.6	18.2
U233T	3.5	17.2
Th232F	4.5	18.3
U233F	3.3	22.3
U233HE	9.1	17.6
U236F	11.7	27.9
Pu239H	6.7	12.2
Pu240F	7.1	18.4
Pu241F	7.7	20.2
Pu242F	12.0	28.5
Th232H	5.3	7.1
Np237F	3.4	10.9
Cf252S	8.0	20.3
AVERAGE	5.3	16.4

FIGURE 11A. Average Error Distribution

NUCLIDE	MEAN σ PEAKS, %	MEAN σ VALLEY, %
U234F	13.2	27.2
U237F	27.9	28.8
Pu240H	11.2	22.4
U234HE	14.4	24.6
U236HE	13.6	23.7
Pu238F	18.9	28.0
Am241F	18.5	27.8
Am243F	18.9	29.0
Np238F	17.7	27.6
Cm242F	19.1	28.8
Th227T	14.9	25.8
Th229T	4.2	13.4
Pa231F	15.0	24.8
Am241T	7.6	21.3
Am241H	7.6	31.3
A242MT	11.3	23.5
Cm245T	9.4	22.8
Cf249T	11.6	22.6
Cf251T	12.3	24.6
Es254T	11.6	23.6
AVERAGE	13.5	24.5

FIGURE 11B. Average Error Distribution (concluded)

MASS	INDIV. σ, %	N	σ OF MEAN, %
83	1.86	8	0.7
85	2.56	34	0.4
86	1.32	14	0.4
131	4.20	26	0.8
132	2.82	26	0.6
133	1.86	23	0.4
134	2.38	13	0.7
135	2.97	13	0.8
136	1.31	9	0.4
137	1.40	19	0.3
143	3.38	29	0.6
144	2.72	23	0.6
145	2.12	16	0.5
146	3.00	17	0.5
147	4.13	16	1.0
148	1.40	21	0.3
150	3.22	19	0.7
MEAN	2.39	19	0.6

FIGURE 12. Individual Measurement Errors for Most Accurate U235T FP Masses

MASS	ENDF/B-III 1971 REV. 0	ENDF/B-IV 1974 REV. 1	ENDF/B-V 1978 REV. 2E	ENDF/B-VI 1980 REV. 3B	σ, %
83	0.535	0.531	0.536	0.537	0.5
85	1.330	1.314	1.311	1.318	0.6
86	1.937	1.951	1.969	1.966	0.8
131	2.772	2.835	2.884	2.892	1.9
132	4.124	4.217	4.299	4.313	2.1
133	6.760	6.774	6.703	6.696	0.6
134	7.187	7.681	7.818	7.869	4.1
135	6.719	6.635	6.542	6.536	1.3
136	6.123	6.278	6.317	6.317	1.5
137	6.224	6.263	6.223	6.183	0.5
143	5.987	5.969	5.938	5.963	0.3
144	5.444	5.457	5.475	5.493	0.4
145	3.949	3.941	3.918	3.939	0.3
146	2.996	2.998	2.975	2.998	0.4
147	2.253	2.282	2.254	2.270	0.6
148	1.639	1.689	1.670	1.674	0.6
150	0.649	0.649	0.648	0.653	0.3
				AVERAGE	1.0

FIGURE 13A. Consistency of Yields Over Time for U235T

MASS	ENDF/B-III 1972 REV. 0	ENDF/B-IV 1974 REV. 1	ENDF/B-V 1978 REV. 2E	ENDF/VI 1980 REV. 3B	σ, %
83	0.293	0.295	0.295	0.296	0.4
85	0.601	0.561	0.573	0.608	3.8
86	0.746	0.758	0.759	0.763	1.0
131	3.839	3.745	3.845	3.865	1.6
132	5.164	5.274	5.391	5.401	2.1
133	6.839	6.973	6.973	6.991	1.0
134	7.225	7.447	7.626	7.648	2.6
135	7.223	7.473	7.615	7.588	2.4
136	6.654	6.732	6.708	7.167	3.5
137	6.535	6.694	6.696	6.685	1.2
143	4.459	4.558	4.426	4.428	1.4
144	3.775	3.832	3.736	3.735	1.2
145	3.016	3.076	2.991	2.989	1.3
146	2.481	2.536	2.461	2.460	1.4
147	1.947	2.075	2.042	2.019	2.7
148	1.659	1.692	1.634	1.639	1.6
150	0.998	0.996	0.966	0.968	1.8
				AVERAGE	1.8

FIGURE 13B. Consistency of Yields Over Time for Pu259T

FIGURE 14A. Light Mass Chain Yields Set A

Table of heavy mass chain yields with columns: MASS, U235T, U235F, U235HE, U236F, U236HE, PU239T, PU239F, PU241T, U233T, TH232F.

FIGURE 14B. Heavy Mass Chain Yields Set A

FIGURE 14C. Light Mass Chain Yields Set B

FIGURE 14D. Heavy Mass Chain Yields Set B

FIGURE 14E. Light Mass Chain Yields Set C

FIGURE 14F. Heavy Mass Chain Yields Set C

MASS	U234F	U237F	PU240H	U234HE	U236HE	PU238F	AM241F	AM243F	NP238F	CM242F

FIGURE 14G. Light Mass Chain Yields Set D

MASS	TH227T	TH229T	PA231F	AM241T	AM241H	A242MT	CM245T	CF249T	CF251T	ES254T
119	0.081443M	0.020880L	0.088632M	0.048011M	1.455033M	0.023500M	0.054402M	0.634056M	1.240472M	3.898758L
120	0.062506M	0.019866L	0.072730M	0.024966M	1.528244M	0.023500M	0.035990M	0.368162M	0.763367M	4.437363K
121	0.112906M	0.011817K	0.078329K	0.026461N	1.585583M	0.018680J	0.031736K	0.212228I	0.497394I	2.644993H
122	0.108118N	0.016903L	0.086907N	0.029637N	1.742641M	0.029761N	0.052990N	0.181701N	0.280615N	2.340372L
123	0.310699N	0.014914L	0.097315N	0.040216M	1.890196M	0.039770M	0.062380M	0.127976N	0.200364H	1.949379L
124	0.21720N	0.012933L	0.115935N	0.050662N	1.676555M	0.049622N	0.070182N	0.096633N	0.187081N	1.350195M
125	0.329978L	0.007644K	0.143450M	0.069536M	2.201911M	0.120191M	0.108577K	0.179850K	0.409866K	0.958214K
126	0.556930M	0.009943L	0.169475N	0.169534N	4.072955M	0.158618N	0.160499N	0.043446N	0.304036M	0.832008M
127	0.673308L	0.006357I	0.291273M	0.246341	3.246341	0.249815M	0.590084K	0.063731	0.608411J	0.942712J
128	0.926972M	0.005968L	0.527815N	0.599941N	3.0279411	0.496190N	0.701477N	0.343308M	0.712702N	1.272127M
129	1.415890K	0.012415BI	1.069148J	1.376387H	3.583691L	0.994035M	1.525702K	0.249849M	0.932407I	2.445494M
130	1.855969M	0.216645L	2.080707M	2.251983M	4.572262L	1.690973M	1.80329M	2.249849M	0.932407I	0.977193J
131	2.829940K	0.735761H	2.685885I	3.550119F	4.434851	1.274081	0.603299M	3.00084IJ	1.214920M	7.876991
132	3.519060J	1.248209H	3.589819I	4.745718F	4.077186K	3.01390H	1.394291	3.3364I9J	1.840718I	4.876630J
133	4.857113K	3.543620	5.092357I	5.540400	4.637911H	4.274861	4.214781	4.129336L	3.907183	5.315525L
134	6.851792K	7.048157G	6.386872K	7.207960G	5.259353K	5.877431	5.654225H	4.747724I	3.908718J	5.047134K
135	6.584598M	5.642150	6.734431	6.673450M	5.729045J	5.540391	6.421388K	4.757702L	4.840850L	5.315525L
136	7.661483L	7.136215O	7.489912L	7.692599G	6.152313L	7.561798K	7.816796I	6.018918K	4.407181J	5.619224K
137	6.987593K	6.935720	7.015784I	6.449090H	4.3357421	5.180591J	5.374030J	6.612943M	5.665588L	5.086052L
138	7.210374L	6.3793041	7.442229L	7.2611711	4.372607K	5.981680J	6.2554551	6.640711	5.774956L	4.634330L
139	7.709008L	8.9429771	7.335965L	7.744960	6.038111	5.682726L	3.605691	5.964182L	5.653911I	4.424578L
140	7.647552J	9.3365120	8.730789H	6.002229O	5.556314J	5.528588I	5.929781	4.506213H	4.135311L	
141	7.411593L	8.088327H	6.354431	8.522850G	2.367681	5.279153J	5.547965H	5.919453	4.916892J	3.904026H
142	6.990007J	6.976163I	6.199207L	4.7730DK	2.983672I	5.1279153J	5.206993H	4.725177I	4.461946L	4.5760773
143	5.974398J	6.980007J	3.328096H	3.628260H	2.694303I	4.203277J	4.690105K	4.204221J	5.078056I	4.5630151
144	1.030479M	6.736709F	4.404402F	3.515101H	2.4985011	4.6816993	4.490103H	4.810928I	5.047390L	3.8169971
145	0.163001M	2.580850F	3.78770GF	2.634656L	2.232041M	1.189996L	3.303490L	3.420101	5.042596L	3.880037J
146	0.031318N	1.24135ZO	2.580850F	2.035858H	2.007670L	2.684435M	2.703134M	3.009705L	4.236165L	3.226737M
147	0.010100N	0.163001M	2.028293H	1.843019M	1.8116301	4.000986J	3.3559153J	3.1903080N	3.511249K	2.852905L
148	0.010100N	0.852052I	0.9212801	1.4483501	1.576467M	1.985532M	2.302737M	0.229239N	3.340707M	2.840173M
149	0.002004N	0.2129671	0.550516N	1.163289N	1.171341N	1.665793J	1.972324M	2.4473521	3.018276K	2.6330071
150	0.000505N	0.047746K	0.31651ON	0.847945J	0.680091	1.495259M	1.806020M	1.90184ON	2.421730L	0.959943M
151	0.000101N	0.010736L	0.178801N	0.605135N	0.806135N	0.9544793M	0.351717M	0.865011K	1.250683L	0.885564L
152	4.04E-05N	0.002187L	0.0770573J	0.6061891	0.6680091	1.876377J	1.251517M	0.343141M	1.512560M	0.613388M
153	1.01E-05N	0.002004N	0.041392M	0.3750904M	0.515066N	0.8083583J	1.201484M	1.2324681	1.214613M	0.504226L
154	2.02E-07N	0.0001001N	0.020689N	0.3109093K	0.3405801	0.497213M	0.665144N	0.885282M	0.910979M	0.271733M
155	6.08E-08M	0.0101E-05N	0.010345N	0.2028551	0.515066N	0.327312N	0.686144N	0.698755N	0.712005N	0.277739M
156	5.08E-09M	1.52E-08N	0.005172N	0.165999J	0.2604981	0.3183543J	0.428914L	0.838053J	0.584509K	0.784290L
157	9.97E-10M	7.95E-08L	0.003207N	0.1707421	0.1707421	0.149604K	0.427740N	0.434841I	0.406888N	0.751713K
158	1.01E-10M	1.99E-08L	0.001552N	0.152160N	0.152160N	0.073948N	0.324544N	0.343858N	0.305186N	0.678022N
159	6.08E-0MM	9.97E-07L	0.001552N	0.130761I	0.1307811	0.045890N	0.226378N	0.36770OJ	0.203444N	0.484301N
160	6.10E-0MM	1.01E-07N	0.000735N	0.0300020N	0.000735N	0.034734M	0.177408N	0.227753N	0.152597N	0.387680N
161	3.02E-1MM	9.08E-08N	0.000372N	0.023325J	0.6001691	0.014444K	0.116168N	0.090488N	0.107722N	0.290581N
162	6.08E-0MM	9.1E-05N	0.000197N	0.003752N	0.004246N	0.019030N	0.078733N	0.081378N	0.107722N	0.193721N
163	1.01E-1MM	9.08E-09N	0.000103N	0.001016ON	0.024164N	0.001980N	0.054091N	0.054293N	0.081033N	0.098660N
164	9.08E-1MM	2.94E-09N	4.14E-05M	0.000372N	0.017136N	0.001964N	0.024842N	0.031881N	0.040889N	0.088662N
165	1.91E-11M	9.93E-10N	2.05E-05M	0.000103N	0.017136N	0.0001964N	0.010813M	0.018098N	0.030385M	0.048890M
166	8.08E-0MM	7.01E-10L	1.82E-06M	4.85E-05N	0.007054N	0.000594N	0.008094N	0.010859N	0.020344N	0.088717N
167	2.02E-10N	1.01E-10N	3.82E-06M	8.85E-05N	0.004031N	0.000490N	0.008334N	0.008333N	0.018258N	0.003674N
168	1.08E-11N	8.08E-12L	5.21E-06N	8.31E-06N	0.002922N	0.000198N	0.00220DN	0.003682N	0.010172N	0.001937N
169	1.82E-12N	7.97E-12L	1.11E-07N	1.705E-05N	0.001113N	9.925E-05N	0.000591N	0.000591N	0.008104N	0.000869N
170	1.07E-12N	1.98E-12N	1.31E-07N	8.70E-07N	0.000766N	3.07E-05N	0.000291N	0.000170N	0.004069N	0.000184N
171	1.28E-12L	1.49E-12L	1.03E-07N	1.08E-07N	0.000504N	1.96E-05N	0.000170N	0.000317N	0.004069N	0.000184N
172	1.11E-12L	1.29E-12L	1.03E-07N	1.08E-07N	0.000504N	9.92E-06N	7.91E-05N	9.05E-05N	0.003082N	9.69E-05N

FIGURE 14H. Heavy Mass Chain Yields Set D

Discussion

England (Comment)

Before your questions, I will make these comments. (1) There are only two extensive yield compilations that also attempt a complete evaluation for all fission products, namely the one by Rider in the USA and the one by Crouch in the UK. (2) The models mentioned in this paper are phenomeological and represent average results over all masses; these seem to work very well but can be improved. (3) The evaluation uses only two conservation principles (charge and normalization to 100% under each mass peak). We could use others, such as $\bar{\nu}_t$, but prefer, instead, to reserve these for use in testing the quality of the evaluation.

Rowlands

My question concerns energy dependence. Is it well defined, what one means by a fast reactor spectrum value? The reason I ask this is some years ago it seemed there was a bias towards measurements in very hard spectrum fast reactor systems and if the energy dependence is linear then for commercial fast reactors it might be more appropriate to take the thermal value than the hard spectrum value. But whether its important, I think, depends on whether the variations affect such things as delayed neutron emission and decay heat, so perhaps the first question is, do the differences result in differences in delayed neutron emission data not only the total delayed neutron but the group breakdown and secondly, do you see such differences in decay heat data between the fast and thermal values?

Rider

There is no significant differences in decay heat and there's no difference in delayed neutrons, that is, the calculated delayed neutrons and their spectra agree with the measured values at fast and thermal energies in both cases and they are virtually identical. There's no important difference.

Rowlands

The individual isotope effect, the proton and neutron effects, don't lead to delayed neutron energy dependence for the groups?

England

There are some differences, John, but these are not large; I think they are even within the evaluated uncertainty, depending on which fissile nuclide you are interested in. You would expect large differences in some quantities, particularly in delayed neutron calculations because of the pairing effects you mention. These

effects are energy dependent and vary with the fissile nuclide, but the aggregate delayed neutrons and spectra show only small differences between fast and thermal incident energies. This is probably true for most aggregate quantities, as it is for decay heating. But I don't think you should use thermal yields for fast reactor spectra; there are other quantities that are energy dependent. This is, in fact, one of our prime interests now—the energy dependence of the yields—particularly for nuclides of individual importance such as those used as fission monitors. For such nuclides, it was recently noted in a conference at LASL that yield variations due to changes in the fast spectra exceed some of our assigned uncertainties. To answer your earlier question, the definition of fast has not been made for the yields, except to meet an ENDF/B format requirement where 0.5 MeV is arbitrarily assigned. We know the energy dependence for only a few nuclides. A linear dependence may be a sufficient approximation, but the slope can be positive or negative. The few dependencies we do know have plus and minus slopes depending on the mass chain. So, defining the meaning of fast would still leave us with the problem of specific energy dependence per mass. At the LASL conference it was noted that thermal yield uncertainties are not too large, as was stated at the 1977 Petten Meeting. It's just not true based on recent data we have seen, but I think Ben ought to comment on this.

Rider (Comment)

I worried a lot about whether we assigned too small an error to the yields and it doesn't appear to me that we have. The main question is whether or not there remains any systematic errors. In general, the fission yields that are recommended now are the same as were recommended 35 years ago. There has been no difference in time, no systematic errors have developed other than a low recovery of xenon in some early measurements which have been identified and removed from the data. But even in removing those systematic errors, the recommended errors have not changed over 1%. So whether or not in the year 2000 someone will find some systematic error that has been made is a matter of speculation; no important systematic errors have been found, largely because so many techniques have been used. Absolute gas counting, gas spectrometry, radiochemistry have been done in all nations; Russia, England, Canada, by different experimenters with different techniques and apparently most of these systematic errors have been shaken out. So I think we can count on the fact that we know they are within 1%. I think that is as much as I would claim.

England (Comment)

I would like to ammend that, though. I think that statement applies to thermal chain and doesn't apply to independent yields.

<u>Rider</u> (Comment)

Yes, the independent yields--many things may happen still.

<u>Moore</u>

I have two questions. The first has to do with this calculation
of apparent nu bar; there are no two ways to do it, the way you
showed where you look at differences between the light and heavy
fragment yields; and the other way would be to take the actual
yields, correct them back, and then use the universal curves of
Terrell. Perhaps you could just tell us what you did.

<u>Rider</u>

The apparent nu bar? It's merely the mass of the compound nucleus
minus the average mass of the light fission products minus the
average mass of the heavy fission products. Independent or
cumulative yields could be used; we used independent yields.

<u>Moore</u>

Is your method of determining the "apparent nu-bar" independent of
neutron energy? If so, it would be interesting to determine a
sensitivity for the change in nu-bar with relative mass yields in
the valley. In other words, is the change in nu-bar for ^{239}Pu
below 1 eV completely explained by changes in the mass
distribution or not?

<u>Rider</u>

The apparent nu bar increases from about 2.4 to about 2.9 between
the two spectra. It's about a half a neutron--about 7 parts in
200 or about 3%. That doesn't directly take into account any of
the incident energy dependence; this is just a yield weighted mass
determination of nu bar.

<u>Moore</u> (Comment)

That's the sort of thing that one might expect, for example, for
plutonium thermal to plutonium resonance.

<u>Peelle</u>

Uncertainties have been compiled for the yields, as you
mentioned. Is information available on the correlations among the
output yields?

<u>Rider</u>

No.

Peelle (Comment)

One might assume there would be significant correlations because
of the use of some constraints and the models in the middle
someplace.

Rider (Comment)

Some constraints have been used in the models, right.

England (Comment)

There are only two constraints, summation to a 100 percent under
each peak and the charge balance, but undoubtedly there are
significant correlations from these and from the models.

Schmidt

For the test area actinides such as Cf-249, what is the accuracy
of the fission yields?

Rider

That was on one of the slides. In the peaks they are perhaps 13%;
it's in the slide exactly what it is; and in the valleys they're
on the order of 35%.

Schmidt

So your comment that fission yields are known to 1% applies to
what?

Rider

They are not known 1% except at U-235 thermal and that is because
95% of the measurements have been made for U-235 thermal. I don't
know if its 95 or 90, but certainly virtually all the work has
been done with U-235 thermal. The models are largely based on U-
235 thermal and they're extended to these other fission systems.
And of course we can check how well they are working on these
systems by other data which have been partially measured, such as
for Pu-239, U-233. Some things we know something about show that
the models derived from U-235 thermal seem to work for those data
used as tests for other fissionable nuclides. We assume they will
work for those where we have no experimental comparisons.

England (Comment)

Bill Maeck measures chain yields in this country and he really
feels that we shouldn't assign an uncertaintly of less than one
percent; as a measurer he thinks from his experience that a

systematic error on that order is likely even though his results have resulted in probably the smallest uncertainties we've seen in some of the yields, including less than the 1% that he has published. This is a question we have to resolve; one issue that will come up in CSEWG, I think, is whether we should ⌄rce a lower limit of 1% uncertainty on the cumulative yields.

Rider (Comment)
Kr-85 has been measured to 2% accuracy approximately 35 times. The question is if its been measured by 35 experimenters and all find the same answer and each claims an accuracy of 2% does the average of the mean of 35 measures really make a 2% measurement better than 1%? Statistical errors say that perhaps it should and the other answer is if there are systematic errors it will not. The question is, are there systematic errors that we have not yet suspected or are there not? I don't know the answer. It's best, perhaps, not claim better than 1% even though statistics say it may be.

Poenitz

You kind of dismissed th⌐t the apparent nu-bar could be of any value beyond the test for your fission yields. On the other hand, the agreement in some cases is so fantastic that one would wonder whether the calculations might contain significant information. For example, U-235 and Cf-252 from direct measurements supposedly should be better, but there are problems. So what is the kind of uncertainty in the apparent nu bar calculate?

Rider

I hope Howerton or someone else is an expert on nu bar. I'm not.

Poentiz (Comment

I only mean those you derive from your fission yields, the apparent nu bar.

England

You can derive a lot of things from the yields; in fact, if we knew the yields extremely well, particularly the independent yields, we could derive most fission related quantities we want to know, including the delayed neutrons, fission Q-values, etc. I have done it for the delayed neutrons and I don't believe the small uncertainty in the P_n values rather than the yield uncertainties. P_n values, the delayed neutron emission probabilities, are much smaller than those we have on the independent yields. I did not put on any estimate on the prompt nu or total nu and I don't think Ben has either so I can't really

answer your question. We do use models that seem to work for most systems, as already n ʰed, but you should note that the calculated delayed nu bar for U-238 is low compared to the evaluated value; the reason appears to the the model estimated pairing effect, which is very large near the fission threshold--the pairing parameter was not averaged over an incident neutron spectrum.

FISSION ENERGY RELEASE FOR 16 FISSIONING NUCLIDES

R. Sher

Department of Mechanical Engineering
Stanford University
Stanford, California 94305, U.S.A.

ABSTRACT

Results are presented of the most recent least-squares evaluation of the components of energy release per fission in Th-232, U-233, U-235, U-238, Pu-239, and Pu-241. For completeness, older (1978) results based on systematics are presented for these and ten other isotopes of interest. There have been recent indications that the delayed energy components may be somewhat higher than those used previously, but the LSQ results do not seem to change significantly when modest (~ 1 MeV) increases in the total delayed energy are included in the inputs. Additional measurements of most of the energy components are still needed to resolve remaining discrepancies.

INTRODUCTION

The energy release in fission and its partition into fragment kinetic energy and radioactive decay energy are important for determining reactor power and in safety considerations, which depend on the decay heat. The energy release can be determined in two ways: by mass balance after fission product decay, and by adding the individual components of the fragment and decay energies. The first of these methods has been exploited by Walker [1-3], Unik and Gindler [4], and James [5,6]. With increasing knowledge of fission fragment yields [7,8] and mass defects [9], it is possible to calculate total energy releases from mass balance to within approximately ±0.1 MeV for neutron-induced fission of U-233 and U-235, ±0.2 MeV for U-238, Pu-239, and Pu-241, and ±0.3MeV for Th-232, and to somewhat poorer accuracy for other isotopes.

The individual components of the energy release (kinetic energy of the fragments and prompt neutrons, prompt gamma rays, beta rays, neutrinos, and delayed gamma rays and neutrons) were determined from a combination of experimental values and nuclear

systematics; in general, these were much less precise and did not always correctly add up to the total energy release.

In this report we continue to utilize these methods, analyzing 16 fissioning isotopes in all. For the isotopes listed above ("primary" isotopes), for which relatively good values of yields and other experimental quantities exist, best values of the total and partial energies are determined by a combination of systematics and a least-squares calculation. Systematics are used for the other isotopes. The systematics are checked against the least-squares values for the primary isotopes; agreement between the two methods is always good (~ ±1 MeV).

It is convenient at this point to define various quantities of interest:

QG = the net energy release per fission. This includes the antineutrino energy, but does <u>not</u> include subsequent radiative capture of the fission neutrons in a reactor. Otherwise it is the total energy released minus the incident neutron energy.

ED = the total (delayed) radioactive decay energy per fission. It is the sum of the beta-ray, delayed gamma ray, and antineutrino energies of all the decay products of the fission fragments (delayed neutrons not included).

EB = beta-ray decay energy per fission.

EGD = delayed gamma-ray decay energy per fission.

ENU = antineutrino decay energy per fission.

ER = "effective" energy release per fission; $ER = QG - ENU + EINC$.

EP = the total prompt energy release per fission; it is the sum of the kinetic energies of the fragments and fission neutrons, and the prompt ($\lesssim$ 10 nsec) gamma-ray energy, minus the incident neutron energy.

EFR = fragment kinetic energy per fission (<u>post</u>-neutron emission).

EGP = prompt gamma-ray energy per fission.

ENP = average prompt neutron energy per fission.

EINC = average incident neutron energy (= 0 for thermal fission).

END = average delayed neutron energy per fission.

ET = the conventionally defined Q-value of the fission reac-
tion; ET = QG + EINC.

All of the above quantities are averages over all modes of
fission and are determined for a given fissionable nuclide and
incident neutron energy. For fast-fissioning isotopes, EINC is
taken to be the average energy of a U-235 fission neutron,
weighted by the fission density of the isotope, i.e.,

$$
EINC^{(i)} = \frac{\int Ef_{25}(E)\ \sigma_{fi}(E)\ dE}{\int f_{25}(E)\ \sigma_{fi}(E)\ dE}
\tag{1}
$$

where $f_{25}(E)$ is the U-235 fission spectrum and the index i
refers to the fissionable nuclide. Typically, the value of EINC
for fast fission when averaged according to Eq. (1) is about 3
MeV. Walker [10] has examined the values of the various energy
components calculated from the ENDF/B-5 yield set as a function of
incident neutron energy and has proposed that, for those nuclides
which fission only with fast neutrons, the components be estimated
and listed in the ENDF-B library at zero neutron incident energy.
He gives approximate expressions for determining the zero energy
values from the values at other EINC. However, in this paper, we
continue to report values appropriate to average EINC's as defined
above.

From the above definitions,

$$
QG = EP + ED + END = ER + ENU - EINC
\tag{2}
$$

$$
EP = EFR + EGP + ENP - EINC
\tag{3}
$$

$$
ED = EB + EGD + ENU
\tag{4}
$$

Walker [3] has pointed out that the Q-value, ET (= QG +
EINC), for a given fissible isotope is almost independent of EINC.
Since the biggest change in QG is due to an increase in ν_t,
this can be interpreted as meaning that most of the incident
neutron energy is simply used to produce extra neutrons. It
should be noted that ternary fission is neglected in what follows.

TOTAL ENERGY RELEASE, QG

From the chain yields, QG can be obtained from the mass-
balance equation:

$$
QG = -\langle M_\ell \rangle - \langle M_h \rangle + M(Z_o, A_o) - (\overline{\nu}_t - 1)\ m_n
\tag{5}
$$

Here $\langle M_\ell \rangle$ is the average mass excess of the final decay prod-
ucts of the light fragments:

$$\langle M_\ell \rangle = \sum_i^{(light)} Y_i M_i \quad . \tag{6}$$

$\langle M_h \rangle$ is the average mass excess of the end products of the heavy fragments, Y_i are the chain yields, M_i is the mass excess of the end product i, $M(Z_0,A_0)$ is the mass excess of the target nucleus (Z_0,A_0), and m_n is the mass excess of the neutron $(= 8.07144 \text{ MeV})$.

Beck [11] carefully reviewed the yield and mass data and recalculated QG values; these values are shown in Table I. In obtaining these values, the yield sets of Meek and Rider [7] and Crouch [8] were used with mass data [9] for 12 of the 17 nuclides shown. For Pa-233, U-234, Pu-238, Am-243, and Cm-244, systematics were used to determine the mass defects.

PROMPT ENERGY RELEASE, EP

The quantity EP = QG – ED – END is the prompt energy release. It is equal to the sum of the kinetic energy of the fragments, the kinetic energy of the (prompt) neutrons (minus the mean incident neutron energy), and the prompt gamma-ray energy. It can also be independently determined from the individual fragment direct yields:

$$EP = M(A_0,Z_0) - \langle m_\ell \rangle - \langle m_h \rangle - (\bar{\nu}_p - 1)\, m_n \quad . \tag{7}$$

Here, $\langle m_{\ell,h} \rangle = \Sigma y_i m_i^{\ell,h}$, where y_i is the independent (direct) yield of a fragment, m_i is its mass excess, and $\bar{\nu}_p$ is the average number of prompt neutrons emitted per fission.

Values of EP have been recalculated [11] with the independent yield set of Walker [12], based on Meek and Rider [13]. Since this yield set (and also more recent ones) does not conserve total yields along Z (that is, the sum of the direct yields of fragments with atomic number Z does not in general equal the sum of fragment yields with complementary charge Z' (= Z_A–Z, where Z_A is the atomic number of the fissioning nuclide), the sensitivity of EP to adjustments in the yield sets was investigated. It was found that, although some chain yields changed under the adjustment by substantial amounts, EP calculated from any of the yield sets varied by less than 0.1%. Table II lists the values of EP.

DECAY ENERGY, ED

For the primary isotopes, ED has been calculated by Walker from the direct fission product yields and their known decay properties; in addition, more accurate results have been obtained by him from long-term irradiation calculations using FISSPROD [12]. A striking characteristic of these results is that the fractions

of ED that respectively represent beta energy (EB), gamma energy (EGD), and antineutrino energy (ENU) are nearly constant for all the primary isotopes (see Table III); that is,

$$\frac{EB}{ED} = .3015 \pm .0010 \quad,$$

$$\frac{EGD}{ED} = .2932 \pm .0015 \quad,$$

$$\frac{ENU}{ED} = .4053 \pm .0015 \quad.$$

We assume that this split of ED holds for all fissioning isotopes of interest.

Recently, Walker [3] has slightly revised his values of ED; the new values are shown in Table IV. For other isotopes, ED was obtained from systematics [11].

LEAST-SQUARES CALCULATIONS OF ENERGY RELEASE

The data given in Tables I, II, and IV can be combined with experimental data on EFR and EGP in a least-squares calculation to get "best" values of all the energy-release parameters. We use the following "observational equations" for the primary isotopes (Th-232, U-233, U-235, U-238, Pu-239, and Pu-241):

$$ED + EGP + EFR = QG - (ENP-EINC) - END \qquad (8)$$

The quantities on the l.h.s. are assumed to be unknown; those on the r.h.s. are assumed to be known (QG is taken from Table I).

$$EFR + EGP = EP - (ENP-EINC) \quad. \qquad (9)$$

Again, the quantities on the r.h.s. are assumed known (EP from Table II) and independent of those in the preceding equation.

In addition to these types of observational equations, in which the "experimental" values are those on their right-hand sides, direct measurements of EFR, EGP, ratios of EFR between different isotopes, and a few calculated values of ratios of EDs based on systematics are also used as inputs to the LSQ calculation.

Table V lists all the foregoing data, together with the weight factors assigned to each observational equation. It should be noted that the weight factors are proportional to the inverse squares of the absolute errors of each experimental value. The error values are either as quoted by the author or are estimates made by us. The LSQ calculations then give the best values of EFR, ED, and EGP shown in Table VI. From the ratios given in Table III, EB, EGD, and ENU are then obtained. By summing the appropriate quantities, value⸱ of QG and EP are obtained, but these are not as good as the input values obtained from yield data, which are therefore recommended, as indicated in Table VI.

SYSTEMATICS

Beck [11] has reviewed the systematics of the various quantities, and his results have been applied both to the primary isotopes (where the results are not as good as the LSQ values) and to the other isotopes of interest, for which there are insufficient data to do a LSQ calculation. For the primary isotopes, the values obtained by systematics are also listed in Table VI; for the others they are given in Table VII. For a detailed discussion of the systematics, Beck [11] should be consulted.

DELAYED NEUTRON CONTRIBUTION, END

It should be noted that the values of END shown in Tables VI and VII are obtained by multiplying the delayed neutron yield per fission [14] by the average energy per delayed neutron. For the primary isotopes, the average energy per delayed neutron was computed from the delayed neutron spectra evaluated by Saphier et al. [15]. These averages are shown in Table VIII, together with the values of v_d used and the resulting END.

For all other nuclides, the average energy per delayed neutron was taken as 0.455 MeV. The values of v_d are taken from Tuttle [14], except for Pa-233, Np-237, Am-243, and Cm-244, for which they are assumed to be 0.02, and Am-241, for which it is assumed to be 0.01. These values should only be considered as "ballpark" guesses.

DISCUSSION

The recommended results shown in Table VI form a consistent set. However, problems remain in the experimental values of some of the components, especially the fragment kinetic energies, the decay energies (beta and delayed gamma), and the prompt gamma energies. (It has been tacitly assumed that neutron energies are well determined.)

Fragment Energies

Direct measurements of fragment energies have been generally performed in two ways--by time of flight, in which the velocities of both fragments are measured (double velocity method), and by surface barrier detection of the energy spectrum of the fragments (double energy method). The double velocity results in general are lower by a few MeV than the double energy values. It is usually surmised that the double velocity results may be slightly low because of small angle scattering effects and the double energy results are slightly high by about the same amount because of charge effects on the energy calibration of the semiconductor

detectors. Table IX summarizes the experimental data. For all isotopes except Pu-239, the input values for the least-squares fit was basically a simple average of all the experimental values. For Pu-239, Deruytter's [16] value was used. Recent measurements at Geel [17] (incident neutron energies in the low-lying resolved resonances of Pu-239) are in excellent agreement with Deruytter's value. However, Deruytter's and the Geel experiments were double-energy, so the nagging problem of the detector calibration may still remain. Good (± 0.1 MeV) measurements for all isotopes using both velocity and energy methods are still required, both to resolve the existing discrepancies and to reduce the uncertainties in the final results.

Decay Energies

There are no direct measurements of total (beta and delayed gamma) decay energy. Recent scintillation and calorimetric measurements of decay energy or power at various times following irradiations of various durations suggest that the total decay energy may be slightly higher than the values calculated from the ENDF/B-4 yields. However, the data at short times are difficult to obtain and are incomplete, and the measurements do not directly determine the quantity of interest here. These measurements form the basis of the ANS decay heat standard, and have been taken into account in the least-squares fit by using values calculated from the parameters of the fitted standard function ($F(0,\infty)$, the decay energy at zero time following an infinite irradiation) [18]. Because the decay heat results indicate that some of the ENDF/B-4 data used in the calculated values of ED may be suspect, the weights assigned to the calculated values of ED in the LSQ calculation have been somewhat reduced, as indicated in Table V. Calculations were also done in which the Walker-calculated ED's were given their full weight (ignoring the ANS standard) and in which the calculated ED's were given weights of unity for Th-232, U-233, and Pu-241, zero weight for U-235, U-238, and Pu-239, with the ANS standard values for the latter isotopes given unity weights. The resulting output values with these alternatives are shown in Table X. Here also, improved experiments to determine total beta and gamma decay energy following a fission with accuracies of the order of ± 0.1 MeV would be useful.

Prompt Gamma Energies

Among the principal problems in measurements of the prompt gamma energy are to consistently define the time domain of "prompt" gamma-ray emission, to distinguish accurately between gamma rays emitted in fission and those which result from neutron capture or inelastic scattering at short times, and the possibility of anisotropic gamma emission [19-21]. The so-called "prompt-

prompt" gamma energy (not involving isomeric decay) has been measured to ~ ± 0.3 MeV for U-233, U-235, Pu-239, and Cf-252 (see Table XI), but because of the effects mentioned above, the total uncertainty has been taken as ~ ± 0.5-1 MeV. It should be noted that the average value for the prompt gamma decay energy of these four isotopes, 6.96 ± 1 MeV, has been used for all other isotopes.

Because of the foregoing experimental uncertainties, the LSQ results are dominated by the QG and EP values determined from yield and decay data. Improved experimental data as suggested above would add independent inputs directly on the quantities of interest of the same quality and weight as the yield data and would give increased confidence in the LSQ results; they would also lead to substantial improvements in the systematics used for the other fissioning isotopes.

Finally, it would obviously be desirable to have as many measurements of energy components as possible done as a function of incident neutron energy up to ~ 20 MeV.

ACKNOWLEDGMENTS

REFERENCES

1. W. H. WALKER, Report AECL-3109, Atomic Energy of Canada, Ltd., Chalk River Laboratories (1968).

2. W. H. WALKER, Report AECL-5259, Atomic Energy o f Canada, Ltd., Chalk River Laboratories (1976).

3. W. H. WALKER, private communication to S. Pearlstein, February 6, 1978.

4. J. P. UNIK and J. E. GINDLER, Report ANL-7748, Argonne National Lab (1971).

5. M. F. JAMES, J. Nuc. En., 23, 517 (1969).

6. M F. JAMES, J. Nuc. En., 25, 513 (1971).

7. M. E. MEEK and B. F. RIDER, Report NEDO-12154-2, General Electric Co., Vallecitos Nuclear Center (1977).

8. E. A. C. CROUCH, Atomic Data and Nuclear Data Tables, 19, 417 (1977).

9. A. H. WAPSTRA and N. B. GOVE, Nuclear Data Tables, 9 (1971).

10. W. H. WALKER, Minutes of Nov. 1979 CSEWG Meeting.

11. C. A. BECK, "The Components of Fission Energy Release for 17 Actinide Nuclides," Engineer's thesis, Dept. of Mechanical Engineering, Stanford University (1978).

12. W. H. WALKER, Report AECL-5105, Atomic Energy of Canada, Ltd., Chalk River Laboratories (1975).

13. M. E. MEEK and B. F. RIDER, Report NEDO-12154-1, General Electric Co., Vallecitos Nuclear Center (1974).

14. R. J. TUTTLE, N.S.E., 56, 37 (1974).

15. D. SAPHIER et al., N.S.E., 62, 660 (1977).

16. A. J. DERUYTTER, Proc. of Rochester Symposium on Phys. and Chem. of Fission, Vol. II, p. 19, I.A.E.A. (1974).

17. C. WAGEMANS et al., Annual Progress Report on Nuclear Data, Report NEANDC(E)212, p. 8. Central Bureau for Nuclear Measurements, Geel (Belgium), 1980.

18. V. E. SCHROCK, Prog. Nuc. En. 3, 125 (1979); A. TOBIAS, Prog. Nuc. En. 5, 1 (1980).

19. R. W. PEELE and F. C. MAIENSCHEIN, Phys. Rev. C3, 373 (1971).

20. V. V. VERBINSKI, H. WEBER, and R. E. SUND, Phys. Rev. C7, 1173 (1973).

21. F. PLEASONTON, Phys. Rev. 174, 1500 (1968); F. PLEASONTON, R. L. FERGUSON, and H. W. SCHMITT, Phys. Rev. C6, 1023 (1972); F. PLEASONTON, Nuc. Phys. A213, 413 (1973).

Table I

QG by Mass Balance--Recommended Values[a]

Nuclide	QG (MeV)
Th-232	195.93 ± 0.32
Pa-233	196.62 ± 0.66
U-233	198.02 ± 0.10
U-234	197.78 ± 0.65
U-235	202.53 ± 0.10
U-236	201.82 ± 0.12
U-238	206.01 ± 0.17
Np-237	202.23 ± 0.80
Pu-238	204.66 ± 0.24
Pu-239	207.02 ± 0.14
Pu-240	205.66 ± 0.23
Pu-241	210.73 ± 0.23
Pu-242	209.47 ± 0.82
Am-241	209.51 ± 0.24
Am-243	209.80 ± 0.88
Cm-244	211.52 ± 0.87
Cf-252	217.66 ± 0.11

[a]Ref. 10

Table II

Prompt Energy Release, EP[a]

Nuclide	EINC (MeV)	EP (MeV)
Th-232	3.35	168.73
U-233	thermal	180.76
U-235	thermal	180.76
U-238	3.10	178.24
Pu-239	thermal	189.52
Pu-241	thermal	189.15

[a]Ref. 11.

Table IV

Decay Energies, ED[a]

Nuclide	EINC (MeV)	ED (MeV)
Th-232	3.35	26.82
U-233	thermal	16.84
U-235	thermal	21.26
U-236	2.82	22.95
U-238	3.10	27.24
Np-237	2.37	18.36
Pu-239	thermal	17.49
Pu-240	2.39	19.04
Pu-241	thermal	21.70
Pu-242	2.32	21.96
Cf-252	(spontaneous)	19.99

[a]Ref. 3.

Note: Table III shown on page 846

Table III

Fission Product Decay Energy Partition[a]

Isotope	Total Decay Energy	Beta Energy		Gamma Energy		Neutrino Energy	
	ED (MeV)	EB (MeV)	EB/ED	EGD (MeV)	EGD/ED	ENU (MeV)	ENU/ED
Th-232	27.25	8.27	.304	8.02	.294	10.95	.402
U-233	17.02	5.09	.299	5.07	.298	6.86	.403
U-235	21.37	6.44	.301	6.28	.294	8.65	.405
U-238	27.46	8.31	.303	8.07	.294	11.08	.403
Pu-239	17.28	5.17	.299	5.04	.292	7.07	.409
Pu-241	21.49	6.51	.303	6.17	.287	8.82	.410
Average			.3015 ±.0010		.2932 ±.0015		.4053 ±.0015

[a]Ref. 12.

Table V

LSQ Input Data and Observational Equations

Input Data	Weight	Observational Equation

Th-232:

EFR^{232} = 159.80 ± 2.0 ⟶ 0.25, $0.25\,x_1 = 39.95$

$EFR^{232} + ED^{232} + EGP^{232} = QG^{232} - (ENP^{232} - EINC^{232}) - END^{232}$

= 194.56 ± 0.26 ⟶ 15, $15x_1 + 15x_2 + 15x_3 = 2918.4$

$EFR^{232} + EGP^{232} = EP^{232} - (ENP^{232} - EINC^{232})$

= 167.38 ± 0.30 ⟶ 10, $10x_1 + 10x_3 = 1673.8$

ED^{232} = 26.82 ± 0.27 ⟶ 4^a, $4x_2 = 107.28$

ED^{232}/ED^{235} = 1.19 ± 0.06 ⟶ 0.6, $0.6x_2 - 0.714x_8 = 0$

$(ED^{232} - 1.19\ ED^{235} = 0 ± 0.06\ ED^{235})$

EGP^{232} = 6.96 ± 1.0 ⟶ 1, $x_3 = 6.96$

U-233:

EFR^{233} = 167.36 ± 2 ⟶ 0.25, $0.25x_4 = 41.84$

$EFR^{233} + ED^{233} + EGP^{233} = QG^{233} - ENP^{233} - END^{233}$

= 193.12 ± 0.2 ⟶ 25, $25x_4 + 25x_5 + 25x_6 = 4828$

$EFR^{233} + EGP^{233} = EP^{233} - ENP^{233}$

= 175.85 ± 0.25 ⟶ 16, $16x_4 + 16x_6 = 2813.76$

EFR^{233}/EFR^{238} = 0.9916 ± 0.0015 ⟶ 18, $18x_4 - 17.8488x_{10} = 0$

EFR^{233}/EFR^{235} = 0.9953 ± 0.0025 ⟶ 5.7, $5.7x_4 - 5.6732x_7 = 0$

ED^{233} = 16.84 ± 0.12 ⟶ 10^a, $10x_5 = 168.4$

ED^{233}/ED^{235} = 0.81 ± 0.04 ⟶ 1.4, $1.4x_5 - 1.134x_8 = 0$

EGP = 6.96 ± 1.0 ⟶ 1, $x_6 = 6.96$

---

[a]Reduced weight; see text.

Table V (cont.)

Input Data	Weight	Observational Equation
U-235:		
$EFR^{235} = 167.93 \pm 2.0$	0.25	$0.25x_7 = 41.9825$
$EFR^{235} + ED^{235} + EGP^{235} = QG^{235} - ENP^{235} - END^{235}$		
$= 197.73 \pm 0.12$	70	$70x_7 + 70x_8 + 70x_9 = 12841$
$EFR^{235} + EGP^{235} = EP^{235} - END^{235}$		
$= 175.97 \pm 0.20$	25	$25x_7 + 25x_9 = 4399.25$
$ED^{235} = 21.26 \pm 0.15$	10^a	$10x_8 = 212.6$
$ED^{235} = 23.8 \pm 1.6$	0.4	$0.4x_8 = 9.52$
$ED^{235} = 22.18 \pm 1$	1	$x_8 = 22.18$
$EGP^{235} = 6.73 \pm 1.0$	1	$x_9 = 6.73$
U-238:		
$EFR^{238} = 167.93 \pm 2.0$	0.25	$0.25x_{10} = 41.9825$
$EFR^{235}/EFR^{238} = 0.9968 \pm 0.0014$	18	$18x_7 - 17.9424x_{10} = 0$
$EFR^{235}/EFR^{238} = 0.9996 \pm 0.0025$	5.7	$5.7x_7 - 5.6977x_{10} = 0$
$EFR^{238} + ED^{238} + EGP^{238} = QG^{238} - (ENP^{238}-EINC^{238}) - END^{238}$		
$= 203.58 \pm 0.32$	10	$10x_{10} + 10x_{11} + 10x_{12} = 2035.8$
$EFR^{238} + EGP^{238} = EP^{238} - (ENP^{238}-EINC^{238})$		
$= 175.83 \pm 0.4$	6	$6x_{10} + 6x_{12} = 1054.98$
$ED^{238} = 27.24 \pm 0.19$	10^a	$10x_{11} = 272.4$
$ED^{238} = 27.2 \pm 1.0$	1	$x_{11} = 27.2$
$ED^{238}/ED^{235} = 1.265 \pm 0.06$	0.44	$0.44x_{11} - 0.5566x_8 = 0$
$EGP^{238} = 6.96 \pm 1.0$	1	$x_{12} = 6.96$

[a]Reduced weight; see text.

Table V (cont.)

Input Data	Weight	Observational Equation
Pu-239:		
$EFR^{239} = 175.77 \pm 0.10$	100	$100x_{13} = 17577$
$EFR^{239} + ED^{239} + EGP^{239} = QG^{239} - ENP^{239} - END^{239}$		
$= 201.12 \pm 0.2$	25	$25x_{13} + 25x_{14} + 25x_{15} = 5028$
$EFR^{239} + EGP^{239} = EP^{239} - ENP^{239}$		
$= 183.62 \pm 0.25$	16	$16x_{13} + 16x15 = 2937.92$
$ED^{239} = 17.49 \pm 0.12$	10^a	$10x_{14} = 174.9$
$ED^{239} = 18.36 \pm 1.0$	1	$x_{14} = 18.36$
$ED^{239}/ED^{235} = 0.878 \pm 0.0044$	0.9	$0.9x_{14} - 0.7902x_8 = 0$
$EGP^{239} = 7.05 \pm 1.0$	1	$x_{15} = 7.05$
Pu-241:		
$EFR^{241} = 174.12 \pm 2.0$	0.25	$0.25x_{16} = 43.53$
$EFR^{241}/EFR^{235} = 1.0353 \pm 0.005$	1.4	$1.4x_{16} - 1.4494x_7 = 0$
$EFR^{261} + ED^{241} + EGP^{241} = QG^{241} - ENP^{241} - END^{241}$		
$= 204.74 \pm 0.31$	10	$10x_{16} + 10x_{17} + 10x_{18} = 2047.4$
$EFR^{241} + EGP^{241} = EP^{241} - ENP^{241}$		
$= 183.16 \pm 0.3$	10	$10x_{16} + 10x_{18} = 1831.6$
$ED^{241} = 21.7 \pm 0.15$	10^a	$10x_{17} = 217$
$ED^{241}/ED^{235} = 1.056 \pm 0.053$	0.7	$0.7x_{17} - 0.7392x_8 = 0$
$EGP^{241} = 6.96 \pm 1$	1	$x_{18} = 6.96$

[a]Reduced weight; see text.

Table VI

Results of LSQ Calculations and Systematics for Primary Isotopes[a]

(MeV/fission)

	Th-232		U-233		U-235	
	LSQ	Systematics	LSQ	Systematics	LSQ	Systematics
QG	195.82 ± 1.3	195.93 ± 0.2	197.93 ± 0.8	198.02 ± 0.12	202.48 ± 0.72	202.53 ± 0.06
ED	26.97 ± 0.31	27.19 ± 1.5	17.10 ± 0.21	18.54 ± 1.5	21.60 ± 0.17	22.83 ± 1.00
EP	168.85 ± 0.9	168.73 ± .25	180.84 ± 0.73	180.76 ± 0.15	180.38 ± 0.70	180.76 ± 0.10
EB	8.13 ± 0.10	8.19 ± 0.5	5.16 ± 0.06	5.58 ± 0.5	6.50 ± 0.05	6.87 ± 0.30
EGD	7.91 ± 0.10	8.2 ± 0.75	5.01 ± 0.06	5.47 ± 0.75	6.33 ± 0.05	6.74 ± 0.50
ENU	10.93 ± 0.13	10.99 ± 1.1	6.93 ± 0.09	7.49 ± 1.10	8.75 ± 0.07	9.22 ± 0.80
EFR	160.39 ± 0.92	159.81 ± 2.0	168.21 ± 0.50	167.36 ± 2.0	169.12 ± 0.49	167.93 ± 2.0
EGP	7.11 ± 0.90	6.96 ± 1.0	7.73 ± 0.52	6.96 ± 1.0	6.97 ± 0.50	6.73 ± 1.0
ENP	4.7 ± 0.12	4.7 ± 0.12	4.9 ± 0.1	4.9 ± 0.1	4.79 ± 0.07	4.79 ± 0.07
EINC	3.35 ± 0.10	3.35 ± 0.1	(thermal)	(thermal)	(thermal)	(thermal)
END	0.022 ± 20%	0.022 ± 20%	0.031 ± 15%	0.0031 ± 15%	0.0074 ± 15%	0.0074 ± 15%

[a]Recommended values are underlined.

Table VI (cont.)[a]

	U-238		Pu-239		Pu-241	
	LSQ	Systematics	LSQ	Systematics	LSQ	Systematics
QG	205.87 ± 0.8	206.01 ± .26	207.06 ± 0.33	207.02 ± 0.13	210.83 ± 1.0	210.73 ± 0.22
ED	27.35 ± 0.25	28.93 ± 1.5	17.62 ± 0.21	20.05 ± 1.5	21.84 ± 0.30	24.18 ± 1.5
EP	178.52 ± 0.75	178.24 ± 0.30	189.44 ± 0.26	189.52 ± 0.15	188.99 ± 1.0	189.15 ± 0.25
EB	8.25 ± 0.08	8.71 ± 0.5	5.31 ± 0.06	6.03 ± 0.5	6.58 ± 0.09	7.28 ± 0.5
EGD	8.02 ± 0.07	8.53 ± 0.75	5.17 ± 0.06	5.91 ± 0.75	6.40 ± 0.09	7.13 ± 0.75
ENU	11.08 ± 0.10	11.69 ± 1.1	7.14 ± 0.09	8.10 ± 1.1	8.85 ± 0.12	9.77 ± 1.1
EFR	169.57 ± 0.49	167.93 ± 2.0	175.78 ± 0.1	173.85 ± 2.0	175.36 ± 0.68	174.12 ± 2.0
EGP	6.54 ± 0.53	6.96 ± 1.0	7.76 ± 0.22	7.05 ± 1.0	7.64 ± 0.69	6.96 ± 1.0
ENP	5.51 ± 0.10	5.51 ± 0.10	5.9 ± 0.1	5.9 ± 0.1	5.99 ± 0.13	5.99 ± 0.13
EINC	3.10 ± 0.10	3.10 ± 0.10	(thermal)	(thermal)	(thermal)	(thermal)
END	0.018 ± 15%	0.018 ± 15%	0.0028 ± 15%	0.0028 ± 15%	0.005 ± 20%	0.005 ± 20%

[a]Recommended values are underlined.

Table VII

Results of Systematics for Other Isotopes[a]

(MeV/fission)

	Pa-233	U-234	U-236	Np-237	Pu-238
QG	196.62 ± 0.66	197.78 ± 0.65	201.82 ± .12	202.23 ± .80	204.66 ± 0.24
ED	23.29 ± 1.5	20.16 ± 1.5	24.43 ± 1.5	20.69 ± 1.5	18.01 ± 1.5
EP	175.75 ± 2.32	179.41 ± 2.31	179.89 ± 2.26	183.69 ± 2.35	186.46 ± 2.26
EB	7.01 ± 0.5	6.07 ± 0.5	7.35 ± 0.5	6.23 ± 0.5	5.42 ± 0.5
EGD	6.87 ± 0.75	5.95 ± 0.75	7.21 ± 0.75	6.10 ± 0.75	5.31 ± 0.75
ENU	9.41 ± 1.10	8.14 ± 1.10	9.87 ± 1.10	8.36 ± 1.10	7.28 ± 1.10
EFR	163.5 ± 2.0	167.1 ± 2.0	167.5 ± 2.0	170.6 ± 2.0	173.6 ± 2.0
EGP	6.96 ± 1.0	6.96 ± 1.0	6.96 ± 1.0	6.96 ± 1.0	6.96 ± 1.0
ENP	5.28 ± 0.42	5.36 ± 0.43	5.41 ± 0.29	6.17 ± 0.48	5.92 ± 0.34
EINC	3.0 ± 0.3	2.36 ± 0.10	2.82 ± 0.10	2.37 ± 0.10	(thermal)
END	0.01 ± 25%	0.005 ± 20%	0.01 ± 20%	0.005 ± 25%	0.002 ± 20%

[a]Ref. 11.

Table VII (cont.)

Results of Systematics for Other Isotopes[a]

(MeV/fission)

	Pu-240	Pu-242	Am-241	Am-243	Cm-244
QG	205.66 ± 0.23	209.47 ± 0.82	209.51 ± 0.24	209.80 ± 0.88	211.52 ± 0.87
ED	21.39 ± 1.5	25.60 ± 1.5	18.68 ± 1.5	21.81 ± 1.5	21.03 ± 1.5
EP	187.43 ± 2.27	187.94 ± 2.34	189.82 ± 2.27	191.03 ± 2.37	193.08 ± 2.29
EB	6.44 ± 0.5	7.70 ± 0.5	5.62 ± 0.5	6.56 ± 0.5	6.33 ± 0.5
EGD	6.31 ± 0.75	7.55 ± 0.75	5.51 ± 0.75	6.43 ± 0.75	6.20 ± 0.75
ENU	8.64 ± 1.10	10.34 ± 1.10	7.54 ± 1.10	8.81 ± 1.10	8.50 ± 1.10
EFR	173.7 ± 2.0	174.0 ± 2.0	176.4 ± 2.0	176.3 ± 2.0	178.5 ± 2.0
EGP	6.96 ± 1.0	6.96 ± 1.0	6.96 ± 1.0	6.96 ± 1.0	6.96 ± 1.0
ENP	6.77 ± 0.36	6.98 ± 0.54	6.53 ± 0.36	7.77 ± 0.59	7.62 ± 0.58
EINC	2.39 ± 0.10	2.32 ± 0.10	(thermal)	3.0 ± 0.5	(thermal)
END	0.004 ± 20%	0.010 ± 20%	-	-	-

[a]Ref. 11.

Table VIII
Average Energy Per Delayed Neutron

Nuclide	Average Energy/ Del. Neutron (MeV)[a]	$\bar{\nu}_d$ [b]	E_d (MeV)
Th-232	0.438	~ 0.05	0.022 ± 20%
U-233	0.443	0.007	0.0031 ± 15%
U-235	0.464	0.016	0.0074 ± 15%
U-238	0.460	0.04	0.018 ± 15%
Pu-239	0.463	0.006	0.0028 ± 15%
Pu-241	0.463	0.01	0.005 ± 20%

[a] Ref. 15.
[b] Ref. 14.

Table IX

Summary of Pre-Neutron Emission Fragment Kinetic Energy Data[a]

U-233	U-235	Pu-239	Pu-241	Cf-252	Method	Reference
167.02±1.70	167.68±1.70	174.41±1.70			DV	Milton (1963)
				182.10±1.70	DV	Fraser (1963)
				185.40±2.00	DV	Milton (1963)
				185.70±1.90	DV	Whetstone (1963)
	167.45±1.70				DV(+DE)	Andritsopoulos (1967)
				184.90±2.00	DV	Barashkov (1971)
167.02	167.56	174.41		184.52	Average	of DV Measurements
169.02±2.0		176.22±0.50	176.12±0.50	Rel. to U-235 = 172.25[b]		Vorob'eva (1974)
	171.90±1.40			186.50±1.20	DE	Schmitt (1966)
		177.70±1.80	179.60±1.80		DE	Neiler (1966)
171.20±2.00	172.00±2.00	179.30±2.00		184.30±2.00	DE	Bennett (1967)
172.00±1.80					DE	Pleasonton (1968)
172.10±1.80	172.00±1.80	177.10±2.00		185.80±2.00	DE	Reisdorf (1971)
		175.20±1.50			DE	Toraskar (1974)
		177.95±0.04			DE	Deruytter (1974)
			179.62±2.00		DE	Hipp (1974)
171.77	171.97	177.45	179.61	184.45	Average	of DE Measurements

[a]Ref. 11.

Table IX (cont.)

Th-232	Pa-231	U-238	Np-237	Pu-240	Pu-242	Cm-245	Meth.	Reference
	166.80±2.0	170.10±2.0	174.00±2.0				DE	Bennett (1967)
163.26±2.0							DE	Sergachev (1968)
169.80±2.0							DE	Holubarsch (1971)
						180.20±0.5	DE	Unik (1974)
		170.01±2.0[b]		175.62±2.0[b]	176.02±2.0[b]			Vorob'eva (1974)
		170.82±2.0[c,d]						Okolovich (1963)

[b]Measurement relative to $\overline{E}_k$(U-235) = 172.25; renormalized to $\overline{E}_k$(U-235) = 169.76.

[c]Error estimated.

[d]Relative measurement; ratio $\overline{E}_k$(U-235)/$\overline{E}_k$(U-238) = 0.9938 reported; renormalized to $\overline{E}_k$(U-235) = 169.76

Table X

Effects of Different Weight Factors for ED

	Weight Factors		LSQ Output Values		
	Walker	Decay Heat Standard	EFR	ED	EGP
Th-232	14	--	160.43	26.89	7.12
	4	--	160.39	26.97	7.11
	1	--	160.36	27.04	7.10
U-233	70	--	168.28	16.91	7.77
	10	--	168.21	17.10	7.73
	1	--	168.08	17.31	7.73
U-235	44	0	169.19	21.41	7.03
	10	1	169.12	21.60	6.97
	0	1	168.99	21.78	6.97
U-238	28	0	169.64	27.29	6.51
	10	1	169.57	27.35	6.54
	0	1	169.43	27.58	6.53
Pu-239	70	0	175.78	17.51	7.82
	10	1	175.78	17.62	7.76
	0	1	175.78	17.73	7.69
Pu-241	44	--	175.42	21.73	7.64
	10	--	175.36	21.84	7.64
	1	--	175.15	22.55	7.50

Table XI

Prompt Gamma Energy-Release Data and Recommended Values[a]

Previous Evaluations:

Time range (seconds)	U-235	U-235	Pu-239
$0.0 - \sim 5\times10^{-8}$	7.54 ± 0.84[b]	7.25 ± 0.26[c]	7.96 ± 0.94[c]
$\sim 5\times10^{-8} - 1\times10^{-6}$	0.43 ± 0.22[b]	0.35 ± 0.71[c]	
$1\times10^{-6} - 1\times10^{-3}$	0.04 ± 0.02[b]	0.04 ± 0.02[c]	0.05 ± 0.03[c]
	8.01 ± 0.87	7.64 ± 0.75	8.01 ± 0.94

Data on Prompt-Prompt Fraction:

Nuclide			
U-233			6.69 ± 0.30[f]
U-235	7.25 ± 0.26[d]	6.51 ± 0.30[e]	6.43 ± 0.30[f]
Pu-239		6.82 ± 0.30[e]	6.73 ± 0.35[f]
Cf-252		6.84 ± 0.30[e]	

Recommended Values:

Nuclide	Prompt-Prompt Fraction	Total Prompt Gamma[a]	
U-233	6.69 ± 0.50	6.96 ± 1.0	These used
U-235	6.47 ± 0.43	6.73 ± 1.0	for these
Pu-239	6.78 ± 0.45	7.05 ± 1.0	isotopes
Cf-252	6.84 ± 0.50	7.11 ± 1.0	
Averages	6.70 ± 0.50	6.96 ± 1.0	Used for all others

[a]Ref. 11.

[b]Ref. 5.

[c]Ref. 4.

[d]Ref. 19.

[e]Ref. 20.

[f]Ref. 21.

Discussion

England (Comment)

Pu-241 decay heating has been measured at ORNL by Dickens and U-233 decay heating has been measured at LASL by Yarnell. Perhaps these could be used in place of these calculated components.

Peelle

I do not understand what items had status as input data to the least-squares fit. Could you clarify how unmeasured quantities were included as observations, particularly with respect to prompt gamma release and neutrino energy release?

Sher

There are four types of input data that we use. Two types are data that are derived from yields as was shown by the two equations. The other are direct measurements. The third type are some results that are based on systematics, like the ratio of decay energies between isotopes that w.re calculated by James. The fourth, in some cases, were averages based on observed quantities in other isotopes, and prompt gamma release is one of those. For the isotopes in which direct measurements of prompt gamma were made, we used the measurements. For all other isotopes, we used the average of those measurements. This is just for want of something better. Now with respect to the neutrino energy, there's a table in the written paper (I don't have a slide). We observed that for the six or so primary isotopes, Walker had obtained from yield and decay-scheme data, the individual components of the beta energy, the average beta energy, the average delayed gamma energy, and the neutrino energy. We just found that the ratio of each of these three to the total decay energy was a constant across all these isotopes. The ratio of beta energy to the total decay energy, for example, is about 0.3 and the variation from isotope to isotope is quite small; so again, for want of something better, we assume that the ratio applied to all isotopes. More recently I have taken a closer look at that and I think that's not quite true, but it is not a bad assumption, so the least-squares calculation actually comes out with the total decay energy and then by multiplying by the appropriate ratio for beta decay, we get the beta energy and so on for the others. So they're not independently obtained.

England (Comment)

I've seen the paper and I don't understand the neutrino energy; it is about 8 MeV per fission compared to a little over 6 for the beta. I would think there should be a larger amount for the neutrino energy but I haven't calculated it and it isn't important

for the recoverable fission energy. There is another problem for the user and that's the (n,γ) capture which can be a major problem, a spatial problem, a reactor dependent problem in general. This component may also contribute a significant uncertainty, especially if the user does not account for its spatial dependence in reactor calculations.

PROMPT FISSION NEUTRON SPECTRA AND $\bar{\nu}_p$

David G. Madland

Los Alamos Scientific Laboratory
University of California
Theoretical Division
Los Alamos, New Mexico 87545, U.S.A.

ABSTRACT

Methods used to obtain the evaluated prompt fission neutron spectrum N(E) and the average prompt neutron multiplicity $\bar{\nu}_p$ are reviewed. The relative influence of experimental data; interpolated, extrapolated, and fitted experimental data; systematics; and nuclear theory are considered for the cases where (a) abundant experimental data exist, (b) some experimental data exist, and (c) no experimental data exist. The Maxwellian and Watt distributions, and the determination of the parameters of these distributions by data fitting, are described and compared to recent new theoretical work on the calculation of N(E). Similarly, various expressions for $\bar{\nu}_p$ that have been obtained by data fitting and systematics are described and compared to recent new theoretical work. Complications in the evaluation of N(E) and $\bar{\nu}_p$ due to the onset of multiple-chance fission and the interrelationships between N(E), $\bar{\nu}_p$ and the multiple-chance fission cross section are discussed using the example of the fission of ^{235}U. Some statistics and comments are given on the evaluations of N(E) and $\bar{\nu}_p$ contained in ENDF/B-V, and a number of concluding recommendations are made for future evaluation work.

I. INTRODUCTION

The prompt fission neutron spectrum N(E) and the average prompt neutron multiplicity $\bar{\nu}_p$ are quantities of crucial importance in a number of practical considerations. Accordingly, there is strong interest in the accuracy and detail with which they are described in evaluated nuclear data files. In this work the methods of evaluating these quantities in preparation of such files is reviewed.

In Sec. II a number of methods are reviewed by which prompt fission neutron spectra are evaluated. These methods are then classified according to the amount of experimental data available for the evaluation. In Sec. III models and two new theories of the prompt fission neutron spectrum are discussed and reviewed. Specific recommendations for the evaluation of $N(E)$ in the cases of least-squares fitting of experimental data and direct calculation are made in Sec. IV. Sections V and VI, for the methods of evaluating the average prompt neutron multiplicity $\bar{\nu}_p$, are completely analogous to Secs. II and IV, respectively. A summary together with some concluding remarks is given in Sec. VII and a number of statistics are presented on the evaluation methods used to determine $N(E)$ and $\bar{\nu}$ in ENDF/B-V.

The most recent reviews on prompt fission neutron spectra were held at conferences in 1971 and 1975 [1-2]. A comprehensive review of $\bar{\nu}$ by Manero and Konshin [3] appeared in 1972.

II. METHODS TO EVALUATE PROMPT FISSION NEUTRON SPECTRA

A number of methods exist by which a representation of the prompt fission neutron spectrum $N(E)$ can be obtained from experimental data, theoretical calculation, or a combination of the two. These methods include the following:

A.   **Direct use of experimental data.** $N(E)$, where E is the energy of the secondary or emitted neutron, is usually given by the experimentalist in histogram form, that is, N_i is given for the i'th emitted neutron energy bin (E_i-E_{i-1}) or for some representative energy E_i of that bin, where E_i has either been measured or defined. The spectrum $N(E)$ is usually measured for a fixed incident energy E_n of the neutron inducing fission or for spontaneous fission. Typically, the experimental data are not presented in absolute units, that is, $N(E)$ is usually unnormalized.

The ENDF MF=5 LF=1 law (Arbitrary Tabulated Function) can be used to tabulate a histogram of $N(E)$. The emitted neutron energy bin limits or a representative bin energy can be used to construct the tabulation. A complete experimental data set for such a tabulation would perhaps consist of 10 to 15 fission spectra which span emitted neutron energy ranges of ~10 keV to ~ 20 MeV and which span an incident neutron energy range of thermal energy to ~20 MeV. However, no such data set yet exists. Points to consider in this approach for the data sets that do exist include the following:

1.   The experimental data cover a limited range of the emitted neutron energy E. The problem therefore exists as to what to use in the external regions below the lowest emitted neutron energy cutoff (~200 keV to ~1 MeV) and above the highest emitted neutron energy cutoff (~5 MeV to ~15 MeV).

2. The problem (1) is further compounded by the fact that the integral of N(E) over all emitted neutron energies E must be unity, that is, N(E) is a normalized spectrum.

3. If one is specifying the energy bin of the histogram by a defined representative bin energy E_i some amount of care must be exercised in the definition especially in the tail region (E > ~2-3 MeV) of the spectrum where the behavior is approximately exponential. For example, the choice of the mean energy of the bin in this region would distort the measured shape of the spectrum.

B. Use of experimental data to determine parameters of models which approximate the prompt fission neutron spectrum. Least-squares or "eyeball" fitting procedures of experimental fission neutron spectra can be applied to determine the parameters of a model of the fission neutron spectrum. The parameters extracted from the fitting analysis can then be used in the model expression to represent the fission neutron spectrum at, or near, the incident neutron energy corresponding to the experiment. Of course, if experimental spectra exist for a number of incident neutron energies for the isotope of interest, then the model parameters can be extracted and used in the model expression to represent the fission neutron spectrum on a set of incident neutron energies. In this case, if the experimental spectra are sufficiently extensive and accurate, the dependence of the model parameters upon the incident neutron energy can be determined provided that the model is a realistic physical approximation.

Some of the more widely used model expression include the Maxwellian distribution, the simple form of the evaporation spectrum [4], and the Watt distribution [5]. These expressions will be discussed in more detail in Secs. III. A. and III.B. They are options for representing the fission neutron spectrum in ENDF MF=5 under LF=7, 9, and 11 laws, respectively.

Points to consider in the approach of using experimental fission neutron spectrum data to determine model parameters include the following:

1. The most obvious question is which of the commonly used model expressions best approximates the fission neutron spectrum? This topic will be addressed in Secs. III and IV.

2. A good example of the use of least-squares fitting procedures in the determination of Maxwellian and Watt distribution parameters, on prompt fission neutron spectra measured at a single incident neutron energy, is given by Johansson and Holmqvist [6].

3. If the least-squares minimization procedure involves an experimental data set comprised of measurements from several sources, the possibility exists that quite different experimental error analyses were performed. This condition can lead to over-biased and possibly erroneous results unless

the degree of thoroughness, or lack thereof, of each error analysis is understood by the evaluator. Error adjustment, of course, should only be done in collaboration with the experimentalist.

4. At sufficiently high incident neutron energy (E_n > ~6-7 MeV) multiple-chance fission processes (n,xnf) begin to occur in which x neutrons are sequentially evaporated prior to the fission of the last compound nucleus. In an experiment 0, 1, 2, ... up to x evaporated neutrons are measured together with pure fission spectrum neutrons in the same fission event (coincidence gate) to comprise the total fission neutron spectrum. The model expression used in the least-squares fitting procedure is therefore made up of a certain number of evaporation spectrum terms and a certain number of pure fission spectrum terms, depending upon the magnitude of E_n. The number of terms and how they are combined is explained in Sec. III.C.

C. Direct use of models which approximate the prompt fission neutron spectrum. This approach is identical to the one just discussed (Sec. II.B) except that the parameters of the model expressions are obtained by methods other than least-squares or "eyeball" fitting procedures using experimental fission neutron spectra. Therefore, the comments of Sec. II.B.1 and Sec. II.B.4 apply to the present discussion. The key to this approach is the determination of an expression for the model parameter, such as the Maxwellian temperature T_M, either empirically or by calculation in terms of other known quantities of the fissioning system.

One well known example due to Terrell [7,8] is the relationship between the average energy of the prompt fission neutron spectrum <E> and the average prompt neutron multiplicity $\bar{\nu}_p$, given by

$$\langle E(E_n) \rangle = \alpha + \beta \sqrt{\nu_p(E_n) + 1} \tag{1}$$

where $\alpha \cong 0.75$, $\beta \cong 0.65$, and where α and β vary slowly with E_n and fissioning nucleus. Since the average energy of the Maxwellian distribution is (3/2) T_M, Eq. (1) determines T_M in terms of $\bar{\nu}_p$ which can be accurately measured. In Sec. III.B it will be shown that Eq. (1) is an approximation of a more general expression also calculated on the basis of Terrell's experiments [7].

D. Use of systematics to approximate the prompt fission neutron spectrum. The use of systematics in this case means simply that the fission neutron spectrum desired is identified with an existing fission neutron spectrum, or average of existing fission neutron spectra, for fissioning nuclei that share some property, or properties, in common with the one of interest.

An example might be that thermal fission is a common property and that the mass and charge numbers of the compound fissioning nuclei are very nearly the same. The cautions that need be exercised in the application of this method are obvious.

E. Theoretical calculation of the prompt fission neutron spectrum. Two new theoretical calculations of the prompt fission neutron spectrum exist. The first of these is a statistical model approach by Browne and Dietrich [9,10] which employs a full Hauser-Feshbach calculation for forty fission fragments representative of the fragment mass distribution. The second calculation is an approach based upon nuclear-evaporation theory by Madland and Nix [11-16] which accounts for a number of physical effects which have usually been ignored. Both of these calculations show significant advances in reproducing experimental fission neutron spectra. This gives credence to their use in evaluation work. They will be discussed in more detail in Sec. III.

Evaluation of the prompt fission neutron spectrum for a given isotope will generally involve the use of one or more of the five methods, A through E, just discussed. It is useful to consider the suitability of these methods as a function of the amount of quality experimental data available to the evaluator. We consider three cases: abundant experimental data, some experimental data, and no experimental data. In the case of abundant experimental data the methods A, B, and E may be suitable. If accuracy is the main consideration in the construction of the evaluated file then methods A and E may dominate, whereas if minimal computing time in the use of the file is the main concern then methods B and, to some extent, E may dominate. In the case of some experimental data the methods B, C, and E may be suitable. If methods B and C are both employed, but at different ranges of incident neutron energy, then overlap calculations should be performed to insure continuity. In the case of no experimental data the methods C, D, and E may be suitable. Comparison of the results using methods C and E would perhaps be useful in assessing a confidence level.

III. MODELS AND THEORIES OF THE PROMPT FISSION NEUTRON SPECTRUM

In the following E and N(E) are laboratory expressions, and ε and $\phi(\varepsilon)$ are center-of-mass expressions, where E and ε are secondary or emitted neutron energies. Unless otherwise noted N(E) and $\phi(\varepsilon)$ are normalized to unity when integrated from zero to infinity. All energies and temperatures are in units of MeV.

A. Previous work. The Maxwellian distribution is given by

$$N_M(E) = (2/\sqrt{\pi T_M^3}) \; E^{1/2} \; \exp(-E/T_M) \qquad (2)$$

where T_M is the Maxwellian temperature. The average energy of the Maxwellian distribution is given by

$$\langle E \rangle_M = (3/2) T_M . \tag{3}$$

The Maxwellian distribution is properly a center-of-mass expression and its use to describe fission neutron spectra measured in the laboratory system means that the temperature T_M is accounting not only for the emission of neutrons from the fission fragments, but also the center-of-mass motion of the fragments as well. We use the notation for the laboratory system here because the distribution is used in this way, historically and at present, to describe measured fission neutron spectra.

The center-of-mass neutron evaporation spectrum [4] is given by

$$\phi(\varepsilon) = k(T_e) \sigma_c(\varepsilon) \varepsilon \exp(-\varepsilon/T_e) \tag{4}$$

where $k(T_e)$ is the temperature-dependent normalization, $\sigma_c(\varepsilon)$ is the cross section for the inverse process of compound nucleus formation, and T_e is the temperature of the residual nucleus following neutron emission. The center-of-mass simple neutron evaporation spectrum is obtained by assuming $\sigma_c(\varepsilon)$ constant. In this case $k(T_e) = 1/\sigma_c T_e^2$ and

$$\phi(\varepsilon) = (\varepsilon/T_e^2) \exp(-\varepsilon/T_e) \tag{5}$$

for which the average energy is given by

$$\langle \varepsilon \rangle = 2T_e . \tag{6}$$

One use of Eqs. (4) and (5) is in the description of the evaporation-neutron component of the total fission neutron spectrum in the case of multiple-chance fission, as discussed in Sec. II.B.4.[†]

The Watt [5] distribution is given by

[†]In this circumstance the neutrons are evaporating from a compound fissioning nucleus just prior to fission and the distinction between laboratory and center-of-mass systems is negligible.

$$N_W(E) = [\exp(-E_f/T_W)/\sqrt{\pi E_f T_W}] \times$$

$$[\exp(-E/T_W) \sinh(2\sqrt{EE_f}/T_W)] \tag{7}$$

where T_W is the Watt temperature and E_f is the average fission-fragment kinetic energy per nucleon. The average energy of the Watt distribution is given by

$$\langle E \rangle_W = E_f + (3/2)T_W . \tag{8}$$

The Watt distribution is obtained by assuming that the center-of-mass fission neutron spectrum is Maxwellian, that both fission fragments are moving with the same average kinetic energy per nucleon E_f, and transforming to the laboratory system. In the limit that E_f approaches zero, $N_W(E)$ approaches $N_M(E)$. The Watt distribution is clearly more physical than the Maxwellian distribution because the contributions due to center-of-mass fragment motion and neutron emission from the fragments are separately taken into account.

B. New work. Two new theoretical calculations of the prompt fission neutron spectrum exist. They have been briefly described in Sec. II.E.

The first new calculation is the statistical-model Hauser-Feshbach calculation of Browne and Dietrich [9,10]. This approach may ultimately provide the most exact agreement with experiment. At the present time, however, this is not the case because of insufficient knowledge of three main input quantities to the calculation. These are the initial fragment spin and excitation energy distributions, the fragment nuclear level densities, and the neutron plus fragment transmission coefficients. The status of this work is that fairly good agreement with experiment has been achieved in calculating the [252]Cf spontaneous-fission neutron spectrum. The next step would be to improve the physics content of the three main input quantities. This would perhaps be crucial in using this approach in evaluation work. The Hauser-Feshbach formalism is sufficiently complex that the final expression for the fission neutron spectrum cannot be written without considerable preliminary definition. Accordingly, a reading of Ref. [9] is recommended.

The second new calculation is the approach based upon standard nuclear-evaporation theory by Madland and Nix [11-16] which accounts for the physical effects of (1) the center-of-mass motion of each fission fragment, (2) the distribution of fission-fragment residual nuclear temperature, (3) the energy-dependence of the cross section $\sigma_c(\varepsilon)$ for the inverse process of compound nucleus formation, and (4) the occurrence of multiple-chance fission processes at high excitation energy. This approach is somewhat more easily applied for various

fissioning nuclei and incident neutron energies. Moreover, the formalism simultaneously yields expressions for $N(E)$ and $\bar{\nu}_p$, for high- as well as low-excitation fission. In addition, this work gives formulas for the parameters of the Maxwellian and Watt distributions as a function of fissioning nucleus and incident neutron energy. A cautionary note similar to that for the Hauser-Feshbach approach is that certain input quantities to the calculation, such as nuclear level-density parameter and average fission energy release, could have improved physical content.

The fission neutron spectrum has been calculated for two different assumptions concerning the cross section $\sigma_c(\varepsilon)$. Use of a constant cross section yields a closed expression for the spectrum while use of an energy-dependent cross section, calculated with the optical model, yields a numerical integral expression. The expressions for the prompt fission neutron spectrum $N(E)$, the average energy of the spectrum $<E>$, and the average prompt neutron multiplicity $\bar{\nu}_p$, under the two assumptions are as follows:

$\sigma_c(\varepsilon) = \text{constant}$

$$N(E) = \frac{1}{2}[N(E,E_f^L) + N(E,E_f^H)] \tag{9}$$

where E_f^L and E_f^H are the average fission-fragment kinetic energy per nucleon of the light and heavy fragment, respectively, and

$$N(E,E_f) = (1/3\sqrt{E_f T_m}) \; \{u_2^{3/2} \, E_1(u_2)$$

$$- u_1^{3/2} \, E_1(u_1) + \gamma(3/2,u_2)$$

$$- \gamma(3/2,u_1)\} \tag{10}$$

where

$$u_1 = (\sqrt{E} - \sqrt{E_f})^2/T_m \quad ,$$

$$u_2 = (\sqrt{E} + \sqrt{E_f})^2/T_m \quad ,$$

E_1 is the exponential integral [17], γ is the incomplete gamma function [17], and T_m is the maximum temperature of the fission-fragment residual nuclear-temperature distribution. The average energy of the spectrum is given by

$$\langle E \rangle = \frac{1}{2}[E_f^L + E_f^H] + (4/3)T_m \ . \tag{11}$$

The average prompt neutron multiplicity $\bar{\nu}_p$ is given by

$$\bar{\nu}_p = \frac{\langle E^* \rangle - \langle E_\gamma^{tot} \rangle}{\langle S_n \rangle + (4/3)T_m} \ , \tag{12}$$

where $\langle E^* \rangle$ is the initial total average fragment excitation energy, $\langle E_\gamma^{tot} \rangle$ is the total average prompt gamma-ray energy, and $\langle S_n \rangle$ is the average fission-fragment neutron separation energy.

$\sigma_c(\varepsilon)$ calculated using the optical model

$N(E)$ is given by Eq. (9) where

$$N(E,E_f) = (1/2 \ \sqrt{E_f}T_m^2) \times \tag{13}$$

$$\int_{u_1 T_m}^{u_2 T_m} \sigma_c(\varepsilon) \ \sqrt{\varepsilon} \ d\varepsilon \int_o^{T_m} k(T) \ T \ \exp(-\varepsilon/T)dT$$

The average energy of this spectrum and the average prompt neutron multiplicity are given exactly by Eqs. (11) and (12) with the quantity $(4/3)T_m$ replaced by $\langle \varepsilon \rangle$ which is the average energy of the center-of-mass neutron spectrum obtained by numerical integration (see Ref. [15]).

Equation (10) can be evaluated easily on any modern computer with a scientific program library. Similarly, Eq. (13) can be numerically integrated by a number of techniques; for example, Gaussian quadrature is used in Refs. [12-16].
The initial average fragment excitation energy $\langle E^* \rangle$ and the maximum temperature T_m are related by the Fermi-gas law

$$T_m = (\langle E^* \rangle/a)^{1/2} \tag{14}$$

where a is the nuclear level-density parameter. The average excitation energy is obtained from

$$\langle E^* \rangle = \langle E_r \rangle + B_n + E_n - \langle E_f^{tot} \rangle \ , \tag{15}$$

where $<E_r>$ is the average energy release given by the difference between the ground-state mass of the fissioning compound nucleus and the ground-state masses of the two fission fragments, B_n and E_n are the separation energy and kinetic energy of the neutron inducing fission, and $<E_f^{tot}>$ is the total average fission-fragment kinetic energy. T_m^f is obtained by substitution of Eq. (15) into Eq. (14).

The quantities $<E_r>$ of Eq. (15) and $<S_n>$ of Eq. (12) must be carefully calculated by averaging over the peaks of the fragment mass distribution [15]. The remaining quantities in the two equations together with E_f^L and E_f^H can be obtained directly from experiment or empirically based formulas [13,15, 18, 19].

discussion

Expressions for the Maxwellian and Watt temperatures T_M and T_W in terms of the above physical quantities are obtained by equating the average energies of the two distributions to that of the exact calculation. In the σ_c = constant case, using Eqs. (3) and (11), one obtains

$$T_M = \frac{1}{3}[E_f^L + E_f^H] + (8/9)T_m ,\tag{16}$$

while use of Eqs. (8) and (11) yields

$$T_W = (8/9)T_m ,\tag{17}$$

where T_m is given by Eqs. (14) and (15). Going one step further, a quadratic relation between T_m and $\bar{\nu}_p$ is obtained by substitution of Eq. (14) into Eq. (12) yielding

$$T_m = (2\bar{\nu}_p/3a)$$
$$+ \sqrt{(2\bar{\nu}_p/3a)^2 + (\bar{\nu}_p<S_n> + <E_\gamma^{tot}>)/a} ,\tag{18}$$

which can be used in Eqs. (16) and (17), respectively, to obtain T_M and T_W in terms of $\bar{\nu}_p$. The well-known expression due to Terrell [7] given by Eq. (1) is obtained in the limit that the first term in the square-root expression is negligible compared to the second and that $<S_n> \cong <E_f^{tot}>$. Substitution of the approximate T_m into Eq. (16) and multiplying by (3/2) gives Eq. (1).

The prompt fission neutron spectrum for the fission of ^{235}U induced by 0.53-MeV neutrons is shown in Fig. 1 for the present calculation, where σ_c is assumed constant, given by Eqs. (9) and (10), for the Maxwellian distribution given by Eq. (2), and for the Watt distribution given by Eq. (7). The average energies of the Maxwellian and Watt distributions are identical to that of the exact calculation by construction using Eqs. (16) and (17). In Fig. 2 where the ratios of these two approximations to the exact calculation are plotted, the Watt spectrum is accurate to within ~5% for laboratory neutron energies below ~7 MeV, but for higher energies is less than the exact calculation because T_W is less than the maximum temperature T_m. In fitting experimental fission neutron spectra to the Watt distribution, T_W is usually increased and E_f decreased to somewhat unphysical values, in order to simultaneously optimize the fit at intermediate and higher energies where most of the data exist [6]. The Maxwellian spectrum is a less accurate approximation, especially at high energy because T_M is substantially greater than T_m. In fitting experimental spectra to the Maxwellian distribution, T_M is usually decreased in order to preserve the fit at high energy [6,20,21]. This simultaneously increases the spectrum somewhat at lower energies because of the normalization.

The present calculation predicts a definite dependence of the prompt fission neutron spectrum (and $\bar{\nu}_p$) upon both the fissioning nucleus and the incident energy of the neutron inducing fission. Figure 3 shows the changes in the spectrum, at both low and high energy, as the charge and mass of the fissioning nucleus increases, for thermal-neutron induced fission. Figure 4 shows the dependence of the spectrum upon the incident neutron energy, for the first-chance fission of ^{235}U.

Figures 5 and 6 show comparisons of the present calculations, for the two cases of σ_c = constant and $\sigma_c(\varepsilon)$ calculated using the optical model, with the experimental data of Johansson and Holmqvist [6]. The optical-model parameters of Becchetti and Greenlees [22] are used for reasons given in Ref. [15]. In Fig. 6 it is apparent that the energy-dependent cross section calculation has introduced some structure into the spectrum and has softened the high-energy portion. It is clear that the calculation performed with the energy-dependent $\sigma_c(\varepsilon)$ is more exact than the calculation performed with σ_c = constant. The same effect and the same conclusion is obtained in a comparison to the experimental data of Boldeman [20] for the spontaneous fission of ^{252}Cf, shown in Fig. 7. The calculations shown in Figs. 5-7, together with those in Figs. 1-4 discussed above, have all been performed assuming a nuclear level-density parameter a in Eq. (14) given by

$$a = A/(11 \text{ MeV}) , \tag{19}$$

where A is the mass number of the fissioning compound nucleus (see Ref. [15]).

A final note of this discussion is that the σ_c = constant calculation given by Eqs. (9) and (10) is much simpler, with respect to both computing time and coding time, than is the optical-model $\sigma_c(\varepsilon)$ calculation given by Eqs. (9) and (13). The question arises as to whether the energy dependence of the compound-nucleus formation cross section $\sigma_c(\varepsilon)$ can be simulated. An approximate solution is found by a slight readjustment of the level-density parameter from the value given by Eq. (19) to the value

$$a_{eff} = A/(10 \text{ MeV}) . \tag{20}$$

A comparison of Figs. 5 and 8, which differ only in the choice of the level-density parameter for the σ_c = constant calculations given by the dashed curves, indicates that the approximation is reasonably good.

C. Multiple-chance fission. At high incident neutron energy E_n multiple-chance fission processes (n,xnf) occur in which x neutrons are sequentially evaporated prior to fission where x = 0,1,2, ... In this circumstance the total prompt fission neutron spectrum is comprised of evaporation-spectrum terms and pure fission-neutron spectrum terms depending upon the magnitude of E_n. If $E_n \sim 7$ MeV first- and second-chance fission occur whereas if $E_n \sim 14$ MeV up to third-chance fission is possible. The total prompt fission neutron spectrum where first-, second-, and third-chance fission are energetically possible is given by

$$N(E) = \{P_1 \bar{\nu}_1 N_1(E) + P_2 [\phi_1(E) + \bar{\nu}_2 N_2(E)]$$

$$+ P_3 [\phi_1(E) + \phi_2(E) + \bar{\nu}_3 N_3(E)]\}/\{P_1 \bar{\nu}_1$$

$$+ P_2 (1 + \bar{\nu}_2) + P_3 (2 + \bar{\nu}_3)\} . \tag{21}$$

The average prompt neutron multiplicity, as a function of the incident neutron energy E_n, where first-, second-, and third-chance fission become energetically possible as E_n increases, is given by

$$\bar{\nu}(E_n) = \{P_1(E_n)\bar{\nu}_1(E_n) + P_2(E_n)[1 + \bar{\nu}_2(E_n)]$$

$$+ P_3(E_n)[2 + \bar{\nu}_3(E_n)]\}/\{P_1(E_n)$$

$$+ P_2(E_n) + P_3(E_n)\} . \qquad (22)$$

In these two expressions P_m, N_m, and $\bar{\nu}_m$ are the fission probability, pure fission neutron spectrum, and average prompt neutron multiplicity, respectively, for m'th chance fission whereas ϕ_m is the evaporation spectrum for the m'th evaporation neutron.

A method to calculate the fission probabilities is developed and used in Ref. [15].

Figures 9 and 10 illustrate the influence of multiple-chance fission processes on the prompt fission neutron spectrum. The curve labeled "σ_c = Constant" is calculated using Eqs. (9) and (10) under the assumption of first-chance fission only. The same is true for the curve labeled "$\sigma_c(\varepsilon)$ First-chance fission" except that Eqs. (9) and (13) are used. The curve labeled "$\sigma_c(\varepsilon)$ Multiple-chance fission" is calculated using Eqs. (4), (9), (13), and (21). Figure 9 shows how the high energy tail of the spectrum softens and the evaporation-neutron peak appears as multiple-chance fission processes are switched on. In Fig. 10 the evaporation-neutron peak is seen more clearly as a ~1-2 MeV wide peak centered at ~0.5 MeV.

IV. PROMPT FISSION NEUTRON SPECTRUM RECOMMENDATIONS

General recommendations for evaluating the prompt fission neutron spectrum depending upon the amount of quality experimental data available have been given at the end of Sec. II. More specific recommendations as a consequence of the developments outlined in Sec. III are given here.

A. Least-squares fitting of experimental prompt fission neutron spectra. The recommended expressions to use in fitting procedures are given in decreasing order of physical content:

1. The prompt fission neutron spectrum $N(E)$ for $\sigma_c(\varepsilon) =$ constant given by Eqs. (9) and (10). The three fitting parameters are E_f^l, E_f^H, and T_m.
2. The Watt distribution $N_W(E)$ given by Eq. (7). The two fitting parameters are E_f and T_W.
3. The Maxwellian distribution $N_M(E)$ given by Eq. (2). The single fitting parameter is T_M.

If multiple-chance fission spectrum data are fit, a combination f $N(E)$ terms and neutron evaporation terms $\phi(E)$ must in principle be included in the fitting expression according to Eq. (21).

If extracted T_m, T_w, or T_M values are themselves parameterized in terms of the incident neutron energy E_n or $\bar{\nu}_p$, it is recommended that the dependencies follow those given in Eqs. (14) through (18).

B. Direct calculation of prompt fission neutron spectra. The recommended expressions to use in calculating prompt fission neutron spectra are given in decreasing order of physical content:

1. The prompt fission neutron spectrum $N(E)$ for $\sigma_c(\varepsilon)$ calculated with the optical model and given by Eqs. (9), (13), (14), and (19).
2. The prompt fission neutron spectrum $N(E)$ for $\sigma_c(\varepsilon) = $ constant given by Eqs. (9), (10), (14), and (20).
3. The Watt distribution $N_W(E)$ given by Eqs. (7), (14), (17), and (20). Note that Eq. (18) can be used in place of Eq. (14).
4. The Maxwellian distribution $N_M(E)$ given by Eqs. (2), (14), (16), and (20). Note that Eq. (18) can be used in place of Eq. (14)

Equation (21) should be used when calculating multiple-chance fission neutron spectra. Equation (4) should be used for energy-dependent $\sigma_c(\varepsilon)$ calculations and Eq. (5) should be used for $\sigma_c = $ constant calculations.

V. METHODS TO EVALUATE THE AVERAGE PROMPT FISSION NEUTRON MULTIPLICITY $\bar{\nu}_p$

A number of methods exist by which a representation of the average prompt fission neutron multiplicity $\bar{\nu}_p$ can be obtained from experimental data, theoretical calculation, or a combination of the two. These methods include the following:

A. Direct use of experimental data The experimentalist usually gives $\bar{\nu}_p$ as a function of the incident energy E_n of the neutron inducing fission. A relative measurement is usually performed by which $\bar{\nu}_p$ for the isotope of interest is measured relative to that for some standard reaction such as the spontaneous fission of ^{252}Cf. Accordingly, care must be exercised in the use of experimental $\bar{\nu}_p$-ratio sets from diverse sources because different standard reactions may have been used or the accepted value of $\bar{\nu}_p$ for a common standard may have changed with time.

The ENDF MF=1 LNP=2 law (Tabulated pairs) can be used to tabulate experimental $\bar{\nu}_p$ values directly, as a function of E_n.

B. Use of experimental data and systematics to determine parameters of models which approximate $\bar{\nu}_p$. It is well known experimentally [3] that $\bar{\nu}_p$ varies approximately linearly with the incident neutron energy E_n. The simplest approach of all, therefore, is to fit the experimental data for a given isotope to the linear expression

$$\bar{\nu}_p(E_n) = b + cE_n \qquad (23)$$

by the method of least-squares, where b and c are the parameters to be determined. This approach has been wisely used, a good example being that of Soleilhac [23]. The ENDF MF=1 LNP=1 law (Polynomial representation) can be used to represent $\bar{\nu}_p$ as a polynomial in E_n up to third degree. Note that use of quadratic and cubic terms in this approach can yield unphysical results when extrapolating the fit to high E_n values where, in many instances, little or no experimental data exist. However, a careful and extensive study of the polynomial representation of $\bar{\nu}_p(E_n)$ by least-squares analysis has been performed by Manero and Konshin [3] in which, for some cases, fifth-degree terms were statistically significant. The theoretical energy dependence of $\bar{\nu}_p$ is obtained from Eqs. (12), (14), and (15) and is of the form

$$\bar{\nu}_p(E_n) = (d+E_n)/(f+g\sqrt{h+E_n}) \qquad (24)$$

where d, f, g, and h are approximately constant with E_n [15] The energy-dependence of Eq. (24) is dominated by the linear term of the numerator, but is modified to turn slightly downward with increasing E_n due to the energy-dependent term of the denominator.

Much attention has been given to the determination of the parameters b and c of Eq. (23) by a study of the systematic behavior of $\bar{\nu}_p$ in actinide and trans-actinide nuclei [3]. In particular, Gordeeva and Smirenkin [24] determined a linear expression for b in terms of A and Z of the fissioning nucleus. Their expression, valid for thermal-neutron-induced fission, ultimately proved to be accurate to within ~8-9% [3]. Similarly, Ping-Shin Tu and Prince [25] found that b could be described in terms of Z^2/A with an accuracy of ~10%.

Howerton [26], in a study of the systematics of neutron-induced fission for incident neutron energies ranging from thermal to ~6 MeV determined expressions for both b and c of Eq. (23). The parameter b is described in terms of A and Z of the target nucleus and a quantity E_{Th}. The parameter c is expressed in terms of A. When E_{Th} is optimally adjusted to fit the $\bar{\nu}_p(E_n)$ data of a given isotope the overall agreement is better than ~5% for the data of that isotope. In this approach

E_{Th} simply shifts the zero-energy intercept of Eq. (23) to the optimal value. Obtaining, in this way, a set of E_{Th} values for the $\bar{\nu}_p(E_n)$ data of a set of actinide nuclei, overall agreement is obtained to within ~5% for the entire set of experimental data. The results obtained in Ref. [26] are therefore useful in representing the experimental $\bar{\nu}_p(E_n)$ data that were used to obtain those results.

C. Theoretical Calculation of $\bar{\nu}$. A new theoretical calculation of $\bar{\nu}_p$ exists based upon standard nuclear-evaporation theory. A discussion of the calculations [11-16] and presentation of the results has been given in Sec. III.B and III.C. In summary: $\bar{\nu}_p(E_n)$ is obtained using experimentally known or calculated quantities as input. Calculations of $\bar{\nu}_p(E_n)$ are performed for two different assumptions concerning the cross section $\sigma_c(\varepsilon)$ for the inverse process of compound-nucleus formation. In the case σ_c = constant, $\bar{\nu}_p(E_n)$ is given by Eqs. (12), (14), (15), and (20). In the case $\sigma_c(\varepsilon)$ is calculated using the optical model, $\bar{\nu}_p(E_n)$ is given by Eq. (12) with $(4/3)T_m$ replaced by $<\varepsilon>$, and Eqs. (14), (15), and (19). As shown in Ref. [15], either of these assumptions can be used for the calculation of $\bar{\nu}_p(E_n)$. The energy dependence of $\bar{\nu}_p(E_n)$ is given, approximately, by Eq. (24). When multiple-chance fission occurs Eq. (22) is used to calculate $\bar{\nu}_p(E_n)$. A calculation of $\bar{\nu}_p(E_n)$ is compared to experimental data in Fig. 11. The calculations were performed using the energy-dependent cross section assumption. In one case it is assumed that only first-chance fission occurs whereas in the other case first-, second-, and third-chance fission contributions are combined according to Eq. (22).

As in Sec. II, it is useful to consider the suitability of the methods A, B, and C as a function of the amount of quality experimental data available to the evaluator. In the case of abundant experimental data the methods A and the least-squares fitting procedures of method B may be most suitable. Method C may serve as a guide. In the case of some experimental data the methods B and C may be most suitable. If both are used, overlap calculations are required. In the case of no experimental data method C is preferred.

VI. RECOMMENDATIONS FOR $\bar{\nu}_p$

General recommendations for evaluating $\bar{\nu}_p(E_n)$ as a function of the amount of quality experimental data available have just been given at the end of Sec. V. More specific recommendations are given here.

A. Least-squares fitting of experimental $\bar{\nu}_p(E_n)$ data. The recommended expressions to use in fitting procedures are given in decreasing order of physical content:

1. The expression for $\bar{v}_p(E_n)$ given by Eq. (12). See Eq. (24) for a parametric form.
2. The expression for $\bar{v}_p(E_n)$ given by Eq. (23).

B. Direct calculation of $\bar{v}_p(E_n)$. The recommended expressions to use in calculating $\bar{v}_p(E_n)$ are given in decreasing order of physical content:

1. The expression for $\bar{v}_p(E_n)$ given by Eq. (12) with $(4/3)T_m$ replaced by $<\varepsilon>$, and Eqs. (14), (15), and (19).
2. The expression for $\bar{v}_p(E_n)$ given by Eqs. (12), (14), (15), and (20).
3. The expression for $\bar{v}_p(E_n)$ given by Howerton [26].

Equation (22) is used to calculate $\bar{v}_p(E_n)$ in the multiple-chance fission region.

VII. SUMMARY

General recommendations on the evaluation of the prompt fission neutron spectrum N(E) and the average prompt neutron multiplicity $\bar{v}_p$ as a function of the amount of quality data available have been given at the ends of Secs. II and V, respectively. Specific recommendations with respect to least-squares fitting procedures and direct calculation of N(E) and $\bar{v}$ have been given in Secs. IV and VI, respectively, where the available options are listed in decreasing order of physical content. Recommendations have been given for the evaluation of N(E) and $\bar{v}_p$ at high incident neutron energy where multiple-chance fission processes occur. All of the recommendations given in this work have been made from the perspective of the most accurate physical representation of N(E) and $\bar{v}_p$. In actual practice, however, the evaluator must weigh these recommendations against the other constraints of his task.

A new calculation of N(E) and $\bar{v}_p$ based upon standard nuclear-evaporation theory has been outlined and shown to yield good results in the prediction of N(E) and $\bar{v}_p$ for high- as well as low-excitation fission. The theory has demonstrated the dependence of N(E) and $\bar{v}_p$ upon fissioning nucleus and incident neutron energy. It has been shown by derived relationships that N(E) and $\bar{v}_p$ should be calculated and evaluated simultaneously.

In conclusion, a survey was made of the forty ENDF/B-V actinide and trans-actinide evaluations having MF=1 and MF=5 $\bar{v}$ and N(E) files. The intent was to gather statistics on the methods used to evaluate N(E) and $\bar{v}_p$. The results of the survey are given in Tables I and II, which are self-explanatory. Some noteworthy comments are the following. In Table I (C) for the statistics of the total fission neutron spectrum (MT=18) it is seen that in 35 of 40 cases the Maxwellian distribution is used. In 16 of the 35 cases a single Maxwellian temperature represents the complete energy dependence. Moreover, in 15 of these 16 cases, the single Maxwellian temperature has the same value, namely, T_M = 1.33 MeV. This constitutes an unphysical

description of N(E) for the 15 cases in that the dependence of N(E)
upon fissioning nucleus and incident neutron energy is ignored.
In Table II(B) it is seen that only in 8 cases out of 40 is a dis-
tinction made between the total and prompt $\bar{\nu}$. Other over-simplifi-
cations in the description of N(E) for multiple-chance fission pro-
cesses can be seen in Table I. The two tables illustrate that much
work can be done to improve the physical descriptions of N(E) and
$\bar{\nu}_p$ in future work.

ACKNOWLEDGMENTS

REFERENCES

1. Prompt Fission Neutron Spectra, Proceedings of a Consultants'
    Meeting on Prompt Fission Neutron Spectra in Vienna, 25-27
    August, 1971. International Atomic Energy Agency, Vienna
    (1972).

2. B. H. ARMITAGE and M. G. SOWERBY, EDS. Inelastic Scattering
    and Fission Neutron Spectra, Proceedings of a Specialist
    Meeting Sponsored by the Joint Euratom Nuclear Data and
    Reactor Physics Committee at Harwell, 14-16 April, 1975.
    AERE-R-8636/NEANDC (UK) 170L/NEACRP L176. AERE HARWELL (1977).

3. F. MANERO and V. A. KONSHIN, "Status of the Energy-dependent
    $\bar{\nu}$-Values for the Heavy Isotopes (Z > 90) from Thermal to 15
    MeV and of $\bar{\nu}$-Values for Spontaneous Fission," At. Energy Rev.
    10, 637 (1972).

4. V. WEISSKOPF, "Statistics and Nuclear Reactions," Phys. Rev.
    52, 295 (1937).

5. B. E. WATT, "Energy Spectrum of Neutrons from Thermal Fission
    of U^{235}," Phys. Rev. 87, 1037 (1952).

6. P. I. JOHANSSON and B. HOLMQVIST, "An Experimental Study of the
    Prompt Fission Neutron Spectrum Induced by 0.5-MeV Neutrons
    Incident on Uranium-235," Nucl. Sci. Eng. 62, 695 (1977).

7. J. TERRELL, "Fission Neutron Spectra and Nuclear Temperatures,"
    Phys. Rev. 113, 527 (1959).

8. J. TERRELL, "Prompt Neutrons from Fission," in Proceedings of
    the Symposium on Physics and Chemistry of Fission, Salzburg,
    22-26 March 1965, International Atomic Energy Agency, Vienna
    (1965) Vol. II p. 3.

9. J. C. BROWNE and F. S. DIETRICH, "Hauser-Feshbach calculation
    of the ^{252}Cf spontaneous-fission neutron spectrum," Phys. Rev.
    C10, 2545 (1974).

10. F. S. DIETRICH and J. C. BROWNE, "Hauser-Feshbach Calculation
    of the Fission Neutron Spectrum," Trans. Am. Nucl. Soc. 32,
    728 (1979).

11. D. G. MADLAND and J. R. NIX, "Calculation of Prompt Fission
    Neutron Spectra," Trans. Am. Nucl. Soc. 32, 726 (1979).

12. D. G. MADLAND and J. R. NIX, "Calculation of Prompt Fission
    Neutron Spectra," Bull. Am. Phys. Soc. 24, 885 (1979).

13. D. G. MADLAND and J. R. NIX, "Calculation of Prompt Fission
    Neutron Spectra," in Proceedings of the International Conference
    on Nuclear Cross Sections for Technology, Knoxville, Tennessee,
    October 22-26, 1979, to be published.

14. D. G. MADLAND and J. R. NIX, "Calculation of Neutron Spectra
    and Average Neutron Multiplicities from Fission," in Contribu-
    tions to the International Conference on Nuclear Physics,
    Berkeley, California, August 24-30, 1980, to be published.

15. D. G. MADLAND and J. R. NIX, "New Calculation of Prompt
    Fission Neutron Spectra and Average Neutron Multiplicities,"
    (in preparation).

16. D. G. MADLAND, "FISPEK: A Program to Calculate Prompt Fission
    Neutron Spectra and Average Neutron Multiplicities," (in
    preparation).

17. M. ABRAMOWITZ and I. A. STEGUN, EDS. Handbook of Mathematical
    Functions, National Bureau of Standards, Washington, D.C.
    (1964).

18. J. P. UNIK et al., "Fragment Mass and Kinetic Energy Distri-
    butions for Fissioning Systems Ranging from Mass 230 to 256,"
    in Proceedings of the Third IAEA Symposium on the Physics
    and Chemistry of Fission, Rochester, New York, August 13-17,
    1973, Vol. II, p. 19, International Atomic Energy Agency,
    Vienna (1974).

19. D. C. HOFFMAN and M. M. HOFFMAN, "Post-Fission Phenomena," Ann.
    Rev. Nucl. Sci. 24, 151 (1974).

20. J. W. BOLDEMAN, D. CULLEY, and R. J. CAWLEY, "The Fission Neutron Spectrum from the Spontaneous Fission of ^{252}Cf," Trans. Am. Nucl. Soc. __32__, 733 (1979).

21. J. FREHAUT, A. BERTIN, and R. BOIS, "Fission Neutron Spectrum Measurements for Fast-Neutron-Induced Fission," Trans. Am. Nucl. Soc. __32__, 732 (1979).

22. F. D. BECCHETTI, JR. and G. W. GREENLESS, "Nucleon-Nucleus Optical-Model Parameters, A > 40, E < 50 MeV," Phys. Rev. __182__, 1190 (1969).

23. M. SOLEILHAC, J. FREHAUT, and J. GAURIAU, "Energy Dependence of $\bar{\nu}_p$ for Neutron-Induced Fission of ^{235}U, ^{238}U and ^{239}Pu from 1.3 to 15 MeV," J. Nucl. Energy __23__, 257 (1969).

24. L. D. GORDEEVA and G. N. SMIRENKIN, "An Empirical Formula for the Average Number of Fission Neutrons," At. Energ. __14__, 562 (1963).

25. PING-SHIN TU and A. PRINCE, "Correlation of the Most Probable Kinetic Energy of Fission Fragments and $\bar{\nu}_p$," J. Nucl. Energy __25__, 599 (1971).

26. R. J. HOWERTON, "$\bar{\nu}$ Revisited," Nucl. Sci. Eng. __62__, 438 (1977).

TABLE I

Statistics on the Fission Neutron Spectrum Files of
Forty ENDF/B-V Actinide and Trans-Actinide Evaluations

(A) Nuclide Mass Number and Charge Number Ranges

230 ≤ A ≤ 253   90 ≤ Z ≤ 98

(B) Distribution of Fission Neutron Spectrum Files According to
Total Fission and Multiple-chance Fission Components (MT=18
is total fission, MT=19 is first-chance fission, MT=20 is
second-chance fission, MT=21 is third-chance fission, and
MT=38 is fourth-chance fission)

File Types Included	Number of Cases
MF=5, MT=18	22
MF=5, MT=18,19	0
MF=5, MT=18,19,20	12
MF=5, MT=18,19,20,21	4
MF=5, MT=18,19,20,21,38	2
total number of cases	40

(C) Distribution of Fission Neutron Spectrum Representations Used
for MT=18 Files (Total Fission)

Representation	Number of Cases
Maxwellian spectrum (single temperature)	16
Maxwellian spectrum (array of temperatures)	19
energy-dependent Watt spectrum	5
total number of cases	40

(D) Distribution of Fission Neutron Spectrum Representations Used
for MT=19 Files (First-chance Fission)

Representation	Number of Cases
Maxwellian spectrum (single temperature)	12
Maxwellian spectrum (array of temperatures)	3
energy-dependent Watt spectrum	3
total number of cases	18

(E) Distribution of Fission Neutron Spectrum Representations Used
for MT=20 Files (Second-chance Fission)

Representation	Number of Cases
Maxwellian spectrum (single temperature)	12
Maxwellian spectrum (array of temperatures)	2
Maxwellian spectrum (array of temperatures) and evaporation spectrum (array of temperatures)	1
energy-dependent Watt spectrum and evaporation spectrum (array of temperatures)	3
total number of cases	18

(F) Distribution of Fission Neutron Spectrum Representations Used
for MT=21 Files (Third-chance Fission)

Representation	Number of Cases
Maxwellian spectrum (array of temperatures)	2
Maxwellian spectrum (array of temperatures) and evaporation spectrum (array of temperatures)	1
energy-dependent Watt spectrum and evaporation spectrum (array of temperatures)	2
energy-dependent Watt spectrum and two evaporation spectra (arrays of temperatures)	1
total number of cases	6

(G) Distribution of Fission Neutron Spectrum Representations Used
for MT=38 Files (Fourth-chance Fission)

Representation	Number of Cases
energy-dependent Watt spectrum and evaporation spectrum (array of temperatures)	1
energy-dependent Watt spectrum and three evaporation spectra (arrays of temperatures)	1
total number of cases	2

TABLE II

Statistics on the $\bar{\nu}$ Files of Forty ENDF/B-V
Actinide and Trans-Actinide Evaluations

(A) Nuclide Mass Number and Charge Number Ranges

   $230 \leq A \leq 253$ $90 \leq Z \leq 98$

(B) Distribution of $\bar{\nu}$ Files According to Total $(\bar{\nu}_t)$, Prompt $(\bar{\nu}_p)$, and Delayed $(\bar{\nu}_d)$ Components (MT=452 is $\bar{\nu}_T$, MT=456 is $\bar{\nu}_p$, and MT=455 is $\bar{\nu}_d$)

File Types Included	Number of Cases
MF=1, MT=452	32
MF=1, MT=452,456	1
MF=1, MT=452,456,455	7
total number of cases	40

(C) Distribution of $\bar{\nu}$ Representations Used for MT=452 Files $(\bar{\nu}_t)$

Representation	Number of Cases
linear	25
tabulation	15
total number of cases	40

(D) Distribution of $\bar{\nu}$ Representations Used for MT=456 Files $(\bar{\nu}_p)$

Representation	Number of Cases
linear	2
tabulation	6
total number of cases	8

(E) Distribution of $\bar{\nu}$ Representations Used for MT=455 Files $(\bar{\nu}_d)$

Representation	Number of Cases
tabulation	7
total number of cases	7
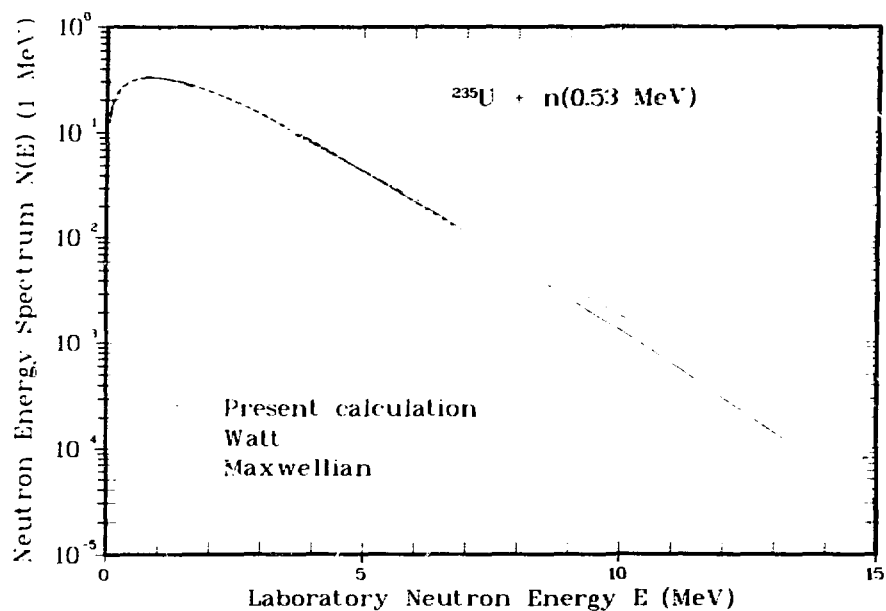
Fig. 1. Prompt fission neutron spectrum in the laboratory system for the fission of ^{235}U induced by 0.53-MeV neutrons. The solid curve gives the present spectrum calculated from Eqs. (9) and (10), the dashed curve gives the Watt spectrum calculated from Eq. (7), and the dot-dashed curve gives the Maxwellian spectrum calculated from Eq. (2). The values of the three constants appearing in the present spectrum are $E_f^L = 1.062$ MeV, $E_f^m = 0.499$ MeV, and $T_m = 1.019$ MeV, whereas those in the Watt spectrum are $E_f^m = 0.780$ MeV and $T_W = 0.905$ MeV. The value of the single constant appearing in the Maxwellian spectrum is $T_M = 1.426$ MeV. The mean laboratory neutron energies of the three spectra are identical.
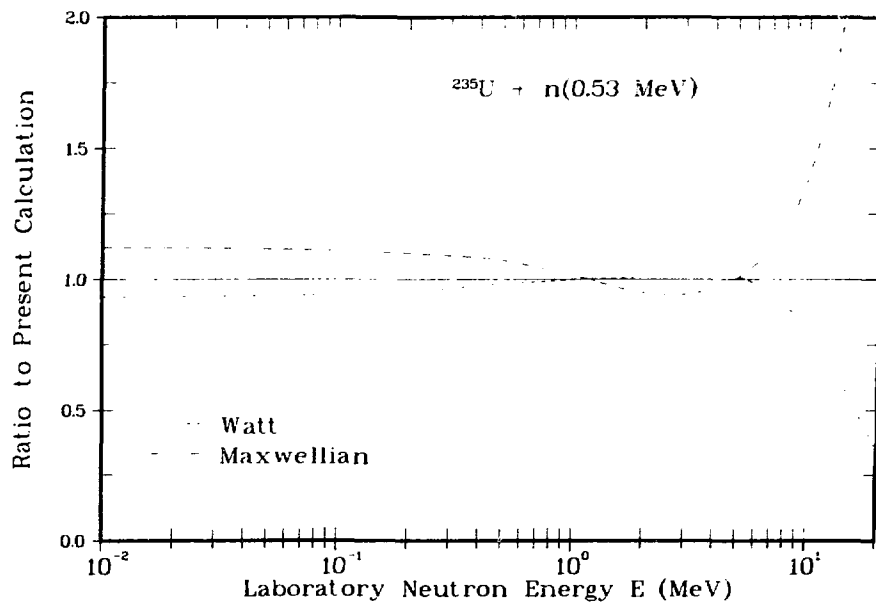
Fig. 2.   Ratio of the Watt spectrum and the Maxwellian spectrum to
          the present spectrum, corresponding to the curves shown in
          Fig. 1.
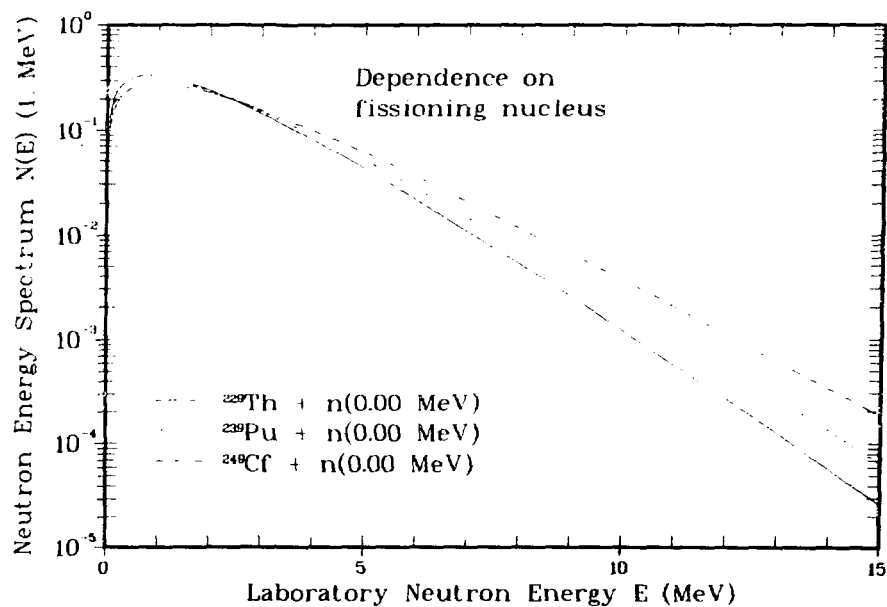
Fig. 3. Dependence of the prompt fission neutron spectrum upon the fissioning nucleus, for thermal-neutron-induced fission. The va.ues of the constants are $E_f^L = 1.106$ MeV, $E_f^H = 0.457$ MeV, and $T_m = 0.989$ MeV for ^{229}Th+n, are $E_f^L = 1.033$ MeV, $E_f^H = 0.527$ MeV, and $T_m = 1.124$ MeV for ^{239}Pu+n, and are $E_f^L = 0.995$ MeV, $E_f^H = 0.575$ MeV, and $T_m = 1.304$ MeV for ^{249}Cf+n.
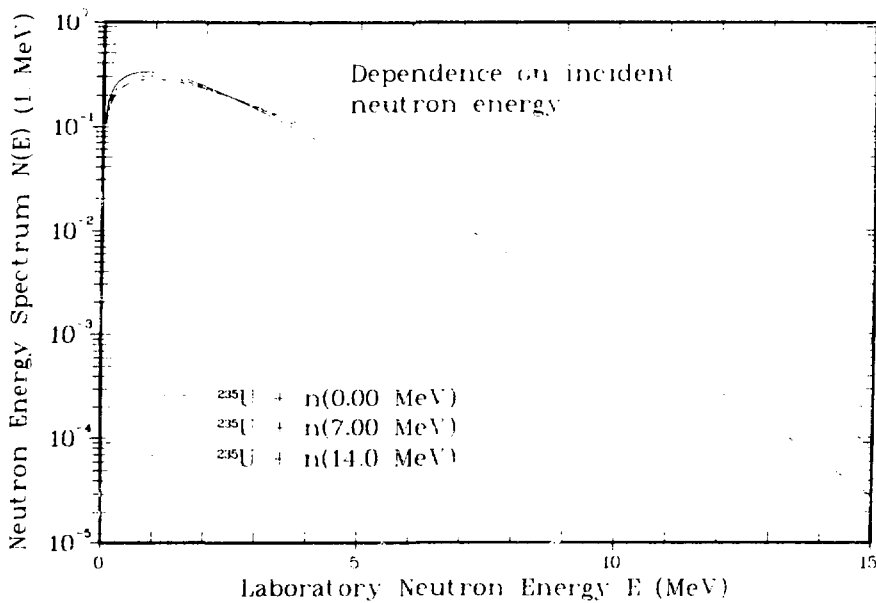
Fig. 4. Dependence of the prompt fission neutron spectrum upon the kinetic energy of the incident neutron, for the fission of ^{235}U. The maximum temperature T_m is 1.006 MeV when the incident neutron energy is 0 MeV, is 1.157 MeV when the incident neutron energy is 7 MeV, and is 1.290 MeV when the incident neutron energy is 14 MeV. The values of the average kinetic energy per nucleon are for each case held fixed at E_f^L = 1.062 MeV and E_f^H = 0.499 MeV. For the latter two cases, the spectra are calculated for first-chance fission only.
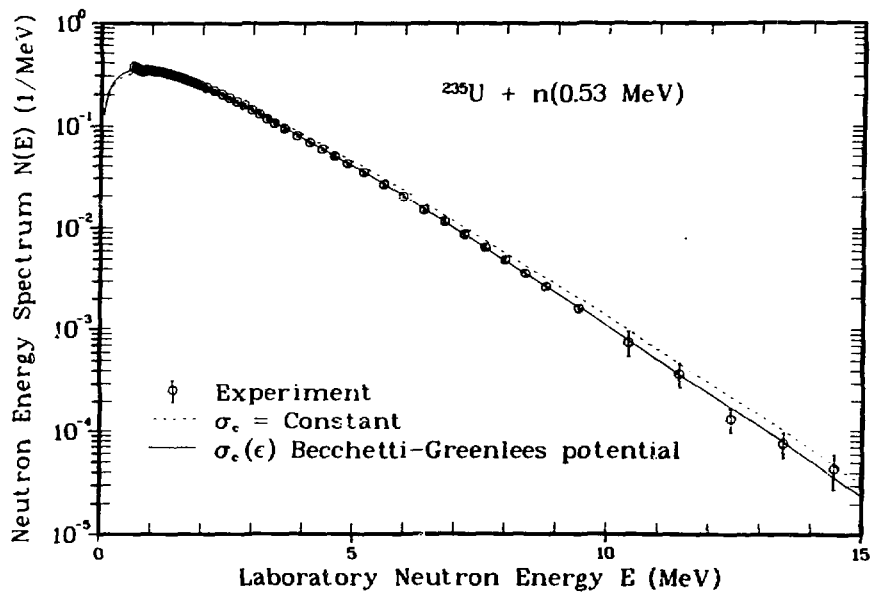
Fig. 5.   Prompt fission neutron spectrum in the laboratory system
for the fission of ^{235}U induced by 0.53-MeV neutrons.
The dashed curve gives the present spectrum calculated
from Eqs. (9) and (10) assuming a constant cross section
whereas the solid curve gives the present spectrum cal-
culated from Eqs. (9) and (13) using the optical-model
parameters of Becchetti and Greenless [22]. The values of
the three constants appearing in the calculated spectra
are in both cases E_f^I = 1.062 MeV, E_f^H = 0.499 MeV, and
T_m = 1.019 MeV. The experimental data are those of
Johansson and Holmqvist [6].
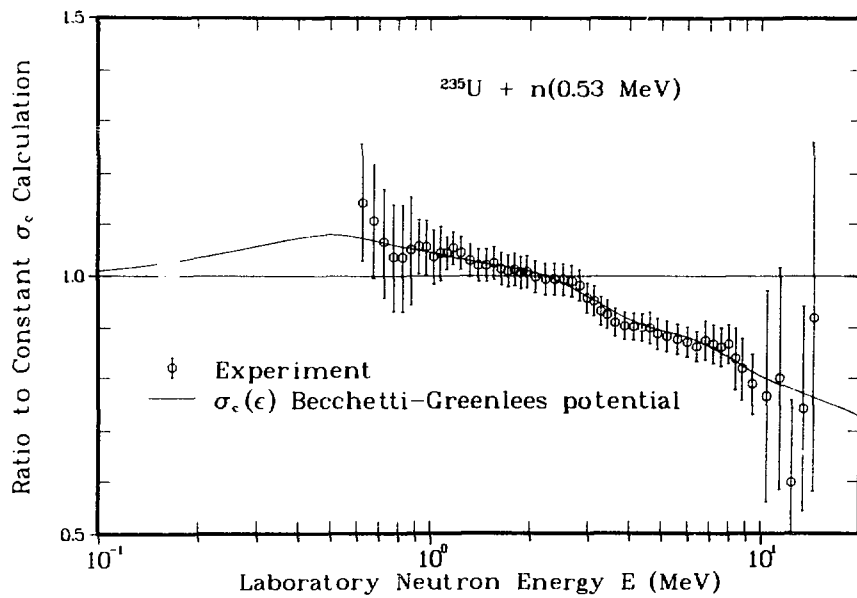
Fig. 6.   Ratio of the present spectrum calculated using the optical-
          model parameters of Becchetti and Greenless [22] and the
          experimental data of Johansson and Holmqvist [6] to the
          present spectrum calculated assuming a constant cross
          section, corresponding to the curves shown in Fig. 5.
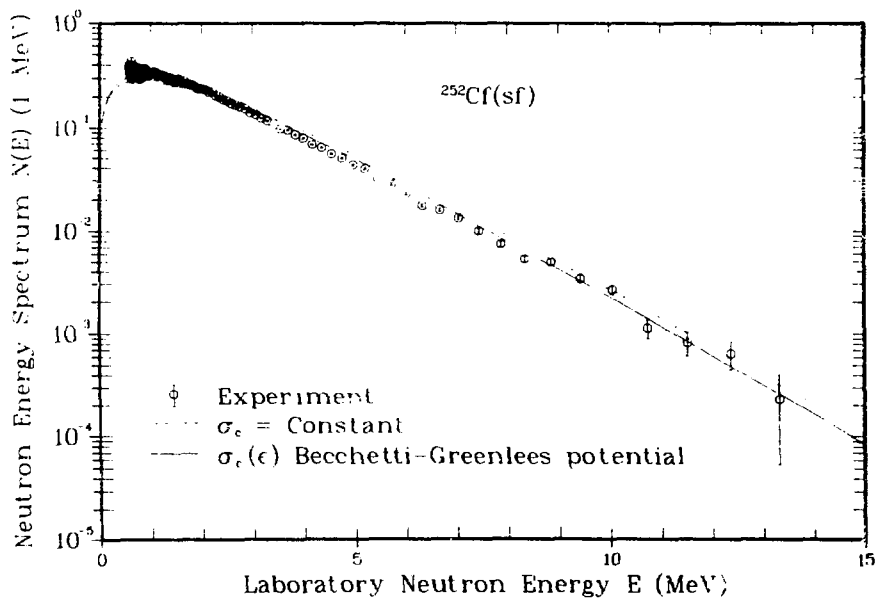
Fig. 7.　Prompt fission neutron spectrum for the spontaneous fission of ^{252}Cf. The dashed curve gives the present calculation calculated assuming a constant cross section whereas the solid curve gives the present calculation using the optical-model parameters of Becchetti and Greenless [22]. The values of the three constants appearing in the calculated spectra are in both cases E_f^L = 0.984 MeV, E_f^H = 0.553 MeV and T_m = 1.209 MeV. The experimental data are those of Boldeman et al [20].
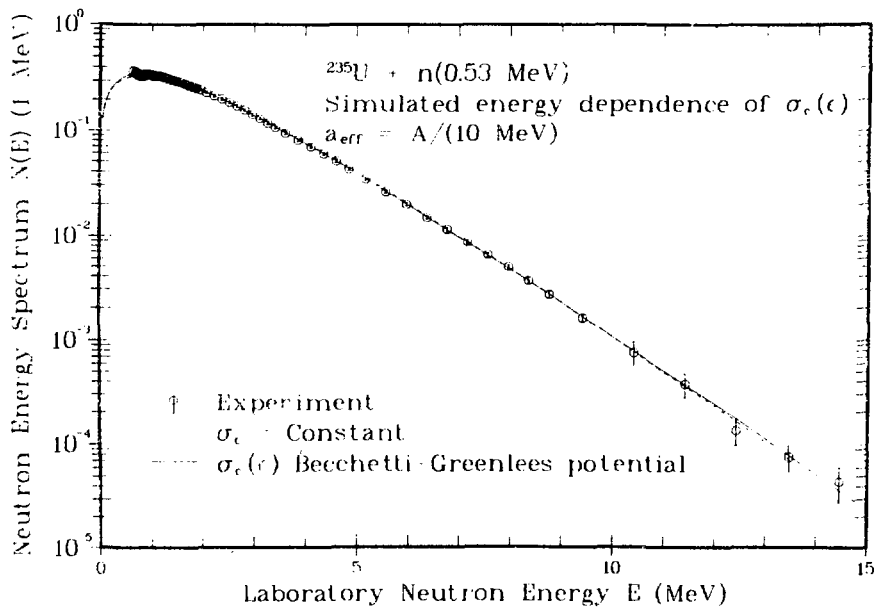
Fig. 8. Prompt fission neutron spectrum for the fission of ^{235}U
induced by 0.53-MeV neutrons illustrating the simulated
energy dependence of $\sigma_c(\varepsilon)$. The two calculated spectra
are in every respect identical to those of Fig. 5 except
that the level-density parameter used in the constant
cross section calculation, shown by the dashed curve, is
given by Eq. (20) instead of Eq. (19).
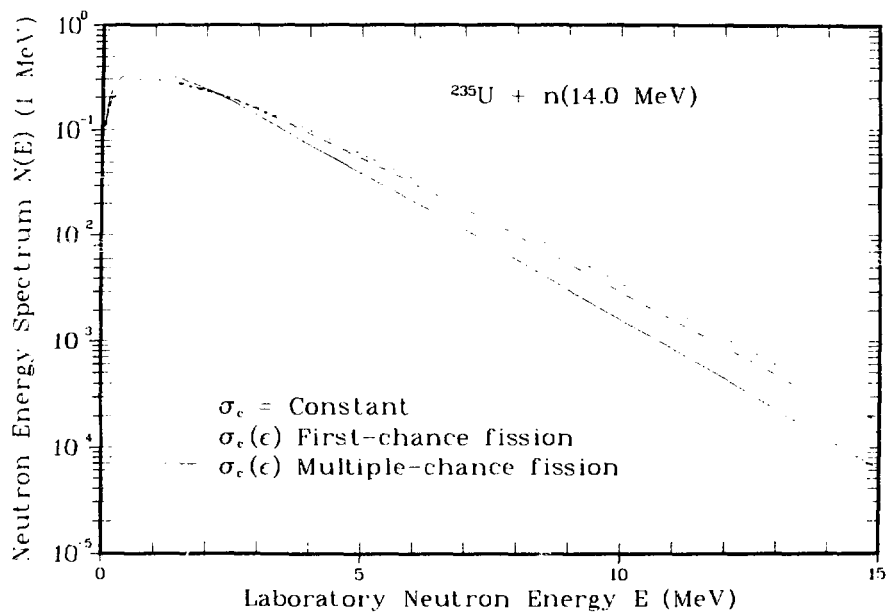
Fig. 9. Prompt fission neutron spectrum for the fission of ^{235}U induced by 14.0-MeV neutrons. The dashed and dot-dashed curves give th· present spectrum calculated for first-chance fission assuming, respectively, a constant cross section and an energy-dependent cross section calculated using the optical-model parameters of Becchetti and Greenless [22]. The solid curve gives the present spectrum calculated for first-, second-, and third-chance fission contributions using Eq. (21) and assuming an energy-dependent cross section calculated with the same optical potential. The values of the three constants appearing in the spectra for the first compound nucleus, ^{236}U, are E_f^L = 1.062 MeV, E_f^H = 0.499 MeV, and T_m = 1.290 MeV.

- 892 -
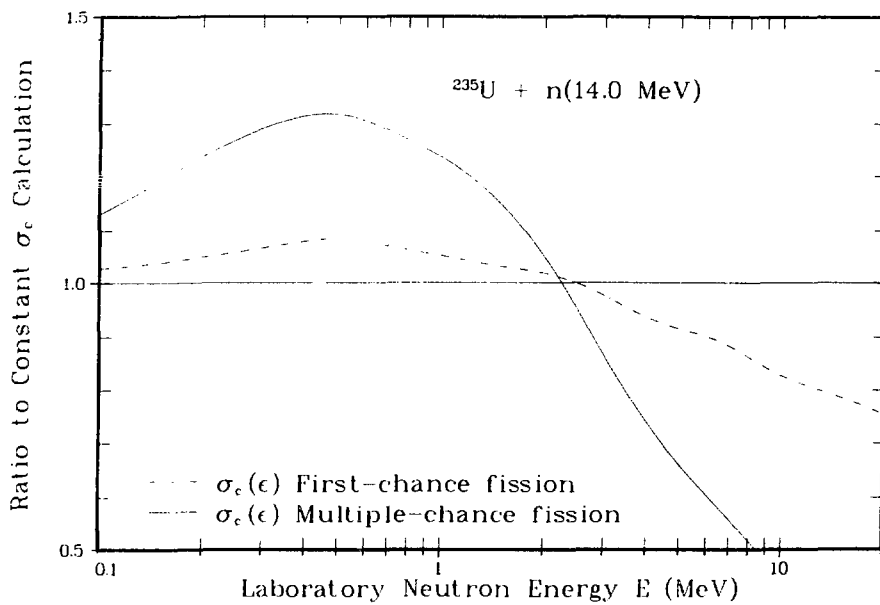
Fig. 10. Ratio of the present spectra calculated using energy-
          dependent cross sections and assuming either first-chance
          or multiple-chance fission to the present spectrum calcu-
          lated using a constant cross section and assuming first-
          chance fission, corresponding to the curves shown in
          Fig. 9.
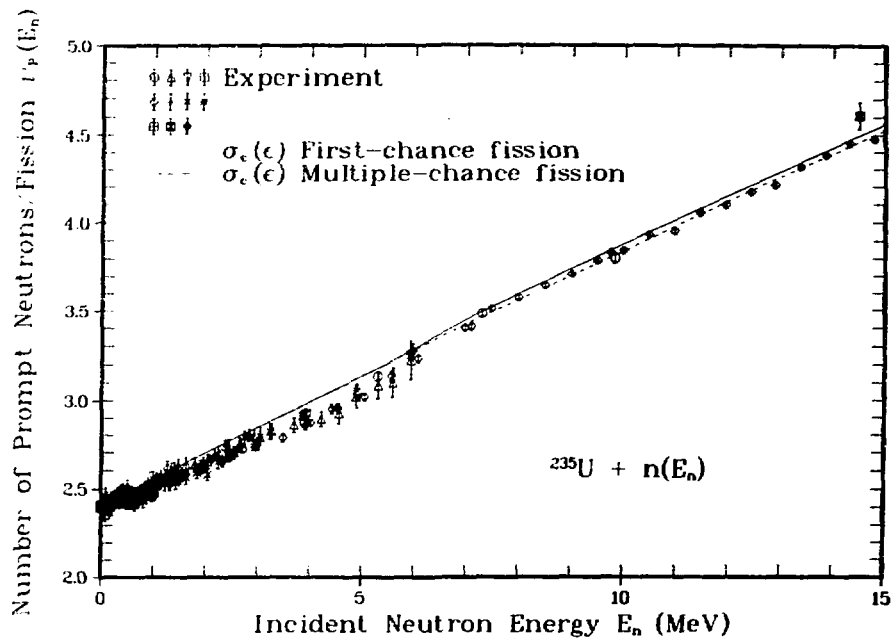
Fig. 11. Average prompt neutron multiplicity as a function of inci-
dent neutron energy for the neutron-induced fission of
235U. The dashed curve, for first-chance fission, is
calculated using Eq. (12), but replacing the term $(4/3)T_m$
with the corresponding quantity obtained by numerical in-
tegration in the energy-dependent cross section calcula-
tion. The solid curve, for first-, second-, and third-
chance fission contributions, is also calculated using
energy-dependent cross sections, but Eq. (22) is used.
The optical-model parameters of Becchetti and Greenless
[22] were used. The experimental data references are
compiled in Ref. [15].

Discussion

England

Dave's paper also includes a review of ν_p that is particularly important for the ENDF/B data. Unfortunatley he did not have sufficient time to cover this in his presentation today.

Sher

Do you take account of neutron-fragment angular distribution measurements in evaluating the prompt neutron spectra?

Madland

We have assumed that the emission of the neutrons in the center-of-mass system of a fission fragment is isotropic. It is true that we could include more physics and look at the angular dependence. That is something that is yet for us to do.

Sher

Measurements of the laboratory angular distribution, the ones that I am familiar with, are quite old and not very good and I wonder if there is any new information that you know about?

Madland

I'm sorry to say that most of the angular distribution information is in fact in the 60's, as far as I am aware, and some in the 50's.

Stewart

We know, of course, that the angular distributions of the fission fragments themselves are vey anisotropic and very mass dependent and you might be able to make some use of that. But the question that I wanted to ask was when you did treat second-chance fission did you include the (n,n') neutrons in your distribution? It did not look like it. If you put it in, too, and say that it is all due to the fission process it would tend to soften the spectrum even more, isn't that correct?

Madland

What we are trying to calculate, is any neutron that is in coincidence with the fission event and we call that a contribution to the fission neutron spectrum. The (n,n'), if you use the label (n,n'f) as a notation, that n' is the bump that you saw in the

transparency; however, in the context and limitations of the assumptions on which the entire model is based, namely the 1937 Weisskopf evaporation model, that n' is there, Lee; it is, however, represented in a very simple way, namely, the evaporation model. That's one of the advantages of the Hauser-Feshbach approach attempted by Brown and Dietrich. More specific detail on the evaporated neutrons would be included and that is one of the reasons I say that ultimately that their approach would probably be a more exact and maybe the very best way to calculate these spectra. In either case, however, there is softening of the high energy tail of the fission spectrum.

Stewart

Well, I was just suprised that your spectra looked so smooth but perhaps that was because it was on a 5 log scale.

Madland

Well, on a linear scale it's really quite a bump, but it will remain relatively smooth so long as the basis for the calculation is such a model as the evaporation model.

Peelle

It wasn't clear from the presentation whether you put in any information at all obtained from the fissioning material or whether all the information relates to the fission fragments. Is anything fitted? Did you put in the velocities?

Madland

I was unable to put down all the formalism but the excitation energy of the fission fragments, the distribution of that excitation energy, is in our distribution function. What we specify is the maximum temperature because we transform from an excitation energy distribution to a temperature distribution. That maximum temperature is calculated from the Q value from prompt fission, that is, the mass differences, together with the binding energy of the neutron when you make the compound nucleus; and substracted from it, of course, is the total fission fragment kinetic energy which is a measured quantity as you know. Those quantities are related to the compound nucleus that is fissioning only through the mass and charge of the compound nucleus. We do have some influence from the level density parameter for the compound system.

Peelle

I seem to recall discussion some years ago of something that was probably called the prescission neutron. Something like an evaporation but below the threshold for second chance fission.

Madland

Prescission neutron, or there is another word used which is scisston neutron, and a scission neutron one might refer to also as a component in the total description of all the ternary fiss'on products. Our feeling is that the prescission and scission neutron question has not yet been answered experimentally. We did not include those effects. There is a paper by Kapoor which estimates that the maximum effect is 10%. We did not include such a term in our calculation because, as I say, we don't think it has been completely experimentally verified at this time.

Takahaski

When you calculated these neutron spectra, did you take into account all of the competition between the neutron emission and gammas? Because when the fission fragment has a quite large angular momentum, then the gamma emission probability is much higher than it is for low angular momentum.

Madland

The total excitation energy of the fragments just at the scission point is dissipated by neutron emission and gamma emission, and we take into account of that gamma emission via the use of experimental measurements, which, if you are interested, are summarized in the article by Hoffman and Hoffman in Annual Reviews of Nuclear Science. So yes, we take account of that gamma emission. There is no angular momemtum in this calculation. We do take account of the total prompt gamma ray energy. We don't go into the detail of a cascade calculation of the number of those gammas or their distribution in numbers or the energies of those gammas, but we make use of the total prompt gamma ray energy which is of the order of 6 to 7 MeV, depending upon the nucleus that is fissioning.

Rowlands

A question of concern in fast reactor calculations is the low energy component of the fission spectrum below say 100 keV. Do you think that one can be confident of the shape of that component in this region, or is it necessary to make measurements? Do you have any comments on the Russina measurements which show structure in the fission spectrum?

Madland

First of all, with regard to the low energy shape of the spectrum, that's probably one of the primary reasons for which we went about this calculation and the reason for that of course is that in most of the measurements that we are aware of, the lower energy cut off where the experiment stops in secondary emitted energy is between 200 keV and 1 MeV. In most of the measurement techniques, what is involved with the experiemntal measurement in this region is a very steep gradient in the efficiency in the neutron detector. This puts huge error bars on the data. As to whether or not we have any confidence in the shape of our spectrum below 1 MeV, let me say I certainly have more confidence than in the circumstance where someone has taken and fit a Maxwellian distribution to an experimental measurement and has adjusted the temperature of the Maxwellian distribution to fit the tail, which is where the experimental data are, at the expense of raising the low energy end of the fitted spectrum. About the Russian measurements:; I know that we have a Cf-252 experiment from an IAEA report. We have not yet compared our calculation to that data; I wasn't too excited to do so because, if I recall correctly, it doesn't go out very far in secondary emitted neutron energy.

Schmidt

The Russian measurements have been withdrawn.

Stewart

The only other thing is that Frehaut would not bet Ray Nix a bottle of good French wine at the Atlanta meeting that those low energy neutrons that he observed at 600 keV, when he was bombarding with 600 keV, were real fission spectrum neutrons.

Madland

Perhaps he was willing to bet a bottle of good California wine.

METHODS AND PROCEDURES FOR EVALUATION OF
NEUTRON-INDUCED ACTIVATION CROSS SECTIONS

M. A. Gardner

Lawrence Livermore National Laboratory
Livermore, CA 94550, U.S.A.

ABSTRACT

One cannot expect measurements alone to supply all
of the neutron-induced activation cross section data
required by the fission reactor, fusion reactor, and
nuclear weapons development communities, given the wide
ranges of incident neutron energies, the great variety
of possible reaction types leading to activation, and
targets both stable and unstable. Therefore, the eval-
uator must look to nuclear model calculations and sys-
tematics to aid in fulfilling these cross section data
needs. This review presents some of the recent develop-
ments and improvements in the prediction of neutron
activation cross sections, with specific emphasis on
the use of empirical and semiempirical methods. Since
such systematics require much less nuclear information
as input and much less computational time than do the
multistep Hauser-Feshbach codes, they can often provide
certain cross section data at a sufficient level of
accuracy within a minimum amount of time. The cross
section information that these systematics can and can
not provide and those cases in which they can be used
most reliably are discussed.

INTRODUCTION

The needs of various segments of the nuclear community for
neutron activation cross-section libraries are well established
[1-4] and do not have to be elaborated on here. It is also ob-
vious that, given the wide ranges of incident neutron energies,
the great variety of possible reaction types leading to activation,
and targets, both stable and unstable, one cannot expect measure-
ments alone to supply all of the activation cross-section data
required. Therefore, the evaluator must look to nuclear model
calculations and systematics to aid in constructing the extensive,

broad-based activation cross-section libraries needed.

We already have heard a number of talks on cross-section cal-
culations that utilize various highly-developed nuclear models:
optical, Hauser-Feshbach statistical, precompound, and coupled-
channel. We have seen that these nuclear models used alone or in
combination, as appropriate, have the ability to predict cross sec-
tions for different neutron reactions very accurately by correctly
taking into account all the competing physics. We have also seen
that the power and performance of such calculational models is very
dependent on the quality of the nuclear information and parameters
that they require as input. I believe that most of us would agree
with O. N. Jarvis that "a valuable service to the activation com-
munity would be to provide multigroup cross sections for all nu-
clides and reactions relevant to activation calculations using a
modern nuclear model code" [4]. However, I think it is recognized
that this kind of undertaking is a very formidable one, when one
considers the input information, computational time, and manpower
required. In addition, it should be kept in mind that there are
situations either where the accuracy and detail of the activation
cross sections provided by the above nuclear model calculations are
not required, or where less accuracy in cross-section values can be
tolerated for the sake of saving computational time and manpower.

In this review, then, I would like to give specific emphasis
to the use of empirical and semiempirical methods in the prediction
of neutron activation cross sections. Since such systematics re-
quire much less nuclear information as input and much less computa-
tional time than do the multistep Hauser-Feshbach codes, they can
often provide certain cross-section data at a sufficient level of
accuracy within a minimum amount of time. Due to the time limita-
tions of this talk, I will only be able to discuss systematics for
obtaining cross sections for some of the more important activation
reactions: (n,2n), (n,p), and (n,α). And I will only be able to
cover some of the methods that have been developed through the
years, highlighting those systematics either that still appear to
be the most successful or that have been improved in the last
several years. I will try to give some perspective on the use of
these systematics: what kind of accuracies they do provide, in
what cases they can be used most reliably, and what cross-section
information they do not yield. In the last section of this review
I will discuss a method for the prediction of (n,γ) cross sections
that involves the use of gamma-ray strength function systematics
in Hauser-Feshbach statistical model calculations.

Before proceeding to separate discussions of the systematics
for the various neutron activation cross sections, I would like to
draw your attention to Fig. 1, which S. M. Qaim presented at the
1975 Washington Conference on Nuclear Cross Sections and Technology
[5]. It gives a very compact though approximate summary of the
relative contributions of the possible activation reactions for in-
cident 14-15 MeV neutrons and provides one with a "quick" estimate
of general cross-section trends.

(n,2n) CROSS SECTIONS

From the viewpoint of simple systematics, the cross section
for the (n,2n) reaction is, probably, the easiest to describe as a
function of incident neutron energy. The (n,2n) excitation func-
tion exhibits little structure, rising rapidly in a sigmoid shape
above its threshold, reaching a plateau value, and then dropping
off smoothly as other reactions begin to compete, the (n,3n) reac-
tion usually being the most important competitor. This evaluation
approach, therefore, only requires systematics that predict the
plateau cross section and an expression that describes the cross
section's smooth rise to and fall from that plateau. The cross
section at 14-15 MeV usually corresponds to that of the plateau
region, except where either the (n,2n) or (n,3n) threshold is only
a few MeV below 14 MeV.

The widely used empirical formula of Lu and Fink [6],

$$\sigma_{(n,2n)} = 61.6(A^{1/3} + 1)^2$$
$$\times \{1 - 1.319 \exp[-8.744(N - Z)/A]\} \text{ mb },$$

(1)

provides quick estimates of the (n,2n) cross section at 14.4 MeV,
and Lu and Fink state that this expression should predict values to
within ± 20% for stable nuclei from Z = 28 to 82, except for the
lightest stable isotope of even-Z elements. This expression, de-
rived from a least-squares fit to 29 (n,2n) cross sections that Lu
and Fink measured for targets ranging from ^{58}Ni to ^{142}Ce, repro-
duced most of the measurements to within ± 20%. Within the same
error limits, the equation, also reproduced most of the 25 (n,2n)
cross sections previously measured at their laboratory for nuclides
from ^{64}Zn to ^{204}Pb. The cross-section predictions falling outside
the stated error limits were ^{64}Zn, ^{74}Se, ^{78}Kr, ^{84}Sr, and ^{92}Mo; each
is the lightest stable isotope of an even-Z element and all have
high thresholds of ≥ 12 MeV. A Z range over which Lu and Fink did
not test their equation is Z = 60 - 77. I have made a comparison
of the predictions of Eq. 1 with (n,2n) cross-section measurements,
made at 14.76 MeV by Frehaut [7], for 19 isotopes of Nd_{60}, Sm_{62},
Eu_{63}, Gd_{64}, and W_{74} and the results are shown in Fig. 2. The
agreement between the experimental values and the empirically-pre-
dicted ones is quite good, with most of the measured values being
reproduced to ± 10% or better. All of these (n,2n) reactions have
thresholds 5-7 MeV below the 14-15 MeV region, and most of the
(n,3n) thresholds for these nuclides are less than 1 MeV below the
14-MeV region.

Another means of obtaining rough estimates of the (n,2n) cross
section in the 14-15 MeV region is the use of the graphical system-
atics of Qaim [8], as shown in Fig. 3. Using an extensive data
base of measurements from a large number of laboratories and strin-
gent criteria regarding the quality of the (n,2n) values chosen for

the systematics study, Qaim plotted the (n,2n) cross sections as a function of the asymmetry parameter, (N - Z)/A, and obtained the smooth trend as shown. Qaim states that his arbitrarily drawn band has a half-width in the flat portion (for (N - Z)/A values $\geq$ 0.1) that corresponds to a deviation from the mean of about 20% and in the rising part (for (N - Z)/A values < 0.1) that corresponds to a 40% deviation from the mean. He further points out that the predicted values from his curve generally agree with those obtained using the empirical expression of Lu and Fink.

A further improvement to the graphical systematics of Qaim was presented by Sigg and Kuroda [9] and is shown in Fig. 4. Here plotted as a function of the asymmetry parameter is the quantity: $\sigma \epsilon / (A^{1/3} + 1)^2$. This quantity represents an attempt to correct the (n,2n) cross section for nuclear radius and reaction energy (E_{RXN} = E_n - $E_{threshold}$) differences for the same value of the asymmetry parameter. By dividing each (n,2n) cross section by $(A^{1/3} + 1)^2$, Sigg and Kuroda referred all data to the same nuclear radius and significantly reduced the scatter in the (n,2n) data shown in Fig. 3. They further attempted to reduce the scatter for nuclei with (N - Z)/A values of < 0.12 by making a crude correction for variations in the reaction energy for a given value of the asymmetry parameter. First, they assumed that the (n,2n) excitation function increases in an approximately linear manner for the first few MeV above the threshold energy. Then, they carried out a least-squares fit of the variation of the (n,2n) threshold energy with (N - Z)/A and obtained

$$\log E'_{thres} = -1.3094 \left(\frac{N - Z}{A} \right) + 1.1712 \tag{2}$$

where E'_{thres} (MeV) is the least-square value of the threshold energy and E'_{RXN} = E_n - E_{thres} may be defined. For nuclides having E_{RXN} < 4 MeV, they multiplied the (n,2n) cross section by the factor ϵ = E'_{RXN}/E_{RXN}. For nuclides with E_{RXN} $\geq$ 4 MeV, ϵ = 1. Sigg and Kuroda point out that such a treatment greatly reduces the scatter of the data in the systematics plot, and that one can see from Fig. 4 that all cross-section values fall within a reasonably narrow band, including those for a number of nuclei with high threshold energies: ^{50}Cr, ^{54}Fe, ^{90}Zr, and ^{92}Mo. They further note that for (N - Z)/A values > - 0.12 the spread in the data is about $\pm$ 10% (rather than the $\pm$ 20% shown in Fig. 3), and that such a plot can be used to predict unknown (n,2n) cross sections with more certainty.

Finally, before leaving this discussion on strictly empirical methods of obtaining (n,2n) cross-section values, I would like to point out the reasonably flexible expression that was used to describe the energy dependence of the (n,2n) cross section for a number of the evaluations in the Livermore ACTL activation library [10]:

$$\sigma_{n,2n}(E_n) = \sigma_{n,2n}(\text{plat.})$$

$$x \left(1 - e^{-\left\{\frac{\left(E_n - E_{\text{thres.}(n,2n)}\right)^2}{E_{\text{plat.}(n,2n)} - E_{\text{thres.}(n,2n)}}\right\}}\right), \quad (3)$$

where $E_{\text{thres.}(n,2n)}$ is the threshold energy and where $E_{\text{plat.}(n,2n)}$ is the energy at which the (n,2n) reaction first reaches the plateau cross section, $\sigma_{n,2n}$ (plat.). A similar expression was used to describe the energy-dependence of the (n,3n) cross section. The difference between $\sigma_{n,2n}$ (plat.) and $\sigma_{n,3n}$ (E_n) was set equal to $\sigma_{n,2n}$ (E_n), allowing the n,2n cross section to drop smoothly while the n,3n cross section rose.

I would now like to consider some of the semiempirical methods of predicting (n,2n) cross sections. The hybrid empirical-statistical model approach of Pearlstein [11-13] is, perhaps, the most well known. The wealth of (n,2n) cross-section measurements that were made at 14-15 MeV during the 1960's and early 1970's, were almost always compared with the Pearlstein predictions. His predicted cross sections computed at 13.1, 14.1, and 15.1 MeV for about 500 stable and unstable targets ranging from ^{23}Na to ^{210}Po were made readily available in a 1967 issue of Nuclear Data [12]. I will not try to present the historical development of this method, but merely summarize its present status and incorporation into the computer code, THRES2. Pearlstein's original three-part equation for the prediction of (n,2n) cross sections [11]:

$$\sigma_{n,2n} = \sigma_{ne} \frac{\sigma_{n,N}}{\sigma_{ne}} \frac{\sigma_{n,2n}}{\sigma_{n,N}} \quad (4)$$

has been adapted in THRES2 to calculate neutron-induced reaction cross sections from 0 to 20 MeV for some 19 different reactions involving the emission of various charged particles and up to three neutrons. Since we are primarily concerned here with (n,2n) reactions, I'll only describe Eq. 4 in some detail. THRES2 uses the empirical formula of Flerov and Talyzin [14] to compute σ_{ne}, the nonelastic cross section, while the ratio $\sigma_{n,N}/\sigma_{ne}$ is given by:

$$\frac{\sigma_{n,N}}{\sigma_{ne}} = 1 - C_1 e^{-C_2[(N-Z)/A]} \quad (5)$$

where $\sigma_{n,N}$ is defined as the cross section for processes where only neutrons are emitted, $\sigma_{n,N} = \sigma_{n,n'} + \sigma_{n,2n} + \sigma_{n,3n}$, and $C_1 = e^{0.031C_2}$ and $C_2 = 12.0$. The ratio $\sigma_{n,2n}/\sigma_{n,N}$ is given by the statistical model formula [15]:

$$\frac{\sigma_{n,2n}}{\sigma_{n,N}} = \frac{\int_0^{E-B_n} \epsilon\, \sigma_c(E)\, e^{\sqrt{[4a(E-\epsilon)]}}\, d\epsilon}{\int_0^E \epsilon\, \sigma_c(E)\, e^{\sqrt{[4a(E-\epsilon)]}}\, d\epsilon} \qquad (6)$$

with the notation as defined in [13] and it is assumed that the compound nucleus emits a second neutron whenever it is energetically possible. The level density parameter $\underline{a}$ is calculated according to the formula of Abdelmalek and Stavinsky [16]. THRES2 contains 14 empirically fitted parameters, C_1, C_2, ... C_{14} that are used in the calculation of the 19 possible reaction cross sections for $Z = 21$ through 83 [17]. Any of these parameters may be replaced by the user, if he chooses. Another feature of THRES2 is its ability to compute uncertainty estimates for each kind of reaction cross section that it calculates. The method for estimating these uncertainties is based on parameter uncertainties and correlations and is described by Pearlstein in [17]. The range of uncertainties that he gives [17] for (n,2n), (n,p), and (n,α) cross sections at 14 MeV as a function of (N-Z)/A are shown in Table I.

Through the years there have been a number of efforts to improve and modify Pearlstein's empirically normalized, simple evaporation model. Lu, et al. [18] used σ_{ne} values calculated from the optical model by Mani, et al. [19]; the Abdelmalek and Stavinsky level density parameter formalism [16] (Pearlstein originally had used a level density formalism based on the work of Newton [20]); and revised values for the parameters C_1, C_2 (used to obtain $\sigma_{n,N}/\sigma_{ne}$, Eq. 5) based on their own (n,2n) measurements at 14.4 MeV. In their work, $\sigma_{n,N}$ was defined as the cross section for all reactions involving neutrons rather than the cross section for all reactions involving only neutrons, as Pearlstein defines it. They point out that in evaluating the ratios containing $\sigma_{n,N}$, Pearlstein did not include contributions to neutron emission from reactions such as the (n,pn). Kondaiah made similar modifications [21], including the redetermination of the parameters C_1, C_2 for the $\sigma_{n,N}/\sigma_{ne}$ ratio using all available 14-15 MeV (n,2n) data published up to 1973. He assigns accuracies of about 10% to (n,2n) cross sections computed at 14.5 MeV with his revision of the Pearlstein formalism. He suggests that larger deviations observed between calculated and experimental cross-section values can be attributed to nonstatistical reaction processes. D. Gardner [22] replaced $\sigma_{n,N}/\sigma_{ne}$ by $G(Z)$, derived empirically from the available 14-15 MeV (n,2n) cross sections for the even-N isotope closest to the stability line for a given element Z. Such a procedure appeared valid for predicting unknown (n,2n) cross sections at 14.5 MeV for isotopes near the stability line, but could lead to quite poor cross section estimates for isotopes away from the line of stability, as pointed out by Lu, et al. in the case of (n,2n) cross-section predictions for

the heavier isotopes of Xe [18]. Gilbert and Gomberg [23] revised
the Pearlstein expression for $\sigma_{n,N}/\sigma_{ne}$ by also reevaluating the
parameters C_1, C_2 and suggested that "effective thresholds" be used
for (n,2n) and (n,3n) cross-section calculations to correct for
level density and gamma-ray competition deficiencies in the simpli-
fied statistical model and for pre-equilibrium effects. They pro-
posed adding 1 MeV to (n,2n) thresholds for even-A, even-N pro-
ducts, adding 0.5 MeV to (n,2n) thresholds for odd-A, even-N pro-
ducts, and in all cases adding 2 MeV to the (n,3n) thresholds. Lu
and Fink [6] used a constant-nuclear-temperature approximation for
level densities in a simple evaporation calculation which also in-
corporated the use of "effective thresholds" for second- and
third-emitted neutrons and corrections for competition from charged
particles. They observed ± 15% agreement between their calculated
and experimental measurements for (n,2n) cross sections at 14.4
MeV. Recently, Kumabe, et al. [24] have incorporated the pre-equi-
librium process into a simplified statistical model code which
again uses threshold shifts to compensate for the lack of consider-
ing competition between gamma-ray and particle emission.

At this point, it might be appropriate to make some comment as
to which semiempirical method is the "best" or "preferred" one to
use; which is the most reliable for the prediction of (n,2n) cross
sections. Frankly, it is difficult to make a general recommenda-
tion regarding which of the above formalisms is the best choice.
While this list of attempts to improve the simple evaporation model
description of (n,2n) cross sections is by no means complete, it
does illustrate the types of corrections that are required to ob-
tain agreement with experiment. A further excellent critique on
the deficiencies of a simple compound nucleus statistical model has
been given by Frehaut [25], in which he discusses those additional
processes that must be included to provide a complete description
of the (n,2n) reaction mechanism: competition between gamma-ray
and particle emission, angular momentum conservation, and pre-
equilibrium and direct processes.

In Fig. 5 are shown a set of calculations that I have made
recently for the ^{90}Zr(n,2n) cross section compared with some of the
available experimental measurements [26-29]. All of the calcula-
tions were carried out using the STAPRE Hauser-Feshbach statistical
model code [30] in which there is complete conservation of angular
momentum and parity. The full curve is an unnormalized calculation
obtained when the code's pre-equilibrium modeling and gamma-ray
competition in the ^{90}Zr compound nucleus are allowed. The short
dash curve results from a calculation in which the gamma-ray com-
petition in ^{90}Zr is turned off and the dash-dot curve results from
a calculation in which the pre-equilibrium model is not included.
As you can see, in the region of 14-15 MeV, the effect of not in-
cluding pre-equilibrium processes leads to a cross section calcula-
tion that is about 15% too high while ignoring gamma-ray competi-
tion results in a cross section that is of the order of 10% high.
Since the ^{90}Zr(n,2n) reaction threshold is at about 12 MeV, the

cross section at 14-15 MeV will be fairly sensitive to whether gamma-ray competition is included.

In Fig. 6 is shown a recent unnormalized calculation that I made for the ^{92}Mo(n,2n) cross section compared with experimental measurements [31]. In this case, the cross section is fairly well characterized experimentally in the region of its threshold. The calculated cross section was again obtained with the STAPRE Hauser-Feshbach statistical model code, with pre-equilibrium modeling and gamma-ray competition included in the ^{92}Mo compound nucleus. The "cold" calculation shows excellent agreement with experiment, despite the fact that the reaction threshold is quite high, about 13 MeV. Recall that this is one of a number of the cases involving the lightest stable isotope of an even-Z nuclide where neither the empirical predictions of the Lu and Fink equation [6] nor the Qaim systematics [8] do well. The Pearlstein 1967 tables [12] predict this cross section to be about a factor of two higher in the 14-15 MeV region. Even the Gilbert-Gomberg formalism [23], which specifically attempts to make more accurate predictions of cross sections for targets away from stability, estimates a 14.5-MeV cross section that is about 50% too high.

Upon examination of the proton and neutron separation energies from the ^{92}Mo compound nucleus, one sees that the separation energy of the proton is about 5 MeV less than that of the neutron. Thus, despite the Coulomb barrier, it is the proton competition rather than the gamma-ray competition that must be accurately modeled to yield a correct (n,2n) cross section. A complete calculation of all possible neutron-induced reactons up to 16 MeV incident energy with the STAPRE code confirms this. In Fig. 7 the various calculated cross sections are plotted in percentages of the total compound nucleus reaction cross section versus the incident neutron energy. One sees that in the 14-15 MeV region the (n,np) cross section is 35% and more of the total reaction cross section, while the (n,2n) cross section ranges from 8 to 16% of the total reaction cross section. The calculated sum of the (n,p), (n,pn), and (n,np) cross sections at 15 MeV, 845 mb, agrees well with recent 14.8 MeV (n,xp) measurements made on ^{92}Mo at Livermore by Haight et al. [32]. Their measured value is 967 $\pm$ 140 mb. It should be noted that the calculation was made before the measurement.

Since none of the semiempirical approaches that have been discussed take into account all of the competing physics and reaction mechanisms in the same way that one or a combination of the modern nuclear model codes would, one must be cautious in their use, even in the case of (n,2n) cross-section calculations. In general, once one begins to include more realistic models of the reaction processes and departs from empirical normalization, the more important it becomes to describe all of the competing mechanisms completely.

Short of carrying out detailed nuclear model calculations, perhaps Pearlstein's empirically normalized, evaporation model lends itself most readily to the calculation of (n,2n) cross sections; since his model, now incorporated in the THRES2 code, offers a rather flexible method of normalizing to experimental data. It

allows one to put in a number of parameters of choice and one can reoptimize these parameters over a particular Z,A range of interest. As Pearlstein points out [13], although his method does not include pre-equilibrium or direct reaction models to supplement the statistical model at higher energies, the fact that the input parameters to his model can be chosen to produce agreement with experimental trends should allow predicted cross-section values to be corrected somewhat for these nonstatistical effects. Since his model ignores competition between gamma-ray and particle emission, cross-section values near threshold will not be accurate and because discrete level information is not included, his calculations will not show nuclear structure effects. However, as Pearlstein says [13], "the simplicity of the model precludes cross-section calculations of great accuracy ..." "The method ... is not intended to supplant detailed nuclear model calculations but rather is intended to readily provide additional cross-section information where measurements are discrepant or nonexistent."

(n,p), (n,α) CROSS SECTIONS

The number of empirical equations that are available in the literature for the prediction of (n,p) and (n,α) cross sections at 14 MeV far exceeds those available for the prediction of 14 MeV (n,2n) cross sections. However, unlike the case for (n,2n) cross sections, from the viewpoint of simple systematics, (n,p) and (n,α) excitation functions are not easily described. Since the Coulomb barrier must be overcome before proton or alpha-particle emission can occur, it is difficult to predict accurately the (n,p) or (n,α) cross section around threshold with simple systematics. Further, simple systematics cannot easily predict the structure in (n,p) and (n,α) excitation functions that is due to the competition between charged-particle and neutron emission.

Following the early work of Levkovskii [33] and D. Gardner [34] on the observation of simple systematic trends in 14 MeV (n,p) cross-section data, many other empirical equations for the prediction of both (n,p) and (n,α) cross sections at 14-15 MeV have been proposed [35-40]. In addition, Qaim [41] has presented graphical systematics for both (n,p) and (n,α) cross sections at 14-15 MeV as a function of the residual nuclear charge, Z_R. Recently, Molla and Qaim [42] have reanalyzed the systematics of (n,p) cross sections using a newer and revised base of 14-15 MeV data. Their updated graphical systematics are shown in Fig. 8. They comment that this correlation should prepredict unknown (n,p) cross sections in the medium and heavy mass regions with errors of about 25%.

As Pearlstein [17] points out, the (n,p) cross section at 14 MeV samples a variety of reaction processes, depending on the target nuclide asymmetry parameter value. In general, for nuclides with small (N-Z)/A values (usually light nuclei with a small Coulomb barrier) the (n,p) cross section has already peaked below 14 MeV and at 14 MeV is decreasing due to other competing reactions;

for nuclides with intermediate values of (N-Z)/A the peak (n,p)
cross section should be around 14 MeV. For nuclides with large
(N-Z)/A values, where the Coulomb barrier is high, the (n,p) cross
section at 14 MeV is somewhere between threshold and the peak value
and is dependent on characteristics of the barrier penetration.
Therefore, it is difficult to derive an expression that has one
set of parameters which can yield reliable 14 MeV (n,p) cross
sections over the entire mass range.

Perhaps the most successful, or at least the most widely used,
empirical equations for predicting (n,p) and (n,α) cross sections
at 14-15 MeV are those of Levkovskii [38].

$$\sigma_{n,p} \text{ (mb)} = 45.2 \ (A^{1/3} + 1)^2 \exp \ [- \ 33(N-Z)/A] \tag{7}$$

$$\sigma_{n,\alpha} \text{ (mb)} = 18.1 \ (A^{1/3} + 1)^2 \exp \ [- \ 33(N-Z)/A] \tag{8}$$

Recently, Kumabe and Fukuda [43] observed, for both (n,p) and (n,α)
reactions, that there were rather large discrepancies between ex-
perimental cross sections and those calculated by the Levkovskii
formulas for nuclei with relatively small or large values of (N-Z)/
A for a given value of Z. Therefore, they reparameterized the Lev-
kovskii formulas over three more limited mass ranges by carrying
out least-squares fits to experimental data. The empirical equa-
tions that they derived for 14-15 MeV (n,p) and (n,α) cross-
section predictions and the corresponding mass ranges are given in
Table II. These revised expressions gave considerably better
agreement with experiment for all isotopes of a given element.

Lu and Fink [6] applied their simple statistical model with
the constant-temperature-approximation for the level densities and
"threshold shifts" to the calculation of (n,p) and (n,α) cross sec-
tions as well as to that of (n,2n) cross sections. Upon comparison
of their calculated results to experimental measurements that they
had made at 14.4 Mev, they observed ± 20% agreement for (n,p) cross
sections and ± 30% agreement for (n,α) cross sections. However, as
in the case of the empirical procedures for predicting a complete
excitation function, a semiempirical calculation based on a simpli-
fied statistical model generally will not describe well the (n,p)
or (n,α) cross section over the entire incident neutron energy
range. It is only with the use of a more developed nuclear model
code which contains an optical model routine that one can describe
proton and alpha-particle Coulomb barrier tunneling properly and
thus obtain accurate cross sections around threshold. In addi-
tion, the inclusion of pre-equilibrium and direct-reaction mechan-
isms are very necessary to correctly predict the (n,p) and (n,α)
cross sections at higher energies, as pointed out by Cindro [44]
and Braga-Marcazzan, et al. [45].

An excellent example of how empirical and semiempirical meth-
ods can effectively contribute to the prediction of (n,p) and (n,α)
cross sections is some recent work by Gruppelaar and van den Bos
[46]. Upon comparison of various data files of fission-product
neutron cross sections, they noted rather large differences in the

neutron capture cross sections for some individual fission product isotopes, particularly above incident energies of 1 MeV. They decided to determine what contribution (n,p) and (n,α) reactions made to these capture cross sections. They noted that very few (n,p) and (n,α) cross sections were included in the various fission-product cross section files, and that they would somehow have to provide full excitation functions for a large number of reactions in order to carry out their investigation. Since it was not practical to carry out Hauser-Feshbach statistical model calculations for all of these cross sections, they chose to use Pearlstein's THRES2 code, which has the capability of providing (n,p) and (n,α) excitation functions.

Originally, they used the systematics built into the code to obtain estimates of the magnitude of the various cross sections. However, since the (n,p) and (n,α) cross section parameters in the code were fitted mainly to data in another mass range, the predicted (n,p) values were factors of 2 to 3 too high and the predicted (n,α) values ranged from being 20% too low to 60% too high. They decided to renormalize the THRES2 calculations at 14.5 MeV to experimen..al values recommended by Qaim [47] or where data were lacking, to the predicted values from the Kumabe and Fukuda empirical expressions that were described above and listed in Table II. Figure 9 was taken from the Gruppelaar and van den Bos report [46] and shows the good agreement between the experimental values recommended by Qaim and the Kumabe and Fukuda systematics. The shapes of the excitation functions, of course, were calculated from the empirical formulas contained in the THRES2 code. Wherever possible, these shapes were checked against available experimental data and it appeared that the THRES2-generated shapes were adequate. The scarcity of (n,p) and (n,α) experimental data over the the full energy range, however, precluded a thorough check. In Fig. 10 is shown an example provided in their report: the ^{90}Zr(n,p) cross section as calculated by THRES2 and renormalized to a 14.5 MeV value recommended by Qaim (the full curve). Other experimental data is that of Carroll and Stooksbury [48] near threshold and that of Bayhurst and Prestwood [49] at higher energies. In this figure, I have also plotted a recent calculation which I made using the STAPRE code (long dash curve) and the results of the same calculation if no pre-equilibrium modeling is used (short dash curve). Note how well the cross section in the threshold region is reproduced by the Hauser-Feshbach calculation. If no pre-equilibrium processes are allowed, the statistical model would predict a cross section that is about 45% too low at 14.5 MeV. The apparent "underestimation" of the threshold by the THRES2 code must result when the overestimated cross section is normalized at 14.5 MeV. Overall, the normalized THRES2 calculation provides a reasonable excitation function for this reaction and is certainly of the accuracy necessary for the study that Gruppelaar and van den Bos carried out.

(n,γ) CROSS SECTIONS

Due to time limitations and the fact that a number of speakers at this Workshop have already addressed various topics that are pertinent to the evaluation of neutron capture cross sections, I would like to take the liberty of discussing only one method for the prediction of neutron capture cross sections. This is the method that we have been developing at Livermore involving the use of gamma-ray strength function systematics in Hauser-Feshbach statistical model calculations. This approach, in its simplest form, proposes using E1 and M1 gamma-ray strength functions, extracted from measured capture cross sections in a limited Z,A range to predict unknown capture cross sections for that range. As such, it should be a valuable tool in predicting (n,γ) cross sections for unstable targets.

The usual Hauser-Feshbach statistical model formulation for the neutron capture cross section, in the region of overlapping resonances, requires a knowledge of the ratio of $\bar{\Gamma}_\gamma/D_{obs}$, where $\bar{\Gamma}_\gamma$ is the average s-wave radiation width and D_{obs} is the observed s-wave resonance spacing, both at the neutron separation energy, S_n. Suppressing spin and parity notation and considering only dipole transitions,

$$2\pi \frac{\Gamma_\gamma}{D} = \int_0^{S_n} (T_\gamma^{E1} + T_\gamma^{M1}) \, \rho(S_n - E_\gamma) \, dE_\gamma \tag{9}$$

The level density $\rho(U)$ is the reciprocal of the level spacing $D(U)$ and T_γ^{E1} and T_γ^{M1} are the gamma-ray transmission coefficients. The normalization of these transmission coefficients may be accomplished by performing the integration indicated in Eq. 9 for each compound spin state produced by s-wave neutron capture, and then equating the results to the quotient of the measured quantities $\bar{\Gamma}_\gamma$ and D_{obs}. When experimental data are lacking, these quantities must be estimated and in regions of closed shells, such as the mass-90 region, the typical errors involved in predicting $\bar{\Gamma}_\gamma$ and D_{obs} separately make it difficult to compute their ratio to within a factor of 2. Depending on the size of $\bar{\Gamma}_\gamma$ relative to the widths of other open channels, this might correspond to a 50% uncertainty in the capture cross section at low energies and to larger uncertainties as the neutron energy increases.

An alternate form of Eq. 9 is

$$\frac{\Gamma_\gamma}{D} = \int_0^{S_n} [f_{E1}(E_\gamma) + f_{M1}(E_\gamma)] \, E_\gamma^3 \rho(S_n - E_\gamma) \, dE_\gamma \tag{10}$$

where the gamma-ray transmission coefficients are expressed in terms of gamma-ray strength functions, $f_{X\ell}(E_\gamma)$. The El gamma-ray strength function may be expressed in terms of the classical dipole sum rule if we assume a single Lorentz function for the shape of the giant dipole resonance:

$$f_{E1}(E_\gamma) = 3.3 \times 10^{-6} \frac{NZ}{A} F_{SR} \frac{E_\gamma \Gamma_R}{(E_\gamma \Gamma_R)^2 + (E_\gamma^2 - E_R^2)^2} \tag{11}$$

where E_R and Γ_R are the energy and width of the giant dipole resonance and F_{SR} is the fraction of the dipole sum rule that is exhausted. In our work, we usually assume that the Ml gamma-ray strength function is single particle in character (independent of energy) and contributes about 15-20% to the total s-wave radiation width, $\bar{\Gamma}_\gamma$. In addition, we assume that the strength functions are independent of the excitation energy of the nucleus. Since the gamma-ray strength function is an averaged quantity, it is appropriate to extract it from capture cross sections in the overlapping resonance region. Our approach has been to adjust the value of $\bar{\Gamma}_\gamma/D_{obs}$, used in the normalization of the El and Ml gamma-ray transmission coefficients, until agreement with the experimental data is achieved; then from this ratio calculate the effective El strength function. This, in turn, can be compared with the prediction from Eq. 11, in order to obtain a value for the parameter F_{SR}.

The method is illustrated in Fig. 11 for the target nuclei, ^{85,87}Rb. The points are the experimental data [50,51] and the curves are our adjusted calculations. The inset shows the single extracted El strength function that represents both isotopes. The power of the strength function approach is obvious; while the capture cross sections for the two isotopes differ by a factor of 10 and the $\bar{\Gamma}_\gamma/D_{obs}$ values differ by a factor of 27, the same strength function is applicable. The neutron separation energy in compound nucleus ^{86}Rb exceeds that for ^{88}Rb by 2.5 MeV. Thus the larger cross section for the target ^{85}Rb is due primarily to the fact that in Eq. 10 one is integrating 2.5 MeV further up the strength function curve.

Our original gamma-ray strength function studies [52] were carried out for 12 target nuclei in the mass-90 region, from ^{75}As to ^{103}Rh. Most of the values of F_{SR} that were extracted over this range showed only small variations with mass - being about 0.75 for compound nuclei with A=90 and about 1.1 for A=94. The two marked exceptions were for compound nuclei ^{76}As and ^{104}Rh, where the F_{SR} values were about 2.6 and 1.6, respectively. These early studies used the following systematics for estimating unmeasured values of E_R and Γ_R:

$$E_R = 35.4/A^{1/6} \tag{12a}$$

$$\Gamma_R = (A^{1/3}/1.227)(1. + 12.78 \; \beta_2^2) \tag{12b}$$

where β_2 is the nuclear deformation parameter.

An example of how this gamma-ray strength function approach can be applied to the prediction of unknown neutron capture cross sections was recently presented for a series of Nb isotopes, ^{93,94,95}Nb [53]. The total capture cross sections for the ground state targets of ^{93}Nb, ^{94}Nb, and ^{95}Nb are shown in Fig. 12. The ^{93}Nb cross section was fitted to experimental data during the derivation of the strength function systematics; the ^{94}Nb and ^{95}Nb cross sections were predicted on the basis of these systematics. The inset shows the E1 and M1 strength functions derived from the ^{93}Nb calculational fit. Nearly identical strength functions were predicted for the other two compound nuclei. Since $\bar{\Gamma}_\gamma/D_{obs}$ is proportional to the integral over the strength functions and dependent on the integration limit, S_n, the same strength function can readily lead to cross sections differing by a factor of two or more. At incident energies below 0.1 MeV, the cross sections reflect the relative magnitude of the neutron separation energies in each compound nucleus. Above 0.1 MeV, the greater level density in the odd-odd ^{94}Nb nucleus allows more competition from inelastic scattering processes and leads to the lower ^{94}Nb capture cross section.

While this modeling successfully predicts the magnitude of (n,γ) cross sections, it fails, in many cases, to reproduce the observed hardness in associated gamma-ray spectra. Our recent efforts have been directed towards the improvement of gamma-ray spectra calculations by modeling the E1 gamma-ray strength function in terms of a double-peak, energy-dependent Breit-Wigner model [54-56].

ACKNOWLEDGMENTS

REFERENCES

1. J. L. Rowlands, "Nuclear Data for Reactor Design, Operation and Safety," in Proc. Int. Conf. Neutron Physics and Nuclear Data for Reactors and Other Applied Purposes, Harwell (1978) p. 7.

2. M. R. Bhat, "Evaluated Files of Nuclear Cross-Sections for Fusion Reactor Calculations," BNL-NCS-25295 (1979).

3. R. C. Haight, "Neutron Cross Sections for Fusion," UCRL-83005, Oct.1979; Int. Conf. Nuclear Cross Sections for Technology, Knoxville (1979).

4. O. N. Jarvis, "Transmutation and Activation of Fusion Reactor Wall and Structural Materials," AERE-R9298 (1979).

5. S. M. Qaim, "A Survey of Fast-Neutron Induced Reaction Cross-Section Data," Proc. Conf. Nuclear Cross Sections and Technology, Washington, D.C., NBS-Special Publication 425 (1975) p. 664.

6. W. Lu and R. W. Fink, Phys. Rev., $\underline{C4}$, 1173 (1971).

7. J. Frehaut and G. Mosinski, "Measurement of (n,2n) and (n,3n) Cross-Sections for Incident Energies Between 6 and 15 MeV," Proc. Conf. Nuclear Cross Sections and Technology, Washington, D.C., NBS-Special Publication 425 (1975) p. 855 and private communication (1980).

8. S. M. Qaim, Nucl. Phys., $\underline{A185}$, 614 (1972).

9. R. A. Sigg and P. K. Kuroda, J. Inorg. Nucl. Chem., $\underline{37}$, 631 (1975).

10. M. A. Gardner and R. J. Howerton, "ACTL: Evaluated Neutron Activation Cross Section Library - Evaluation Techniques and Reaction Index," UCRL-50400, Vol. 18 (1978).

11. S. Pearlstein, Nucl. Sci. Eng., $\underline{23}$, 238 (1965).

12. S. Pearlstein, Nuclear Data, $\underline{3}$, 327 (1967).

13. S. Pearlstein, J. Nucl. Energy, $\underline{27}$, 81 (1973).

14. N. N. Flerov and V. M. Talyzin, J. Nucl. Energy, $\underline{4}$, 529 (1957).

15. J. M. Blatt and V. F. Weisskopf, Theoretical Nuclear Physics, Wiley, New York (1952).

16. N. N. Abdelmalek and V. S. Stavinsky, Nucl. Phys., 58, 601 (1964).

17. S. Pearlstein, "Neutron Cross Sections and Their Uncertain-ties Obtained From Nuclear Systematics," Proc. Conf. Nuclear Cross Sections and Technology, Washington, D.C., NBS-Special Publication 425 (1975) p. 332.

18. Lu, et al., Phys. Rev., C1, 350 (1970).

19. G. Mani, et al., CEA-2380 (1963).

20. T. D. Newton, Can. J. Phys., 34, 804 (1956).

21. E. Kondaiah, J. Phys. A., 7, 1457 (1974).

22. D. G. Gardner, UCRL-14575 (1966).

23. A. Gilbert and R. Somberg, UCRL-50736 (1969).

24. I. Kumabe, et al., J. Nucl. Sci. Technol., 14, 319 (1977).

25. J. Frehaut, "Neutron Induced Cascade Reactions," Int. Conf. Interaction of Neutrons with Nuclei, Lowell (1976).

26. D. R. Nethaway, Nucl. Phys., A190, 635 (1972) and private communication.

27. Y. Kanda, Nucl. Phys., A185, 177 (1972).

28. A. Abboud, et al., Nucl. Phys., A139, 42 (1969).

29. B. P. Bayhurst, et al., Phys Rev., C12, 451 (1975).

30. M. Uhl, Acta Physica Austriaca, 31, 245 (1970).

31. P. Cuzzocrea, et al., Nucl. Phys., A103, 616 (1967); P. Stro-hal, et al., Nucl. Phys., 30, 49 (1962).

32. R. C. Haight, S. M. Grimes, R. G. Johnson, and H. H. Bar-shall, Lawrence Livermore National Laboratory (to be pub-lished).

33. V. N. Levkovskii, Soviet Physics JETP, 4, 291 (1957).

34. D. G. Gardner, Nucl. Phys., 29, 373 (1962).

35. E. Havlik, Acta Physica Austriaca, 34, 209 (1971).

36. S. R. Choudhury and O. N. Kaul, J. Pure and Applied Phys., 10, 197 (1973).

37. G. Eder, et al., Z. Physik, 253, 335 (1972).

38. V. N. Levkovskii, Sov. J. Nucl. Phys., 18, 361 (1974).

39. D. G. Gardner and Y. Yu, Nucl. Phys., 60, 49 (1964).

40. D. G. Gardner and S. Rosenblum, Nucl. Phys., A96, 121 (1967).

41. S. M. Qaim, Z. Naturf., 25a, 1977 (1970).

42. N. I. Molla and S. M. Qaim, Nucl. Phys., A283, 269 (1977).

43. I. Kumabe and K. Fukuda, NEANDC(J) - 65/U (1978) p. 45.

44. N. Cindro, "Neutron Induced Reactions II: (n,x) Reactions on Medium and Heavy Nuclei," Int. Conf. Interaction of Neutrons with Nuclei, Lowell (1976).

45. G. M. Braga-Marcazzan, et al., Phys. Rev., C6, 1398 (1972).

46. H. Gruppelaar and B. P. J. van den Bos, "The Contribution of (n,p) and (n,α) Reactions to Fission-Product Capture Cross Sections," Proc. Specialists' Meeting on Neutron Cross Sections of Fission Product Nuclei, Bologna (1979).

47. S. M. Qaim, "14-MeV Neutron Activation Cross-Sections," Handbook of Spectroscopy, 3, The Chemical Rubber Company Press, Inc., West Palm Beach, Fla., to be published.

48. E. Carroll and R. W. Stooksberry, Nucl. Sci. Eng., 25, 285 (1966).

49. B. P. Bayhurst and R. J. Prestwood, J. Inorg. Nucl. Chem., 23, 173 (1961).

50. D. C. Stupegia, et al., J. Nucl. Energy, 22, 267 (1968).

51. N. D. Dudey, et al., J. Nucl. Energy, 24, 181 (1970).

52. D. G. Gardner and M. A. Gardner, "Gamma-Ray Strength Functions for Medium-Weight Nuclei," Third International Symposium on Neutron Capture Gamma-Ray Spectroscopy and Related Topics, Plenum Press, New York (1979) p. 612.

53. M. A. Gardner and D. G. Gardner, "Calculated Neutron Capture Cross Sections for the Ground States and Isomers of 93,94,95Nb," Proc. Int. Conf. Neutron Physics and Nuclear Data for Reactors and Other Applied Purposes, Harwell (1978) p. 1121.

54. D. G. Gardner and F. S. Dietrich, "A New Parameterization of the El Gamma-Ray Strength Function," Proc. Int. Conf. Nucl. Cross Sections for Technology, Knoxville (1979).

55. M. A. Gardner and D. G. Gardner, "Capture Cross Sections and Gamma-Ray Spectrum Calculations for Medium-Weight Nuclei," ibid.

56. D. G. Gardner, M. A. Gardner, and F. S. Dietrich, UCID-18759 (1980).

TABLE I

RANGE OF UNCERTAINTIES (%)[a]

| Reaction | $\frac{N-Z}{A}$ | | | |
	.03-.05	.05-.10	.10-.15	.15-.20
n,2n	20-50	10	10	10
n,p	20-25	20-30	20-40	30-150
n,α	25	25-40	30-60	40-150

[a]Cross section uncertainties as computed from parameters built into THRES2 code.

TABLE II

EMPIRICAL FORMULAS FOR (n,p) AND (n,α) CROSS SECTIONS AT 14 MeV
DERIVED BY KUMABE AND FUKUDA

A	$\sigma_{n,p}$ (mb)
40 - 62	$21.8A \exp[-34(N-Z)/A]$
63 - 89	$0.75A^2 \exp[-43.2(N-Z)/A]$
90 - 160	$0.75A^2 \exp[-45.0(N-Z)/A]$

A	$\sigma_{n,\alpha}$ (mb)
30 - 60	$51.0A^{1/2} \exp[-30(N-Z)/A]$
61 - 105	$55.0A^{1/2} \exp[-33(N-Z)/A]$
106 - 150	$7.6 \times 10^{-4} A^3 \exp[-40(N-Z)/A]$
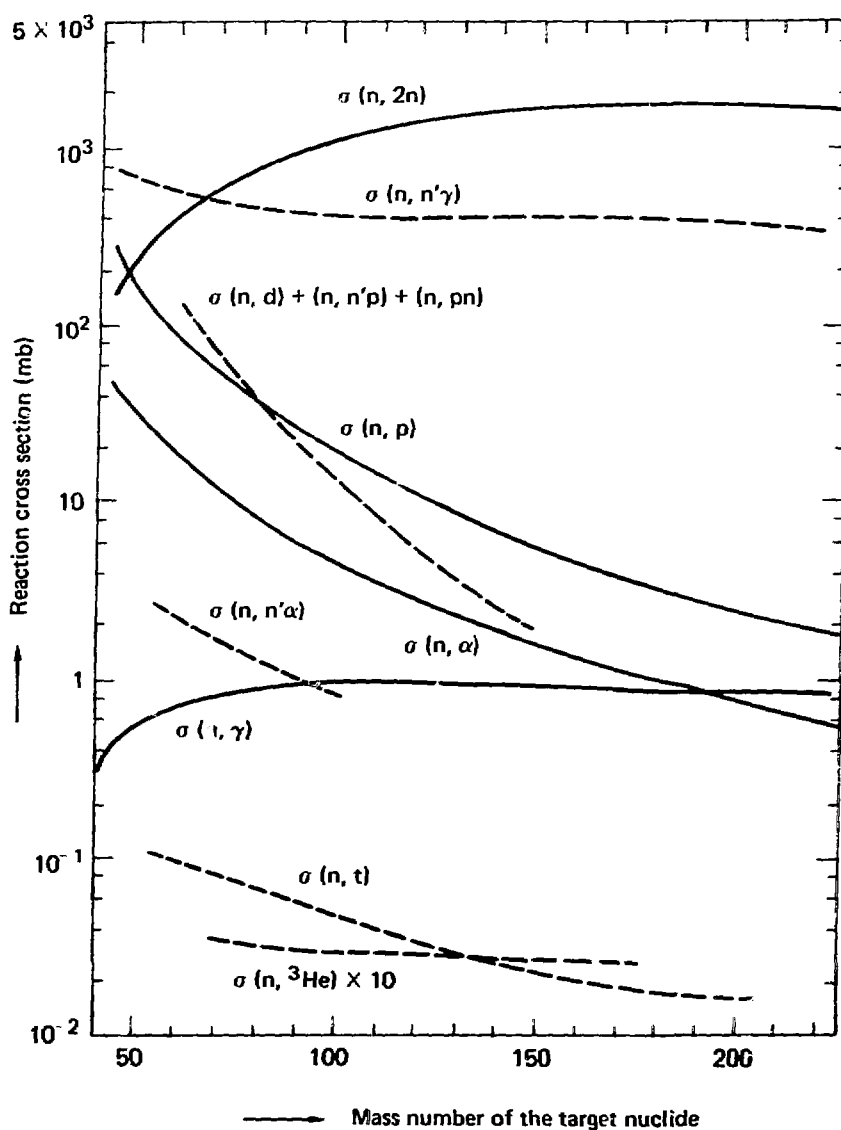
1. From Ref. 5. Relative contributions of nuclear reactions induced by 14-MeV neutrons.
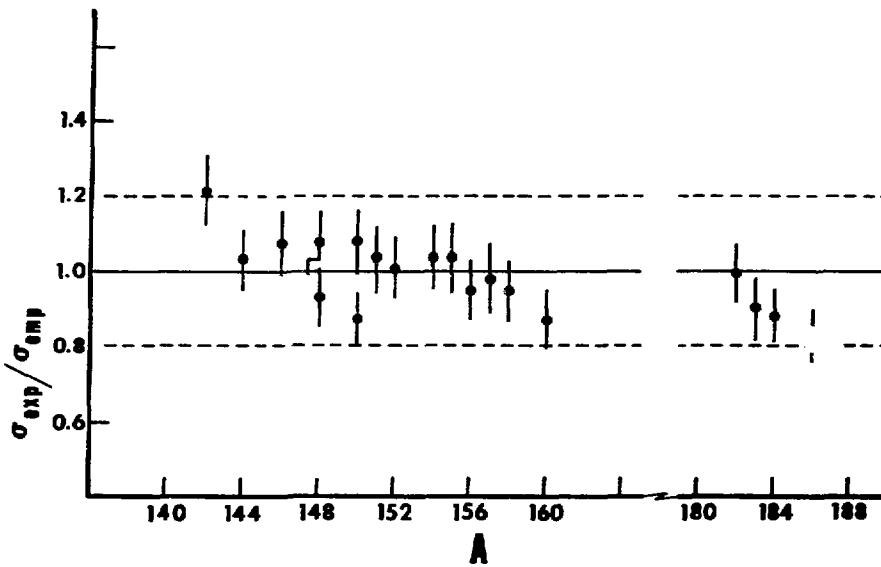
2. Comparison of (n,2n) cross sections predicted from the empirical equation of Lu and Fink (Eq. 1) with experimental measurements made at 14.76 MeV by Frehaut [7] for isotopes of Nd, Sm, Eu, Gd, and W.

Figure axes and legend (as shown in figure):

- Y-axis: σ (n,2n) mb — values 1, 10, 100, 1000, 10000
- X-axis: Asymmetry parameter, (N-Z)/A — values 0, 0.04, 0.08, 0.12, 0.16, 0.20, 0.24

Systematics of (n,2n) reaction
Cross-sections induced
by 14-15MeV neutrons

- o   Normal nuclei
- •   Nuclei with magic neutron numbers
- (o)   Nuclei with magic proton numbers
- ≤   Doubly magic nuclei
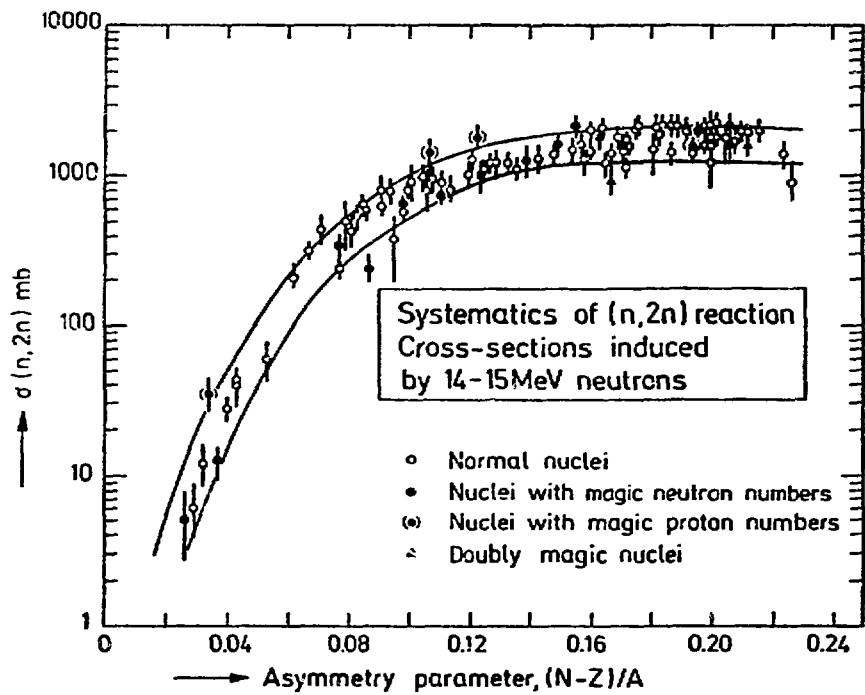
3. From Ref. 8. Systematics of (n,2n) reaction cross sections induced by 14- to 15-MeV neutrons.
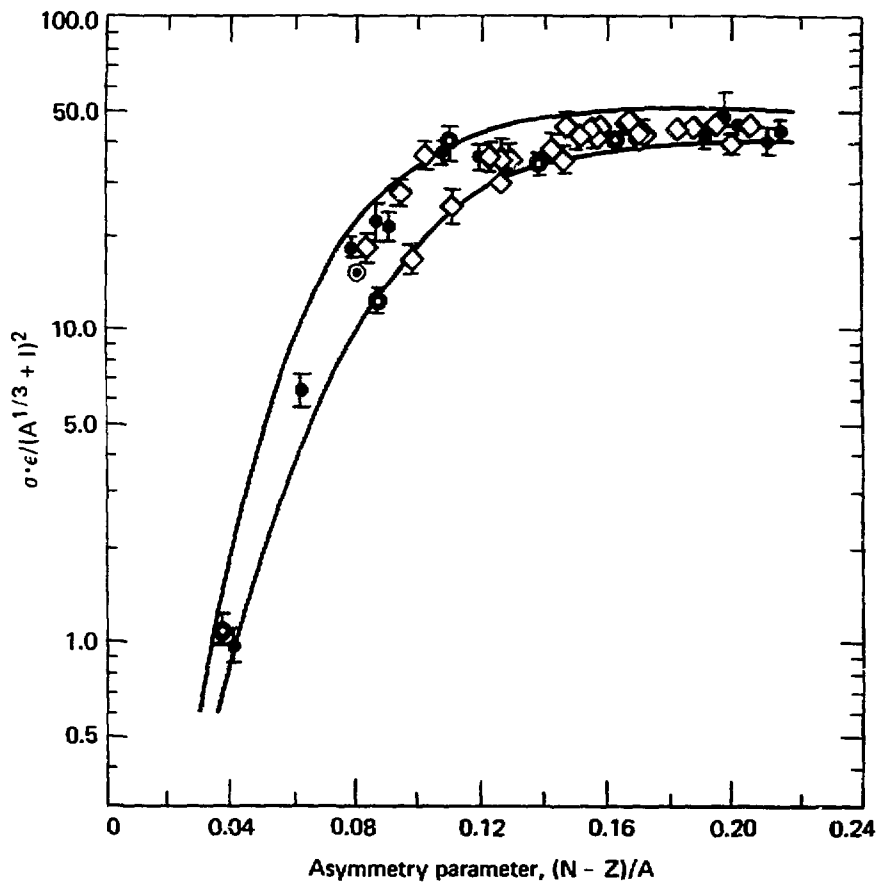
4. From Ref. 9. 14.8-MeV (n,2n) cross sections including linear
   energy and nuclear radius corrections plotted against (N-Z)/A.
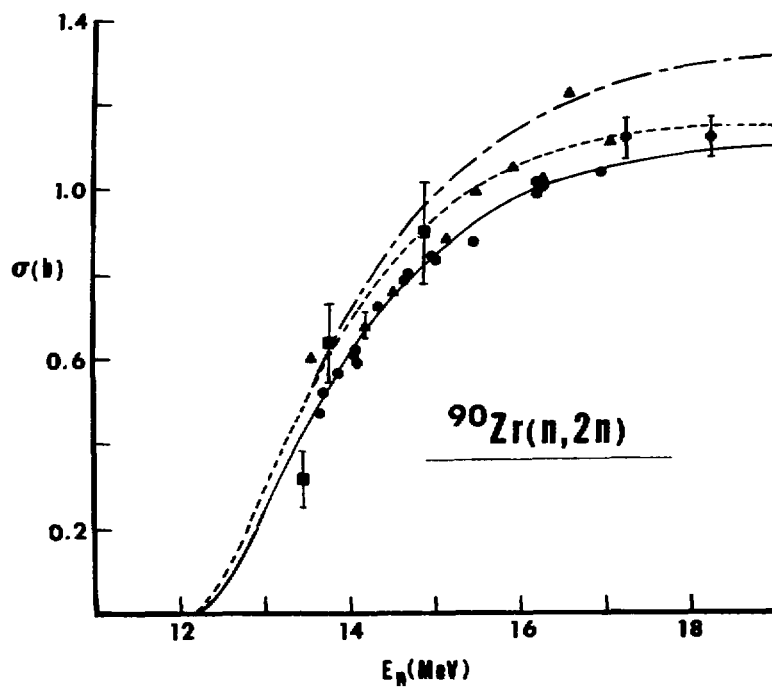
5. The ^{90}Zr(n,2n) cross section calculated as a function of neutron energy with the STAPRE code (————— with pre-equilibrium modeling and gamma-ray competition in ^{90}Zr compound nucleus; – – – – with no gamma-ray competition in ^{90}Zr compound nucleus; – —— – —— – —— with no pre-equilibrium modeling in ^{90}Zr compound nucleus) compared with experimental data [26-29].
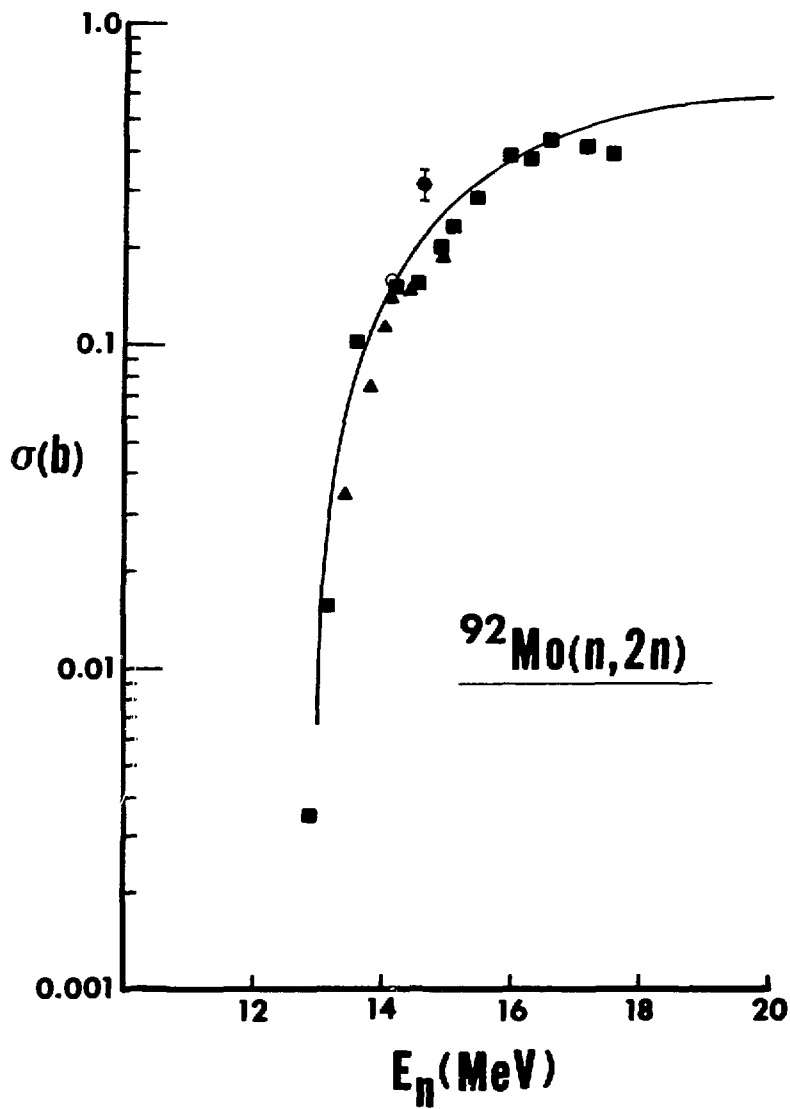
6. The ^{92}Mo(n,2n) cross section calculated as a function of neutron energy with the STAPRE code (————) compared with experimental data [27,28,31].
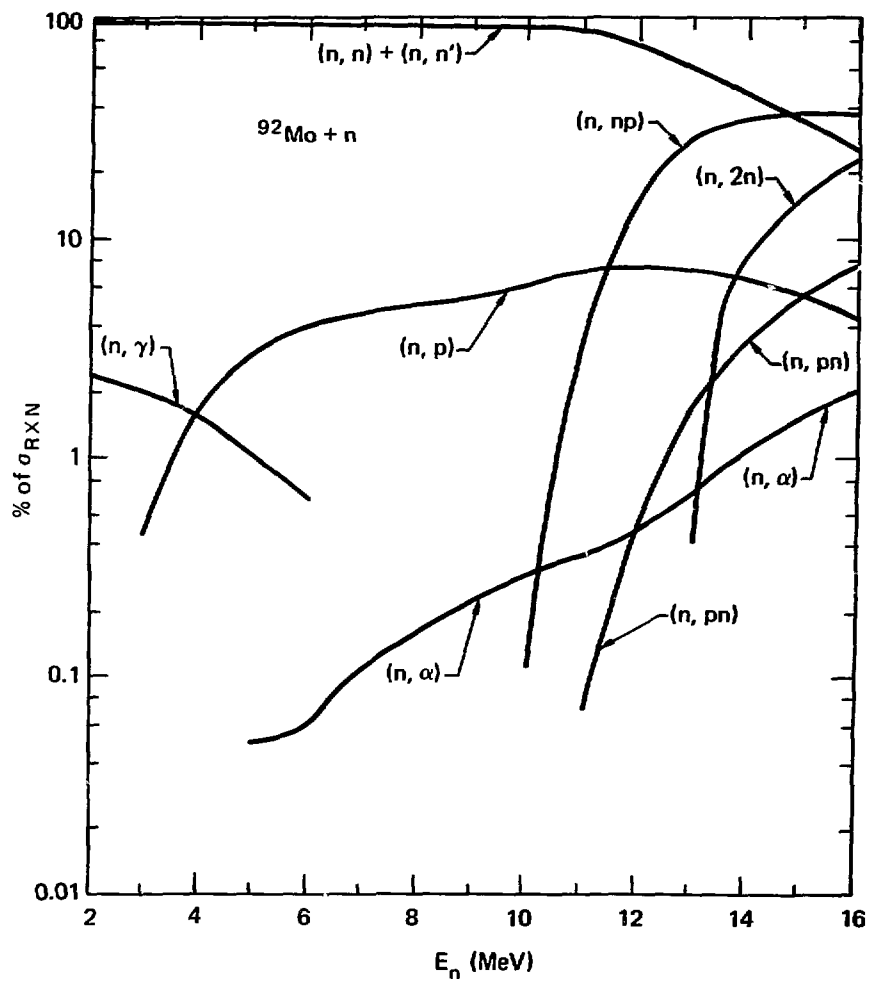
7. The STAPRE-calculated cross sections for ^{92}Mo plotted in percentages of the total compound nucleus reaction cross section versus the incident neutron energy.
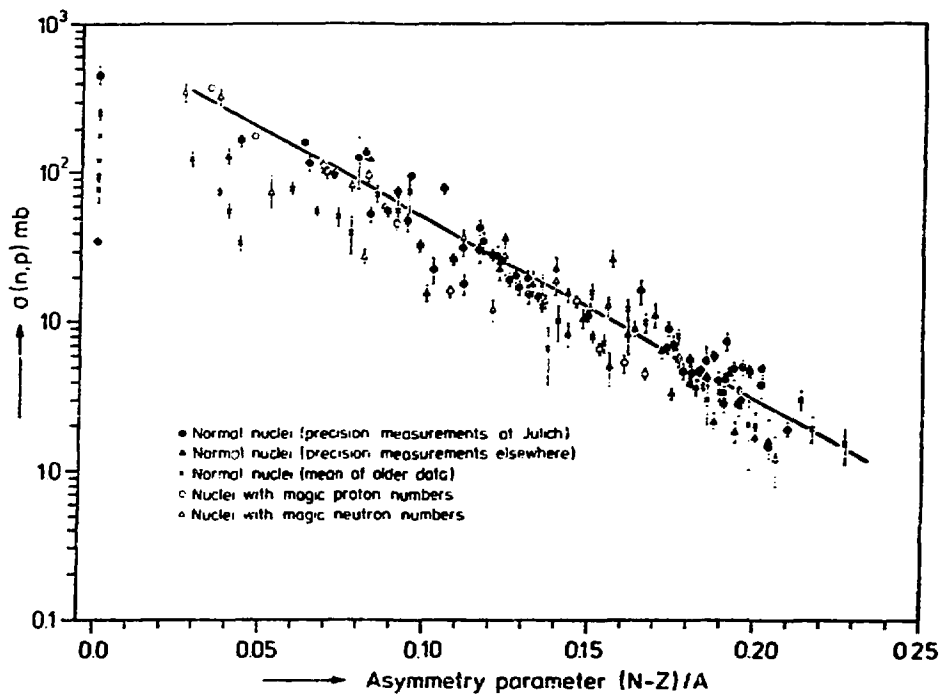
8. From Ref. 42. Systematics of (n,p) reaction cross sections induced by 14- to 15-MeV neutrons.
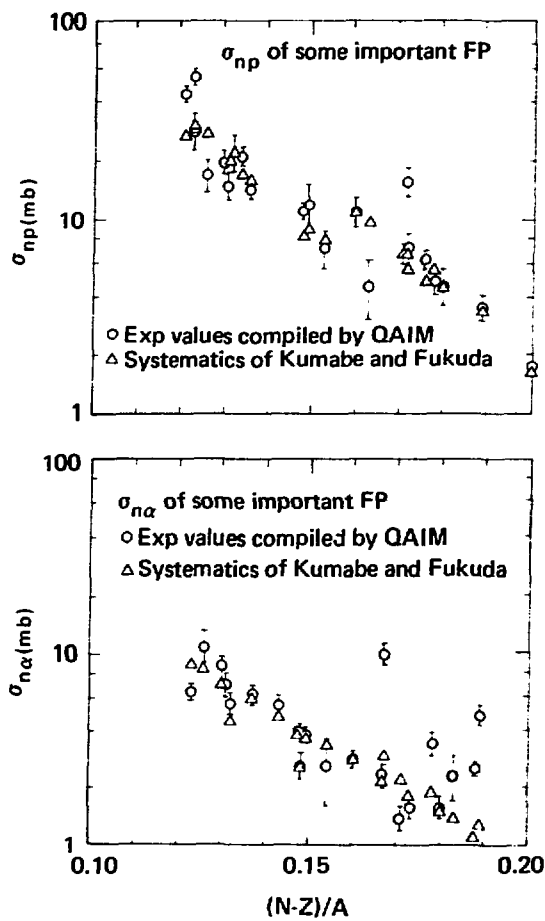
9. From Ref. 46. Comparison of experimental and calculated 14.5-MeV values of (n,p) and (n,α) cross sections.

100.

10.

σ(mb)

STAPRE

NORM.
THRES2

STAPRE
(no
precomp.)

1.

$^{90}Zr(n,p)$

0.1

2   6   10   14   18

$E_n(MeV)$
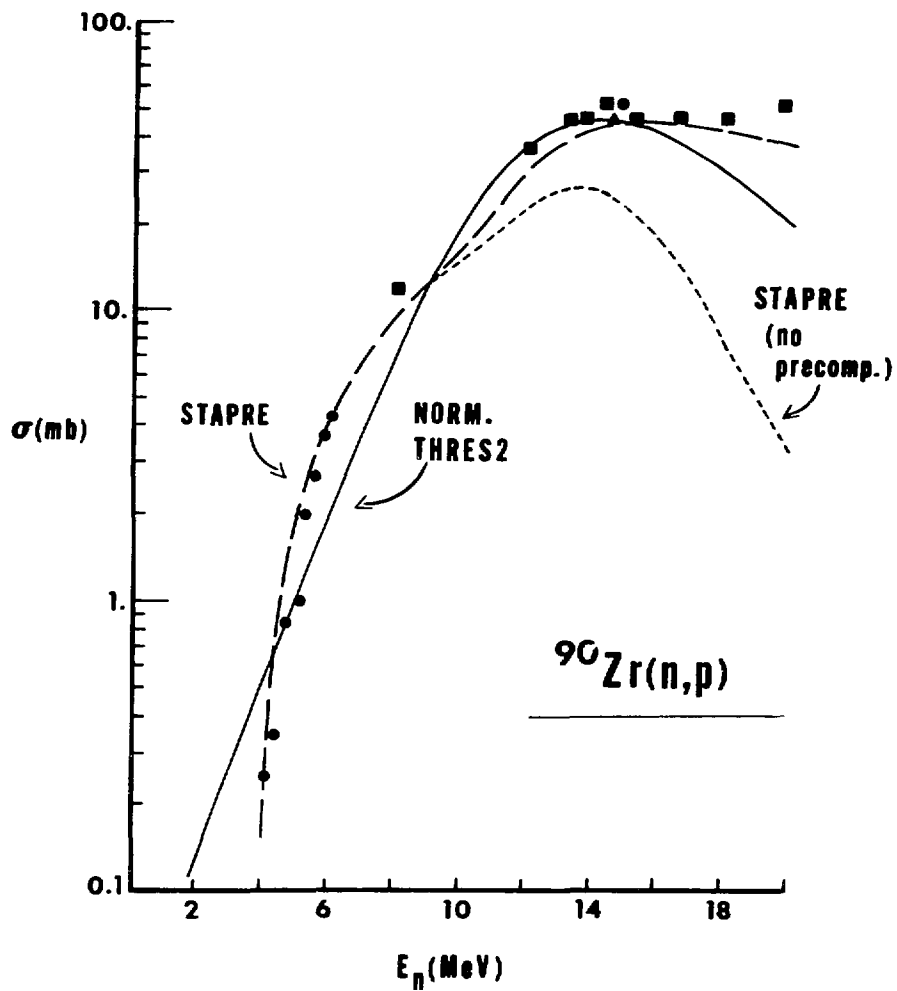
10. The $^{90}Zr(n,p)$ cross section calculated as a function of neu-
tron energy (————— with THRES2 and normalized to a 14.5-MeV
value recommended by Qaim ▲ (from Ref. 46);— —— ——with
STAPRE; – – – – – with STAPRE but without precompound model-
ing) compared with experimental data [48,49].
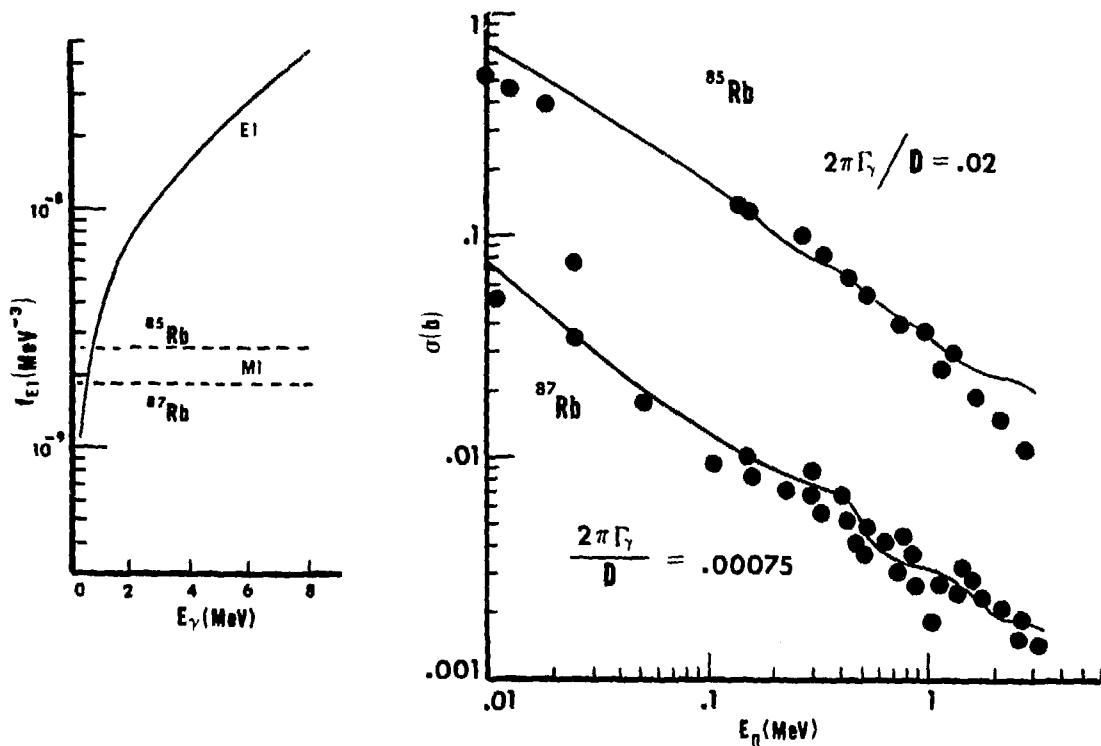
11. The ^{85,87}Rb(n,γ) cross sections versus incident neutron energy, E_n. The points are experimental data [50,51] and the curves are calculational fits that yield the $2\pi\Gamma_\gamma/D$ values indicated. The inset shows the single extracted E1 strength function that represents both isotopes versus E_γ.
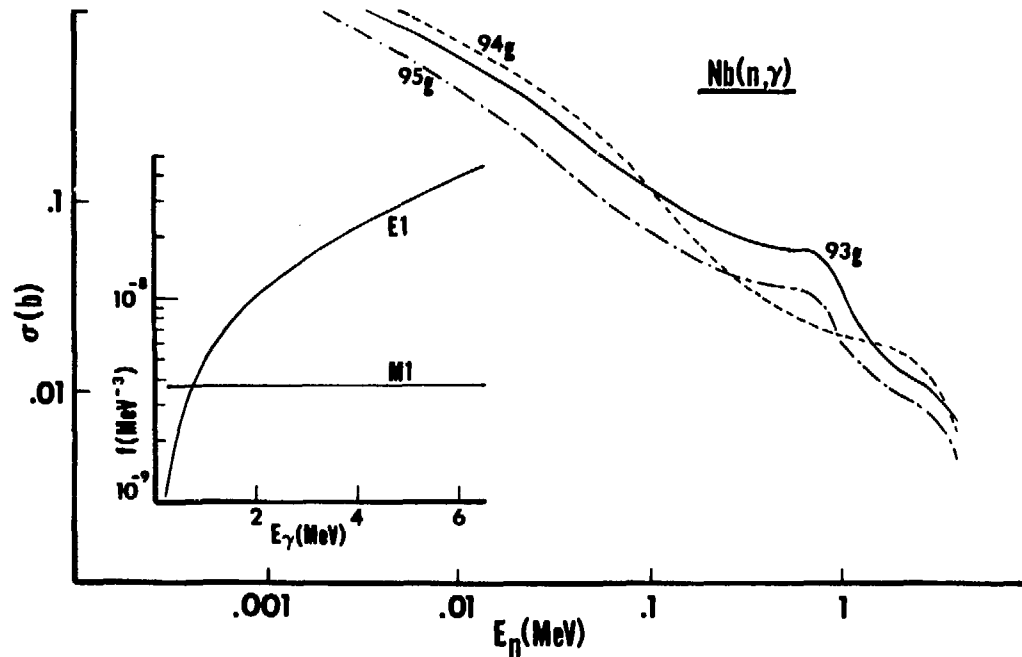
12. The calculated total neutron capture cross sections for $^{93,94,95}Nb$ versus incident neutron energy, E_n. The ^{93}Nb cross section was fitted to experimental data; the ^{94}Nb and ^{95}Nb cross sections were predicted on the basis of gamma-ray strength function systematics. The inset shows the E1 and M1 strength functions derived from the ^{93}Nb calculational fit.

Discussion

Howerton

Before proceeding to the questions I should like to comment that it must be obvious to everyone that we have moved into a different realm when we discuss evaluation methods that agree with experiment to 20%, 30%, 50% or factors of two. It is equally obvious from allusions made by Dr. Gardner and other speakers that the cost in terms of manpower and computer time often precludes making as detailed calculations as should be done for any specific reaction when we are faced by the necessity of providing for a large number of reactions. Thus we must fall back on a less precise method for providing estimates of the required cross sections. While none of us are happy with the necessity to use less precise methods, we must live with the world as it is.

Pearlstein

While I did a lot to parameterize and automate the cross sections that could be calculated specifying only the nuclide charge and mass, the possibility to factorize the $(n,2n)$ cross section was first pointed out to me by the work of Barr, Browne and Gilmore of LASL.

Poenitz

I was suprised about the integration limit in your expression for Γ_γ/D. I would expect for activation cross sections an integration to the excitation energy which is $S_n + E_n$.

Lone

Dr. Poenitz you are correct. The numerator Γ_γ in the expression Γ_γ/D is the total radiative width of the capturing state and thus the integration is carried out to the excitation energy of the capturing state.

Gardner

The ratio, Γ_γ/D, as given in Eq. 9, when used to normalize the gamma-ray transmission coefficients is actually $\overline{\Gamma}_\gamma/D_{obs}$ where $\overline{\Gamma}_\gamma$ is the average s-wave radiation width and D_{obs} is the observed s-wave resonance spacing, both at the neutron separation energy. Eq. 10 is an alternate form of Eq. 9, where the gamma-ray transmission coefficients are expressed in terms of gamma-ray strength functions. Once this normalization is achieved, then for every incident energy, En, the integration is carried out form zero to $S_n + E_n$.

Lup

CHARGED-PARTICLE CROSS SECTION DATA
FOR FUSION PLASMA APPLICATIONS

George H. Miley

Fusion Studies Laboratory
University of Illinois, Urbana, Illinois 61801, U.S.A.

ABSTRACT

Cross-section data for fusion plasma calculations are reviewed for three categories: fusion reactions, nuclear elastic and inelastic scattering. While the data base for the basic D-T fuel cycle seems adequate for present purposes, continued refinement appears warranted. Further, increasing emphasis on advanced-fuel fusion introduces requirements for new reaction rate and charged-particle scattering data over a wider range of reacting species (light elements through ^{11}B) and over a larger energy range (to several MeV). These new needs are discussed along with suggestions for increased emphasis on providing the user with more convenient compilations. In particular, the extension of reactivities ($<\sigma v>$) to non-Maxwellian distributions, scattering matrix data, and development of computer based files are noted.

INTRODUCTION

Charged-particle cross section data are important to four aspects of fusion studies: plasma energetics, beam stopping in inertial confinement targets, first wall erosion, and radiation interactions in blanket materials. The latter three areas involve charged-particle interactions with solids. This will not be considered in any detail in the present review which concentrates on data needs for fusion plasma calculations.

To date D-T fusion has achieved almost exclusive attention in fusion research. Consequently, data needs seemed quite straight-forward, dealing with D-T fusion reactions, slowing down of the resulting fusion product (3.5-MeV alpha) and, to some extent, parasitic D-D fusion reactions. Recently, however, there has been a growing interest in "advanced" or "alternate" fusion fuels which

would eliminate the need for tritium breeding and reduce induced radioactivity and materials damage problems associated with large neutron fluxes.[1-5]

The advent of the advanced fuels (AFs) has greatly increased the data needs for fusion studies. As outlined in Table I, these fuels can be broadly separated into two groups: (1) deuterium (D)-based, and (2) proton (p)-based. In addition to introducing a multitude of new reaction species, some AF reactions result in fusion products that are at a higher energy than the 3.5-MeV alpha from D-T fusion, e.g., the D-^{3}He reaction yields a 14.7-MeV proton while a multitude of energetic charged particles are involved in the chain reactions that occur in a p-^{6}Li plasma. Since AF fusion represents an important new direction in fusion research, the associated data needs will receive special attention here.

GENERAL REQUIREMENTS

Data required for fusion plasma calculations are outlined in Table II. In the present review we will concentrate on fusion reactions (fusion reactivities) and high-energy scattering (including Coulombic and nuclear collisions associated with the slowing down of energetic particles in plasmas). While charge-exchange and ionization reactions also play a crucial role in many plasma calculations, these data are generally classified under atomic data[6].

Broadly speaking, fusion cross section activities can be divided into four general categories: basic meansurements, evaluation, interpolation/extrapolation, and tabulation (Fig. 1). Experiments result in microscopic cross sections, hopefully including data on differential angular and energy distributions. Evaluation of these data should not only involve a comparison of independent experiments but also a comparison of experimental vs. theoretical predictions. While such evaluations have attained a fairly sophisticated level in other fields such as neutronics, there remains a noticeable lack of critical reviews in areas of interest for fusion.

It is generally desirable to have reaction cross-sections cover an energy range up to 5 or 6 kT where T is the background plasma temperature. Since advanced fuels may burn at ion temperatures of 400 or 500 keV, this implies a data range to ~ 3 MeV. Of course, data for interactions involving fusion products during slowing must extend to their birth energy, e.g., up to 14 MeV for the D-^{3}He proton. In view of other uncertainties in plasma calculations, an accuracy better than 20-30% does not generally seem warranted. However, as the field continues to mature, continued refinement of the data base is highly desirable.

Tabulation and reduction of fusion cross section data is complicated by the variety of averages that are of interest. As indicated in Table II, the user may have need for speed-averaged fusion reaction data for various ion distributions (Maxwellian, mirror loss-cone, etc.) in addition to data related to charged-particle slowing in plasmas.

1) Fusion Reactivities

As the name *thermonuclear* fusion implies, fusion confinement concepts frequently involve reactions between ions comprising Maxwellian velocity distributions. Thus the "reactivity" $\langle \sigma v \rangle$, required to calculate the reaction rate R between species 1 and 2

$$R \equiv n_1 n_2 \langle \sigma v \rangle \quad , \tag{1}$$

most commonly assumes a Maxwellian distribution. This average, $\langle \sigma v \rangle_m$, is defined as

$$\langle \sigma v \rangle_m = \frac{4}{(2\pi m_1)^{1/2}} \left(\frac{\mu}{m_1 kT}\right)^{3/2} \int_0^\infty dE \, E \, \sigma(E) \, \exp\left(\frac{\mu E}{m_1 kT}\right) \quad , \tag{2}$$

where   T = the temperature of both species
m_i = mass of an ion of species i
μ = reduced mass of the two fusing ions.

This form for $\langle \sigma v \rangle_m$ assumes that both ion distributions can be assigned the same temperature T.

Several variations of the basic Maxwellian "reactivities" are of interest in particular projects. For example, in some confinement concepts fusion largely occurs by interaction of an energetic ion beam with a target plasma. The TFTR "breakeven" experiment at Princeton is an example. Corresponding calculations typically assume an isotropic angular distribution for the ion beam and a Maxwellian distribution for the background or target plasma ions. Then the appropriate averaged reactivity for the beam ions at speed v_b is

$$\langle \sigma v \rangle_b = \frac{\beta}{\sqrt{\pi}} \frac{1}{v_0} \int_0^\infty \sigma(\tfrac{1}{2} m_1 v^2) \, v^2 \, \{\exp[-\beta^2(v_0-v)^2] \tag{3}$$
$$-\exp[-\beta^2(v_0+v)^2]\}dv \quad ,$$

where the various quantities are

$$\beta^2 = \frac{m_2}{2kT}$$

v_0 = velocity of injected particle
m_2 = mass of background particle
m_1 = mass of incident particle.

Note that in order to employ $\langle\sigma v\rangle_b$ in a practical case, the user must still integrate over the speed distribution corresponding to slowing down $f_b(v_0)$ of the incident beam; that is, an integration $\int dv_0 f_b(v_0)\langle\sigma v\rangle_b$ remains while evaluation of $f_b(v_0)$ requires a knowledge of the particular fusion concept involved.

Graphical and tabular presentations for $\langle\sigma v\rangle_m$ are available in various reports [7-11] while $\langle\sigma v\rangle_b$ is presented in Ref. 7. The reactions included in the most recent compilation by Howerton[11] are indicated in Table III, along with information about the base data used for the averaging.

In a mirror reactor, instead of a Maxwellian, the ions assume a loss-cone distribution.[12] Essentially this distribution corresponds to a Maxwellian with a void in the region of velocity space where ions escape through the loss cone (Fig. 2). To date, however, workers in mirror research and also in other areas where the deviation from a Maxwellian are not too severe have ignored these effects and used $\langle\sigma v\rangle_m$ in calculations. The reason is simply that other uncertainties in the analysis have been too large to warrant the added detail in $\langle\sigma v\rangle$. However, it appears to the author that we are now rapidly approaching an era where the added accuracy will be desired and important. Indeed, this will pose a new challenge for those carrying out tabulations; namely $\langle\sigma v\rangle$ tables should be enlarged to handle more cases.

If carried to the extreme, however, such tabulations could become unwieldly. The alternative of leaving the averaging to the user doesn't seem practical either. Thus, a conscious effort, involving both tabulators and users, should be undertaken to develop a list of generic distribution functions other than Maxwellian for use in future tables. An alternate approach is to develop utility processing routines that can be employed by the user to carry out the averaging over an arbitrary distribution.

2) Fast Fusion Probabilities

As noted above, integration of beam-target reactivities over the slowing down distribution of the incident beam gives the fusion rate during slowing. This is commonly expressed in terms of the fast fusion probability p_{ij} for ion j slowing in a background plasma of species i. Thus,

$$p_{ij} = 1 - \exp(p_{ij}^*) \qquad (4a)$$

where

$$p_{ij}^* = \int_{E_{0j}}^{3/2T_i} n_i \langle\sigma v(E)\rangle_{ij} (dt/dE)_j dE . \qquad (4b)$$

The energy loss rate for ion j in the plasma, $(dE/dt)_j$, is a strong function of the plasma electron temperature T_e. For example, an approximate relation assuming only Coulomb scattering is:

$$\left(\frac{dE}{dt}\right)_j \sim -\frac{4\pi e^4 \ell n\Lambda}{v_j}\left[\frac{n_i}{m_i} + \frac{4}{3\sqrt{\pi}}\frac{n_e}{m_e}\left(\frac{m_e E}{m_j T_e}\right)^{3/2}\right], \qquad (5)$$

where the quantity $\ell n\Lambda$ is about 20 for typical magnetic plasmas and about 10 for the denser inertial confinement plasmas. Assuming, as implied earlier, a plasma with $Z = 1$ and $n_i = n_e$, we have $(dE/dt)_j \propto n_i$. Consequently, the integral in Eq. (4b) turns out to be independent of target density.

An illustration of the fast fusion probability for energetic protons slowing down in a ^{6}Li plasma is shown in Fig. 3 for T_e ranging from 100 keV to 300 keV. If, for example, the proton occurs by a ^{3}He-^{6}Li reaction, it would have a birth energy of ~ 11 MeV. From Fig. 3, this proton would have a 5% probability of fusing while slowing in a 100-keV ^{6}Li plasma. At higher electron temperatures the slowing down time is increased so that in this example, if $T_e = 300$ keV, the probability increases to ~ 21%.

3) Scattering Cross Sections Data

The slowing down of energetic fusion products in a plasma becomes increasingly important as the achievement of a "fusion grade" plasma becomes closer. As indicated in Table II, three types of "scattering" data are required: Coulombic, nuclear elastic, and nuclear inelastic. Coulombic interactions are typically treated analytically, leaving the main data needs to nuclear scattering.[13-18] The latter are particularly important for AF plasmas, and this has resulted in an increasing effort to generate nuclear elastic data in the past few years. However, virtually no data exist in the key area of nuclear inelastic scattering in a regime of interest to fusion systems.

4) Theoretical Methods

Fairly comprehensive reaction R-matrix analyses of select fusion reactions have been carried out and continued studies are in progress.[19-22] Results have been presented for T(d,n), D(d,n) D(d,p), T(t,2n) and ^{6}Li(p,^{3}He) reactions. Future extensions to nuclear elastic scattering are planned. As pointed out by G. Hale,[19] R-matrix theory provides a framework for fitting and extrapolating cross sections whereby both long-range effects (like penetration of the Coulomb-angular momentum barrier) and short-range (nuclear) effects arise in a simple and physically meaningful way. Moreover, the interaction of these effects in the theory generally leads to a different energy dependence for the low-

energy cross sections than that obtained from the representations of fusion cross sections commonly used. Indeed, there are indications from T(d,n) and T(t,2n) comparisons that the R-matrix dependence is more nearly correct.[19,20]

At higher energies, the reactions appear to be dominated by broad, overlapping structures, a few of which appear as definite bumps in the integrated cross sections. These structures can be associated with definite R-matrix levels, however, with the help of angular distribution measurements, particularly those for polarization observables. Use of all the available experimental data in these analyses offers statistical advantages, especially in cases where direct measurements of the cross sections are conflicting or incomplete. In those cases, this may even allow a resolution of the difficulties.

The use of R-matrix calculations then appears as a valuable technique for interpretation, extension, and evaluation of fusion data. In principle such calculations can yield a unified cross-section data set in which both nuclear elastic scattering and reaction cross sections are calculated from the same R-matrix parameters. Such calculations should provide a most valuable aid as evaluators attempt to further resolve and refine fusion cross section data.

FUSION REACTION AND SCATTERING DATA

In the following sections we will consider reaction and scattering data in more detail, outlining sources of available information and indicating some serious gaps in the data.

1) Reaction Data

The recent review of fusion reaction data for fusion applications by G. Shuy[4] is relied on here heavily. A summary of reaction data is presented in Table IV where it is observed that a majority of the measurements for relevant reactions contain relatively large uncertainties. This is clearly an unsatisfactory situation as the search for attractive AF systems continues. On the other hand, the situation for select key reactions is not so serious. These include:

a) D-T, D-D, and D-^{3}He reactions

While there has only been one measurement of the basic D-T reaction:[4]

$$D + T \rightarrow \alpha + n \ (17.59 \text{ MeV}) \tag{6}$$

since 1960, the integral data seem adequate from 0.01 to
15 MeV. However, as noted by Shuy [4], discrepancies in
angular distributions exist above 5 MeV. These data
could eventually become important and consequently
deserve more attention. Further, due to the vital role
of D-T in fusion, it would seem prudent to remeasure
this reaction over the entire energy range in order to
reduce the existing 10-20% uncertainty.

Measurements for the two D-D reactions

$$D + D \rightarrow {}^3He + n \text{ (3.27 MeV)} \tag{7a}$$

$$\rightarrow p + T \text{ (4.03 MeV)} \tag{7b}$$
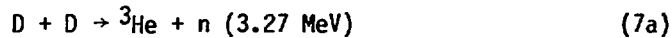
have been evaluated by Liskien and Paulsen [23] for the
range of 0.013 to 10 MeV. Results appear adequate for
fusion uses at this time.

The D-^{3}He reaction,

$$D + {}^3He \rightarrow p + \alpha \text{ (18.35 MeV)} \tag{8}$$

has received no measurements since 1960. A fairly large
uncertainty (25-35%) exists in the neighborhood of the
430 keV resonance. In view of its key position as an
AF, this question deserves attention. Hale's review
[19] suggests, however, that integral data is reasonably
good up to 15 MeV.

b) p-Based Reactions

Considerable uncertainty exists for many of the
multitude of p-based reactions. Two key fuel cycles
that are of particular interest as candidates for almost
"neutronless" fuels are p-^{6}Li and p-^{11}B. The fact
that these fuels can approach ignition[4] makes them
especially attractive.

As indicated in Table V, a p-^{6}Li fusion plasma
would involve a number of reactions in addition to the
basic reaction:

$$p + {}^6Li \rightarrow {}^3He + \alpha \text{ (4.02 MeV)} . \tag{9}$$
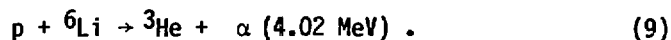
Recent measurements of the latter reaction by Elwyn[24]
over the range 0.14-3 MeV appear fairly definitive, but as
summarized in Table VI, many of the other p-^{6}Li plasma
reactions need careful attention. Indeed, recent measure-
ments of the key ^{3}He-^{6}Li reaction[25] indicate that
this cross section (with all decay channels included) is

lower than originally estimated. The result is that
ignition of p-^{6}Li for T_i below ~ 500 keV is now in
doubt.[4]

Uncertainties in the p-^{11}B reaction

$$p + {}^{11}B \rightarrow 3\alpha \qquad\qquad (10)$$

drew strong attention in recent years as interest grew
in this nearly ideal "neutronless" fusion fuel. The
recent measurement by Davidson[26] over the range 0.08-
1.4 MeV resolved some of the questions, although uncer-
tainties in the region of higher lying resonances (7
pronounced resonances are observed up to 5 MeV) require
more attention.

In addition to reaction cross sections (10),
evaluation of parasitic gamma and neutron production
requires, as indicated in Fig. 4, data for other
reactions such as ^{11}C branching ratio and ^{11}B-^{11}B
reactions. Norbeck[27] has reported recent measures of
these cross sections. Indeed, as shown in Fig. 4, the
corresponding reactivities are several orders of
magnitude lower than for p-^{11}B itself. Still, this
is important since even low levels of radioactivity must
be considered in evaluating this nearly ideal fuel.

2) Nuclear Elastic Scattering

As pointed out earlier, nuclear elastic scattering
can become an especially important mechanism in AF
plasmas due to the combination of high electron tempera-
ture and more energetic fusion products. (See, for
example, Fig. 5.) In that case, hard collisions between
energetic (MeV) fusion products and fuel plasma ions can
"knock-up" the latter to relatively high energies,
causing a bump on the tail of the otherwise Maxwellian
ion distribution. Since ions in the tail of the distri-
bution are major contributors to fusion reactions, this
"bump" can result in an important enhancement in fusion
reactivities, i.e., fusion rates. For example, the
ratio of $\langle \sigma v \rangle_{eff}$ calculated for p-^{11}B reactions in-
cluding this effect normalized by the normal Maxwellian
$\langle \sigma v \rangle$ is shown in Fig. 6. This result has led Shuy[4] to
predict ignition against Bremsstrahlung losses is
possible for p-^{11}B with T_i ~ 250 keV and T_e ~ 150 keV.

Similar enhancements in $\langle \sigma v \rangle$ have been noted for
D-D and D-^{3}He plasmas. As illustrated in Table VII,
in D-D and catalyzed-D plasmas, a variety of energetic

fusion products çan undergo nuclear elastic effects. The tritium and ^{3}He can also undergo fast fusion events during slowing, although this contribution to fusion is generally small compared to fusion reactions that occur after they thermalize. As shown in Fig. 7, when "knock-up" ions due to nuclear elastic scattering are included, the reactivity is increased by ~ 20% at T_i ~ 40 keV where ignition occurs for catalyzed-D fusion.

As outlined in Table VIII, based on Shuy's review[4], data on nuclear elastic scattering is generally available for reactions through ^{3}He-^{3}He. However, there are significant gaps in data involving heavier elements.

The most comprehensive data bank for nuclear elastic scattering is that compiled by Perkins and Cullen[13]. They have considered the 25 projectile-target combinations of the particles, p, D, T, ^{3}He, and α, based on data from about 100 references (the differential cross section data used were sent to the National Nuclear Data Center at BNL and are available from that center). They obtained nuclear (plus interference) elastic cross sections from these data by subtracting out calculated Coulombic interaction contributions. Results are presented for the following quantities integrated over the center-of-mass scattering cosine: reaction rate, average fractional energy loss per collision, average fractional energy loss per unit path length, and average laboratory scattering cosine. A typical plot of these results is shown in Fig. 8 for an alpha particle impinging on a tritium target. (This particular case has a sharp peak at an α energy of ~ 5 MeV while the behavior of other projectile-target combinations may be more or less smooth.

A basic problem encountered in the treatment of the nuclear elastic data is that the differential cross section $d\sigma/d\Omega_{NE}$ (including interferences) exhibits poles at the extreme scattering cosine (η) values, hence is nonintegrable. Consequently, Perkins and Cullen, in their analysis, define a new cross section:

$$\left(\frac{d\sigma}{d\Omega}\right)_E \equiv (1-\eta) \left(\frac{d\sigma}{d\Omega}\right)_{NE} \quad , \quad \text{(11a)}$$

$$\text{where} \quad \eta = \begin{cases} \geq 0 \text{ for like particles} \\ \geq -1 \text{ for unlike particles,} \end{cases} \quad \text{(11b)}$$

which is integrable over the entire range of interest. Then, the various quantities of interest can be obtained by direct integration. For example, the average energy loss per unit path length, $dE(E)/dx$, is simply:

$$\frac{1}{n_i} \frac{1}{E} \frac{dE(E)}{dx} = \frac{4\pi A_1 A_2}{(A_1+A_2)^2} \int_{n_1}^{n_2} \left(\frac{d\sigma}{d\Omega}\right)_E dn \qquad (12)$$

where n_1 is the target-ion number density, A_1 is the atomic mass of the projectile of energy E incident on a stationary target of atomic mass A_2 and $n_1 = -1$ for unlike particles, $n_1 = 0$ for like particles, and $n_2 = 1$.

Likewise, the average fractional energy loss per collision is:

$$\frac{D(E)}{E} = \frac{4\pi A_1 A_2}{(A_1+A_2)^2} = \frac{1}{\sigma_{NE}(E)} \int_{n_1}^{n_2} \left(\frac{d\sigma}{d\Omega}\right)_E dn \qquad (13)$$

where σ_{NE} is the total nuclear elastic (plus interference) cross section defined by

$$\sigma_{NE}(E) = 2\pi \int_{n_1}^{n_2} \frac{1}{(1-n)} \left(\frac{d\sigma}{d\Omega}\right)_E dn \quad , \qquad (14a)$$

$$n_2 \equiv \max (n_+, n_{CO}) \qquad . \qquad (14b)$$

Here n_{CO}, representing the boundary between large-angle and small-angle scattering, is taken as ~ 20° (c.m. angle). The cosine n_+ corresponds to the point where the cross section (including interference effects) goes through zero. Indeed, for most cases $n_+ \sim n_{CO}$.

Expressions for the reaction rate and average laboratory scattering cosine can be derived in similar fashion (see Ref. 13).

As pointed out by Perkins and Cullen[13], results such as presented in Fig. 8 can be used to correct energy loss rates due to Coulomb scattering, or in more exact transport calculations, to account for large-angle nuclear scattering. A problem discussed later is that present trends in these calculations involve use of scattering matrix techniques, and convenient data forms are desirable for such approaches.

3) Nuclear Inelastic Scattering

Energetic ions from AF reactions can, in addition to nuclear elastic scattering, excite nuclear levels, losing energy by inelastic scattering. For example, for the 14-MeV proton from D-^{3}He slowing against deuterium, the inelastic cross section is ~ 0.15 barns vs.~0.65 barns for elastic events.[28] Thus, while inelastic scattering does not appear to be a dominant effect, it could be significant, especially in some AF cases where ignition is marginal.

Thus far, however, inelastic scattering has not been included in any burn calculations that the author knows of, nor does an adequate data base exist. Consequently, this represents an important area for future work.

DATA REDUCTION

To understand the type of data required for fusion plasma calculations, we review the typical AF burn code flow chart of Fig. 9. Basically this program requires reactivity data (as a function of ion temperature T_i), both nuclear elastic and inelastic scattering data, and fast fusion probabilities. AF codes now being developed typically use a multigroup energy approach to handle the variety of particles, interactions, and large energy range involved. Consequently, a format consistent with such an approach should be one of the options available from data banks.

Most calculations for magnetic confinement studies have been centralized on the computers available at the National Magnetic Fusion Energy Computer Center (NMFECC) at LLL. Future data compilations could take advantage of this by making files available through this center. (Alternate access would still be necessary since a few users and the ICF community do not yet use the NMFECC facilities.)

To date most data have been distributed through reports and a standard format has not been developed. Consequently, this appears to be an opportune time for compilers, evaluators, and users to set up guidelines for development of a national data bank and format for fusion applications.

CONCLUSIONS

Based on the review presented here, we conclude that:

- The existing data for the basic fusion fuel cycles are "adequate" for present calculations, but should be improved as the field matures.

- The growing interest in AF fuel introduces new needs due to gaps in both reaction rate and scattering cross sections for the variety of ion species and energy range of interest.

- Evaluations of the accuracy of charged-particle cross sections in the regime of interest to fusion have been "sparse" to date and should be intensified in the future.

- Thus far no attempt has been made to develop a guideline for presentation of data in a form that is most convenient to workers doing plasma calculations. The use of the NMFECC computer for files appears as an important opportunity in this respect. The variety of data and various averaged quantities of interest require careful consideration by both compilers and users.

In summary, the opportunity to establish a national data bank in the rapidly growing area of charged-particle cross sections for fusion represents an exciting challenge for the nuclear data community.

REFERENCES

1. G. H. MILEY, Fusion Energy Conversion, Am. Nuclear Society, LaGrange, Illinois (1976).

2. G. H. MILEY, "Status and Prospects for Advanced-Fuel Fusion," IASTED International Symposia on Modelling, Policy and Decision in Energy Systems, Montreal, Canada, May 28-30, 1980.

3. J. R. McNALLY, JR. and K. E. ROTHE, "Advanced Fusion Fuels - A Review," Second Int'l Conf. Emerging Nuclear Energy Systems, Lausanne, Switzerland, April 1980.

4. G. W. SHUY, "Advanced Fusion Fuel Cycles and Fusion Reaction Kinetics," Report UWFDM-335, U of Wisc., Madison, Wisc, Dec. 1979.

5. R. CONN, et al., "Alternate Fusion Cycle Research," IAEA-CN-38/V5, 1980.

6. C. F. BARNETT, W. B. GAUSTER, and J. A. RAY, "Atomic and Molecular Collision Cross Sections of Interest in Controlled Thermonuclear Research," Report ORNL-3113, Oak Ridge National Laboratory, Oak Ridge, TN.

7. G. H. MILEY, et al., "Fusion Cross Sections and Reactivities, Report COO-2218-17, U of Illinois, Urbana, IL (June 1974).

8. B. H. DUANE, "Fusion Cross Section Theory," BNWL-1685, Battelle Northwest Laboratories, (1972).

9. N. JARMIE and R. SEAGRAVE (eds.), "Charged Particle Cross Sections," LA-2014, Los Alamos Scientific Laboratory (1957).

10. S. L. GREEN, "Maxwell-Averaged Cross Sections for Some Thermonuclear Reactions on Light Isotopes," UCRL-70522 (1967).

11. R. J. HOWERTON, "Maxwell-Averaged Reaction Rates $\langle \sigma v \rangle$ for Selected Reactions between Ions with Atomic Mass $\leq$ 11," Report UCRL-50400, Vol. 21, Pt. A, Lawrence Livermore Laboratory, Feb. 1979.

12. B. I. COHEN (ed.), "Status of Mirror Fusion Research 1980," UCAR 10049-80, Lawrence Livermore Laboratory (1980).

13. S. T. PERKINS and D. E. CULLEN, "Elastic Nuclear (Plus Interference) Cross Sections for Light Charged Particles," UCRL-83468, Lawrence Livermore Laboratory (January 1980).

14. D. E. CULLEN and S. T. PERKINS, "Multigroup Constants for Charged Particle Elastic Nuclear (plus Interference) Scattering of Light Isotopes," Lawrence Livermore Laboratory, Livermore, CA, UCID-17564 (1977).

15. S. T. PERKINS, "NSCAT - A Code to Obtain Charged Particle Nuclear (plus Interference) Differential Scattering Cross Sections from Experimental Data," Lawrence Livermore Laboratory, Livermore, CA, UCID-17608 (1977).

16. D. E. CULLEN and S. T. PERKINS, "Elastic Nuclear (plus Interference) Cross Sections for Light Charged Particles, Tables and Plots," to be published, Lawrence Livermore Laboratory, Livermore, CA (1980).

17. J. E. DEVANEY and M. L. STEIN, "Energy Loss by Nuclear Elastic Scattering," Nucl. Sci. Eng., 46, 323 (1971).

18. E. GREENSPAN, "Large Energy Transfer Reactions in Ion Slowing Problems," MATT-1235, Princeton Plasma Physics Laboratory (May 1976).

19. G. M. HALE and D. C. DODDER, "R-Matrix Analysis of Light-Element Reactions for Fusion Applications," LA-UR 79-2896, Los Alamos Scientific Laboratory (1979). Also see Int. Conf. on Nuclear Cross Sections for Technology, Knoxville, TN (Oct. 1979).

20. G. M. HALE, "R-Matrix Analysis of the Light Element Standards," NBS Special Publication 425, p. 302 (1975).

21. D. C. DODDER, et al., "Models Based on Multichannel R-Matrix Theory," JAERI-M 5984, p. 1 (1975).

22. G. M. HALE, "R-Matrix Methods for Light Systems," IAEA-90, Vol II, p. 1 (1976).

23. H. LISKIEN and A. PAULSEN, "An Evaluation for Cross Sections of the Reactions $T(D,n)^4He$, $D(D,n)^3He$ and $D(D,p)T$," Report EANDC(E)-144 "L", 1972.

24. A. ELWYN, R. E. HOLLAND, C. N. DAVIDS, L. MEYER-SCHUTZMEISTER, F. P. MOORING, and W. RAY, JR., "Cross Sections for the $^6Li(p,^3He)^4He$ Reaction at Energies Between 0.1 and 3.0 MeV," Phys. Rev., $\underline{C20}$, 1984 (1979).

25. A. ELWYN, et al., "Cross Sections for the $^6Li(^3He,p)$ Reaction at Energies Below 2 MeV," submitted to Phys. Rev. (1980).

26. J. DAVIDSON, H. L. BERG, and M. M. LOWRY, "Low Energy Cross Sections for $p-^{11}B(p,3\alpha)$," Report LAP-165, Calif. Institute of Technology, Pasadena, CA (1978).

27. E. NORBECK, "Neutrons from $^{11}B + ^{11}B$ Compared with Other Sources of Neutrons from an $^{11}B + p$ Burn," Report 80-32, Univ. of Iowa, August 1980.

28. R. FRANK and J. GAMMEL, "Inelastic Scattering of Protons and Neutrons by Deuterons," Phys. Rev., $\underline{93}$, 463 (1954).

Table I

Some Key Advanced Fuel Reactions

CONVENTIONAL D—T		Q_F, MeV	f_c
D + T → n + α		17.6	0.2

Advanced

			Q_F, MeV	f_c
Prime	D—D	D + D ⟨ n + ^{3}He / p + T	3.6	0.33
	D—^{3}He	D + ^{3}He → α + p	18.3	1.0
	CAT—D	Burn product T & ^{3}He in situ	21.6	0.62
Exotic	p,D — ^{6}Li	{p / D} + ^{6}Li → {α + ^{3}He / p + ^{7}Li + ⋯}	< 5.0	~0.9
	p + ^{11}B	p + ^{11}B → 3 α	8.7	1.0

Note

Q_F : total fusion energy released

f_c : fraction of energy to charged particles

TABLE II

Data Requirements

Discussed here

Fusion Cross Sections σ_f

     Reactivities (Maxwellian) $\langle\sigma v\rangle_m$

     Beam-Target (Maxwellian Target) $\langle\sigma v\rangle_b$

     Specialized Reactivities $\langle\sigma v\rangle_j$
       (j:non-Maxwellian distribution)

High-Energy Scattering

     Coulombic σ_s

     Nuclear Elastic σ_{SE}

     Nuclear Inelastic σ_{SI}

- -

Charge-Exchange σ_{c-x}

Ionization σ_I

TABLE III

Evaluated Charged Particle Induced Reactions in
The LLL Evaluated Charged Particle Library (ECPL). Ref. 11

Reaction	Q-Value (MeV)	Range (MeV)	Properties
$D(d,n)^3He$	3.37	.001-20.	c/s, ang. dist. of n
$D(t,n)^4He$	17.59	.001-20.	c/s
$D(d,p)T$	4.034	.001-20	c/s
$T(p,n)^3He$	- 0.764	1.025-20.	c/s, ang. dist. of n
$T(d,n)^4He$	17.59	.001-20.	c/s, ang. dist of n
$^3He(d,p)T$	18.354	.005-20.	c/s, ang. dist. of p
$^6Li(d,n)^7Be$	3.382	.001-20.	c/s
$^6Li(T,2n)^7Be$	- 2.87	4.31 -20.	c/s
$^6Li(d,p)^7Li$	5.027	.001-20.	c/s
$^6Li(He^3,d)$	0.11	.2 -20.	c/s
$^6Li(d,p+t+^4He)$	2.558	.001-20.	c/s
$^6Li(d,^4He)^4He$	22.374	.001-20.	c/s
$^7Li(p,n)^7Be$	- 1.64	1.88 -20.	c/s
$^7Li(p,2n)^7Be$	- 3.86	4.97 -20.	c/s
$^7Li(t,3n)^7Be$	-10.13	14.47 -20.	c/s
$^7Li(^3He,t)^7Be$	- 0.88	1.25 -20.	c/s
$^{10}B(d,n)^{11}C$	6.47	.001-20.	c/s
$^{10}B(d,p)^{11}B$	9.23	.1 -20.	c/s
$^{10}B(p,^3He+2^4He)$	- 0.44	.484-20.	c/s
$^{10}B(p,^4He)^7Be$	1.15	.1 -20.	c/s
$^{10}B(d,3^4He)$	17.914	.001-20.	c/s
$^{11}B(p,n)^{11}C$	- 2.77	3.02 -20.	c/s
$^{11}B(d,n)^{12}C$	13.73	.001-20.	c/s
$^{11}B(d,p)^{12}B$	1.14	.1 -20.	c/s
$^{11}B(p,3^4He)$	8.683	.068-20.	c/s

TABLE IV

Overview of Fusion Reaction Data

	D	T	^{3}He	p
D	0.013-14† (50-90)*	/	/	-
T	0.01 -15 (94-112,	0.04-2.2 (143-146)	/	1.1 -10 (31-45)
^{3}He	0.25-15 (117-125)	.15-1.9 (149-154)	0.06-2.2 (159-163)	~
^{6}Li	0.1 -1.0 (213-225)	0.3- 20^x (226-230)	1.2 -4.2^x (232-245)	0.14-12 (197-210)
^{7}Li	0.6 -2.6^x (287-300)	0.23-2.5^x (301-310)	0.8 -6.0^x (312-325)	0.8 -15^x (255-285)
^{7}Be	0.8 -1.7^x (331-332)	None^x	None^x	-^{x}
^{9}Be	0.15-19 (351-370)	0.52-2.1 (371-372)	1.6-20^x (376-380)	0.028-2.0 (341-345)
^{10}B	0.14-12^x (394-415)	0.8-2.0^x (416)	2.0-19^x (424-430)	0.06-6.3^x (388-390)
^{11}B	0.3 -10^x (441-453)	1.0-2.1^x (454,455)	0.9-18^x (456-460)	0.17-10^x (434-440)

Based on data in Ref. 4.

†Energy range of measurements, MeV

*Reference numbers (keyed to listing in Ref. 4)

^{x}Measurements insufficient and/or inconsistent

TABLE V

Summary of Key Reactions for the p-^{6}Li Fuel Cycle

Primary •

$$p + {}^6Li \rightarrow {}^3He \ (2.3 \ MeV) + \alpha \ (1.7 \ MeV)$$

$$^3He + {}^6Li \rightarrow p \ (11.3 \ MeV) + 2\alpha \ (2.81 \ MeV)$$

$$\rightarrow p + {}^8Be \ (various \ nuclear \ levels)$$

$$\rightarrow d \ (.088 \ MeV) + {}^7Be \ (.026 \ MeV)$$
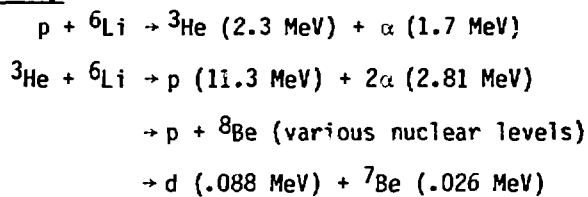
Secondary and Tertiary Reactions

$$d + {}^6Li \begin{cases} \rightarrow n + {}^7Be \ (.42 \ MeV) \\ \rightarrow p \ (4.4 \ MeV) + {}^7Li \ (.63 \ MeV) \\ \rightarrow p \ (1.6 \ MeV) + t + \alpha \\ \rightarrow n + {}^3He + \alpha \\ \rightarrow 2\alpha \ (11.2 \ MeV) \end{cases}$$

$$d + {}^3He \rightarrow p \ (14.6 \ MeV) + \alpha \ (4.7 \ MeV)$$

$$d + d \begin{cases} \rightarrow n + {}^3He \ (.82 \ MeV) \\ \rightarrow p \ (3 \ MeV) + t \ (1.01 \ MeV) \end{cases}$$

$$d + {}^7Be \rightarrow p \ (11.2 \ MeV) + 2\alpha \ (2.8 \ MeV)$$

$$d + t \rightarrow n + {}^4He \ (3.5 \ MeV)$$

$$t + {}^3He \begin{cases} \rightarrow d \ (9.6 \ MeV) + \alpha \ (4.8 \ MeV) \\ \rightarrow p + n + \alpha \end{cases}$$

$$^3He + {}^3He \rightarrow 2p \ (5.7 \ MeV) + \alpha \ (1.4 \ MeV)$$

$$^3He + {}^7Be \rightarrow 2p \ (4.5 \ MeV) + 2\alpha \ (1.1 \ MeV)$$

$$t + {}^7Be \rightarrow p \ (4.2 \ MeV) + 2\alpha$$

$$d + {}^7Li \rightarrow n + 2d \ (2.52 \ MeV)$$
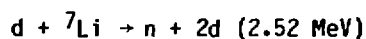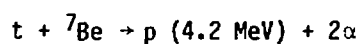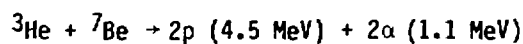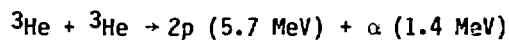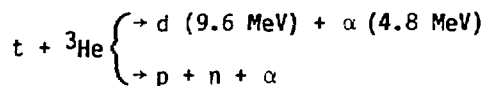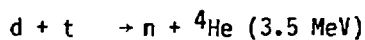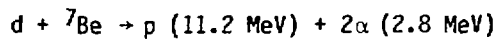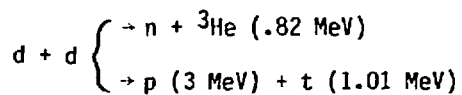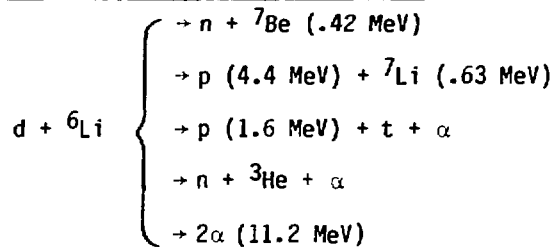
Other Reactions: over 30 side reactions plus thirteen ^{6}Li + ^{6}Li exothermic reactions

TABLE VI

Key Cross-Section Requirements for the p-^{6}Li Reactor

REACTION	REASON FOR IMPORTANCE	ADEQUATE X-SECTION DATA
^{3}He + ^{6}Li → d + ^{7}Be	A,B,	INCOMPLETE
^{3}He + ^{6}Li → n + ^{8}Be	B	INCOMPLETE
^{3}He + ^{6}Li → p + 2α	A,C,D	INCOMPLETE
^{6}Li + ^{6}Li → p + α + ^{7}Li	A,C,D	NO
"　　→ ^{3}He + ^{9}Be	A	NO
"　　→ 2p + ^{10}Be	A,B,C,D	NO
"　　→ n + ^{3}He + 2α	A,B	NO
d + ^{7}Be → p + 2α	A,C,D	NO
^{3}He + ^{7}Be → 2p + 2α	A,C,D	NO
$\bar{\alpha}$ + ^{3}He → α + $^3\bar{\text{He}}$	D	NO
$\bar{\alpha}$ + t → α + $\bar{\text{t}}$	D	NO
d + ^{6}Li → 5 channels	A,B,C,D	NO DATA ABOVE 1 MeV
^{3}He + ^{3}He → 2p + α	A,C,D	NO DATA ABOVE 2.2 MeV

A - HAS IMPORTANT EFFECT ON EQUILIBRIUM PLASMA PARAMETERS
    THROUGH $\langle\sigma v\rangle th$

B - NEUTRON AND RADIOACTIVE MATERIAL PRODUCTION

C - AFFECTS FAST FUSION PROBABILITY

D - NUCLEAR ELASTIC SCATTERING

TABLE VII

Energetic Fusion Products in D-D and Catalyzed-D Reactors*

$$d + d \begin{cases} \rightarrow n(2.45 \text{ MeV}) + {}^3\overline{\text{He}} \ (.87 \text{ MeV}) \\ \rightarrow \overline{p}(3.01 \text{ MeV}) + \overline{t}(1. \text{ MeV}) \end{cases}$$

$$d + t \quad \rightarrow n(14.06 \text{ MeV}) + \overline{\alpha}(3.5 \text{ MeV})$$

$$d + {}^3\text{He} \quad \rightarrow \overline{p}(14.68 \text{ MeV}) + \overline{\alpha}(3.67 \text{ MeV})$$

---
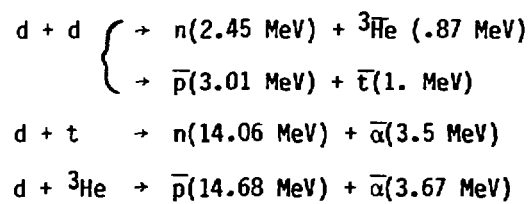
*A bar signifies an energetic ion capable of undergoing nuclear elastic scattering. The tritium and ^{3}He can also undergo fast fusion.

TABLE VIII

Summary of Nuclear Elastic Scattering

	D	T	^{3}He	^{4}He	p
D	2.0 -20[†] (46-49)[*]	/	/	0.3 -20 (164-178)	0.2 -30 (1-20)
T	0.013-10 (91-93,	1.58-2 (141-142)	/	1.2 -18.2[x] (179-182)	0.05-8.3 (21-30)
^{3}He	0.38-20 (113-116)	5.0 -19 (147-148)	5.0 -20 (155-158,	1.72-20 (183-190)	0.1 -20 (126-140)
^{6}Li	2.0 -7 (211-213)	None[x]	8.0 -20[x] (231)	2. -7.5 (246-250)	0.5 -16 (191-196)
^{7}Li	0.4 -1.8[x] (286)	None[x]	10 - 11[x] (311)	1.6 -20[x] (326-330)	0.4 -20[x] (251-254)
^{7}Be			No Measurement[x]		
^{9}Be	0.4 -7 (346-350)	0.6 -2.1 (371-372)	1.2-20[x] (373-375)	1.4 -20 (381-384)	0.2 -10 (333-340)
^{10}B	1. -16[x] (391-393)	1.5-3.3[x] (416-418)	4.0-20[x] (419-423)	2.0 -20[x] (431-433)	0.15-10.5[x] (385-387)
^{11}B			No Data[x] Reported		

Based on information in Ref. 4.

[†]Energy range of measurements, MeV

[*]Reference numbers (keyed to listing in Ref. 4)

[x]Data insufficient and/or inconsistent
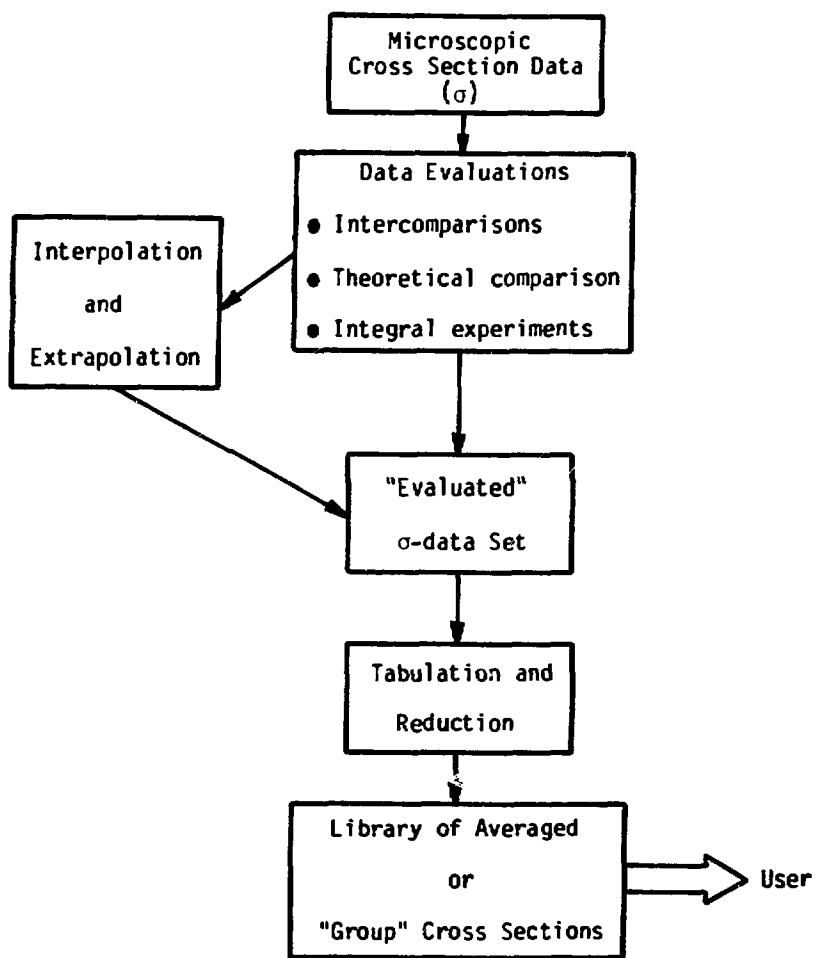
Figure 1. Data Flow Chart
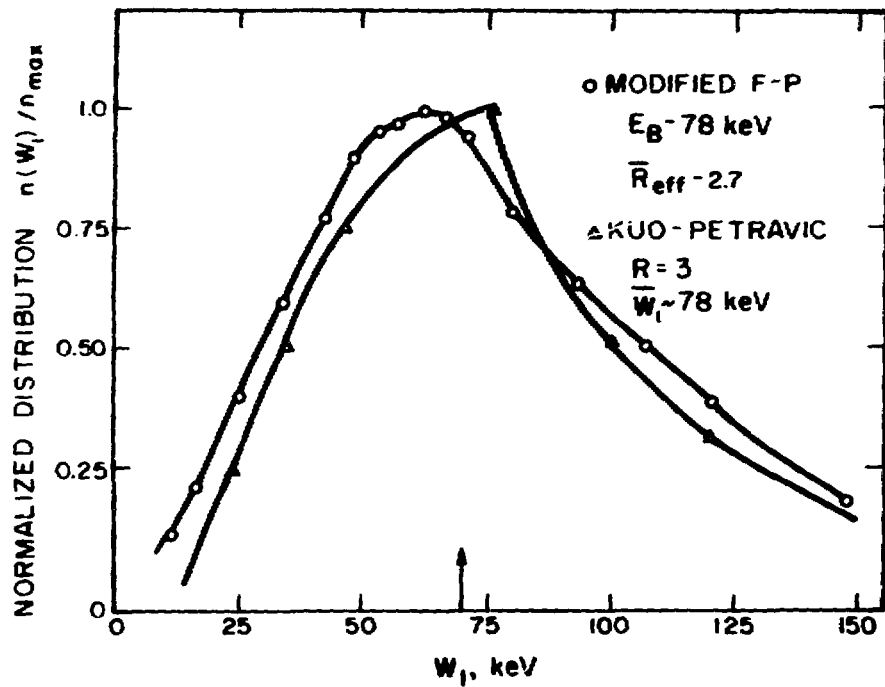
Figure 2. Mirror Loss Cone Distribution. Results from two calculations, one using a modified Fokker-Planck (F-P) method and one using a semi-empirical fit (Kuo-Petravic) are shown for injection at ~ 78 keV into a conventional mirror with effective mirror ratio ~ 3.
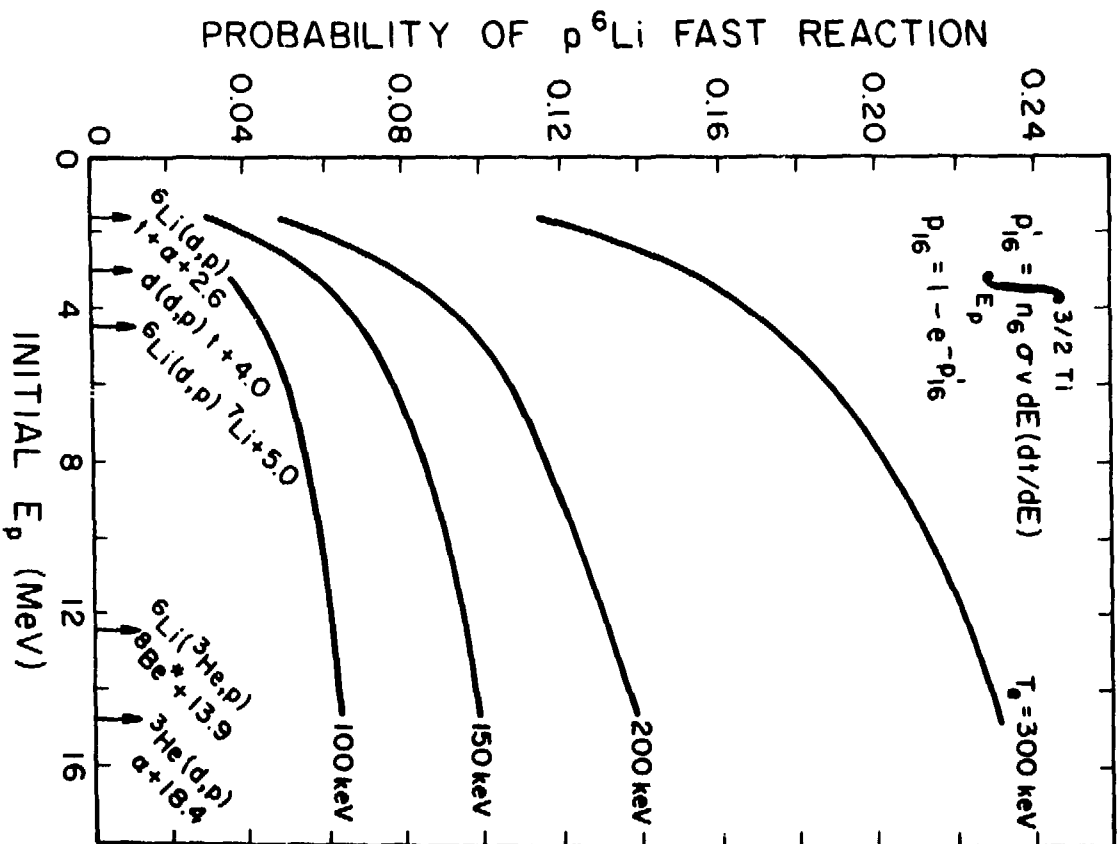
Figure 3. Fast Fusion Probabilities for Protons Slowing in a
6Li Plasma (From McNally and Rothe, Ref. 3).
Arrows on E_p axis indicate initial proton energies
from various reactions.
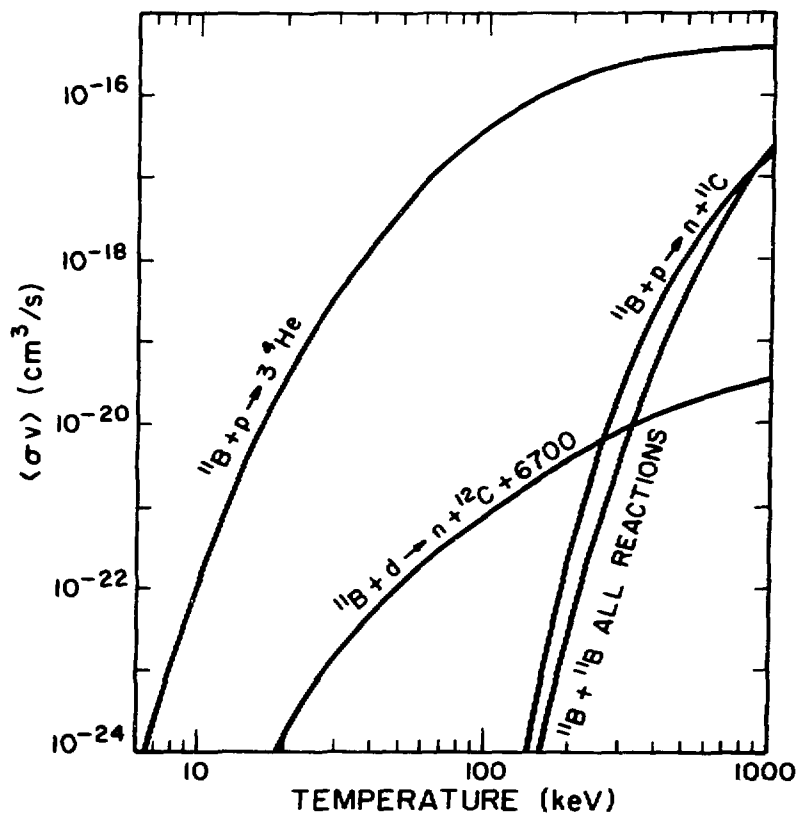
Figure 4. Reaction rates for ^{11}B reactions. The primary ^{11}B + p → 3^{4}He reaction is given to facilitate comparison with the various nuisance reactions.
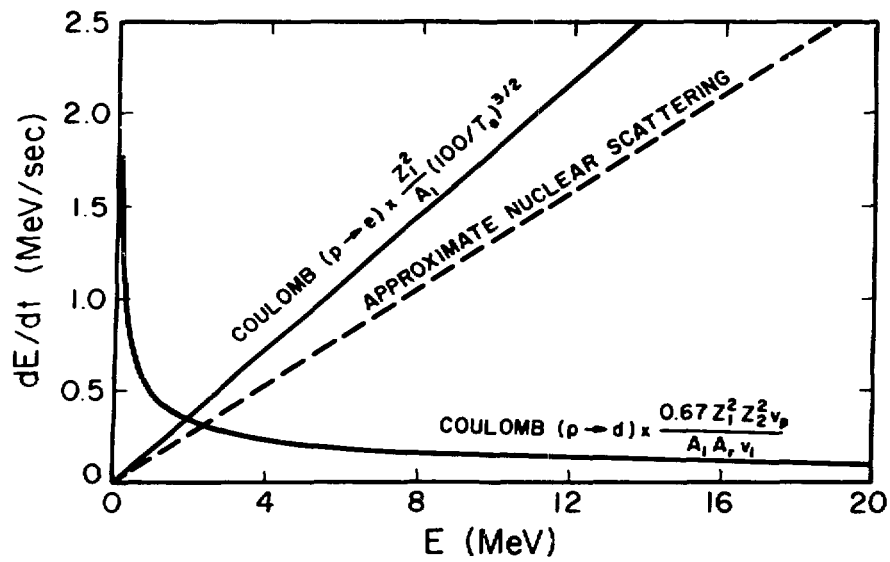
Figure 5. Energy Loss Rates for Test Ions in D-Plasma (n_e = n_d = 10^{14} particles/cm^3). From Ref. 3. Assumes $\ln \Lambda_{ie} \sim \ln \Lambda_{ii} \sim 20$. Note that at higher energies where electron "drag" is the predominant Coulombic loss rate, nuclear elastic scattering is comparable in magnitude with electron drag.
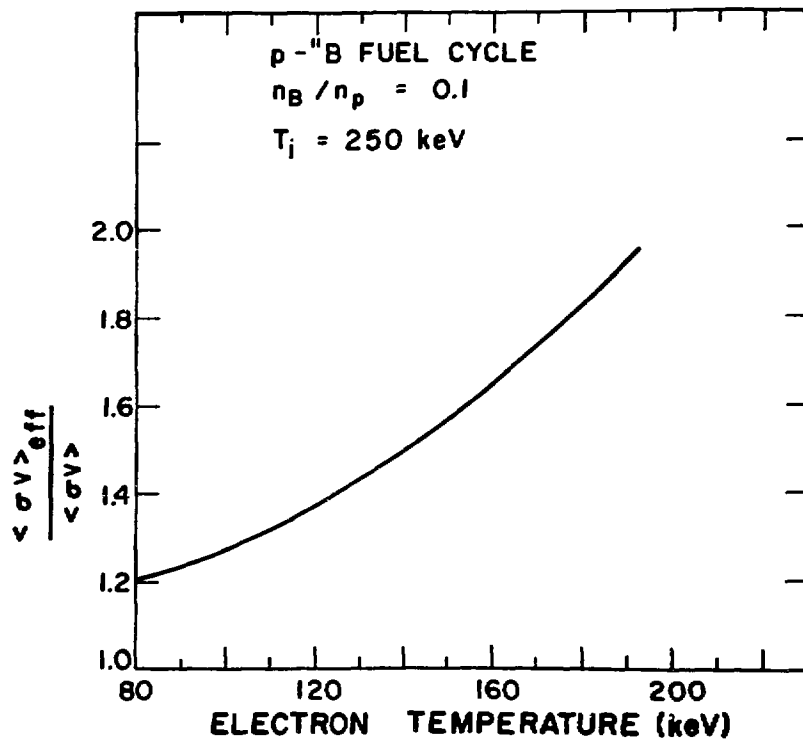
Figure 6. Effective reactivity for p-^{11}B including a non-Maxwellian distribution due to hard collisions from nuclear elastic scattering of fusion products. (From Ref. 4).
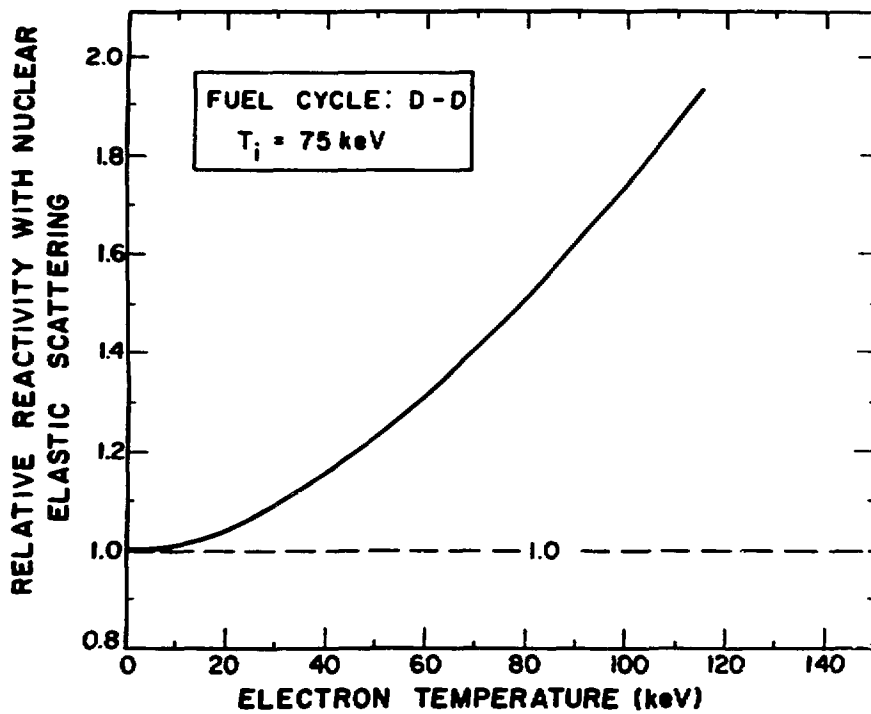
Figure 7. Ratio of $\langle\sigma v\rangle_{eff}$ to the Maxwellian value for the D-D cycle. (From Ref. 4).
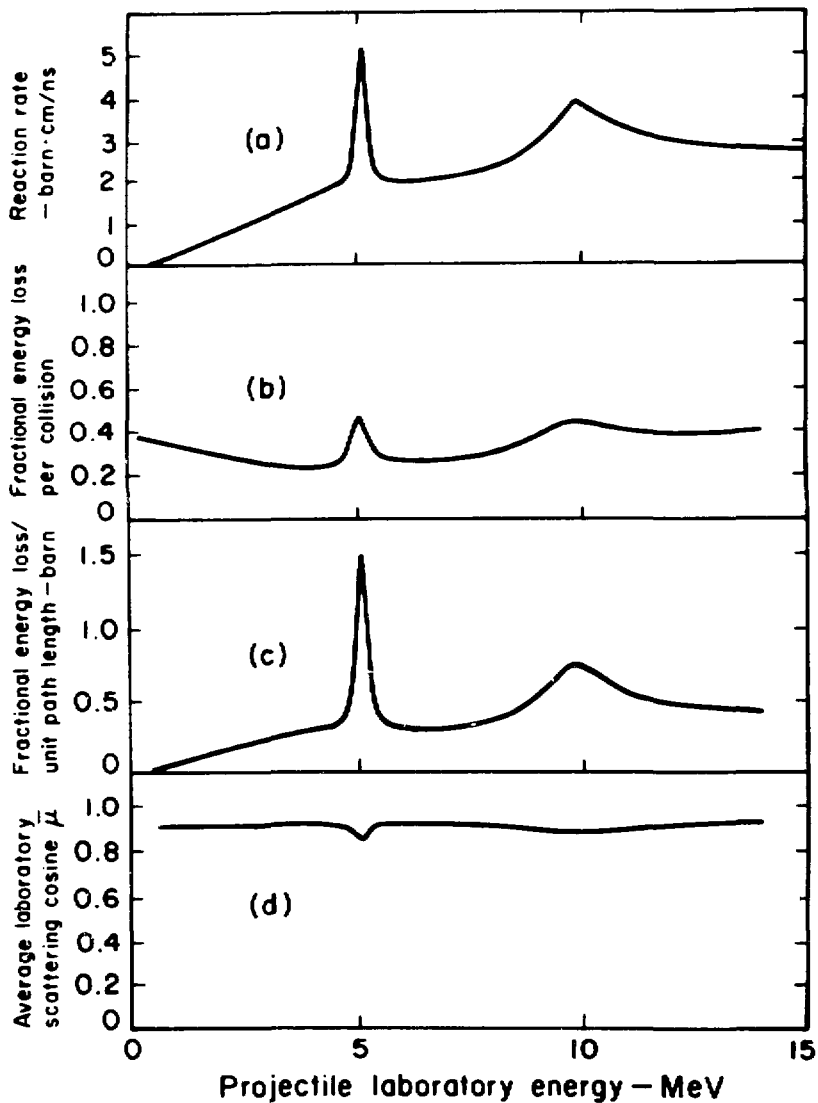
Figure 8. Evaluated Nuclear (plus Interference) Elastic Data From Scattering Integration Over the Center-of-Mass Scattering Cosine for an Alpha Particle Impinging on a Tritium Target. (Ref. 13).
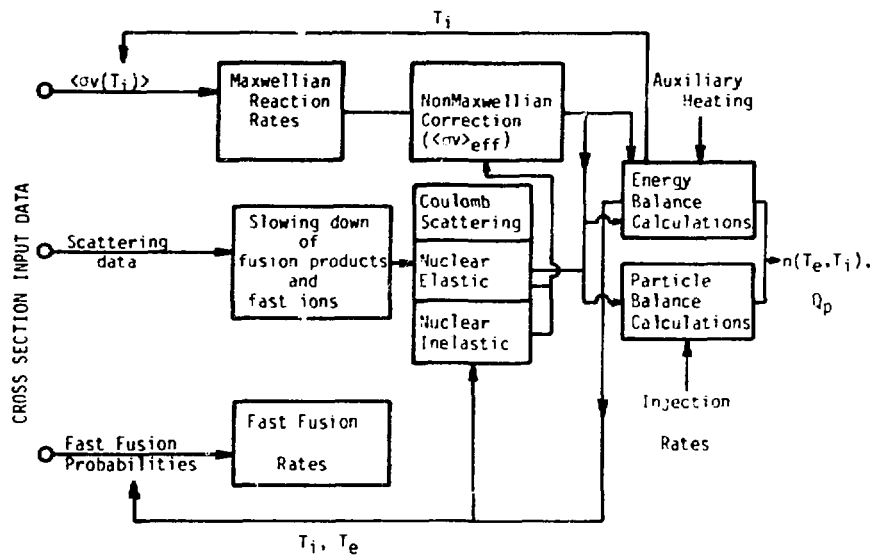
Figure 9. Flow Diagram for a Typical AF Burn Code.

Discussion

Burrows

I believe that there have been several measurements for the D+D and D+T reactions (MeV range) since 1960.

Miley

I am glad to hear that. Also, one of the attendees at the meeting pointed out to me that some new measurements are in progress. Let me hasten to add that the literature review of this paper was simply done by me as a user to quickly survey the field. Indeed, for reaction rate data I largely depended on Shuy's excellent earlier survey (Ref. 4). Some important work may have been overlooked by me in this process. Still one purpose of having a user present this view was to find out what information is generally known by workers in the field. I would hope that this will provide an incentive to others to point out oversights.

Bhat

Can you comment on the use of nuclear reaction for plasma diagnostics especially for short time response?

Miley

Actually, atomic phenomena are most frequently involved in plasma diagnostics. Examples include detection of charge-exchange neutrals escaping the plasma and spectroscopic studies of radiation from partially ionized impurities and from fuel at the cold outer layer of the plasma. Two measurements involving nuclear reactions come to mind--detection of alpha particles and also of neutrons from fusion reactions. In inertial confinement experiments, the use of magnetic spectrometer and time of flight measurements of the energy spectrum of alphas created by D-T reactions has enabled a measurement of fuel ion temperature, tamper ρR, and the buildup of electrostatic potential on the target. Measurements of neutrons can also yield ion temperature data, either based on the spread of the D-T energy distribution or on the ratio of 2.54-MeV D-D neutrons to 14-MeV D-T neutrons. In conclusion, though, I would agree that more thought should be devoted to the possible use of nuclear reactions for diagnostics.

Bhat

For p+^{11}B reactions, are the nuclear data reaction needs less for inertial confinement as opposed to plasma reactions?

Miley

The potential use of $p-^{11}B$ as a "neutronless" fuel was initially
stressed by Wood and Weaver at LLL who were interested in its use
in inertial confinement fusion (ICF) pellets. A major advantage
of the ICF approach is that losses due to synchrotron radiation
are eliminated since no confining magnetic fields are used. The
disadvantage is the large input energy required to burn $p-^{11}B$
(assuming ignition is indeed possible). One approach that we have
been considering at Illinois is the use of a small D-T "seed" in
the center of the pellet that is shock heated to ignition. It
then, in turn, heats a surrounding $p-^{11}B$ layer. This compromises
some of the advantage of $p-^{11}B$ since neutrons are produced by the
D-T seed. However, the neutron flux is still relatively low. To
attempt to burn $p-^{11}B$ with magnetic confinement would require a
very high β (plasma pressure/magnetic pressure) device such as the
Surmacs under study at UCLA. Regardless of the approach, the
nuclear data needs are much the same. As pointed out in the talk,
continued refinement of data for the basic reaction as well as
parasitic reaction data are needed. Distortion of the tail of the
ion distribution faction due to nuclear elastic scattering events
is especially important, so refinement of scattering cross section
data also becomes crucial.

Larson

The importance of specification of and inclusion of variances and
covariances in evaluation of neutron data has been stressed at
this meeting. Are you considering inclusion of this information
in charged-particle evaluations from the beginning of this effort?

Miley

I have not considered this possibility in any detail. Off-hand,
however, its inclusion sounds good to me, speaking mainly as a
user of the data. We are in a fortunate position since, compared
to the area of neutron reaction data, we are just at the beginning
of formularizing charged particle data "banks" for fusion.
Consequently, this is a good time to incorporate new procedures
that take advantage of experience gained in the neutron area.

Hale

You mentioned the possible need for new measurements of the T(d,n)
cross section since it had not been done since around 1960. As
you may know, these measurements are being carried out now at Los
Alamos for T(d,n) and also for D(d,n) and T(t,2n) at energies in
the 10-100 keV range. The results of these measurements should be
available in about a year.

Miley

I was not aware of this work and am certainly pleased to hear that
it is being done. As I stated in the paper, continued refinement
of these basic cross sections is very desirable.

Hale

When you talk about "inelastic" scattering, do you really mean
scattering from excited levels in the light targets, or do you
refer to secondary reactions induced by the products of the
(primary) fusion reactions?

Miley

I refer to collisions that result in excited levels in the
target. These levels can, in principle, decay in a variety of
ways e.g., emission of gamma rays or via "break-up" into charged
products.

SUMMARY REVIEW FOURTH DAY (25 September)

(Photon Production, Special Fission Properties, Neutron
Activation Cross Sections, Charged Particle Induced Reactions)

J.J. Schmidt

Nuclear Data Section
International Atomic Energy Agency
Vienna, Austria

Today's talks again reviewed several interesting and
important evaluation topics ranging from photon production data to
light-charged particle reaction data of interest to fusion with
most of the papers dealing with fission properties. Let me
consider with you some of the high-lights contained in these
papers.

Photon production data form an important part of evaluated
nuclear data libraries since photon production constitutes a
significant portion of the overall reaction energy output. From
Fu's concise review of the major methods for the evaluation and
estimation of photon production data the large progress in recent
years in the understanding of photon spectra became apparent,
particularly, through the introduction of the precompound model.
It appears, however, that only part of the present day's detailed
knowledge and methodical capability has entered into the evaluated
data libraries.

In his lucid review of problems encountered in the evaluation
of fission cross sections for secondary actinides Weigmann
contested the assertion by the Harwell group that present fission
theory predictions of σ_f can be as accurate as $\pm 25\%$ by pointing
out the large systematic discrepancies in data on the fission
barrier heights as deduced from resolved resonance, (d,pf) and
other measurements. In the subthreshold range a 0.5 MeV
discrepancy in barrier height may lead to an uncertainty of a
factor of five in the fission width. He furthermore emphasized
that the question of the transition state density above the
fission barrier is still far from being solved and expressed the
hope that this problem would find adequate attention at the
planned IAEA meeting (1983) on nuclear level density.

Rider reminded us of the importance of accurate fission
product yield data for the calculation of reliable decay heat
curves which are indispensable for emergency cooling design for
nuclear power reactor cores.

An impressive amount of experimental and theoretical model
data has been accumulated in the 1980 version of ENDF fission
product yields, for thermal, fission spectra and 14 MeV
neutrons. While little work has yet been devoted to modelling
yield data outside these three energy regions, Rider warned
against over-emphasizing the importance of the energy dependence
of fission yields which affected essentially only the rather
unimportant low-yield region around symmetric fission.

The energy release in fission and its partition into fragment kinetic energy and radioactive decay energy are important for determining nuclear reactor power and for considerations of nuclear safety, Sher pointed out. He demonstrated that with the recent improved knowledge of fission product yields and mass defects, fission energy releases for the major fissile and fertile isotopes can presently be calculated to accuracies of fractions of one MeV, and to somewhat poorer accuracy for other actinide isotopes. However, some problems remain in the accurate knowledge of some of the components such as fission fragment kinetic energies, beta and delayed gamma decay energies, and the prompt gamma energies.

Madland gave a fine review of the methods used in evaluating prompt fission neutron energy spectra and prompt neutron multiplicities. Particularly, his and Nix's recent work based upon a physically refined application of standard nuclear evaporation theory allows a fairly simple yet accuarate simultaneous description of the energy dependence of these two quantities and promises to lead to a considerable improvement of prompt fission spectrum data as contained in present evaluated data files. As far as the low-energy part of the spectra is concerned recent experimental work at Leningrad and other places seems definitely to rule out the existence of any structure in the energy dependence.

Maureen Gardner underlined the important role which nuclear model calculations and systematics play in interpreting and complementing the available experimental material on neutron activation cross sections. Users' accuracy needs and available money should determine the choice of using more sophisticated, accurate and expensive model calculation or less expensive semi-empirical methods. In special cases e.g., the estimation and summation of reaction cross sections over many fission product nuclides, the use of a semi-empirical approach such as that contained in Pearlstein's THRESH-2 code has proven to be successful and continues to be adequate.

Miley ended the workshop by reviewing the requirements and status of charged particle nuclear data for conventional and advanced nuclear fusion reactor concepts. While the data for the basic (d,t) fusion reaction are rather adequately known, advanced fuels introduce new needs for still largely unknown charged particle reaction and scattering data. Miley expressed the hope that the LASL R-matrix analysis of light isotope cross sections would help to fill the gap. He also emphasized the need to include, from the beginning, variance-covariance data in the evaluation.

CHARGED PARTICLE REFERENCES

No.	Lab	Work Type	Reference	Emin (MeV)	Emax (MeV)	Author, Comments

$^2H(p.2p)n$ $\sigma(E,E',\theta)$

1 LAS Revw S BNL-NCS-51363 517 81 1.4+1   Stewart. CURV.PHASE CALC.CFD EXP

$^3H(p,n)^3He$ $\sigma(E)$

2 LAS Revw S BNL-NCS-51363 517 81 NDG   Stewart. DEDUCED INVERSE

3 UI Revw S BNL-NCS-51363 915 81 1.1+0 1.0+1 Miley NDG.SURVEY-DATA FOR FUSION

$^3He(p.elastic)^3He$ $\sigma(E)$

4 LAS Revw S BNL-NCS-51363 494 81 1.0-2 1.1+1 Hale. R-MATRIX.CHARGE SYMMETRY

$^6Li(p.x)$ $\sigma(E)$

5 UI Revw S BNL-NCS-51363 915 81 1.4-1 1.2+1 Miley. NDG.SURVEY-DATA FOR FUSION

$^6Li(p.^3He)^4He$ $\sigma(E)$

6 UI Revw S BNL-NCS-51363 915 81 NDG   Miley. NDG.KEY SIGS FOR P-LI6.

$^7Li(p.x)$ $\sigma(E)$

7 UI Revw S BNL-NCS-51363 915 81 6.0-1 1.5+1 Miley NDG.SURVEY-DATA FOR FUSION

$^7Be(p.x)$ $\sigma(E)$

8 UI Revw S BNL-NCS-51363 915 81 NDG   Miley. NDG.SURVEY-DATA FOR FUSION

$^9Be(p.x)$ $\sigma(E)$

9 UI Revw S BNL-NCS-51363 915 81 2.8-2 2.0+0 Miley. NDG.SURVEY-DATA FOR FUSION

$^{10}B(p.n)^{10}C$ $\sigma(E)$

10 UI Revw S BNL-NCS-51363 915 81 6.0-2 6.3+0 Miley. NDG.SURVEY-DATA FOR FUSION

$^{11}B(p.n)^{11}C$ $\sigma(E)$

11 UI Revw S BNL-NCS-51363 915 81 1.7-1 1.0+1 Miley. NDG.SURVEY-DATA FOR FUSION

$^2H(d.p)^3H$ $\sigma(E)$

12 UI Revw S BNL-NCS-51363 915 81 NDG   Miley. NDG.KEY SIGS FOR P-LI6

$^2H(d.n)^3He$ $\sigma(E)$

13 UI Revw S BNL-NCS-51363 915 81 1.3-2 1.4+1 Miley. NDG.SURVEY-DATA FOR FUSION
       Revw S BNL-NCS-51363 915 81 NDG   Miley. NDG.KEY SIGS FOR P-LI6

$^3H(d.n)^4He$ $\sigma(E)\cdot factor$

14 LAS Revw S BNL-NCS-51363 494 81 0.0+0 3.5-2 Hale. CURV.R-MAT.S-FCT. CFD OTH

$^3H(d.n)^4He$ $\sigma(E)$

15 UI Revw S BNL-NCS-51363 915 81 1.0-2 1.5+1 Miley. NDG.KEY SIGS FOR P-LI6.
       Revw S BNL-NCS-51363 915 81 NDG   Miley. NDG.KEY SIGS FOR P-LI6

$^3He(d.elastic)^3He$ $\sigma(E)$

16 UI Revw S BNL-NCS-51363 915 81 NDG   Miley. NDG.KEY SIGS FOR P-LI6.

$^3He(d.p)^4He$ $\sigma(E)$

17 UI Revw S BNL-NCS-51363 915 81 2.5-1 1.5+1 Miley. NDG.SURVEY-DATA FOR FUSION
       Revw S BNL-NCS-51363 915 81 NDG   Miley. NDG.KEY SIGS FOR P-LI6.

$^6Li(d.n+^3He)^4He$ $\sigma(E)$

18 UI Revw S BNL-NCS-51363 915 81 NDG   Miley. NDG.KEY SIGS FOR P-LI6.

CHARGED PARTICLE REFERENCES

No.	Lab	Work Type	Reference	Emin (MeV)	Emax (MeV)	Author, Comments

$^6Li(d,p+:)^4He$ $\sigma(E)$

19 UI Revw S BNL-NCS-51363 915 81 NDG   Miley NDG.KEY SIGS FOR P LI6

$^6Li(d,\alpha)^4He$ $\sigma(E)$

20 UI Revw S BNL-NCS-51362 915 81 NDG   Miley NDG.KEY SIGS FOR P-LI6

$^6Li(d,p)^7Li$ $\sigma(E)$

21 UI Revw S BNL-NCS-51363 915 81 NDG   Miley. NDG.KEY SIGS FOR P LI6

$^6Li(d,n)^7Be$ $\sigma(E)$

22 UI Revw S BNL-NCS-51363 915 81 1.0-1 1.0+0 Miley NDG.SURVEY DATA FOR FUSION
       Revw S BNL-NCS-51363 915 81 NDG   Miley NDG.KEY SIGS FOR P-LI6

$^7Li(d,n+2d)^4He$ $\sigma(E)$

23 UI Revw S BNL-NCS-51363 915 81 NDG   Miley. NDG.KEY SIGS FOR P-LI6

$^7Li(d,n)^8Be$ $\sigma(E)$

24 UI Revw S BNL-NCS-51363 915 81 6.0-1 2.6+0 Miley. NDG.SURVEY -DATA FOR FUSION

$^7Be(d,x)$ $\sigma(E)$

25 UI Revw S BNL-NCS-51363 915 81 8.0-1 1.7+0 Miley. NDG.SURVEY DATA FOR FUSION

$^7Be(d,p+\alpha)^4He$ $\sigma(E)$

26 UI Revw S BNL-NCS-51363 915 81 NDG   Miley. NDG.KEY SIGS FOR P-LI6

$^9Be(d,x)$ $\sigma(E)$

27 UI Revw S BNL-NCS-51363 915 81 1.5-1 1.9+1 Miley. NDG.SURVEY-DATA FOR FUSION
28 UI Revw S BNL-NCS-51363 915 81 1.4-1 1.2+1 Miley. NDG.SURVEY DATA FOR FUSION

$^{11}B(d,n)^{12}C$ $\sigma(E)$

29 UI Revw S BNL-NCS-51363 915 81 3.0-1 1.0+1 Miley. NDG.SURVEY-DATA FOR FUSION

$^3H(t,2n)^4He$ $\sigma(E)$

30 UI Revw S BNL-NCS-51363 915 81 4.0-2 2.2+0 Miley NDG.SURVEY DATA FOR FUSION

$^3He(t,x)$ $\sigma(E)$

31 UI Revw S BNL-NCS-51363 915 81 1.5-1 1.9+0 Miley. NDG SURVEY-DATA FOR FUSION

$^3He(t,n+p)^4He$ $\sigma(E)$

32 UI Revw S BNL-NCS-51363 915 81 NDG   Miley. NDG.KEY SIGS FOR P-LI6.

$^3He(t,d)^4He$ $\sigma(E)$

33 UI Revw S BNL-NCS-51363 915 81 NDG   Miley NDG.KEY SIGS FOR P LI6.

$^6Li(t,x)$ $\sigma(E)$

34 UI Revw S BNL-NCS-51363 915 81 3.0 1 2.0+1 Miley. NDG.SURVEY-DATA FOR FUSION

$^7Li(t,x)$ $\sigma(E)$

35 UI Revw S BNL-NCS-51363 915 81 2.3-1 2.6+0 Miley. NDG SURVEY-DATA FOR FUSION

$^7Be(t,x)$ $\sigma(E)$

36 UI Revw S BNL-NCS-51363 915 81 NDG   Miley. NDG.SURVEY DATA FOR FUSION

$^7Be(t,n+p+\alpha)^4He$ $\sigma(E)$

37 UI Revw S BNL-NCS-51363 915 81 NDG   Miley. NDG.KEY SIGS FOR P LI6.

CHARGED PARTICLE REFERENCES

No	Lab	Work Type	Reference	Emin (MeV)	Emax (MeV)	Author, Comments

$^9Be(t,x)$ $\sigma(E)$

38 UI Revw S BNL-NCS-51363 915 81 5.2-1 2.1+0 Miley. NDG.SURVEY-DATA FOR FUSION

$^{10}B(t,x)$ $\sigma(E)$

39 UI Revw S BNL-NCS-51363 915 81 1.6+0 2.0+1 Miley. NDG.SURVEY-DATA FOR FUSION

$^{11}B(t,x)$ $\sigma(E)$

40 UI Revw S BNL-NCS-51363 915 81 1.0-0 2.1+0 Miley. NDG.SURVEY-DATA FOR FUSION

$^3He(^3He,x)$ $\sigma(E)$

41 UI Revw S BNL-NCS-51363 915 61 6.0-2 2.2+0 Miley. NDG.SURVEY-DATA FOR FUSION

$^3He(^3He,2p)^4He$ $\sigma(E)$

42 UI Revw S BNL-NCS-51363 915 81 NDG   Miley. NDG.KEY SIGS. FOR P-LI6.

$^6Li(^3He,x)$ $\sigma(E)$

43 UI Revw S BNL-NCS-51363 915 81 1.2+0 4.2+0 Miley. NDG.SURVY-DATA FOR FUSION

$^6Li(^3He,p+\alpha)^4He$ $\sigma(E)$

44 UI Revw S BNL-NCS-51363 915 81 NDG   Miley. NDG.KEY SIGS FOR P-LI6

$^6Li(^3He,d)^7Be$ $\sigma(E)$

45 UI Revw S BNL-NCS-51363 915 81 NDG   Miley. NDG.KEY SIGS FOR P-LI6

$^6Li(^3He,n)^8B$ $\sigma(E)$

46 UI Revw S BNL-NCS-51363 915 81 NDG   Miley. NDG.KEY SIGS FOR P-LI6

$^7Li(^3He,x)$ $\sigma(E)$

47 UI Revw S BNL-NCS-51363 915 81 8.0-1 6.0+0 Miley. NDG.SURVEY-DATA FOR FUSION

$^7Be(^3He,x)$ $\sigma(E)$

48 UI Revw S BNL-NCS-51363 915 81 NDG   Miley. NDG.SURVEY-DATA FOR FUSION

$^7Be(^3He,2p+\alpha)^4He$ $\sigma(E)$

49 UI Revw S BNL-NCS-51363 915 81 NDG   Miley. NDG.KEY SIGS FOR P-LI6

$^9Be(^3He,x)$ $\sigma(E)$

50 UI Revw S BNL-NCS-51363 915 81 1.6+0 2.0+1 Miley. NDG.SURVEY-DATA FOR FUSION

$^{10}B(^3He,x)$ $\sigma(E)$

51 UI Revw S BNL-NCS-51363 915 31 2.0+0 1.9+1 Miley. NDG.SURVEY-DATA FOR FUSION

$^{11}B(^3He,x)$ $\sigma(E)$

52 UI Revw S BNL-NCS-51363 915 81 9.0-1 1.8+1 Miley. NDG.SURVEY-DATA FOR FUSION

$^3H(\alpha,elastic)^3H$ $\sigma(E)$

53 UI Revw S BNL-NCS-51363 915 81 NDG   Miley. NDG.KEY SIGS FOR P-LI6

$^6Li(^6Li,n+^3He+\alpha)^4He$ $\sigma(E)$

54 UI Revw S BNL-NCS-51363 915 81 NDG   Miley. NDG.KEY SIGS FOR P-LI6

$^6Li(^6Li,p+\alpha)^7Li$ $\sigma(E)$

55 UI Revw S BNL-NCS-51363 915 81 NDG   Miley. NDG.KEY SIGS FOR P-LI6

$^6Li(^6Li,^3He)^9Be$ $\sigma(E)$

56 UI Revw S BNL-NCS-51363 915 81 NDG   Miley. NDG.KEY SIGS FOR P-LI6

CHARGED PARTICLE REFERENCES

No	Lab	Work Type	Reference	Emin (MeV)	Emax (MeV)	Author, Comments

$^6Li(^6Li\ 2p)^{10}Be$ $\sigma(E)$

57 UI Revw S BNL NCS-51363 915 81 NDG   Miley NDG KEY SIGS FOR P LI6

NEUTRON DATA REFERENCES

Element	Quantity	Energy (eV) Min	Max	Type	Documentation Ref	Vol	Page	Date	Lab
^{1}H	σ_{tot}	1.0+6	2.0+7	Revw	BNL-51363		517	Sep80	LAS
					Stewart.EVAL CS CFD H.HE GRPHS REVW				
^{1}H	σ_{el}	1.0+3	2.0+7	Revw	BNL-51363		282	Sep80	BNL
					Bhat.EVAL METHODS REVIEWED				
^{2}H	σ_{tot}	1.0+6	2.0+7	Revw	BNL-51363		517	Sep80	LAS
					Stewart.EVAL CS CFD H.HE GRPHS REVW				
^{2}H	σ_{el}	5.5+6		Revw	BNL-51363		517	Sep80	LAS
					Stewart.N-D ANGDIST FROM P D GRAPH				
^{2}H	$\sigma_{n.2n}$	1.4+7		Revw	BNL-51363		517	Sep80	LAS
					Stewart.P SPEC PHASE SPACE CALC.GRPH				
^{3}H	σ_{tot}	1.0+6	2.0+7	Revw	BNL-51363		517	Sep80	LAS
					Stewart.EVAL CS CFD H.HE.GRPHS REVW				
^{3}H	σ_{tot}	1.0-2	1.0+1	Revw	BNL-51363		494	Sep80	LAS
					Hale.R-MATRIX CALC.GRPH CFD EXPT				
^{3}He	σ_{tot}	1.0+6	2.0+7	Revw	BNL-51363		517	Sep80	LAS
					Stewart.EVAL CS CFD H.HE.GRPHS REVW				
^{3}He	$\sigma_{n.p}$	2.5-2	5.0+4	Revw	BNL-51363		282	Sep80	BNL
					Bhat.EVAL METHODS REVIEWED.				
^{3}He	$\sigma_{n.p}$	1.0+1	5.0+3	Revw	BNL-51363		494	Sep80	LAS
					Hale.B-10 NA 'HE 3 NP R MATRIX.CFD				
^{3}He	$\sigma_{n.p}$	5.0+3	2.0+6	Revw	BNL-51363		517	Sep80	LAS
					Stewart EVAL CS CFD H.HE.GRPHS REVW				
^{4}He	σ_{tot}	1.0+6	2.0+7	Revw	BNL-51363		517	Sep80	LAS
					Stewart.EVAL CS CFD H.HE.GRPHS REVW				
^{6}Li	σ_{tot}	5.0+4	5.0+5	Revw	BNL-51363		494	Sep80	LAS
					Hale R-MATRIX CALC.GRPH CFD EXPT				
^{6}Li	σ_{tot}	1.0+6	2.0+7	Revw	BNL-51363		517	Sep80	LAS
					Stewart.EVAL LI.BE CS CFD.GRPF				
^{6}Li	σ_{el}	1.0+6	2.0+7	Revw	BNL-51363		517	Sep8.	LAS
					Stewart.EVAL CFD EXPT GRPHS RE.W				
^{6}Li	σ_{inl}	2.5+6	2.0+7	Revw	BNL-51363		517	Sep80	LAS
					Stewart.EVAL CFD EXPT.GRPHS.REVW.				
^{6}Li	$\sigma_{n.nd}$	2.5+6	2.0+7	Revw	BNL-51363		517	Sep80	LAS
					Stewart.EVAL CFD EXPT GRPHS.REVW				
^{6}Li	$\sigma_{n.t}$	2.5-2	1.0+5	Revw	BNL-51363		282	Sep80	BNL
					Bhat.EVAL METHODS REVIEWED				
^{6}Li	$\sigma_{n.t}$	5.0+4	5.0+5	Revw	BNL-51363		494	Sep80	LAS
					Hale.R-MATRIX CALC.GRPH.CFD EXPT				

NEUTRON DATA REFERENCES

Element	Quantity	Energy (eV) Min	Max	Type	Documentation Ref Vol	Page Date	Lab
^{6}Li	$\sigma_{n,t}$	1.0+0	1.0+3	Revw	BNL-51363	494 Sep80	LAS
					Hale.B-10 NA/LI-6 NA.R-MATRIX.CFD.		
^{7}Li	σ_{tot}	1.0+6	2.0+7	Revw	BNL-51363	517 Sep80	LAS
					Stewart.EVAL LI,BE CS CFD.GRPHS.REVW		
^{7}Li	$\sigma_{n,n'\gamma}$	5.0+5	1.0+7	Revw	BNL-51363	517 Sep80	LAS
					Stewart.EVAL CS CURVE DISCUSSED.		
^{7}Li	$\sigma_{n,nt}$	1.0+7	2.0+7	Revw	BNL-51363	517 Sep80	LAS
					Stewart.EVAL CFD EXPT.GRPHS.REVW.		
^{9}Be	σ_{tot}	1.0+6	2.0+7	Revw	BNL-51363	517 Sep80	LAS
					Stewart.EVAL LI,BE CS CFD.GRPHS.REVW		
^{9}Be	$\sigma_{n,2n}$	2.5+6	2.0+7	Revw	BNL-51363	517 Sep80	LAS
					Stewart.EVAL LI,BE CS CFD.GRPHS.REVW		
^{10}B	σ_{tot}	1.0+5	2.0+7	Revw	BNL-51363	517 Sep80	LAS
					Stewart.EVAL ENDF-B/V.GRPH.REVW.		
^{10}B	$\sigma_{n,\alpha}$	2.5-2	1.0+5	Revw	BNL-51363	282 Sep80	BNL
					Bhat.EVAL METHODS REVIEWED.		
^{10}B	$\sigma_{n,\alpha}$	1.0+1	5.0+3	Revw	BNL-51363	494 Sep80	LAS
					Hale.B-10 NA/HE-3 NP.R-MATRIX.CFD.		
^{10}B	$\sigma_{n,\alpha}$	1.0+0	1.0+3	Revw	BNL-51363	494 Sep80	LAS
					Hale.B-10 NA/LI-6 NA.R-MATRIX.CFD.		
^{11}B	σ_{tot}	1.0+5	2.0+7	Revw	BNL-51363	517 Sep80	LAS
					Stewart.EVAL ENDF-B/V.GRPH.REVW.		
^{11}B	$\sigma_{n,\gamma}$	Maxw			Revw BNL-51363	331 Sep80	BNL
					Mughabghab.PARTIAL CS CALC.CFD.TBL.		
^{11}B	γ Spectra	Maxw			Revw BNL-51363	331 Sep80	BNL
					Mughabghab.G INT CALC CFD EXPT.TBL.		
^{12}C	σ_{tot}	1.0+5	2.0+7	Revw	BNL-51363	517 Sep80	LAS
					Stewart.EVAL ENDF-B/V.GRPH.REVW.		
^{12}C	$\sigma_{el}(\theta)$		1.8+6	Revw	BNL-51363	282 Sep80	BNL
					Bhat.EVAL METHODS REVIEWED.		
^{12}C	$\sigma_{n,x}$	5.0+6	2.0+7	Revw	BNL-51363	517 Sep80	LAS
					Stewart.EVAL.PARTIAL REACTIONS.GRPH		
^{12}C	$\sigma_{n,\gamma}$	Maxw			Revw BNL-51363	331 Sep80	BNL
					Mughabghab.PARTIAL CS CALC.CFD.TBL.		
^{12}C	γ Spectra	Maxw			Revw BNL-51363	331 Sep80	BNL
					Mughabghab.G INT CALC CFD EXPT.TBL.		
^{12}C	$\sigma_{n,n'\gamma}$	4.8+6	2.0+7	Revw	BNL-51363	517 Sep80	LAS
					Stewart.EVAL. 4.4 MEV STATE.GRPH.		

NEUTRON DATA REFERENCES

Element	Quantity	Energy (eV) Min	Max	Type	Documentation Ref Vol	Page	Date	Lab
^{13}C	$\sigma_{n,\gamma}$	Maxw			Revw BNL-51363	331	Sep80	BNL
					Mughabghab.PARTIAL CS CALC.CFD.TBL.			
^{14}N	$\sigma_{n,x}$	1.0+6	2.0+7	Revw	BNL-51363	517	Sep80	LAS
					Stewart.EVAL.PARTIAL REACTIONS.GRPH			
^{16}O	$\sigma_{n,x}$	1.0+6	2.0+7	Revw	BNL-51363	517	Sep80	LAS
					Stewart.EVAL.PARTIAL REACTIONS.GRPH			
^{19}F	$\sigma_{n,x}$	1.0+6	2.0+7	Revw	BNL-51363	517	Sep80	LAS
					Stewart.EVAL.PARTIAL REACTIONS.GRPH			
^{19}F	Res.Params.	2.7+5			Revw BNL-51363	331	Sep80	BNL
					Mughabghab.WN.WG CALC FROM THERMAL.			
^{20}Ne	$\sigma_{n,\gamma}$	Maxw			Revw BNL-51363	331	Sep80	BNL
					Mughabghab.PARTIAL CS CALC.CFD.TBL.			
^{22}Ne	$\sigma_{n,\gamma}$	Maxw			Revw BNL-51363	331	Sep80	BNL
					Mughabghab.PARTIAL CS CALC.CFD.TBL.			
^{23}Na	$\sigma_{n,2n}$	1.3+7	2.1+7	Revw	BNL-51363	241	Sep80	ANL
					Poenitz.VARIOUS EVALS CFD.GRPH.			
^{26}Mg	$\sigma_{n,\gamma}$	Maxw			Revw BNL-51363	331	Sep80	BNL
					Mughabghab.PARTIAL CS CALC.CFD.TBL.			
^{27}Al	σ_{nem}	1.5+7			Revw BNL-51363	647	Sep80	LAS
					Arthur.HF CFD EXPT.EVAL REVW.GRPH.			
^{34}S	$\sigma_{n,\gamma}$	Maxw			Revw BNL-51363	331	Sep80	BNL
					Mughabghab.PARTIAL CS CALC.CFD.TBL.			
Ca	$\sigma_{n,x\gamma}$	8.0+6	2.0+7	Revw	BNL-51363	738	Sep80	ORL
					Fu.HF CALC CFD EXPT.GRPH.REVW.			
^{40}Ca	$\sigma_{n,\gamma}$	Maxw			Revw BNL-51363	331	Sep80	BNL
					Mughabghab.CALC CS CFD EXPT.			
^{42}Ca	$\sigma_{n,\gamma}$	Maxw			Revw BNL-51363	331	Sep80	BNL
					Mughabghab.CALC CS CFD EXPT.			
^{44}Ca	$\sigma_{n,\gamma}$	Maxw			Revw BNL-51363	331	Sep80	BNL
					Mughabghab.CALC CS CFD EXPT.			
^{46}Ca	$\sigma_{n,\gamma}$	Maxw			Revw BNL-51363	331	Sep80	BNL
					Mughabghab.COH SCT AMP CALC.			
^{48}Ca	$\sigma_{n,\gamma}$	Maxw			Revw BNL-51363	331	Sep80	BNL
					Mughabghab.COH SCT AMP CALC.			
^{45}Sc	$\sigma_{n,2n}$	1.0+7	1.8+7	Revw	BNL-51363	647	Sep80	LAS
					Arthur.CALC/EXPT RATIO.EVAL REVW.			
Ti	$\sigma_{n,x\gamma}$	3.3+6	1.8+7	Revw	BNL-51363	738	Sep80	ORL
					Fu.EVAL CFD EXPT.GRPH.REVW.			

NEUTRON DATA REFERENCES

Element	Quantity	Energy (eV) Min	Max	Type	Documentation Ref Vol	Page	Date	Lab
Ti	σ_{nem}	1.5+7		Revw	BNL-51363	647	Sep80	LAS
					Arthur.HF CFD EXPT.EVAL REVW.GRPH.			
^{48}Ti	σ_{tot}	1.0+4	8.0+4	Revw	BNL-51363	365	Sep80	KFK
					Froehner.MLBW,R-M,KAPUR-PIERLS CFD.			
^{51}V	σ_{nem}	1.5+7		Revw	BNL-51363	647	Sep80	LAS
					Arthur.HF CFD EXPT.EVAL REVW.GRPH.			
Cr	σ_{tot}	1.0+6	1.5+6	Revw	BNL-51363	561	Sep80	ANL
					Guenther+GRPH.CS EXTRAP FOR EVAL.			
Cr	σ_{nem}	1.5+7		Revw	BNL-51363	647	Sep80	LAS
					Arthur.HF CFD EXPT.EVAL REVW.GRPH.			
Fe	σ_{tot}	1.0+6	2.8+6	Revw	BNL-51363	561	Sep80	ANL
					Guenther+GRPH.CS EXTRAP FOR EVAL.			
Fe	$\sigma_{el}(\theta)$	1.5+7	1.8+7	Revw	BNL-51363	647	Sep80	LAS
					Arthur.CALC VS EXPT.EVAL REVW.			
Fe	σ_{nem}	1.5+7		Revw	BNL-51363	647	Sep80	LAS
					Arthur.HF CFD EXPT.EVAL REVW.GRPH.			
^{56}Fe	Evaluation	1.0+7	4.0+7	Revw	BNL-51363	647	Sep80	LAS
					Arthur.GNASH CALC.EVAL REVW.			
^{56}Fe	σ_{tot}	2.2+4	2.5+4	Revw	BNL-51363	401	Sep80	RPI
					Block.FILTERED BEAM METHOD.REVW.			
Ni	σ_{tot}	1.3+6	4.8+6	Revw	BNL-51363	561	Sep80	ANL
					Guenther+GRPH.CS EXTRAP FOR EVAL.			
Ni	σ_{tot}	1.0+6	4.0+6	Revw	BNL-51363	561	Sep80	ANL
					Guenther+BEST VALUE EVAL EXAMPLE.			
Ni	σ_{el}	1.0+6	4.0+6	Revw	BNL-51363	561	Sep80	ANL
					Guenther+BEST VALUE EVAL EXAMPLE.			
Ni	σ_{inl}	1.0+6	4.0+6	Revw	BNL-51363	561	Sep80	ANL
					Guenther+BEST VALUE EVAL EXAMPLE.			
Ni	σ_{nem}	1.5+7		Revw	BNL-51363	647	Sep80	LAS
					Arthur.HF CFD EXPT.EVAL REVW.GRPH.			
^{58}Ni	$\sigma_{n,2n}$	1.3+7	2.2+7	Revw	BNL-51363	647	Sep80	LAS
					Arthur.GNASH CALC VS EXPT.EVAL REVW.			
^{60}Ni	σ_{tot}	5.0+5	5.0+6	Revw	BNL-51363	561	Sep80	ANL
					Guenther+GRPH.OPTMDL CALC FOR EVAL.			
^{60}Ni	$\sigma_{el}(\theta)$	1.5+6	4.0+6	Revw	BNL-51363	561	Sep80	ANL
					Guenther+ANGDIST.GRPH.OPTMDL FOR EVL			
Cu	$\sigma_{n,x\gamma}$	1.2+7	1.8+7	Revw	BNL-51363	738	Sep80	ORL
					Fu.ENDF/B-V CFD EXPT.GRPH.REVW.			

NEUTRON DATA REFERENCES

Element	Quantity	Energy (eV) Min	Max	Type	Documentation Ref	Vol	Page	Lab Date
Cu	σ_{nem}	1.5+7		Revw	BNL-51363	647	Sep80	LAS
					Arthur.HF CFD EXPT.EVAL REVW.GRPH.			
^{63}Cu	$\sigma_{n,2n}$	1.2+7	2.0+7	Revw	BNL-51363	614	Sep80	IRK
					Vonach+EVAL,METHODS,PROCEDURES.GRPH.			
^{64}Zn	$\sigma_{n,p}$	3.0+6	1.5+7	Revw	BNL-51363	614	Sep80	IRK
					Vonach+EVAL,METHODS,PROCEDURES.GRPH.			
^{85}Rb	$\sigma_{n,\gamma}$	1.0+4	3.0+6	Revw	BNL-51363	647	Sep80	LAS
					Arthur.CS CALC FROM G STF.CFD.			
^{85}Rb	$\sigma_{n,\gamma}$	1.0+4	3.0+6	Revw	BNL-51363	882	Sep80	LRL
					Gardner.CALC FROM G STF VS EXPT.GRPH			
^{87}Rb	$\sigma_{n,\gamma}$	1.0+4	3.0+6	Revw	BNL-51363	647	Sep80	LAS
					Arthur.CS CALC FROM G STF.CFD.			
^{87}Rb	$\sigma_{n,\gamma}$	1.0+4	3.0+6	Revw	BNL-51363	882	Sep80	LRL
					Gardner.CALC FROM G STF VS EXPT.GRPH			
^{89}Y	$\sigma_{n,2n}$	1.0+7	1.8+7	Revw	BNL-51363	647	Sep80	LAS
					Arthur.CALC/EXPT RATIO.EVAL REVW.			
^{89}Y	$\sigma_{n,2n}$	1.2+7	2.0+7	Revw	BNL-51363	647	Sep80	LAS
					Arthur.GNASH CALC VS EXPT.EVAL REVW.			
^{90}Zr	$\sigma_{n,2n}$	1.2+7	1.8+7	Revw	BNL-51363	882	Sep80	LRL
					Gardner.CALC CFD EXPT.GRPH.REVW.			
^{90}Zr	$\sigma_{n,2n}$	1.2+7	1.9+7	Revw	BNL-51363	614	Sep80	IRK
					Vonach+EVAL,METHODS,PROCEDURES.GRPHS			
^{90}Zr	$\sigma_{n,p}$	2.0+6	2.0+7	Revw	BNL-51363	882	Sep80	LRL
					Gardner.CS SYSTEMATICS.GRPH.REVW.			
^{93}Nb	$\sigma_{n,\gamma}$	1.0+3	3.0+6	Revw	BNL-51363	882	Sep80	LRL
					Gardner.CS CALC FROM G STF.GRPH.			
^{93}Nb	σ_{nem}	1.5+7		Revw	BNL-51363	647	Sep80	LAS
					Arthur.HF CFD EXPT.EVAL REVW.GRPH.			
^{94}Nb	$\sigma_{n,\gamma}$	1.0+3	3.0+6	Revw	BNL-51363	882	Sep80	LRL
					Gardner.CS CALC FROM G STF.GRPH.			
^{95}Nb	$\sigma_{n,\gamma}$	1.0+3	3.0+6	Revw	BNL-51363	882	Sep80	LRL
					Gardner.CS CALC FROM G STF.GRPH.			
^{92}Mo	σ_{el}	2.0+6	1.6+7	Revw	BNL-51363	882	Sep80	LRL
					Gardner.PCT CS OF REACTION CALC.GRPH			
^{92}Mo	σ_{inl}	2.0+6	1.6+7	Revw	BNL-51363	882	Sep80	LRL
					Gardner.PCT CS OF REACTION CALC.GRPH			
^{92}Mo	$\sigma_{n,\gamma}$	2.0+6	5.0+6	Revw	BNL-51363	882	Sep80	LRL
					Gardner.PCT CS OF REACTION CALC.GRPH			

NEUTRON DATA REFERENCES

Element	Quantity	Energy (eV) Min	Max	Type	Documentation Ref	Vol	Page	Date	Lab
^{92}Mo	$\sigma_{n,2n}$	1.3+7	2.0+7	Revw	BNL-51363		882	Sep80	LRL
					Gardner.CALC CFD EXPT.GRPH.REVW.				
^{92}Mo	$\sigma_{n,p}$	2.0+6	1.6+7	Revw	BNL-51363		882	Sep80	LRL
					Gardner.PCT CS OF REACTION CALC.GRPH				
^{92}Mo	$\sigma_{n,np}$	1.0+7	1.6+7	Revw	BNL-51363		882	Sep80	LRL
					Gardner.PCT CS OF REACTION CALC.GRPH				
^{92}Mo	$\sigma_{n,\alpha}$	4.0+6	1.6+7	Revw	BNL-51363		882	Sep80	LRL
					Gardner.PCT CS OF REACTION CALC.GRPH				
^{103}Rh	σ_{el}	2.0+5	1.6+6	Revw	BNL-51363		592	Sep80	BRC
					LaGrange.OPT-STATMDL CALC.GRPH.CFD				
^{103}Rh	σ_{pot}	2.0+5	1.6+6	Revw	BNL-51363		592	Sep80	BRC
					LaGrange.OPT-STATMDL CALC.TBL.CFD.				
^{103}Rh	$\sigma_{dif.inl}$	2.0+5	1.6+6	Revw	BNL-51363		592	Sep80	BRC
					LaGrange.OPT-STATMDL CALC.GRPH.CFD				
^{103}Rh	$<\Gamma>/D$	2.0+5	1.6+6	Revw	BNL-51363		592	Sep80	BRC
					LaGrange.OPT-STATMDL CALC.TBL.CFD.				
^{107}Ag	σ_{tot}	1.0+5	1.0+7	Revw	BNL-51363		592	Sep80	BRC
					LaGrange.CC.OPTMDL CFD.GRPHS.REVW.				
^{126}Sn	$\sigma_{n,\gamma}$	Maxw		Revw	BNL-51363		331	Sep80	BNL
					Mughabghab.LANE-LYNN TH CALC				
^{132}Te	$\sigma_{n,\gamma}$	Maxw		Revw	BNL-51363		331	Sep80	BNL
					Mughabghab.LANE-LYNN TH CALC				
^{136}Xe	$\sigma_{n,\gamma}$	Maxw		Revw	BNL-51363		331	Sep80	BNL
					Mughabghab.PARTIAL CS CALC.CFD.TBL.				
^{136}Xe	γ Spectra	Maxw		Revw	BNL-51363		331	Sep80	BNL
					Mughabghab.LANE-LYNN TH VERIFIED.				
^{142}Nd	$\sigma_{n,2n}$	1.5+7		Revw	BNL-51363		882	Sep80	LRL
					Gardner.CALC CFD EXPT.GRPH.REVW.				
^{144}Nd	$\sigma_{n,2n}$	1.5+7		Revw	BNL-51363		882	Sep80	LRL
					Gardner.CALC CFD EXPT.GRPH.REVW.				
^{146}Nd	$\sigma_{n,2n}$	1.5+7		Revw	BNL-51363		882	Sep80	LRL
					Gardner.CALC CFD EXPT.GRPH.REVW.				
^{148}Nd	$\sigma_{n,2n}$	1.5+7		Revw	BNL-51363		882	Sep80	LRL
					Gardner.CALC CFD EXPT.GRPH.REVW.				
^{150}Nd	$\sigma_{n,2n}$	1.5+7		Revw	BNL-51363		882	Sep80	LRL
					Gardner.CALC CFD EXPT.GRPH.REVW.				
^{148}Sm	$\sigma_{n,2n}$	1.5+7		Revw	BNL-51363		882	Sep80	LRL
					Gardner.CALC CFD EXPT.GRPH.REVW.				

NEUTRON DATA REFERENCES

Element	Quantity	Energy (eV) Min	Max	Type	Documentation Ref	Vol	Page	Date	Lab
^{150}Sm	$\sigma_{n,2n}$	1.5+7		Revw	BNL-51363		882	Sep80	LRL
				Gardner.CALC CFD EXPT.GRPH.REVW					
^{152}Sm	$\sigma_{n,2n}$	1.5+7		Revw	BNL-51363		882	Sep80	LRL
				Gardner.CALC CFD EXPT.GRPH.REVW					
^{154}Sm	$\sigma_{n,2n}$	1.5+7		Revw	BNL-51363		882	Sep80	LRL
				Gardner.CALC CFD EXPT.GRPH.REVW					
^{151}Eu	$\sigma_{n,2n}$	1.5+7		Revw	BNL-51363		882	Sep80	LRL
				Gardner.CALC CFD EXPT.GRPH.REVW					
^{155}Gd	$\sigma_{n,2n}$	1.5+7		Revw	BNL-51363		882	Sep80	LRL
				Gardner.CALC CFD EXPT.GRPH.REVW					
^{156}Gd	$\sigma_{n,2n}$	1.5+7		Revw	BNL-51363		882	Sep80	LRL
				Gardner.CALC CFD EXPT.GRPH.REVW.					
^{158}Gd	$\sigma_{n,2n}$	1.5+7		Revw	BNL-51363		882	Sep80	LRL
				Gardner.CALC CFD EXPT.GRPH.REVW.					
^{160}Gd	$\sigma_{n,2n}$	1.5+7		Revw	BNL-51363		882	Sep80	LRL
				Gardner.CALC CFD EXPT.GRPH.REVW.					
^{168}Er	Res.Params.	0.0+0	4.7+3	Revw	BNL-51363		450	Sep80	BNL
				Liou.METHODS TO CALC D.TBLS.GRPHS.					
^{168}Er	$<\Gamma>/D$	1.4+2	4.6+3	Revw	BNL-51363		450	Sep80	BNL
				Liou.METHODS TO CALC D.TBLS.GRPHS.					
^{182}W	σ_{tot}	1.0+5	2.5+6	Revw	BNL-51363		561	Sep80	ANL
				Guenther+GRPH.FLUCT CORRC FOR EVAL.					
^{182}W	$\sigma_{n,2n}$	1.5+7		Revw	BNL-51363		882	Sep80	LRL
				Gardner.CALC CFD EXPT.GRPH.REVW.					
^{183}W	$\sigma_{n,2n}$	1.5+7		Revw	BNL-51363		882	Sep80	LRL
				Gardner.CALC CFD EXPT.GRPH.REVW.					
^{184}W	σ_{tot}	1.0+5	2.5+6	Revw	BNL-51363		561	Sep80	ANL
				Guenther+GRPH.FLUCT CORRC FOR EVAL.					
^{184}W	σ_{inl}	1.5+7		Revw	BNL-51363		647	Sep80	LAS
				Arthur.N SPEC.ENDF.CALC VS EXPT.					
^{184}W	$\sigma_{n,2n}$	1.5+7		Revw	BNL-51363		647	Sep80	LAS
				Arthur.N SPEC ENDF.CALC VS EXPT.					
^{184}W	$\sigma_{n,2n}$	1.5+7		Revw	BNL-51363		882	Sep80	LRL
				Gardner.CALC CFD EXPT.GRPH.REVW.					
^{184}W	$\sigma_{n,xn}$	1.5+7		Revw	BNL-51363		647	Sep80	LAS
				Arthur.N SPEC.ENDF.CALC VS EXPT.					
^{184}W	$\sigma_{n,em}$	1.5+7		Revw	BNL-51363		647	Sep80	LAS
				Arthur.N SPEC ENDF.CALC VS EXPT.					

NEUTRON DATA REFERENCES

Element	Quantity	Energy (eV) Min	Max	Type	Documentation Ref	Vol	Page	Date	Lab
^{184}W	$\sigma_{n,np}$	1.5+7		Revw	BNL-51363		647	Sep80	LAS
					Arthur.N SPEC.ENDF VS EXPT.GRPH				
^{186}W	σ_{tot}	1.0+5	2.5+6	Revw	BNL-51363		561	Sep80	ANL
					Guenther+GRPH.FLUCT CORRC FOR EVAL				
^{186}W	σ_{el}	3.0+6		Revw	BNL-51363		561	Sep80	ANL
					Guenther+TBLS.MULT EVENT SCT CORRC				
^{186}W	$\sigma_{dif.inl}$	3.0+6		Revw	BNL-51363		561	Sep80	ANL
					Guenther+TBLS.MULT EVENT SCT CORRC				
^{186}W	$\sigma_{n,2n}$	1.5+7		Revw	BNL-51363		882	Sep80	LRL
					Gardner.CALC CFD EXPT.GRPH.REVW				
^{197}Au	σ_{tot}	1.0-1	1.2+7	Revw	BNL-51363		647	Sep80	LAS
					Arthur.CC CALC VS EXPT.EVAL REVW.				
^{197}Au	$\sigma_{n,\gamma}$	2.0+5	3.5+6	Revw	BNL-51363		282	Sep80	BNL
					Bhat.EVAL METHODS REVIEWED.				
^{208}Pb	$\sigma_{el}(\theta)$	2.4+6	2.5+6	Revw	BNL-51363		592	Sep80	BRC
					LaGrange.GRPH OPTMDL VS EXPT.REVW.				
^{209}Bi	$\sigma_{n,2n}$	1.0+7	1.8+7	Revw	BNL 51363		647	Sep80	LAS
					Arthur.CALC/EXPT RATIO.EVAL REVW.				
^{227}Th	Fiss.Yield	Maxw		Eval	BNL-51363		779	Sep80	GEV
					Rider+HEAVY.LIGHT MASS YLDS.TBLS.				
^{229}Th	Spect.fiss n	Maxw		Revw	BNL-51363		843	Sep80	LAS
					Madiand.SPEC CALC 3 NUCLIDES.REVW.				
^{229}Th	Fiss.Yield	Maxw		Eval	BNL-51363		779	Sep80	GEV
					Rider+HEAVY.LIGHT MASS YLDS.TBLS.				
^{232}Th	σ_{tot}	6.0-3	2.0+1	Revw	BNL-51363		401	Sep80	RPI
					Block.CORRC REVW.GRPHS.CFD.				
^{232}Th	σ_{sct}	6.0-3	2.0+1	Revw	BNL-51363		401	Sep80	RPI
					Block.SCT=TOT-NG.GRPHS.CALC CFD EXPT				
^{232}Th	ν_d	3.4+6		Eval	BNL-51363		817	Sep80	STF
					Sher.LEAST SQ EVAL OF E RELEASE.TBL				
^{232}Th	Spect.fiss n	3.4+6		Eval	BNL-51363		817	Sep80	STF
					Sher LEAST SQ EVAL OF E RELEASE.TBL.				
^{232}Th	Fiss.Prod γ	3.4+6		Eval	BNL-51363		817	Sep80	STF
					Sher.LEAST SQ EVAL OF E RELEASE.TBL				
^{232}Th	Fiss Prod β	3.4+6		Eval	BNL-51363		817	Sep80	STF
					Sher.LEAST SQ EVAL OF E RELEASE.TBL.				
^{232}Th	Fiss.Yield	Fiss	1.4+7	Eval	BNL-51363		779	Sep80	GEV
					Rider+2ES.HEAVY.LIGHT MASS YLDS.TBLS				

NEUTRON DATA REFERENCES

Element	Quantity	Energy (eV) Min	Max	Type	Documentation Ref	Vol	Page	Date	Lab
^{232}Th	Frag Spectra	3.4+6		Eval	BNL-51363	817	Sep80	STF	
	Sher.LEAST SQ EVAL OF E RELEASE.TBL.								
^{231}Pa	Fiss.Yield	Fiss		Eval	BNL-51363	779	Sep80	GEV	
	Rider+HEAVY.LIGHT MASS YLDS.TBLS.								
^{233}U	ν_d	Maxw		Eval	BNL-51363	817	Sep80	STF	
	Sher.LEAST SQ EVAL OF E RELEASE.TBL.								
^{233}U	Spect.fiss n	Maxw		Eval	BNL-51363	817	Sep80	STF	
	Sher.LEAST SQ EVAL OF E RELEASE.TBL.								
^{233}U	Fiss.Prod γ	Maxw		Eval	BNL-51363	817	Sep80	STF	
	Sher.LEAST SQ EVAL OF E RELEASE.TBL.								
^{233}U	Fiss Prod β	Maxw		Eval	BNL-51363	817	Sep80	STF	
	Sher.LEAST SQ EVAL OF E RELEASE.TBL.								
^{233}U	Fiss.Yield	Fiss	1.4+7	Eval	BNL-51363	779	Sep80	GEV	
	Rider+THR E ALSO.HEAVY. LIGHT MASSES								
^{233}U	Frag Spectra	Maxw		Eval	BNL-51363	817	Sep80	STF	
	Sher.LEAST SQ EVAL OF E RELEASE.TBL.								
^{234}U	Fiss.Yield	Fiss		Eval	BNL-51363	779	Sep80	GEV	
	Rider+HEAVY.LIGHT MASS YLDS.TBLS.								
^{235}U	Evaluation	1.0+2	5.0+5	Revw	BNL-51363	683	Sep80	ORL	
	Weston.ENDF/B-V CS GRPH.REVW.								
^{235}U	σ_{tot}	5.0+5	1.5+7	Revw	BNL-51363	702	Sep80	HAR	
	Patrick.CS SHAPE 3 NUCLIDES CFD.REVW								
^{235}U	$\sigma_{n,f}$	1.0+5	2.0+7	Revw	BNL-51363	241	Sep80	ANL	
	Poenitz.VARIOUS EVALS CFD.GRPH.								
^{235}U	$\sigma_{n,f}$	1.0+5	2.0+7	Revw	BNL-51363	282	Sep80	BNL	
	Bhat.THR E ALSO.EVAL REVW.GRPHS.								
^{235}U	ν_p	0.0+0	1.5+7	Revw	BNL-51363	843	Sep80	LAS	
	Madland.CALC CFD EXPT.GRPH.REVW.								
^{235}U	ν_d	Maxw		Eval	BNL-51363	817	Sep80	STF	
	Sher.LEAST SQ EVAL OF E RELEASE.TBL.								
^{235}U	Spect.fiss n	5.3+6	1.4+7	Revw	BNL-51363	843	Sep80	LAS	
	Madland.EVAL RECOMMENDATIONS.GRPH.								
^{235}U	Spect.fiss n	Maxw		Eval	BNL-51363	817	Sep80	STF	
	Sher.LEAST SQ EVAL OF E RELEASE.TBL.								
^{235}U	Fiss.Prod γ	Maxw		Eval	BNL-51363	817	Sep80	STF	
	Sher.LEAST SQ EVAL OF E RELEASE.TBL.								
^{235}U	Fiss Prod ρ	Maxw		Eval	BNL-51363	817	Sep80	STF	
	Sher.LEAST SQ EVAL OF E RELEASE.TBL.								

NEUTRON DATA REFERENCES

Element	Quantity	Energy (eV) Min	Max	Type	Documentation Ref	Vol	Page	Date	Lab
^{235}U	Fiss.Yield	Fiss	1.4+7	Eval	BNL-51363		779	Sep80	GEV
				Rider+THR E ALSO.HEAVY, LIGHT MASSES					
^{235}U	Frag Spectra	Maxw		Eval	BNL-51363		817	Sep80	STF
				Sher.LEAST SQ EVAL OF E RELEASE.TBL.					
^{236}U	Fiss.Yield	Fiss		Eval	BNL-51363		779	Sep80	GEV
				Rider+HEAVY,LIGHT MASS YLDS.TBLS.					
^{238}U	Evaluation	5.0+3	5.0+5	Revw	BNL-51363		683	Sep80	ORL
				Weston.ENDF/B-V CS GRPH.REVW.					
^{238}U	σ_{tot}	5.2-1	1.0+5	Revw	BNL-51363		401	Sep80	RPI
				Block.CORRC REVW.GRPHS.CFD.2 E RANGE					
^{238}U	σ_{tot}	5.0+5	1.5+7	Revw	BNL-51363		702	Sep80	HAR
				Patrick.CS SHAPE 3 NUCLIDES CPD.REVW					
^{238}U	$\sigma_{n.\gamma}$	1.0+5	3.0+6	Revw	BNL-51363		241	Sep80	ANL
				Poenitz.EVAL FROM MDL+EXPT.GRPH.					
^{238}U	$\sigma_{n.\gamma}$	1.0+4	1.0+6	Revw	BNL-51363		531	Sep80	ANL
				Guenther+CS DIFFERENCE FROM 2 CALCS.					
^{238}U	ν_d	3.1+6		Eval	BNL-51363		817	Sep80	STF
				Sher.LEAST SQ EVAL OF E RELEASE.TBL.					
^{238}U	Spect.fiss n	3.1+6		Eval	BNL-51363		817	Sep80	STF
				Sher.LEAST SQ EVAL OF E RELEASE.TBL.					
^{238}U	Fiss.Prod γ	3.1+6		Eval	BNI-51363		817	Sep80	STF
				Sher.LEAST SQ EVAL OF E RELEASE.TBL.					
^{238}U	Fiss Prod β	3.1+6		Eval	BNL-51363		817	Sep80	STF
				Sher.LEAST SQ EVAL OF E RELEASE.TBL.					
^{238}U	Fiss.Yield	Fiss	1.4+7	Eval	BNL-51363		779	Sep80	GEV
				Rider+2%S.HEAVY,LIGHT MASS YLDS.TBLS					
^{238}U	Frag Spectra	3.1+6		Eval	BNL-51363		817	Sep80	STF
				Sher.LEAST SQ EVAL OF E RELEASE.TBL.					
^{238}U	Res.Params.	1.0+2	4.5+3	Revw	BNL-51363		450	Sep80	BNL
				Liou.METHODS TO CALC D.GRPHS.					
^{238}U	Res.Params.	NDG		Revw	BNL-51363		760	Sep80	GEL
				Weigmann.WF CALC CFD EXPT.TBL.REVW.					
^{238}U	$<\Gamma>/D$	1.0+2	4.5+3	Revw	BNL-51363		450	Sep80	BNL
				Liou.METHODS TO CALC D.GRPHS.					
^{237}Np	$\sigma_{n.\gamma}$	1.0+2	1.1+5	Revw	BNL-51363		683	Sep80	ORL
				Weston.EVAL.RES FIT CFD EXPT					
^{237}Np	Fiss.Yield	Fiss		Eval	BNL-51363		779	Sep80	GEV
				Rider+HEAVY,LIGHT MASS YLDS.TBLS.					

NEUTRON DATA REFERENCES

Element	Quantity	Energy (eV) Min	Max	Type	Documentation Ref	Vol	Page	Date	Lab
^{237}Np	Res.Params.	NDG			Revw BNL-51363		760	Sep80	GEL
					Weigmann.WF CALC CFD EXPT.TBL.REVW.				
^{238}Np	Fiss.Yield	Fiss			Eval BNL-51363		779	Sep80	GEV
					Rider+HEAVY,LIGHT MASS YLDS.TBLS.				
^{239}Pu	Evaluation	1.0+2	5.0+5		Revw BNL-51363		683	Sep80	ORL
					Weston.ENDF/B-V CS GRPH.REVW.				
^{239}Pu	σ_{tot}	5.0+5	1.5+7		Revw BNL-51363		702	Sep80	HAR
					Patrick.CS SHAPE 3 NUCLIDES CFD.REVW				
^{239}Pu	α	1.0+3	2.0+5		Revw BNL-51363		683	Sep80	ORL
					Weston.EXPTS GRPH.EVAL REVW.				
^{239}Pu	ν_d	Maxw			Eval BNL-51363		817	Sep80	STF
					Sher.LEAST SQ EVAL OF E RELEASE.TBL.				
^{239}Pu	Spect.fiss n	Maxw			Revw BNL-51363		843	Sep80	LAS
					Madland.SPEC CALC 3 NUCLIDES.REVW.				
^{239}Pu	Spect.fiss n	Maxw			Eval BNL-51363		817	Sep80	STF
					Sher.LEAST SQ EVAL OF E RELEASE.TBL.				
^{239}Pu	Fiss.Prod γ	Maxw			Eval BNL-51363		817	Sep80	STF
					Sher.LEAST SQ EVAL OF E RELEASE.TBL.				
^{239}Pu	Fiss Prod β	Maxw			Eval BNL-51363		817	Sep80	STF
					Sher.LEAST SQ EVAL OF E RELEASE.TBL.				
^{239}Pu	Fiss.Yield	Fiss	1.4+7		Eval BNL-51363		779	Sep80	GEV
					Rider+THR E ALSO.HEAVY, LIGHT MASSES				
^{239}Pu	Frag Spectra	Maxw			Eval BNL-51363		817	Sep80	STF
					Sher.LEAST SQ EVAL OF E RELEASE.TBL.				
^{240}Pu	$\sigma_{n.\gamma}$	1.0+3	3.0+5		Revw BNL-51363		683	Sep80	ORL
					Weston.EVAL CFD EXPT.GRPH				
^{240}Pu	Fiss.Yield	Fiss			Eval BNL-51363		779	Sep80	GEV
					Rider+HEAVY,LIGHT MASS YLDS.TBLS.				
^{240}Pu	Res.Params.	NDG			Revw BNL-51363		760	Sep80	GEL
					Weigmann.WF CALC CFD EXPT.TBL.REVW.				
^{241}Pu	Evaluation	1.0+2	5.0+5		Revw BNL-51363		683	Sep80	ORL
					Weston.ENDF/B-V CS GRPH.REVW.				
^{241}Pu	σ_{tot}	4.0+0	2.7+1		Revw BNL-51363		365	Sep80	KFK
					Froehner.MLBW,R-M.KAPUR-PIERLS CFD.				
^{241}Pu	$\sigma_{n.\gamma}$	4.0+0	2.7+1		Revw BNL-51363		365	Sep80	KFK
					Froehner.3 CHANNEL R-M,TURING METHOD				
^{241}Pu	$\sigma_{n.f}$	1.0+4	1.1+7		Revw BNL-51363		683	Sep80	ORL
					Weston.EVAL CFD EXPT.GRPH				

NEUTRON DATA REFERENCES

Element	Quantity	Energy (eV) Min	Max	Type	Documentation Ref	Vol	Page	Date	Lab
^{241}Pu	$\sigma_{n,f}$	4.0+0	2.7+1	Revw	BNL-51363		365	Sep80	KFK
					Froehner.3 CHANNEL R-M,TURING METHOD				
^{241}Pu	ν_d	Maxw			Eval BNL-51363		817	Sep80	STF
					Sher.LEAST SQ EVAL OF E RELEASE.TBL				
^{241}Pu	Spect.fiss n	Maxw			Eval BNL-51363		817	Sep80	STF
					Sher.LEAST SQ EVAL OF E RELEASE.TBL.				
^{241}Pu	Fiss.Prod γ	Maxw			Eval BNL-51363		817	Sep80	STF
					Sher.LEAST SQ EVAL OF E RELEASE.TBL.				
^{241}Pu	Fiss Prod β	Maxw			Eval BNL-51363		817	Sep80	STF
					Sher.LEAST SQ EVAL OF E RELEASE.TBL.				
^{241}Pu	Fiss.Yield	Maxw	Fiss		Eval BNL-51363		779	Sep80	GEV
					Rider+2ES.HEAVY.LIGHT MASS YLDS.TBLS				
^{241}Pu	Frag Spectra	Maxw			Eval BNL-51363		817	Sep80	STF
					Sher.LEAST SQ EVAL OF E RELEASE.TBL.				
^{242}Pu	σ_{tot}	3.0+4	2.0+7	Revw	BNL-51363		561	Sep80	ANL
					Guenther+GRPH.OPTMDL CALC FOR EVAL.				
^{242}Pu	Fiss.Yield	Fiss			Eval BNL-51363		779	Sep80	GEV
					Rider+HEAVY,LIGHT MASS YLDS.TBLS.				
^{242}Pu	Res.Params.	NDG			Revw BNL-51363		760	Sep80	GEL
					Weigmann.WF CALC CFD EXPT.TBL.REVW.				
^{241}Am	σ_{tot}	1.0-5	1.0+1	Revw	BNL-51363		365	Sep80	KFK
					Froehner.MEAS AND EVAL CS CFD.GRPH.				
^{241}Am	$\sigma_{n,f}$	4.0+6	2.0+7	Revw	BNL-51363		702	Sep80	HAR
					Patrick.CALC CS GRPH.EVAL REVW				
^{241}Am	$\sigma_{n,f}$	1.0-5	1.0+1	Revw	BNL-51363		365	Sep80	KFK
					Froehner.MEAS AND EVAL CS CFD.GRPH.				
^{241}Am	Fiss.Yield	Maxw			Eval BNL-51363		779	Sep80	GEV
					Rider+HEAVY,LIGHT MASS YLDS.TBLS.				
^{241}Am	Fiss.Yield	Fiss	1.4+7	Eval	BNL-51363		779	Sep80	GEV
					Rider+2ES.HEAVY,LIGHT MASS YLDS.TBLS				
^{242}Am	Fiss.Yield	Maxw			Eval BNL-51363		779	Sep80	GEV
					Rider+HEAVY,LIGHT MASS YLDS.TBLS.				
^{243}Am	Fiss.Yield	Fiss			Eval BNL-51363		779	Sep80	GEV
					Rider+HEAVY,LIGHT MASS YLDS.TBLS.				
^{242}Cm	Fiss.Yield	Fiss			Eval BNL-51363		779	Sep80	GEV
					Rider+HEAVY,LIGHT MASS YLDS.TBLS.				
^{245}Cm	Fiss.Yield	Maxw			Eval BNL-51363		779	Sep80	GEV
					Rider+HEAVY,LIGHT MASS YLDS.TBLS.				

NEUTRON DATA REFERENCES

Element	Quantity	Energy (eV) Min	Max	Type	Documentation Ref	Vol	Page	Date	Lab
^{249}Cf	Spect.fiss n	Maxw			Revw BNL-51363		843	Sep80	LAS
					Madland.SPEC CALC 3 NUCLIDES.REVW.				
^{249}Cf	Fiss.Yield	Maxw			Eval BNL-51363		779	Sep80	GEV
					Rider+HEAVY,LIGHT MASS YLDS.TBLS.				
^{251}Cf	Fiss.Yield	Maxw			Eval BNL-51363		779	Sep80	GEV
					Rider+HEAVY,LIGHT MASS YLDS.TBLS.				
^{252}Cf	Spect.fiss n	Spon			Revw BNL-51363		843	Sep80	LAS
					Madland.SPEC CALC CFD EXPT.GRPH.				
^{252}Cf	Fiss.Yield	Spon			Eval BNL-51363		779	Sep80	GEV
					Rider+HEAVY,LIGHT MASS YLDS.TBLS.				
^{254}Es	Fiss.Yield	Maxw			Eval BNL-51363		779	Sep80	GEV
					Rider+HEAVY,LIGHT MASS YLDS.TBLS.				
Many	σ_{pot}	NDG			Revw BNL-51363		331	Sep80	BNL
					Mughabghab.LOW E.POT VS A GRPH.CFD.				
Many	$\sigma_{n,2n}$	1.5+7			Revw BNL-51363		882	Sep80	LRL
					Gardner.CALC METHODS REVW.GRPHS.				
Many	$\sigma_{n,p}$	1.5+7			Revw BNL-51363		882	Sep80	LRL
					Gardner.CS SYSTEMATICS.GRPH.REVW.				
Many	$\sigma_{n,\alpha}$	1.5+7			Revw BNL-51363		882	Sep80	LRL
					Gardner.CALC VS EXPT.GRPH.REVW.				